Western Washington University
Western CEDAR

WWU Graduate School Collection | WWU Graduate and Undergraduate Scholarship

Fall 1980

Geology, Petrology, and Paleomagnetism of Eocene Basalts from the Black Hills, Washington Coast Range

Brian R. Globerman
Western Washington University, bgloberman@gmail.com

Follow this and additional works at: https://cedar.wwu.edu/wwuet

 Part of the Geology Commons

Recommended Citation

Globerman, Brian R., "Geology, Petrology, and Paleomagnetism of Eocene Basalts from the Black Hills, Washington Coast Range" (1980). *WWU Graduate School Collection*. 660.
https://cedar.wwu.edu/wwuet/660

This Masters Thesis is brought to you for free and open access by the WWU Graduate and Undergraduate Scholarship at Western CEDAR. It has been accepted for inclusion in WWU Graduate School Collection by an authorized administrator of Western CEDAR. For more information, please contact westerncedar@wwu.edu.

GEOLOGY, PETROLOGY, AND PALEOMAGNETISM OF EOCENE BASALTS FROM THE BLACK HILLS, WASHINGTON COAST RANGE

by

Brian R. Globerman

Accepted in Partial Completion

of the Requirements for the Degree

Master of Science

Dean of Graduate School

Advisory Committee

Chairman

MASTER'S THESIS

In presenting this thesis in partial fulfillment of the requirements for a master's degree at Western Washington University, I grant to Western Washington University the non-exclusive royalty-free right to archive, reproduce, distribute, and display the thesis in any and all forms, including electronic format, via any digital library mechanisms maintained by WWU.

I represent and warrant this is my original work, and does not infringe or violate any rights of others. I warrant that I have obtained written permissions from the owner of any third party copyrighted material included in these files.

I acknowledge that I retain ownership rights to the copyright of this work, including but not limited to the right to use all or part of this work in future works, such as articles or books.

Library users are granted permission for individual, research and non-commercial reproduction of this work for educational purposes only. Any further digital posting of this document requires specific permission from the author.

Any copying or publication of this thesis for commercial purposes, or for financial gain, is not allowed without my written permission.

Brian Globerman
February 15, 2018

GEOLOGY, PETROLOGY, AND PALEOMAGNETISM OF EOCENE BASALTS FROM THE BLACK HILLS, WASHINGTON COAST RANGE

A thesis

Presented to

The Faculty of

Western Washington University

In partial Fulfillment

Of the Requirements for the Degree

Master of Science

---

by

Brian R. Globerman

December 1980

ABSTRACT

Geology, petrology, and paleomagnetism of
Eocene basalts from the Black Hills, Washington Coast Range

Brian R. Globerman

Geologic mapping in the Black Hills area strongly suggests that the middle Eocene basalts of the Crescent Formation and overlying upper Eocene and Oligocene sedimentary rocks constitute a structurally coherent terrane that is bounded by northeast- and northwest-trending faults. I interpret the Black Hills as a homocline which dips about 10^{o} to 15^{o} to the west. Units within the block are commonly cut by normal and reverse faults, but are not appreciably folded.

Major- and trace-element geochemical analyses indicate that the Black Hills suite is co-magmatic, and is composed of hypersthene-normative tholeiites which were apparently derived by plagioclase — clinopyroxene — olivine ± magnetite fractionation. The suite is petrochemically similar to basalts from the upper part of the Crescent Formation of the Olympic Peninsula, and the upper flows of the lower member of the Siletz River Volcanics of coastal Oregon. An island arc origin for the Black Hills rocks, and by analogy the Crescent basalts, is not supported by field and petrochemical evidence. Discriminant plots of incompatible element data for the Black Hills rocks indicate that the suite is nearly identical to tholeiites from an oceanic island (Hawaiian-type) setting, although the lavas approach mid-ocean ridge basalt compositions as well. These intermediate incompatible-element compositions of the Black Hills rocks, along with Sr isotopic ratios,

resemble those of tholeiites from Iceland and Galapagos, both of which are oceanic islands that were erupted at, or close to, the ridge crest of an active oceanic spreading center. I suggest that the Black Hills lavas, and possibly the tholeiitic and overlying alkalic flows of Eocene age in the Oregon-Washington Coast Range, may reflect generation of the seamount chain on the crest or flanks of an active or fossil spreading center. The composition of the erupting lavas probably evolved toward progressive enrichment in certain incompatible elements (i.e. Ti, Zr, Y, Nb) as the chain moved away from the spreading center axis. The Coast Range oceanic island chain was subsequently sutured to the leading edge of North America by late Eocene to early Oligocene time.

Paleomagnetic study of 35 sites in the Black Hills and adjacent areas indicates that most of the lava flows have declinations of remanent magnetizations that are significantly more easterly-directed than expected for cratonic North America, both before and after application of tectonic corrections. Using the preferred procedure for tilt-correction, the mean Black Hills paleomagnetic direction is: Dec.= 16.3°, Inc.= 67.3°, α_{95}= 4.9°. A rotation of 25.9° ±15° clockwise since middle Eocene time is inferred from these data; there is no evidence of north-south translation. The Black Hills show significantly less clockwise rotation than coeval rocks in the Oregon Coast Range, such as the Siletz River Volcanics, Tyee-Flournoy sediments, and Tillamook Volcanic Series. Data from the Willapa Hills south of the study area confirm the differential rotations the Oregon and Washington coastal blocks.

The paleomagnetic results suggest that the entire Coast Range terrane, extending from the Olympic Peninsula to north of the Klamath

Mountains, has not been a coherent terrane since middle Eocene time. A tectonic model more consistent with available paleomagnetic data involves accretion, and independent clockwise rotation of two or more Coast Range blocks, or "microplates", in response to oblique subduction of the Farallon plate beneath western North America during Paleogene time.

MASTER'S THESIS

In presenting this thesis in partial fulfilment of the requirements for a master's degree at Western Washington University, I agree that the Library shall make its copies freely available for inspection. I further agree that extensive copying of this thesis is allowable only for scholarly purposes. It is understood, however, that any copying or publication of this for commercial purposes, or for financial gain, shall not be allowed without my written permission.

Signature _____

Date 23 December 1980

TABLE OF CONTENTS

LIST OF TABLES

LIST OF FIGURES

ACKNOWLEDGMENTS

I gratefully acknowledge the support and supervision provided by Dr. Myrl E. Beck, Jr., my thesis advisor. He read earlier drafts of this manuscript, and made numerous suggestions for its improvement. In addition, he provided my training in paleomagnetism, and sparked my enthusiam for paleomagnetic investigation of tectonic problems in western North America. Dr. R. Scott Babcock contributed substantially to the geochemistry section through his critical review of earlier drafts, and his instruction in the methods of analytical geochemistry and interpretation of the data. Dr. David R. Pevear reviewed the entire manuscript and provided extremely helpful criticism. He also conducted x-ray diffraction studies on some Black Hills basalt samples, and identified the important zeolites and alteration minerals.

Dr. Parke D. Snavely, Jr. (U.S. Geological Survey) supported the geologic field studies, critically reviewed that section of the manuscript, and contributed to my understanding of the geology and tectonics of the Coast Range through our numerous conversations. Dr. Weldon W. Rau (U.S. Geological Survey and Washington Division of Geology and Earth Resources) identified Foraminifera from the Black Hills, and Dr. Richard L. Armstrong (University of British Columbia) provided Sr isotopic ratios and access to UBC's x-ray fluorescence spectrometer. Dr. David A. Clague (U.S. Geological Survey) critically reviewed the geochemistry section and helped me interpret the petrography of the basalts. Dr. C. Sherman Gromme (U.S. Geological Survey) allowed me to use his Tektronix computer for graphing paleomagnetic and petrochemical data, and provided

very helpful advice on programming and interpretation of paleomagnetic statistics.

Field assistance and logistical support were provided by the following people: Charles and Eleanor Adler, John Day, David Engebretson, Lynn Hertz, Peter Lombardi, Richard Straw, and Gordon White. The Washington State Department of Natural Resources gave me maps of the Capitol Forest Multiple Use Area (Black Hills).

My understanding of the geology of the Black Hills, paleomagnetic and geochemical techniques and interpretation, and the tectonic history of the Coast Range, were greatly enhanced through communication with the following people: John Armentrout, Richard Armstrong, Roger Bates, Rodey Batiza, Russell Burmester, Robert Carson III, Robert Duncan, David Engebretson, Thomas Ewing, Lee Fairchild, Robert Forbes, Ralph Haugerud, Linn Hoover, Edward Irving, Terry Jones, Norman MacLeod, James Pearl, Maurice Pease, Weldon Rau, William Rogers, Donald Swanson, Rowland Tabor, Grant Valentine, Joseph Vance, and Ray Wells. However, I take sole responsibility for all errors in this manuscript.

Financial support was provided by The Geological Society of America Penrose Foundation, United States Geological Survey—Branch of Pacific-Arctic Marine Geology, and National Science Foundation Grant EAR76-24109. The technical help provided by Ruth Schoonover (Western Washington Univ.) and Krista Scott (Univ. of British Columbia) for paleomagnetic and geochemical lab work is gratefully acknowledged.

I. INTRODUCTION

Recent tectonic investigations in western North America suggest that accretion, rotation, and possibly large scale translation of continental and oceanic crustal fragments have been essential processes in the development of the western Cordillera during Mesozoic and Cenozoic time (e.g. Wise, 1963; Hamilton and Myers, 1966; Monger et al., 1972; Jones et al., 1977; Davis et al., 1978; Beck and Cox, 1979; Irving, 1979; Travers and Ladd, 1979). These studies indicate that the Cordillera is an extensive composite of generally unrelated, accreted terranes (Davis et al., 1978). The Cordillera thus may be envisioned as a "collage" (Helwig, 1974) or, more graphically, as in the case of south-central Alaska, a "garbage heap" (D. L. Jones, 1977, oral comm.) into which crustal fragments, derived from distant sources, were emplaced by subduction processes and/or transcurrent faulting.

During the past few years, considerable efforts have been directed toward identifying the pieces of the collage, and delineating their boundaries. These crustal fragments, variously termed "microcontinents" (Beck et al., 1977; Churkin and Eberlein, 1977), "miniplates" (Irving, 1979), and "schollen" (Dewey and Sengor, 1979), are frequently bounded by major faults, pronounced linear gravity and magnetic anomalies, or distinct isotopic transition zones (Davis, 1977; R. L. Armstrong, 1979, oral comm.), and may differ considerably in stratigraphy, lithology, and petrochemistry from adjacent terranes. Many appear to be allochthonous with respect to the North American craton, in that their paleomagnetic poles are appreciably discordant with respect to the apparent polar wandering path for

"stable" North America (Fig. 1).

Latitudinal shifts of sizable magnitude have been proposed for certain units, such as the Triassic Nikolai Greenstone in south-central Alaska (Hillhouse, 1977), and the mid-Cretaceous "Layton-ville limestone" blocks within the Franciscan mélange in northern California (Alvarez et al., 1980). Large scale longitudinal shifts are indicated in the Cordillera as well, since Permian fusulinids of Tethyan affinities have been collected from several localities in central British Columbia. These fauna are characteristic of a shallow water equatorial environment (W. R. Danner, 1979, oral comm.), and are thought to be exotic to North America (Monger and Ross, 1971; Monger et al., 1972). Furthermore, geologic investigations of Paleozoic and Mesozoic ophiolites and volcanic complexes in eastern Oregon (Thayer, 1977; Dickinson, 1979), and in the interior of British Columbia (Schau, 1970; Anderson, 1976; Monger, 1977; Travers, 1978) suggest that suturing of oceanic crust and island arcs to the leading edge of North America, followed by transposition of the subduction zone to the outboard side of the accreted terranes, were important and recurrent processes in the evolution of the Cordillera. In situ rotation of crustal blocks, as suggested by the discordant paleomagnetic directions observed in predominantly Cenozoic igneous and sedimentary rocks (Beck, 1976; Basham and Larson, 1978; Beck and Cox, 1979; Greenhaus and Cox, 1979; Kamerling and Luyendyk, 1979) also appears to have been a widespread phenomenon.

A final and almost insurmountable complication in Cordilleran reconstructions is the presence of numerous strike slip faults with tens to hundreds of kilometers of displacement (Fig. 2), such as the San Andreas (Hill and Hobson, 1978); Straight Creek (Misch, 1966);

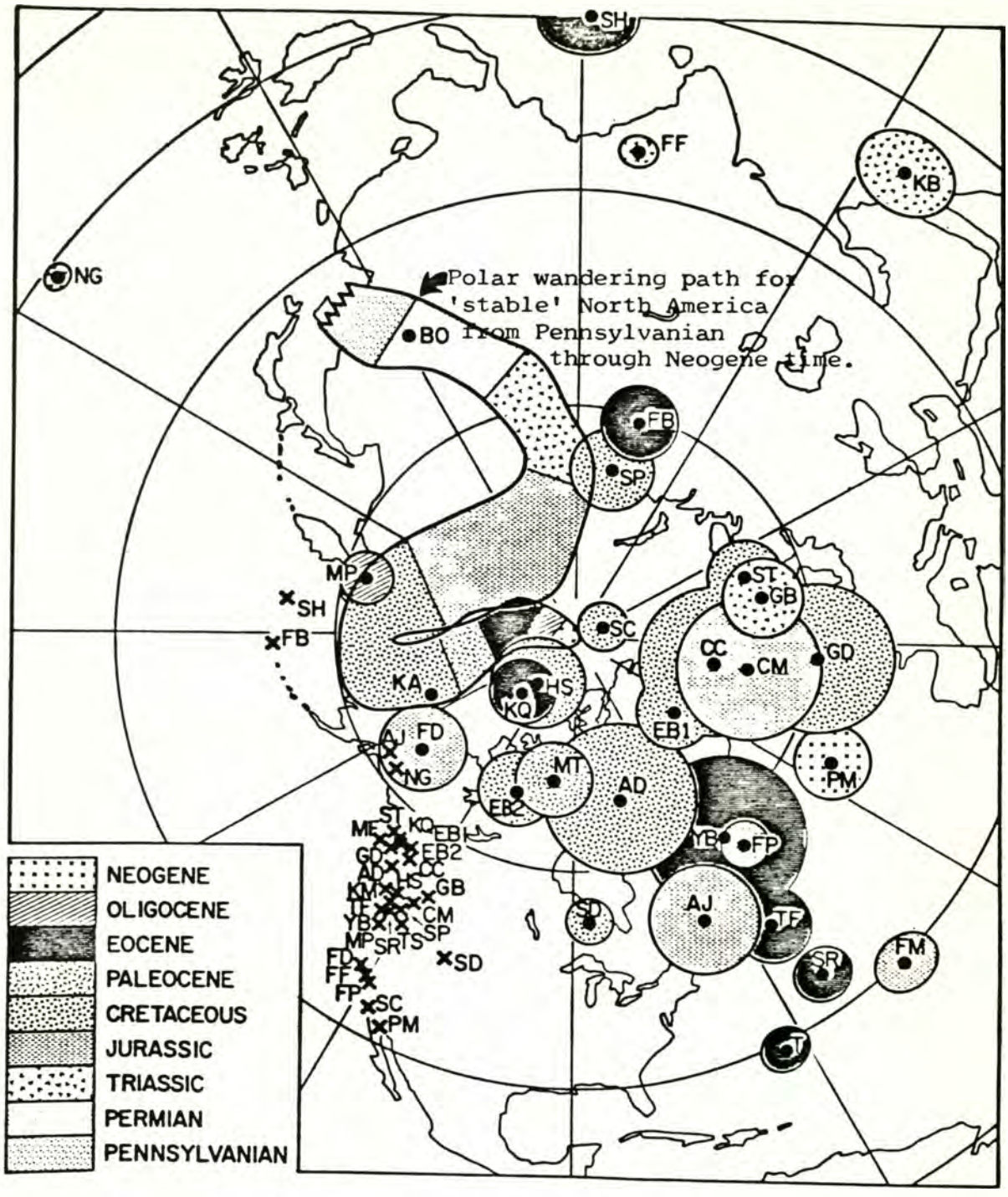

FIGURE 1 - Aberrant paleopoles from the western Cordillera compared with the apparent polar wandering path for stable North America. Selected poles are: NG= Nikolai greenstone, Alaska (Hillhouse, 1977); SR= Siletz River Series, Oregon, TF= Tyee-Fluornoy Fm., Oregon, and YB= Yachats basalt, Ore. (Simpson and Cox, 1977). For complete reference of poles shown above see Appendix F. Diagram from Irving, 1979.

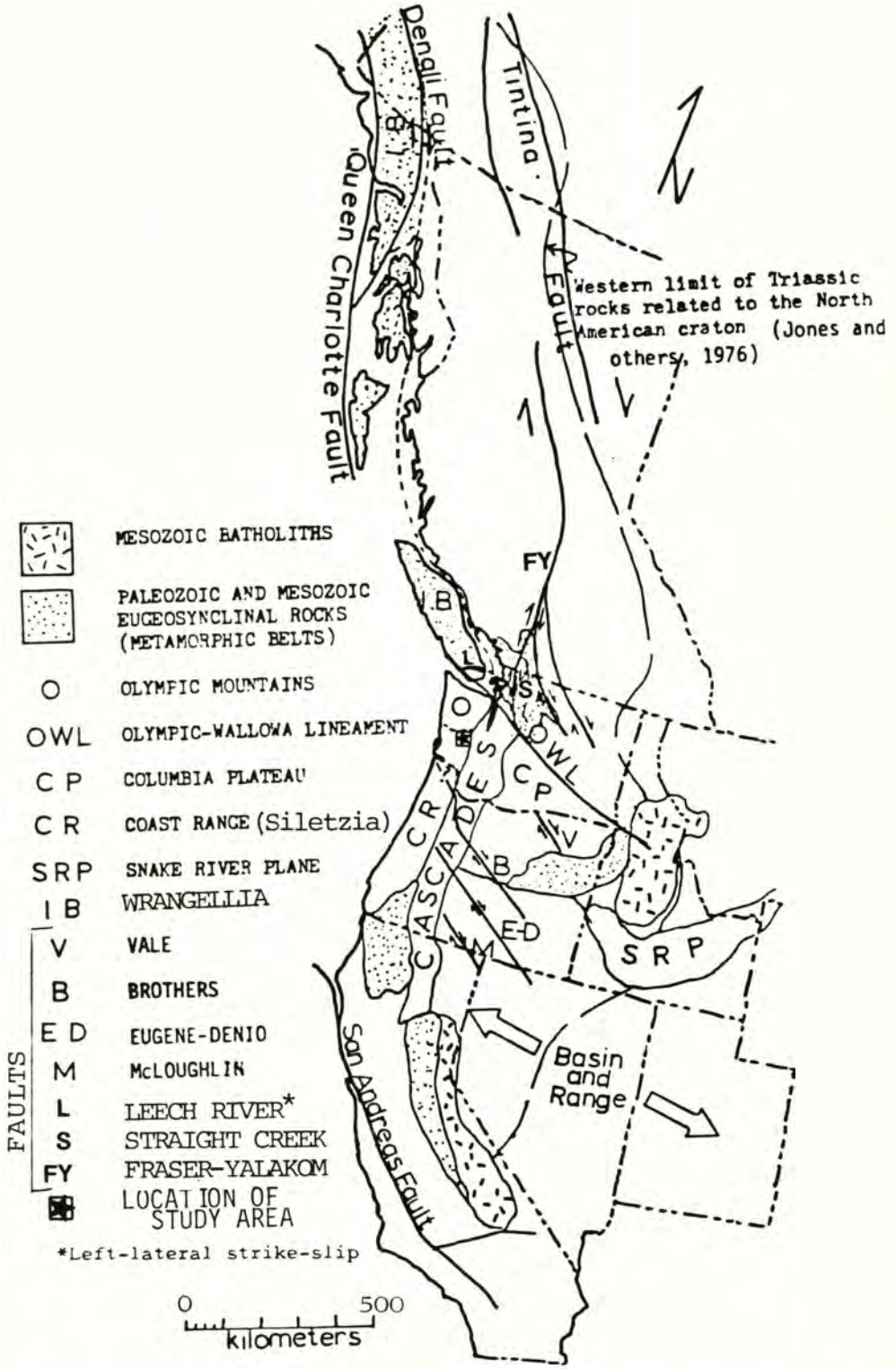

Figure 2: Generalized geologic and tectonic map of the western North American Cordillera from California to Alaska. Modified from Burr, 1978.

Leech River (Fairchild, 1979a); Fraser River, Yalakom, Tintina–Northern Rocky Mountain Trench System (Monger and Price, 1979); Denali (Lanphere, 1978); and Queen Charlotte - Fairweather (Chase and Tiffin, 1972). These faults may redistribute large segments of a terrane after its accretion, further complicating the interpretation of its initial extent, derivation, and tectonic significance.

Despite these complexities, it has been possible to recognize several discrete "microcontinental" blocks, some of them dismembered and separated by appreciable distances, but with nearly identical stratigraphies, geochemical trends, and paleomagnetic inclinations. One example is Wrangellia (Jones et al., 1977), a sizable terrane extending along the Pacific margin from south-central Alaska to Vancouver Island, and possibly to the Hells Canyon region of eastern Oregon and western Idaho. It is characterized in its entirety by similar sequences of Triassic volcanic rocks and carbonates, and is juxtaposed against unrelated sequences of Triassic and older rocks along major faults. A paleomagnetic pole determined for Wrangellia suggests derivation from a source region of between 30 to 45 degrees south latitude (Jones et al., 1977), possibly the Equadorian coast (Irving, 1979).

Another displaced terrane is Stikinia (Monger and Irving, 1979) in the northern Intermontane Belt of British Columbia. It is composed of andesite, basalt, and minor clastic sedimentary rocks, presumably a volcanic arc assemblage of Early Triassic age. It was accreted to the western margin of North America in latest Triassic time (Monger and Irving, 1979).

A more recently emplaced terrane is Siletzia (Irving, 1979), a thick sequence of Eocene through Oligocene submarine pillow lavas,

dikes, and sills with overlying marine sediments which, together with Miocene basalt flows and coastal plain deposits, comprise the Oregon Coast Range (Snavely and Wagner, 1964). Simpson and Cox (1977) reported 55 to 75 degrees of clockwise rotation since middle Eocene time for the Siletz River Volcanics, Tyee-Flournoy sediments, and Yachats Basalt in the Oregon Coast Range. Siletzia had been thought to extend north through Washington to the southern tip of Vancouver Island (Simpson and Cox, 1977; Irving, 1979), implying that the entire Coast Range, from north of the Klamath Mountains in Oregon to south of the Leech River fault on Vancouver Island, rotated as a single, coherent unit. However, no paleomagnetic data were available in the Washington Coast Range with which this assumption could be tested, although Burr (1978) and Beck and Burr (1979) have demonstrated that the Goble volcanics of southwest Washington (which may be Coast Range or Cascade volcanic arc) rotated about 25 degrees clockwise since middle Oligocene time. More recent work by Bates (1980) in the Ohanapecosh Formation of the southern Washington Cascades is consistent with Beck and Burr's (1979) interpretation. Several preliminary studies have been conducted in the Eocene volcanic rocks of the Olympic Peninsula, which lie in the northern part of the Washington Coast Range, but most samples were highly altered and did not yield stable remanent magnetizations (M. E. Beck, Jr., 1979, oral comm.).

The present investigation was undertaken to extend paleomagnetic sampling of the coastal block(s) north into west-central Washington, where relatively unaltered volcanic rocks of middle Eocene age are exposed in a gently dipping basement uplift known as the Black Hills, located south of the Olympic Mountains and

about 15 km west of the city of Olympia. This study has several objectives. The first is to determine a paleomagnetic pole position for the basalts of the Black Hills, and to compare it with the expected middle Eocene pole for cratonic North America, in order to ascertain the amount and direction of any significant rotation. Secondly, this pole position is to be compared with data for coeval rocks in the Oregon Coast Range, in order to test the assumption that Siletzia is a single, coherent terrane. If statistically different pole positions are found, then the Washington - Oregon Coast Range would more reasonably be modelled by two or more independently rotating sub-units. Finally, major- and trace-element petrochemical analyses will be presented for the Black Hills basalts. These data, coupled with discrimination diagrams of several immobile elements, provide additional constraints on the petrotectonic setting of the Eocene volcanic flows. This is particularly important because the origin of broadly coeval and lithologically similar volcanic sequences in the Olympic Peninsula and Oregon Coast Range is equivocal: they are variously interpreted as products of island arc (Lyttle and Clarke, 1975), ocean ridge (Glassley, 1974; Loeschke, 1979), and oceanic island (Snavely et al., 1968; Glassley, 1974; Cady, 1975) magmatism. Another possibility is that the basalts are a hybrid of the latter two environments (Globerman and Babcock, 1980), resembling the eruption of tholeiitic seamounts on active spreading ridge crests that has been described by Menard (1969) and Batiza (1977).

II. GEOLOGY

INTRODUCTION

Reconnaissance geologic mapping in the Black Hills and adjacent areas was conducted during the summers of 1978 and 1979. The objectives of this study were to obtain data on the structural geology of the area to complement the paleomagnetic studies of the Eocene basalts in the Black Hills; to establish better age control for the volcanic rocks; and to interpret the eruptive history of these lavas through detailed field observations, petrographic studies, and chemical analyses.

The southern and western sections of the Black Hills were studied in greatest detail; virtually all road outcrops and numerous stream bed exposures were examined. In the northern and eastern sections, only exposures along the improved roads and railroad grades were studied. South of the Chehalis River and the Black Hills, geologic data were mainly compiled from published mapping, although reconnaissance studies were made along county roads and railroad grades.

Observed field data, such as contacts and structural measurements, were plotted on aerial photographs and transferred to a base map consisting of the Rochester, Malone, Shelton, and Olympia (eastern portion) 15-minute quadrangles. Additional geologic information was obtained from LANDSAT and side-looking airborne radar (SLAR) imagery, aeromagnetic and gravity maps, and soil maps of the Capitol Forest Multiple Use Area, in which much of the Black Hills area is located.

Structural data are based on geologic mapping, interpretation of aerial photography, and investigations of earlier workers. Mapping

involved the measurement of attitudes on sedimentary rocks, silty interbeds or breccia units within lava flows, and horizontal cross-joints. The latter features are recognizable in columnar-jointed basalt flows, and are perpendicular to the lengths of the columns (Williams and McBirney, 1979, p. 114). Attitudes of well developed cross-joints were measured at columnar basalt outcrops which lacked recognizable interbeds. Between 5 and 15 cross-joints were measured at a single outcrop, with the mean taken to represent the strike and dip of the lava flow at that locality. Most of these cross-joints have shallow dips which do not exceed 10 to 15 degrees and are consistent with the more accurately measured dips of flows based upon such features as saprolitic zones, abrupt changes in column thicknesses, and breccia layers between columnar-jointed flows. It is assumed that the cross-joints formed parallel to the near horizontal surface upon which the flows were erupted, and that any observed dip was produced strictly by tectonic processes subsequent to cooling of the lava flow. It is assumed that no component of the (total) dip of the joints was due to cooling phenomena or the existence of steep pre-eruption topography, primarily because these variables are unknown.

This is not a very precise method of structural mapping, since the orientations of the columns and cross-joints may not necessarily represent actual dips which are produced by folding or some other deformation. However, no alternative method is available to obtain attitudes for the basalt flows as the flows which constitute most of the eastern and interior regions of the Black Hills lack sedimentary interbeds or overlying clastic deposits. Henriksen (1956)

was faced with a similar problem in mapping the structure of thick Eocene basalt flows in the Willapa Hills, about 75 km south of the Black Hills. He elected to use joint orientations in the absence of other, more reliable features, and stated:

> "Well-developed columnar jointing serves in determination of the attitudes of the flows where the tops are not exposed, and other indications of bedding are absent."

The validity of this method is supported by the fact that the mean attitudes of all measured cross-joints and of the more accurately measured sedimentary units overlying and interbedded with the flows are virtually identical.

Location

This investigation includes most of the Black Hills and the surrounding area between meridians 123° and 123° 30' W., and parallels 46° 45' and 47° 15' N. The study area lies about 90 km southwest of Seattle, Washington, and about 45 km east of Hoquiam within Thurston, Grays Harbor, Lewis, and Mason Counties (Fig. 3), and comprises the cities of Olympia-Tumwater, Shelton, McCleary, Elma, Oakville, Rochester, and Little Rock (Sheet 1).

The Black Hills constitute one of several large basement uplifts in the central part of the Washington Coast Range (Fig. 4), an area roughly bordered by the Pacific Ocean on the west, the Puget-Willamette trough on the east, Hood Canal and the southernmost Olympic Peninsula on the north, and the Columbia River on the south. The Washington Coast Range is part of a larger tectonic province extending from just north of the Klamath Mountains in Oregon northward to the southern end of Vancouver Island. The Black Hills comprise about 200

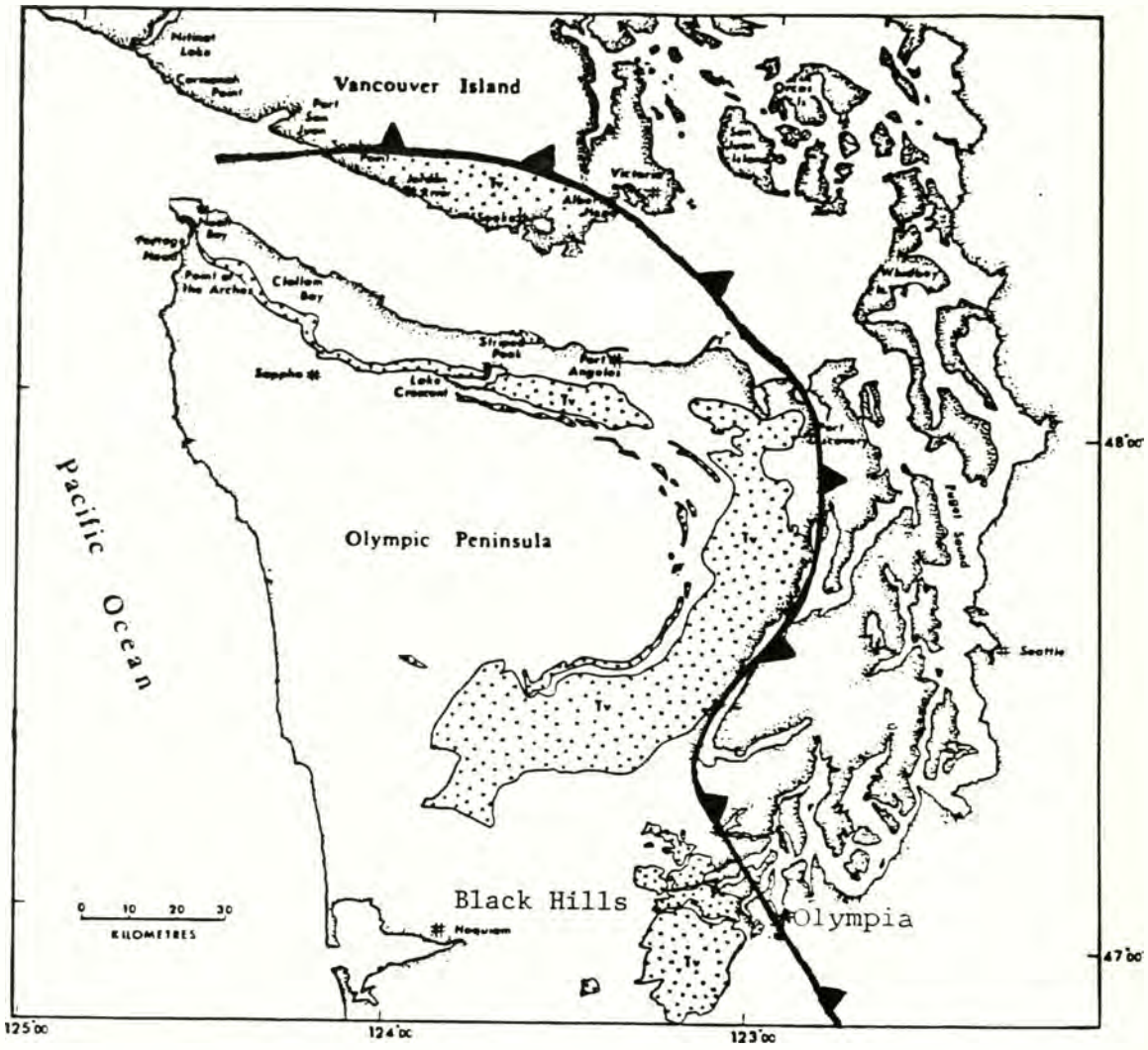

Figure 3 : Index map of Strait of Juan de Fuca, Olympic Peninsula, southern Vancouver Island, and southern Puget Sound lowland, showing outcrops of Metchosin Volcanics on Vancouver Island and Crescent Formation (Tv) in the Olympic Peninsula and southern Puget Sound. The study area (Black Hills) is situated at the southwestern end of Puget Sound. Map from MacLeod and others (1977). Thick barbed line represents an inferred early Eocene underthrust (P. D. Snavely, Jr., written comm., 1978).

Figure 4: Simplified geologic map of Black Hills and nearby basement uplifts. Patterned areas represent exposures of Eocene volcanic rocks; heavy black lines represent faults. Geology after Huntting and others, 1961.

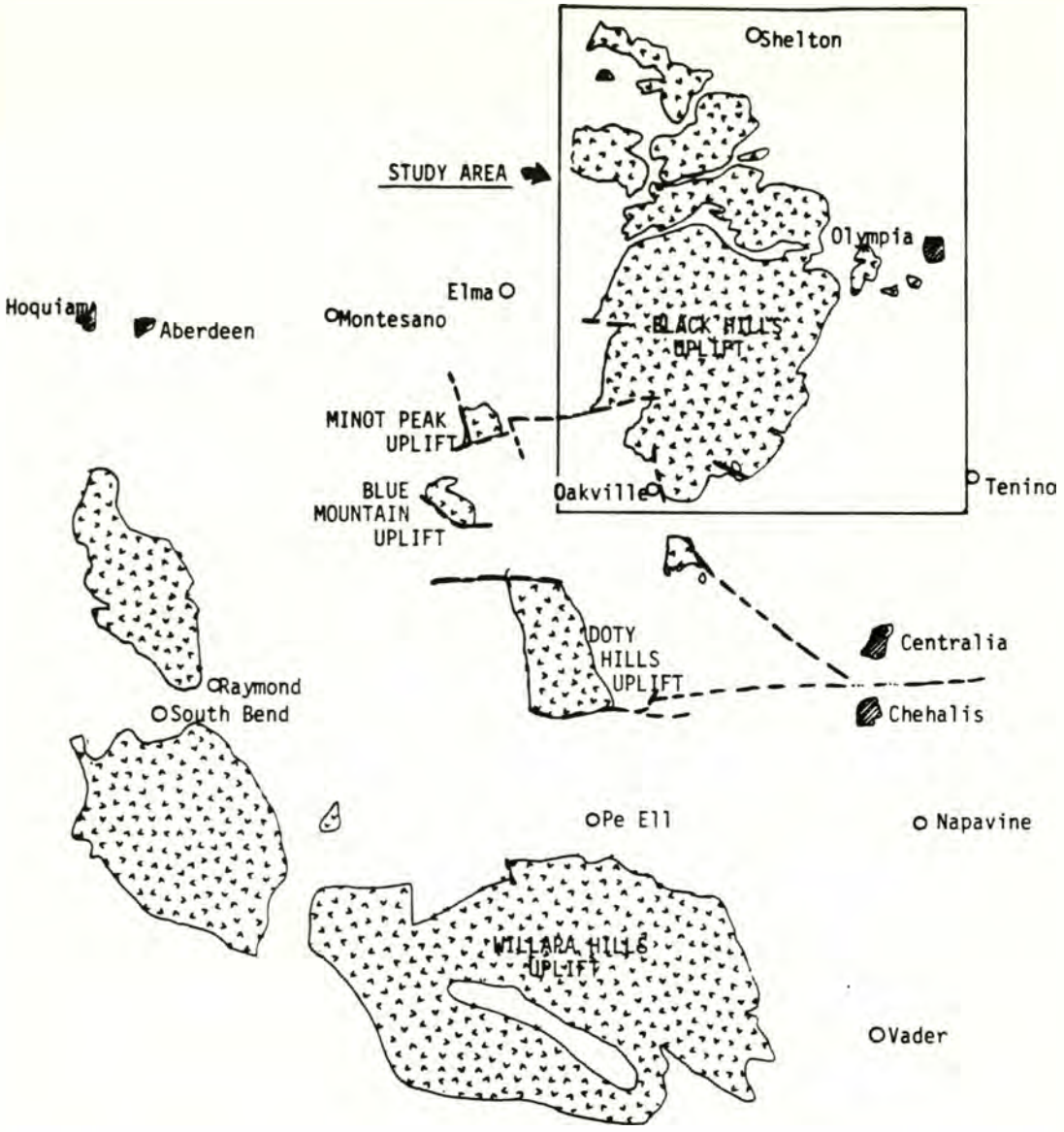
Shelton
STUDY AREA
Olympia
Elma
Hoquiam
Aberdeen
Montesano
BLACK HILLS UPLIFT
MINOT PEAK UPLIFT
BLUE MOUNTAIN UPLIFT
Oakville
Tenino
DOTY HILLS UPLIFT
Centralia
Chehalis
Raymond
South Bend
Pe Ell
Napavine
WILLAPA HILLS UPLIFT
Vader

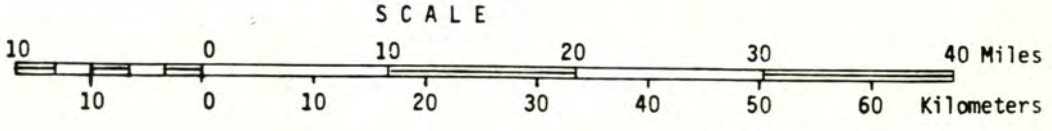
SCALE
10 0 10 20 30 40 Miles
10 0 10 20 30 40 50 60 Kilometers

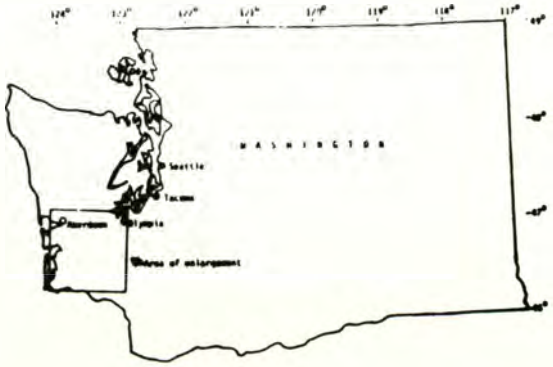

square km of heavily forested uplands between Summit Lake and U.S. Highway 101 on the north, the Black River and Interstate 5 on the east, and the Chehalis River and U.S. 12 on the south. Major drainages include Waddell, Sherman, Cedar, McLean, Perry, Porter, Mox Chehalis, and Kennedy Creeks. Elevations range from approximately 60 m along the Chehalis River to 808 m at Capitol Peak, 805 m at Larch Mountain, and 716 m at Rock Candy Mountain.

Physiography

The Black Hills area consists of steep escarpments and sub-rounded peaks surrounded by glacial outwash prairies and broad alluvial stream valleys. Within the highlands small creeks head and flow outwards through deep, narrow canyons cut in basalt. This characteristic physiography developed in part during the retreat of the Puget lobe of the Fraser glacier toward the end of the Vashon Stade (Noble and Wallace, 1966), some 13,000 radiocarbon years b.p. (Easterbrook and Rahm, 1972). The physiography of the eastern portion of the Black Hills and adjacent glacial outwash prairies is shown diagramatically in Figure 5. The western and southern margins of the study area are characterized by more subdued topography, reflecting the more readily eroded Tertiary sandstones and siltstones which constitute much of this area.

PREVIOUS INVESTIGATIONS

Earliest geologic investigations in the study area were conducted by Weaver (1916, 1937), who described the lithology and structure of Tertiary formations and their correlation with similar units in the Willapa Hills to the south, and the Olympic Mountains and hills of Kitsap County to the north. He suggested that

the volcanic rocks of the Black Hills were erupted near the continent on a submerged coastal plain, and proposed an early to middle Eocene age for this 600+ m thick basaltic pile (Weaver, 1937).

G. M. Valentine mapped portions of the Black Hills in 1950 while conducting geologic studies for the Shell Oil Company. He collected Foraminifera from basaltic sandstone that crops out below a pillow lava flow on the north flank of Rock Candy Mountain. These Foraminifera indicated a middle Eocene age and an inner neritic environment of deposition for these strata. Pease and Hoover (1957) mapped the southern and western portions of the Black Hills, and most of the Doty Hills and Minot Peak area to the southwest. Snavely and others (1958) mapped the southeastern corner of the Black Hills as far west as the Grays Harbor - Thurston County boundary, in connection with a detailed geological and resources investigation of the Centralia-Chehalis coal district to the southeast. Wallace and Molenaar (1961) and Noble and Wallace (1966) mapped the Quaternary deposits and exposures of volcanic basement in northern Thurston County. Molenaar and Noble (1970) conducted related mapping in southeastern Mason County. Rau (1967) investigated the geology and paleontology of the Wynoochee Valley quadrangle in the extreme western section of the Black Hills area. Quaternary deposits in the southern Olympic Peninsula were mapped by Carson (1970); his study extended into the northwesternmost part of the Black Hills area. Fossiliferous Oligocene siltstones and sandstones at the Porter Bluffs in the southwestern flank of the Black Hills were studied by Rau (1948) and Armentrout (1973), who provided further age control on strata that unconformably overlie the Eocene basalts.

Figure 5: Physiography of eastern Black Hills and adjacent Puget Sound lowland. After Wallace and Molenaar, 1961.

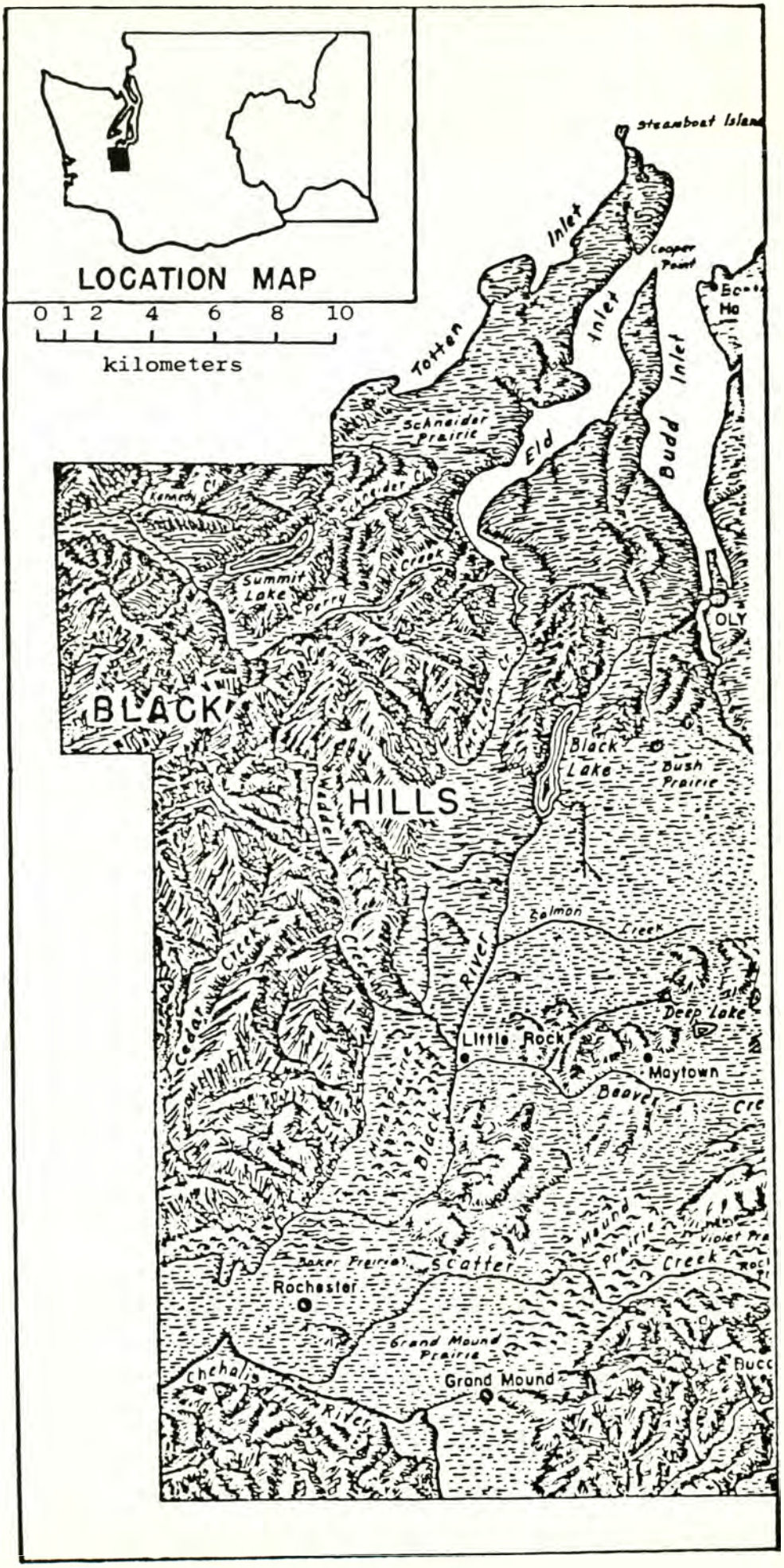
LOCATION MAP
0 1 2 4 6 8 10
kilometers
Steamboat Island
Inlet
Cooper Point
Totten
Inlet
Budd Inlet
Schneider Prairie
Eld
Summit Lake
Perry
OLY
BLACK
HILLS
Black Lake
Bush Prairie
Salmon Creek
Cedar Creek
Black River
Deep Lake
Little Rock
Maytown
Beaver
Mound Prairie
Violet Prairie
Creek
Baker Prairie
Scatter
Rochester
Grand Mound Prairie
Grand Mound
Chehalis River

Two major faults bordering the Black Hills on the southeast and northeast were proposed by Bromery (1962) and Rogers (1970) on the basis of aeromagnetic and gravity surveys. Additional studies of the northeastern structure, termed the "Olympia lineament" on the geologic map (Sheet 1), were made by the Washington Public Power Supply System (1975) during site evaluations for two proposed nuclear power generating plants just west of the Black Hills area.

STRATIGRAPHY

Crescent Formation

Distribution and thickness: The oldest rocks exposed in the Black Hills area are a sequence of lava flows with pyroclastic and sedimentary interbeds which are tentatively correlated on the basis of lithology and age with the Crescent Formation (Fig. 3) in the northern Olympic Peninsula of Washington (Arnold, 1906; Weaver, 1937; Pease and Hoover, 1957). Most of the lower "member" of the Crescent Formation at the type locality consists of predominantly augite-rich submarine pillow lava flows and lesser intercalations of marine siltstone. The upper "member" consists of columnar-jointed, massive, and lesser pillow basalt flows, volcanic breccia, and marine tuffaceous sedimentary rocks (Arnold, 1906; Brown et al., 1960; Cady et al., 1972; Glassley, 1974; Cady, 1975; Tabor and Cady, 1978a).

The Crescent Formation is exposed in the Black Hills along logging roads, railroad grades, stream beds, highway embankments, and quarries. Excellent exposures are found in a quarry 1.5 km northwest of Oakville (NE¼ sec. 25, T. 16 N., R. 4 W.), a quarry on U.S. 101 10 km south of Shelton (NW¼ sec. 17, T. 19 N., R. 3 W.)

in southeastern Mason County, the Burlington Northern railroad grade between Gate and Oakville along the southern slope of the Black Hills, and the steep escarpment at Kennedy Falls just north of State Route 8 (S.R. 8) in the NE¼ sec. 1, T. 18 N., R. 4 W. Numerous outcrops of columnar-jointed and pillow lava flows and breccias occur along the freeway cuts of U.S. 101 and S.R. 8 which traverse the northern part of the area. The maximum exposed thickness of the Crescent Formation in the Black Hills is estimated to be at least 600 m (Weaver, 1937) to 1500 m (Pease and Hoover, 1957).

Lithology: The augite-rich basalt flows of the Crescent Formation are commonly massive, although pillow and columnar structures occur in places. Hyaloclastite, lapilli tuff, lapilli-breccia, and basaltic sandstone are subordinant, while intercalations of hemipelagic siltstone are rare. In contrast, thick intercalations of marine siltstone and sandstone are common in correlative lava flows mapped in the Willapa Hills to the south (Henriksen, 1956; Wolfe and McKee, 1968; R. E. Wells, 1979, oral comm.).

Within the Black Hills the Crescent Formation can be subdivided into five major lithologic units:

(1) Pillow basalt with subordinant breccia and hyaloclastite

(2) Breccia with or without subordinant pillows

(3) Basalt flows with prominent columnar jointing

(4) Massive basalt flows

(5) Lithic tuff with subordinant volcanic breccia

The relationship between these groups is usually gradational. Pillow lavas and breccias predominate along the northern and northeastern slopes, while columnar-jointed and massive flows generally

crop out in the interior of the Black Hills, and along the southern flank. The stratigraphic relations of the various units are not well understood.

Pillow basalt: Pillows range from about 0.5 to 1.0 m in diameter, and frequently display well developed radial jointing (Fig. 6). Between the pillows are thin interstices filled with volcanic breccia, devitrified glass, and well-indurated marine siltstone and basaltic sandstone (Fig. 7). These interstices rarely exceed 15 cm in thickness. In the Black Hills sedimentary interbeds are extremely rare, although they are abundant in the Doty Hills and Minot Peak area to the southwest, and range from 1 to 15 m in thickness (Pease and Hoover, 1957). The best exposures of hemipelagic siltstone interbeds in pillow lavas are at the Mottman quarry east of the Black Hills and southwest of Olympia (NW¼ sec. 27, T. 18 N., R. 2 W.), in a small quarry on State Route 108 near the intersection with the Burlington Northern railroad grade (NE¼ NW¼ sec. 19, T. 19 N., R. 3 W.), and along a roadcut on S.R. 8 (westbound lanes), about 2.5 km east of McCleary. I collected a foraminiferal assemblage characteristic of open-sea bathyal conditions (W. W. Rau, 1979, written comm.) from a siltstone interbed in this roadcut.

The pillow lavas are generally dense and vesicular, and contain amygdaloidal fillings of calcite and zeolite minerals such as natrolite, analcite, and heulandite, laumontite, stilbite, and scolecite (D. R. Pevear, 1979, oral comm.). Pillows are frequently encrusted by thick rinds and altered glassy selvages, are ellipsoidal to subrounded in shape, and are intercalated with more or less horizontal breccia layers. Pillows were rarely observed in the higher elevation areas.

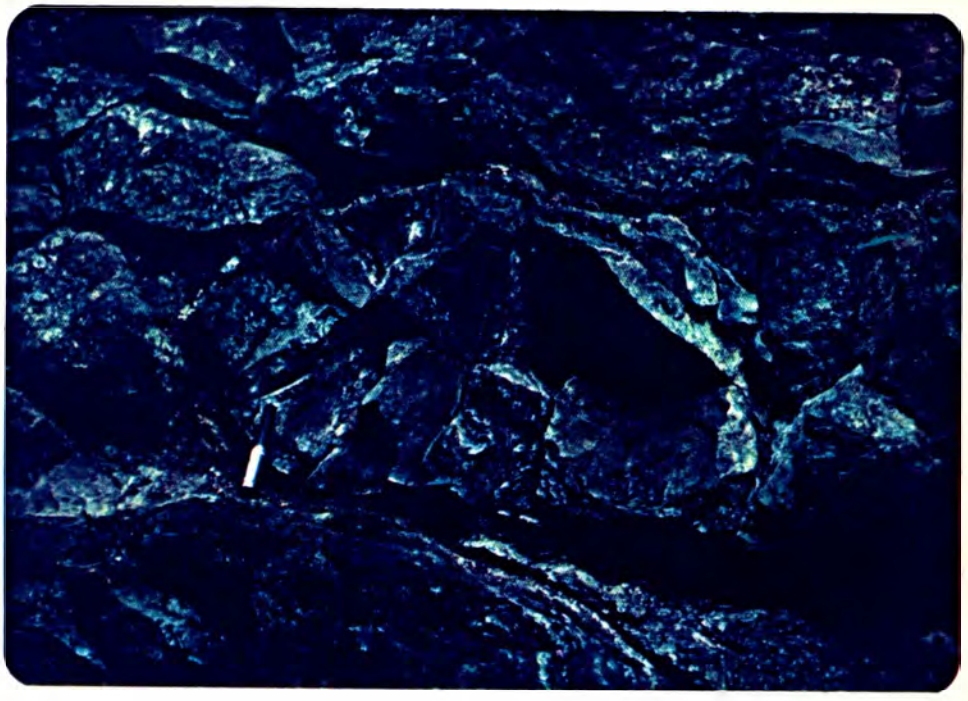

Figure 7 (above): Subrounded to ellipsoidal pillow basalt of the Crescent Formation, Black Hills. Pillow in center of photograph is surrounded by matrix of siltstone, basaltic sandstone, and devitrified glass.

Figure 6 (right): Pillow basalt of lower member of the Crescent Formation. Hurricane Ridge Road, northern Olympic Peninsula.

Pillow breccia: This unit comprises mainly fine-grained brecciated basalt which completely surrounds isolated pillows. Abrupt chilling of fluid lavas erupted in the sea probably produced the variety of fragmental deposits observed in roadcuts along S.R. 8 between Olympia and McCleary, and at Summit Lake, in the northern part of the area. The breccia is compositionally similar to the radially-jointed pillows which it surrounds, and presumably formed as pillow margins coalesced and shattered during submarine extrusion. Some pillow cores were apparently well insulated and preserved within the breccia matrix. Fragments of palagonitized basaltic glass, termed hyaloclastite (Williams and McBirney, 1979), and alteration products such as zeolite and carbonate minerals are intermixed with the breccia. These exposures resemble a volcanic sequence described on Quadra Island, British Columbia (Carlisle, 1963), in which pillow lavas grade upward into an unstratified mass of isolated, unbroken pillows of quite variable size and shape, within a matrix of breccia and hyaloclastite.

Columnar-jointed basalt flows: Thick lava flows with prominent columnar jointing predominate in the highlands and along the southern and eastern flanks of the Black Hills (although they are a less conspicuous feature on the northern flank as well). Pillow lavas, in contrast, are almost always confined to the lowland areas. Amygdaloidal, augite-rich aphanitic to phaneritic basalts make up the majority of these flows, whose surfaces are commonly reddish or brown due to oxidation of iron-rich minerals. The basalts, however, are internally fresh. Elongate laths of plagioclase and augite are recognizable on fresh surfaces

of some of the coarse grained rocks. Vesicles are commonly filled with zeolite minerals and calcite.

Columnar-jointed flows at several localities are separated by breccia layers and thin saprolite zones (Fig. 8). In general, the typical three-fold division of flows into lower colonnade, entablature, and upper colonnade (e.g. Williams and McBirney, 1979) is not recognized in the Black Hills. The colonnade, consisting of vertical to steeply inclined hexagonal columnar joints, is usually overlain by a thick layer of highly oxidized basalt and/or basaltic sand (Fig. 9), rather than by an entablature. Cross-joints form more or less orthogonal to the primary columnar joints, and are generally horizontal to slightly inclined. These cross-joints therefore can be used to determine the tectonic tilt of flows where sedimentary interbeds and flow contacts are lacking, as they frequently are in the Black Hills (Figs. 10, 11). Column inclinations at most localities are fairly consistent along the length of the exposure, although some display prominent fanning (Fig. 12) and/or rosette patterns (Fig. 13) which make it impossible to deduce structural information. A highly chaotic jointing pattern is observed in flows at the Kelly quarry on U.S. 101, about 15 km northwest of Olympia (NE¼ sec. 2, T. 18 N., R. 3 W.). This complex unit overlies highly altered columnar basalt, and appears to be composed of either pillows or filled lava tube rosettes (Fig. 13). It was impossible to infer structural information from such chaotic jointing.

Massive basalt flows: Thick sequences of highly vesicular, massive basalt flows constitute the dominant lithologic type in

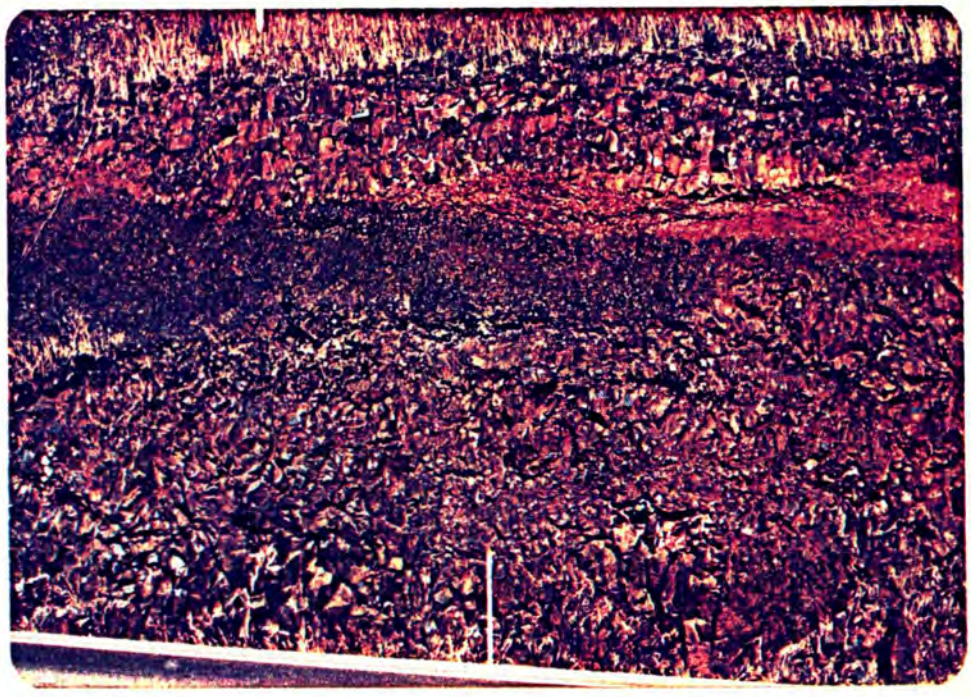

Figure 8: Two columnar basalt flows separated by a breccia zone which dips about 15^{0} to the northwest. Note weathering horizon between breccia and overlying columns in the upper right-hand corner of photograph. Road sign at bottom center provides scale. State Route 8 (westbound lanes), about 2.5 km east of McCleary.

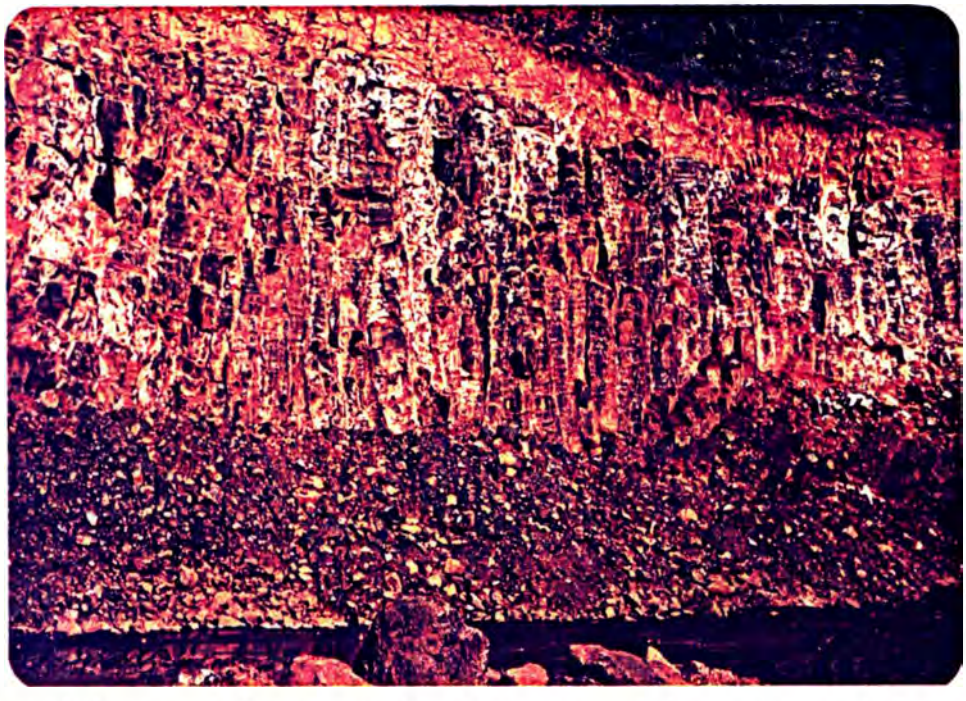

Figure 9: Columnar-jointed basalt flow exposed in a quarry 1.5 km northwest of Oakville. Note thickness and near verticality of the columns. Lava flow is unconformably overlain by highly oxidized basaltic sandstone.

Figure 10: Roadcut of relatively unweathered columnar-jointed Crescent basalt flow, which is virtually flat lying. Note drill holes in roadcut (arrow) from which paleomagnetic core samples were obtained. Black Lake Boulevard, east side of Black Hills (SW¼ SW¼ sec. 29, T. 18 N., R. 2 W.).

Figure 11: Highly vesicular columnar-jointed basalt flow which dips about 18° to the east (right). Note drill hole (arrow) from which paleomagnetic sample no. 258 was obtained. Bordeaux Road, east side of Black Hills (NW¼ NW¼ sec. 9, T. 16 N., R. 2 W.).

Figure 12: Black Lake Boulevard quarry (NE¼ sec. 29, T. 18 N., R. 2 W.) about 3.5 km southwest of Olympia, in which columnar-jointed Crescent basalt flows are exposed. Note that some columns are nearly vertical, while others display prominent fanning patterns.

Figure 13: Kelly Quarry on U.S. 101 and Steamboat Island Road (NE¼ sec. 2, T. 18 N., R. 3 W.). Highly altered columnar-jointed basalt flow is exposed in lower right section of the quarry wall, and appears to be relatively flat lying. It is overlain by a complex radially-jointed unit (arrow) consisting of either pillows or filled lava tube rosettes. Columnar unit may represent a feeder for the overlying flow, or perhaps a later sill.

the Black Hills, and typically crop out in the highlands and along the southern flank of the hills. Unaltered exposures of massive basalt are rare; they are more commonly internally partitioned by a rectilinear network of highly zeolitized selvages between joints. Volcanic blocks produced by this joint pattern subsequently undergo spheroidal weathering, with the joints eventually coalescing into a matrix of basaltic sand- and silt-sized detrital material. Figures 14 and 15 illustrate one such internally altered outcrop of poorly indurated, highly oxidized detrital volcanic material containing isolated masses of exfoliating basaltic clasts of various sizes and shapes. Eventually all that remains of the outcrop is a reddish pile of loosely consolidated sand, containing abundant clasts of altered basalt. These totally decomposed basalt outcrops are especially common in the vicinity of suspected fault zones, suggesting that the original joint network may have been related to tectonism rather than to cooling phenomena. Soils formed by the decomposition of basaltic lava flows have been locally termed the Katula, Crim, and Boistfort Series (McMurphy and Anderson, 1968), and are diagnostic indicators of bedrock geology where outcrops are not present.

Lithic tuffs with subordinant breccia: Tuffaceous deposits are the least conspicuous lithologic unit in the Crescent Formation of the Black Hills (Weaver, 1916). One exposure west of Gate on the southern flank of the hills (NW¼ sec. 26, T. 16 N., R. 4 W.) consists of lapilli-tuff and lapilli-breccia cemented by chalcedony, calcite, zeolites, and palagonite. To the north of the highlands and west of Shelton (NW¼ sec. 2, T. 19 N., R. 4 W.), a

Figure 14: Spheroidal weathering of columnar-jointed Crescent basalt flow. Volcanic rock decomposes to loosely-consolidated basaltic sand- and silt-sized material. Independence Road, south of Black Hills (SW¼ NW¼ sec. 15, T. 15 N., R. 4 W.). Close-up of area in box is reproduced below.

Figure 15: Close-up of portion of Figure 14, showing exfoliation of angular to subrounded basalt fragments.

highly altered outcrop of porphyritic, palagonitic tuff overlies a thin layer of basaltic, micaceous siltstone. The tuff contains abundant grains of augite, plagioclase, zeolite minerals, and lithic fragments, and is cut by thick veins of calcite and phillipsite. The tuff is distinctively banded, probably due to alteration, and is locally so well indurated that it may be easily mistaken for a basalt flow. Contact relations in the northern part of the area suggest that these "volcaniclastic" deposits are stratigraphically the highest part of the Crescent Formation.

Mode of origin: Thick basalt flows of the Crescent Formation are partly submarine in origin, as indicated by the presence of pillow lavas and lesser hemipelagic siltstone interbeds, some of which contain deep water foraminiferal assemblages. Pillow breccias and hyaloclastites in the Crescent evidently formed by rapid cooling and internal shattering of lava flows during submarine extrusion. Palagonitic tuffs associated with many of these breccias indicate rapid quenching, followed by submarine alteration of the glass. As magmatism continued, the flows eventually built up above sea level, particularly around one or more eruptive centers. Evidence for this transition is the presence of columnar-jointed basalt flows and pyroclastic deposits in the upland sections of the Black Hills. Although columnar basalt is generally characteristic of subaerial eruptions (e.g. Columbia River Basalt), its occurrence along active ridge crests has been well established (D. A. Swanson, 1979, oral comm.). However, the presence of mollusc-bearing basaltic (coquina) sandstone interbedded with some Black Hills lava flows (P. D. Snavely, Jr., 1978, written

comm.; G. M. Valentine, 1980, written comm.) suggests that most of the columnar basalts were erupted either subaerially or in a shallow water (littoral) environment.

Age and correlation: Fossils are scarce in the Crescent basalts of the Black Hills, owing to the paucity of sedimentary interbeds. Where interbeds occur, they are highly oxidized and do not contain well preserved fossils. However, somewhat better preserved Foraminifera were recovered from two of the more than 30 localities sampled, and were identified by Dr. W. W. Rau, U. S. Geological Survey. The road cut on the north side of S.R. 8 near McCleary (see page 18) consists of pillow basalt and pillow breccia separated by a thin siltstone interbed. A poorly preserved foraminiferal assemblage within the siltstone was referred to the middle Eocene Ulatisian Stage by Dr. Rau (1979, written comm.), and indicates open-sea conditions at bathyal depths. The Ulatisian Stage ranges from 49 to 46.5 m.y. b.p. according to Berggren's (1972) time scale. A foraminiferal assemblage was collected by Dr. Rau from coquina sandstone beneath an outcrop of columnar basalt on the north flank of Rock Candy Mountain (NW¼ SW¼ sec. 30, T. 18 N., R. 3 W.), about 12 km southeast of the McCleary locality. A Ulatisian age was also suggested by the fauna (W. W. Rau, 1980, written comm.), although this assemblage is more characteristic of a shallow water (50 m or less) littoral environment. It comprises the following species:

Nummulites (operculina) cushmani (Cole) (F)
Discocyclina cf. D. psila Woodring (F)
Amphistegina californica Cushman and M.A. Hanna (F)
Nodosaria latejugata Gumbel (R)

Globigerina sp. (R)
?Valvulineria sp. (R)

Pease and Hoover (1957) have proposed a middle Eocene to early late Eocene age for the Crescent Formation on the basis of Foraminifera collected from silty interstices in pillow lavas about 5 km east of Oakville, and a megafossil assemblage collected from basaltic sandstone interbedded with a pillow basalt flow near Capitol Peak. Dr. J. M. Armentrout of Mobil Oil Company has reported three whole-rock K/Ar ages of Crescent lavas in the Black Hills (1980, written comm.; Armentrout et al., 1980). The dates are: 38.9 ±1.2 m.y. from a roadcut along U.S. 12 north of Oakville; 40.7 ±0.7 m.y. from a cut on Interstate 5 at Tumwater; and 47.5 ±1.7 m.y. (middle Eocene) from a roadcut on S.R. 8. This latter date is consistent with the middle Eocene faunal ages described in the Black Hills, although the first two K/Ar dates suggest that the Crescent Formation is younger than earliest late Eocene in age. Since there is no faunal evidence for this young age, I suggest that the first two dates be considered minimum ages for the times of crystallization.

Middle to upper mid-Eocene volcanic rocks of the Black Hills correlate temporally and lithologically with the Crescent Formation of the Olympic Peninsula (Arnold, 1906), the Metchosin Volcanics of southern Vancouver Island (Clapp, 1917), the basalts of the Bald Hills in central Kitsap County (Weaver, 1916, 1937), the "Metchosin" lavas of the Willapa Hills in southwestern Washington (Henriksen, 1956); and the Siletz River Volcanics (Snavely and Baldwin, 1948), the lower part of the Tillamook Volcanics (Warren et al.,

1945), and the Roseburg Formation volcanics (Baldwin, 1974), all of the Oregon Coast Range. Petrochemical studies of the Black Hills basalts (Globerman, 1979) support their correlation with at least the upper "member" of the Crescent Formation in the Olympic Peninsula, as described by Glassley (1974) and Cady (1975). This consanguinity of Eocene volcanic sequences along the axis of the northwest coast suggests that the region was the site of extensive submarine and subaerial volcanism beginning about latest Paleocene (Roseburg Formation) to early Eocene time, although temporal and spatial variations were locally present.

Field evidence suggests that these volcanic piles were isolated and randomly distributed, since several of them grade laterally into coeval deep water sediments (Snavely et al., 1980). The oldest lavas contain thick siltstone interbeds with associated open-sea Foraminifera (Rau, 1966). Depths probably decreased as the lavas accumulated, since shallow water fauna appear immediately above the highest lava flows and suggest the inception of warm, shallow water reef conditions (Rau, 1966). In some areas subsidence of the ocean floor apparently coincided with eruptive activity, although elsewhere local tectonism and rapid accumulation of the lavas produced emergent volcanic highlands (Henriksen, 1956).

Volcanism continued until about the end of middle Eocene time, with the latest eruptions producing flows interbedded with equal volumes of lowermost upper Eocene marine sediments (Henriksen, 1956). Following the onset of magmatic quiescence and the partial erosion of the volcanic highlands, the area subsided and became submerged during late Eocene time. This transgression is indicated

by the more than two kilometers of deep water turbidites unconformably overlying subaerial lava flows of the Siletz River Volcanics in the Oregon Coast Range (Snavely et al., 1980), and the littoral sandstones and siltstones which unconformably overlie the Black Hills basalts along the western and southern slopes. Most of these basalts are probably the uppermost part of a major volcanic accumulation, as suggested by the highly vesicular, massive basalts and columnar-jointed flows relative to pillow lavas. Many of these pillows are brecciated and interbedded with palagonitic tuffs and hyaloclastites, and contain sparse intercalations of marine siltstone. Such an association often characterizes shallow water eruptions in Hawaii (Moore and Fiske, 1969). In contrast, very thick sequences of pillow lavas and interbeds of hemipelagic siltstone occur in equivalent basalts of southwestern Washington (Henriksen, 1956; Wolfe and McKee, 1968; R. E. Wells, 1979, oral comm.), and the Olympic Peninsula (Cady, 1975; Tabor and Cady, 1978a), suggesting deeper water eruption in these regions. Since the Black Hills basalts are definitely younger than the latest Paleocene to early middle Eocene Roseburg Formation (Baldwin, 1974) and lower part of the Siletz River Volcanics (Snavely et al., 1968) of the Oregon Coast Range, it is reasonable to assume that volcanism was somewhat diachronous throughout the entire Coast Range and Olympic Peninsula, and may have persisted longer at certain eruptive centers such as the Black Hills. It is also possible that the Black Hills did not undergo the same degree of tectonic deformation that affected adjacent regions such as the Willapa Hills and Olympic Peninsula, which resulted in the exposure of the deeper submarine sections of

these volcanic piles, and the denudation of the youngest lava flows.

Contact relations: Since the base of the Crescent Formation is not exposed anywhere in the Coast Range and Olympic Peninsula, the nature of this basal contact is not known. The uppermost flows of the volcanic sequence are locally interbedded with and conformably overlain by siltstone of the upper part of the McIntosh Formation (Pease and Hoover, 1957; Snavely et al., 1958). Deposition of these marine tuffaceous sediments occurred during the waning stages of volcanism, and apparently continued after volcanism had ceased. This resulted in a thick contact between the Crescent and McIntosh Formations characterized by several hundreds of meters of thin basalt flows and siltstone interbeds (Henriksen, 1956). In the southern Black Hills near Gate, two types of sedimentary deposits occur near the top of the basalts. One deposit distinctly overlies the lava flows and contains fossils of late Eocene age, while the other is interbedded with the lavas and contains middle Eocene fossils. Rau (1963, personal comm., cited in Noble and Wallace, 1966) assigns the latter to the uppermost part of the Crescent Formation, and the former to the lowermost part of the upper member of the McIntosh Formation. The contact between the Crescent and overlying Lincoln Creek Formation is an unconformity; along U.S. 12 basaltic sandstone of the Lincoln Creek Formation occurs at the contact. Lincoln Creek sediments also occur in fault contact with the lava flows.

McIntosh Formation

Rocks of the McIntosh Formation, named by Snavely and others (1951a) for the type locality along the south shore of McIntosh Lake near Tenino, crop out sparcely along the southern flank of the

Black Hills near Gate, but are more extensive in the Doty Hills and Minot Peak area to the southwest (Sheet 1). The McIntosh may be divided into a lower member, comprising alternating beds of basaltic sandstone, tuffaceous siltstone, mudstone, and waterlaid breccia; and an upper member of massive, well indurated greenish-gray to dark olive-gray tuffaceous siltstone (Pease and Hoover, 1957). The latter is exposed in a stream bed beneath a steep escarpment of massive basalt flows and lapilli-breccia deposits just northwest of Gate (NW¼ sec. 26, T. 16 N., R. 4 W.). A thick transition zone occurs between the lowermost McIntosh and the underlying Crescent Formation, in which thin lava flows alternate with siltstone interbeds. Pease and Hoover (1957) mapped the base of the McIntosh as the horizon below which volcanic rocks predominate.

The thickness of the lower member averages 275 m in the Doty Hills, but decreases rapidly to the west. The upper member averages about 450 m in thickness, but locally reaches 660 m in the southwestern part of the Doty Hills. Because low relief and poor exposure are characteristic of areas underlain by siltstone of the McIntosh Formation (Pease and Hoover, 1957), the contact between the Crescent and the upper member of the McIntosh in the southern Black Hills was inferred by the writer from the distinctive topographic differences observable in the field and in air photos.

Rau (1956) has proposed an early late Eocene (Narizian) age for the upper part of the McIntosh Formation on the basis of abundant Foraminifera within siltstones and mudstones, which apparently become progressively younger toward the west. According to Armentrout and others (1980), the McIntosh is equivalent to parts of the Aldwell

Formation of the Olympic Peninsula, and to late Eocene units both in the Satsop River area and along the Willapa River. In Oregon, the Tyee and Yamhill Formations also correlate with the McIntosh Formation.

The sediments of the McIntosh were probably derived from two sources. Basaltic sandstones and conglomerates of the lower member were apparently eroded from emergent volcanic piles, and accumulated in embayments and troughs between the highlands formed by the Crescent Formation. Arkoses and tuffaceous siltstones of the upper member which contain abundant quartz and mica grains were probably derived from ancestral Cascade volcanic rocks to the east (Henriksen, 1956). Since arc-derived earliest late Eocene sedimentary rocks are interbedded with the uppermost part of the Crescent Formation in the Black Hills, it follows that the area was in close proximity to the continental margin during that time. Cady (1975) also suggested a proximal location for the upper member of the Crescent Formation in the Olympic Peninsula, since some lava flows contain intercalations of clasts of terrigenous origin. These relationships have important implications for various mobilistic models of the early Tertiary history of the Oregon - Washington Coast Range, and will be discussed in a later section.

Skookumchuck Formation

The Skookumchuck Formation is typified by interbedded shallow marine and continental facies, and was first described by Snavely and others (1951b) as a sequence of coal-bearing rocks of late Eocene age in the Centralia-Chehalis district. The Skookumchuck Formation does not crop out in the Black Hills, but is found in the Doty Hills and Minot Peak area to the south (Sheet 1). It consists of medium-gray to dark greenish-gray massive to poorly bedded sandstone and siltstone

(Pease and Hoover, 1957). Lower and upper basaltic and arkosic sandstone members are separated by carbonaceous siltstones which thicken westward. Coal beds are abundant in the lower and upper members (Snavely et al., 1951b), suggesting that coastal plain conditions prevailed during the period of deposition. The McIntosh and Skookumchuck Formations are separated by the Northcraft volcanics; the Skookumchuck is conformably overlain by the Lincoln Creek Formation. A late Eocene age for the Skookumchuck Formation has been suggested by Snavely and others (1958) on the basis of molluscan and foraminiferal fauna.

Lincoln Creek Formation

The Lincoln Creek Formation is a thick sequence of massive tuffaceous mudstone, siltstone, and sandstone which unconformably overlies the Crescent Formation (Rau, 1967). It was originally named the Lincoln Formation by Weaver (1912, 1937) for the type locality along the Chehalis River near Lincoln Creek, just northwest of Galvin, and was considered to be early Oligocene in age. The formation was subsequently redefined by Weaver and others (1944) and Beikman and others (1967) as the Lincoln Creek Formation.

Within the Black Hills, the Lincoln Creek Formation is exposed on the southern and western flanks along U.S. 12 between Oakville and Malone (Sheet 1), where it is typically in fault contact with the Crescent Formation, although at a few localities (e.g. the Oakville quarry) the Lincoln Creek sediments rest unconformably on the jointed lava flows. It consists of massive, well indurated, light-gray to white, very fine grained basaltic and tuffaceous sandstones and siltstones which generally weather a dark brown to rust-red and

orange. Following prolonged weathering it frequently forms very fine grained, sticky soils locally termed the Garrard and Lytell Series (McMurphy and Anderson, 1968).

Highly oxidized, basaltic, coarse grained sandstone, conglomerate, and sedimentary breccia of the Lincoln Creek Formation locally overlie outcrops of Crescent Formation with apparent unconformity; this relationship may be observed along U.S. 12 just north of Gibson Creek (SW¼ SE¼ sec. 34, T. 17 N., R. 5 W.), and in a quarry 1.5 km northwest of Oakville (see Fig. 9). Discontinuous beds of calcareous sandstone, altered tuff, and concretions overlie the basaltic sandstone base of the Lincoln Creek Formation, and are present at several localities, particularly along Porter Bluffs on U.S. 12 near the town of Porter (Sheet 1). Rounded pebbles of basalt and andesite occur sporadically in the sandstone and occasionally form thin conglomeratic lenses. These lenses tend to weather out of the more friable tuffaceous sandstone, and serve as excellent attitude markers. Where these lenses are absent, it is difficult to recognize any structure, since the unit is massive and unstratified (Rau, 1967).

Armentrout and others (1980) report fossil molluscs of late Eocene age from conglomeratic sandstone at the Oakville quarry, and shallow water epifaunal bivalves from basaltic sandstone at the Gibson Creek locality. Elsewhere molluscs of early and late Oligocene age indicative of a moderately deep water environment were collected by Pease and Hoover (1957) at several sites. Hence the age of the Lincoln Creek Formation probably ranges from latest Eocene to early Oligocene near the base, to late Oligocene near the top.

Astoria(?) Formation

The Astoria(?) Formation overlies the Lincoln Creek Formation with apparent unconformity, except in the Doty Hills to the southwest, where the relationship appears to be conformable (Pease and Hoover, 1957). No exposures of this formation occur in the Black Hills, although outcrops are abundant along the Delezene Creek syncline to the west, across the Chehalis River valley (Sheet 1).

Sedimentary rocks of the Astoria(?) Formation consist chiefly of friable coarse- to fine-grained feldspathic, basaltic, slightly micaceous sandstone. The sandstone is massive to crossbedded, except for occasional beds of calcareous sandstone and pebble conglomerate. Strata containing abundant fragments of carbonized wood are distributed throughout the unit (Pease and Hoover, 1957). The Astoria(?) Formation is easily differentiated from the underlying Lincoln Creek Formation by its more conspicuous bedding and abundance of mica and carbonaceous material, which suggests deposition in a coastal plain.

Two microporphyritic basalt members with columnar jointing and pillow structures are interbedded with the sedimentary rocks of the Astoria(?) Formation in the Doty-Minot Peak area: the lower basalt member near the base of the formation, and the upper basalt member about 1000 m stratigraphically higher (Pease and Hoover, 1957). Snavely and others (1973) correlate these tholeiitic basalt flows and breccias with Miocene lavas of the Columbia River Plateau.

Foraminifera of the Astoria(?) Formation are considered by Rau (1967) to be early to middle Miocene in age. Radiometric age dating by Dr. R. B. Forbes of the Geophysical Institute, University of Alaska, indicates that sand grains of the Astoria(?) are approximately

60 - 65 m.y. in average age, and are of plutonic-metamorphic origin (R. B. Forbes, 1979, oral comm.). This suggests that they were derived from the crystalline rocks of the northern Cascades province, rather than from the Tertiary volcanic rocks of the southern Cascades region.

Columbia River Basalt

Isolated exposures of tholeiitic basalt flows have been described south of the Chehalis River by Snavely and others (1958). These Miocene lavas are widespread in coastal Oregon and southwestern Washington, and correlate temporally and petrochemically with the Yakima Basalt of the Columbia River Plateau (Snavely et al., 1973). In coastal Washington these flows frequently display columnar jointing, have a uniform thickness of about 20-25 m, and both rest unconformably on, and are interbedded with, sedimentary rocks of the Astoria(?) Formation (Snavely et al., 1958). The lavas also unconformably overlie sedimentary rocks of the Lincoln Creek Formation. They crop out only in the western part of the Centralia-Chehalis area south of the Chehalis River and the Black Hills (Sheet 1). The basalt unit has been dated at 15.7 ±0.8 m.y. (K/Ar) by Turner (1970), and therefore correlate with the Yakima Basalt of the Columbia River Group, which is middle Miocene in age (Snavely et al., 1973).

STRUCTURAL GEOLOGY

The dominant structures in the central Washington Coast Range are five major basement uplifts and several minor ones that expose the Eocene basalts of the Crescent Formation; the Black Hills are one of the largest of these uplifts (Fig. 4). Most of these highs probably existed since middle to late Eocene time, since sedimentary units are generally observed onlapping or offlapping and thickening

away from the uplifts. Northwest- and northeast-trending normal and reverse faults form the boundaries of most uplifts.

Within each uplift the stratigraphy is disrupted by faulting of lesser magnitude than along the boundary structures. These interior faults are all high angle features and commonly form contacts between rocks of the Crescent Formation and younger sedimentary deposits (Pease and Hoover, 1957). In general, internal faulting is more intense in the basaltic basement complexes, and declines with decreasing age in the overlying units. The age of faulting is probably no younger than early Pliocene, since the youngest offset strata are sedimentary rocks of Miocene age (Pease and Hoover, 1957) mapped as the Montesano Formation west of the Black Hills area (Rau, 1966, 1967). However, Pease and Hoover (1957) reported that some movement may have occurred along a fault about 5 km southeast of Oakville (sec. 9, T. 15 N., R. 4 W.) during the 13 April 1949 Olympia earthquake (intensity= VIII). The earthquake evidently caused lateral displacement on the fault boundary between the Crescent and Lincoln Creek Formations, which may have resulted in warpage of the Union Pacific railroad tracks along the south bank of the Chehalis River (M. H. Pease, Jr., 1979, written comm.). It is uncertain whether this event represents reactivation of older basement structures, or landslides in the vicinity of inactive faults zones that were caused by earthquake-induced ground acceleration. Most earthquake activity in the area is confined to the Puget Sound lowland to the northeast (Crosson, 1972). There is no strong evidence for recent faulting in either the Black Hills, Chehalis Valley, or southwestern Washington Coast Range (Washington Public Power Supply System, 1975), although several Quaternary

faults were reported by Carson (1973) along the southeastern flank of the Olympic Peninsula near Lilliwaup Lake.

Weaver (1916) suggested that the western boundary of the Black Hills is a northwest-trending syncline whose axis is nearly parallel to and slightly east of the Chehalis River valley between Oakville and Elma; the basalts along the west side of the uplift would form the eastern synclinal limb. Evidence for this is the nearly north - south strike and 10 degree west dip of Lincoln Creek sedimentary rocks unconformably overlying the basalts of the western slope (Weaver, 1916), and interpretations of local Bouguer gravity profiles by Bromery (1962). In addition, Pease and Hoover (1957) stated that the Chehalis River downwarp is divided by faults into two major synclines: the Garrard Creek at the southern end of the downwarp, and the Delezene Creek syncline to the north.

Structural relationships along the northern and eastern boundaries of the Black Hills uplift are even more equivocal, owing to the thick mantle of glacial drift. The distribution of volcanic exposures in the northeastern corner of the mapped area (Sheet 1), and isopachs showing depth to bedrock in the southern Puget Sound area (Fig. 16), suggest that the basement uplift is abruptly truncated along a northwest- to southeast-trending zone roughly coincident with the southern reaches of Budd, Eld, Totten, and Hammersley Inlets of southernmost Puget Sound (see King, 1969). This zone also coincides with a belt of steepened gravity gradients extending from the southern end of Hood Canal southeastward about 90 km into the eastern foothills of the Cascades (Danes et al., 1965; Rogers, 1970), and forms the southern limit of the block-faulted Puget Sound tectonic province

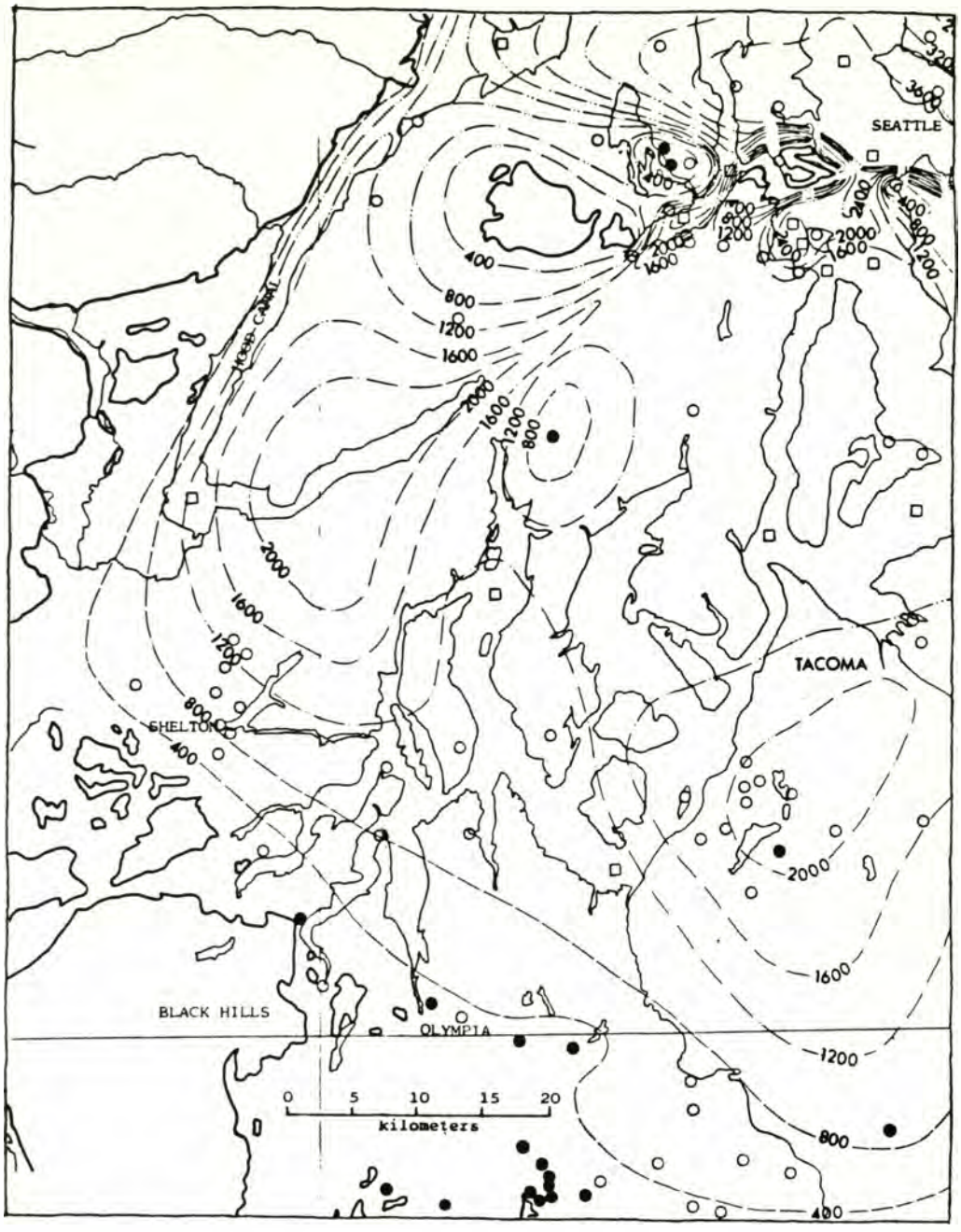

Figure 16: Isopach map of southern and central Puget Sound lowland and vicinity, showing thickness of unconsolidated sediments. Contours are in feet. Note the nearly rectilinear pattern of the 400 foot (120 m) and 800 foot (240 m) contours northwest and southeast of Shelton. Circles denote well locations. Closed circles indicate drilling penetrated bedrock; open circles indicate deep drilling did not penetrate base of unconsolidated deposits, hence thickness is less accurately known. After Hall and Othberg, 1974.

to the north. Although topographic evidence for this feature is strongly suggested by SLAR imagery, no corroborative field data are available; its existence is based solely on geophysical evidence because of the cover of glacial debris.

Figure 17 is a regional structural interpretation of the Puget Sound lowland and adjacent basement highs. The lowland is both bordered and internally disrupted by a nearly rectilinear set of major northwest- and northeast-trending faults (Rogers, 1970). The major boundary structure between the Black Hills and the Puget lowland is shown to lie just south of Olympia, and is termed the "Olympia lineament" on the geologic map (Sheet 1). According to testimony presented before the Nuclear Regulatory Commission hearings (1975) by the Washington Public Power Supply System, the Olympia lineament is considered to be seismically active, capable of generating a magnitude 7.5 earthquake.

Along the southern edge of the Black Hills uplift, an east-trending linear magnetic anomaly passing just north of Rochester (T. 16 N., R. 3 W.) is interpreted as a major fault, downthrown to the south (Bromery, 1962). This anomaly is termed the "Rochester lineament" on the geologic map (Sheet 1). According to Bromery (1962), the depth to buried Crescent volcanic rocks 3 km southwest of Rochester is approximately 700 to 800 m.

Although the suspected Rochester fault is totally concealed by thick glacial and alluvial deposits in the Chehalis River valley, there is some geologic evidence for its existence. For example, several northwest-trending faults and a syncline mapped in the Black Hills between Oakville and Gate are apparently truncated by the linea-

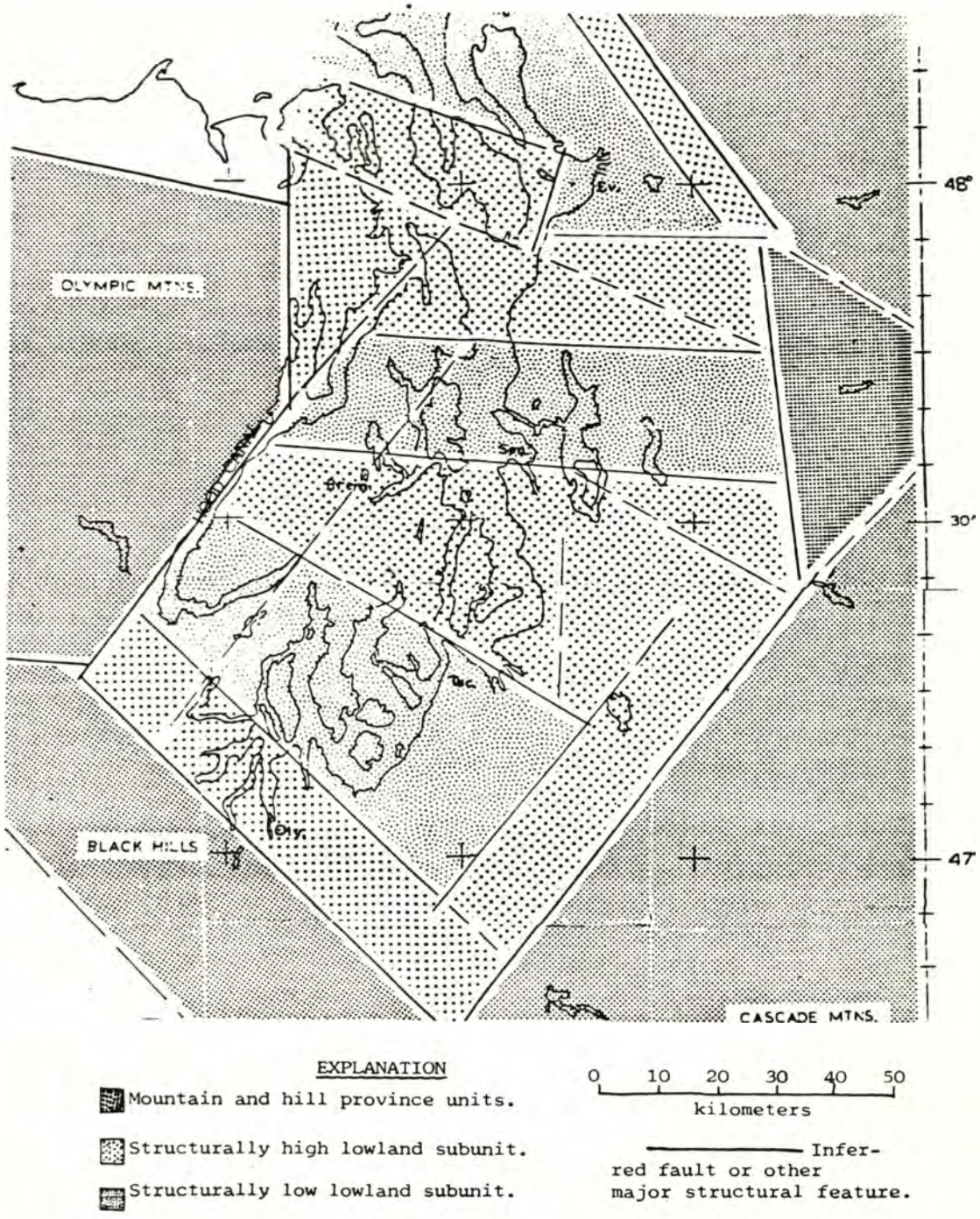

Figure 17: Regional structural interpretation of the Puget Sound lowland and vicinity. Note fault bounded blocks within the lowland and rectilinear pattern of the structures. Faults are concealed by extensive deposits of Pleistocene sediments, but are recognizable in aeromagnetic and gravimetric surveys. After Rogers, 1970.

ment, since they are not recognized south of the Chehalis valley (Sheet 1). Most basalts exposed along the railroad grade in this area are extremely sheared and slickensided. In addition, the trend of the north fork of Garrard Creek, about 4 km southwest of Oakville (T. 15 N., R. 5 W.) may be controlled by the southwestern continuation of the lineament.

In summary, limited geophysical and geological data suggest that the basement uplift is bordered on the southwest and west by the northwest-trending Chehalis River downwarp; on the northeast and north by the northwest-trending Olympia lineament; and on the southeast and south by the northeast-trending Rochester lineament. One explanation for this tectonic configuration is that the Black Hills uplift represents a north-, to northeast-trending homocline, gently dipping to the west. Evidence for this is an equal area plot of 52 poles to bedded sedimentary units and cross-jointed columnar basalt flows in the Black Hills (Fig. 18). The small radius of the circle of 95% confidence (3.5^{o}) around the mean of the 52 poles, and the near overlap of the mean poles to bedding and to joints, suggests that the structural data are internally consistent, even when attitudes on basalt flows are combined with measurements from overlying and interbedded sediments. According to Figure 18, the mean of 52 poles has a declination of 97^{o} and an inclination of 83^{o}. This corresponds to a plane striking 7^{o} northeast and dipping about 7.5^{o} to the northwest, consistent with my interpretation of the uplift as a north-trending homocline that dips gently to the west.
Another possible interpretation is that the Black Hills uplift was originally a northwest-trending anticline (Weaver,

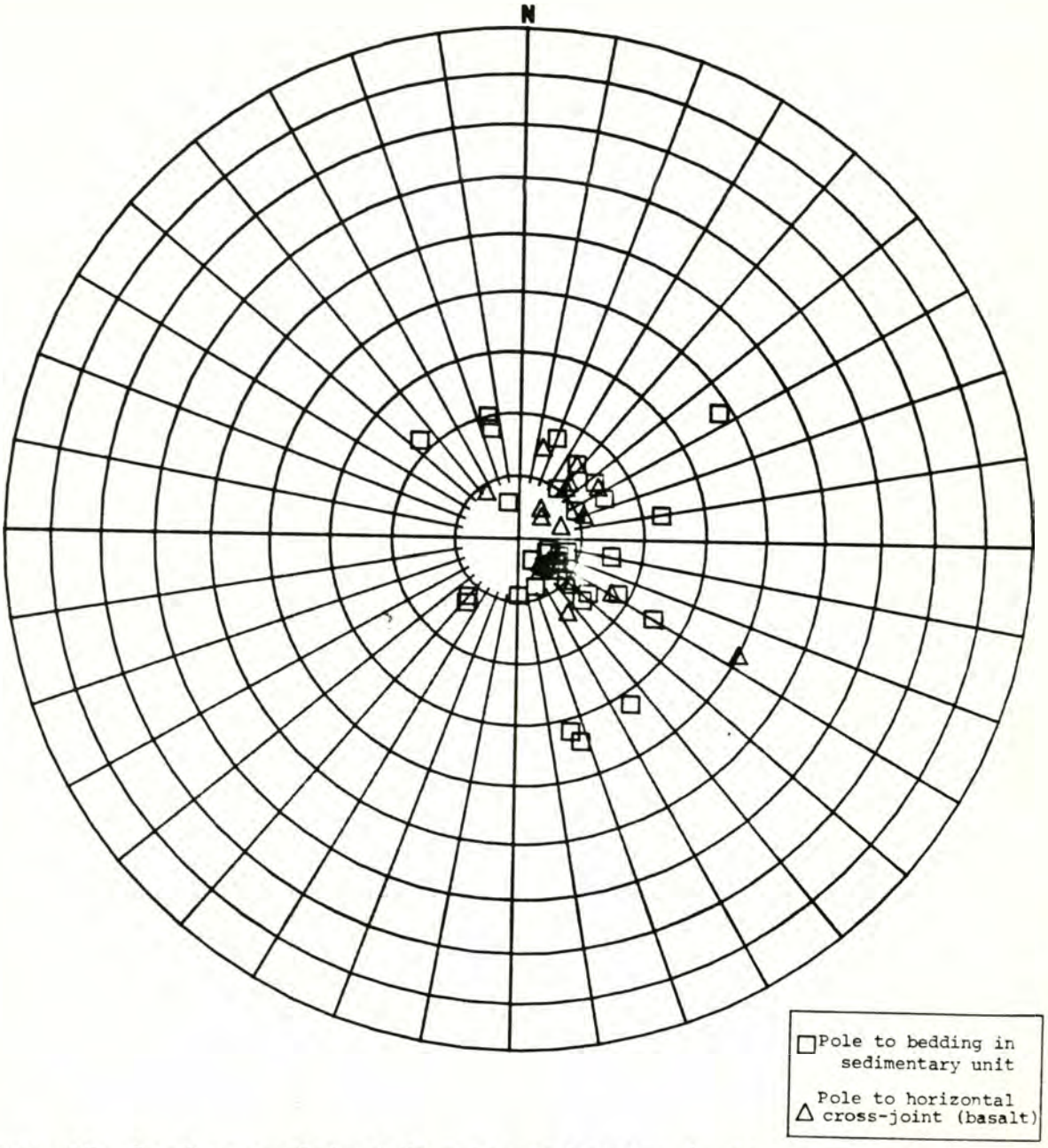

Figure 18: Equal area plot of 52 poles to bedding (sedimentary units) and horizontal cross-joints (columnar basalt flows) in the Black Hills and adjacent area. The mean pole to bedding is Dec.= 106°, Inc.= 83°, α95= 4.4°, while the mean pole to cross-joints is Dec.= 80°, Inc.= 82°, α95= 5.4°. The mean of all 52 poles is Dec.= 97°, Inc.= 83°, α95= 3.5°. This corresponds to a mean Black Hills attitude of N7°E 7.5°NW.

1916), whose northeastern limb was subsequently downdropped along the Olympia lineament. Although local deviations from this structural pattern are present, such as the small northwest-trending syncline just north of Oakville, and the more steeply dipping beds of McIntosh Formation sedimentary rocks near Gate, the Black Hills uplift as a whole is structurally quite coherent.

III. PETROLOGY

INTRODUCTION

Geochemical study of 30 Black Hills samples was undertaken with two fundamental objectives in mind:

(1) To compare the volcanic rocks of the Crescent Formation in the Black Hills with coeval and lithologically similar basalts from the Olympic Peninsula, southwestern Washington, and the Oregon Coast Range. Comparison of the Black Hills basalts with rocks of the type Crescent Formation in the Olympic Peninsula is critical to any correlation between these two suites; their similarities have been previously described by Weaver (1937) and Pease and Hoover (1957). Furthermore, it was suggested by R. S. Babcock (1978, oral comm.) that if the Black Hills rocks proved to be geochemically similar to the type Crescent Formation, then the paleomagnetic data for the Black Hills might have some applicability to the more enigmatic Olympic Peninsula. Since previous paleomagnetic investigations in the Olympic Mountains produced inconclusive results (C. S. Gromme, 1979, written comm.), perhaps some useful paleomagnetic information for the Olympics could be inferred from a study of strongly magnetized coeval basalts on the periphery of the range.

(2) To better constrain the petrotectonic setting of the Black Hills basalts. To this end, numerous discriminant functions have been used, particularly those utilizing the more reliable, relatively immobile elements such as Ti, Zr, Y, and Nb (Cann, 1970; Pearce, 1975; Pearce and Cann, 1971, 1973; Smith and Smith, 1976). The three possible tectonic settings tested in this study are mid-oceanic ridge, oceanic island (also termed seamount), and island arc.

A continental flood basalt origin is also possible, as basalts from such a province are difficult to distinguish geochemically from tholeiites erupted in oceanic island settings. A flood basalt origin is not considered plausible for the Black Hills rocks due to the presence of pillow basalts and pillow breccias containing sparse intercalations of hemipelagic siltstones and shales with bathyal Foraminifera (W. W. Rau, 1979, 1980, written comm.). These features indicate that at least part of the volcanic sequence was erupted in a submarine setting.

PETROGRAPHY

All of the Black Hills samples selected for major- and trace-element analysis were carefully examined in thin section. Several additional samples which were not analyzed have also been petrographically studied. A complete description of the mineralogy, texture, and alteration of these samples appears in Appendix A. The locations of the 30 geochemistry samples are given in Appendix B. All but three of the 35 samples are plagioclase–augite basalts containing minor amounts of olivine, iron-titanium (Fe-Ti) oxides, and altered interstitial glass, and have coarse- to medium-grained, intergranular textures (Fig. 19). The other three samples are basaltic lithic tuffs composed of plagioclase, augite, Fe-Ti oxides, interstitial palagonite, and lithic fragments. One basalt sample contains large aggregates of cumulus plagioclase, augite, and olivine. The absence of interstitial melt phases in these aggregates suggests that they are xenoliths or cognate inclusions, rather than phenocrysts.

Plagioclase phenocrysts and microphenocrysts range from andesine to labradorite in composition, are generally normally zoned,

and are ubiquitous in the Black Hills suite. Augite phenocrysts and microphenocrysts are less abundant; they partially to wholly surround plagioclase laths, and approach subcalcic compositions. Even fewer olivine microphenocrysts are present; they range from about Fo_{95} to Fo_{90} in composition. Groundmass plagioclase microlites are usually surrounded by augite and lesser olivine grains. These entire clusters are in turn partially to wholly surrounded by interstitial Fe-Ti oxides and small amounts of altered glass. Plagioclase was presumably the earliest phase to crystallize, and was closely followed by augite and olivine. Most of the Fe-Ti oxides apparently crystallized last.

A fine-grained, intergranular texture is dominant in the Black Hills suite. Several samples have quenched textures indicative of rapid (possibly submarine) cooling (Fig. 20), whereas a few others are porphyritic to diabasic (Figs. 21, 22). These samples are probably from flow interiors, although they may also be from dikes or sills. The lithic tuffs are characterized by their highly vesicular, hemicrystalline trachytic textures.

Alteration of the Black Hills basalts ranges from very slight to extreme. Samples which are only slightly altered contain recognizable relict olivine grains which are partially to wholly pseudomorphed by saponitic clays. Moderately altered samples contain abundant groundmass saponite, and plagioclase phenocrysts and microlites which show incipient alteration to sericite. Some zeolites are present in fractures and vesicles. In the extremely altered samples, abundant zeolites, clays, and lesser carbonate occur as vesicle and fracture fillings. Plagioclase grains are more extensively albitized. Inter-

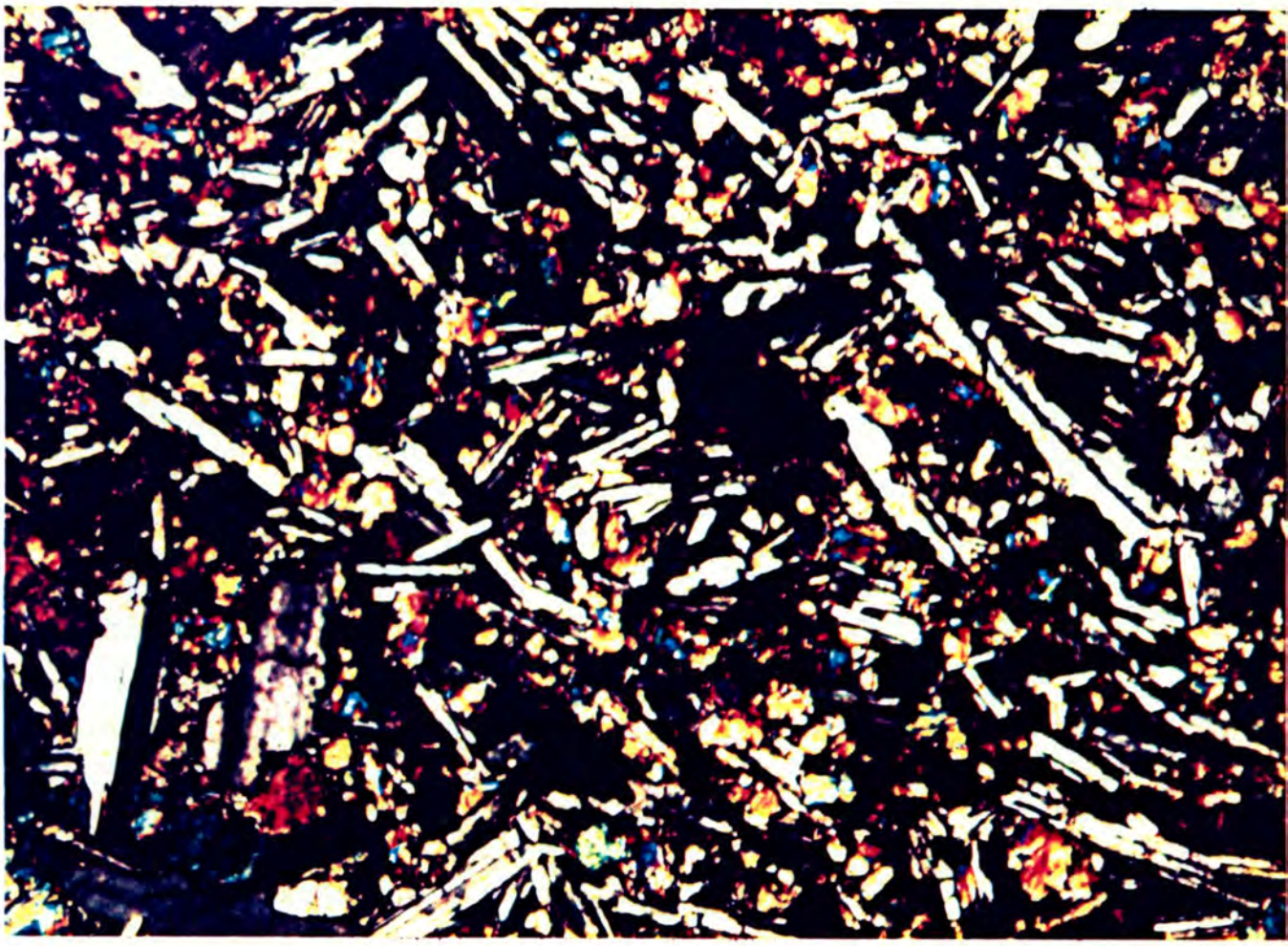

Figure 19 (above): Photomicrograph of Crescent basalt. Grains of augite and plagioclase appear to be directionless and very homogeneous. Fe-Ti oxides constitute most of the opaque material. Note that this sample appears to lack significant alteration products. X80. Crossed nicols.

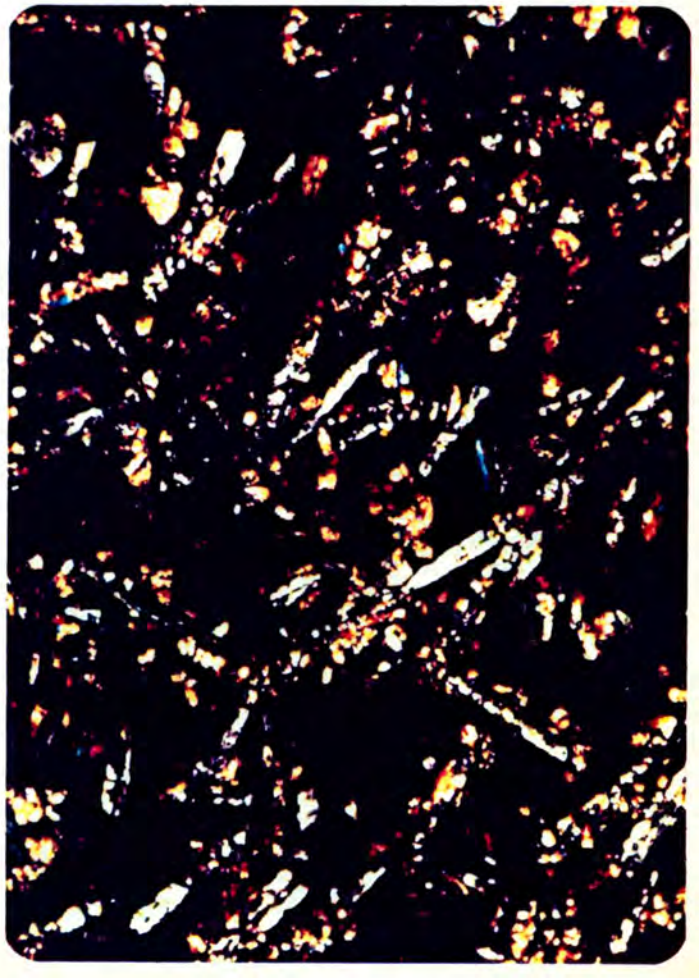

Figure 20 (right): Photomicrograph of Crescent basalt, showing quenched texture characteristic of submarine lavas. Stringy appearance of groundmass pyroxene grains and abundance of devitrified glass (opaque material) are evidence of rapid quenching. X20. Crossed nicols.

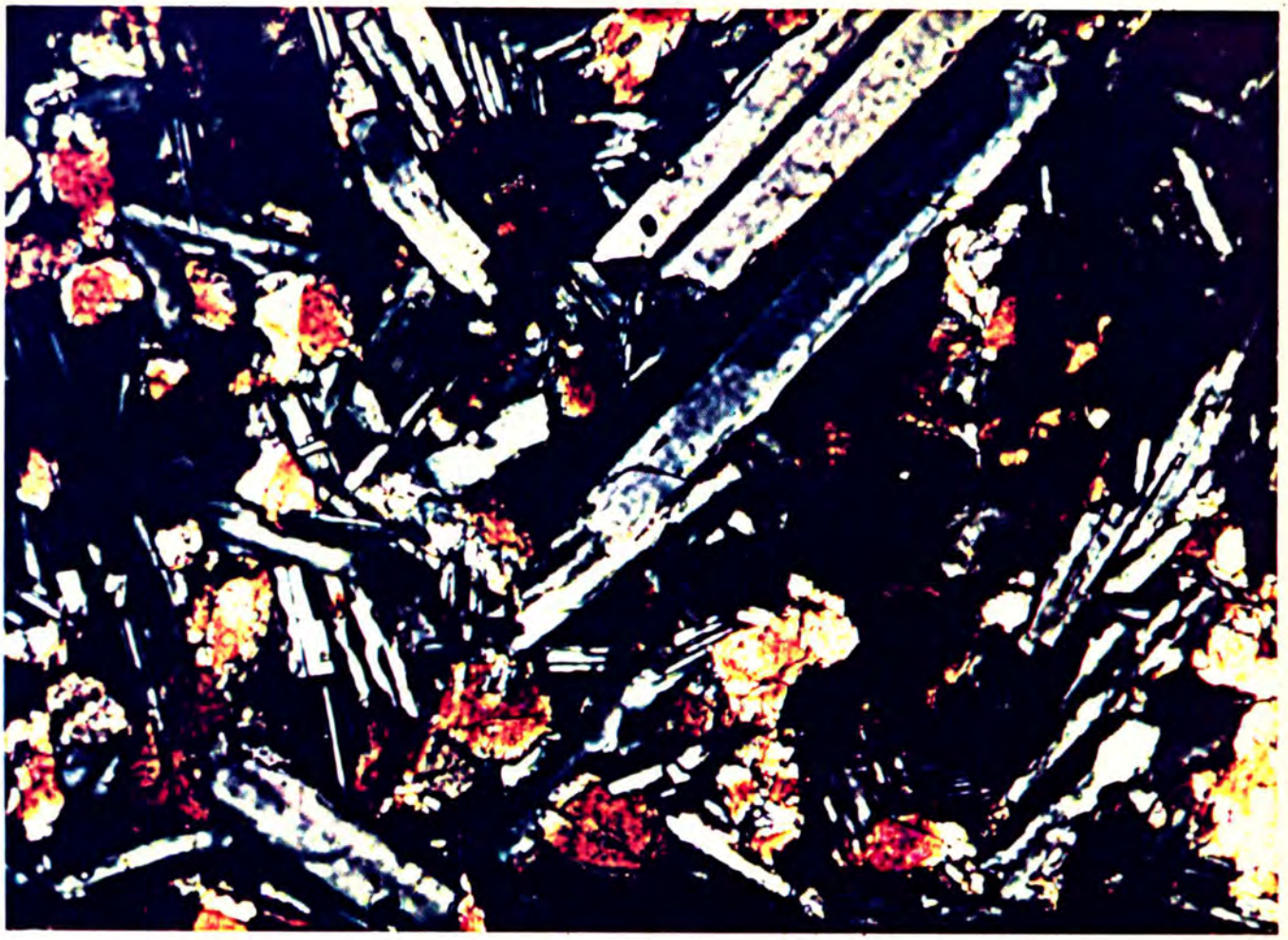

Figure 21(above): Photomicrograph of relatively unaltered Crescent basalt with distinctive diabasic texture. Large plagioclase laths are partially surrounded by subhedral to euhedral augite grains. Opaque material consists predominantly of Fe-Ti oxides and lesser amounts of glass. X80. Crossed nicols.

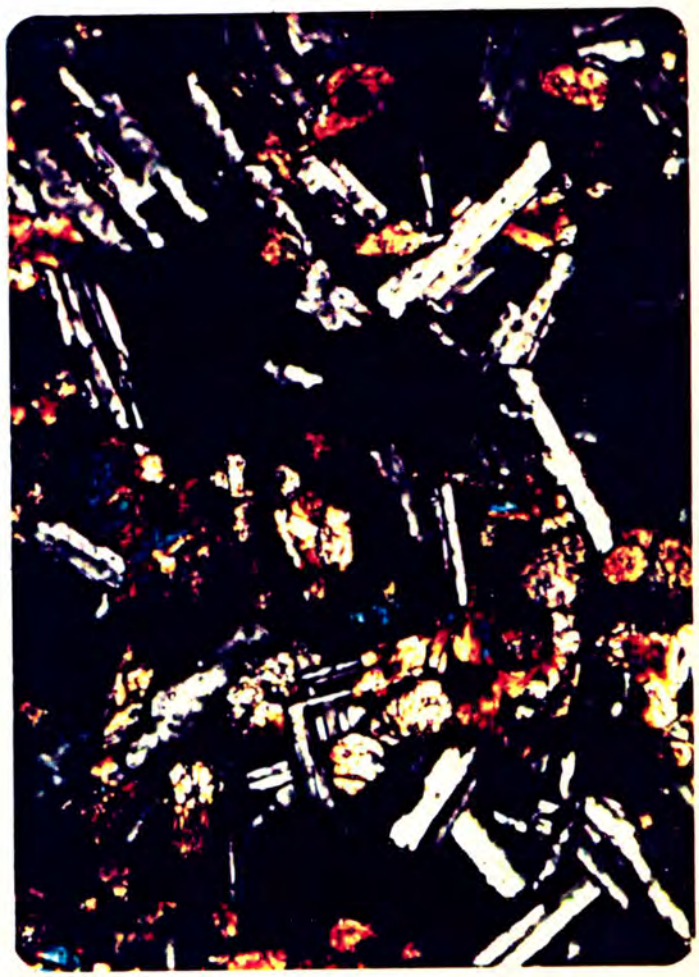

Figure 22(right): Photomicrograph of Crescent basalt. Augite grains partially surround laths of plagioclase. Note diabasic texture and relatively fresh appearance of the grains. X20. Crossed nicols.

stitial glass, if originally present, has been altered to palagonite, while some opaque grains appear to have been entensively fragmented.

ANALYTICAL PROCEDURE

Major elements for 30 Black Hills samples were determined using a Perkin Elmer Model 306 atomic absorption spectrophotometer. The trace elements Zr, Rb, Sr, Y, Nb, V, and Cr were measured in 29 samples using a Philips Model 1410 x-ray fluorescence spectrometer. The analytical procedure is more fully described in Appendix C. In addition, $^{87}Sr/^{86}Sr$ ratios for four samples were kindly provided by Dr. R. L. Armstrong, Dept. of Geological Sciences, University of British Columbia. Error limits determined for the major- and trace-element analyses are reported with the chemical data. The table of petrochemical data, including CIPW norms and Sr isotopic ratios, appears in Appendix D.

NORMS AND CLASSIFICATION

CIPW norm calculations indicate that virtually all samples are hypersthene normative, although a few contain up to seven percent normative olivine and some up to nine percent normative quartz. Virtually all Black Hills basalts plot in the tholeiitic fields on alkali versus silica, Al_2O_3 vs. normative plagioclase composition, and normative nepheline-olivine-quartz diagrams (Figs. 23,24,25) of Macdonald and Katsura (1964) and Irvine and Baragar (1971). Most samples that appear alkalic may be tholeiites modified by secondary alteration.

ALTERATION

Alteration of the Black Hills basalts was probably a low temperature

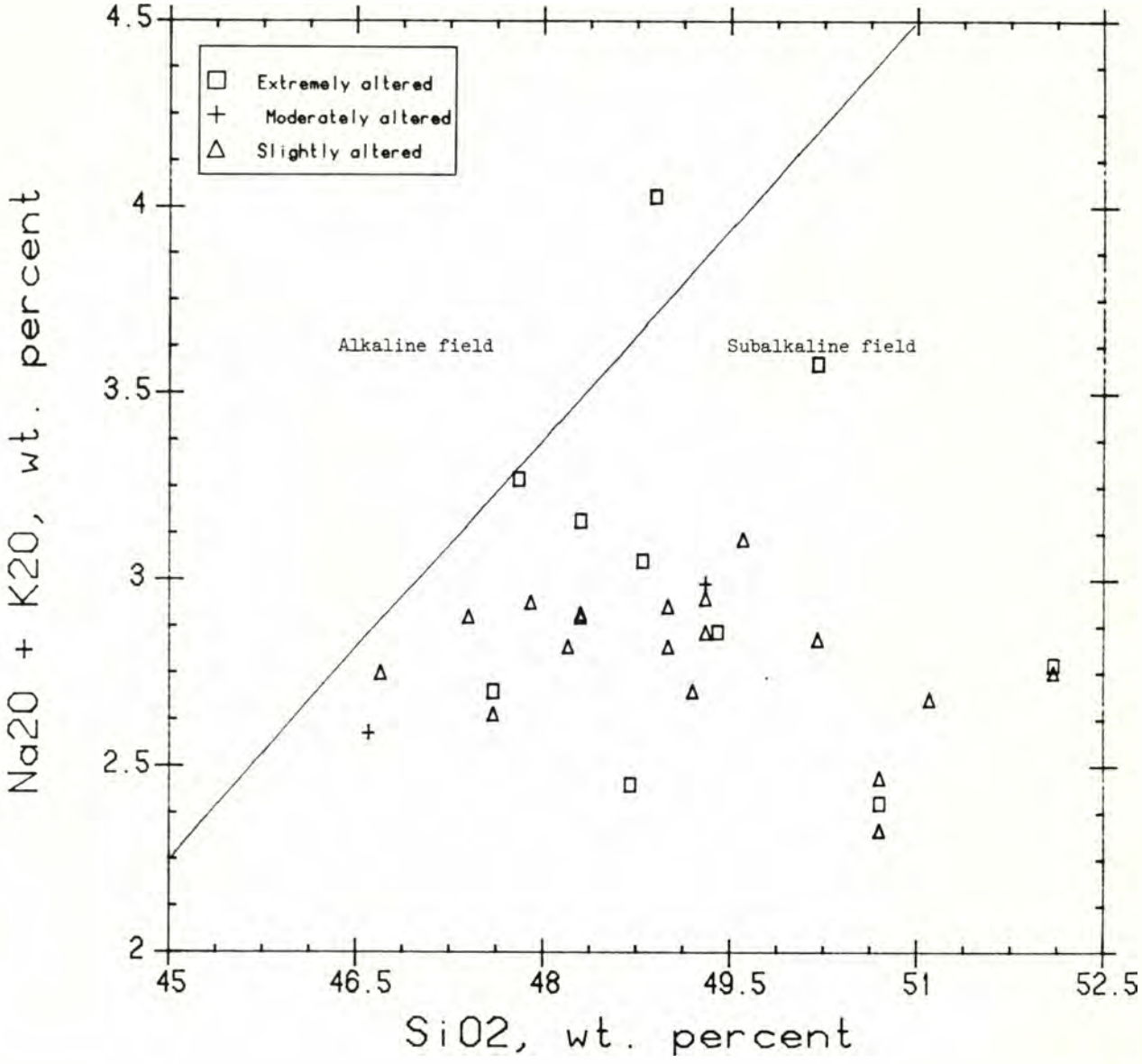

Figure 23: Total alkalis versus silica plot for 30 Black Hills samples. After Macdonald and Katsura, 1964.

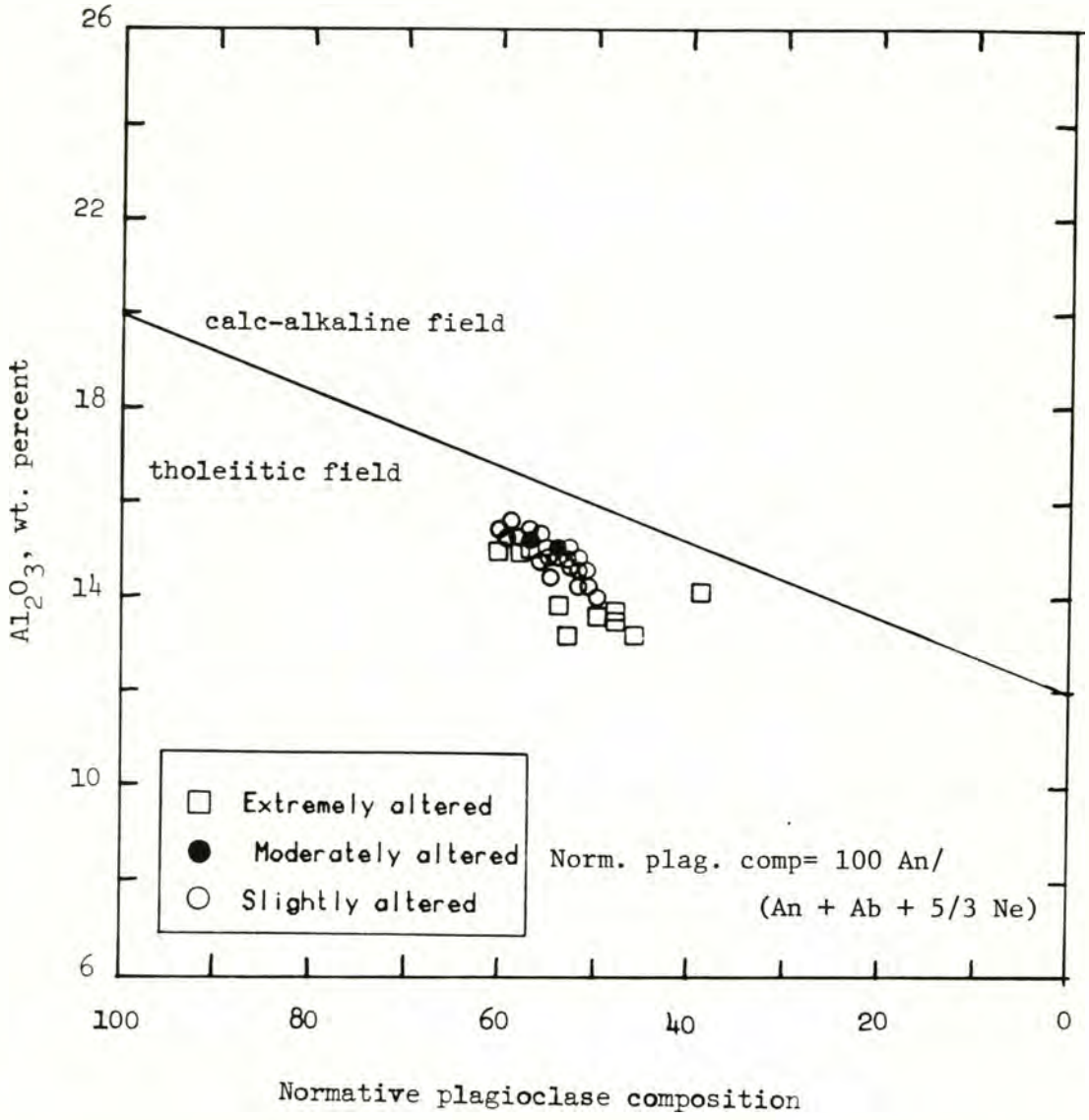

Figure 24: Al_2O_3 versus normative plagioclase composition plot for 30 Black Hills rocks. After Irvine and Baragar, 1971.

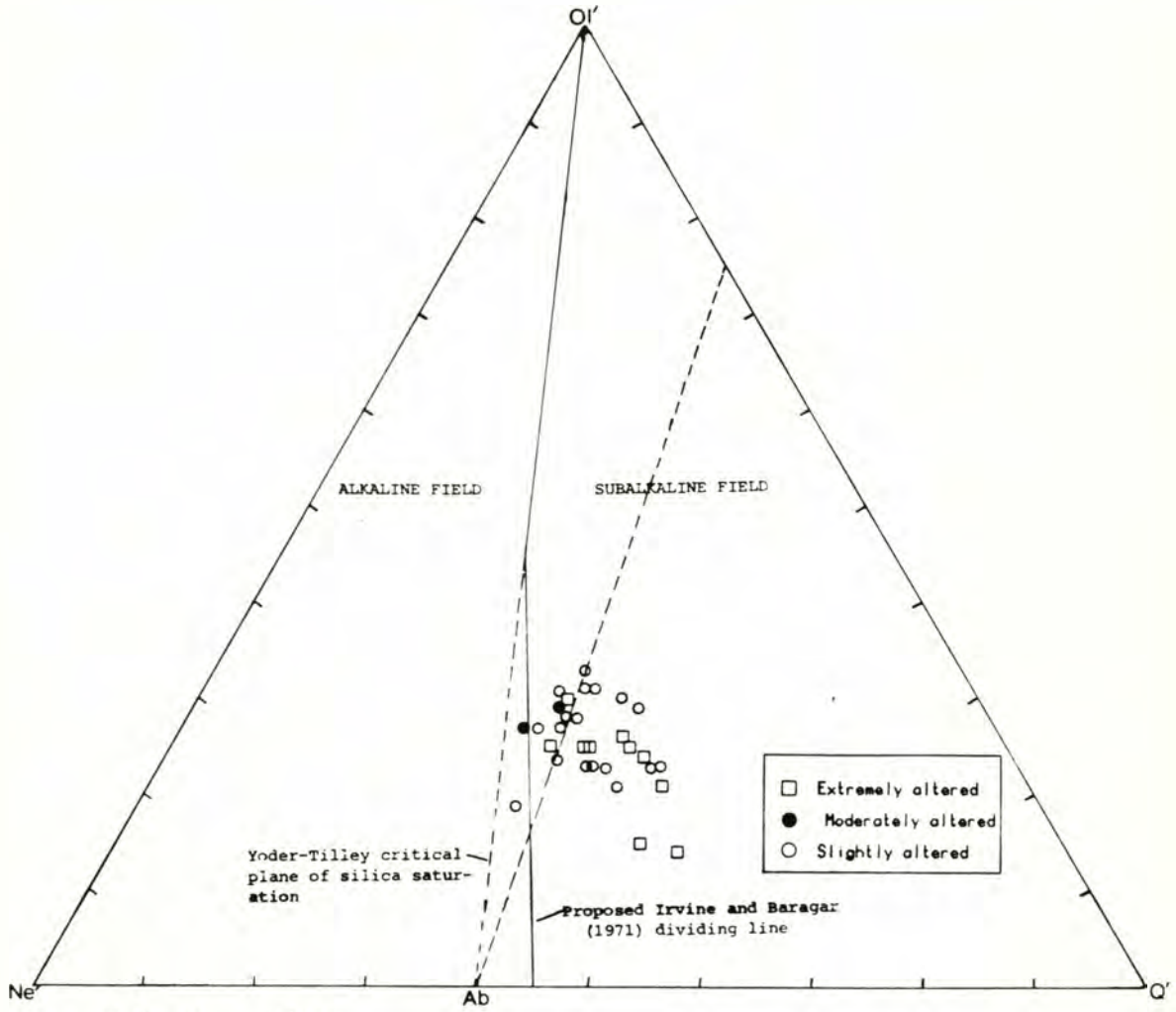

Ne'= Ne + 3/5Ab
Q'= Q + 2/5Ab + 1/4 Opx
Ol'= Ol + 3/4 Opx

Figure 25: Normative Ne'-Ol'-Q' ternary diagram for 30 Black Hills rocks, showing division into alkaline and subalkaline fields. Field boundaries after Irvine and Baragar (1971) and Yoder and Tilley (1962).

(sea-floor) diagenetic process (e.g. Dunoyer de Segonzac, 1970; Hall and Robinson, 1979), in contrast to the prehnite-pumpellyite facies metamorphism reported in the lower member of the Crescent Formation in the Olympic Peninsula (Glassley, 1974). This possibly explains why the Black Hills basalts have stable remanent magnetizations, while the Olympic Peninsula Crescent basalts are unstably magnetized.

In most of the chemical diagrams, the Black Hills rocks are divided into three groups: (1) slightly altered- 18 samples, (2) moderately altered- 2 samples, and (3) extremely altered- 10 samples. These designations were made on the basis of petrographic criteria discussed earlier. Standard magnesia-based variation diagrams (Fig. 26a-n) indicate that the most altered samples contain greater amounts of total iron (as Fe_2O_3), K_2O, V, Y, Rb, Sr, and Zr; and lesser Cr, compared to fresher samples. Observed fractionation trends of the immobile-element ratios Zr/TiO_2 and Zr/Y (Fig. 27b-c) for 29 Black Hills rocks indicate good correlation of the data, even when the most altered samples are included. They suggest that the Black Hills basalts are a comagmatic suite, and that the TiO_2/Zr and Y/Zr enrichment observed in the most altered samples probably reflects their greater degree of fractionation in a magma chamber, rather than the effects of weathering on the sea floor. Apparently the most fractionated members of the magma suite had higher initial ratios of TiO_2/Zr and Y/Zr, and following eruption underwent more alteration than the less fractionated samples. Perhaps a higher volatile content in the more fractionated lavas, or certain characteristics of their eruptive environment, increased their susceptibility to low temperature alteration. All of the Black Hills samples are included in the dis-

Figure 26a-n: Standard variation diagrams for 30* Black Hills rocks, in which MgO is plotted against:

(a) SiO_2
(b) Al_2O_3
(c) Fe_2O_3 (total iron)
(d) CaO
(e) K_2O
(f) Na_2O
(g) Rb
(h) V
(i) Y
(j) TiO_2
(k) Cr
(l) Sr
(m) Nb
(n) Zr

*Only 29 samples are plotted where trace elements are compared with MgO.

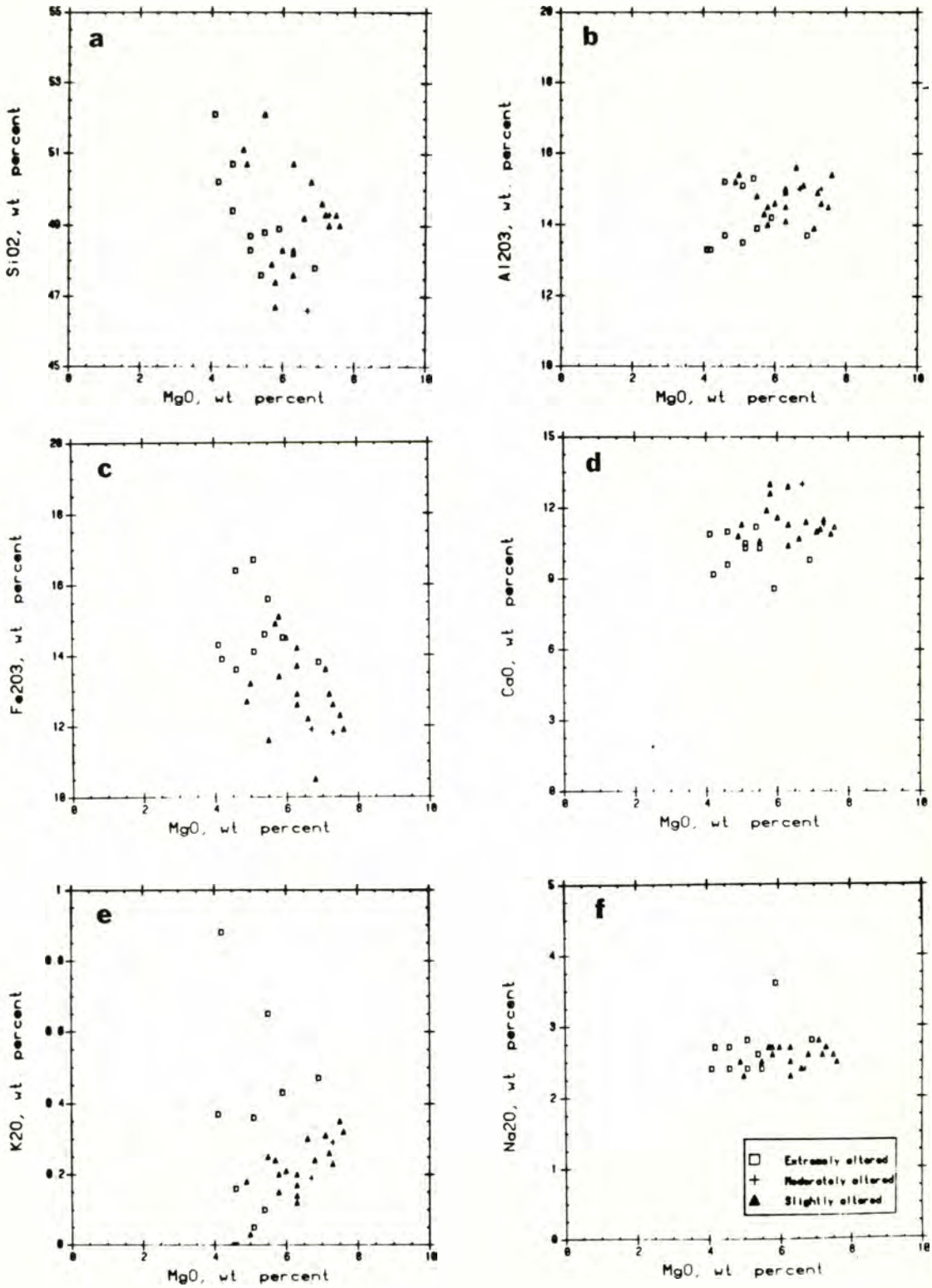
a
SiO2, wt percent
MgO, wt percent
b
Al2O3, wt percent
MgO, wt percent
c
Fe2O3, wt percent
MgO, wt percent
d
CaO, wt percent
MgO, wt percent
e
K2O, wt percent
MgO, wt percent
f
Na2O, wt percent
MgO, wt percent
Extremely altered
Moderately altered
Slightly altered

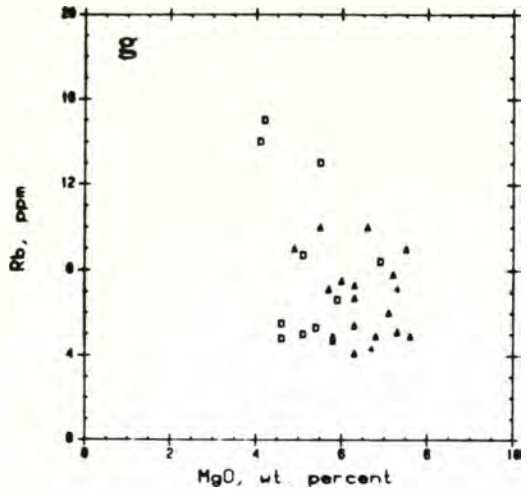
g
Rb, ppm
MgO, wt percent

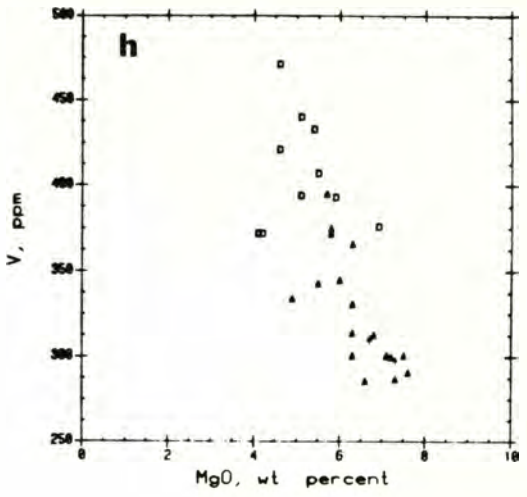
h
V, ppm
MgO, wt percent

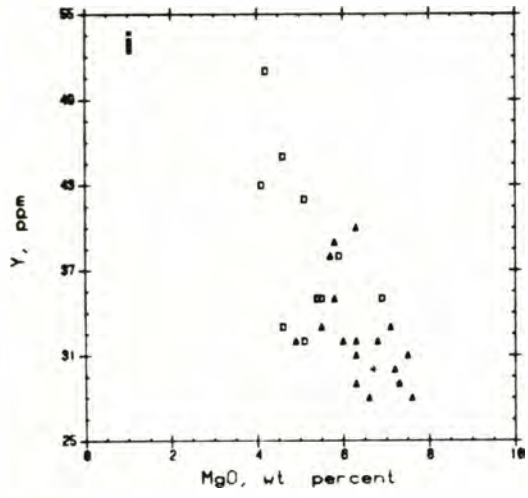
i
Y, ppm
MgO, wt percent

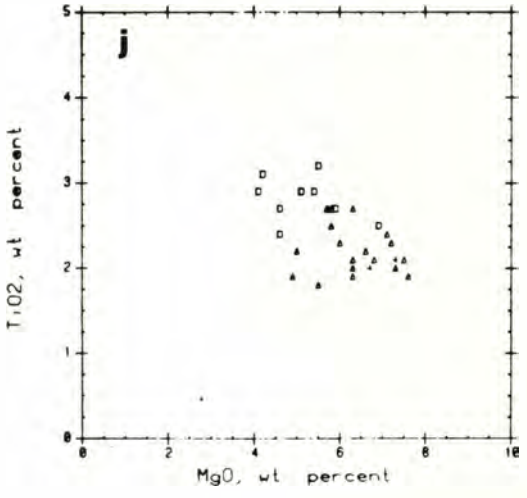
j
TiO2, wt percent
MgO, wt percent

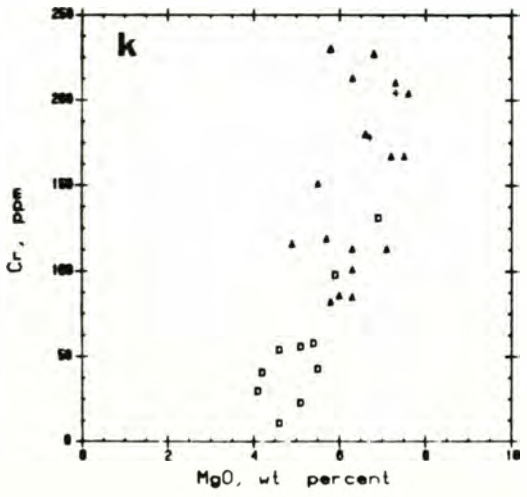
k
Cr, ppm
MgO, wt percent

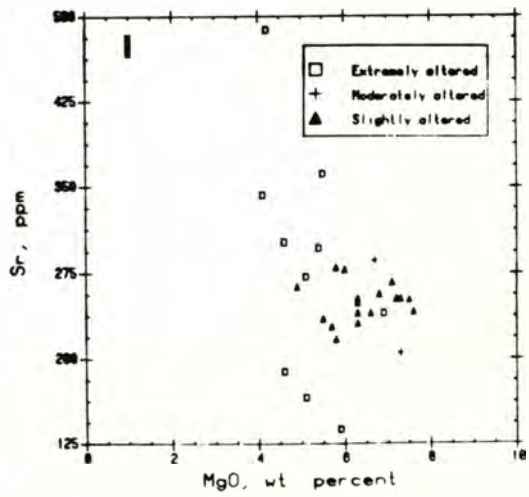
l
Extremely altered
Moderately altered
Slightly altered
Sr, ppm
MgO, wt percent

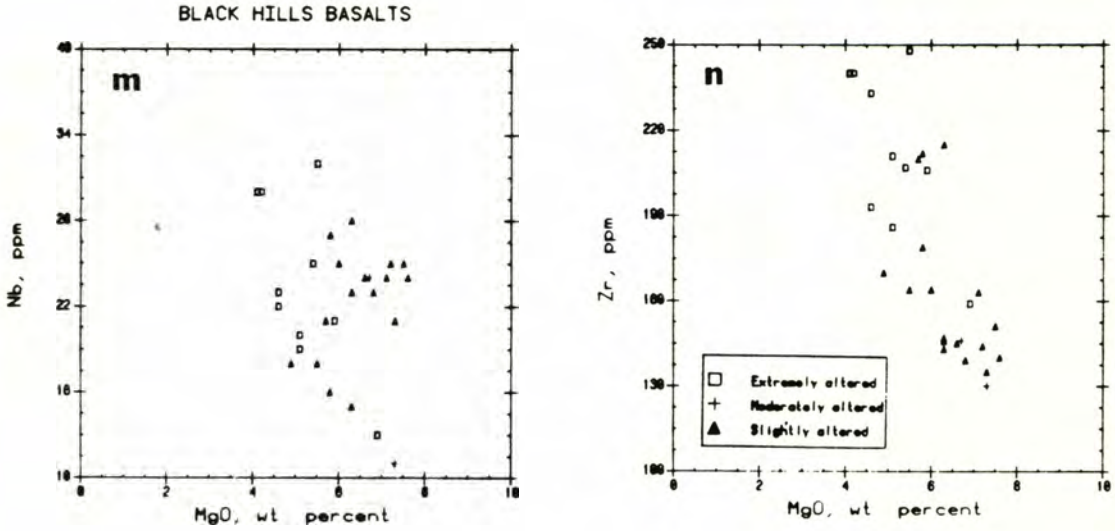
BLACK HILLS BASALTS
m
Nb, ppm
MgO, wt percent
n
Zr, ppm
MgO, wt percent
Extremely altered
Moderately altered
Slightly altered

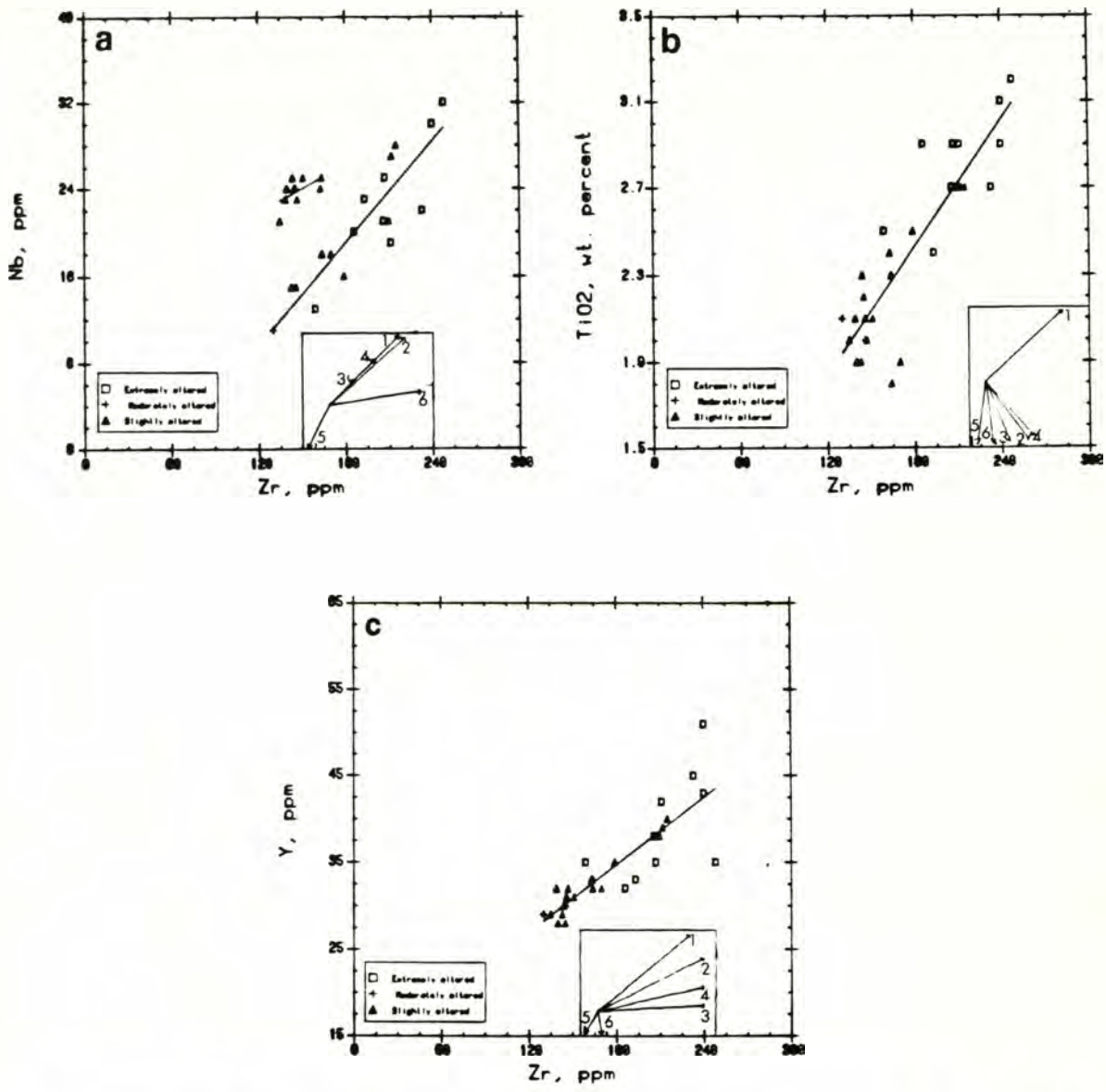

Figure 27a-c: Observed and modelled fractionation trends on Zr-Nb (a), Zr-TiO_2 (b), and Zr-Y (c) diagrams. Least-squares best-fit lines drawn through plots of 29 Black Hills rocks. Note that Zr-Nb diagram defines two separate groups of samples. Modelled fractionation vectors (in boxes) are:

(1) $pl_{0.5}\ cpx_{0.3}\ ol_{0.2}$

(2) $pl_{0.5}\ cpx_{0.3}\ ol_{0.1}\ mt_{0.05}$

(3) $pl_{0.6}\ am_{0.35}\ mt_{0.05}$

(4) $pl_{0.55}\ am_{0.2}\ cpx_{0.2}\ mt_{0.05}$

(5) $(ksp, pl)_{0.6}\ bi_{0.15}\ am_{0.2}\ mt_{0.05}$

(6) $pl_{0.6}\ cpx_{0.2}\ am_{0.15}\ mt_{0.05}$

Fractionation vectors after Pearce and Norry, 1979.

crimination diagrams, since they constitute a comagmatic suite, and their incompatible element compositions were largely unchanged following even extreme alteration (e.g. Hart et al., 1974). However, SiO_2, Al_2O_3, CaO, Fe_2O_3, Na_2O, K_2O, Sr, and Rb compositions of the most altered samples were probably moderately to substantially modified by secondary processes (e.g. Hart et al., 1974; Menzies and Seyfried, 1979), although this is not important here since the various discriminant functions are based primarily on the immobile elements, and are not significantly influenced by the more mobile ones such as K_2O, Na_2O, and Rb.

The Zr/Nb fractionation diagram (Fig. 27a) appears to define two sample groups with different ratios and fractionation trends. The major group contains less Nb at a given Zr level, and includes all of the most altered samples and eight less altered ones. The data show good correlation, suggesting that the rocks represent a comagmatic suite, and that alteration probably had little effect on the Nb/Zr ratio. The higher Nb/Zr group, consisting only of slightly altered samples, may reflect greater initial concentrations of Nb in the parental magma, possibly due to compositional heterogeneities in the mantle source region.

The observed fractionation trends for all three ratios (Zr/Nb, Zr/TiO_2, and Zr/Y) closely match Pearce and Norry's (1979) modelled fractionation trends, shown as lines 1 and 2 in Figures 27a-c (insets). These lines represent $Plag_{0.5}\ Cpx_{0.3}\ Ol_{0.2}$ and $Plag_{0.5}\ Cpx_{0.3}\ Ol_{0.1}\ Mt_{0.05}$ fractionation, respectively. The similarity of the observed Black Hills trends to the Pearce and Norry (1979) models suggests that the Black Hills basalts were derived by plagioclase-clinopyroxene-

olivine ±magnetite fractionation of a tholeiitic parental magma.

PETROCHEMICAL COMPARISONS

Chemical analyses of the Black Hills basalts are compared with data from various Eocene volcanic suites in the Oregon Coast Range, Olympic Peninsula, and southern Vancouver Island, in order to supplement earlier correlations using lithologic and stratigraphic criteria (Clapp, 1917; Weaver, 1937; Pease and Hoover, 1957; Muller, 1980). Comparison of the Black Hills basalts with average compositions of the upper and lower members of the Crescent Formation in the Olympic Peninsula, and the Metchosin Volcanics of southern Vancouver Island (Table 1) suggests that the Black Hills suite closely resembles the upper Crescent Formation member, particularly with respect to TiO_2 content. They both are consistently higher in TiO_2 (by a factor of two to three) compared to the lower member of the Crescent Formation. This pattern is reflected in a plot of TiO_2 versus total iron (as Fe_2O_3)/MgO (Fig. 28) for Black Hills and Crescent basalts, using data from Glassley (1974) and Cady (1975). Note that most of the Black Hills samples plot in the "upper Crescent" field. The Metchosin Volcanics show similarities to the lower Crescent unit in terms of TiO_2 and gross lithology (Clapp, 1917; Muller, 1974, 1977, 1980).

Table 2 compares the average Black Hills composition with chemical data for the Siletz River Volcanics (Snavely et al., 1968), Yachats Basalt (Snavely and MacLeod, 1974), and basalts in the Marys Peak and North Umpqua areas (Loeschke, 1979), all in the Oregon Coast Range. Black Hills rocks are also compared with samples from the Goble volcanic series in southwestern Washington (Burr, 1978).

The Siletz River Volcanics display a characteristic pattern of

Table 1: Comparison of major element petrochemistry of Black Hills basalts with data from the Crescent Formation (Olympic Peninsula) and Metchosin Volcanics (southern Vancouver Island).

element	1	2	3	4	5	6*	7	8*	9
SiO_2	49.1	50.38	49.14	48.5	51.0	50.4	47.0	47.8	47.8
Al_2O_3	14.6	15.37	14.99	14.6	14.6	15.5	13.9	13.9	14.5
$Fe_2O_3(t)$	13.5	12.50	13.05	13.2	9.5	10.9	14.5	12.0	12.6
MgO	6.0	7.04	7.18	7.2	7.7	7.7	6.6	6.9	6.9
CaO	11.1	9.80	10.83	11.8	10.8	11.3	10.9	10.3	12.1
Na_2O	2.6	3.44	3.02	2.6	3.3	3.0	2.8	3.4	2.6
K_2O	0.26	0.47	0.34	0.22	0.25	0.44	0.12	0.56	0.17
TiO_2	2.4	1.62	2.08	2.2	2.1	1.4	1.7	1.3	1.38
MnO	0.22	nd	nd	0.21	0.3	0.3	0.22	0.19	0.20
P_2O_5	nd	0.29	0.24	0.26	0.2	0.1	0.18	0.19	0.16
volatiles	0.14	nd	nd	nd	nd	nd	3.0	4.02	2.47

Explanation of column headings

1 Black Hills volcanic rocks, average of 30 analyses
2 Lower member of Crescent Formation, average of 37 analyses (Cady, 1975)
3 Upper member of Crescent Formation, average of 32 analyses (Cady, 1975)
4 Crescent Formation, average of 10 analyses (Snavely et al., 1968)
5 Upper member of Crescent Formation, average of 8 analyses (Glassley, 1974)
6 Lower member of Crescent Formation, average of 14 analyses (Glassley, 1974)
7 Upper member of Crescent Formation, average of 3 analyses (Lyttle and Clarke, 1975)
8 Lower member of Crescent Formation, average of 13 analyses (Lyttle and Clarke, 1975)
9 Metchosin Volcanics, average of 10 analyses (Muller, 1980)

*Data from intrusive samples were eliminated from averages

Table 2: Comparison of major element petrochemistry of Black Hills basalts with data from the Siletz River Volcanics, Yachats Basalt, basalts from Marys Peak and North Umpqua areas (Oregon Coast Range), and Goble volcanics (southwestern Washington).

element	1	2	3	4	5	6	7	8
SiO_2	49.1	48.3	48.3	47.8	46.99	47.51	49.7	52.6
Al_2O_3	14.6	14.5	14.6	15.1	14.56	14.49	16.9	16.3
$Fe_2O_3(t)$	13.5	12.4	14.7	14.0	12.36	13.08	11.8	10.3
MgO	6.0	8.3	5.8	6.3	7.39	6.65	3.7	5.5
CaO	11.1	12.2	11.5	11.5	11.92	11.71	8.6	9.5
Na_2O	2.6	2.3	2.6	2.7	2.30	2.39	3.3	2.8
K_2O	0.26	0.17	0.14	0.58	0.26	0.22	1.0	0.58
TiO_2	2.4	1.6	2.7	2.6	1.65	1.83	2.6	2.2
MnO	0.22	0.19	0.25	0.21	0.20	0.22	0.15	0.12
P_2O_5	nd	0.15	0.31	0.33	0.21	0.23	0.52	nd
volatiles	0.14	nd	nd	nd	0.03	0.02	2.40	nd

Explanation of column headings

1 Black Hills volcanic rocks, average of 30 analyses
2 Older flows of lower unit, Siletz River Volcanics, average of 3 analyses (Snavely et al., 1968)
3 Younger flows of lower unit, Siletz River Volcanics, average of 5 analyses (Snavely et al., 1968)
4 Tholeiites from upper unit, Siletz River Volcanics, average of 4 analyses (Snavely et al., 1968)
5 Basalts from Marys Peak area (Oregon Coast Range), average of 22 analyses (Loeschke, 1979)
6 Basalts from North Umpqua area (Oregon Coast Range), average of 10 analyses (Loeschke, 1979)
7 Yachats Basalt, average of 5 analyses (Snavely and MacLeod, 1974)
8 Goble volcanics, average of 13 analyses (Burr, 1978)

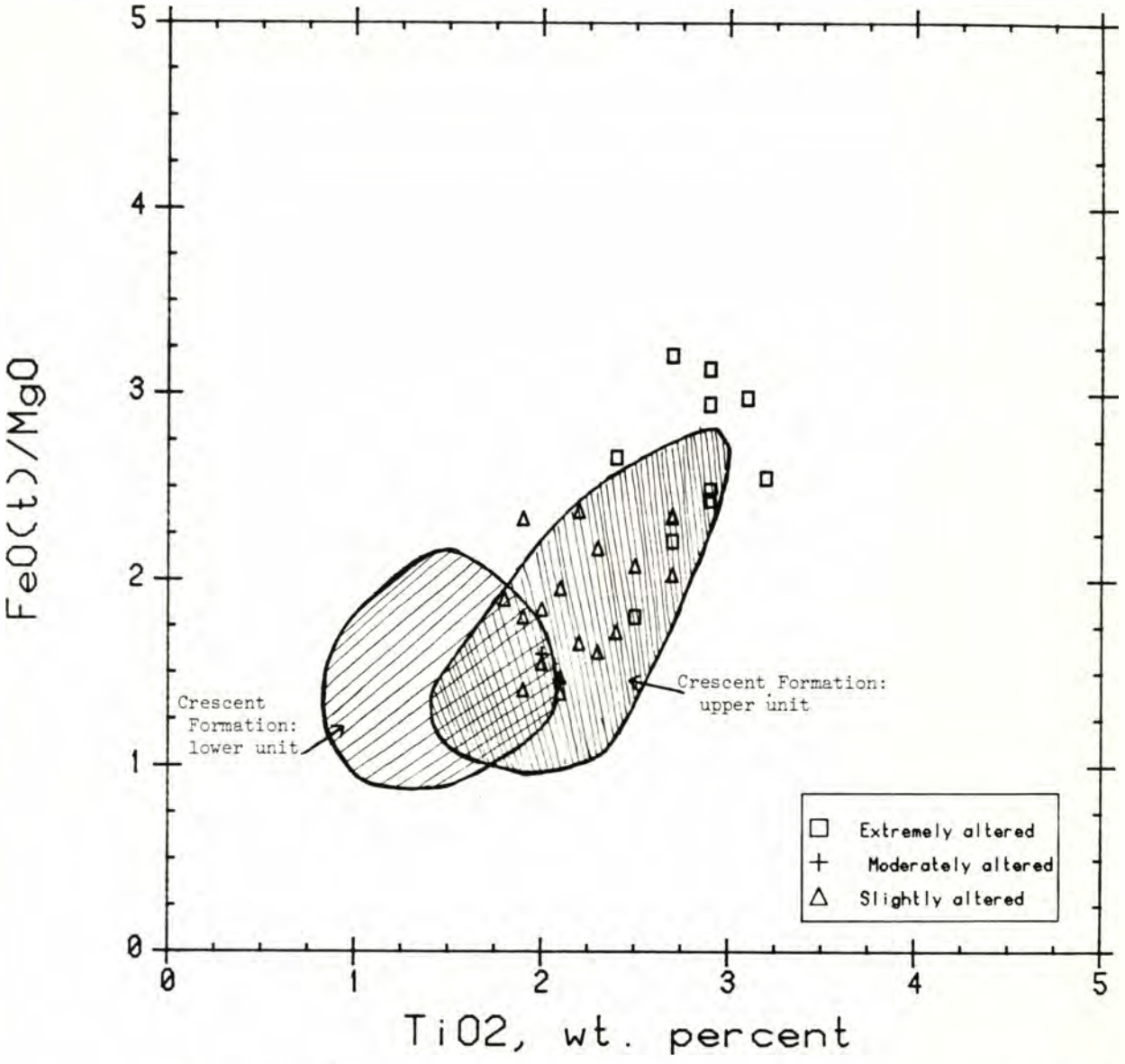

Figure 28: Titania versus total iron/magnesia-ratio plot for Black Hills rocks. Crescent Formation analytical data from Glassley, 1974, and Cady, 1975.

TiO_2 enrichment with decreasing age, which is similar to that observed in the Crescent Formation. The upper section of the lower unit, along with the upper unit of the Siletz River Volcanics, contain about one to two weight percent more TiO_2 than basalts from the lower flows of the lower unit. The Black Hills samples are similar to the upper section of the lower unit of the Siletz River Volcanics with respect to TiO_2, MgO, CaO, Na_2O, and K_2O. The Yachats Basalt also closely resembles the Black Hills suite in terms of TiO_2, although it has considerably higher alkali contents and lower FeO, MgO, and CaO. Basalts from the Marys Peak and North Umpqua areas in the northern and southern sections of the Oregon Coast Range, respectively, have comparatively lower SiO_2 and TiO_2, and are intermediate in composition between the rocks of the lowest part of the Siletz River Volcanics and the Black Hills. The Goble volcanics have higher SiO_2 than other units and are more appropriately termed basaltic andesites, using Streckeisen's (1979) classification.

In summary, the Black Hills suite is chemically similar to basalts from the upper member of the Crescent Formation, the upper flows of the lower member of the Siletz River Volcanics, and the Yachats Basalt. The suite less closely resembles the Metchosin Volcanics, the lower member of the Crescent Formation, and the lower flows of the lower member of the Siletz River Volcanics. The most prominent difference between the two groups is their TiO_2 contents: Black Hills and upper Crescent basalts are TiO_2-enriched, while lower Crescent and older Siletz River lavas have comparatively less TiO_2. The significance of these associations will be discussed in the following sections.

PETROTECTONIC SETTING

Volcanic arc or ocean floor origin?

The petrotectonic setting of the basalts of the study area may be constrained by a number of discriminant functions. The island arc hypothesis, which was proposed by Lyttle and Clarke (1975) to explain the origin of the Crescent Formation in the Olympic Peninsula, is tested by plotting the relationship of Ti to Cr. Jakes and Gill (1970) and Pearce (1975) have shown that discrimination between island arc tholeiites and ocean floor basalts can be made on the basis of Cr and Ti contents. Thompson (1973) and Hart and others (1974) have shown that Cr is immobile during low grade metamorphic and alteration reactions, while Cann (1970) and Pearce (1975) have reported that Ti is immobile during most alteration processes. Figure 29, a Ti versus Cr plot, indicates that the Black Hills basalts are typical eruptive products of an ocean floor setting, and do not appear to have originated in a volcanic arc.

Field evidence also argues against an arc origin for the Black Hills suite. Volcanic arc accumulations contain a high proportion of fragmental rocks relative to basalts from oceanic islands and spreading ridges. Rittman (1962) and Rittman and Rittman (1976) have estimated that the volume percentage of fragmental material in island and continental volcanic arcs averages about 92%, while in ocean basins and oceanic islands the average is much lower (4% and 16%, respectively). Fragmental rocks develop in volcanic arcs without regard for magma type, since tholeiitic, calc-alkaline, and alkalic magmas all display a prominent fragmental texture (Garcia, 1978). This texture is commonly preserved, even in altered or slightly metamorphosed volcanic rocks (Bond, 1973).

The Black Hills rocks, in contrast, consist predominantly of

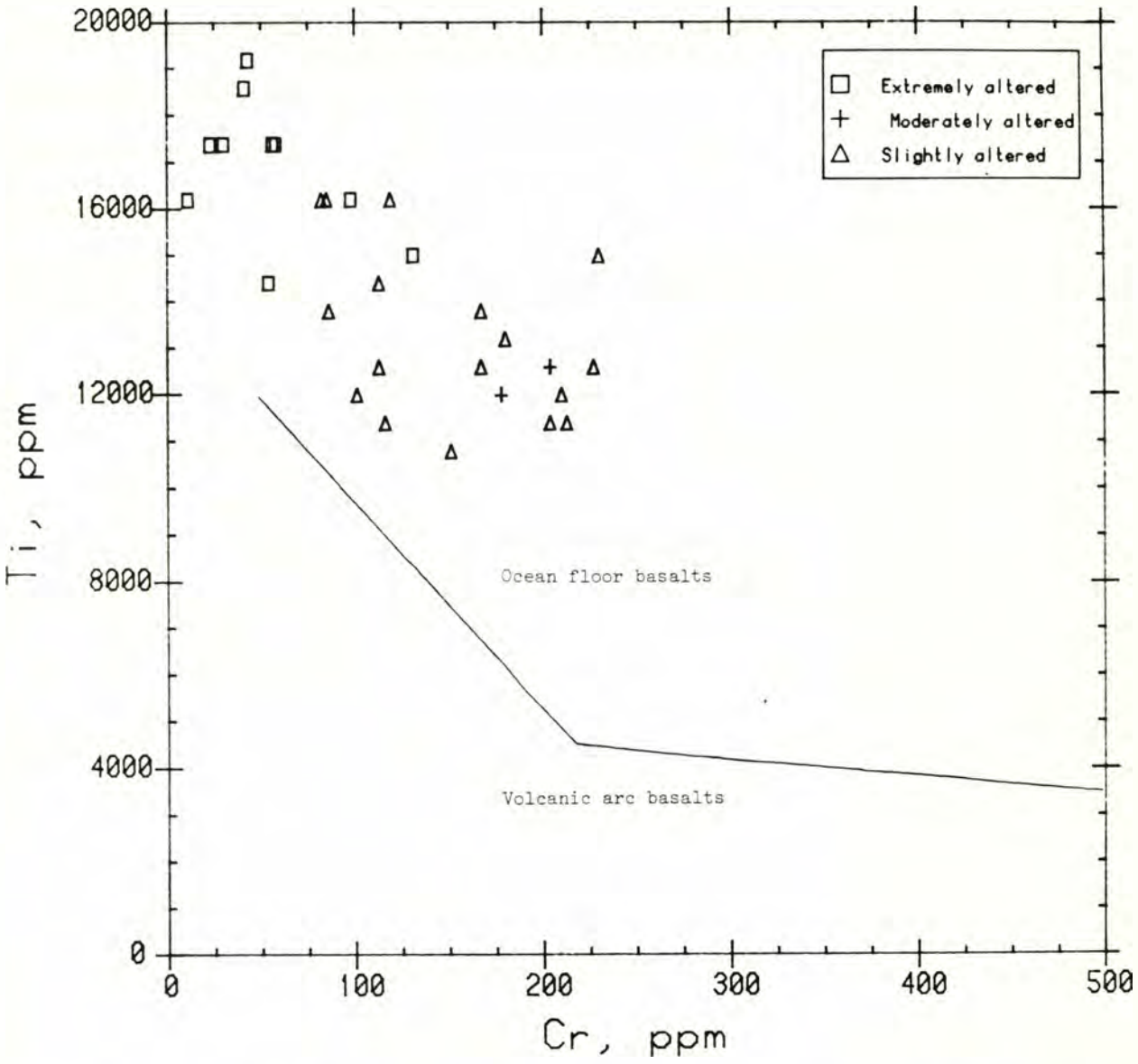

Figure 29: Chromium versus titanium discrimination plot for 29 Black Hills rocks. After Pearce, 1975.

massive and columnar flows, with subordinant pillow lavas, pillow breccias, and hyaloclastites. The breccias and hyaloclastites presumably formed by fragmentation of the lava by friction during flow and by rapid cooling of lava in water, a process that has been described by Lajoie (1979). Fragmentation of volcanic arc lavas, however, is related to the high volatile content of the magma (Macdonald, 1972), which results in relatively explosive eruptions. For example, Hawaiian tholeiitic volcanism is mainly non-violent and is characterized by low volatile contents (Macdonald, 1972), whereas Mt. Shasta (Cascade volcanic arc) has had extremely violent eruptions with high volatile contents (Anderson, 1973).

Cady (1975) has estimated that interpillow breccias, flowfoot breccias, and hyaloclastites constitute only about 15% of the lower member of the Crescent Formation in the Olympic Peninsula. This is considerably less fragmental material than is found in most volcanic arc accumulations (Rittman, 1962; Rittman and Rittman, 1976). Hence the field evidence, together with several geochemical discriminators, preclude an island arc origin for the volcanic rocks of the Black Hills and lithologically similar rocks of the Olympic Peninsula. Extensive field investigations in the Crescent Formation and Siletz River Volcanics by Snavely (1978, written comm.) led him to a similar conslusion.

Mid-oceanic ridge or oceanic island origin?

Several generalizations about the geochemistry of oceanic island (or seamount) basalt (OIB) vis-à-vis mid-oceanic ridge basalt (MORB) are widely recognized (Engel et al., 1965; Hubbard, 1969; Cann, 1970; Pearce and Cann, 1971, 1973; Pearce, 1975; Floyd and Winchester, 1975; Hekinian and Thompson, 1976; Pearce, 1976; Pearce et al., 1977; Pearce,

1979). Most OIBs have significantly higher abundances of incompatible elements (Ti, Ba, Sr, Rb, Zr, Y, Pb, and K) than MORBs (e.g. Bryan et al., 1976). For example, basalts from oceanic islands such as Hawaii (Macdonald and Katsura, 1964), the Galapagos Islands (McBirney and Williams, 1969), Tahiti (McBirney and Aoki, 1968), St. Helena (Baker, 1969), Mauritius (Shand, 1933), the Canary Islands (Ibarrola, 1969; Munoz, 1969; Ridley, 1970), Tristan da Cunha (Baker et al., 1964), and Gough (Le Maitre, 1962) are all enriched in TiO_2/Mg# ratio (Mg#= 100* Mg/(Mg+Fe)) relative to MORBs. Incompatible elements are not preferentially incorporated into the earliest crystallizing rock-forming minerals due to their large ionic radii and strong positive charges, and become concentrated in residual liquids relative to parental material during magmatic differentiation (Clague, 1974; Bence et al., 1980, in press). In general, this enrichment of large cations in residual liquids accounts for the higher abundances of incompatible elements in OIBs relative to MORBs, although chemical heterogeneities in the upper mantle source region may also be a significant factor. Possibly these chemical heterogeneities evolved during repeated magmatic differentiation events, which resulted in a stratified mantle consisting of enriched and depleted source regions. The differences in incompatible element abundances between MORBs, and tholeiites and alkalic basalts of oceanic islands, may reflect these compositional differences in mantle source regions. For example, MORBs are probably derived from sources that are depleted in large cations (Gast, 1968).

Contrasting incompatible element abundances in OIBs and MORBs are accompanied by differences in radiogenic isotope ratios (Gast et

al., 1964; Powell et al., 1965; Tatsumoto et al., 1965; Hedge, 1966; Powell and Delong, 1966; Gast, 1968). Ridge tholeiites are unique in their low $^{87}Sr/^{86}Sr$ ratios, while basalts from oceanic islands within about 2500 km of the East Pacific Rise (EPR) have $^{87}Sr/^{86}Sr$ ratios of 0.7034 $\pm$0.0004. Basalts in the south-central Pacific Basin (more than 2500 km from the EPR) have relatively higher Sr isotopic ratios (Hedge, 1978). Large scale vertical and lateral compositional heterogeneities within the mantle may account for these isotopic differences as well. The best documented example of this large scale ($\sim$400 km) heterogeneity is the Reykjanes Ridge - Iceland rift system (Hart et al., 1973; Schilling, 1973; O'Nions and Pankhurst, 1974; Sun et al., 1975; O'Nions et al., 1976). Another example is the basalts along the central and northern Mid-Atlantic Ridge, which show systematic variations in trace element abundances and radiogenic isotopic ratios as a function of latitude (Schilling, 1975; White and Schilling, 1978).

The characteristic geochemical and isotopic compositions of basalts from OI and MOR environments may be used to reconstruct the petrotectonic setting of the Black Hills rocks. Discriminant functions utilize a set of elements or ratios which are generally specific to one of the three major tectonic settings of terrestrial volcanism: (1) Plate convergent zones= island arc tholeiites and calc-alkaline lavas, (2) Plate divergent zones= ocean ridge tholeiites, and (3) Zones of intraplate volcanism= ocean island and continental flood basalts of tholeiitic and alkalic compositions. Thus there is a characteristic range of magma compositions which can be used to better constrain the specific petrotectonic setting with which a given rock suite may be associated.

The results of any discrimination diagram should be used with caution, since the particular element abundances and ratios of the set of rocks being investigated cannot always be related to their eruptive settings. Rock compositions within a certain setting may represent a composite of several factors, including:(1) composition, (2) processes of magma genesis, such as partial melting, fractional crystallization in magma chambers, magma mixing, and assimilation (Haskin and Dungan, 1980, in press), (3) conditions of melting and magma evolution, including pressure, temperature, and volatile composition, and (4) subsequent weathering or alteration. Because of the extreme variability of magmatic conditions occurring within a particular source region, and because of the likelihood of low grade alteration of basalts following submarine eruption, discriminant analysis of OIB and MORB suites may produce inconclusive or spurious results.

In this study, I use a number of discriminant functions on the grounds that together they provide a more reliable indication of a rock suite's petrotectonic setting than any individual function. Thus the important point is not so much the results of any one diagram, but the consistency of the results when a number of appropriate discriminators are used. Most of these discriminant functions utilize those major- and trace-elements which have been found to be the least affected by sea-floor alteration (Pearce, 1970; Pearce and Cann, 1971, 1973; Pearce, 1975; Smith and Smith, 1976).

Seven discrimination plots of mainly incompatible element data from the Black Hills rocks (Figs. 30-36) show that the suite is most similar to tholeiites from oceanic island (also termed "Hawaiian") and

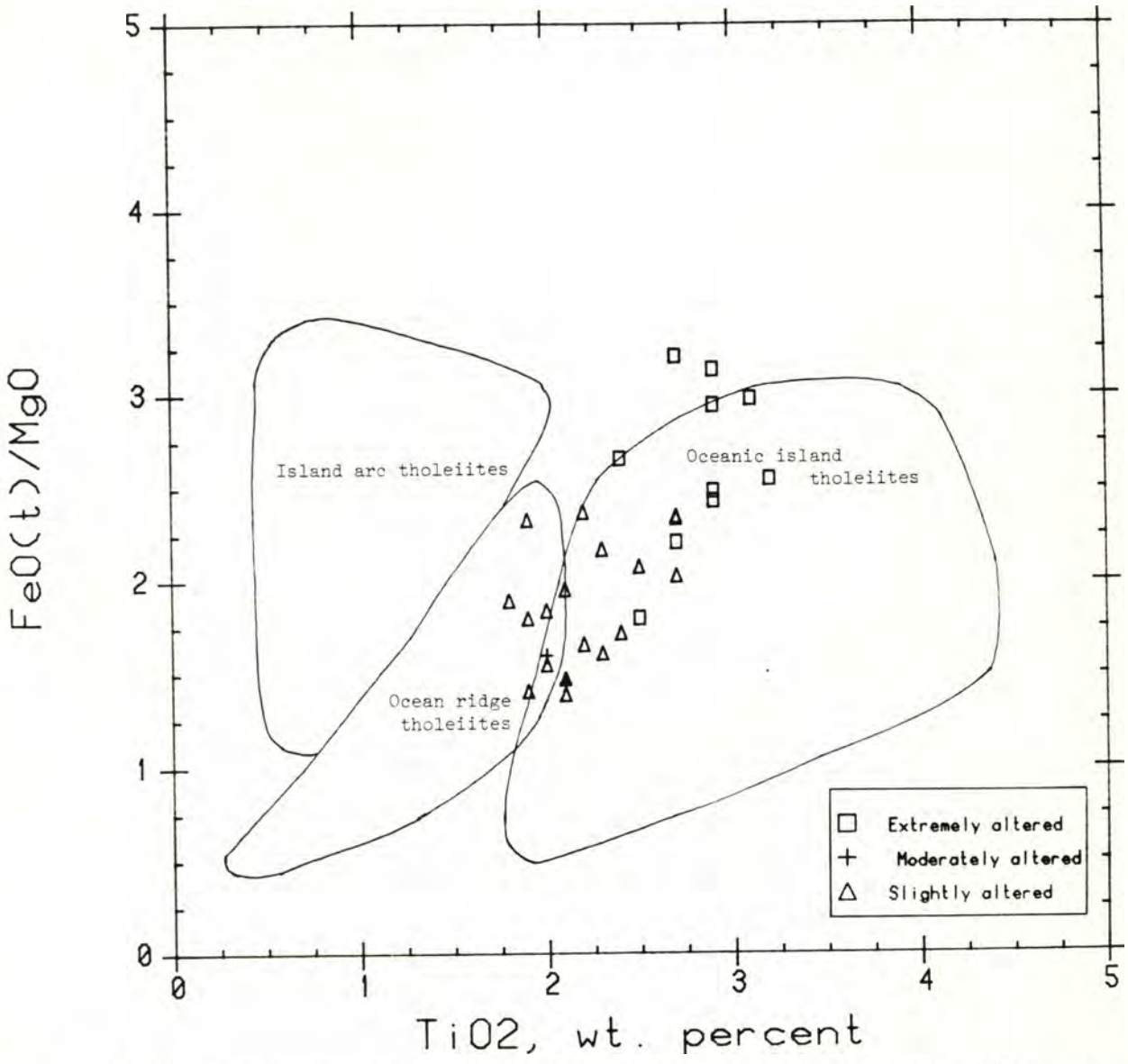

Figure 30: Titania versus total iron/magnesia-ratio discrimination plot for 30 Black Hills samples. After Glassley, 1974.

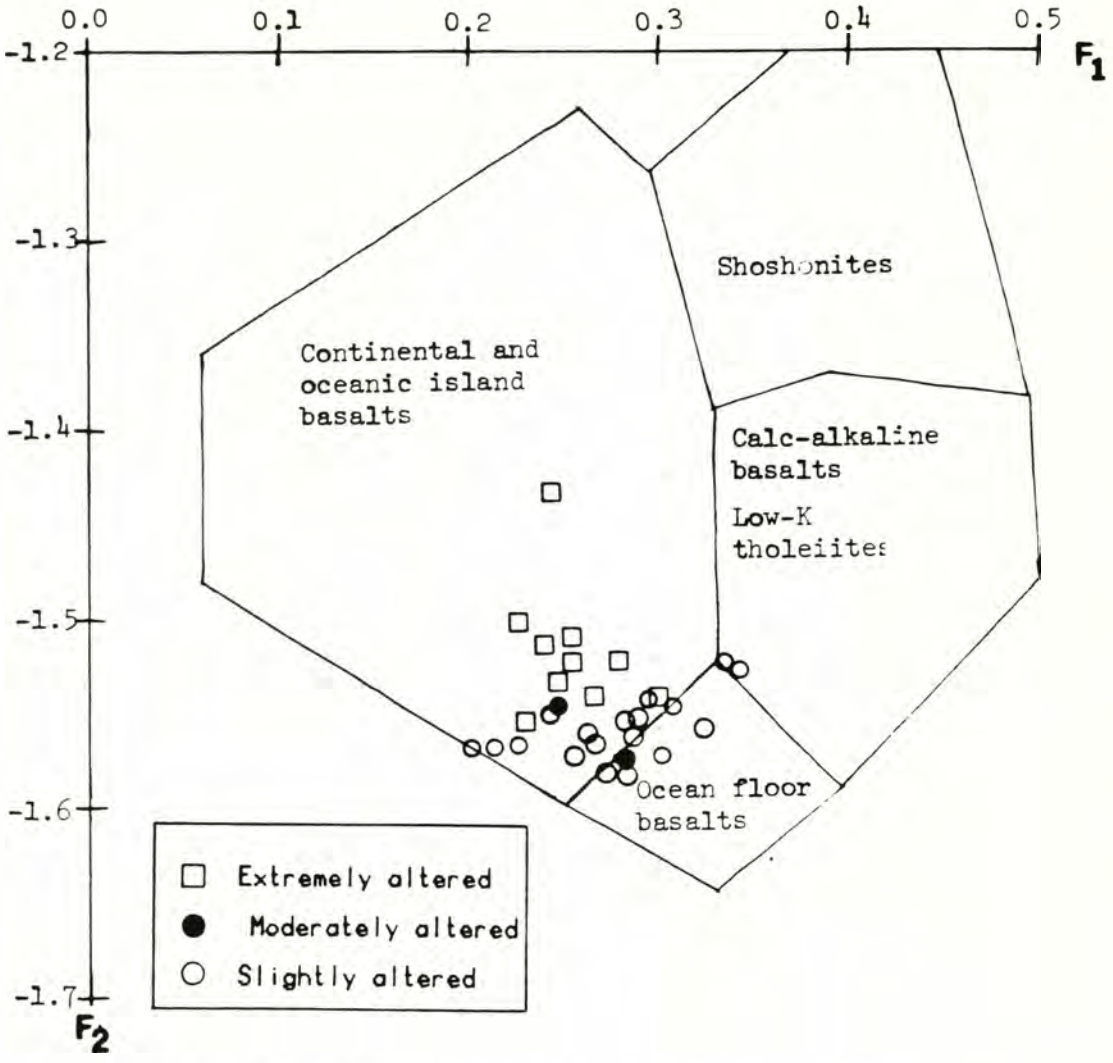

Definition of eigenvectors:

$F_1 = 0.0088\ SiO_2 - 0.0774\ TiO_2 + 0.0102\ Al_2O_3 + 0.0066\ FeO - 0.0017\ MgO - 0.0143\ CaO - 0.0155\ Na_2O - 0.0007\ K_2O.$

$F_2 = -0.0130\ SiO_2 - 0.0185\ TiO_2 - 0.0129\ Al_2O_3 - 0.0134\ FeO - 0.0300\ MgO - 0.0204\ CaO - 0.0481\ Na_2O + 0.0715\ K_2O.$

Figure 31: F_1 versus F_2 discrimination plot for 30 Black Hills rocks. After Pearce, 1976.

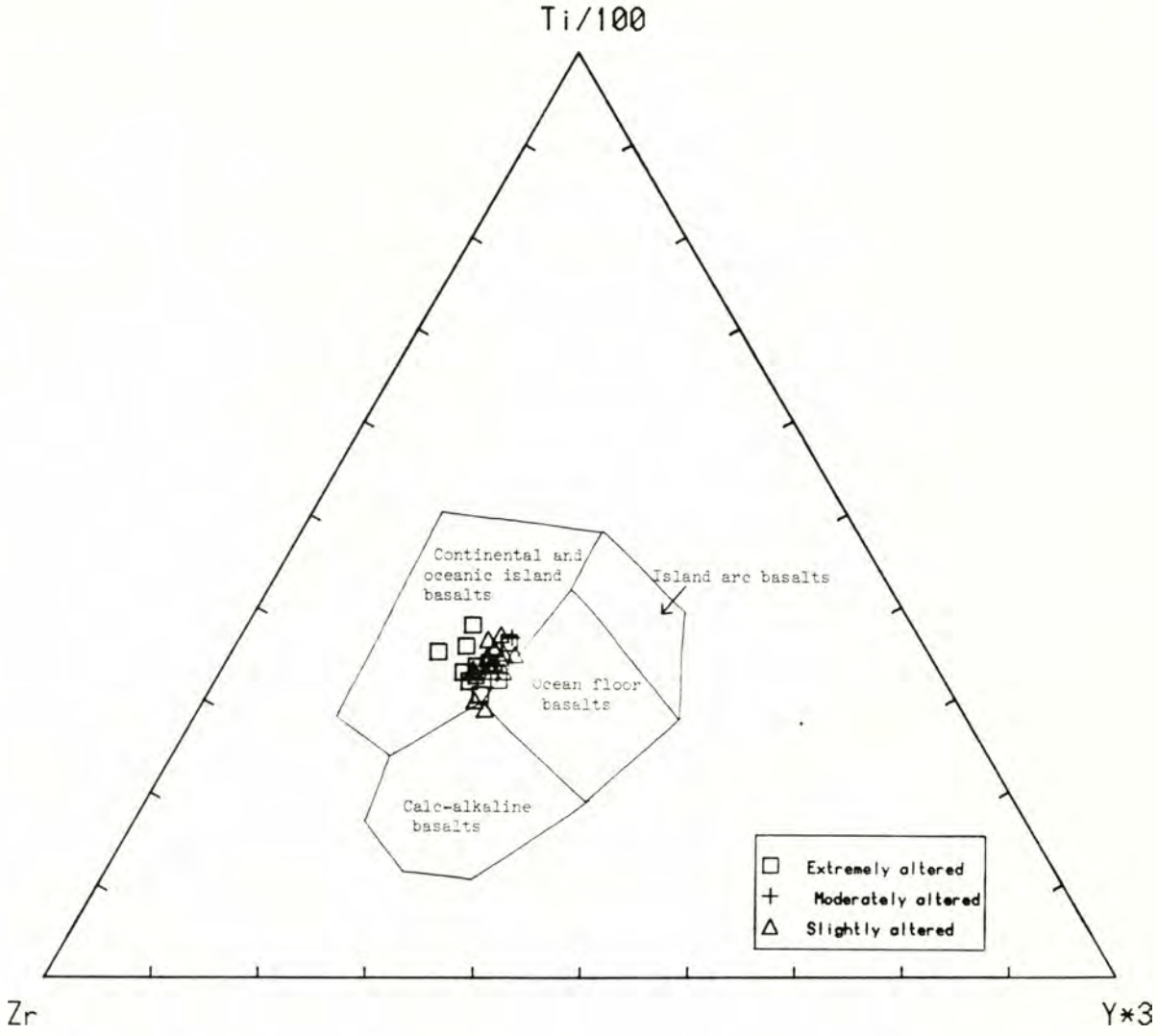

Figure 32: Zirconium-titanium-yttrium discrimination plot of 29 Black Hills rocks. After Pearce, 1975.

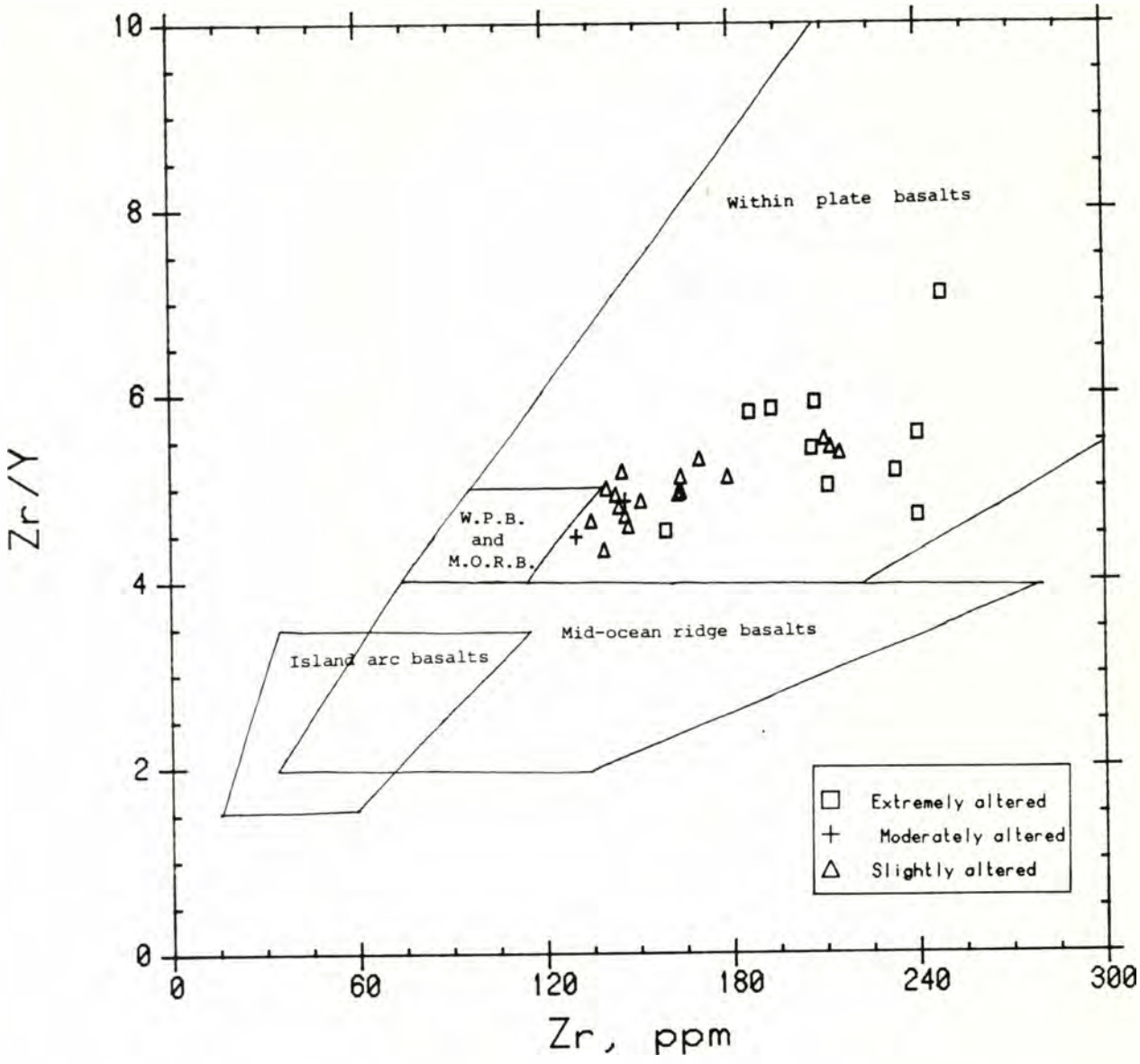

Figure 33: Zirconium versus zirconium/yttrium ratio discrimination plot for 29 Black Hills rocks. After Pearce and Norry, 1979.

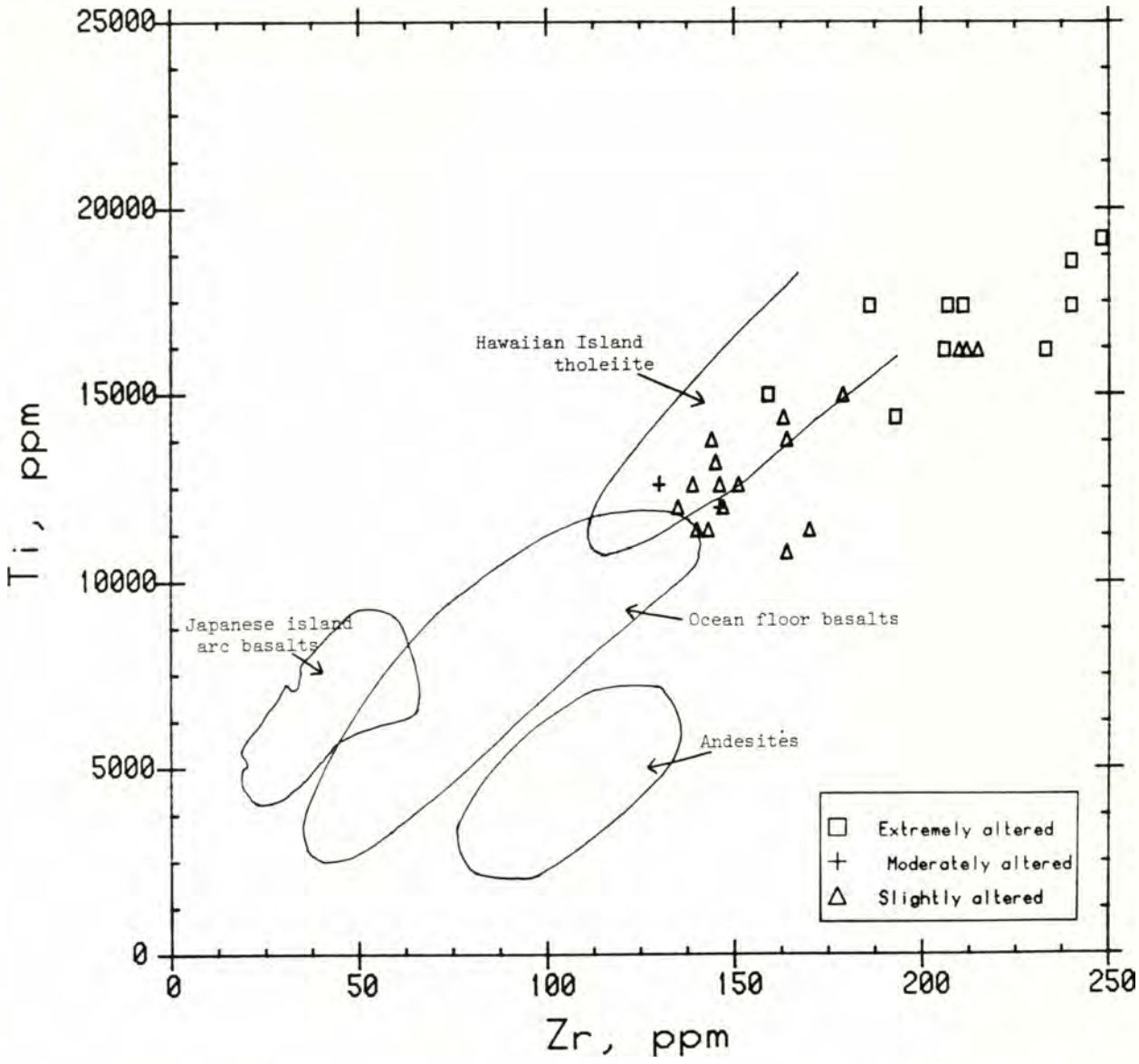

Figure 34: Titanium versus zirconium discrimination diagram for 29 Black Hills rocks. After Pearce and Cann, 1971.

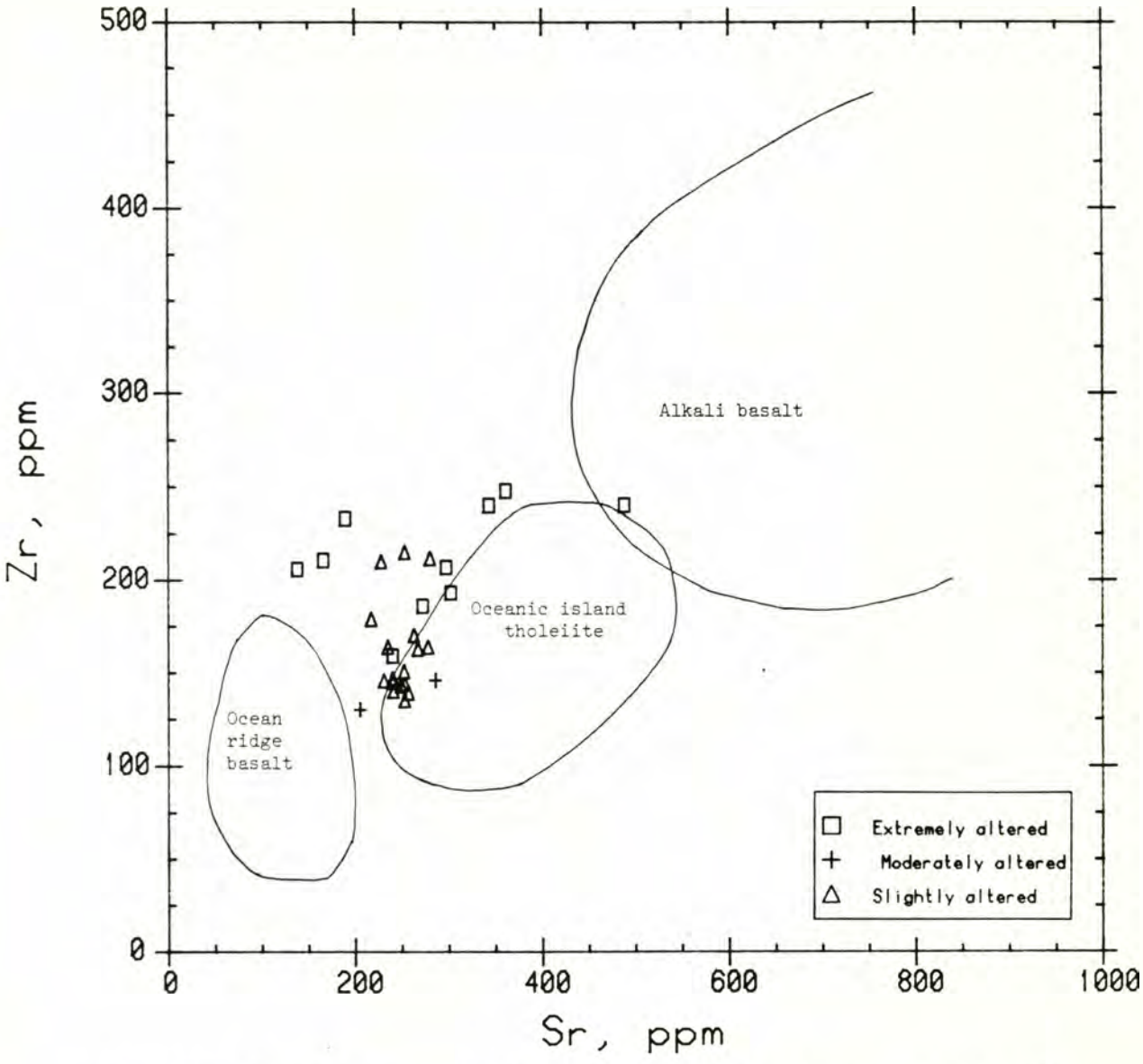

Figure 35: Strontium versus zirconium discrimination plot for 29 Black Hills rocks. After Bass et al., 1973.

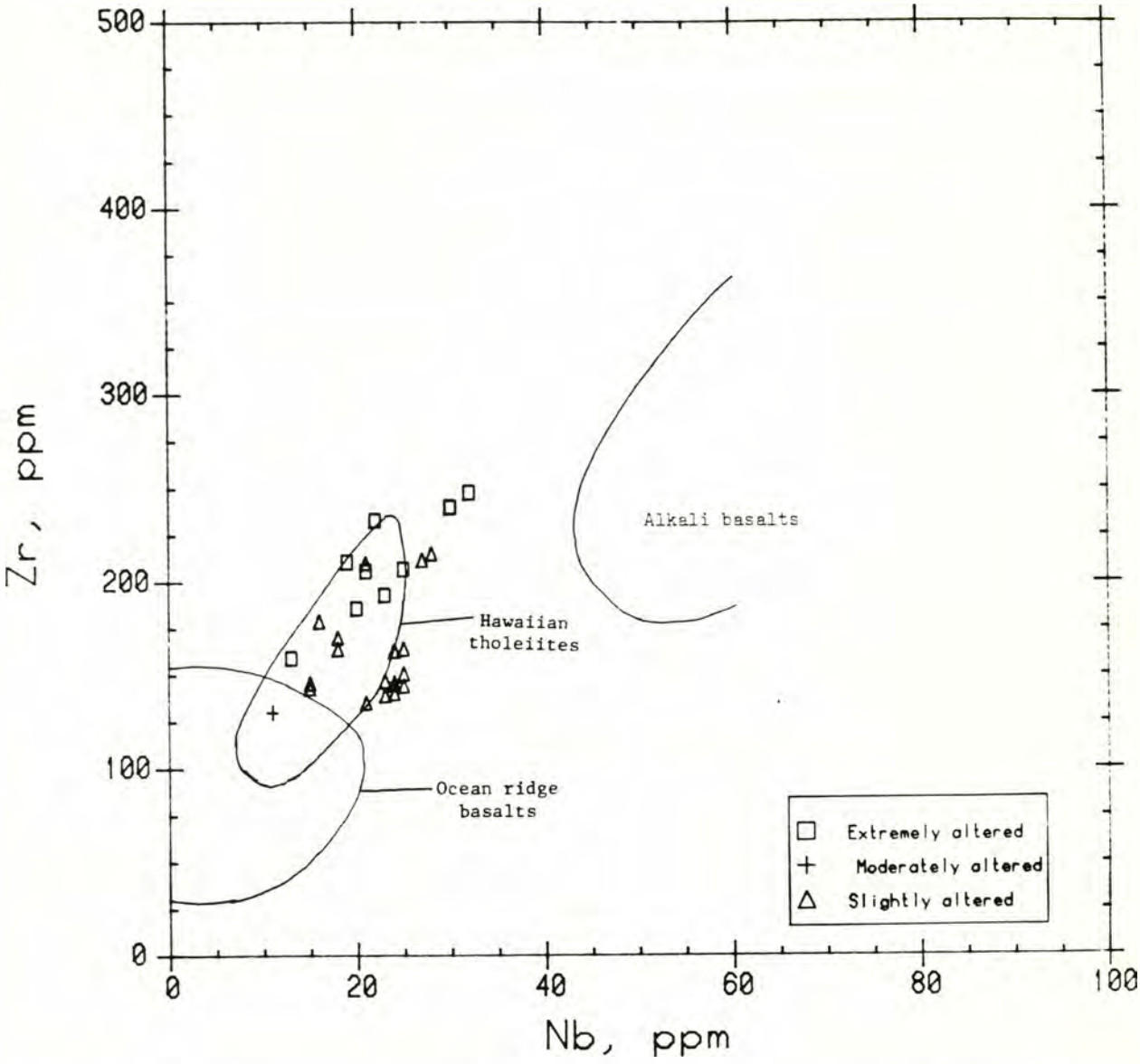

Figure 36: Niobium versus zirconium discrimination plot for 29 Black Hills rocks. The fields outlined for ocean ridge and alkali basalts are after Bass et al., 1973. Hawaiian tholeiite field is based on data from Bence et al., in press.

continental (flood basalt) settings. The presence of pillow lavas, pillow breccias, and hemipelagic siltstones with bathyal Foraminifera in the Black Hills make an OI origin for the suite more plausible. However, the crucial point here is that in most diagrams, the Black Hills basalts approach MORB compositions, despite their basic similarities to OI tholeiites. For example, in the TiO_2 versus Fe_2O_3/MgO plot (Fig. 30), the F_1 versus F_2 eigenvector diagram (Fig. 31), and the Zr vs. Ti plot (Fig. 34), the data points define a trend which extends from the edge of the MORB field well into the OIB range. Because the Black Hills basalts contain significantly more K, Ti, Sr, Ti, Zr, and V than normal MORBs, but much less of these elements than alkalic basalts from oceanic islands, they are termed "transitional" tholeiites, as defined by Johnson (1979). This characteristic of the Black Hills rocks- their overall petrochemical similarity to OIBs though slight resemblance to MORB compositions- has important implications for the petrogenesis of this suite and for analogous basalts in the Washington-Oregon Coast Range. For example, Globerman and Babcock (1980) suggest that the somewhat intermediate incompatible element composition of the Black Hills suite (between MORB and OIB) may reflect its generation by some "hybrid" magmatic process, or simply heterogeneities in the mantle source region. Perhaps some mixing of magmas associated with spreading ridges and with mantle plumes occurred which produced the apparently transitional characteristics of these rocks. Such a mixing model has been suggested to explain the intermediate abundances of incompatible elements and $^{87}Sr/^{86}Sr$ ratios in basalts from Iceland (Schilling, 1973), Galapagos (Hedge, 1978), and Siqueiros basalts near the EPR (Johnson, 1979). Alternatively, the suite may have progressively

evolved from MORB- to OIB-type in chemical composition without any significant mixing of mantle sources.

DISCUSSION

I propose the following model for the evolution of Oregon-Washington Coast Range volcanism during Eocene time, based on a synthesis of field investigations, petrochemical variations, and isotopic data for the Black Hills suite, the Siletz River Volcanics and analogous basalts in coastal Oregon, the Metchosin Volcanics of southern Vancouver Island, and the Crescent Formation of the Olympic Peninsula. The earliest stages of volcanism produced tholeiitic basalts depleted in incompatible elements, which closely resemble lavas erupted at oceanic spreading centers. Subsequent eruptions produced tholeiitic basalts whose compositions were somewhat more enriched in incompatible elements. As magmatism continued the lavas evolved toward OIB compositions; enrichments of most incompatible elements and increases in the Sr isotope ratio probably characterized this phase of volcanism. Continued construction of the volcanic piles resulted in deep water pillow basalts and breccias with intercalated abyssal siltstones grading upward into highly vesicular, massive and columnar flows which in part erupted subaerially. Finally, extremely differentiated alkalic lavas such as mugearites, nephelinites, and camptonites were locally produced, although in far less abundance than the earlier tholeiites. These alkalic magmas resemble the later-stage eruptions of Hawaii (Macdonald and Katsura, 1964) and other older seamounts.

Snavely and others (1968) report that the older basaltic pillow lavas of the lower member of the Siletz River Volcanics in the Oregon

Coast Range have the most primitive compositions. These lavas, which have close affinities to primitive oceanic tholeiitic basalt (Snavely et al., 1968), are overlain by younger basaltic flows and breccias of the lower member. The latter are somewhat enriched in TiO_2, P_2O_5, and total iron, depleted in SiO_2 and MgO, and are more similar in composition to the bulk of the Hawaiian shield-forming tholeiitic basalts (Snavely et al., 1968). The upper part of the Siletz River assemblage consists of shallow marine and subaerial tholeiitic flows and sills, along with a differentiated alkalic suite containing pillow flows and breccias of alkalic basalt, porphyritic augite basalt, picrite basalt, and feldspar-phyric basalt. Snavely and others (1968) suggest that the older basalts of the Siletz River Volcanics represent the parental magma, with the remainder of the SRV constituting the differentiation products of this magma.

Several occurrences of younger alkalic basalts overlying older tholeiites have been reported in the Washington Coast Range, mainly in the Olympic Peninsula (Glassley, 1974; Cady, 1975), although they do not form the extensive flows that occur in the upper Siletz River Volcanics. Several alkalic basalt flows are present in the upper part of the Crescent Formation in the Willapa Hills, about 75 km south of the study area (R. E. Wells, 1979, oral comm.). The presence of alkalic basalts at various localities in the Coast Range suggests that the Eocene volcanic sequences of coastal Oregon and Washington are grossly similar, and are characterized by relatively thin alkalic flows capping more extensive tholeiitic submarine and subaerial accumulations. In Hawaii the voluminous flows of tholeiitic basalt produced during the main shield-building stage are subsequently covered by a thin layer of

alkalic basalt produced during the final stages of volcanism (Macdonald and Katsura, 1964; Presnall et al., 1979).

In the Olympic Peninsula Glassley (1974), Cady and others (1972), Cady (1975) and Tabor and Cady (1978a) have divided the Crescent Formation into two members: (1) a lower unit, consisting of deep water basalts characterized by pillow and massive flows with interbeds of pelagic limestone (Cady et al., 1972; Garrison, 1973) resembling MORB in composition (Glassley, 1974; Cady, 1975), and (2) an upper unit, consisting of shallow marine and locally subaerial, massive and columnar basalt flows and breccias with intercalated terrigenous clasts (Cady, 1975). The upper part of the Crescent Formation is chemically similar to OI tholeiites (Glassley, 1974; Cady, 1975). This unusually thick sequence has been interpreted as one or more seamounts either erupted in situ on top of lower Crescent oceanic crust (Cady, 1975), or isolated from the lower Crescent sea floor during eruption, with subsequent tectonism juxtaposing the two Crescent units (Glassley, 1974). The former interpretation is more plausible, since field investigations by Wilson (1975) show that the fault separating the two units, which Glassley interpreted as a suture, postdates the major Olympic folding and thrusting events which affected the entire formation. These events have been dated at 29 m.y. and 17 m.y. B.P. (Tabor, 1972); hence the fault could not have been an Eocene suture zone. In addition, reexamination of Glassley's (1974) data by Fairchild (1979b) indicates that the lower Crescent is crosscut by dikes compositionally similar to the upper Crescent, suggesting that the two units were probably part of a continuous volcanic succession. Analogous rocks of the Oregon Coast

Range, such as the Siletz River Volcanics, also appear to be a continuous succession (Snavely et al., 1968).

The "hybrid" petrochemistry of the Black Hills basalts, the widely prevalent association of incompatible-element depleted (MOR-type) tholeiites grading up into incompatible-element enriched (OI-type) tholeiitic lavas and lesser alkalic flows in the Oregon-Washington Coast Range, and the prodigious quantities of magma associated with widespread "eugeoclinal" volcanic centers, may all reflect eruption of the seamount chain on the crest or flanks of a north- to northwest-trending oceanic spreading center during latest Paleocene and Eocene time. This chain was subsequently sutured to the leading edge of North America by late Eocene (Magill et al., 1980, in press) to early Oligocene time (Fairchild, 1980).

The evolution of volcanic edifices at ridge crests has been described by Menard (1969), who proposed that these seamounts continue to develop after moving away from the ridge on the new oceanic plate (Fig. 37). Subaerial eruptions occur if the edifice grows to sufficient size. Numerous occurrences of young seamounts either on or peripheral to active mid-oceanic ridges have been reported. Barr (1974) has described two northwest-trending seamount chains (Heck and Heckle chains) on the western flank of the Juan de Fuca Ridge. These chains originated on the ridge crest, where most of the volcanism occurred. Cobb Seamount is located near these seamount chains, and is also situated relatively close to the ridge crest (Menard, 1969). Isla Tortuga is a recently formed volcanic island located on a fracture zone of an active spreading trough in the Gulf of California (Batiza, 1978; Batiza et al., 1979a). Batiza (1979) has described nine small

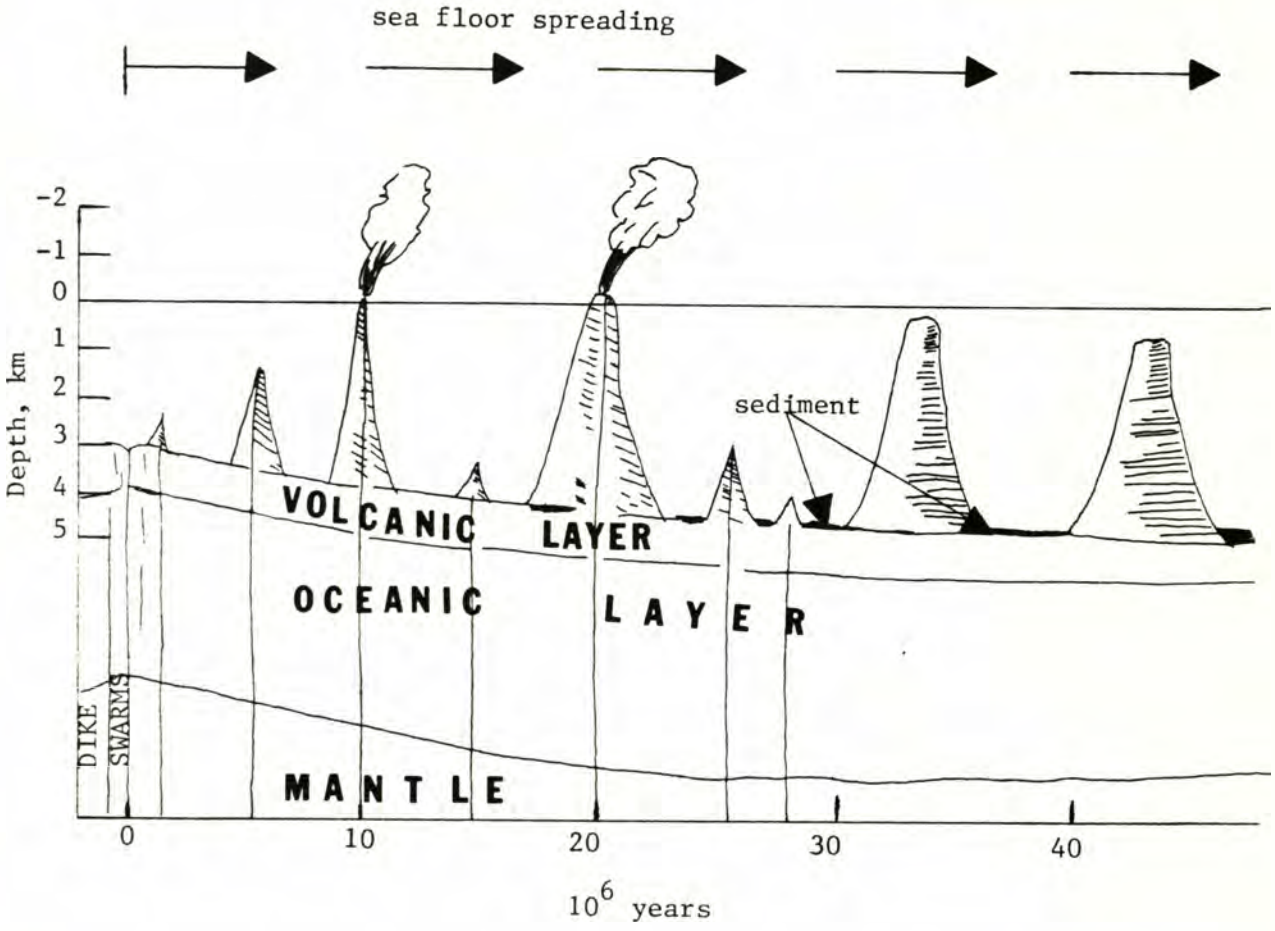

Figure 37: Menard (1969) model of typical growth and subsidence of drifting oceanic central volcanoes (seamounts). The volcanoes erupt first on the crest or flanks of a mid-oceanic spreading center. They may continue erupting for several millions of years as they are carried away from the ridge on the new oceanic plate.

volcanoes near the East Pacific Rise at 9^{o} - 14^{o}N; Lonsdale and Spiess (1979) have described a pair of small seamounts flanking the East Pacific Rise at $8^{o}50'$N, which apparently had a common origin at a "hotspot" on the spreading axis. These seamounts continued to grow for a brief time after they were separated by seafloor spreading. Tutu Seamount is positioned directly on the crest of the Cocos Ridge (Fornari et al., 1979) near the Panama Basin. Iceland is perhaps the best example of a volcanic edifice built up on the crest of an active oceanic spreading center (Schilling, 1973).

A progressive shift in the magmatic compositions of ridge-formed oceanic islands has been described by Batiza (1977, 1980), who showed that many small isolated oceanic central volcanoes (seamounts) located on young oceanic crust (less than 10 m.y. old) are composed of primitive incompatible-element depleted (MOR-type) tholeiitic basalts. Seamounts located on older oceanic crust are composed mainly of transitional to alkalic and differentiated lavas (Batiza, 1977). Presumably seamount eruptions along the axial zones of spreading centers tap the same incompatible-element depleted tholeiitic mantle source from which the underlying oceanic crust was derived (Batiza, 1979; Lonsdale and Spiess, 1979). Isla Tortuga is one example of a recently formed tholeiitic volcanic island on an active spreading trough; major element, trace element, and isotopic compositions of Tortuga basalts are almost identical to MOR tholeiites (Batiza, 1978; Batiza et al., 1979a). Johnson (1979) has described basalts from a small seamount on 1.5 m.y. old crust west of the East Pacific Rise, whose chemical and isotopic compositions are intermediate between MORB and OI alkalic basalt.

If volcanism continues after the seamounts have drifted away from the vicinity of the ridge crest, the earlier MOR-type tholeiitic flows will be capped successively by transitional and alkalic basalts and differentiated lavas which reflect a mantle source region that is less depleted in the incompatible elements (Batiza, 1977, 1980). Such a source region is usually associated with OIBs (Bryan et al., 1976). The Siletz River Volcanics and the Crescent Formation are possible examples of this idealized compositional sequence. However, the specific compositional changes associated with seamount evolution are not well constrained, and the relationship of most seamount compositions to the age of the underlying oceanic crust (and hence distance from the ridge crest) require further study (Batiza et al., 1979b).

Assuming that the chemistry of erupted seamount lavas changes systematically with distance from the ridge crest, some portion of the volcanic suite should be intermediate in composition between depleted and undepleted mantle sources. Samples from this portion of the sequence could be expected to plot in both the OIB and MORB fields of most discrimination diagrams. Since the Black Hills suite primarily resembles OI tholeiites, but approaches MORB compositions, particularly with regard to the incompatible elements, it may represent some intermediate stage in the evolution of ridge-formed seamounts.

In contrast to the Crescent and Siletz River lavas, the Black Hills suite does not include a distinct MORB-type member; even the most incompatible-element depleted samples plot close to the boundary between the MORB and OIB groups on most diagrams. One possible ex-

planation is that the Black Hills region was not as extensively deformed as the Olympic Peninsula. This deformation, characterized by imbricate thrust faulting, folding, and doming (Park, 1950; Stewart, 1970; Tabor, 1972, 1975; Tabor et al., 1970; Tabor and Cady, 1978b), probably exposed the thick, older submarine section of the Crescent Formation. The basalt flows of the Black Hills are too shallow-dipping to expose a very large stratigraphic section through the volcanic pile. Hence the lowermost flows of predominantly MORB composition are not observed in the study area.

I suggest that the Eocene volcanic piles of the Washington-Oregon Coast Range may represent a linear chain of oceanic islands erupted more or less contemporaneously at or near a spreading center. The spreading center may have been active during the time of seamount eruption, or may have been an extinct ridge crest which served as a zone of crustal weakness along which basaltic volcanism preferentially occurred. Alternatively, the chain of oceanic islands may have been generated along a transform fault separating two spreading ridge segments during realignment of spreading (Plumley, 1980), although it seems unlikely that such a large volume of magma could be explained by a simple "leaky transform".

The composition of the erupting lavas probably evolved as the oceanic island chain moved away from the spreading center, or as the ridge segments became further separated by transform faulting. The inferred temporal transition from MOR- to OI-type tholeiite may reflect this changing geometry of ridges and proximal seamounts. Alkalic basalts and strongly differentiated lavas which cap parts of the older tholeiitic flows were probably erupted in the final

stages of Coast Range volcanism during middle to late Eocene time. The fact that these late-stage flows constitute a relatively small proportion of the total sequence may be explained by some abrupt termination of magmatism before significant quantities of alkalic lavas could be produced. Cessation of magmatism probably coincided with the accretion of the Coast Range to the leading edge of North America, and may have occurred not long after the shift from tholeiitic to alkalic volcanism.

Isotopic data from the Black Hills basalts, although limited, provide strong supporting evidence for the near-ridge origin of the seamount province. According to the $^{87}Sr/^{86}Sr$ versus Rb/Sr diagram of Hedge (1978), the four Black Hills samples analyzed are distinctly different from average rocks from the East Pacific Rise, but are analogous to basalts from the Galapagos Islands (Fig. 38). This correspondence is significant since the Galapagos Islands consist of predominantly OI-type tholeiitic basalts, and were erupted in close proximity to the Cocos Ridge (McBirney and Williams, 1969; Pearce, 1975). According to Clague (1980, oral comm.), seamounts which originate close to spreading ridges are characterized by low initial Sr isotope ratios, in the range of approximately 0.7030. The mean Sr isotope ratio of four Black Hills basalts is 0.7030 $\pm$0.0004 (Appendix D). One other example of a tholeiitic oceanic island originating at an active mid-oceanic spreading center is Iceland (Schilling, 1973; Sigvaldason, 1974; O'Nions et al., 1976), which is also characterized by a relatively low $^{87}Sr/^{86}Sr$ ratio (Hart et al., 1973; O'Nions and Pankhurst, 1973). Subbarao and others (1973) report $^{87}Sr/^{86}Sr$ ratios ranging from 0.7022 to 0.7034

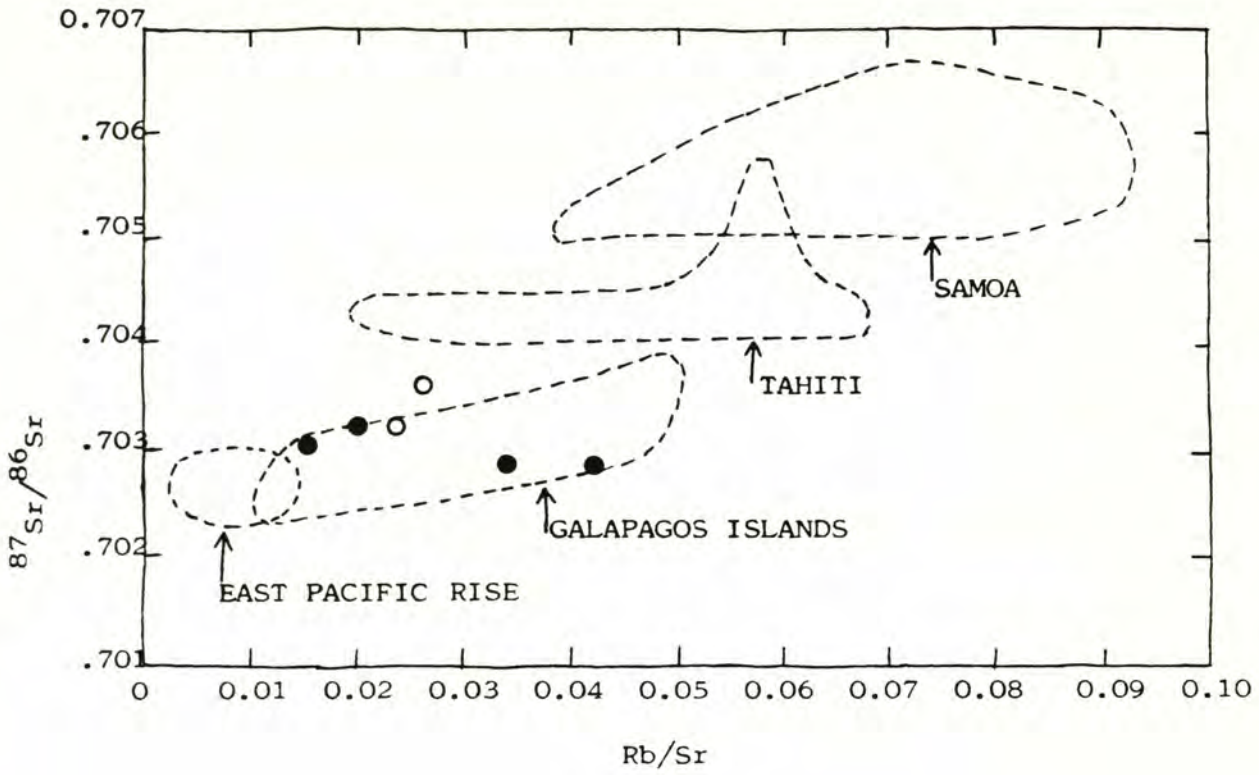

Figure 38: $^{87}Sr/^{86}Sr$ versus Rb/Sr diagram comparing four Black Hills samples with fields of data for several Pacific Basin settings, and average compositions from Hawaii and Oahu. Field boundaries and Hawaiian data after Hedge, 1978.

in basalts from three seamounts in the Gulf of Alaska (Giacomini, Kodiak, and Hodgkins), and one in the Juan de Fuca area (Cobb). They state that: "These basalts seem to be similar to oceanic island basalts in alkali element concentrations (and) $^{87}Sr/^{86}Sr$... However, in places, seamount basalts also appear to resemble ridge tholeiites." Turner and others (1979) suggest that trace element signatures and radiometric ages of Davidson and Denson guyots (Kodiak-Bowie chain) are more compatible with an origin at or near an oceanic spreading center.

Further supporting evidence for my interpretation is a recent geochemical study of the Metchosin Volcanics of southern Vancouver Island by Muller (1980), who arrived at a similar conclusion for the petrogenesis of these middle Eocene basalts. According to him: "...(T)he Iceland-type ridge-island setting is the most probable mode of origin for Metchosin as well as Crescent Formations, with the Hawaiian-type intra-plate setting as a second alternative" (emphasis added). Muller's (1980) interpretation closely parallels my hypothesis for the origin of the Black Hills basalts and other Eocene volcanic suites of the Coast Range.

In summary, major- and trace-element analyses indicate that the Black Hills basalts constitute a comagmatic suite and, although basically similar to OI tholeiites, approach MORB compositions as well. They are lithologically and petrochemically similar to the upper member of the Crescent Formation of the Olympic Peninsula (Glassley, 1974; Cady, 1975), and the upper flows of the lower member of the Siletz River Volcanics of the Oregon Coast Range (Snavely et al., 1968). These two units overlie the MORB-like lower Crescent

member and lower member of the SRV, respectively. The intermediate incompatible element compositions and Sr isotope ratios of the Black Hills basalts resemble those of tholeiites from Iceland, Galapagos, and possibly Easter Island, all of which are oceanic islands that were erupted at or close to the ridge crest of an active spreading center.

The hypothesized petrochemical evolution of the Black Hills basalts and other Eocene lavas of the Coast Range is not unlike that described at certain oceanic central volcanoes formed at ridge crests. These seamounts initially erupt depleted tholeiitic lavas resembling MORB in composition, but subsequently produce less depleted transitional tholeiites, alkali basalts, and alkalic differentiated lavas (all typical of oceanic islands) after the seamounts have drifted away from the ridge crest on young oceanic lithosphere (Batiza, 1977, 1979, 1980).

One difficulty with a ridge origin for the Coast Range is that a recent early Tertiary reconstruction of Byrne (1979) has the Pacific-Farallon spreading center situated too far from the leading edge of North America to have enabled the Coast Range to erupt near the ridge and be emplaced by late Eocene time, assuming geologically reasonable rates of plate convergence. Possibly an active or "fossil" ridge segment (the latter serving as a zone of crustal weakness) existed in close proximity to the western margin of North America, which generated the voluminous lava piles of the Coast Range before its consumption at a trench during the waning stages of rapid Eocene plate convergence.

IV. PALEOMAGNETISM

SAMPLING

A total of 263 core samples were collected from 37 sites in the Black Hills and adjacent areas, using drilling and orientation procedures described by Doell and Cox (1965). The cores were drilled in the field using portable rock drills, and oriented with a magnetic compass. Weather conditions and forest cover did not permit corroboration with sun compass orientation. As a result, spurious magnetizations of the outcrop, such as those resulting from lightning strikes, may have introduced some error into these orientations. These should be rare, however, since most are located in heavily forested, low- to moderate-elevation areas, rather than on exposed high ridges.

Each site consists of between six and eight individually oriented samples, generally drilled at least one meter apart. Most suitable exposures are found along roadcuts, with the remainder in quarries and stream beds. Appendix B gives the locations of all paleomagnetic sampling sites.

LABORATORY PROCEDURE

Following collection, samples cores were cut into specimens approximately 2.3 cm in length, according to standard paleomagnetic laboratory procedure. Natural remanent magnetization (NRM) of each specimen was then measured on a Schonstedt Model SSM-1A spinner magnetometer. Secondary components of NRM were removed by alternating field (AF) demagnetization, using a Schonstedt Model GSD-5

AC tumbling specimen demagnetizer. Optimum demagnetization field strength used for each site was determined with two pilot specimens. The demagnetization level which resulted in the least angular divergence between two pilot specimens was the level selected for all other cores in the site. Most specimens were demagnetized at field strengths ranging from 100 to 400 oersted (Fig. 39). This technique follows methods described by McElhinny (1973) and Tarling (1971).

In eleven sites, one or more specimens remained far outside the cluster defined by the other samples, following AF demagnetization. Such specimens that diverged from the mean direction by at least twice the angular standard deviation were eliminated. Generally these aberrant samples were highly oxidized, cracked, or questionably oriented in the field because they fragmented during drilling. A total of 25 samples were eliminated by this process.

Two entire sites were eliminated from the Black Hills population following demagnetization and the application of tilt corrections. Equal area plots of these and all other sites are given in Appendix E. Site 78-03 was eliminated because the six specimen directions failed to cluster (radius of 95% circle of confidence= 37.4^{o}). Site 7.7.79.1 was rejected due to lack of adequate structural control at the sampling locality. According to geologic mapping in the Doty - Minot Peak area (Pease and Hoover, 1957), this site is located near the axis of a northwest-trending anticline just south of the Chehalis River. When the mapped attitude nearest to the sampling site was used for making the tilt correction, an inclination of nine degrees was obtained. Such an inclination is very much too flat for the

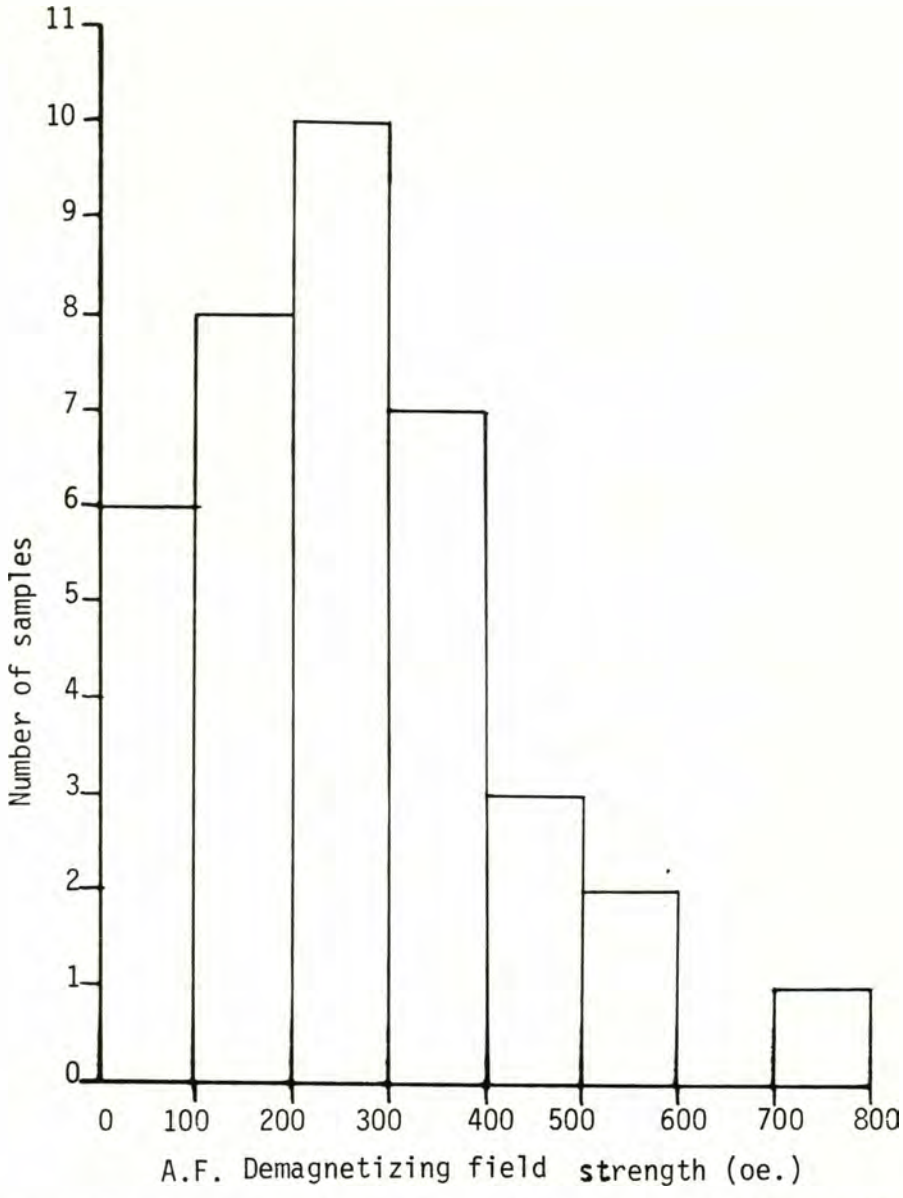

Figure 39: Demagnetizing field strength used for 37 Black Hills sites. The number of sites demagnetized at a given field strength (in oersteds) is represented by the vertical bars. The majority of samples were demagnetized at between 100 and 400 oe.

latitude of the Black Hills, and suggests that there are structural complications at the drilling site which are not apparent in the field or on the geologic map. I therefore decided to eliminate this site from the Black Hills population, even though the radius of its 95% circle of confidence (α_{95}) was below the maximum cut-off value of 15^{o}. Demagnetization of all sites and elimination of the two aberrant sites result in an increase in Fisher's (1953) precision parameter (k) from 8.1^{o} to 18.7^{o} (Figs. 40,41).

TILT CORRECTIONS

Obtaining structural measurements for tilt-correcting the paleomagnetic data proved to be the most intractable problem of this investigation. Mapping by Pease and Hoover (1957), Snavely and others (1958), and myself along the southern and western flanks of the Black Hills provided sufficient structural data for siltstones and sandstones of the Lincoln Creek Formation, which nonconformably overlie the Crescent Formation (Sheet 1). Snavely and others (1958) measured several attitudes in siltstones of the McIntosh Formation. These siltstones are intercalated with the uppermost flows of the Crescent Formation in the southern part of the Black Hills near Rochester. No sedimentary rocks have been observed overlying the basalts in the interior of the Black Hills or along the northern and eastern margins. For this reason, the extent of tilting of the interior flows is unknown. Furthermore, the paucity of sedimentary interbeds in the basalts makes it virtually impossible to obtain accurate attitudes from the flows directly. Consequently, it was necessary to determine the geologic structure of the Black Hills by compiling available sedimentary

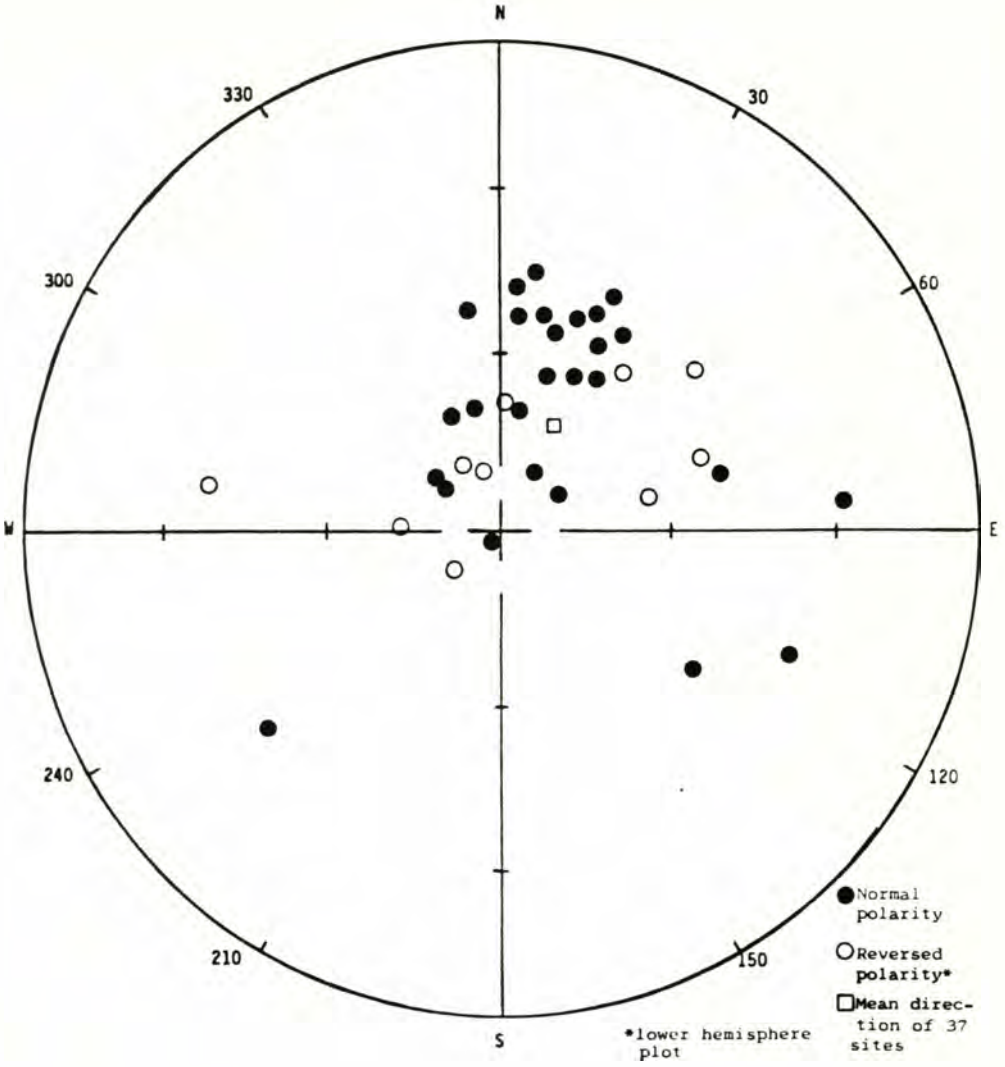

Figure 40: Equal area plot of 37 Black Hills sites before demagnetization and the application of tectonic corrections.
Declination= 25.7°
Inclination= 68.9°
kappa= 8.08
α_{95}= 8.10°

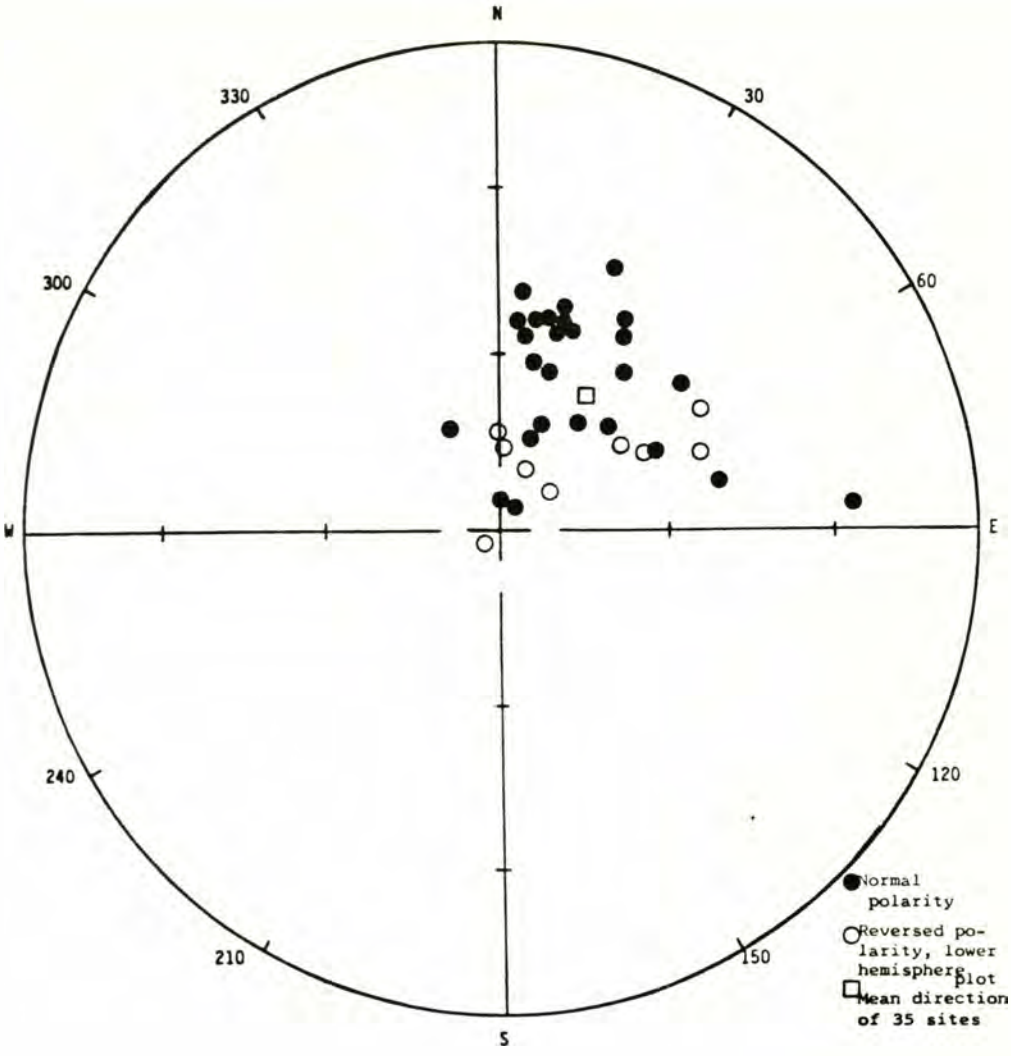

Figure 41: Equal area plot of 35 Black Hills sites after demagnetization but before application of tectonic corrections.
Declination= 32.1°
Inclination= 62.5°
kappa= 18.7
α_{95}= 5.47°

attitudes and by measuring various marker horizons in lava flows, such as breccia layers, saprolite zones, and cross-joints in columnar basalt outcrops. A total of 52 attitudes were obtained by this method, which is more fully described in Chapter II. Compilation of previous mapping in sections of the McIntosh and Lincoln Creek Formations (Pease and Hoover, 1957; Snavely et al., 1958), and reconnaissance mapping of columnar-jointed flows of Crescent basalts throughout the Black Hills, suggest that dips at most outcrops do not exceed 10 to 15 degrees. In general, attitudes of both sedimentary layers and lava flows are virtually identical: the mean Black Hills attitude is N 7^{o} E, 7.5^{o} W. Most outcrops dip west to slightly northwest and southwest, although some flows appear to be flat-lying.

After these attitudes were plotted on the geologic map (Sheet 1), all sampling localities within a two kilometer radius of each attitude were tilt-corrected. A sampling locality between two mapped attitudes was corrected using an interpolated attitude. It was possible to tilt-correct 17 out of 35 sites in this manner. These corrections resulted in a slight increase in k from 18.7 to 20.1 for the 17 sites with "known" attitudes. However, this increase is not significant, according to a test described by Cox (1968). The mean directions of these 17 sites were essentially unchanged: D= 31.9^{o}, I= 62.5^{o} for the non-tilt-corrected mean direction; and D= 29.1^{o}, I= 66.6^{o} for the tilt-corrected mean direction. Note that the 95% circles of confidence around the mean directions overlap (Fig. 42), indicating that they are statistically similar. The absence of a significant increase in the precision of site directions following

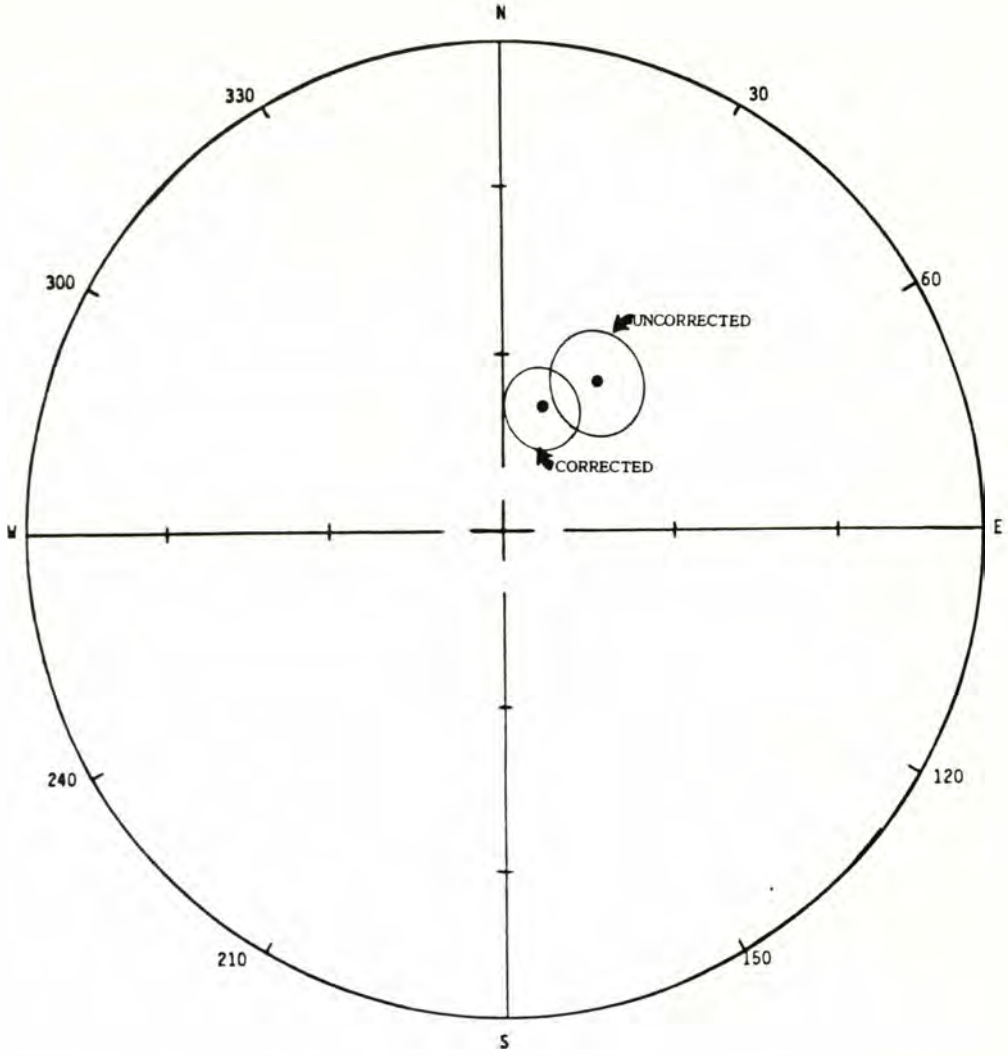

Figure 42: Equal area plot of mean directions and 95 percent circles of confidence for 17 Black Hills sites whose attitudes have been measured. The directions plotted are with and without tectonic corrections. The fact that these circles overlap suggests that there is no statistically significant difference in the directions of the tectonically corrected and uncorrected groups.

tilt correction has been observed in other paleomagnetic studies of gently dipping lava flows (M. E. Beck, Jr., 1979, oral comm.), and suggests that uncorrected shallow dips do not introduce serious errors into the data.

Applying tilt corrections to the remaining 18 sampling localities, termed the "attitudes unknown" sites, was more difficult, since these sites are located more than two kilometers from any mapped attitude. These "attitudes unknown" sites may either be combined with the 17 tilt-corrected sites without themselves being corrected (Method I), eliminated entirely from the Black Hills population (Method II), or arbitrarily tilt-corrected using the mean Black Hills attitude of N 7^{o} E, 7.5^{o} W, and then combined with the remaining 17 sites (Method III). The latter technique results in the highest value of k when all 35 sites are combined, although the increase is not significant.

Method III is preferred because the 52 measured or inferred poles to sedimentary layers and lava flow cross-joints throughout the Black Hills are tightly clustered ($\alpha 95 = 3.5^{o}$), and indicate rather uniform dips of 10 to 15 degrees or less, generally to the west, northwest, and southwest (Fig. 18). This consistency does not support the assumption implicit in Method I that the 18 "attitudes unknown" sites between the measured outcrops are flat-lying and do not require tectonic correction. Method II is not preferred because it eliminates more than half of the data set, including most of the reversely-magnetized sites. This would tend to increase secular variation in the remaining 17 sites. Although Method III is preferred, the mean Black Hills paleomagnetic direc-

tions and amounts of discordance from the expected direction determined by each of the three methods are reported here.

In summary, the structural relations in the Black Hills area, although imprecisely known, have been inferred from a combination of geologic mapping along the southern and western flanks (Pease and Hoover, 1957; Snavely et al., 1958), where overlying and intercalated sedimentary units are exposed, and from field measurements of cross-joints in columnar basalt flows in the interior and along the northern and eastern flanks. These structural data are not inconsistent with the results of earlier geologic studies in the Black Hills and nearby areas, where basalts of the Crescent Formation and overlying clastic rocks of the Lincoln Creek Formation crop out. They suggest that the basalts are gently dipping at most localities, and strike in the same north to northeasterly direction as the Lincoln Creek Formation. For example, Weaver (1916) reported that:

> "(A)long the western contact of the basalt in the Black Hills area, sandstones and shales of Oligocene age (Lincoln Creek Formation) are resting unconformably upon the former. The sediments have a strike approximately parallel to the contact. This is nearly north and south with a low dip to the west ranging from 9 to 11 degrees."

Henriksen (1956) mapped analogous volcanic flows in the Willapa Hills, about 70 km to the southwest, and also noted that relatively shallow dipping flows were most common:

> "Locally, dips as high as 30^{o} to 40^{o} were measured in outcrops of the (Crescent) volcanic series, but such steep dips are rare. Most dips are lower, ranging from 10^{o} to 20^{o}."

The paleomagnetic data tend to support this interpretation, since the relatively small value of $\alpha 95$ of the mean non-tilt-corrected Black Hills direction (5.5^{o}) would be unlikely if the region were more extensively folded. An equal area plot of 52 poles to bedding and cross-joints (Fig. 18), along with other geologic evidence discussed in Chapter II, indicates that the rocks dip about eight degrees west to slightly northwest and southwest, and that the Black Hills area is probably a gently dipping homocline which lacks major internal structural complications. The very slight increase in the precision parameter, and the corresponding reduction in the radius of the 95% circle of confidence which result from the application of tilt corrections, suggest that tectonic deformation of the lava flows is insignificant between sampling sites. Since the sites are well distributed throughout the Black Hills area (Sheet 1), the paleomagnetic results presented in this study are considered to be valid, although random, undetected tilt may have decreased precision to a small degree.

RESULTS

Three sets of equal area plots for the Black Hills sites are presented in Appendix E. These sets represent directions of remanent magnetizations before and after AF demagnetization of 37 sites, and following tectonic correction of the 17 "attitudes known" sites. A summary of directions of remanent magnetizations and site virtual geomagnetic poles (VGPs) before and after demagnetization and tilt correction (using Method III) is given in Table 3. Note that sites 78.03 and 7.7.79.1 are excluded from the Black Hills population for reasons discussed earlier. The locations of the 35 acceptable sites

Table 3 : Paleomagnetic results for the Black Hills volcanic rocks treated as site means.

SITE	LOCATION	LONG.	LAT.	N	N R M D̄	N R M Ī	α95	N	H (oe)	L B A N E D D̄	L B A N E D Ī	Q(95	SITE V.G.P. PLONG.	SITE V.G.P. PLAT.	TECTONIC ATTITUDE	CORRECTION D̄	CORRECTION Ī	CORRECTED SITE V.G.P. PLONG.	CORRECTED SITE V.G.P. PLAT.
78.01	SR8, Perry Creek	123.12W	47.12N	7	3.53	47.06	17.34	7	100	5.14	52.78	10.27	39.25E	75.69N	N7E 7.5**	354.5	52	74.94E	74.91N
78.02	SR8, Perry Creek	123.12W	47.12N	7	10.19	68.57	9.97	7	100	20.91	69.79	4.97	67.01W	75.23N	N7E 7.5**	359	71	127.03W	81.65N
78.03*	SR8, Perry Creek	123.12W	47.12N	6	307.52	76.48	31.49	6	150	236.40	-70.1	37.37	65.80W	54.53S	- - - - - -	- - - - -	- - - - -	- - - - -	- - - - -
78.04	US101, Kamiche	123.12W	47.12N	6	32.97	48.99	21.28	5	100	16.59	49.22	4.16	14.03E	68.70N	N7E 7.5**	7.5	50	34.75E	72.68N
78.05	US101, Kamiche	123.12W	47.12N	7	12.38	51.42	14.20	7	200	18.41	61.46	2.55	20.68W	70.23N	N7E 7.5**	4	62	19.44E	85.20N
78.06	US101, Kamiche	123.12W	47.12N	7	347.13	68.78	7.74	7	150	11.87	60.47	5.15	3.60W	79.79N	N7E 7.5**	359	60	63.82E	83.73N
7.8.78.1	Black Lake Blvd.	123.00W	47.00N	7	300.52	77.85	8.35	7	200	357.82	84.83	6.36	123.72W	57.25N	N7E 7.5**	316	78.5	154.13W	59.58N
7.8.78.2	Black Lake Blvd.	123.00W	47.00N	8	207.26	88.43	14.72	8	100	26.81	84.92	4.09	114.94W	55.73N	N52E 6W	331.5	80.64	129.27W	64.93N
7.9.78.1	US101, Mud Bay	123.00W	47.05N	8	336.09	69.42	16.23	7	300	334.33	70.99	6.51	175.83W	72.02N	N56E 9E	331.78	82.06	146.62E	69.87N
7.9.78.2	Capitol Peak Road	123.25W	46.88N	7	26.88	43.99	5.74	7	100	24.48	39.07	4.29	9.78E	58.31N	N43W 9W	21.0	47.28	7.73E	65.33N
7.9.78.3	Iron Creek Road	123.25W	46.88N	7	230.08	35.38	23.08	6	100	36.63	66.65	2.61	52.29W	65.64N	N56W 3W	37.31	71.64	69.75W	65.20N
7.9.78.4	Summit Lake South	123.00W	47.00N	7	149.17	-76.83	3.52	7	800	178.45	-73.45	0.84	126.73W	77.69S	N7E 7.5**	157	-71	173.94W	73.42S
7.10.78.1	Shaker Church Road	123.00W	47.00N	6	163.39	-80.29	10.25	5	200	201.30	-78.28	12.37	102.32W	66.78S	N7E 7.5**	165.5	-78	138.61W	68.65S
7.10.78.2	Bordeaux Road	123.00W	46.90N	8	51.38	-79.93	27.01	6	200	230.34	-78.51	1.67	90.71W	57.21S	N7E 7.5**	189.5	-81.5	116.98W	63.20S
7.10.78.3	Sherman Valley Road	123.12W	46.90N	7	58.82	77.70	24.82	6	300	17.68	73.30	5.05	88.69W	73.96N	N23W 7W	354.61	76.78	130.48W	71.83N
7.10.78.4	Sherman Valley Road	123.12W	46.90N	6	17.42	61.58	22.78	5	300	11.28	51.82	3.32	22.10E	73.18N	N7E 7.5**	1	52	53.47E	75.70N
8.6.78.1	US12, Oakville	123.25W	46.83N	7	219.39	-54.71	21.02	7	300	238.66	-48.44	5.84	33.69W	41.93S	N7E 7.5**	232	-54	34.84W	49.50S
8.6.78.2	US12, Gibson Creek	123.30W	46.88N	7	20.79	49.91	11.86	7	300	20.18	51.54	9.56	3.15E	68.72N	N30E 10W	9.36	47.57	31.54E	70.39N
8.7.78.1	Cedar Creek Road A	123.25W	46.88N	7	16.01	53.67	3.18	7	600	18.31	50.95	3.41	7.60E	69.29N	N30W 15W	3.14	62.35	21.14E	86.10N
8.7.78.2	Cedar Creek Road B	123.25W	46.88N	6	350.74	50.78	33.07	5	600	6.21	48.21	9.27	39.26E	71.69N	N30W 15W	350.18	57.19	98.80E	78.39N
8.7.78.3	Cedar Creek Road C	123.12W	46.90N	6	25.37	47.60	12.33	6	400	31.58	47.01	7.21	7.11W	59.10N	N7E 7.5**	23	49.5	1.73E	65.74N
8.23.78.1	Monroe Creek	123.12W	46.90N	7	4.87	52.07	5.85	7	300	7.82	54.96	4.20	26.92E	77.18N	N42W 13W	351.29	63.69	135.39E	83.76N
8.23.78.2	Countyline	123.12W	46.90N	7	29.10	53.04	6.58	7	400	18.46	52.99	4.84	3.97E	70.68N	N42W 13W	6.09	63.62	13.98E	85.46N
9.8.78.1	Capitol Peak	123.12W	46.90N	6	27.43	60.07	10.22	6	200	40.55	57.05	3.11	30.68W	58.99N	N7E 7.5**	29	61	30.49W	68.88N
9.8.78.2	Hell Creek	123.12W	46.90N	7	113.42	33.48	23.24	7	400	51.62	48.53	4.72	28.25W	46.78N	N60W 13W	59.50	60.29	47.95W	47.90N
9.11.78.1	Porter Ck. campground	123.25W	46.90N	7	76.21	50.15	4.02	7	500	77.41	49.89	4.19	47.42W	30.05N	N19E 9W	70.38	57.27	50.10W	30.01N
9.27.78.1	Porter Creek Road B	123.25W	46.90N	7	125.84	47.85	28.88	7	400	63.18	59.15	3.53	48.45W	44.84N	N7E 7.5**	53	63	53.41W	54.53N
10.9.78.1	Wedekind campground	123.25W	46.83N	7	31.01	78.49	13.99	7	400	47.43	64.43	4.50	49.99W	57.88N	N60W 13W	63.10	76.31	83.56W	53.30N
10.9.78.2	Porter Creek Road A	123.25W	46.90N	7	85.25	27.38	12.22	7	300	86.11	25.79	4.58	39.86W	12.51N	N30E 40W	60.26	54.46	60.86W	44.14N
10.15.78.1	Cloquallum Ck. Road	123.30W	47.12N	6	231.12	-44.74	21.45	6	300	249.11	-52.35	4.77	44.19W	37.02S	N7E 7.5**	243.2	-58.5	47.44W	44.51S
10.22.78.1	SR108, Kamiche	123.12W	47.12N	7	32.88	59.42	24.54	7	200	30.86	69.83	6.25	9.34W	61.17N	N20E 17W	11.35	47.74	27.11E	69.68N
10.23.78.1	SR108, McCleary	123.25W	47.00N	7	249.60	-51.64	25.61	7	300	241.55	-60.55	4.47	49.44W	46.73S	N7E 7.5**	231.5	-66	54.90W	55.93S
10.23.78.2	Summit Lake North	123.00W	47.00N	7	258.03	-62.58	15.37	6	500	235.68	-63.81	8.38	51.79W	52.28S	N54W 12W	250.05	-74.61	79.46W	68.84S
10.28.78.1	Kennedy Falls	123.12W	47.00N	7	92.07	-72.66	22.01	5	500	56.07	-87.49	14.26	129.90W	44.05S	N7E 7.5**	85.5	-80.5	148.57W	42.38S
7.7.78.1*	Independence Valley	123.25W	46.75N	7	98.97	-37.15	31.37	5	400	135.90	-52.27	11.09	140.17E	53.96S	- - - - - -	- - - - -	- - - - -	- - - - -	- - - - -
7.8.78.1	Gate Quarry	123.12W	46.85N	6	9.06	43.91	11.36	5	400	12.36	52.41	7.20	18.31E	73.27N	N48W 28W	329.67	71.54	175.11W	69.13N
7.8.78.1	Gate-Mine Road	123.12W	46.83N	7	183.05	-67.68	10.06	7	300	183.10	-75.01	6.78	117.50W	74.90S	N7E 7.5**	158	-73	183.38W	72.39S

N - number of samples used in calculating a site mean
D - mean direction, degrees from true north
I - mean inclination, degrees, positive downwards
α95 - radius of the circle of 95 percent confidence
H - alternating current demagnetizing field in oersteds yielding least dispersion

ATTITUDE - measured strike and dip on tilted flows
PLONG. - paleolongitude of site virtual geomagnetic pole (V.G.P.)
PLAT. - paleolatitude of site virtual geomagnetic pole
* - site directions rejected from Black Hills mean for reasons discussed in text
** - estimated strike and dip on tilted flows

are plotted on the geologic compilation map of the Black Hills area (Sheet 1). These locations, with their magnetic polarities and tectonically corrected magnetic declinations, are also plotted on the modified Black Hills map (Fig. 43). From these plots several important relationships may be inferred:

(1) All of the paleomagnetic sampling sites with reversed polarity occur in the lowlands. Some normally-magnetized sites are found in the lowlands as well, but the majority occur in the higher elevation areas.

(2) Most of the sites have mean declinations of remanent magnetizations which are significantly more easterly-directed than expected for cratonic North America, both before and after tectonic corrections have been applied.

(3) Out of a total of 35 sites used in the determining the mean Black Hills direction, 26 sites (74%) are of normal polarity, while 9 sites (26%) are of reversed polarity.

This observed predominance of normally-magnetized sites is not unexpected for the Crescent lava flows of the Black Hills. These rocks have been assigned to the Ulatisian Stage (middle Eocene) on the basis of Foraminifera collected from sedimentary interbeds within the volcanic flows (Henriksen, 1956; Pease and Hoover, 1957; Snavely et al., 1958; Rau, 1966, 1967, and written communications, 1979, 1980). The Ulatisian Stage extended from 49 to 46.5 m.y. b.p., according to the revised Cenozoic time scale of Berggren (1972). The magnetic polarity scale of McElhinny (1973) shows that the earth's magnetic field was normal during most of the Ulatisian Stage (Fig. 44). Hence the predominance of normally-magnetized sites in the Black Hills probably

Figure 43: Locations, polarities, and mean declinations of paleomagnetic sampling sites in the Black Hills area. Arrows indicate observed mean declinations of remanent magnetizations at each site following tilt correction by Method III. Antipoles of mean declinations are plotted for all reversely-magnetized sites. Lines without arrowheads are expected mid-Eocene declinations for cratonic North America.

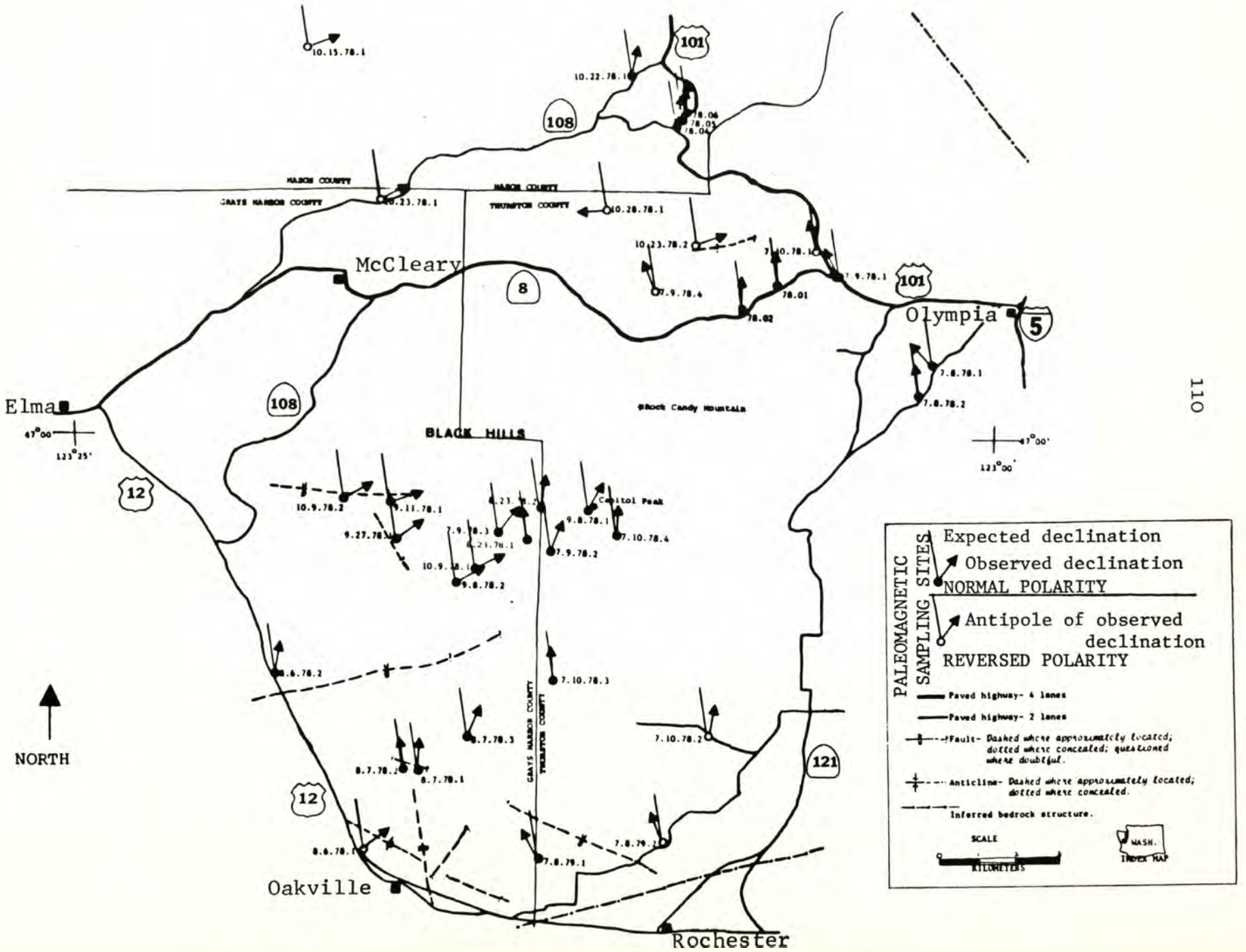
McCleary
Olympia
Elma
Oakville
Rochester
BLACK HILLS
Capitol Peak
Rock Candy Mountain
MASON COUNTY
GRAYS HARBOR COUNTY
THURSTON COUNTY
PACIFIC COUNTY
47°00'
123°25'
123°00'
101
108
8
12
5
121
NORTH
PALEOMAGNETIC SAMPLING SITES
Expected declination
Observed declination
NORMAL POLARITY
Antipole of observed declination
REVERSED POLARITY
Paved highway- 4 lanes
Paved highway- 2 lanes
Fault- Dashed where approximately located; dotted where concealed; questioned where doubtful.
Anticline- Dashed where approximately located; dotted where concealed.
Inferred bedrock structure.
SCALE
KILOMETERS
WASH.
INDEX MAP

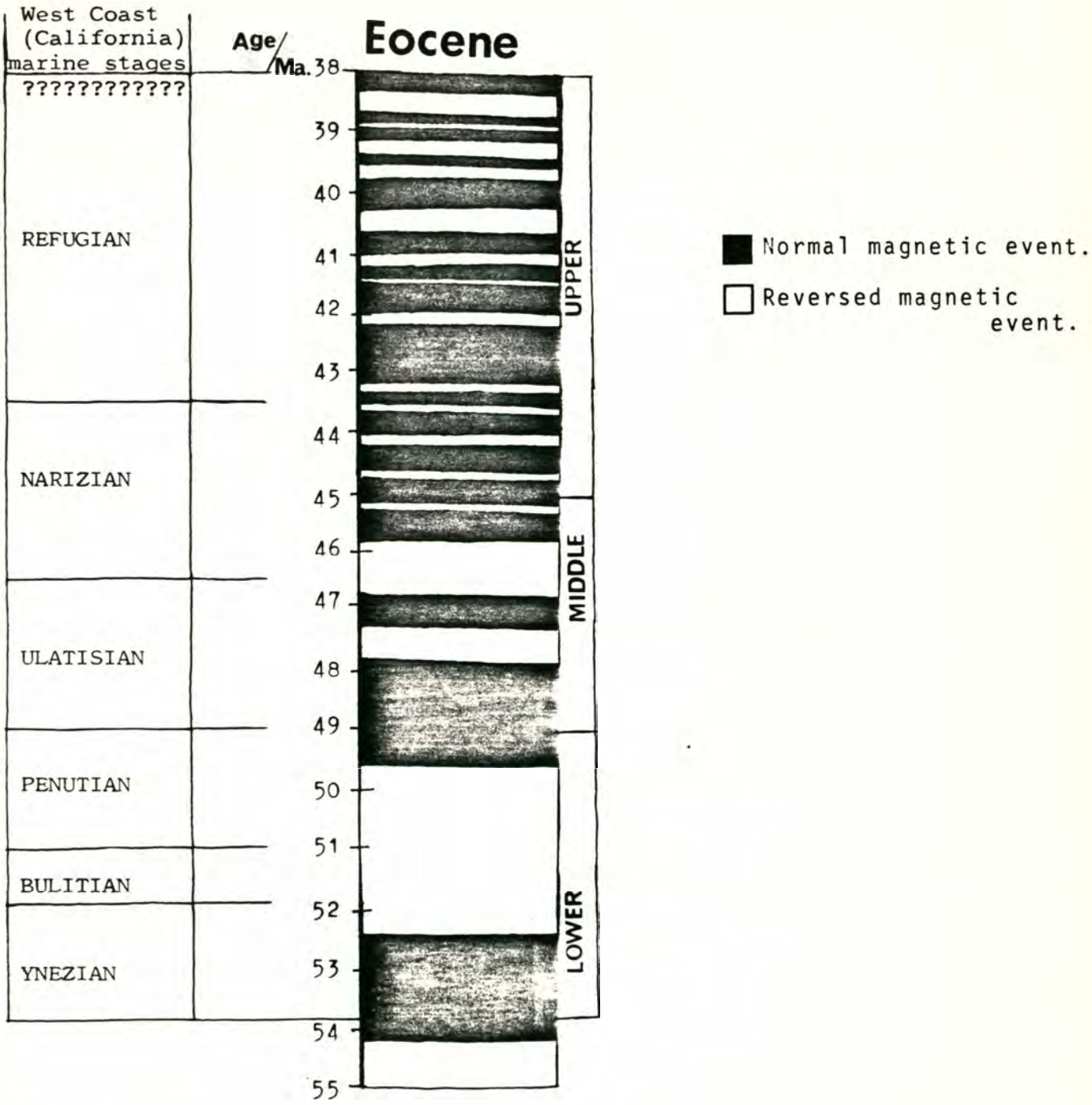

Figure 44: Correlation of absolute ages and magnetic stratigraphy of various stages of the Eocene epoch. Eocene magnetostratigraphy after McElhinny, 1973, p. 169. Absolute ages of Eocene stages after Berggren, 1972, p. 202.

reflects the bias of the earth's field during the time the Crescent basalts were erupted.

Mean paleomagnetic directions, Fisher (1953) statistics, and paleopole positions for cratonic North America and the Black Hills are presented as six separate groups of data in Table 4, along with the varying amounts of clockwise rotation estimated for the study area. The first group is for the expected middle Eocene direction for stable North America (Irving, 1979), calculated for the latitude and longitude of the central part of the Black Hills area (47^{o}N, 123.13^{o}W). The middle Eocene paleomagnetic pole and direction were interpolated from early and late Eocene paleopole positions. The second group pertains to the mean of 37 site NRMs. The third group is for the mean of 35 acceptable Black Hills sites following AF demagnetization but prior to the application of tilt corrections. The fourth and sixth groups correspond to the means of 35 sites following demagnetization and tectonic correction using Methods I and III, respectively, while the fifth group represents the mean of 17 sites after demagnetization and tectonic correction by Method II. Individual site directions for groups four and six are plotted on equal area diagrams (Figs. 45 and 46, respectively). Note that k increases from 18.7 (third group) to 22.9 (sixth group) after all sites have been tilt-corrected. However, the sites do not pass the fold test of Graham (1949), since the ratio of $k_{\text{group 3}} / k_{\text{group 6}}$ (1.22) is less than the value of f (1.37) at which the two groups are significantly different at the 95% confidence level. The similarity of the two groups indicates that correcting all of the sites for recognizable and inferred tilt improves the precision of the

Table 4: Mean directions, paleopole positions, and degrees of clockwise rotation for the Black Hills volcanic rocks using different methods of tectonic correction.

DESCRIPTION	N	$\bar{D}$	$\bar{I}$	kappa	$\alpha 95$	PLONG.	PLAT.	ROTATION (clockwise)
1. Middle Eocene (45 Ma.) pole position for stable North America*	29	$350.4^{\circ} \pm 7.74^{\circ}$	$68.68^{\circ} \pm 3.5^{\circ}$	60	5.0°	170.5°E	82.0°N	- - - - - - -
2. Black Hills rocks: no tilt correction, no demagnetization	37	$25.68^{\circ} \pm 23.0^{\circ}$	$68.89^{\circ} \pm 8.1^{\circ}$	8.08	8.1°	60.35°W	72.65°N	$35.28^{\circ} \pm 24.3^{\circ}$
3. Black Hills rocks: following A-F demagnetization; no tilt correction	35	$32.11^{\circ} \pm 11.9^{\circ}$	$62.45^{\circ} \pm 5.47^{\circ}$	18.71	5.47°	36.68°W	67.38°N	$39.01^{\circ} \pm 14.2^{\circ}$
4. Black Hills rocks: demagnetized; tilt-corrected according to Method I.	35	$25.31^{\circ} \pm 12.57^{\circ}$	$66.39^{\circ} \pm 5.0^{\circ}$	22.35	5.0°	48.55°W	73.02°N	$34.9^{\circ} \pm 14.76^{\circ}$
5. Black Hills rocks: demagnetized; tilt-corrected according to Method II.	17	$18.75^{\circ} \pm 18.84^{\circ}$	$66.73^{\circ} \pm 7.33^{\circ}$	21.45	7.33°	50.34°W	77.32°N	$28.35^{\circ} \pm 20.37^{\circ}$
6. Black Hills rocks: demagnetized; tilt-corrected according to Method III	35	$16.28^{\circ} \pm 12.9^{\circ}$	$67.3^{\circ} \pm 4.94^{\circ}$	22.9	4.94°	54.98°W	78.81°N	$25.88^{\circ} \pm 15.04^{\circ}$

N - the number of sites used in calculating mean directions and paleopoles

$\bar{D}$ - mean declination, measured from true north

$\bar{I}$ - mean inclination, positive downwards

kappa - precision parameter (Fisher, 1953)

$\alpha 95$ - radius of the circle of 95 percent confidence

ROTATION - easterly discordance of the mean Black Hills direction from the expected middle Eocene direction for cratonic North America

*Middle Eocene pole position interpolated from early and late Eocene pole positions of Irving (1979, p. 671).

TILT-CORRECTION:

Method I- Tectonic corrections are made on 17 sites where the attitudes of sedimentary interbeds, overlying clastic units, or horizontal cross-joints in basalt flows are reasonably well known. An additional 18 sites are included in this group for which no structural information is available. These latter sites have not been tectonically corrected.

Method II- Tectonic corrections are applied to the 17 "attitudes known" sites, and only these sites are used in calculating the mean direction of the Black Hills.

Method III- Tectonic corrections are made on the 17 "attitudes known" sites. The remaining 18 sites have been arbitrarily corrected for tilt using the mean Black Hills attitude determined from 52 poles to bedding and cross-joints; the mean attitude is $N7^{\circ}E$ 7.5° W. These 18 "attitudes inferred" sites have been combined with the 17 "attitudes known" sites in calculating the mean direction of the Black Hills.

BLACK HILLS LOCATION:
47.0°N, 123.13°W

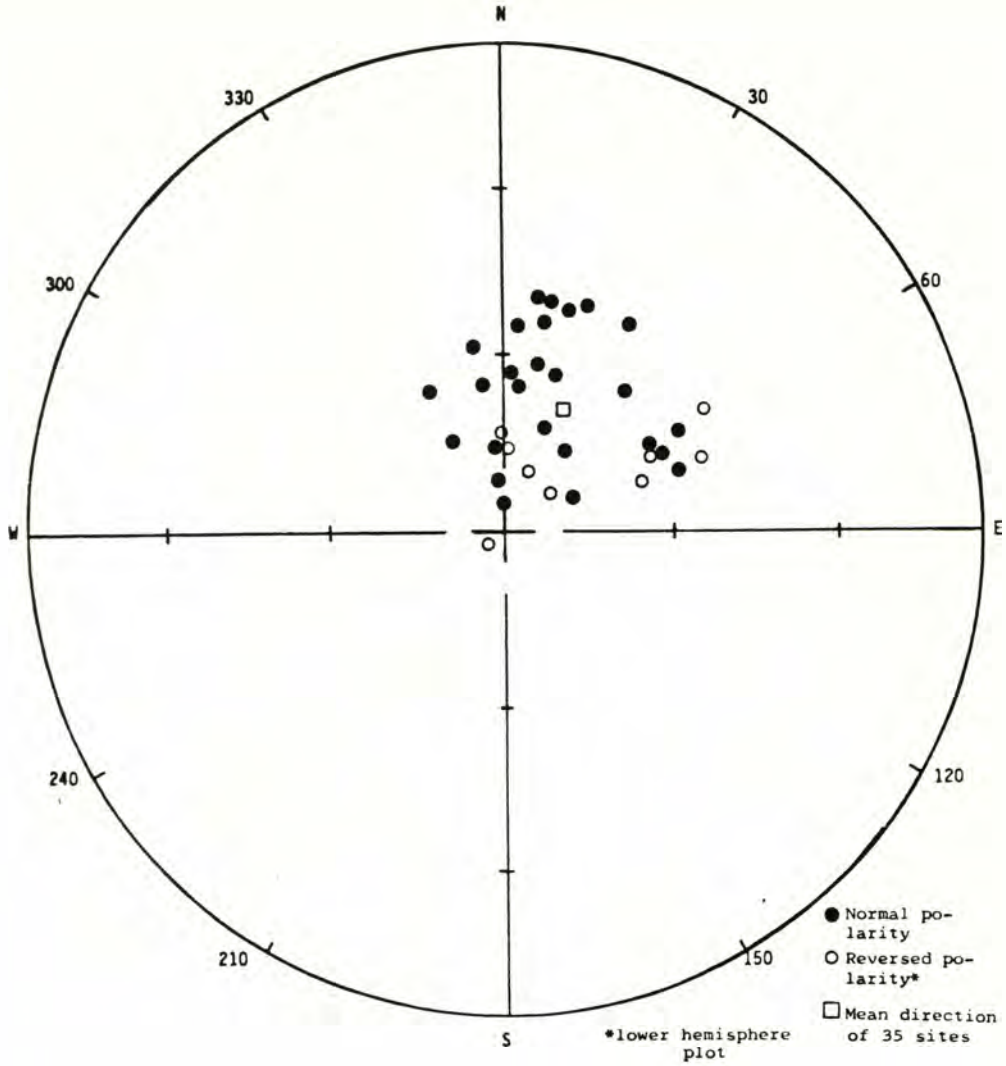

Figure 45: Equal area plot of 35 Black Hills sites after demagnetization, and tectonic correction on 17 sites with known attitudes, using Method I. The mean direction is:

Dec.= 25.3°
Inc.= 66.4°
kappa= 22.4
α_{95}= 5.0°

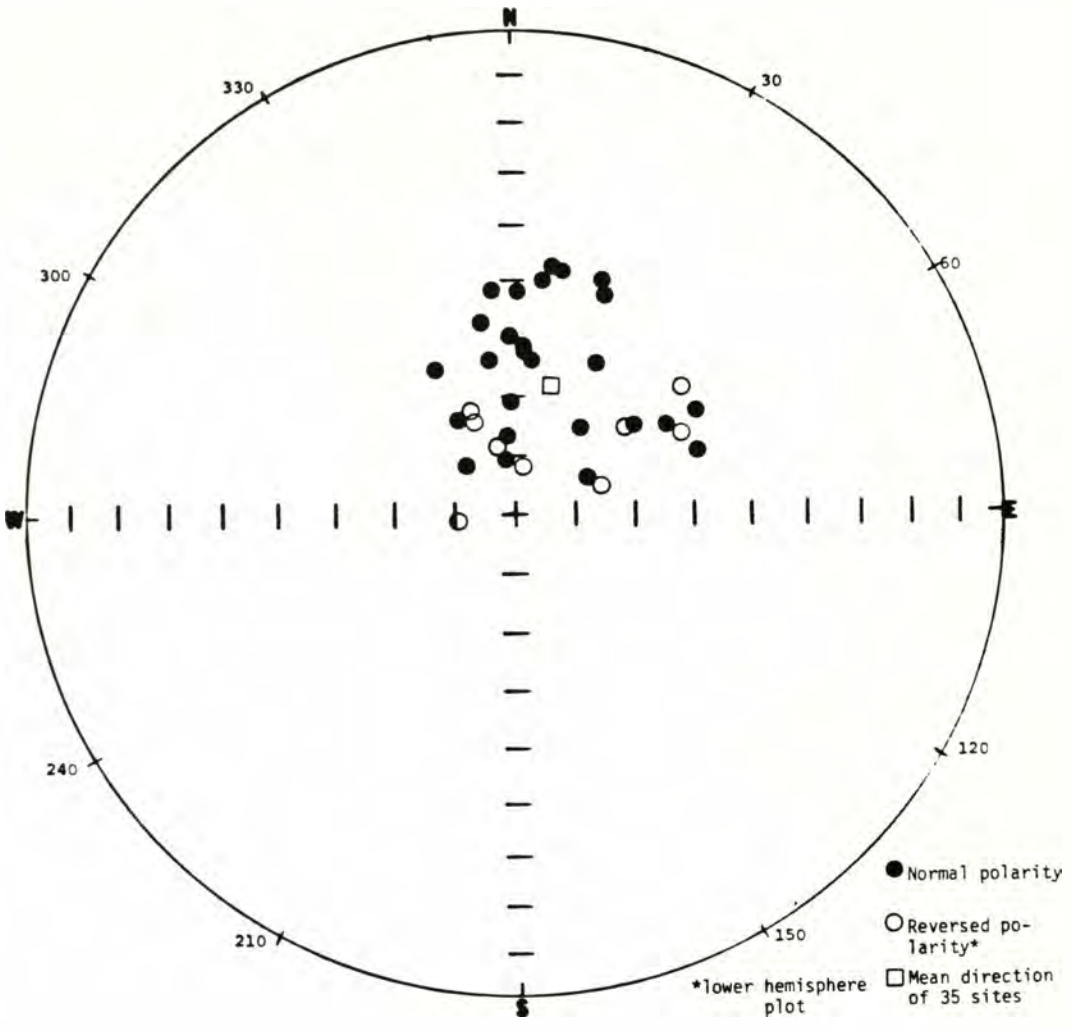

Figure 46: Equal area plot of 35 Black Hills sites after demagnetization, and tectonic correction on 17 sites with known attitudes plus 18 sites with inferred attitudes, using Method III. The mean direction is:

Dec.= 16.3°
Inc.= 67.3°
kappa= 22.9°
α_{95}= 4.9°

data only slightly. I conclude that tectonic deformation of the Black Hills area was minor, and had an insignificant effect on the remanent magnetizations of the Crescent volcanic flows.

The observed mean Black Hills direction may be compared with the expected middle Eocene direction for stable North America to test for discordances in declination and/or inclination of remanent magnetization. Any discordance would be significant tectonically if secular variation of the earth's magnetic field has been sufficiently averaged out, and local tilting of the sampling sites has been corrected for. I have already discussed how the latter requirement is probably satisfied by the third method of tectonic correction. It is less certain whether secular variation has been completely averaged out. The slight overlap of the circles of 95% confidence around the mean directions of the normal- and reversed-polarity groups (the latter plotted in the lower hemisphere),following tectonic correction by Method III, would suggest that the two groups are approximately antipolar (Fig. 47), and that the effects of secular variation are probably insignificant. Despite this overlap, the two groups are not similar at the 95% confidence level, according to an f-test. Therefore there is no statistical evidence that secular variation has been completely averaged out. This may be attributable to inadequate sampling of the reversed polarity interval(s), since the reversely-magnetized group consists of only nine sites, all of which occur at approximately the same elevation in the lowlands (Sheet 1). One of these reversed sites (10.28.78.1) appears to be anomalous (Fig. 43): the antipole of its magnetic direction following tilt correction ($D= 265^{o}$, $I= 80^{o}$) is westerly-discordant with respect to the other

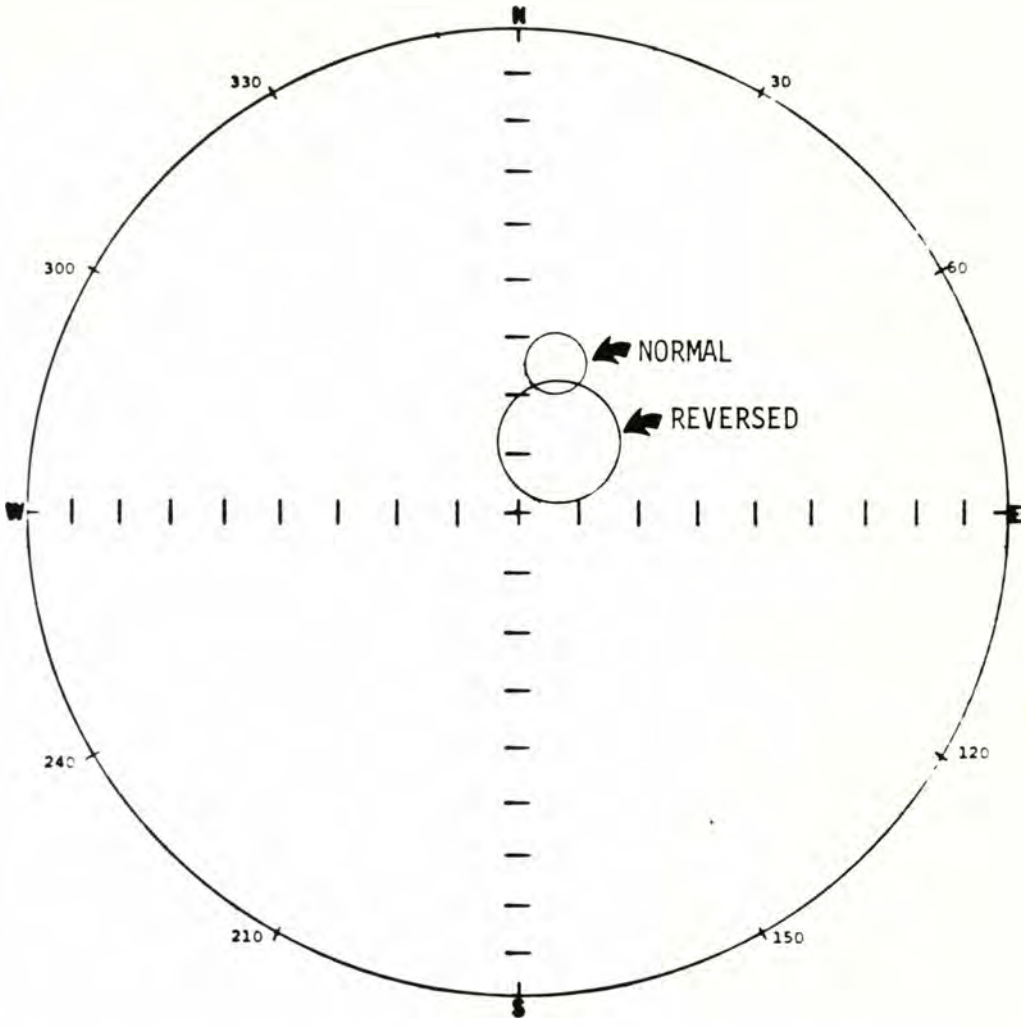

Figure 47: Equal area plot of mean directions and 95 percent circles of confidence for normally- and reversely-magnetized Black Hills volcanic rocks following tectonic correction of all 35 sites, using Method III. The mean direction of the normal polarity group is Dec.= 13.6^{o}, Inc.= 64.2^{o}, $\alpha 95 = 5.5^{o}$ (26 sites). The antipole of the mean direction of the reversed polarity group is Dec.= 30.1^{o}, Inc.= 75.8^{o}, $\alpha 95 = 9.6^{o}$ (9 sites), and is plotted in the lower hemisphere.

reversed sites by at least 70° (Fig. 47). An excursion of the earth's magnetic field, orientation error, or unrecognized deformation of the outcrop may be responsible for this single aberrant direction. If site 10.28.78.1 is eliminated from the Black Hills population, then the normal- and reversed-polarity groups are statistically similar and antipolar. However, since α_{95} of site 10.28.78.1 (14.3°) is below the maximum cut-off value of 15°, and its mean direction is within two angular standard deviations of the mean Black Hills direction, there are no statistical or geological grounds for eliminating it. I suggest that the apparently incomplete averaging out of secular variation is probably attributable to one reversely-magnetized site, whose anomalous direction strongly influences the mean direction of the reversed polarity group (which comprises only nine sites).

Any latitudinal shift of the Black Hills area would be recognized by a flattening or steepening of the observed inclination relative to the expected middle Eocene inclination for stable North America. According to Table 4, the expected inclination is 68.7° ± 3.5°, while the observed mean inclination of 35 Black Hills sites, following demagnetization and tectonic correction by Methods I, II, and III, is 66.4° ±5°, 66.7° ±7.3°, and 67.3° ±4.9°, respectively. Since these inclinations are not significantly different at the 95% confidence level, any large latitudinal shift of the Black Hills relative to the North American craton may be effectively ruled out.

Rotation of the Black Hills about a vertical axis would result in its observed declination being different from the expected middle Eocene declination. According to Table 4, the expected declination

is $350.4^{o} \pm 7.7^{o}$. If no tilt corrections are made, the mean Black Hills declination is $32.1^{o} \pm 11.9^{o}$. Tectonic correction results in a mean declination of $25.3^{o} \pm 12.6^{o}$ using Method I, $18.8^{o} \pm 18.4^{o}$ using Method II, and $16.3^{o} \pm 12.9^{o}$ using Method III. These declinations are easterly-discordant with respect to the expected declination by $39.0^{o} \pm 14.2^{o}$, $34.9^{o} \pm 14.8^{o}$, $28.4^{o} \pm 20.4^{o}$, and $25.9^{o} \pm 15^{o}$, respectively. Since Method III is the preferred one for tilt-correcting the sites, the paleomagnetic data suggest that the Black Hills area has undergone $25.9^{o} \pm 15^{o}$ of clockwise rotation with respect to cratonic North America since middle Eocene time (Fig. 48).

DISCUSSION

The suggested rotation of the Black Hills basalts may be compared with paleomagnetic results from other Eocene rocks in western Oregon and Washington, and southern British Columbia. In coastal Oregon, the early to middle Eocene Siletz River Volcanics, Tyee-Flournoy sediments, and Yachats Basalt have undergone between 55 and 76 degrees of clockwise rotation (Simpson and Cox, 1977), whereas the Eocene Tillamook Volcanic Series points 46^{o} clockwise from the expected Eocene field direction (Magill et al., 1980, in press). Oligocene dikes and sills of coastal Oregon are rotated clockwise by between 44^{o} (Beck and Plumley, 1980) and 27^{o} (Clark, 1969).

In order to determine if two separate sampling regions (A and B) of similar age have undergone significant differential rotation (R), the following equation is used:

$$ {}_{A}R_{B} = R_{A} - R_{B}, \qquad \Delta {}_{A}R_{B} = (\Delta R_{A}^{2} + \Delta R_{B}^{2})^{\frac{1}{2}} $$

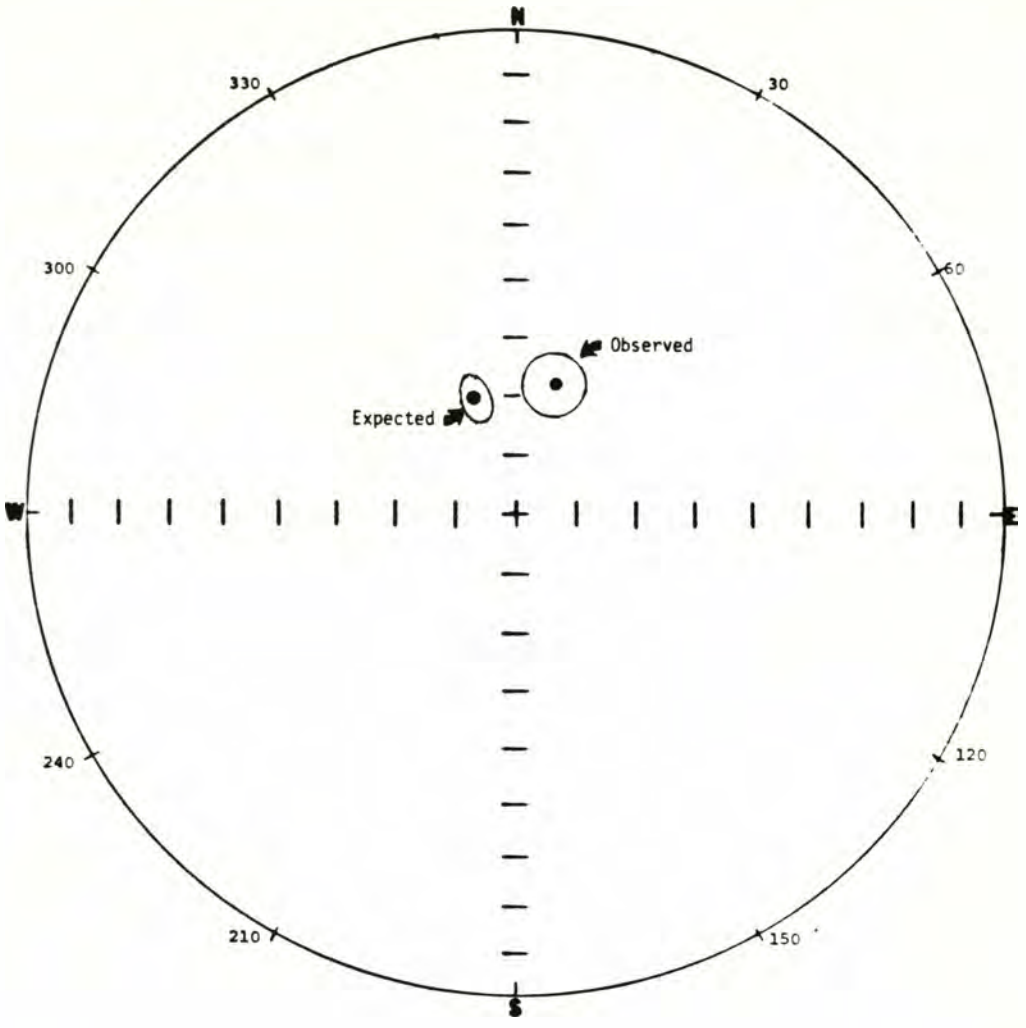

Figure 48: Equal area plot of expected middle Eocene direction for cratonic North America (Dec.= 350.4°, Inc.= 68.7°, α95= 5.0°), and observed direction of Black Hills volcanic rocks after tectonic correction using Method III (Dec.= 16.3°, Inc.= 67.3°, α95= 4.9°). The discordance between the expected and observed directions is 25.9° ± 15.0°.

A value of ${}_{A}R_{B} > \Delta_{A}R_{B}$ would indicate that the two sampling regions underwent differential rotation. Applying this equation to the rotations inferred for the Siletz River Volcanics ($R = 76.8^{\circ}$, $\Delta R = 15.7^{\circ}$ - Simpson and Cox, 1977) and the Black Hills basalts yields the result ${}_{S}R_{BH} = 50.9^{\circ} \pm 21.7^{\circ}$, indicating that the larger amount of rotation of the coeval Siletz River unit is significant at the 95% confidence level. The clockwise rotation of the middle Eocene Tyee-Flournoy sediments ($R = 69.7^{\circ}$, $\Delta R = 17.2^{\circ}$ - Simpson and Cox, 1977) is also significantly greater than that of the Black Hills basalts by the angle $43.8^{\circ} \pm 22.8^{\circ}$. Differential clockwise rotation is also indicated for the middle Eocene Tillamook Volcanic Series of northwestern coastal Oregon ($R = 46.4^{\circ}$, $\Delta R = 12.7^{\circ}$ - Magill et al., 1980, in press) and the Black Hills basalts, although the angle $20.5^{\circ} \pm 19.7^{\circ}$ is just barely significant.

It is concluded that the Black Hills basalts of the Washington Coast Range underwent less rotation than rocks of similar age in the Oregon Coast Range, although all of these rotations are clockwise. Further evidence for differential rotation between the Oregon and Washington coastal blocks is provided by Wells and Coe (1979), who report that the mid-Eocene "oceanic" basement of southwestern Washington has undergone much less clockwise rotation than the Oregon Coast Range basement.

The differential rotations of the Oregon-Washington coastal blocks are readily apparent in Figure 49, as is the nearly ubiquitous clockwise sense of rotation in the Coast Range and Cascades. The only exception to this pattern is the Oligocene East Sooke Gabbro of southern Vancouver Island, which intrudes tilted rocks of late Eocene age, is overlain by undeformed late Eocene rocks, and has apparently

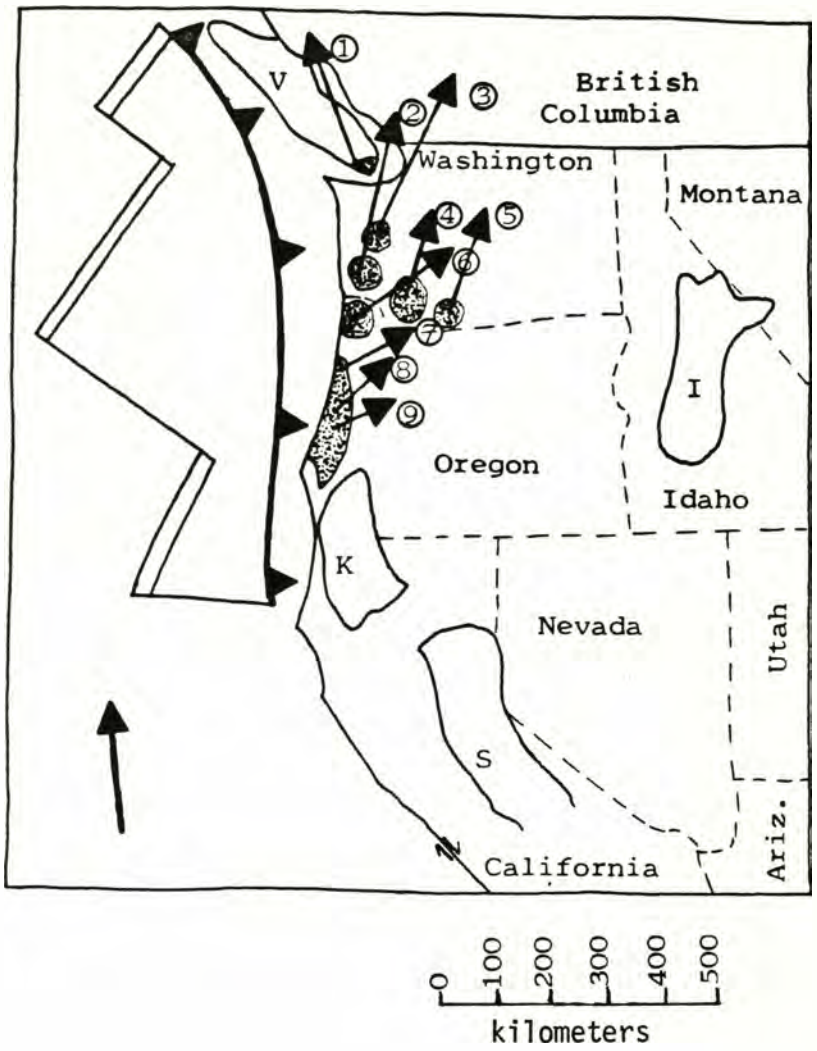

Figure 49: Tectonic setting of the Siletz River Volcanics, Yachats Basalt, Tyee-Flournoy sediments, and Tillamook Volcanic Series of western Oregon; Ohanapecosh Formation, Goble volcanics, and Crescent Formation lavas in the Willapa and Black Hills of western Washington; and Metchosin Volcanics of southern Vancouver Island. Stippled pattern indicates paleomagnetic study areas. Small arrows show present declinations of remanent magnetizations observed at these areas. Circled numbers to the right of the arrowheads identify the study areas: 1= Metchosin Volcanics (Symons, 1973); 2= Willapa Hills (Wells and Coe, 1979); 3= Globerman and Beck, this study; 4= Goble volcanics (Beck and Burr, 1979); 5= Ohanapecosh Formation (Bates, 1980); 6= Tillamook Volcanic Series (Magill et al., 1980, in press); 7= Siletz River Volcanics, 8= Yachats Basalt, and 9= Tyee-Flournoy sediments (Simpson and Cox, 1977). Large arrow denotes expected Eocene direction for the North American craton. I= Idaho batholith, K= Klamath Mountains, S= Sierra Nevada batholith, V= Vancouver Island.

rotated about 20° counterclockwise (Symons, 1973). However, Beck (1976) suggests that the westward deflection of declination would be eliminated if tilt corrections are applied, since Symons assumed that deformation pre-dated intrusion of the gabbro, and did not correct the unit for tilt. Unless additional paleomagnetic studies in southern Vancouver Island confirm Symons' (1973) interpretation of the East Sooke Gabbro, it is more reasonable to conclude that all significant rotations of Tertiary rocks in the Coast Range and western Cascades are in the clockwise sense.

The rotations of coastal Oregon and Washington, while uniform in direction, differ significantly in amount, suggesting that the entire Coast Range block, from the Olympic Peninsula to north of the Klamath Mountains, has not been a coherent terrane since middle Eocene time. Figure 50 shows that the Black Hills, Ohanapecosh Formation, and Goble volcanics of southwest Washington are considerably less rotated than the Siletz River Volcanics, Tyee - Flournoy sedimentary units, and Yachats Basalt of coastal Oregon. Plumley and Beck (1977) propose a constant rotation rate for the Oregon Coast Range for the interval between 50 and 30 m.y. b.p., although it is uncertain whether rotation continued at this rate through Miocene time (Beck and Plumley, 1980). Magill and others (1980, in press) favor rotation of coastal Oregon in two discrete steps with different rates.

A tectonic model which is more consistent with available paleomagnetic data involves accretion and independent clockwise rotation of two or more Coast Range terranes, or "microplates", in response to oblique subduction of the Farallon plate beneath North America during Early and Middle Cenozoic time (Beck et al., 1979). This in-

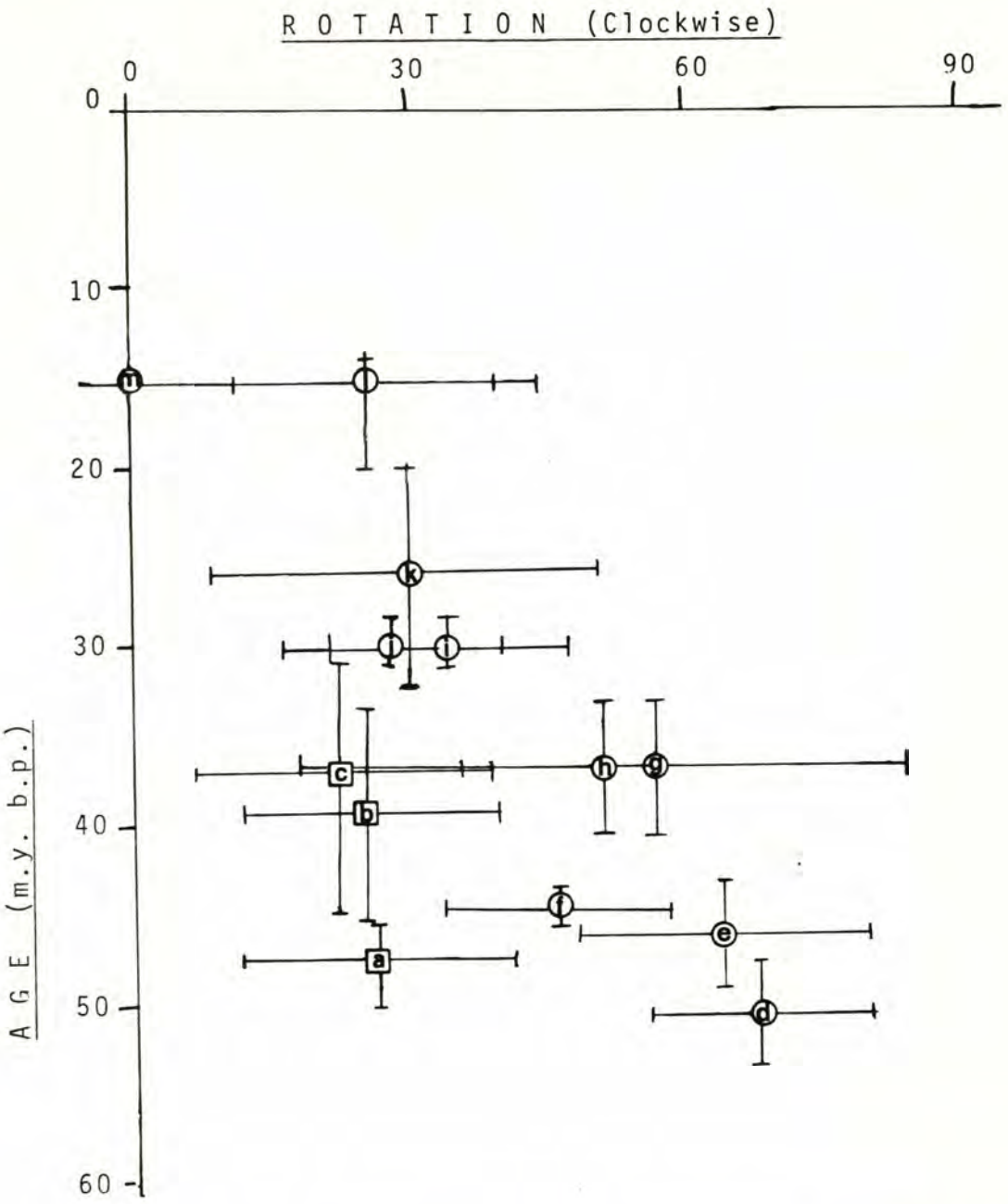

Figure 50: Rotation versus age for volcanic and sedimentary rocks in western Washington and Oregon. Horizontal bars are uncertainties in rotation, while vertical bars represent errors in age determinations. Letters in boxes correspond to Washington study areas: a- Black Hills (Globerman, this study); b- Goble volcanics (Beck and Burr, 1979); c- Ohanapecosh Formation (Bates et al., 1979). Circles letters are Oregon study areas: d and e- Siletz River Volcanics and Tyee-Flournoy sediments, respectively (Simpson and Cox, 1977); f- Tillamook Volcanic Series (Magill et al., 1980, in press); g- Yachats Basalt (Simpson and Cox, 1977); h and i- Oligocene sills (Plumely, 1980); j- Mary's Peak sills (Clark, 1969); k- Cascade volcanics (J. Magill, 1979, oral comm.); l and m- Miocene basalt (Plumley, 1980).

terpretation requires a reevaluation of current models for the emplacement and rotation of the Coast Range. For example, Hammond's (1979) model of the Tertiary rotation of the Coast Range about a pivot near the northern end of the Olympic Peninsula (Fig. 51) treats the block as a coherent unit as far south as the Klamath Mountains. Similarly, Model 2 of Simpson and Cox (1977) envisages the Coast Range as a northwest trending aseismic ridge that clogged a parallel early Tertiary subduction zone, causing it to step outboard and initiating the rotation of the block about a pivot near the Olympic Peninsula (Fig. 52). Both models involve early Tertiary rifting of the Klamath Mountains from the Sierra Nevada province, although Schweickert (1976), Irwin (1977), and Blake and Jones (1977) suggest that rifting occurred during Late Mesozoic time. In addition, the late Eocene Clarno Formation of central Oregon shows only $17^{o} \pm 13^{o}$ of clockwise rotation (M. E. Beck, Jr., 1980, oral comm.), which is considerably less than the 50 to 70 degree rotations described in coastal Oregon (Simpson and Cox, 1977). A serious problem with both models is that the Coast Range must somehow slide past the relatively stationary Clarno block during its rotation about a pivot in the Olympic Peninsula. Alternatively, all of the Coast Range rotation could have been accomplished before the late Eocene eruption of the Clarno Formation, although the clockwise rotation of Oligocene sills in coastal Oregon (Plumley, 1980) is inconsistent with this hypothesis.

Model 1 of Simpson and Cox (1977) attempts to avoid these problems by rotating the coastal block trenchward (clockwise) about a pivot point near the Klamath Mountains at its southern end (Fig. 52). If the block is coherent as far north as the Olympic Peninsula, then the

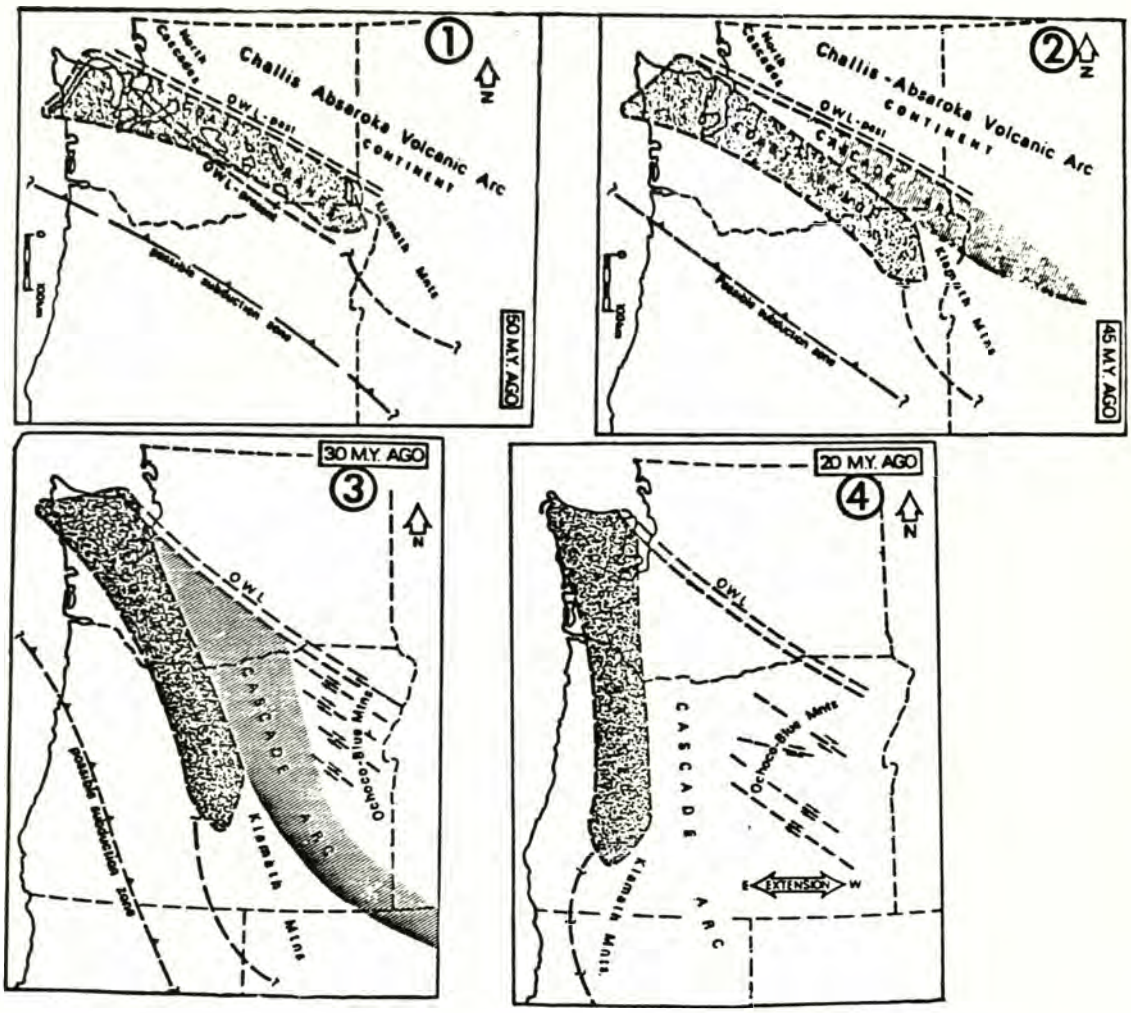

Figure 51: Idealized paleogeographic reconstruction of the Pacific Northwest from 50 through 20 m.y. b.p., showing rotation of the Cascade arc and the Oregon-Washington Coast Range. The Challis - Absaroka volcanic arc formed inboard of a presumed northwest-trending subduction zone during early Eocene time. After Hammond, 1979.

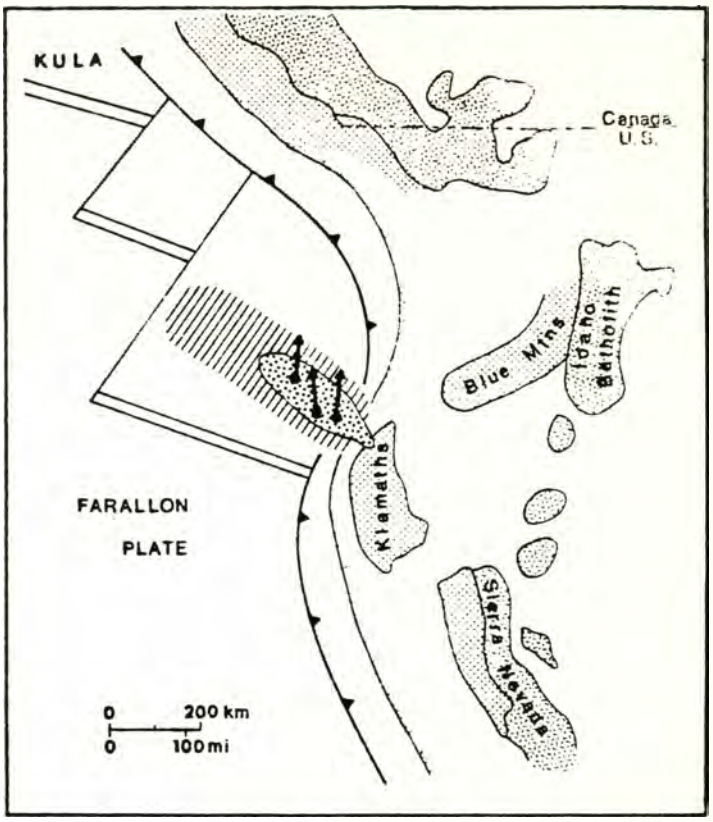

MODEL 1- The coastal block initially extended northwest into the Pacific from the Klamaths, then rotated clockwise about a pivot near its southern end toward an early Tertiary subduction zone. A similar rotation of younger microplates is suggested by the fanning of magnetic stripes off the coast of Oregon.

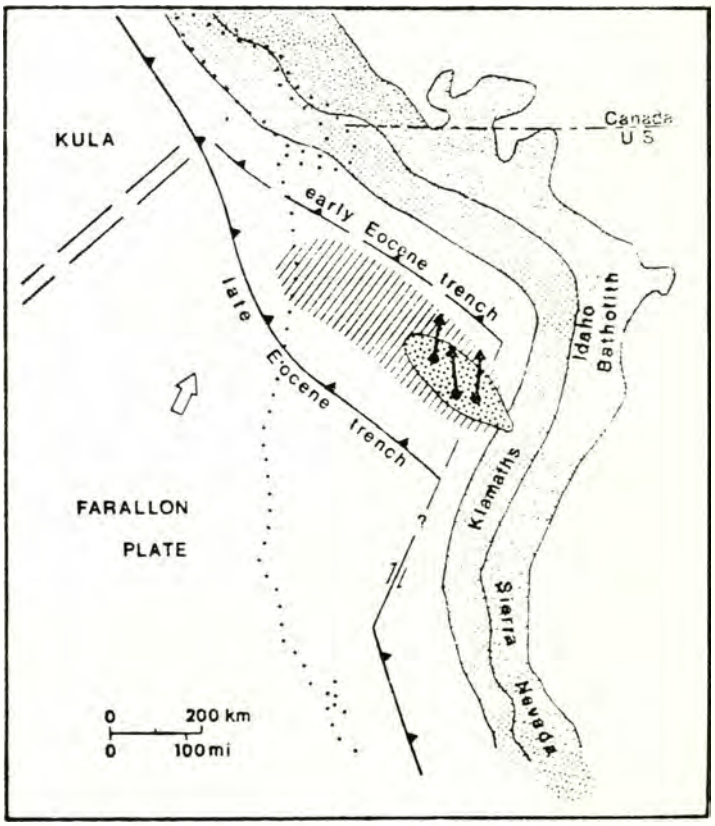

MODEL 2- The block is an oceanic aseismic ridge which clogged a northwest-trending early Tertiary subduction zone located to the east of the present coastline. The trench jumped southwest in the middle Eocene isolating the present coastal block which then began to rotate westward with the Klamath Mountains attached to the southern end, about a pivot near the Olympic Peninsula at its northern end.

Figure 52: Models 1 and 2 of Simpson and Cox (1977), illustrating emplacement and rotation of the Coast Range block during Eocene time.

northern end could not have been adjacent to the continental margin during eruption of the Crescent Formation. However, since these lavas are intercalated with terrigenous sediments and locally contain large quartz diorite clasts (Cady, 1975), it is more probable that the northern end of the Coast Range was proximal to the continental margin as the basalts were extruded. In addition, two major submarine fan systems of the late Eocene Lyre Formation (Ansfield, 1972) are exposed in the northern Olympic Peninsula. Paleocurrent, paleoslope, and provenance studies indicate that the source region for the igneous and metasedimentary clasts was probably central Vancouver Island, immediately to the north (Ansfield, 1972). The Makah Formation, a late Eocene to Oligocene submarine fan complex in the northwestern Olympic Peninsula, also appears to have been derived from a Vancouver Island source area (Snavely et al., 1979). These geologic relationships make Simpson and Cox's (1977) Model 1 less plausible.

Simpson (1977) speculates that if the Coast Range was not a coherent terrane during its rotation, then the complications inherent in Models 1 and 2 could be avoided. If the block is separated somewhere to the south of the Olympic Peninsula, then the southern (Oregon) Coast Range could rotate about a Klamath pivot, while the northern (Washington) Coast Range could rotate about a pivot in the northern Olympic Peninsula. My paleomagnetic data provide strong confirmation of this interpretation, although it remains possible that the Coast Range comprises more than two "microplates".

The precise location of the boundary between the Oregon and Washington coastal blocks is problematical. Since the Tillamook Highlands of northwestern Oregon are rotated 46^{o} clockwise (Magill et al.,

1980, in press), whereas slightly older volcanic rocks in the Willapa Hills of southwestern Washington show considerably less rotation (Wells and Coe, 1979), it is likely that the Coast Range is separated between these two areas. Burr (1978) proposes that this break occurs near the Columbia River, and may be recognized by offsets in gravity anomalies produced by the northwest trending Portland Hills fault zone. The presence of this structure is indicated by LANDSAT and SLAR photolinears in Washington and Oregon, field and structural mapping, geochemical and stratigraphic correlations, and microseismic monitoring (Jones, 1977), although gravity studies by Bromery and Snavely (1964) show no evidence of a major fault trending northwest from Portland to the mouth of the Columbia River. According to Jones (1977), the predominant motion on the Portland Hills fault is dextral strike-slip, with as much as 20 km of movement since late Eocene time. Schmela and Palmer (1972) extend the Portland Hills fault southward through the Clackamas River alignment to the Brothers fault zone, which trends southeastward across Oregon to Steens Mountain.

In summary, this study provides additional evidence for segmentation of the Coast Range into two or more smaller blocks which have had independent rotational histories, although none show significant northward translation. The blocks are broadly coeval, stratigraphically similar, and display identical petrochemical trends, indicating that they are not exotic relative to each other. Segmentation of the Coast Range most probably occurred during or subsequent to its accretion to western North America, and may have been accomplished by one of several possible mechanisms. For example, Menard (1978) suggests that since early Tertiary time the Farallon plate has been complexly frag-

mented by the formation of ridge-trench transforms, paired ridges, leaky transforms, and transverse spreading centers, as well as by ridge jumps and ridge and fracture zone reorganizations. These phenomena may reflect pivoting of fragments of the Farallon plate during subduction around points located near the ridge-trench-transform triple junctions. Presumably the fragmented coastal blocks underwent differential clockwise rotation in response to pivoting subduction of the Farallon plate. This model does not satisfactorily explain the observed rotations of the Oregon and Washington Cascades (e.g. Burr, 1978; Beck and Burr, 1979; Bates, 1980), which were associated with the North American plate, rather than the Farallon plate.

A second possibility, informally termed the "ball-bearing model", involves rotation of rigid crustal fragments which are caught in a broad right-lateral shear zone (Fig. 53). These fragments, which may be visualized as ball bearings (or more accurately, roller bearings), rotate clockwise and translate northwestward as independent units in a broad zone of distributed dextral shear. The model was first proposed by Teissere and Beck (1973) to explain the rotation of the southern California batholith, and was further expounded by Beck (1976) in interpreting the differential clockwise rotations found throughout the western Cordillera (Beck et al., 1977). According to Atwater (1970), much of the westernmost Cordillera during Tertiary time was a "broad transform fault zone", implying that the continental margin behaved as a zone of simple shear across which relative (oblique) motion between the North American and Farallon plates was distributed. Within the zone, the rotating fragments are bounded by northwest trending dextral strike slip faults, and northeast trending sinistral faults.

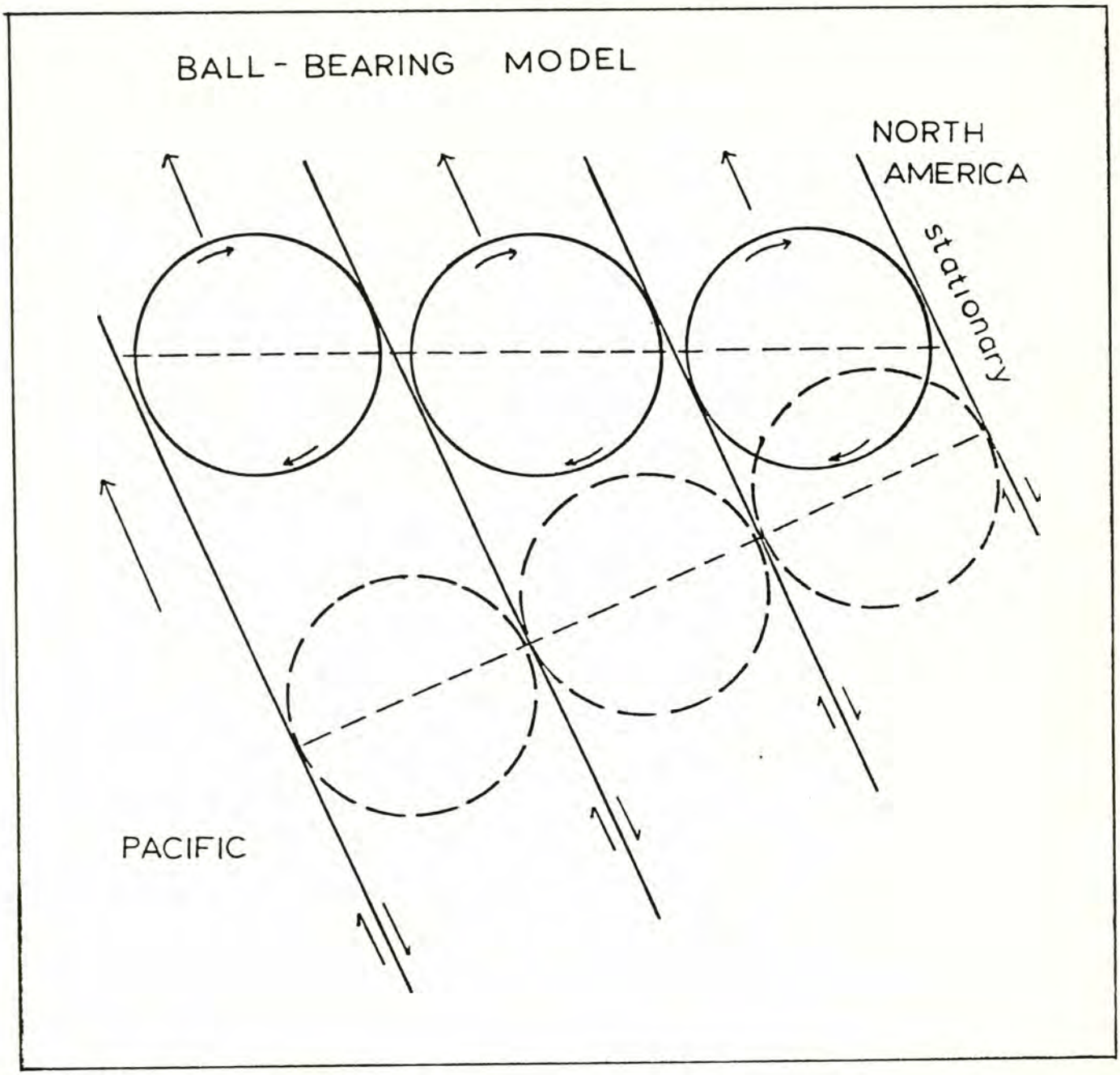

Figure 53:
Ball-bearing method for rotation of continental fragments in a zone of right-lateral shear (Beck, 1976). Circles represent idealized fragments of continental crust which are displaced northwestward and rotated in a clockwise sense. Dashed circles represent initial positions of crustal fragments prior to shearing motion.

Possibly the Portland Hills - Clackamas River fault zone (Schmela and Palmer, 1972), Brothers fault zone (Lawrence, 1976), and Olympic-Wallowa lineament (Raisz, 1945; Skehan, 1965) are examples of these major boundary structures. The northwest trending Olympia lineament and northeast trending Rochester lineament in the Black Hills area (Sheet 1) are consistent with the predicted configuration of faults bounding the rotating crustal blocks, although nothing is known about the sense of displacement, if any, along these particular structures.

Paleomagnetic studies of crustal blocks within right-lateral shear zones support a roller bearing interpretation of the tectonics of the Coast Range. For example, Greenhaus and Cox (1978) report varying amounts of clockwise rotation for upper Oligocene intrusive rocks in central coastal California, and suggest that right-lateral shearing applied to extensionally loosened crustal fragments within a pull-apart basin may best explain the differential rotations. Kamerling and Luyendyk (1979) report up to 80^{o} of clockwise rotation for Miocene igneous rocks on Anacapa, Santa Cruz, San Miguel, and Catalina Islands in southern California. These rotations are also ascribed to distributed right-lateral shear within the Pacific - North American plate boundary zone.

Beck (1976) does not specify the maximum width of the zone of distributed shear, although there is no reason to assume that it is confined to the continental margin. Rotations in the Oregon and Washington Cascades, opening of the Chiwaukum graben in north-central Washington beginning about 46 m.y. b.p. (Gresens, 1979), and occurrences of bimodal extensional volcanism (e.g. Teanaway dike swarms) in

the eastern Cascades of Washington during Eocene time (Vance, 1979) are indications that the shear zone extended considerably inland. However, the absence of significant clockwise rotation in the Republic graben of northeastern Washington (Schwimmer et al., 1979) appears to limit how far into the Cordilleran interior the stress regime extended.

A third possibility involves development of a right lateral strike-slip fault inboard of an active trench along which oblique subduction is occurring. According to Fitch (1972), recent crustal movements in the western Sunda arc region provide convincing evidence for the coexistence of oblique convergence, active volcanism, and transcurrent faulting on the continental side of a zone of plate consumption. Beck and Plumley (1977, personal comm., cited in Burr, 1978) have expanded this model to explain clockwise rotation of roughly equant crustal blocks caught in the shear zone between the trench and the transcurrent fault (Fig. 54). The revised model predicts that elongate blocks will primarily translate northward within the shear zone, while equant blocks will both translate northward and rotate clockwise in a manner similar to roller bearings if relative convergence is northeast directed, and transcurrent faulting is right lateral. According to Fitch (1972), the development of a strike slip fault along the axis of a volcanic arc is easily achieved, since the axial zone is extensionally weakened and would likely be weak in horizontal shear as well. The only evidence of large scale Tertiary dextral movement in the Cascades is the Straight Creek fault (Misch, 1966), although this structure is terminated near Kachess Lake (about 85 km southeast of Seattle) by the Miocene Snoqualmie batholith (Tabor and Frizzell, 1979). However, Weaver and others (1980) report that earthquake focal mechanisms

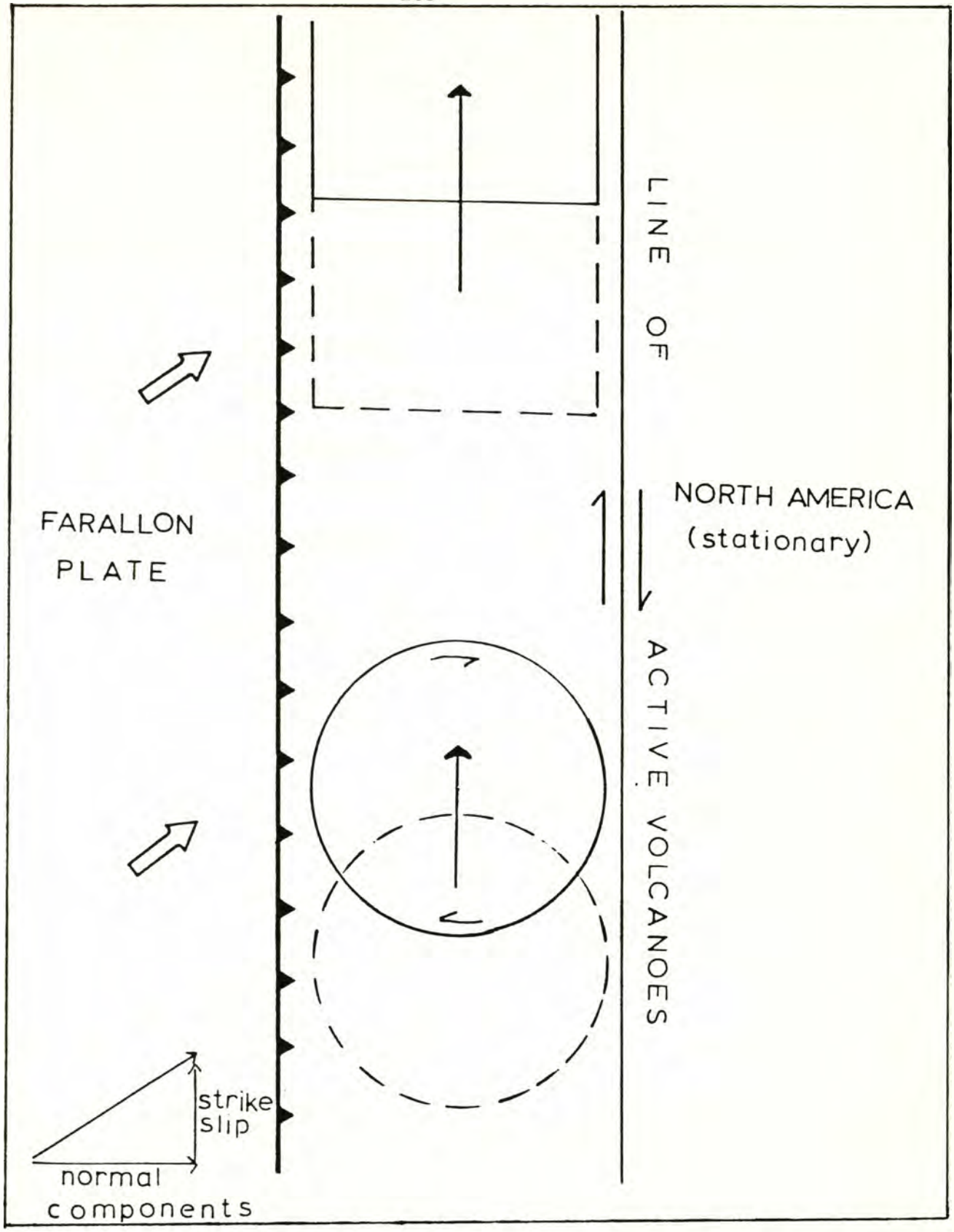

Figure 54: Fitch Model.
Development of dextral strike-slip fault inboard of an active trench along which oblique subduction is occurring (Fitch, 1972). The model illustrates the predicted kinematics of crustal blocks caught between the trench and the transcurrent fault: northward translation only for elongate blocks, while equant blocks both rotate clockwise and translate northward. The zone of transucrrent faulting may follow the line of active volcanoes, since this is a zone of crustal weakness. After Burr, 1978.

associated with the 1980 Mount Saint Helens eruptive sequence suggest right lateral strike slip faulting on northwest-striking planes. It is possible that further detailed monitoring of seismic activity in connection with volcanic hazards assessment in Washington and Oregon will reveal a more complicated tectonic pattern in the western Cascades.

A fourth interpretation of discordant clockwise rotations in the Coast Range combines accretion of thick fragments of oceanic volcanic piles by plate convergence with rotation of the fragments (at the continental margin) about a vertical axis. This model involves the decoupling of island arcs and aseismic ridges from the underlying oceanic crust along a basal décollement zone consisting of hemipelagic and terrigenous siltstones. The detachment occurs when the volcanic pile impinges upon a subduction zone, due to the high fluid pressure and ductility in the sedimentary horizon (D. C. Engebretsen and M. E. Beck, Jr., 1979, unpub. manuscript). Evidence in the Marianas area supports the possibility that seamounts are sheared off the downgoing plate without being subducted (Vogt et al., 1976). It is likely that these elongate volcanic piles break into smaller, more equant crustal fragments during accretion. Following detachment and accretion, the crustal blocks undergo rotation, particularly if subduction is markedly oblique. However, rotations well inboard of the trench, such as in the Cascade Range, are not satisfactorily explained by this model.

Obviously, further detailed geologic mapping of suspected "microplates" in the Coast Range is essential in order to elucidate the nature of the structures bounding them, and to place additional constraints on the various interpretations of the origin, accretion, and tectonic relations of the blocks. For example, detailed structural

mapping and paleomagnetic investigation of Eocene basalts in the Willapa Hills of southwestern Washington indicate that the block is divisible into five structurally distinct subunits, some of which give significantly different paleomagnetic directions (Wells and Coe, 1980). The data imply that the Washington Coast Range has not only undergone differential rotation with respect to coastal Oregon, but may be segmented into even smaller crustal fragments that have rotated independently. A critical area for further paleomagnetic study lies between the Willapa and Black Hills, and comprises the Minot Peak, Doty Hills, and Blue Mountain volcanic highlands (Fig. 4). It is essential to ascertain whether these uplifts show rotations similar to that of the Black Hills. If they do not, then the structures which separate them should be identified and their displacement histories carefully investigated. Another key area lies just east of the Black Hills, where late Eocene to early Oligocene basaltic, andesitic, and pyroclastic flows of the Northcraft Formation have been described (Snavely et al., 1951b). These volcanic rocks correlate with the Goble volcanics (Snavely et al., 1958) and were apparently erupted during incipient Cascade arc activity (Burr, 1978). Paleomagnetic study of these volcanic flows, which crop out in close proximity to the Black Hills, would be a further test of Hammond's (1979) model involving clockwise rotation of the active Cascade arc together with the accreted coastal block. Finally, the Olympic Peninsula remains enigmatic in paleomagnetic interpretations because of its greater structural complexity, and the absence of stable remanent magnetizations in basalts of the Crescent Formation. If overlying sedimentary rocks such as the Lincoln Creek Formation prove to be more stably

magnetized, then paleomagnetic study of these strata should be undertaken to further elucidate the tectonics of the northern end of the Coast Range.

V. CONCLUSIONS

1) The Black Hills uplift is a structurally coherent terrane which is bounded by northwest- and northeast-trending lineaments that are presumed to be faults. Within the uplift, middle Eocene (Ulatisian) basalts of the Crescent Formation and overlying late Eocene and Oligocene sedimentary rocks are faulted, but are not appreciably deformed. The uplift is interpreted as a homocline dipping west about 10 to 15 degrees.

2) Major- and trace-element analyses incidate that the Black Hills basalts are comagmatic hypersthene-normative tholeiites that were apparently derived by plagioclase– clinopyroxene– olivine ± magnetite fractionation.

3) The Black Hills suite is petrochemically similar to basalts from the upper member of the Crescent Formation of the Olympic Peninsula, and the upper flows of the lower member of the Siletz River Volcanics of coastal Oregon.

4) Field and petrochemical evidence does not support an island arc origin for the Black Hills basalts. If the basalts are indeed correlative with the upper member of the Crescent Formation of the Olympic Peninsula, then my data are more consistent with a Hawaiian-type oceanic island origin for the upper Crescent, as proposed by Glassley (1974) and Cady (1975), than with an island arc origin, as suggested by Lyttle and Clarke (1975).

5) Seven discrimination plots of mainly incompatible element data for the Black Hills rocks indicate that the suite is most similar

to tholeiites from oceanic island (Hawaiian) and continental (flood basalt) settings. However, the presence of pillow lavas, pillow breccias, and hemipelagic siltstones in the Black Hills suite makes an oceanic island origin more plausible.

6) Despite the overall affinities with oceanic island tholeiites, the Black Hills lavas approach mid-ocean ridge basalt compositions as well. The somewhat intermediate incompatible element composition of the suite (between MORB and OIB) may either reflect its generation by some "hybrid" magmatic process (i.e. mixing of magmas associated with spreading ridges and with mantle plumes), or simply heterogeneities in the mantle source region.

7) The intermediate incompatible element compositions and Sr isotope ratios of the Black Hills basalts resemble those of tholeiites from Iceland, Galapagos, and possibly Easter Island, all of which are oceanic islands that were erupted at, or close to, the ridge crest of an active oceanic spreading center. I suggest that the "hybrid" petrochemistry of the Black Hills basalts, and the widely prevalent association of incompatible-element depleted (MOR-type) tholeiites grading up into incompatible-element enriched (OI-type) tholeiitic lavas and lesser alkalic flows in the Oregon-Washington Coast Range may reflect eruption of the seamount chain on the crest or flanks of an oceanic spreading center.

8) The composition of the erupting lavas probably evolved as the chain moved away from the spreading center axis. This evolution may have resembled the compositional changes shown by several younger oceanic central volcanoes formed at ridge crests. These seamounts

initially erupt depleted tholeiitic lavas resembling MORB in composition, but subsequently produce less depleted transitional tholeiites, alkali basalts, and alkalic differentiated lavas (all typical of oceanic islands) after the seamounts have drifted away from the ridge crest on young oceanic lithosphere. The Coast Range oceanic island chain was subsequently sutured to the leading edge of North America by late Eocene to early Oligocene time (Vance, 1979).

9) Paleomagnetic study of 35 sites in the Black Hills and adjacent areas indicates that most of the lava flows have declinations of remanent magnetizations that are significantly more easterly-directed than expected for cratonic North America, with or without application of tectonic corrections. Using the preferred procedure for tilt-correction (Method III), the mean Black Hills paleomagnetic direction is: D= 16.3^{o}, I= 67.3^{o}, $\alpha 95 = 4.9^{o}$. A rotation of $25.9^{o} \pm 15^{o}$ in the clockwise direction since middle Eocene time is inferred from these data; there is no evidence of north-south translation.

10) The Black Hills basalts show significantly less clockwise rotation than Eocene rocks of the Oregon Coast Range, such as the Siletz River Volcanics, Tyee-Flournoy sediments, and Tillamook Volcanic Series. Data from the Willapa Hills south of the study area confirm the differential rotation between the Oregon and Washington coastal blocks (Wells and Coe, 1979).

11) It is suggested that the entire Coast Range block, extending from the Olympic Peninsula to north of the Klamath Mountains, has not been a coherent terrane since middle Eocene time. A tectonic model

which is more consistent with available paleomagnetic data involves accretion, and independent clockwise rotation of two or more Coast Range terranes, or "microplates", in response to oblique subduction of the Farallon plate beneath North America during early and middle Cenozoic time. This interpretation requires reevaluation of Simpson and Cox's (1977) and Hammond's (1979) models for the emplacement and rotation of the Coast Range.

12) Segmentation of the Coast Range and independent clockwise rotation of the crustal fragments probably occurred during or subsequent to its accretion to western North America, and may have been accomplished by one of several possible mechanisms:

A. Fragmentation of the Farallon plate and pivoting of these fragments during subduction around points located near ridge– trench–transform triple junctions (Menard, 1978).

B. Differential clockwise rotation of rigid crustal fragments (analogous to roller bearings) caught in a broad zone of distributed right lateral shear (Beck, 1976). The shear zone formed in response to oblique convergence between the North American and Farallon plates during early and middle Cenozoic time.

C. Development of a strike slip fault inboard of an active trench along which oblique convergence is occurring. Roughly equant crustal blocks caught in the shear zone between the trench and the parallel transcurrent fault translate northward and rotate clockwise if relative convergence is oblique and northeast directed (Fitch, 1972; modified by Beck and Plumley, 1977, cited in Burr, 1978).

D. Accretion of thick fragments of oceanic volcanic piles by

plate convergence, with rotation of the fragments at the continental margin. The fragments are easily decoupled from the underlying oceanic crust along a basal décollement consisting of hemipelagic and terrigenous siltstones. Following detachment the fragments break into smaller, more equant crustal blocks which rotate independently, especially if plate convergence is markedly oblique (D. C. Engebretsen and M. E. Beck, Jr., 1979, unpub. manuscript).

13) Further geologic mapping and paleomagnetic study of suspected "microplates" in the Coast Range is essential in order to elucidate the nature of the structures bounding them, and to determine the scale on which independent block rotation has operated. Specifically, the question of whether all of coastal Washington is a coherent terrane, or composed of separate blocks which have had independent rotational histories, may be resolved by paleomagnetic investigations in the volcanic highlands south of the Black Hills and in the late Eocene through Oligocene strata overlying the Crescent Formation in the Olympic Peninsula.

REFERENCES CITED

Alvarez, Walter, Kent, D. V., Silva, I. P., Schweickert, R. A., and Larson, R. A., 1980, Franciscan Complex limestone deposited at 17° south paleolatitude: Geol. Soc. America Bull., Pt. I, v. 91, p. 476-484.

Anderson, A. T., 1973, The before-eruption water content of some high-alumina magmas: Bull. Volcanol., v. 37, p. 530-552.

Anderson, Phillip, 1976, Oceanic crust and arc-trench gap tectonics in southwestern British Columbia: Geology, v. 4, p. 443-446.

Ansfield, V. J., 1972, Eocene cone-fan deposits and their significance, northern Olympic Peninsula, Washington: Geol. Soc. America Abs. with Programs, v. 4, p. 435.

Armentrout, J. M., 1973, Molluscan paleontology and biostratigraphy of the Lincoln Creek Formation (late Eocene-Oligocene), southwestern Washington: Seattle, Univ. Washington, unpub. Ph.D. dissertation, 479 p.

Armentrout, J. M., McDougall, K., Jefferis, P. T., and Nesbitt, E., 1980, Geologic field trip guide for the Cenozoic stratigraphy and late Eocene paleoecology of southwestern Washington: Ore. Dept. Geology and Mineral Industries Bull. 101, p. 79-119.

Arnold, R., 1906, Geological reconnaissance of the coast of the Olympic Peninsula, Washington: Geol. Soc. America Bull., v. 17, p. 451-468.

Atwater, Tanya, 1970, Implications of plate tectonics for the Cenozoic tectonic evolution of western North America: Geol. Soc. America Bull., v. 81, p. 3513-3536.

Baker, I., 1969, Petrology of the volcanic rocks of St. Helena Island, South Atlantic: Geol. Soc. America Bull., v. 80, p. 1283-1310.

Baker, P. E., Gass, I. G., Harris, P. G., and Le Maitre, R. W., 1964, The volcanological report of the Royal Society expedition to Tristan da Cunha: Phil. Trans. Royal Soc. London, Series A, v. 256, p. 439-578.

Baldwin, E. M., 1974, Eocene stratigraphy of southwestern Oregon: Ore. Dept. Geology and Mineral Industries Bull. 83, 40 p.

Barr, S. M., 1974, Seamount chains formed near the crest of the Juan de Fuca Ridge, northeast Pacific Ocean: Marine Geol., v. 17, p. 1-19.

Basham, W. L., and Larson, E. E., 1978, Paleomagnetic evidence for clockwise rotation in western Idaho, eastern Oregon, and northern Nevada: Geol. Soc. America Abs. with Programs, v. 10, p. 210.

Bass, M. N., Moberly, R., Rhodes, J. M., Shih, C. Y., and Church, S. E., 1973, 14. Volcanic rocks cored in the central Pacific, Leg 17, Deep Sea Drilling Project, in Winterer, E. L., Ewing, J. L., et al., Initial Reports of the Deep Sea Drilling Project, Volume XVII, Washington, D. C. (U. S. Government Printing Office), p. 429-503.

Bates, R. G., 1980, Tectonic rotations in the Cascade Mountains of southern Washington: Bellingham, Western Washington Univ., unpub. M.S. thesis, 86 p.

Bates, R. G., Beck, M. E., Jr., and Simpson, R. W., 1979, Preliminary paleomagnetic results from the southern Cascade Range of southwestern Washington (abs.): EOS, Trans. American Geophys. Union, v. 60, p. 816-817.

Batiza, Rodey, 1977, Age, volume, compositional and spatial relations of small isolated oceanic central volcanoes: Marine Geology, v. 24, p. 169-183.

Batiza, Rodey, 1978, Geology, petrology, and geochemistry of Isla Tortuga, a recently formed tholeiitic island in the Gulf of California: Geol. Soc. America Bull., v. 89, p. 1309-1324.

Batiza, Rodey, 1979, Geologic evolution of small oceanic islands: Preliminary results: Geol. Soc. America Abs. with Programs, v. 11, p. 385.

Batiza, Rodey, 1980, Are most small oceanic volcanoes tholeiitic? (abs.): EOS, Trans. American Geophys. Union, v. 61, p. 406.

Batiza, Rodey, Futa, K., and Hedge, C. E., 1979a, Trace element and strontium isotope characteristics of volcanic rocks from Isla

Tortuga: A young seamount in the Gulf of California: Earth and Planet. Sci. Lett., v. 43, p. 269-278.

Batiza, Rodey, and others, 1979b, Origin and evolution of small oceanic volcanoes near mid-ocean ridges: St. Louis, Washington University-McDonnell Center for the Space Sciences, Cruise Report, Rise III Leg 3 R/V NEW HORIZON (29 March to 22 April 1979, Mazatlan, Mexico to Mazatlan, Mexico), 38 p.

Beck, M. E., Jr., 1976, Discordant paleomagnetic pole positions as evidence of regional shear in the western Cordillera of North America: American Jour. Sci., v. 276, p. 694-712.

Beck, M. E., Jr., Plumley, P. W., and Burr, C. D., 1977, Microcontinental tectonics in the western North American Cordillera (abs.): EOS, Trans. American Geophys. Union, v. 58, p. 743.

Beck, M. E., Jr., and Burr, C. D., 1979, Paleomagnetism and tectonic significance of the Goble Volcanic Series, southwestern Washington: Geology, v. 7, p. 175-179.

Beck, M. E., Jr., and Cox, A., 1979, Paleomagnetic evidence for large-scale tectonic rotations and translations along the western edge of North America (abs.), in Armentrout, J. M., Cole, M. R., and Terbest, H., Jr., eds., Cenozoic Paleogeography of the Western United States: Soc. Econ. Paleontol. and Mineral., Pacific Coast Paleogeography Symposium 3, p. 325.

Beck, M. E., Jr., Engebretson, D. C., and Globerman, B. R., 1979, Cenozoic microplate tectonics in Washington State: A progress report: Geol. Soc. America Abs. with Programs, v. 11, p. 386.

Beck, M. E., Jr., and Plumley, P. W., 1980, Paleomagnetism of intrusive rocks in the Coast Range of Oregon: Microplate rotations in middle Tertiary time: Geology, v. 8, p. 573-577.

Beikman, H. M., Rau, W. W., and Wagner, H. C., 1967, The Lincoln Creek Formation, Grays Harbor Basin, southwestern Washington: U. S. Geol. Survey Bull. 1244-I, p. I1-I14.

Bence, A. E., Haskins, L. A., and Rhodes, J. M., 1980, Oceanic intraplate volcanism, in Basaltic Volcanism on the Terrestrial Planets:

Houston, NASA, Lunar and Planet. Sci. Instit., in press.

Berggren, W. A., 1972, A Cenozoic time-scale— Some implications for regional geology and paleobiogeography: Lethaia, v. 5, p. 195-215.

Blake, M. C., Jr., and Jones, D. L., 1977, Tectonics of the Yolla Bolly junction and its significance to the plate tectonic history of northern California: Geol. Soc. America Abs. with Programs, v. 9, p. 391.

Bond, G. C., 1973, A late Paleozoic volcanic arc in the eastern Alaska Range, Alaska: Jour. Geol., v. 81, p. 557-575.

Bromery, R. W., 1962, Aeromagnetic and gravimetric interpretation of the geology of the Malone, Rochester, Pe Ell, and Adna quadrangles, Washington: Washington, D. C., The American Univ., unpub. M.S. thesis, 44p.

Bromery, R. W., and Snavely, P. D., Jr., 1964, Geologic interpretation of reconnaissance gravity and aeromagnetic surveys in northwestern Oregon: U. S. Geol. Survey Bull. 1181N, p. N1-N13.

Brown, R. D., Jr., Gower, H. D., and Snavely, P. D., Jr., 1960, Geology of the Port Angeles— Lake Crescent area, Clallam County, Washington: U. S. Geol. Survey Oil and Gas Investigations Map OM-203.

Bryan, W. B., Thompson, G., Frey, F. A., and Dickey, J. S., 1976, Inferred geologic settings and differentiation in basalts from the Deep Sea Drilling Project: Jour. Geophys. Res., v. 81, p. 4285-4304.

Burr, C. D., 1978, Paleomagnetism and tectonic significance of the Goble volcanics of southern Washington: Bellingham, Western Washington Univ., unpub. M.S. thesis, 66p.

Byrne, Tim, 1979, Late Paleocene demise of the Kula-Pacific spreading center: Geology, v. 7, p. 341-344.

Cady, W. M., 1975, Tectonic setting of the Tertiary volcanic rocks of the Olympic Peninsula, Washington: U. S. Geol. Survey Jour. Res., v. 3, p. 573-582.

Cady, W. M., Sorenson, M. L., and MacLeod, N. S., 1972, Geologic map of The Brothers quadrangle, Washington: U. S. Geol. Survey, Geol.

Quad. Map GQ-969.

Cann, J. R., 1970, Rb, Sr, Y, and Nb in some ocean floor basaltic rocks: Earth and Planet. Sci. Lett., v. 10, p. 7-11.

Carlisle, D., 1963, Pillow breccias and their aquagene tuffs, Quadra Island, British Columbia: Jour. Geol., v. 71, p. 48-71.

Carson, R. J., III, 1970, Quaternary geology of the south-central Olympic Peninsula, Washington: Seattle, Univ. Washington, unpub. Ph.D. dissertation, 67p.

Carson, R. J., 1973, Holocene faulting, southeastern Olympic Peninsula, Washington: Geol. Soc. America Abs. with Programs, v. 5, p. 568-569.

Chase, R. L., and Tiffin, D. L., 1972, Queen Charlotte fault zone, British Columbia: 24th International Geological Congress, Marine Geology and Geophysics Section, v. 8, p. 17-28.

Churkin, Michael, Jr., and Eberlein, G. D., 1977, Ancient borderland terranes of the North American Cordillera: Correlations and microplate tectonics: Geol. Soc. America Bull., v. 88, p. 769-786.

Clague, D. A., 1974, The Hawaiian-Emperor Seamount chain: Its origin, petrology, and implications for plate tectonics: San Diego, Univ. California, unpub. Ph.D. dissertation, 319p.

Clapp, C. H., 1917, Sooke and Duncan Map-Areas, Vancouver Island: Geol. Survey Canada Memoir 96, 445p.

Clark, H. C., 1969, Remanent magnetization, cooling history, and paleomagnetic record of the Mary's Peak sill, Oregon: Jour. Geophys. Res., v. 74, p. 3143-4160.

Cox, Allan, 1968, Confidence limits for the precision parameter kappa: Geophys. Jour. Royal. Astro. Soc., v. 18, p. 545-549.

Crosson, R. S., 1972, Small earthquakes, structure, and tectonics of the Puget Sound area: Bull. Seis. Soc. America, v. 62, p. 1133-1171.

Danes, Z. F., Bonno, E. M., Brau, E., Gilham, W. D., Hoffman, T. F., Johansen, D., Jones, M. A., Malfait, B., Maston, J., and Teague, G. O., 1965, Geophysical investigations of the southern Puget Sound area, Washington: Jour. Geophys. Res., v. 70, p. 5573-5580.

Davis, G. A., 1977, Tectonic evolution of the Pacific Northwest: Precambrian to present: Washington Public Power Supply System, Nuclear Project No. 1, Subappendix 2RC, PSAR, Amendment 23, p. i-2R C-46.

Davis, G. A., Monger, J. W. H., and Burchfiel, B. C., 1978, Mesozoic construction of the Cordilleran "collage", central British Columbia to central California, in Howell, D. G., and McDougall, K. A., eds., Mesozoic Paleogeography of the Western United States: Soc. Econ. Paleontol. and Mineral., Pacific Coast Paleogeography Symposium 2, p. 1-32.

Dewey, J. F., and Sengor, A. M. C., 1979, Aegean and surrounding regions: Complex multiplate and continuum tectonics in a convergent zone: Geol. Soc. America Bull., Pt. I, v. 90, p. 84-92.

Dickinson, W. R., 1979, Mesozoic forearc basin in central Oregon: Geology, v. 7, p. 166-170.

Doell, R. R., and Cox, A., 1965, Measurement of the remanent magnetization of igneous rocks: U. S. Geol. Survey Bull. 1203-A, p. 1-32.

Dunoyer de Segonzac, G., 1970, The transformation of clay minerals during diagenesis and low-grade metamorphism— a review: Sedimentology, v. 15, p. 281-346.

Easterbrook, D. J., and Rahm, D. A., 1972, Landforms of Washington: Bellingham, Wash., Union Printing,

Engebretson, D. C., and Beck, M. E., Jr., 1979, Accretion and rotation at obliquely subducting plate margins: Unpublished manuscript.

Engel, A. E. J., Engel, C. G., and Havens, R. G., 1965, Chemical characteristics of oceanic basalts and the upper mantle: Geol. Soc. America Bull., v. 76, p. 719-734.

Fairchild, L. H., 1979a, Leech River unit and Leech River fault, southern Vancouver Island: Seattle, Univ. Washington, unpub. M.S.

thesis, 169p.

Fairchild, L. H., 1979b, A reinterpretation of the eruptive environment of the Crescent Formation basalt (abs.): Northwest Science, Proceedings 52nd Annual Meeting, Bellingham, Wash., p. 33.

Fairchild, L. H., 1980, A model for the post-39 MY tectonic evolution of northwestern Washington and southern Vancouver Island: Geol. Soc. America Abs. with Programs, v. 12, p. 105-106.

Fisher, Sir Ronald, F. R. S., 1953, Dispersion on a sphere: Proceedings Royal Soc. London, Series A, p. 295-305.

Fitch, T. J., 1972, Plate convergence, transcurrent faults, and internal deformation adjacent to southeast Asia and the western Pacific: Jour. Geophys. Res., v. 77, p. 4432-4460.

Floyd, P. A., and Winchester, J. A., 1975, Magma type and tectonic setting using immobile elements: Earth and Planet. Sci. Lett., v. 27, p. 211-218.

Fornari, D. J., Malahoff, A., and Heezen, B. C., 1979, Visual observations of the volcanic micromorphology of Tortuga, Lorraine, and Tutu Seamounts; and petrology and chemistry of ridge and seamount features in and around the Panama Basin: Marine Geol., v. 31, p. 1-30.

Garcia, M. O., 1978, Criteria for the identification of ancient island arcs: Earth Sci. Reviews, v. 14, p. 147-165.

Garrison, R. E., 1973, Space-time relations of pelagic limestones and volcanic rocks, Olympic Peninsula, Washington: Geol. Soc. America Bull., v. 84, p. 583-594.

Gast, P. W., 1968, Trace element fractionation and th origin of tholeiitic and alkaline magma types: Geochim. Cosmochim. Acta, v. 32, p. 1057-1070.

Gast, P. W., Tilton, G. R., and Hedge, C. E., 1964, Isotopic composition of lead and strontium from Ascension and Gough Islands: Science, v. 145, p. 1181-1183

Glassley, W. E., 1974, Geochemistry and tectonics of the Crescent

volcanic rocks, Olympic Peninsula, Washington: Geol. Soc. America Bull., v. 85, p. 785-794.

Globerman, B. R., 1979, Geochemistry of Eocene basalts from the Black Hills, Washington Coast Range: Geol. Soc. America Abs. with Programs, v. 11, p. 80.

Globerman, B. R., and Beck, M. E., Jr., 1979, Cenozoic tectonic rotations in the western Cordillera: New evidence from the Washington Coast Range (abs.): EOS, Trans. American Geophys. Union, v. 60, p. 817.

Globerman, B. R., and Babcock, R. S., 1980, New geochemical data and their significance from the Washington Coast Range: Geol. Soc. America Abs. with Programs, v. 12, p. 107-108.

Graham, J. W., 1949, The stability and significance of magnetism in sedimentary rocks: Jour. Geophys. Res., v. 54, p. 131-167.

Greenhaus, M. R., and Cox, A., 1979, Paleomagnetism of the Morro Rock-Islay Hill Complex as evidence for crustal block rotations in central coastal California: Jour. Geophys. Res., v. 84, p. 2393-2400.

Gresens, R. L., 1979, Timing of igneous and tectonic events on the eastern flank of the Cascade Range in central Washington: Geol. Soc. America Abs. with Programs, v. 11, p. 80.

Hall, J. B., and Othberg, K. L., 1974, Thickness of unconsolidated sediments, Puget Lowland, Washington: Wash. Div. Geol. and Earth Resources, Geol. Map GM-12.

Hall, J. M., and Robinson, P. T., 1979, Deep srustal drilling in the North Atlantic: Science, v. 204, p. 573-586.

Hamilton, Warren, and Myers, W. B., 1966, Cenozoic tectonics of the western United States: Reviews Geophys., v. 4, p. 509-549.

Hammond, P. E., 1979, A tectonic model for evolution of the Cascade Range, in Armentrout, J. M., Cole, M. R., and Terbest, H., Jr., eds., Cenozoic Paleogeography of the Western United States: Soc. Econ. Paleontol. and Mineral., Pacific Coast Paleogeography Symposium 3, p. 219-237.

Hart, S. R., Schilling, J.-G., and Powell, J. L., 1973, Basalts from Iceland and along the Reykjanes Ridge: Sr isotope geochemistry: Nature, v. 246, p. 104-107.

Hart, S. R., Erlank, A. J., and Kable, E. J. D., 1974, Sea floor basalt alteration: Some chemical and Sr isotopic effects: Contrib. Mineral. Petrol., v. 44, p. 219-230.

Haskin, L., and Dungan, M., 1980, Processes that affect basaltic magma composition: American Jour. Sci., in press.

Hedge, C. E., 1966, Variations in radiogenic strontium found in volcanic rocks: Jour. Geophys. Res., v. 71, p. 6119-6126.

Hedge, C. E., 1978, Strontium isotopes in basalts from the Pacific Ocean basin: Earth and Planet. Sci. Lett., v. 38, p. 88-94.

Hekinian, Roger, and Thompson, G., 1976, Comparative geochemistry of volcanics from rift valleys, transform faults and aseismic ridges: Contrib. Mineral. Petrol., v. 57, p. 145-162.

Helwig, James, 1974, Eugeosynclinal basement and a collage concept of orogenic belts: Soc. Econ. Paleontol. and Mineral. Spec. Pub. 19, p. 359-376.

Henriksen, D. A., 1956, Eocene stratigraphy of the lower Cowlitz River— eastern Willapa Hills area, southwestern Washington: Wash. Div. Mines and Geol., Bull. 43, 122p.

Hill, M. L., and Hobson, H. D., 1968, Possible post-Cretaceous slip on the San Andreas fault zone, in Dickinson, W. R., and Grantz, A., eds., Proceedings of Conference on Geologic Problems of San Andreas Fault System: Stanford Univ. Pub. in Geol. Sci., v. XI, p. 123-127.

Hillhouse, J. W., 1977, Paleomagnetism of the Triassic Nikolai Greenstone, McCarthy Quadrangle, Alaska: Can. Jour. Earth Sci., v. 14, p. 2578-2592.

Hubbard, N. J., 1969, A chemical comparison of oceanic ridge, Hawaiian tholeiitic, and Hawaiian alkalic basalts: Earth and Planet. Sci. Lett., v. 5, p. 346-352.

Huntting, M. T., Bennett, W. A. G., Livingston, V. E., Jr., and Moen,

W. S., 1961, Geologic map of Washington: Wash. Dept. Conservation, Div. Mines and Geol., scale 1:500,000.

Ibarrola, E., 1969, Variation trends in volcanic rocks of the Canary Islands: Bull. Volcanol., v. 33, p. 729-777.

Irvine, T. N., and Baragar, W. R. A., 1971, A guide to the chemical classification of the common volcanic rocks: Can. Jour. Earth Sci., v. 8, p. 523-548.

Irving, E., 1979, Paleopoles and paleolatitudes of North America and speculations about displaced terranes: Can. Jour. Earth Sci., v. 16, p. 669-694.

Irwin, W. P., 1977, Review of Paleozoic rocks of the Klamath Mountains, in Stewart, J. H., Stevens, C. H., and Fritsche, A. E., eds., Paleozoic Paleogeography of the Western United States: Soc. Econ. Paleontol. and Mineral., Pacific Coast Paleogeography Symposium 1, p. 441-454.

Johnson, J. R., 1979, Transitional basalts and tholeiites from the East Pacific Rise, 9° North: Jour. Geophys. Res., v. 84, p. 1635-1651.

Jakes, P., and Gill, J. B., 1970, Rare earth elements and the island arc tholeiitic series: Earth and Planet. Sci. Lett., v. 9, p. 17-28.

Jones, D. L., Silberling, N. J., and Hillhouse, J. W., 1977, Wrangellia— A displaced terrane in northwestern North America: Can. Jour. Earth Sci., v. 14, p. 2565-2577.

Jones, T. D., 1977, Analysis of a gravity traverse south of Portland, Oregon: Portland, Portland State Univ., unpub. B.S. thesis, 54p.

Kamerling, M. J., and Luyendyk, B. P., 1979, Tectonic rotations of the Santa Monica Mountains region, western Transverse Ranges, California, suggested by paleomagnetic vectors: Geol. Soc. America Bull., Pt. I, v. 90, p. 331-337.

King, P. B., 1969, Tectonic map of North America, in The Tectonics of North America— A discussion to accompany the Tectonic Map of North America: U. S. Geol. Survey Prof. Paper 628, scale 1:5,000,000.

Lajoie, Jean, 1979, Facies models 15. Volcaniclastic rocks: Geoscience Canada, v. 6, p. 129-139.

Lanphere, M. A., 1978, Displacement history of the Denali fault system, Alaska and Canada: Can. Jour. Earth Sci., v. 15, p. 817-822.

Lawrence, R. D., 1976, Strike-slip faulting terminates the Basin and Range province in Oregon: Geol. Soc. America Bull., v. 87, p. 846-850.

LeMaitre, R. W., 1962, Petrology of volcanic rocks, Gough Island, South Atlantic: Geol. Soc. America Bull., v. 73, p. 1309-1340.

Loeschke, Jorg, 1979, Basalts of Oregon (U.S.A.) and their geotectonic environment I. Petrochemistry of Tertiary basalts of the Oregon Coast Range: N. Jb. Mineral. Abh., v. 134, p. 225-247.

Lonsdale, Peter, and Spiess, F. N., 1979, A pair of young cratered volcanoes on the East Pacific Rise: Jour. Geol., v. 87, p. 157-173.

Lyttle, N. A., and Clarke, D. B., 1975, New analyses of Eocene basalt from the Olympic Peninsula, Washington: Geol. Soc. America Bull., v. 86, p. 421-427.

McBirney, A. R., and Aoki, K., 1968, Petrology of the Island of Tahiti: Geol. Soc. America Memoir, v. 116, p. 523-556.

McBirney, A. R., and Williams, H., 1969, Geology and Petrology of the Galapagos Islands: Geol. Soc. America Memoir, v. 118, p. 1-197.

Macdonald, G. A., 1972, Volcanoes: Englewood Cliffs, N. J., Prentice-Hall, 509p.

Macdonald, G. A., and Katsura, T., 1964, Chemical composition of Hawaiian lavas: Jour. Petrol., v. 5, p. 82-133.

McElhinny, M. W., 1973, Paleomagnetism and Plate Tectonics: Cambridge, University Press, 358p.

MacLeod, N. S., Tiffin, D. L., Snavely, P. D., Jr., and Currie, R. G., 1977, Geologic interpretation of magnetic and gravity anomalies in the Strait of Juan de Fuca, United States and Canada: Can. Jour. Earth Sci., v. 14, p. 223-238.

McMurphy, C. J., and Anderson, H. W., 1968, Soil survey report of the

Capitol Forest area: Wash. Dept. Natural Resources, Report no. DNR-14, 45p.

Magill, J., Cox, A., and Duncan, R. A., 1980, Tillamook volcanic series: Further evidence for tectonic rotation of the Oregon Coast Range: Jour. Geophys. Res., in press.

Menard, H. W., 1969, Growth of drifting volcanoes: Jour. Geophys. Res., v. 74, p. 4827-4837.

Menard, H. W., 1978, Fragmentation of the Farallon plate by pivoting subduction: Jour. Geophys. Res., v. 86, p. 99-110.

Menzies, M., and Seyfried, W., 1979, Experimental basalt-seawater interaction: Implications for K, Rb, and Sr mobility and Sr isotopic variation within the oceanic crust (abs.): IAVCEI Hawaiian Symposium on Intraplate Volcanism and Submarine Volcanism, Hilo, p. 66.

Misch, Peter, 1966, Tectonic evolution of Northern Cascades of Washington State— A West-Cordilleran case history, in Gunning, H. C., ed., A Symposium on the Tectonic History and Mineral Deposits of the Western Cordillera in British Columbia and Neighboring Parts of the United States: Can. Instit. Mining and Metallurgy, Spec. Vol. 8, p. 101-148.

Molenaar, Dee, and Noble, J. B., 1970, Geology and related groundwater occurrence, southeastern Mason County, Washington: Wash. Dept. Water Resources, Water Supply Bull. 29, 145p.

Monger, J. W. H., 1977, Ophiolitic assemblages in the Canadian Cordillera, in Coleman, R. G., and Irwin, W. P., eds., North American Ophiolites: Ore. Dept. Geology and Mineral Industries, Bull. 95, p. 59-66.

Monger, J. W. H., and Ross, C. A., 1971, Distribution of fusulinaceans in the western Canadian Cordillera: Can. Jour. Earth Sci., v. 8, p. 259-278.

Monger, J. W. H., Souther, J. G., and Gabrielse, H., 1972, Evolution of the Canadian Cordillera: A plate tectonic model: American Jour. Sci., v. 272, p. 577-602.

Monger, J. W. H., and Irving, E., 1979, The Canadian Cordilleran collage: Geol. Soc. America Abs. with Programs, v. 11, p. 482.

Monger, J. W. H., and Price, R. A., 1979, Geodynamic evolution of the Canadian Cordillera— Progress and problems: Can. Jour. Earth Sci., v. 16, p. 770-791.

Moore, J. G., and Fiske, R. S., 1969, Volcanic substructure inferred from dredge samples and ocean-bottom photographs, Hawaii: Geol. Soc. America Bull., v. 80, p. 1191-1202.

Muller, J. E., 1974, Victoria Map-Area, British Columbia (92B): Geol. Survey Canada, Paper 75-1, Pt. A, p. 21-26.

Muller, J. E., 1977, Evolution of the Pacific Margin, Vancouver Island, and adjacent regions: Can. Jour. Earth Sci., v. 14, p. 2062-2085.

Muller, J. E., 1980, Chemistry and origin of the Eocene Metchosin Volcanics, Vancouver Island, British Columbia: Can. Jour. Earth Sci., v. 17, p. 199-209.

Munoz, M., 1969, Estudio petrologico de las formationes alcalinas de fuerte ventura (Islas Canarias): Estud. Geol. Instit. Mallada, v. 25, p. 257-310.

Noble, J. B., and Wallace, E. F., 1966, Geology and groundwater resources of Thurston County, Washington: Wash. Dept. Water Resources, Water Supply Bull. 10, v. 2, 141p.

Nuclear Regulatory Commission (U. S.), 1975, Advisory Committee on Reactor Safeguards, Subcommittee review of WPPSS 3 and 5, Elma, Washington, August 4, 1975.

O'Nions, R. K., and Pankhurst, R. J., 1973, Secular variation in Sr isotope composition of Icelandic volcanic rocks: Earth and Planet. Sci. Lett., v. 21, p. 13-21.

O'Nions, R. K., and Pankhurst, R. J., Petrogenetic significance of isotope and trace element variations in volcanic rocks from the mid-Atlantic: Jour. Petrol., v. 15, p. 603-634.

O'Nions, R. K., Pankhurst, R. J., and Gronvold, K., 1976, Nature and development of basaltic magma sources beneath Iceland and the

Reykjanes Ridge: Jour. Petrol., v. 17, p. 315-338.

Park, C. F., Jr., 1950, Structure of the volcanic rocks of the Olympic Peninsula, Washington (abs.): Geol. Soc. America Bull., v. 61, p. 1529.

Pearce, J. A., 1975, Basalt geochemistry used to investigate past tectonic environments on Cyprus: Tectonophysics, v. 25, p. 41-67.

Pearce, J. A., 1976, Statistical analysis of major element patterns in basalts: Jour. Petrol., v. 17, p. 15-43.

Pearce, J. A., and Cann, J. R., 1971, Ophiolite origin investigated by discriminant analysis using Ti, Zr, and Y: Earth and Planet. Sci. Lett., v. 12, p. 339-349.

Pearce, J. A., and Cann, J. R., 1973, Tectonic setting of basic volcanic rocks determined using trace element analyses: Earth and Planet. Sci. Lett., v. 19, p. 290-300.

Pearce, J. A., and Norry, M. J., 1979, Petrogenetic implications of Ti, Zr, Y, and Nb variations in volcanic rocks: Contrib. Mineral. Petrol., v. 69, p. 33-47.

Pearce, T. H., 1979, The effects of tectonics on major element chemistry of intraplate volcanics (abs.): IAVCEI Hawaiian Symposium on Intraplate Volcanism and Submarine Volcanism, Hilo, p. 95.

Pearce, T. H., Gorman, B. E., and Birkett, T. C., 1977, The relationship between major element chemistry and tectonic environment of basic and intermediate volcanic rocks: Earth and Planet. Sci. Lett., v. 36, p. 121-132.

Pease, M. H., and Hoover, L., 1957, Geology of the Doty—Minot Peak area, Washington: U. S. Geol. Survey Oil and Gas Explorations Map OM-188, scale 1:62,500.

Plumley, P. W., 1980, Paleomagnetism of Tertiary intrusive rocks in the Oregon Coast Range: Timing and mechanism of tectonic rotation: Bellingham, Western Washington Univ., unpub. M.S. thesis, 239p.

Plumley, P. W., and Beck, M. E., Jr., 1977, Tectonic rotation of Oligo-

cene intrusive rocks in the Coast Range of Oregon: A constant rate of rotation for the period 50– 30 M.Y.B.P. (abs.): EOS, Trans. American Geophys. Union, v. 58, p. 1126.

Powell, J. L., Faure, G., and Hurley, P. M., 1965, Strontium-87 abundance in a suite of Hawaiian volcanic rocks of varying silica content: Jour. Geophys. Res., v. 70, p. 1509-1513.

Powell, J. L., and Delong, S. E., 1966, Isotopic composition of strontium in volcanic rocks from Oahu: Science, v. 153, p. 1239-1242.

Presnall, D. C., Jackson, E. D., and Dixon, S. A., 1979, A model for the origin of the tholeiitic to alkalic basalt transition in Hawaiian volcanoes (abs.): IAVCEI Hawaiian Symposium on Intraplate Volcanism and Submarine Volcanism, Hilo, p. 96.

Raisz, Erwin, 1945, The Olympic– Wallowa lineament: American Jour. Sci., v. 243A, p. 479-485.

Rau, W. W., 1948, Foraminifera from the Porter Shale (Lincoln Formation), Grays Harbor County, Washington: Jour. Paleon., v. 22, p. 152-174.

Rau, W. W., 1956, Foraminifera from the McIntosh Formation (Eocene) at McIntosh Lake, Washington: Cushman Foundation for Foraminiferal Research Contributions, v. 7, pt. 3, p. 69-78.

Rau, W. W., 1966, Stratigraphy and Foraminifera of the Satsop River area, southern Olympic Peninsula, Washington: Wash. Div. Mines and Geol., Bull. 53, 66p.

Rau, W. W., 1967, Geology of the Wynoochee Valley quadrangle, Grays Harbor County, Washington: Wash. Div. Geol. and Earth Resources, Bull. 56, 51p.

Ridley, W. I., 1970, The petrology of Las Canadas volcanoes, Tenerife, Canary Islands: Contrib. Mineral. Petrol., v. 26, p. 124-160.

Rittman, A., 1962, Volcanoes and their Activity: New York, Wiley, 305p.

Rittman, A., and Rittman, L., 1976, Volcanoes: New York, G. P. Putnam's Sons, 97p.

Rogers, W. P., 1970, A geological and geophysical study of the northern part of the Puget Sound Lowland, Washington: Seattle, Univ. Washington, unpub. Ph.D. dissertation, 123p.

Schau, Mikkel, 1970, Stratigraphy and structure of the type area of the Upper Triassic Nicola Group in south-central British Columbia: Geol. Assoc. Canada, Spec. Pub. 6, p. 123-135.

Schilling, J.-G., 1973, Iceland mantle plume: Geochemical study of the Reykjanes Ridge: Nature, v. 242, p. 565-571.

Schilling, J.-G., 1975, Rare-earth variations across 'normal segments' of the Reykjanes Ridge, 60°– 53°N, mid-Atlantic Ridge, 29°S, and East Pacific Rise, 2°– 19°S, and evidence on the composition of the underlying low-velocity layer: Jour. Geophys. Res., v. 80, p. 1459-1473.

Schmela, R. J., and Palmer, L. A., 1972, Geologic analysis of the Portland Hills– Clackamas River alignment, Oregon: The Ore Bin, v. 34, p. 93-103.

Schweickert, R. A., 1976, Early Mesozoic rifting and fragmentation of the Cordilleran orogen: Nature, v. 260, p. 586-591.

Schwimmer, P. M., Beck, M. E., Jr., and Fox, K. F., 1979, The western extent of stable North American craton during the Eocene: Evidence from the paleomagnetism of the Sanpoil volcanics (abs.): EOS, Trans. American Geophys. Union, v. 60, p. 817.

Shand, S. J., 1933, The lavas of Mauritius: Quaterly Jour. Geol. Soc. London, v. 89, p. 1-13.

Sigvaldason, G. E., 1974, Basalts from the center of the assumed Icelandic mantle plume: Jour. Petrol., v. 15, pt. 3, p. 497-524.

Simpson, R. W., 1977, Paleomagnetic evidence for the tectonic rotation of the Oregon Coast Range: Stanford, Calif., Stanford Univ., unpub. Ph.D. dissertation, 156p.

Simpson, R. W., and Cox, A., 1977, Paleomagnetic evidence for the tectonic rotation of the Oregon Coast Range: Geology, v. 5, p. 585-589.

Skehan, J. W., 1965, The Olympic-Wallowa lineament— A major deep-seated tectonic feature of the Pacific Northwest (abs.): Trans. American Geophys. Union, v. 46, p. 71.

Smith, R. E., and Smith, S. E., 1976, Comments on the use of Ti, Zr, Y, Sr, K, P, and Nb in classification of basaltic magmas: Earth and Planet. Sci. Lett., v. 32, p. 114-120.

Snavely, P. D., Jr., and Baldwin, E. M., 1948, Siletz River volcanic series, northwestern Oregon: American Assoc. Petroleum Geol. Bull., v. 32, p. 805-812.

Snavely, P. D., Jr., Rau, W. W., Hoover, L., Jr., and Roberts, A. E., 1951a, McIntosh Formation, Centralia-Chehalis coal district, Washington: American Assoc. Petroleum Geol. Bull., v. 35, p. 1052-1061.

Snavely, P. D., Jr., Roberts, A. E., Hoover, L., Jr., and Pease, M. H., Jr., 1951b, Geology of the eastern part of the Centralia-Chehalis coal district, Lewis and Thurston Counties, Washington: U. S. Geol. Survey Coal Investigations Map C8.

Snavely, P. D., Jr., Brown, R. D., Jr., Roberts, A. E., and Rau, W. W., 1958, Geology and coal resources of the Centralia-Chehalis district, Washington: U. S. Geol. Survey Bull. 1053, 159p.

Snavely, P. D., Jr., and Wagner, H. C., 1964, Geologic sketch of northwestern Oregon: U. S. Geol. Survey Bull. 1181-M, p. M1-M17.

Snavely, P. D., Jr., MacLeod, N. S., and Wagner, H. C., 1968, Tholeiitic and alkalic basalts of the Eocene Siletz River Volcanics, Oregon Coast Range: American Jour. Sci., v. 266, p. 454-481.

Snavely, P. D., Jr., MacLeod, N. S., and Wagner, H. C., 1973, Miocene tholeiitic basalts of coastal Oregon and Washington and their relations to coeval basalts of the Columbia Plateau: Geol Soc. America Bull., v. 84, p. 387-424.

Snavely, P. D., Jr., and MacLeod, N. S., 1974, Yachats Basalt— an upper Eocene differentiated volcanic sequence in the Oregon Coast Range: U. S. Geol. Survey Jour. Res., v. 2, p. 395-403.

Snavely, P. D., Jr., Niem, A. R., MacLeod, N. S., Pearl, J. E., and

Rau, W. W., 1979, Makah Formation— A deep marginal basin sedimentary sequence of late Eocene and Oligocene age in the northwestern Olympic Peninsula, Washington: U. S. Geol. Survey, Open File Report 79-581, 75p.

Snavely, P. D., Jr., Wagner, H. C., and Lander, D. L., 1980, Interpretation of the Cenozoic geologic history of central Oregon continental margin: Cross-section summary: Geol. Soc. America Bull., Pt. I, v. 91, p. 143-146.

Stewart, R. J., 1970, Petrology, metamorphism, and structural relations of graywackes in the western Olympic Peninsula, Washington: Stanford, Calif., Stanford Univ., unpub. Ph.D. dissertation, 123p.

Streckeisen, A., 1979, Classification and nomenclature of volcanic rocks, lamprophyres, carbonatites, and melitic rocks: Recommendations and suggestions of the IUGS Subcommission on the Systematics of Igneous Rocks: Geology, v. 7, p. 331-335.

Subbarao, K. V., Clark, G. S., and Forbes, R. B., 1973, Strontium isotopes in some seamount basalts from the northeastern Pacific Ocean: Can. Jour. Earth Sci., v. 10, p. 1479-1483.

Sun, S.-S., Tatsumoto, M., and Schilling, J.-G., 1975, Mantle plume mixing along the Reykjanes Ridge axis: lead isotopic evidence: Science, v. 190, p. 143-147.

Symons, D. T. A., 1973, Paleomagnetic zones in the Oligocene East Sooke gabbro, Vancouver Island, British Columbia: Jour. Geophys. Res., v. 78, p. 5100-5109.

Tabor, R. W., 1972, Age of Olympic metamorphism, Washington: K-Ar dating of low-grade metamorphic rocks: Geol. Soc. America Bull., v. 83, p. 1805-1816.

Tabor, R. W., 1975, Guide to the Geology of Olympic National Park: Seattle, Univ. Washington Press, 144p.

Tabor, R. W., Cady, W. M., and Yeats, R. S., 1970, Broken formations and thrust faulting in the northeastern Olympic Mountains, Washington: Geol. Soc. America Abs. with Programs, v. 2, p. 153.

Tabor, R. W., and Cady, W. M., 1978a, Geologic map of the Olympic Penin-

sula, Washington: U. S. Geol. Survey Misc. Investigations Series Map I-994, scale 1:125,000.

Tabor, R. W., and Cady, W. M., 1978b, The structure of the Olympic Mountains, Washington— Analysis of a subduction zone: U. S. Geol. Survey Prof. Paper 1033, 37p.

Tabor, R. W., and Frizzell, V. A., Jr., 1979, Tertiary movement along the southern segment of the Straight Creek fault and its relation to the Olympic Wallowa Lineament in the central Cascades, Washington: Geol. Soc. America Abs. with Programs, v. 11, p. 131.

Tarling, D. H., 1971, Principles and Applications of Paleomagnetism: London, Chapman and Hall, 164p.

Tatsumoto, M., Hedge, C. E., and Engel, A. E. J., 1965, Potassium, rubidium, strontium, uranium, and the ratio of strontium-87 to strontium-86 in oceanic tholeiitic basalt: Science, v. 150, p. 886-888.

Teissere, R. F., and Beck, M. E., Jr., 1973, Divergent Cretaceous paleomagnetic pole position for the southern California batholith, U. S. A.: Earth and Planet. Sci. Lett., v. 18, p. 296-300.

Thayer, T. P., 1977, The Canyon Mountain Complex, Oregon, and some problems of ophiolites, in Coleman, R. G., and Irwin, W. P., eds., North American Ophiolites: Ore. Dept. Geology and Mineral Industries, Bull. 95, p. 93-106.

Thompson, G., 1973, A geochemical study of the low-temperature interaction of seawater and oceanic igneous rocks: EOS, Trans. American Geophys. Union, v. 54, p. 1015-1019.

Travers, W. B., 1978, Overturned Nicola and Ashcroft strata and their relation to the Cache Creek Group, southwestern Intermontane Belt, British Columbia: Can. Jour. Earth Sci., v. 15, p. 99-116.

Travers, W. B., and Ladd, J. H., 1979, Microplate accretion by obduction— The age and nature of Cache Creek thrust faulting near Cache Creek, British Columbia: Geol. Soc. America Abs. with Programs, v. 11, p. 529.

Turner, D. L., 1970, Potassium-argon dating of Pacific Coast Miocene foraminiferal stages, in Bandy, O. L., ed., Radiometric Dating and Paleontological Zonation: Geol. Soc. America Spec. Paper 124, p. 91-129.

Turner, D. L., Jarrard, R. D., Forbes, R. B., Hedge, C. E., and Naeser, C. W., 1979, Geochronology and genesis of the Kodiak-Bowie Seamount Chain, Gulf of Alaska (abs.): IAVCEI Hawaiian Symposium on Intraplate Volcanism and Submarine Volcanism, Hilo, p. 128.

Vance, J. A., 1979, Early and middle Cenozoic arc magmatism and tectonics in Washington State: Geol. Soc. America Abs. with Programs, v. 11, p. 132.

Vogt, P. R., Lowrie, A., Bracey, D. R., and Hey, R. N., 1976, Subduction of aseismic oceanic ridges: Effects on shape, seismicity, and other characteristics of consuming plate boundaries: Geol. Soc. America Spec. Paper 172, p. 1-59.

Wallace, E. F., and Molenaar, D., 1961, Geology and groundwater resources of Thurston County, Washington: Wash. Div. Water Resources, Water Supply Bull. 10, v. 1, 254p.

Warren, W. C., Norbisrath, H., and Grivetti, R. M., 1945, Geology of northwestern Oregon, west of Willamette River and north of latitude 45°N 15': U. S. Geol. Survey Oil and Gas Investigations, Preliminary Map 42.

Washington Public Power Supply System, 1975, Preliminary Safety Analysis Report for Washington Nuclear Projects 3 and 5, Amendment 19, p. 2.5.I-6c— 2.5.I.12.

Weaver, C. E., 1912, A preliminary report on the Tertiary paleontology of western Washington: Wash. Geol. Survey Bull. 15, 80p.

Weaver, C. E., 1916, The Tertiary formations of western Washington: Wash. Geol. Survey Bull. 13, 327p.

Weaver, C. E., 1937, Tertiary stratigraphy of western Washington and northwest Oregon: Univ. Washington Publications in Geology, v. 4, 266p.

Weaver, C. E., and others, 1944, Correlation of the marine Cenozoic formations of western North America: Geol. Soc. America Bull., v. 55, p. 569-598.

Weaver, C. S., Malone, S. D., Endo, E. T., and Noson, L. T., 1980, Seismicity patterns of the Mount Saint Helens eruptive sequence (abs.): EOS, Trans. American Geophys. Union, v. 61, p. 1133.

Wells, R. E., and Coe, R. S., 1979, Paleomagnetism and tectonic significance of the Eocene Crescent Formation, southwestern Washington: Geol. Soc. America Abs. with Programs, v. 11, p. 537.

Wells, R. E., and Coe, R. S., 1980, Tectonic rotations in southwest Washington (abs.): EOS, Trans. American Geophys. Union, v. 61, p. 949.

White, W. M., and Schilling, J.-G., 1978, The nature and origin of geochemical variation in mid-Atlantic Ridge basalts from the central North Atlantic: Geochim. Cosmochim. Acta, v. 42, p. 1501-1516.

Williams, Howell, and McBirney, A. R., 1979, Volcanology: San Francisco, Freeman Cooper, 384p.

Wilson, J. R., 1975, Geology of the Price Lake area, Mason County, Washington: Raleigh, North Carolina State Univ., unpub. M.S. thesis, 79p.

Wise, D. U., 1963, An outrageous hypothesis for the tectonic pattern of the North American Cordillera: Geol. Soc. America Bull., v. 74, p. 357-362.

Wolfe, E., and McKee, E. H., 1968, Geology of the Grays River quadrangle, Wahkiakum and Pacific Counties, Washington: Wash. Div. Mines and Geol., Geol. Map GM-4.

Yoder, H. C., and Tilley, C. E., 1962, Origin of basaltic magmas: An experimental study of natural and synthetic rock systems: Jour. Petrol., v. 3, p. 512-532.

APPENDIX A: Petrography

SAMPLE NUMBER	ROCK NAME	PHENOCRYSTS/MICRO-PHENOCRYSTS	G R O U MINERALS	N D M A DOMINANT TEXTURE	S S ALTERATION	REMARKS
6.4.1A	basalt	plag (andesine to labradorite)	plag, augite, Fe-Ti oxides, olivine	medium-grained, intergranular	very slight	Plagioclase phenocrysts occur as glomerocrysts and in cruciform twins. A xenolith of cumulus plagioclase-augite-olivine is found in the sample, although they are quite rare. Olivine is partially altered to saponite and chlorite.
7.8.2D	basalt	plag, augite, olivine	plag, augite, olivine, Fe-Ti oxides	very fine-grained, intergranular	very slight	Olivine has been mainly replaced by saponite, although unaltered grains are still recognizable. These range from phenocryst to groundmass in size.
7.9.2A	basalt	plag	plag, augite, Fe-Ti oxides, olivine(?)	fine-grained, intergranular	very slight	Most olivine, if originally present, has been completely altered to saponite. Small amounts of zeolite occur as vesicle fillings.
7.9.3A	basalt	plag and lesser olivine	plag, augite, olivine, Fe-Ti oxides	fine-grained, intergranular	very slight	This sample is extremely fresh in that it contains some unaltered olivine as both groundmass and phenocryst phases. Olivine grains mainly occur in clusters, partially to completely altered to saponite.
7.9.4A	basalt	plag, lesser augite	plag, augite, olivine, Fe-Ti oxides	fine-grained, intergranular	very slight	Olivine grains are completely altered to saponite. Plagioclase grains are mainly fresh, although a few laths show incipient corrosion and sericitization.
7.10.1A	basalt	normally-zoned plag (andesine to labradorite)	plag, augite (slightly subcalcic), Fe-Ti oxides, olivine(?)	aphyric, fine-grained intergranular	very slight	Plagioclase phenocrysts occur in glomerocrysts. Olivine is mainly replaced by saponite. Slight alteration of plagioclase occurs near fractures.
7.10.3A	basalt	plag	plag, augite, Fe-Ti oxides, olivine	fine-grained, intergranular	very slight	Some Fe-Ti oxides display trellis structures. Overall, sample is not very altered despite almost complete replacement of olivine by saponite- these tend to occur in clusters.
7.11.1A	basalt	plag (labradorite), augite	plag, augite, olivine (Fo80-90), Fe-Ti oxides	fine-grained, intergranular	very slight	Saponite is randomly distributed through the groundmass, and is replacing olivine. Along fractures, alteration of plagioclase laths is occurring as well.
8.6.1A	basalt	plag	plag, augite, Fe-Ti oxides, olivine(?)	fine-grained, intergranular	moderate	Plagioclase laths show incipient sericitization along fractures. Saponite is abundant in the groundmass, presumably replacing olivine. Some zeolite is present as vesicle fillings
8.6.2A	basalt	plag (labradorite) augite, olivine	plag, augite, olivine, Fe-Ti oxides	fine-grained, intergranular	moderate	Plagioclase phenocrysts occur in glomerocrysts. Most olivine is altered to saponite, although some fresh surfaces may be observed. Groundmass plagioclase laths show incipient corrosion.

SAMPLE NUMBER	ROCK NAME	PHENOCRYSTS/MICRO-PHENOCRYSTS	GROUNDMASS MINERALS	DOMINANT TEXTURE	ALTERATION	REMARKS
8.7.1A	basalt	plag (labradorite), augite (slightly subcalcic), opaques	plag, augite, Fe-Ti oxides, olivine(?)	fine-grained, intergranular	slight	Plagioclase phenocrysts occur in glomerocrysts. Groundmass augite grains enclose plagioclase microlites. Some plagioclase grains are altering to sericite, particularly along fractures. Clusters of saponite are rare but quite large in size, presumably replacing olivine.
8.7.2A	basalt	rare plagioclase	plag, augite, Fe-Ti oxides, olivine	very fine-grained, intergranular	slight	Rock is relatively unaltered compared with other samples in the suite, although some plagioclase phenocrysts show slight corrosion. Groundmass grains are quite fresh, except for olivine, which has been completely altered to saponite. Fe-Ti oxides surround small plag microlites.
8.7.3A	basalt	plag	plag, augite, olivine, Fe-Ti oxides	medium- to fine-grained, intergranular	very slight	Clusters of fresh olivine appear to be surrounded by saponite. Plagioclase phenocrysts are slightly fractured and corroded. Groundmass is quite fresh. Some unaltered olivine grains are present. Groundmass plagioclase microlites show incipient corrosion and sericitization. Augite grains enclose small microlites of plagioclase. Fe-Ti oxides enclose minute grains of augite and plag. The saponite patches partially enclose augite grains.
8.23.1A	basalt	plag (andesine to labradorite), augite (subcalcic)	plag, augite, olivine, Fe-Ti oxides	fine-grained, intergranular	very slight	Plagioclase phenocrysts occur in glomerocrysts. One of the least altered samples in the suite. Olivine grains are rimmed by iddingsite and partially replaced by saponite, but are otherwise quite fresh. Augite grains typically surround plag microlites, while anhedral opaque grains surround both plag and augite.
8.23.1C	basalt	plag, lesser augite	plag, augite, olivine, Fe-Ti oxides	fine-grained, intergranular	very slight	Augite phenocrysts are somewhat elongate in habit. Olivine is recognizable in the groundmass, generally rimmed by iddingsite, and is being replaced by saponite.
8.23.2C	basalt	rare plag	plag, augite, Fe-Ti oxides, olivine(?)	very fine-grained, intergranular	very slight	Groundmass plagioclase is quite fresh. No primary olivine is observed, but abundant chlorophaite patches in the groundmass are presumably alteration products of olivine. These patches enclose both plag microlites and augite grains.
9.8.2A	basalt	plag, olivine (Fo90-93)	plag, augite, Fe-Ti oxides, olivine	fine-grained, plagioclase-phyric, intergranular	very slight	Relatively fresh sample. Plagioclase phenocrysts show incipient corrosion, but are otherwise unaltered. Some relict olivine is present as both microphenocryst and groundmass phases. Olivine grains are partially to wholly replaced by saponite.

SAMPLE NUMBER	ROCK NAME	PHENOCRYSTS/MICRO-PHENOCRYSTS	GROUNDMASS MINERALS	DOMINANT TEXTURE	ALTERATION	REMARKS
9.11.1A	basalt	rare plag	plag, augite, Fe-Ti oxides, olivine(?)	fine-grained, intergranular	moderate	Plagioclase phenocrysts are almost completely replaced by sericite. Zeolitic clusters are present which surround groundmass-size plag and augite grains. Thin reaction rims have developed around these grains. The plag laths in contact with the zones of zeolitic alteration are moderately to completely sericitized. Clusters of saponite are presumably replacement products of olivine.
9.27.1A	basalt	rare plag	plag, augite, Fe-Ti oxides, olivine	very fine-grained, intergranular	very slight	Quite fresh in appearance, although patches of saponite are distributed throughout the sample. Some olivine is recognizable in the centers of these saponite clusters. Augite grains partially enclose plag microlites, while Fe-Ti oxides enclose plag and augite grains. Augite grains are partially incorporated in saponite clusters as well. Some of the plag microlites show incipient corrosion and sericitization.
10.15.1A (lower part of outcrop)	basalt- plagioclase phyric	plag (andesine to labradorite), augite microphenocrysts	plag, autite, Fe-Ti oxides, olivine(?)	fine- to medium-grained, intergranular to ophitic	very slight	The sample is relatively fresh despite complete replacement of olivine grains by saponite. Plagioclase phenocrysts occur in glomerocrysts and as cruciform twins. One of the coarsest-grained rocks observed in this suite.
10.15.1B (upper part of outcrop)	basalt	plag	sodic plagioclase, augite, olivine(?), Fe-Ti oxides, rare interstitial glass (altered to palagonite)	medium- to fine-grained, intergranular. Very vesicular	extreme	Very altered, zeolitized sample. Vesicles are partially to wholly filled by clays and zeolites (natrolite and clinozoisite). Olivine grains, if originally present, have been completely replaced by saponite. Groundmass plag microlites are moderately to severely corroded. Augite grains envelop small plag microlites.
10.18.1B	basaltic lithic tuff	lithic fragments of plag and augite	plag, augite, Fe-Ti oxides, interstitial palagonite	fine-grained, semi-trachytic, hemicrystalline. Highly vesicular.	extreme	Plagioclase lithic inclusions are highly sericitized. This sample is extremely altered. Vesicles are filled with clays and zeolites. Some groundmass opaque grains occur as anhedral patches, others display prominent trellis structures.
10.18.1C	basaltic lithic tuff	lithic fragments of plag and augite	plag, augite, Fe-Ti oxides, interstitial palagonite	fine-grained, semi-trachytic, hemicrystalline. Highly vesicular	extreme	Very altered sample. The vesicles are partially to completely filled in by clays and zeolites, Plagioclase lithic inclusions are highly corroded and sericitized. Some groundmass opaque grains display prominent trellis structures.
10.18.1G	basaltic lithic tuff	lithic fragments of plag and augite	plag, augite, Fe-Ti oxides, saponite, and interstitial palagonite	fine-grained, semi-trachytic, hemi-crystalline. Highly vesicular	extreme	The sample is highly altered and vesicular. Plagioclase lithic inclusions are corroded, while augite inclusions are highly fractured but otherwise unaltered. Vesicles are partially to wholly filled in by clays and zeolites. Microlites of plag in the groundmass are extremely corroded.

SAMPLE NUMBER	ROCK NAME	PHENOCRYSTS/MICRO-PHENOCRYSTS	G R O U N D MASS MINERALS	DOMINANT TEXTURE	ALTERATION	REMARKS
10.22.1A	basalt	plag (andesine to labradorite)	plag, augite, Fe-Ti oxides, olivine(?)	medium-grained, intergranular	extreme	This sample is extremely altered. Vesicles are filled with zeolites and clays. Plagioclase microlites show incipient corrosion and sericitization, particularly where they are close to fractures. Olivine, if originally present, has been completely altered to saponite. Opaque grains display prominent trellis structures.
10.22.1B	basalt	plag (andesine to labradorite)	plag, augite, Fe-Ti oxides, olivine(?)	medium-grained, intergranular	extreme	Sample is extremely altered. Vesicles are filled with zeolites and clays. Plagioclase microlites show incipient corrosion and sericitization, particularly where they are close to fractures. Olivine, if originally present, has been completely altered to saponite. Opaque grains display prominent trellis structures.
10.22.1C	basalt	plag (andesine to labradorite)	plag, augite, Fe-Ti oxides, olivine(?)	medium-grained, intergranular	extreme	Sample is extremely altered. Vesicles are filled with zeolites and clays. Plagioclase microlites show incipient corrosion and sericitization, particularly where they are close to fractures. Olivine, if originally present, has been completely altered to saponite. Opaque grains display prominent trellis structures.
10.22.1D	basalt	plag (andesine to labradorite)	plag, augite, Fe-Ti oxides, olivine(?)	medium-grained, intergranular	extreme	Sample is extremely altered. Vesicles are filled with zeolites and clays. Plagioclase microlites show incipient corrosion and sericitization, particularly where they are close to fractures. Olivine, if originally present, has been completely altered to saponite. Opaque grains display prominent trellis structures.
10.23.1A	basalt	plag	plag, augite, Fe-Ti oxides, olivine, interstitial glass	coarse-grained, intergranular. Hemicrystalline. Highly vesicular	extreme	Plagioclase phenocrysts show incipient corrosion and sericitization. Vesicles are partially to wholly filled with clays and zeolites. Groundmass olivine has been completely altered to saponite, while interstitial glass has been altered to palagonite. Opaque grains display trellis structures.
10.23.1B	basalt	plag	plag, augite, Fe-Ti oxides, olivine, interstitial glass	coarse-grained, intergranular. Hemicrystalline. Highly vesicular	extreme	Plagioclase laths are relatively unaltered. Vesicles are partially to wholly filled with zeolites and clays. Groundmass olivine has been completely altered to saponite, while glassy interstitial material has been altered to palagonite. Opaque grains display trellis structures.

SAMPLE NUMBER	ROCK NAME	PHENOCRYSTS/MICRO-PHENOCRYSTS	GROUNDMASS MINERALS	GROUNDMASS DOMINANT TEXTURE	ALTERATION	REMARKS
10.23.1C	basalt	plag	plag, augite, Fe-Ti oxides, olivine, interstitial glass	coarse-grained, intergranular. Hemicrystalline. Very vesicular.	extreme	Very altered sample. Vesicles are partially to wholly filled with zeolites, clays, and carbonate. Plagioclase laths show incipient corrosion. Groundmass olivine has been completely altered to saponite, while glassy material has been altered to palagonite. Opaque grains display trellis structures.
10.23.2A	basalt	plag (labradorite) with lesser augite	plag, augite, Fe-Ti oxides, lesser olivine and interstitial glass	fine-grained, intergranular	moderate to extreme	Plagioclase phenocrysts occur in glomerocrysts. Sample is extremely altered in some parts, though less altered in other sections. Alteration appears to be deuteric, since it is strongest in close proximity to throughgoing fractures. Plagioclase laths are corroded and sericitized near fractures, while olivine is completely altered to saponite. Interstitial glass has been altered to palagonite. Natrolite fills in most of the fractures which cut through the sample. Augite grains are corroded near these fractures. Opaque grains display prominent trellis structures.
10.23.2B	basalt	plag and augite	plag, augite, Fe-Ti oxides, lesser olivine(?)	fine-grained, intergranular	slight	Plagioclase phenocrysts occur in glomerocrysts and as cruciform twins. One of the larger plag phenocrysts contains euhedral to subhedral opaque grains which are oriented parallel to the cleavage direction. A small amount of saponite is present, presumably replacing olivine. Some opaque grains display trellis structures.
10.23.2C	basalt	plag (labradorite) and augite	plag, augite, Fe-Ti oxides, minor olivine(?)	fine-grained, intergranular	slight	This sample is relatively fresh. Little to no alteration of plagioclase has occurred. Saponite clusters are abundant, however, and are presumably replacement products of olivine.
10.28.1A	porphyritic basalt	xenoliths of cumulus plag-augite-olivine	plag, augite, olivine, and Fe-Ti oxides (abundant relative to other Black Hills samples)	cumulophyric; groundmass is fine-grained, intergranular	very slight	This sample contains xenoliths of cumulate olivine-augite-plagioclase. These clusters contain no interstitial melt. The typical xenolith contains about 70% plag, 20-25% augite, and 5-10% olivine. Virtually no Fe-Ti oxides occur in these xenoliths. This abundance of cumulate xenoliths is unusual in the Black Hills suite. Plagioclase laths and augite grains within the xenoliths are virtually unaltered, although the olivine grains are partially to wholly replaced by saponite. Within the groundmass, alteration of olivine grains is more extensive. Groundmass augite grains surround plag microlites, while clusters of saponite partially surround both augite and plagioclase.

APPENDIX B: Paleomagnetic and geochemical site locations

PALEOMAG. SITE	GEOCHEM. SAMPLES	USGS 15' QUAD	SECTION	COUNTY	DESCRIPTION
78.01	- - - - -	Shelton	NE¼ NE¼ sec. 15, T18N R3W	Thurston	Aberdeen-Olympia freeway (SR 8), about 4 km west of interchange with US 101
78.02	- - - - -	Shelton	NE¼ NE¼ sec. 15, T18N R3W	Thurston	0.8 km west of site 78.01
78.03	- - - - -	Shelton	NE¼ NE¼ sec. 15, T18N R3W	Thurston	0.4 km west of site 78.02
78.04	6.4.1A	Shelton	NW¼ NW¼ sec. 17, T19N R3W	Mason	Quarry on north side of US 101 at intersection of Hurley-Waldrup Road
78.05	- - - - -	Shelton	NW¼ NW¼ sec. 17, T19N R3W	Mason	50 m north of site 78.04
78.06	- - - - -	Shelton	NE¼ SE¼ sec. 18, T19N R3W	Mason	US 101 near Kamilche Valley cut-off
7.8.78.1	- - - - -	Olympia	NE¼ sec. 29, T18N R2W	Thurston	Quarry on west side of Black Lake Blvd., south of Tumwater
7.8.78.2	7.8.2D	Olympia	SW¼ SW¼ sec. 29, T18N R2W	Thurston	Roadcut on west side of Black Lake Blvd. just north of the north shore of Black Lake
7.9.78.1	- - - - -	Olympia	SE¼ SW¼ sec. 12, T18N R3W	Thurston	Secondary road above US 101 and SR 8 freeway interchange
7.9.78.2	- - - - -	Rochester	SW¼ sec. 14, T17N R4W	Thurston	Capitol Peak access road, Capitol Forest
7.9.78.3	7.9.3A	Rochester	NE¼ sec. 16, T17N R4W	Grays Harbor	Iron Creek Rd. at intersection with Porter Creek Rd., Capitol Forest
7.9.78.4	7.9.4A	Shelton	NW¼ NE¼ sec. 18, T18N R3W	Thurston	Summit Lake Lakeshore Rd. Outcrop on east side of road
7.10.78.1	7.10.1A	Shelton	NE¼ NE¼ sec. 11, T18N R3W	Thurston	Shaker Church Road junction with eastbound lanes of US 101
7.10.78.2	- - - - -	Rochester	NW¼ NW¼ sec. 9, T16N R3W	Thurston	Bordeaux Road entrance to Capitol Forest, 3.2 km west of junction with Gate - Mima Road
7.10.78.3	7.10.3A	Rochester	SW¼ sec. 35, T17N R4W	Thurston	Sherman Valley Rd. about 2 km north of junction with Cedar Creek Rd., Capitol Forest
7.10.78.4	7.10.4A	Rochester	NE¼ sec. 13, T17N R4W	Thurston	Sherman Creek Rd. about 0.5 km south of intersection with Waddell Creek Rd., Capitol Forest

PALEOMAG. SITE	GEOCHEM. SAMPLES	USGS 15' QUAD	SECTION	COUNTY	DESCRIPTION
8.6.78.1	- - - - -	Rochester	NW¼ NE¼ sec. 25, T16N R4W	Grays Harbor	Quarry on north side of US 12, 2 km west of Oakville
8.6.78.2	8.6.2A	Malone	NW¼ sec. 34, T17N R5W	Grays Harbor	North side of US 12 near Gibson Creek, about 10.5 km northwest of Oakville
8.7.78.1	8.7.1A	Rochester	SW¼ sec. 8, T16N R4W	Grays Harbor	Cedar Creek Rd., about 1 km NE of junction with North Creek Rd., Capitol Forest
8.7.78.2	- - - - -	Rochester	SE¼ SE¼ sec. 7, T16N R4W	Grays Harbor	Shelton Creek streambed just south of Cedar Creek Rd., Capitol Forest
8.7.78.3	8.7.3A	Rochester	NW¼ sec. 9, T16N R4W	Grays Harbor	Cedar Creek Rd. about 0.5 km north of North Creek campground, Capitol Forest
8.23.78.1	8.23.1A	Rochester	SW¼ NE¼ sec. 15, T17N R4W	Grays Harbor	Sherman Valled Rd. near Monroe Creek, Capitol Forest
8.23.78.2	8.23.2A	Rochester	sections 10-11, T17N R4W	Thurston-Grays Harbor	Capitol Peak access road at section boundary, Capitol Forest
9.8.78.1	- - - - -	Rochester	SW¼ sec. 12, T17N R4W	Thurston	Auxillary road south of Capitol Peak, Capitol Forest
9.8.78.2	9.8.2A	Rochester	SW¼ sec. 21, T17N R4W	Grays Harbor	Porter Creek Rd., about 0.8 km west of North Creek Rd., Capitol Forest
9.11.78.1	9.11.1A	Malone	NW¼ NW¼ sec. 12, T17N R5W	Grays Harbor	Buck Ridge Rd., about 0.8 km NE of Porter Creek Rd, Capitol Forest
9.27.78.1	9.27.1A	Rochester	NE¼ SW¼ sec. 18, T17N R4W	Grays Harbor	Porter Creek Rd., 6.4 km west of North Creek Rd., Capitol Forest
10.9.78.1	- - - - -	Rochester	SE¼ NW¼ sec. 21, T17N R4W	Grays Harbor	Porter Creek Rd., 0.3 km NE of North Creek Rd., Capitol Forest
10.9.78.2	10.9.2D	Malone	SE¼ sec. 12, T17N R4W	Grays Harbor	Porter Creek Rd., 8.5 km west of North Creek Rd., Capitol Forest
10.15.78.1	10.15.1A	Shelton	SW¼ sec. 14, T19N R5W	Mason	Cloquallum Rd., 1.5 km west of Highland Rd.
- - - - -	10.18.1A, 10.18.1B, 10.18.1C, 10.18.1G	Shelton	NE¼ NW¼ sec. 2, T19N R4W	Mason	Secondary road north of Cloquallum Rd., 2 km west of Isabelle Lake

PALEOMAG. SITE	GEOCHEM. SITE	USGS 15' QUAD	SECTION	COUNTY	DESCRIPTION
10.22.78.1	10.22.1A, 10.22.1B, 10.22.1C	Shelton	NW¼ NW¼ sec. 19, T19N R3W	Mason	Quarry on NW side of SR 108 just north of railroad tracks
10.23.78.1	10.23.1B, 10.23.1C	Elma	SW¼ NE¼ sec. 1, T18N R5W	Grays Harbor	SR 108, about 1.5 km NE of junction with McCleary-Hillgrove Rd.
10.23.78.2	10.23.2A, 10.23.2B, 10.23.2C	Shelton	NW¼ NE¼ sec. 8, T18N R3W	Thurston	Summit Lake Lakeshore Rd., NE end of lake
10.28.78.1	10.28.1A	Shelton	SE¼ NE¼ sec. 1, T18N R4W	Thurston	Kennedy Falls, north of SR 8
7.9.79.1	- - - - -	Rochester	SW¼ NW¼ sec. 15, T15N R4W	Lewis	Independence Rd., junction with Hyppa Rd.
7.8.79.1	- - - - -	Rochester	SW¼ NW¼ sec. 26, T16N R4W	Thurston	Quarry west of Gate, north of railroad tracks
7.8.79.2	- - - - -	Rochester	SW¼ SW¼ sec. 20, T16N R3W	Thurston	Gate - Mima Road, 8.5 km SW of Little Rock

APPENDIX C:

GEOCHEMISTRY- SAMPLING AND ANALYTICAL PROCEDURES

A total of 30 samples of Crescent Formation basalts from the Black Hills and peripheral areas to the north have been analyzed for whole rock major element compositions. Of these 30 samples, 29 have been analyzed for the trace elements Cr, V, Sr, Zr, Rb, Y, and Nb. Volatile loss determinations were performed as well, although no attempt was made to determine ferrous/ferric iron ratios by the iron titration method. Laboratory methods will be described in some detail, since they are non-standard.

Numerous hand specimens were collected in the field for geochemical study, the majority of which came from the same localities as the paleomagnetic core samples. Generally the most coherent, least oxidized, and least vesicular material was collected. Thin sections of the specimens were examined and, where possible, only those specimens showing the least chloritization and/or zeolitization were selected for analysis. Figure 55 shows the locations at which the selected specimens were collected.

In the laboratory each selected sample was cut into rectangular chips on a diamond saw. The chips were polished on a lapidary wheel to remove saw marks, and cleaned with alcohol to remove any scouring grit. The chips were next reduced in size using the Braun Chipmunk rock crusher. Several replicate chips of each sample were processed through the crusher before the sample actually used in the analysis was crushed. This practice, combined with thorough cleaning of the instrument before each sample reduction, served to minimize cross-contamination. The sample fragments were then further

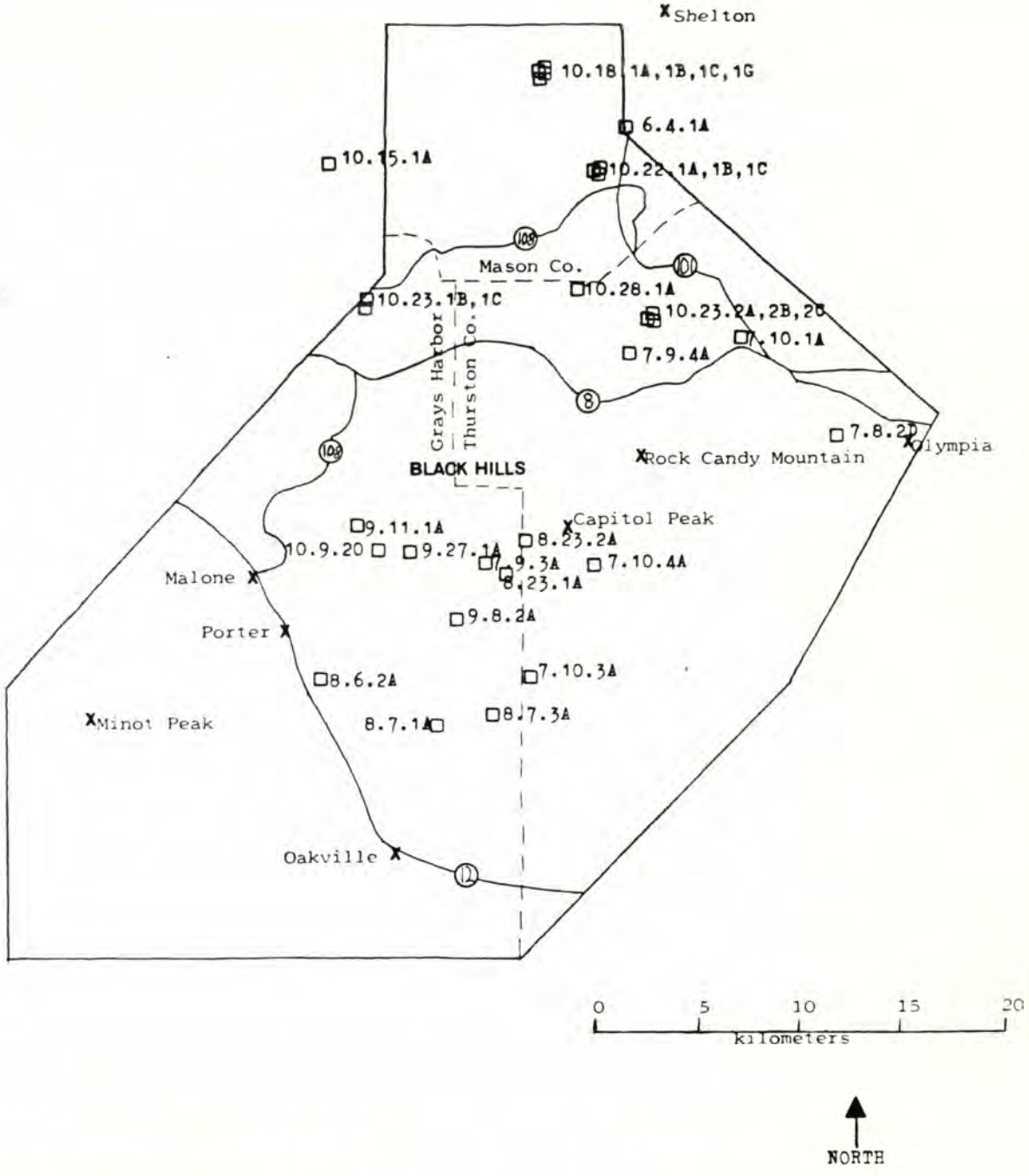

Figure 55: Locations of geochemical sampling sites in Black Hills area.

pulverized using a Spex shatterbox, and made to pass through a -200 mesh nylon cloth. Sample powders were transferred to plastic containers and homogenized by being shaken for 20 minutes in a Spex mixer/mill.

Major element analyses: Chemical stock solutions of each sample were prepared by fusing 0.3 g rock powder with 1.8 g lithium metaborate for 15 minutes in a muffle furnace at 1000° C. The molten beads were next dissolved in 50 ml hydrochloric acid, and brought to 100 ml with distilled deionized water. Two solutions were prepared:

(1) 25 ml were withdrawn from the stock solution, and combined with 7.0 ml lithium solution consisting of 1.23 g lithium chloride per 10 ml H_2O. This solution was diluted to 100 ml with H_2O, and was used to analyze for SiO_2 and Al_2O_3.

(2) 5 to 10 ml of the above solution were combined with 10 ml of the lithium solution and 1 ml of lanthanum solution (0.254 g lanthanum chloride/ 10 ml H_2O), and diluted to 100 ml. This solution was used to analyze for total iron as Fe_2O_3, MgO, CaO, Na_2O, K_2O, TiO_2, and MnO.

The lithium and lanthanum solutions minimized inter-element absorption and enhancement effects. Several, but not all of the samples, were prepared and analyzed in duplicate to verify analytical precision.

Elemental compositions of the samples were determined by comparing them with a set of whole rock standards, which were prepared in the same manner as the samples. The following standards were used in the analyses: QLO-1, NIM-N, NIM-D, NIM-G, BA, TON, GRAN,

JB-1, ARHCO-1, BC-4, TP, and DIOR. Not all of these standards were used in the final calculations. The latter three standards are Western Washington University in-house standards whose major element compositions are given in Table 5.

The samples were analyzed on a Perkin-Elmer Model 306 atomic absorption spectrophotometer. The nitrous oxide/acetylene flame was used in analyzing for SiO_2, Al_2O_3, CaO, TiO_2, and MnO. The air/acetylene flame was used for Fe_2O_3, MgO, Na_2O, and K_2O. In order to minimize instrument drift, the mean of five integrated counting intervals of 10 seconds duration was recorded. Calibration solutions were analyzed after every fifth sample to construct a curve of machine drift as a function of time. This curve was used for correcting sample and standard absorption values. In addition, one or more of the standards were run as unknowns during each experiment as a check on analytical accuracy. Data were reduced using least-squares best-fit curves relating concentration to absorption values. Samples whose totals were less than 97.0% or greater than 101.0% were re-analyzed.

Trace element analyses: Homogenized powders of 29 samples were pressed into pellets and analyzed for trace elements on a Philips Model 1410 x-ray fluorescence spectrometer, which is housed in the Geochronology Laboratory, Department of Geological Sciences, University of British Columbia. The following rock standards were used in the analyses (although not all of them were entered into the data reduction program): AGV-1, BCR-1, GH, W-1, GSP, JB-1, JG-1, NIM-N, NIM-D, and NIM-S. Data were reduced using several computer programs which determined least-squares best-fit regression lines for a cer-

Table 5 : Major element compositions of three Western Washington University in-house standards: BC-4, TP, and DIOR.

Element	BC-4	TP	DIOR
SiO_2	50.9	62.2	56.1
Al_2O_3	14.9	16.4	15.7
Fe_2O_3*	14.3	5.4	8.7
MgO	4.5	2.3	9.3
CaO	8.4	4.6	8.1
Na_2O	2.7	4.3	2.7
K_2O	0.9	2.1	0.4
TiO_2	2.1	0.8	0.7
MnO	0.24	0.10	0.15
TOTAL	98.81	98.40	101.81

*Total iron as Fe_2O_3

tain number of standards. These standards were selected by an iterative process which eliminated those standards with abnormally high or low values of a given element, thereby minimizing the total standard deviation. Samples which showed unacceptable background fits or standard deviations were re-analyzed.

CIPW norms were calculated according to the standard procedure. Since the calculation requires that the ratio of ferrous to ferric iron by known, arbitrary values had to be assigned since an iron titration was not performed. I omitted the titration because the FeO/Fe_2O_3 ratio is extremely susceptible to secondary alteration. For example, a significant change in this ratio was observed as a linear function of the duration of crushing time for a sample in the Spex mixer/mill (J. A. Ashelman, 1977, oral comm.). It was decided that the FeO/Fe_2O_3 ratio determined by the iron titration method would not reflect the original composition of the sample, and would be of limited usefulness in the CIPW norm calculation. For this reason values of Fe_2O_3 and FeO were assigned according to the following method, as first suggested by Irvine and Baragar (1971):

Wt. % Fe_2O_3= wt. % TiO_2 + 1.5

The remaining iron was converted to FeO.

The average FeO/Fe_2O_3 ratio in the Black Hills suite is 2.2, and ranges from 1.7 to 2.6. Macdonald (1968) reports an average FeO/Fe_2O_3 ratio of 2.8 for 200 tholeiites and olivine tholeiites from Hawaii. The normative classification depends heavily on the ratio of FeO/Fe_2O_3 used in the CIPW norm calculation. Under-estimation of this ratio results in higher amounts of normative nepheline,

and lesser amounts of hypersthene or quartz (Clague, 1974).

APPENDIX D: Major- and trace-element analyses.

Major element (wt. percent)	6.4.1A	7.8.2D	7.9.3A	7.9.4A	7.10.1A
SiO_2	48.3	47.4	49.0	47.6	46.7
Al_2O_3	14.6	14.5	14.6	14.5	14.0
Fe_2O_3(t)	14.5	13.4	12.6	13.7	15.1
MgO	6.0	5.8	7.3	6.3	5.8
CaO	11.6	13.0	11.5	12.9	12.6
Na_2O	2.7	2.7	2.7	2.5	2.6
K_2O	0.21	0.20	0.23	0.14	0.15
TiO_2	2.3	2.5	2.0	2.1	2.7
MnO	0.20	0.19	0.20	0.19	0.19
TOTAL	100.41	99.69	100.13	99.93	99.84
LOI	0	0.05	0.03	0.07	0.04
CIPW norm					
Qz	0	0	0	0	6.07
Or	1.27	1.22	1.38	0.85	0.92
Ab	24.78	25.24	24.34	23.15	24.28
An	27.96	27.63	27.77	28.62	27.05
Mt	4.09	4.35	3.73	3.91	4.50
Il	3.30	3.64	2.84	3.06	3.83
Di	24.99	31.19	24.34	29.79	30.23
Hy	12.40	2.49	13.56	6.12	4.04
Ol	1.22	4.23	2.04	4.50	5.16
Ne	0	0	0	0	0
Trace element (ppm)					
Cr	86.	230.	210.	113.	82.
V	345.	375.	287.	331.	372.
Sr	278.	217.	253.	231.	280.
Zr	164.	179.	135.	146.	212.
Y	32.	35.	29.	31.	39.
Rb	7.5	4.7	5.1	6.7	4.9
Nb	25.	16.	21.	15.	27.
Ratios					
Na_2O/K_2O	12.8	13.7	11.6	17.9	17.4
Rb/Sr	0.027	0.022	0.020	0.029	0.018
K/Rb	232.	353.	374.	173.	254.
$^{87}Sr/^{86}Sr$	--	--	0.7033, 0.7033	--	--

Major element (wt.percent)	7.10.3A	7.10.4A	8.6.2A	8.7.1A	8.7.3A
SiO_2	50.7	50.7	46.6	49.3	49.2
Al_2O_3	15.4	15.0	15.0	14.5	15.6
Fe_2O_3(t)	13.2	12.6	11.9	12.3	12.2
MgO	5.0	6.3	6.7	7.5	6.6
CaO	11.3	11.3	13.0	10.9	10.7
Na_2O	2.3	2.3	2.4	2.6	2.4
K_2O	0.03	0.17	0.19	0.35	0.30
TiO_2	2.2	1.9	2.0	2.1	2.2
MnO	0.36	0.23	0.17	0.20	0.17
TOTAL	100.49	100.50	97.96	99.75	99.37
LOI	0.11	0.16	0.16	0.06	0.25
CIPW norm					
Qz	6.07	4.23	0	0.20	2.57
Or	0.18	1.03	1.15	2.11	1.81
Ab	21.47	20.94	22.87	24.22	22.14
An	32.35	30.76	30.58	27.29	31.80
Mt	4.00	3.64	3.71	3.87	4.02
Il	3.17	2.71	2.86	3.02	3.21
Di	20.41	21.23	29.28	22.10	18.21
Hy	12.32	15.46	3.03	17.19	16.25
Ol	0	0	6.52	0	0
Ne	0	0	0	0	0
Trace element (ppm)					
Cr	--	213.	178.	167.	180.
V	--	314.	310.	301.	286.
Sr	--	249.	286.	252.	240.
Zr	--	143.	146.	151.	145.
Y	--	29.	30.	31.	28.
Rb	--	7.3	4.3	9.0	10.0
Nb	--	15.	24.	25.	24.
Ratios					
Na_2O/K_2O	77.3	13.4	12.8	7.5	8.0
Rb/Sr	--	0.029	0.015	0.036	0.042
K/Rb	--	193.	367.	322.	250.
$^{87}Sr/^{86}Sr$	--	--	0.7031	--	0.7028, 0.7029

Major element (wt. percent)	8.23.1A	8.23.2A	9.8.2A	9.11.1A	9.27.1A
SiO_2	49.6	49.0	50.2	49.3	52.1
Al_2O_3	13.9	15.4	15.1	15.0	14.8
Fe_2O_3(t)	13.6	11.9	10.5	11.8	11.6
MgO	7.1	7.6	6.8	7.3	5.5
CaO	11.0	11.2	11.4	11.3	10.6
Na_2O	2.8	2.5	2.6	2.7	2.5
K_2O	0.31	0.32	0.24	0.29	0.25
TiO_2	2.4	1.9	2.1	2.1	1.8
MnO	0.22	0.19	0.18	0.19	0.29
TOTAL	100.93	100.01	99.12	99.98	99.44
LOI	0	0.23	0.15	0.23	0.09
CIPW norm					
Qz	0.22	0	2.83	0	6.66
Or	1.88	1.92	1.44	1.74	1.52
Ab	25.38	22.90	24.26	24.55	23.31
An	24.97	30.33	29.29	28.52	29.31
Mt	4.10	3.65	3.82	3.79	3.54
Il	3.35	2.75	2.96	2.93	2.57
Di	24.46	20.84	22.97	22.86	20.17
Hy	15.64	16.70	12.34	15.58	12.92
Ol	0	0.91	0	0.01	0
Ne	0	0	0	0	0
Trace element (ppm)					
Cr	113.	204.	227.	204.	151.
V	301.	291.	313.	298.	343.
Sr	267.	241.	257.	205.	235.
Zr	163.	140.	139.	130.	164.
Y	33.	28.	32.	29.	33.
Rb	6.0	4.9	4.9	7.1	10.0
Nb	24.	24.	23.	11.	18.
Ratios					
Na_2O/K_2O	9.0	7.8	11.0	9.3	10.0
Rb/Sr	0.022	0.020	0.019	0.035	0.043
K/Rb	428.	542.	406.	340.	208.
$^{87}Sr/^{86}Sr$	--	--	--	--	--

Major element (wt. percent)	10.9.20	10.15.1A	10.18.1A	10.18.1B	10.18.1C
SiO_2	49.3	48.2	48.3	52.1	50.2
Al_2O_3	14.9	14.9	13.5	13.3	13.3
Fe_2O_3	12.9	12.9	16.7	14.3	13.9
MgO	7.2	6.3	5.1	4.1	4.2
CaO	11.1	11.3	10.3	10.9	9.2
Na_2O	2.6	2.7	2.8	2.4	2.7
K_2O	0.26	0.12	0.36	0.37	0.88
TiO_2	2.3	2.0	2.9	2.9	3.1
MnO	0.19	0.20	0.24	0.31	0.21
TOTAL	100.75	98.65	100.20	100.68	97.69
LOI	0	0.03	0.10	0.29	0.27
CIPW norm					
Qz	0.84	0	1.22	9.16	7.08
Or	1.57	0.73	2.21	2.29	5.56
Ab	23.22	25.36	26.41	22.53	26.29
An	28.88	29.21	24.10	25.37	22.80
Mt	4.03	3.80	4.82	4.73	4.97
Il	3.25	2.89	4.26	4.12	4.55
Di	21.51	23.30	23.18	24.82	20.74
Hy	16.70	14.48	13.81	6.98	8.01
Ol	0	0.22	0	0	0
Ne	0	0	0	0	0
Trace element (ppm)					
Cr	167.	101.	23.	30.	41.
V	300.	301.	440.	372.	372.
Sr	253.	240.	166.	343.	488.
Zr	144.	147.	211.	240.	240.
Y	30.	32.	42.	43.	51.
Rb	7.8	4.1	8.7	14.	15.
Nb	25.	23.	19.	30.	30.
Ratios					
Na_2O/K_2O	9.8	22.7	7.9	6.5	3.1
Rb/Sr	0.031	0.017	0.052	0.039	0.030
K/Rb	276.	242.	346.	228.	500.
$^{87}Sr/^{86}Sr$	--	--	--	--	--

Major element (wt. percent)	10.18.1G	10.22.1A	10.22.1B	10.22.1C	10.23.1B
SiO_2	48.8	48.7	47.6	50.7	49.4
Al_2O_3	13.9	15.1	15.3	15.2	13.7
Fe_2O_3(t)	15.6	14.1	14.6	13.6	16.4
MgO	5.5	5.1	5.4	4.6	4.6
CaO	10.3	10.5	11.2	11.0	9.6
Na_2O	2.4	2.4	2.6	2.4	2.7
K_2O	0.65	0.05	0.10	0	0.16
TiO_2	3.2	2.9	2.9	2.4	2.7
MnO	0.19	0.26	0.19	0.31	0.33
TOTAL	100.54	99.11	99.89	100.21	99.59
LOI	0.23	0.16	0.10	0.19	0.09
CIPW norm					
Qz	3.34	5.15	1.50	7.02	4.72
Or	4.01	0.31	0.61	0	0.99
Ab	22.20	22.64	24.19	22.09	25.46
An	26.10	31.77	30.92	31.93	25.95
Mt	5.08	4.75	4.74	4.25	4.65
Il	4.56	4.16	4.16	3.50	4.01
Di	21.48	18.25	21.37	19.62	19.40
Hy	13.22	12.96	12.52	11.58	14.82
Ol	0	0	0	0	0
Ne	0	0	0	0	0
Trace element (ppm)					
Cr	43.	56.	58.	54.	11.
V	407.	394.	433.	421.	471.
Sr	361.	272.	297.	302.	189.
Zr	248.	186.	207.	193.	233.
Y	35.	32.	35.	33.	45.
Rb	13.	5.0	5.3	4.8	5.5
Nb	32.	20.	25.	23.	22.
Ratios					
Na_2O/K_2O	3.7	48.2	26.0	--	16.9
Rb/Sr	0.035	0.018	0.018	0.016	0.029
K/Rb	422.	84.	156.	--	242.
$^{87}Sr/^{86}Sr$	--	--	--	--	--

Major element (wt. percent)	10.23.1C	10.23.2A	10.23.2B	10.23.2C	10.28.1A
SiO_2	47.8	48.9	48.3	47.9	51.1
Al_2O_3	13.7	14.2	14.1	14.3	15.2
Fe_2O_3(t)	13.8	14.5	14.2	14.9	12.7
MgO	6.9	5.9	6.3	5.7	4.9
CaO	9.8	8.6	10.4	11.9	10.8
Na_2O	2.8	3.6	2.7	2.7	2.5
K_2O	0.47	0.43	0.20	0.24	0.18
TiO_2	2.5	2.7	2.7	2.7	1.9
MnO	0.21	0.19	0.22	0.20	0.31
TOTAL	97.98	99.02	99.12	100.54	99.59
LOI	0.40	0.49	0.15	0.04	0
CIPW norm					
Qz	0	0	1.46	0	6.04
Or	2.91	2.63	1.22	1.47	1.10
Ab	26.68	33.61	25.53	24.68	22.80
An	24.19	21.87	26.74	27.10	31.13
Mt	4.37	4.55	4.54	4.49	3.67
Il	3.64	3.90	3.87	3.80	2.73
Di	21.28	17.97	21.37	27.08	19.60
Hy	15.83	13.28	15.26	10.38	12.93
Ol	1.10	2.20	0	1.00	0
Ne	0	0	0	0	0
Trace element (ppm)					
Cr	131.	98.	85.	119.	116.
V	376.	393.	366.	395.	334.
Sr	240.	138.	253.	228.	263.
Zr	159.	206.	215.	210.	170.
Y	35.	38.	40.	38.	32.
Rb	8.4	6.6	5.4	7.1	9.0
Nb	13.	21.	28.	21.	18.
Ratios					
Na_2O/K_2O	6.0	8.4	13.7	11.1	13.6
Rb/Sr	0.035	0.048	0.021	0.031	0.034
K/Rb	464.	540.	308.	280.	166.
$^{87}Sr/^{86}Sr$	--	--	--	--	0.7029

Major element (wt. percent)	Average of 30 samples	Range	Error (2σ)
SiO_2	49.1	46.6 - 52.1	2.8
Al_2O_3	14.6	13.3 - 15.6	1.3
Fe_2O_3(t)	13.5	10.5 - 16.7	2.8
MgO	6.0	4.1 - 7.6	2.0
CaO	11.1	8.6 - 13.0	2.0
Na_2O	2.6	2.3 - 3.6	0.5
K_2O	0.26	0.0 - 0.88	0.34
TiO_2	2.4	1.8 - 3.2	0.80
MnO	0.22	0.17 - 0.36	0.05
TOTAL	99.78	---	--
LOI	0.14	---	--
CIPW norm			
Qz	1.99		
Or	1.59		
Ab	24.29		
An	28.06		
Mt	4.21		
Il	3.45		
Di	22.84		
Hy	13.58		
Ol	0.0		
Ne	0.0		
Trace element (ppm)			
Cr	122.	11. - 245.	132
V	354.	286. - 471.	102
Sr	259.	138. - 489.	124
Zr	178.	130. - 248.	72
Y	34.	28. - 51.	11
Rb	7.3	4.1 - 14.6	5.7
Nb	22.	11. - 32.	10
Ratios			
Na_2O/K_2O	15.1	3.1 - 77.3	
Rb/Sr	0.029	0.015 - 0.052	
K/Rb	296.	84. - 542.	
$^{87}Sr/^{86}Sr$	0.7030	0.7028 - 0.7033	0.0004

*Sample 7.10.3A is not analyzed for trace-elements

APPENDIX E: Paleomagnetic data for all sites and core samples. Data presented as natural remanent magnetizations, and as measurements following demagnetization at optimum field. Equal area plots are for both NRM and demagnetized measurements. Solid circles correspond to lower hemisphere, open circles to upper hemisphere. Square represents site mean, normal polarity; triangle represents site mean, reversed polarity.

Black Hills Project

FISHER ON SAMPLE DIRECTIONS

Site: 78.01 -- SR 8, Perry Creek Demagnetization level: NRM

NE¼ NE¼ sec. 15, T. 18 N., R. 3 W.

Sample number	Declination	Inclination
001	36.5	42.0
002	17.04	32.47
003	3.69	65.81
004	359.48	49.78
005	16.57	46.23
006	295.25	30.95
007	9.21	32.30

R= 6.36 Site declination= 3.53 Site inclination= 47.06

Alpha 95= 17.34 Delta= 24.77 Kappa= 9.31

Site latitude= 47.12° Site longitude= 123.12°

Paleolatitude= 70.93°N Paleolongitude= 47.32°E DELP= 14.50

DECLM= 22.42

Black Hills Project

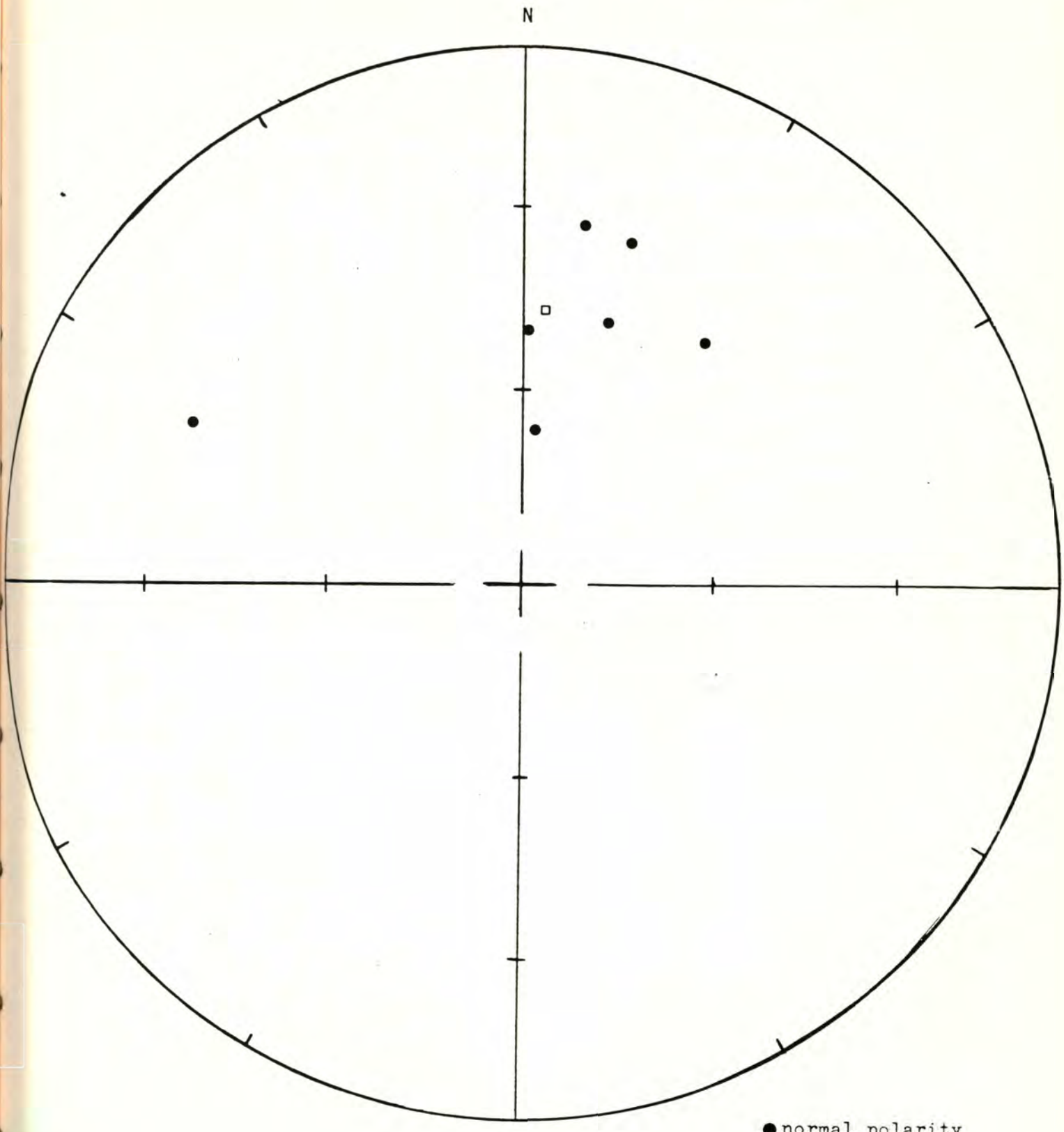

● normal polarity

○ reversed polarity

□ site mean, normal polarit

△ site mean, reversed polarity

Site: 78.01 - SR 8, Perry Creek

Demagnetization level: NRM

FISHER ON SAMPLE DIRECTIONS

Site: 78.01 -- SR 8, Perry Creek Demagnetization level: 100 oe.

NE¼ NE¼ sec. 15, T. 18 N., R. 3 W.

Sample number	Declination	Inclination
001	336.21	61.42
002	3.52	51.85
003	2.5	53.67
004	0.47	33.66
005	345.17	58.23
006	42.57	46.58
007	15.15	52.51

R= 6.77 Site declination= 5.14 Site inclination= 52.78

Alpha 95= 10.27 Delta= 14.59 Kappa= 26.57

Site latitude= 47.12° Site longitude= 123.12°

Paleolatitude= 75.69°N Paleolongitude=39.25°E DELP= 9.79

DECLM= 14.18

Black Hills Project

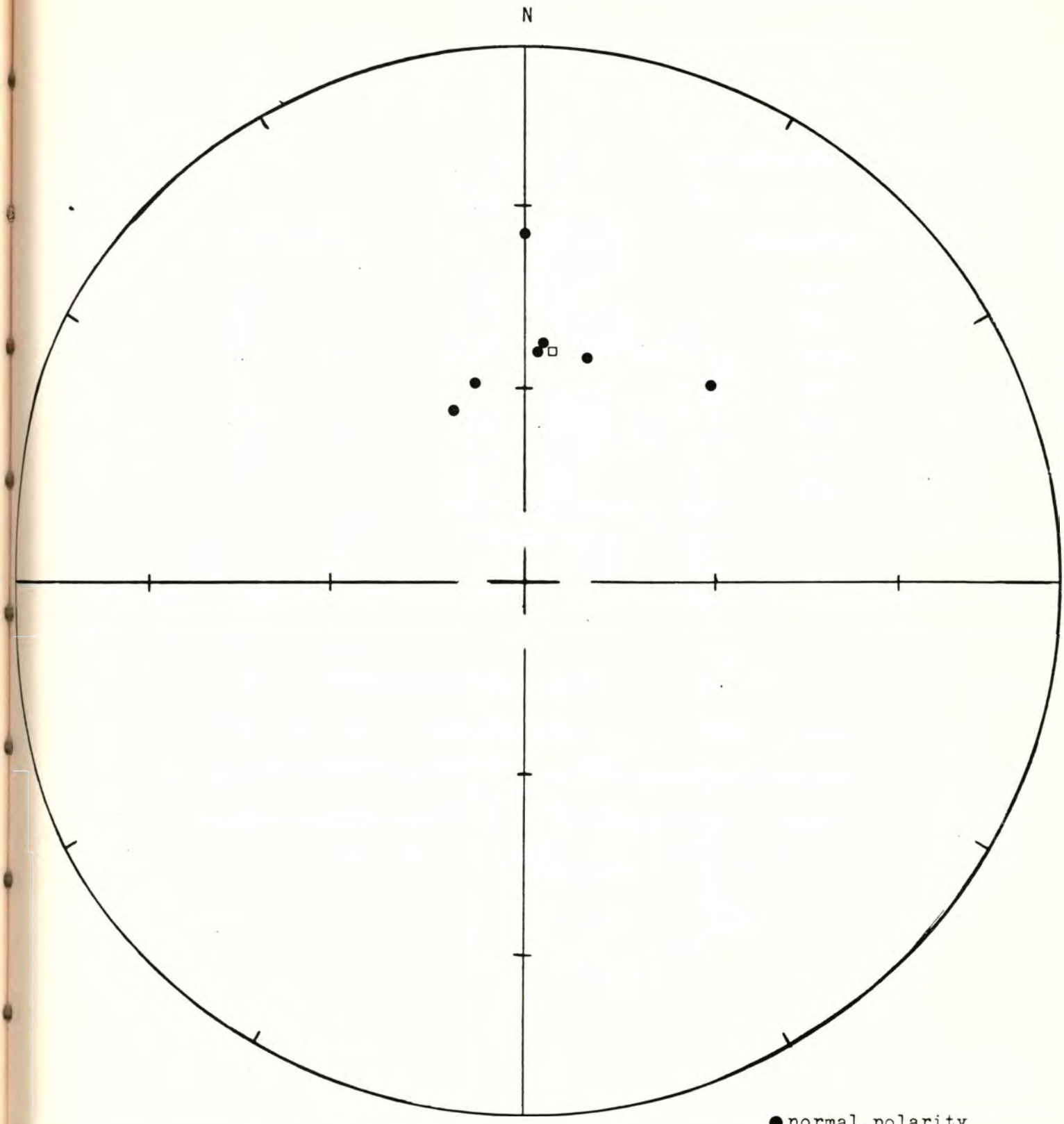

Site: 78-01 - SR 8, Perry Creek

Demagnetization level: 100 oe.

● normal polarity

○ reversed polarity

□ site mean, normal polarity

△ site mean, reversed polarity

FISHER ON SAMPLE DIRECTIONS

Site: 78.02 -- SR 8, Perry Creek Demagnetization level: NRM

NE¼ NE¼ sec. 15, T. 18 N., R. 3 W.

Sample number	Declination	Inclination
011	18.20	47.80
012	6.67	74.53
013	347.55	82.62
014	346.94	62.39
015	57.92	87.03
016	18.63	65.67
017	15.93	55.64

R= 6.79 Site declination= 10.19 Site inclination= 68.57

Alpha 95= 9.97 Delta= 14.17 Kappa= 28.17

Site latitude= 47.12°N Site longitude= 123.12°W

Paleolatitude= 81.87°N Paleolongitude= 72.58°W DELP= 14.24

DECLM= 16.85

Black Hills Project

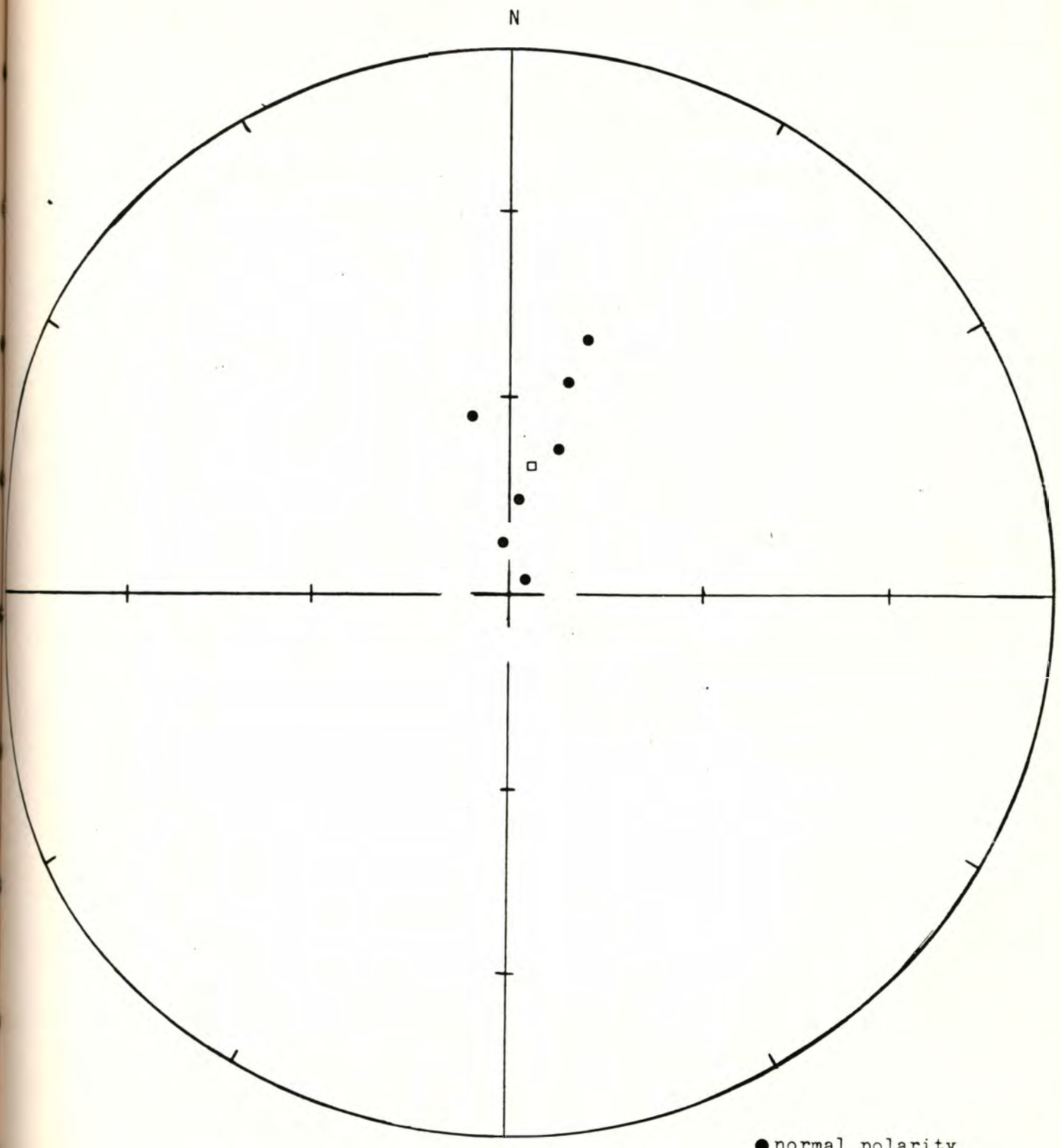

● normal polarity

○ reversed polarity

□ site mean, normal polarit

△ site mean, reversed polarity

Site: 78.02 - SR 8, Perry Creek

Demagnetization level: NRM

FISHER ON SAMPLE DIRECTIONS

Site: 78.02 -- SR 8, Perry Creek Demagnetization level: 100 oe.

NE¼ NE¼ sec. 15, T. 18 N., R. 3 W.

Sample number	Declination	Inclination
011	32.38	78.55
012	11.66	68.92
013	26.03	73.91
014	357.56	73.60
015	36.0	67.54
016	20.94	61.50
017	21.60	62.03

R= 6.95 Site declination= 20.91 Site inclination= 69.79

Alpha 95= 4.97 Delta= 7.05 Kappa= 113.48

Site latitude= 47.12° Site longitude= 123.12°

Paleolatitude= 75.23°N Paleolongitude= 67.01°W DELP= 7.32

DECLM= 8.52

Black Hills Project

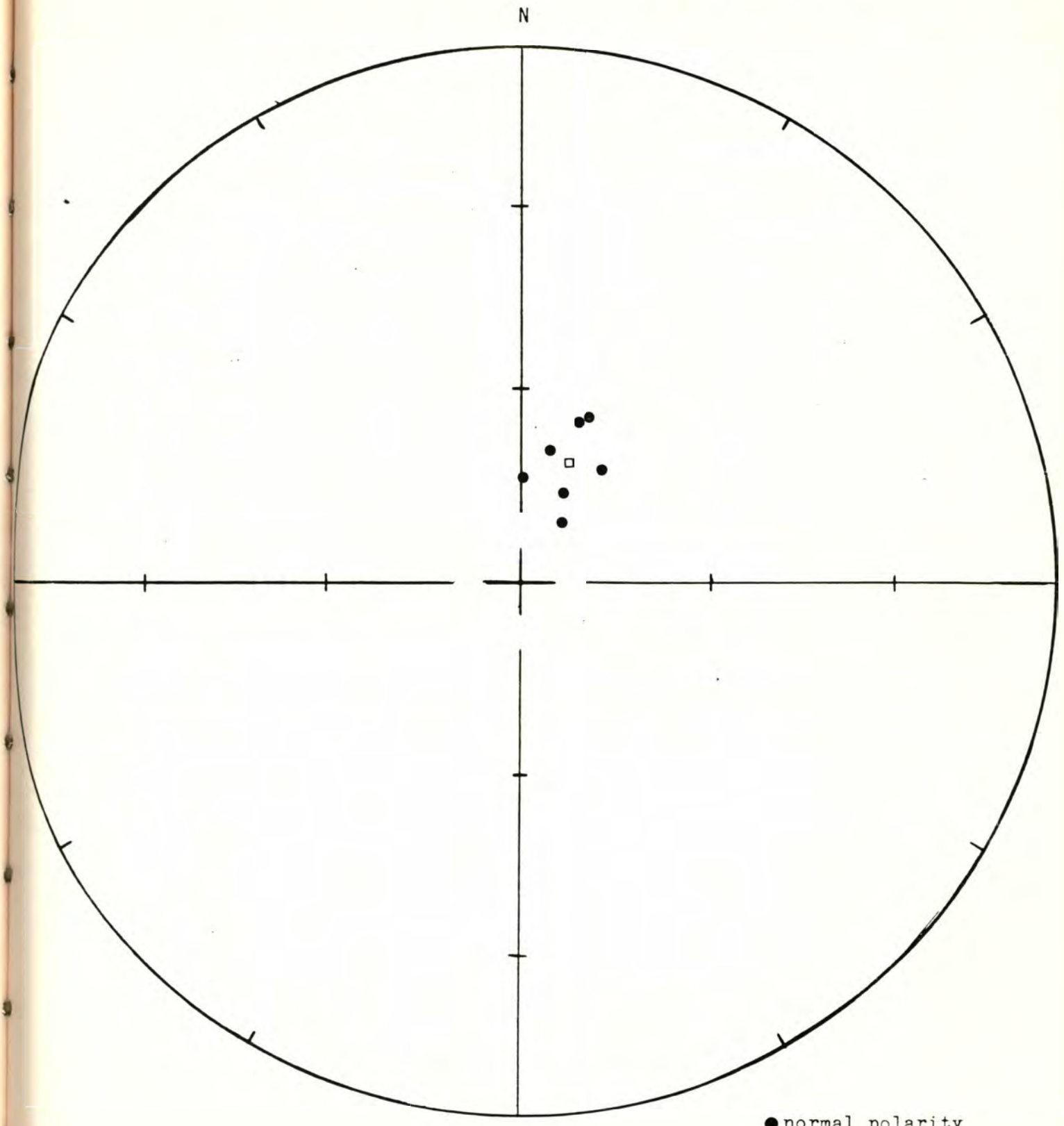

● normal polarity

○ reversed polarity

□ site mean, normal polarit

△ site mean, reversed polarity

Site: 78.02 - SR 8, Perry Creek

Demagnetization level: 100 oe.

Black Hills Project

FISHER ON SAMPLE DIRECTIONS

Site: 78.03 -- SR 8, Perry Creek Demagnetization level: NRM
NE¼ NE¼ sec. 15, T. 18 N., R. 3 W.

Sample number	Declination	Inclination
021	277.2	34.90
022	239.8	-10.24
023	194.37	63.0
024	256.0	68.1
025	290.44	58.89
026	10.0	67.42

R= 4.48 Site declination= 307.52 Site inclination= 76.48

Alpha 95= 31.49 Delta= 41.66 Kappa= 3.30

Site latitude= 47.12° Site longitude= 123.12°

Paleolatitude= 57.14°N Paleolongitude= 162.43°E DELP= 54.10

DECLM= 58.37

Black Hills Project

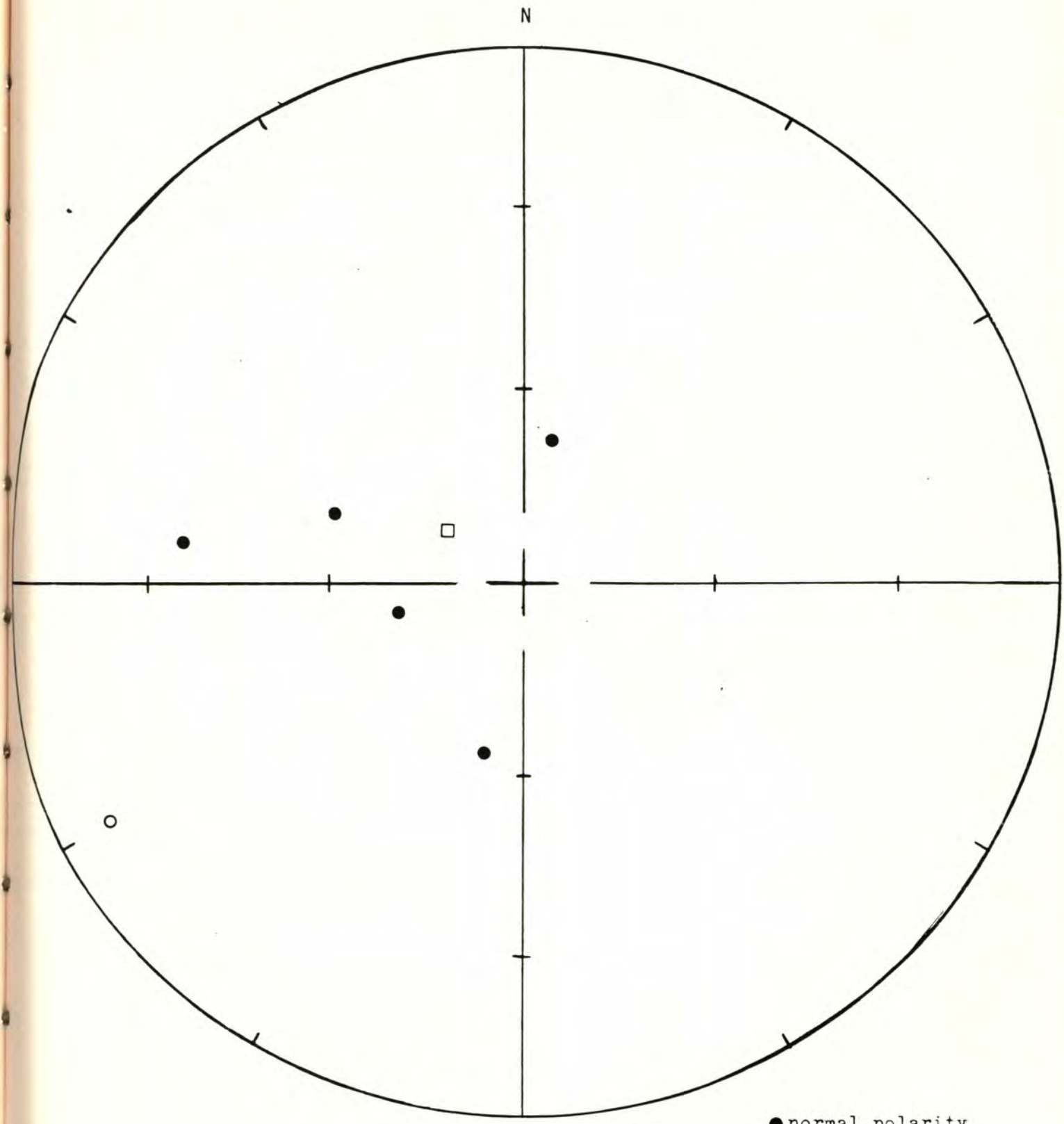

● normal polarity

○ reversed polarity

□ site mean, normal polarit

△ site mean, reversed polarity

Site: 78.03 - SR 8, Perry Creek

Demagnetization level: NRM

FISHER ON SAMPLE DIRECTIONS

Site: 78.03 -- SR 8, Perry Creek Demagnetization level: 150 oe.

NE¼ NE¼ sec. 15, T. 18 N., R. 3 W.

Sample number	Declination	Inclination
021	224.84	60.6
022	255.9	-14.45
023	204.21	-25.66
024	231	-18.5
025	204.45	57.0
026	257.61	67.15

R= 3.86 Site declination= 236.4 Site inclination= -70.1

Alpha 95= 37.37 Delta= 49.94 Kappa= 2.34

Site latitude= 47.12° Site longitude= 123.12°

Paleolatitude= 54.53°N Paleolongitude= 65.80°W DELP= 55.46

DECLM= 64.38

This site is rejected

Black Hills Project

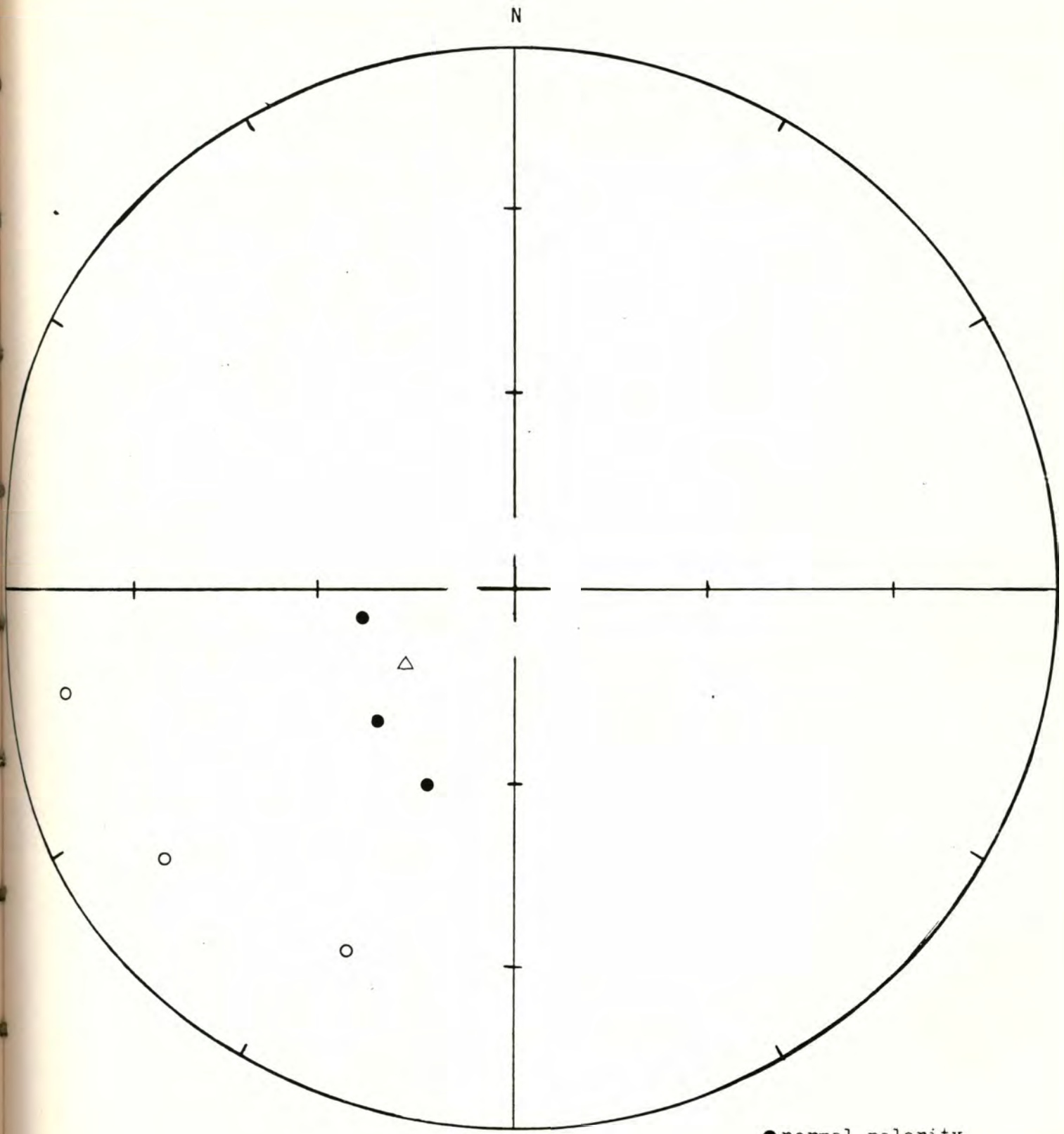

Site: 78.03 - SR 8, Perry Creek

Demagnetization level: 150 oe.

● normal polarity

○ reversed polarity

□ site mean, normal polarit

△ site mean, reversed polarity

This site is rejected.

FISHER ON SAMPLE DIRECTIONS

Site: 78.04 -- US 101, Kamilche quarry Demagnetization level: NRM

NW¼ NW¼ sec. 17, T. 19 N., R. 3 W.

Sample number	Declination	Inclination
030	19.79	46.05
031	18.08	40.79
032	20.42	39.94
033	27.99	46.09
034	19.58	39.00
035	132.0	39.75

R= 5.31 Site declination= 32.97 Site inclination= 48.99

Alpha 95= 21.28 Delta= 27.82 Kappa= 7.21

Site latitude= 47.12° Site longitude= 123.12°

Paleolatitude= 59.34°N Paleolongitude= 10.79°W DELP= 18.57

DECLM=28.12

Black Hills Project

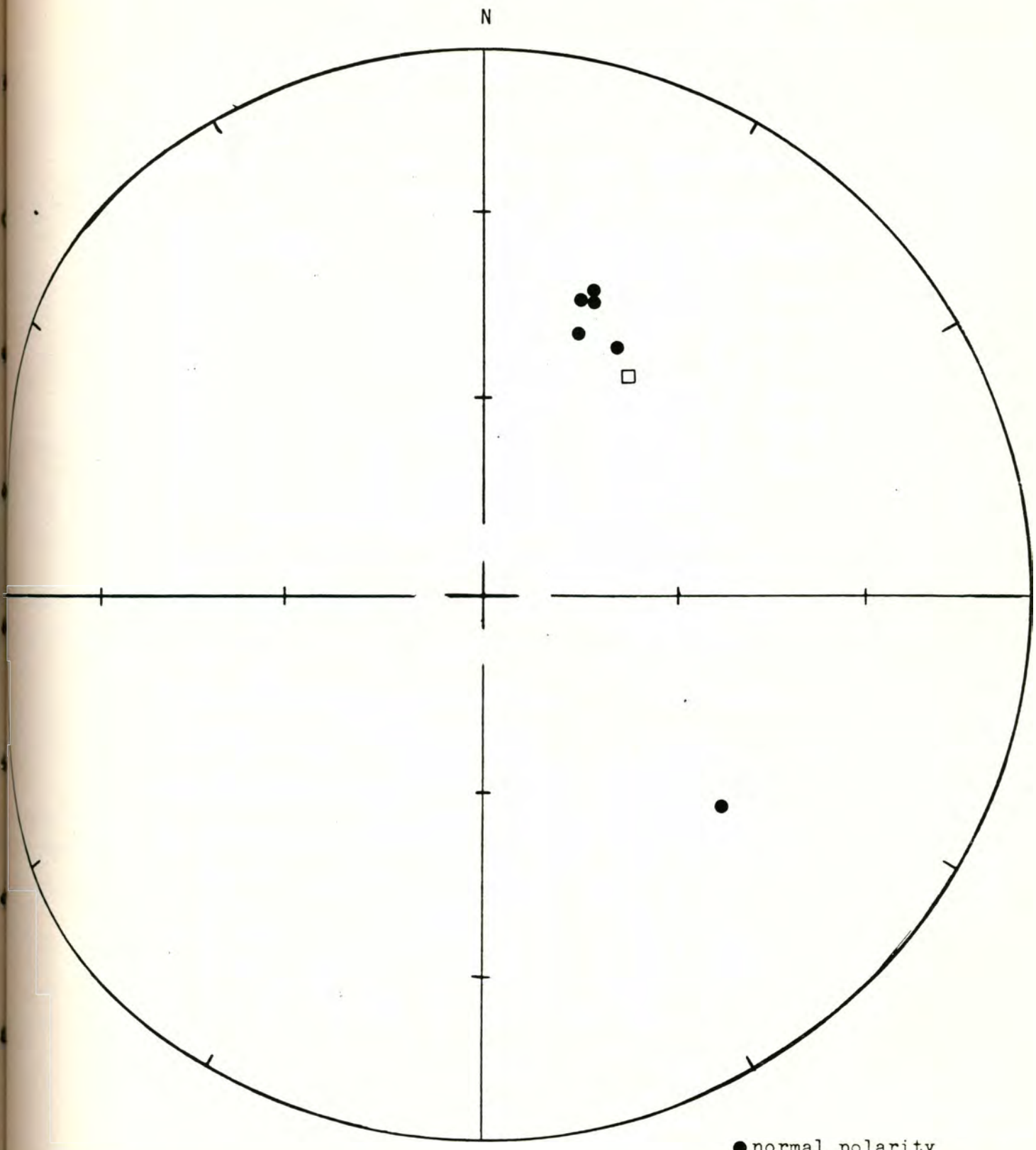

● normal polarity

○ reversed polarity

□ site mean, normal polarit

△ site mean, reversed polarity

Site: 78.04 - US 101, Kamilche quarry.

Demagnetization level: NRM

FISHER ON SAMPLE DIRECTIONS

Site: 78.04 -- US 101, Kamilche quarry Demagnetization level: 100 oe.
NW¼ NW¼ sec. 17, T. 19 N., R. 3 W.

Sample number	Declination	Inclination
030	19.27	50.07
031	19.60	42.63
032	10.61	53.70
033	17.19	53.55
034	15.49	45.91
035*	130.88	30.06

*Sample eliminated from site mean

R= 4.98 Site declination= 16.59 Site inclination= 49.22

Alpha 95= 4.16 Delta= 4.81 Kappa= 226.94

Site latitude= 47.12° Site longitude= 123.12°

Paleolatitude= 68.70°N Paleolongitude= 14.03°E DELP= 3.65

DECLM= 5.51

Black Hills Project

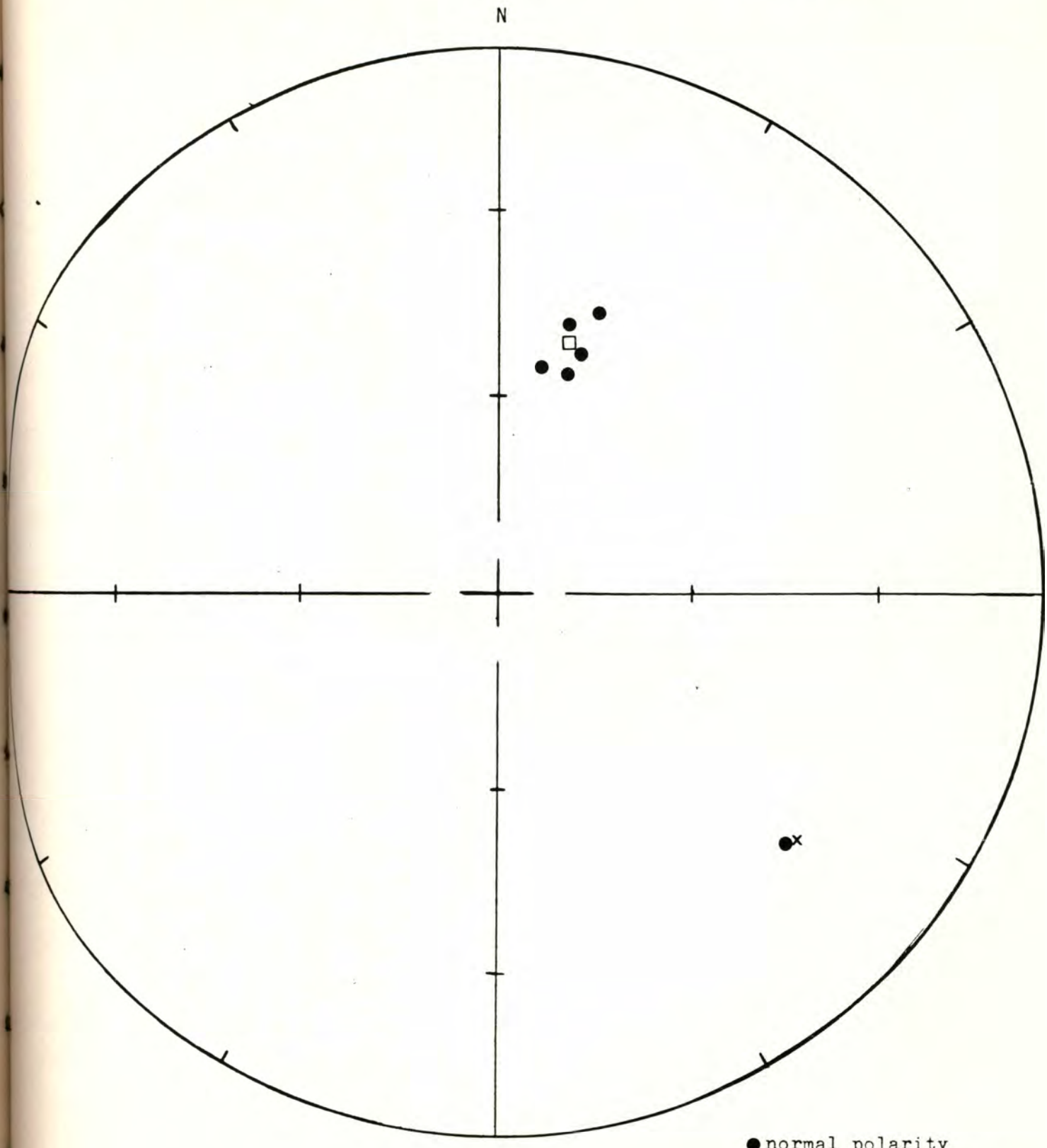

Site: 78.04 - US 101, Kamilche quarry.

Demagnetization level: 100 oe.

● normal polarity

○ reversed polarity

□ site mean, normal polarit

△ site mean, reversed polarity

X Sample 35 is eliminated from site mean.

FISHER ON SAMPLE DIRECTIONS

Site: 78.05 -- US 101, Kamilche quarry, Demagnetization level: NRM

NW¼ NW¼ sec. 17, T. 19 N., R. 3 W.

Sample number	Declination	Inclination
036	3.0	63.23
037	10.53	58.17
038	10.7	49.93
039	20.0	1.83
040	12.13	63.16
041	12.62	56.97
042	2.0	59.75

R= 6.57 Site declination= 12.38 Site inclination= 51.42

Alpha 95=14.20 Delta= 20.24 Kappa= 13.89

Site latitude= 47.12° Site longitude= 123.12°

Paleolatitude= 72.24°N Paleolongitude= 20.33°E DELP=13.11

DECLM= 19.29

Black Hills Project

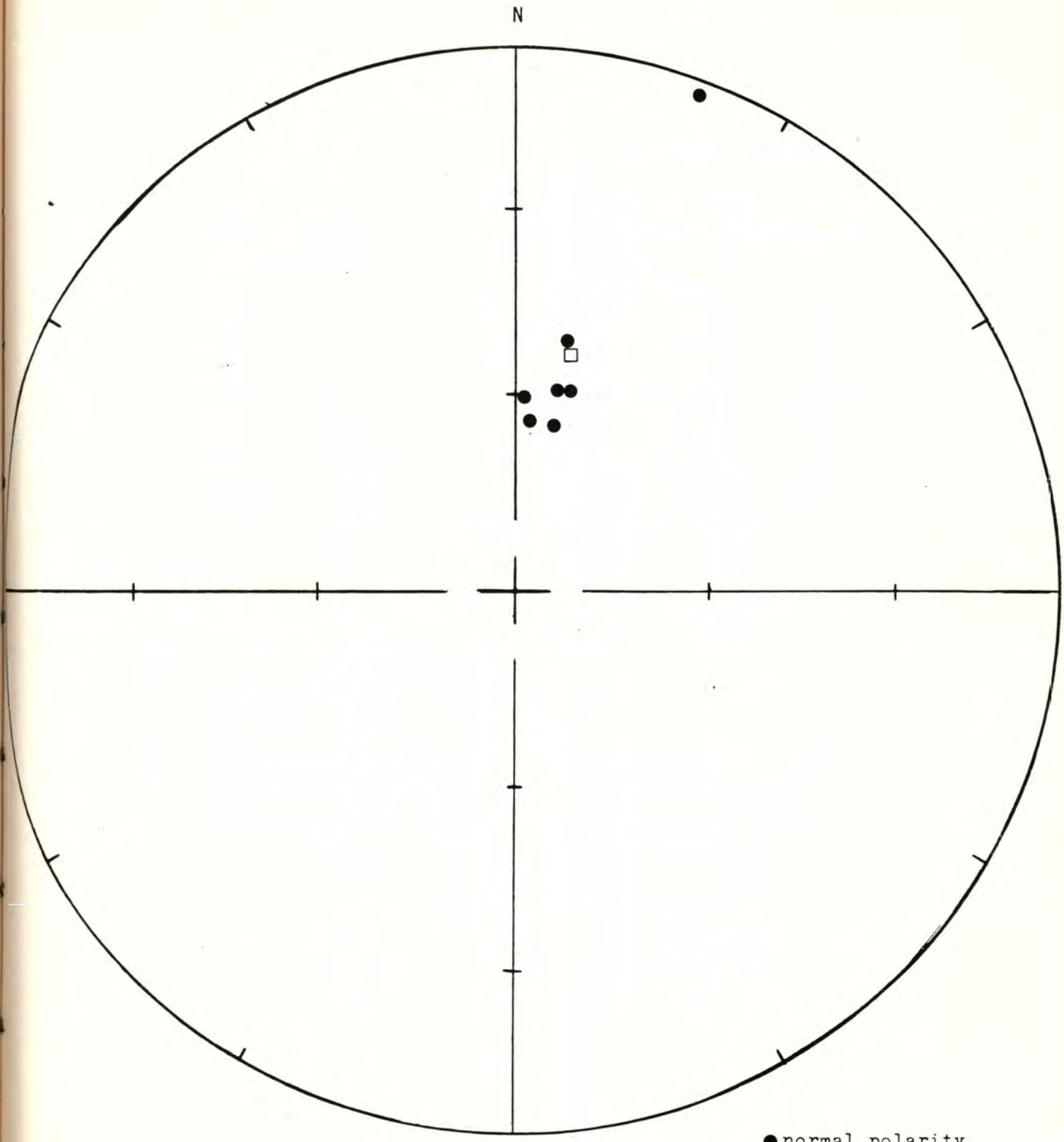

● normal polarity

○ reversed polarity

□ site mean, normal polarit

△ site mean, reversed polarity

Site: 78.05 - US 101, Kamilche quarry.

Demagnetization level: NRM

FISHER ON SAMPLE DIRECTIONS

Site: 78.05 -- US 101, Kamilche quarry Demagnetization level: 200 oe.

NW¼ NW¼ sec. 17, T. 19 N., R. 3 W.

Sample number	Declination	Inclination
036	20.87	63.76
037	24.9	62.0
038	19.79	56.60
039	20.0	63.88
040	21.20	58.18
041	12.47	61.48
042	8.81	63.64

R= 6.99 Site declination= 18.41 Site inclination= 61.46

Alpha 95= 2.55 Delta= 3.62 Kappa= 429.10

Site latitude=47.12° Site longitude= 123.12°

Paleolatitude= 76.23°N Paleolongitude= 20.68°W DELP= 3.03

DECLM= 3.93

Black Hills Project

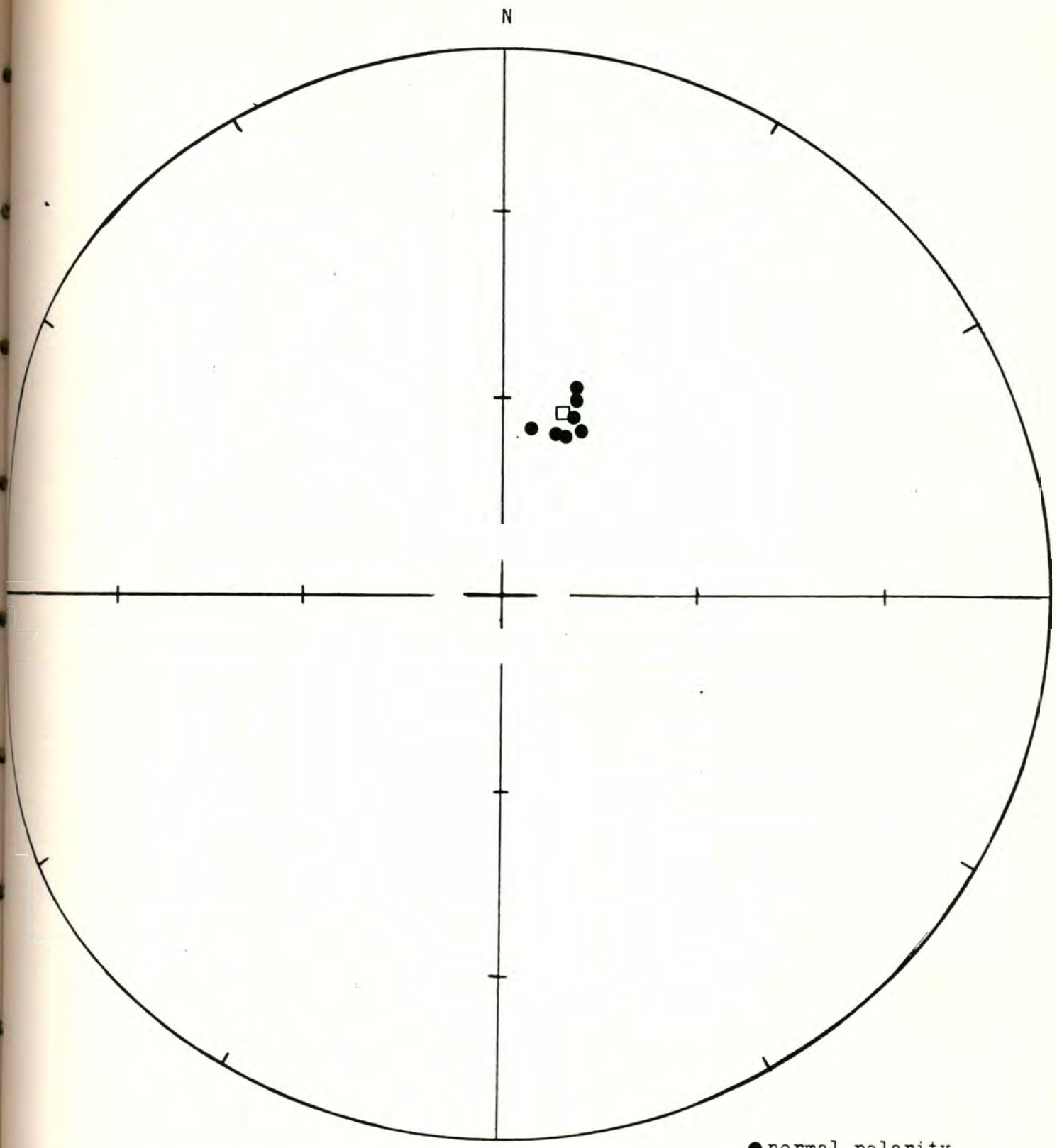

● normal polarity

○ reversed polarity

□ site mean, normal polarit

△ site mean, reversed polarity

Site: 78.05 - US 101, Kamilche quarry.

Demagnetization level: 200 oe.

FISHER ON SAMPLE DIRECTIONS

Site: 78.06 -- US 101, Kamilche cutoff. Demagnetization level: NRM

NE¼ SE¼ sec. 18, T. 19 N., R. 3 W.

Sample number	Declination	Inclination
050	338.04	61.97
051	344.94	83.44
052	314.87	70.54
053	351.55	69.30
054	4.88	65.72
055	54.0	67.0
056	21.49	67.47

R= 6.87 Site declination= 347.15 Site inclination= 68.78

Alpha 95= 7.74 Delta= 10.99 Kappa= 46.74

Site latitude= 47.12° Site longitude= 123.12°

Paleolatitude= 80.29°N Paleolongitude= 177.08°W DELP= 11.11

DECLM= 13.12

Black Hills Project

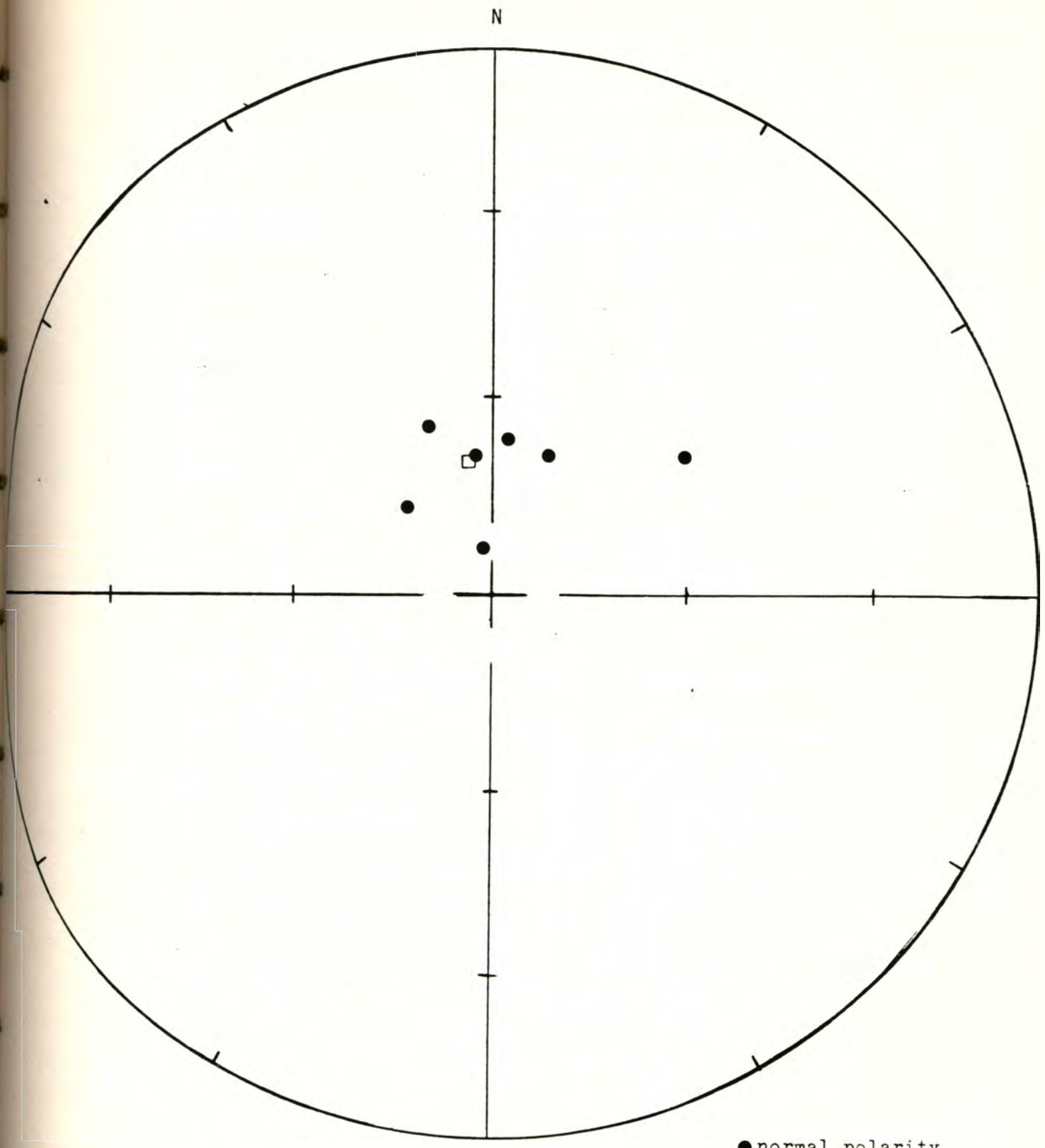

● normal polarity

○ reversed polarity

□ site mean, normal polarit

△ site mean, reversed polarity

Site: 78.06 - US 101, Kamilche cutoff.

Demagnetization level: NRM

FISHER ON SAMPLE DIRECTIONS

Site: 78.06 -- US 101, Kamilche cutoff. Demagnetization level: 150 oe.

NE¼ SE¼ sec. 18, T. 19 N., R. 3 W.

Sample number	Declination	Inclination
050	22.6	61.02
051	2.57	50.96
052	354.24	70.54
053	23.91	59.45
054	4.12	58.24
055	19.43	62.11
056	13.43	58.38

R= 6.94 Site declination= 11.87 Site inclination= 60.47

Alpha 95= 5.15 Delta= 7.31 Kappa= 105.49

Site latitude= 47.12° Site longitude= 123.12°

Paleolatitude= 79.79°N Paleolongitude= 3.60°W DELP= 5.97

DECLM= 7.85

Black Hills Project

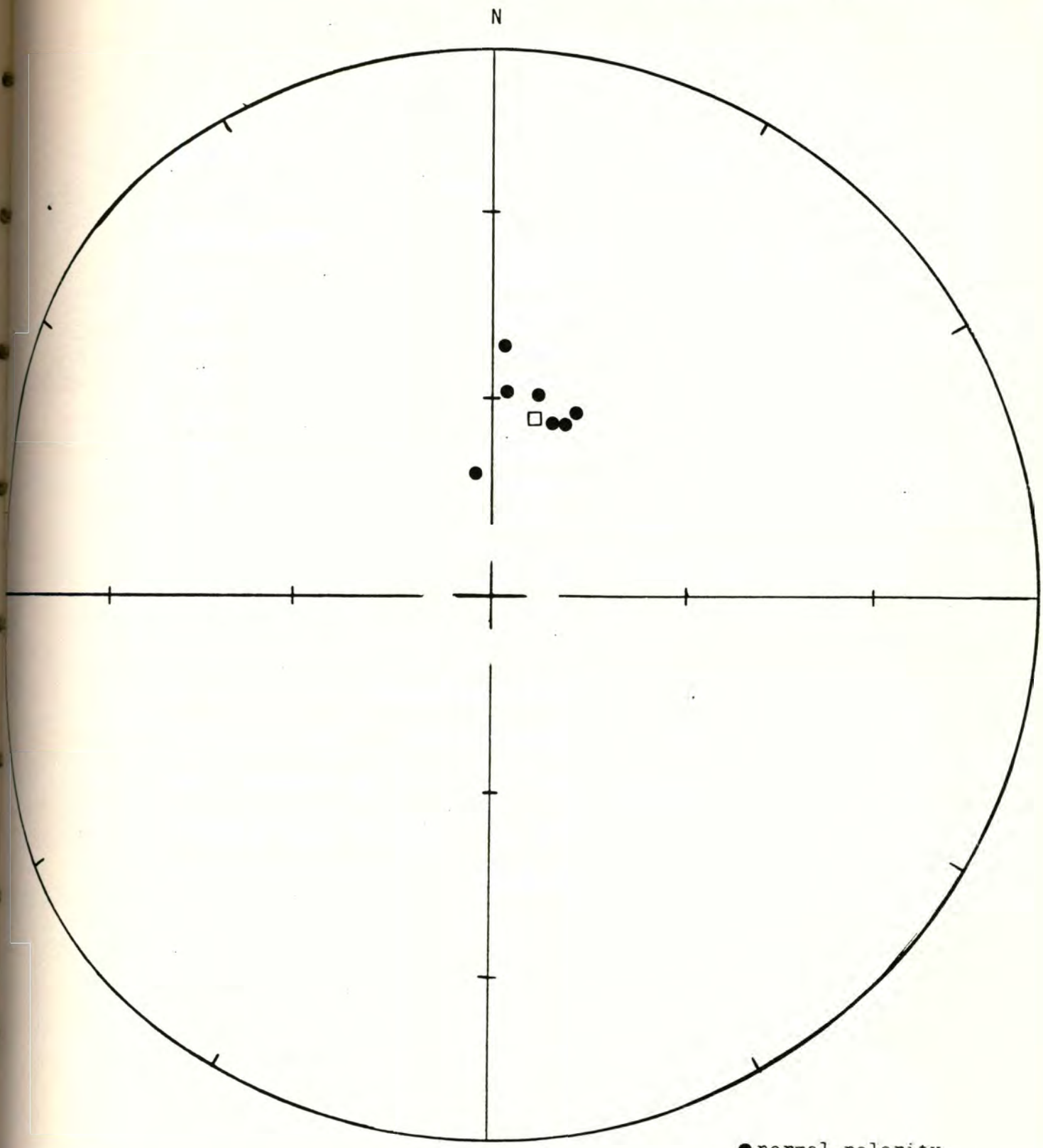

● normal polarity

○ reversed polarity

□ site mean, normal polarit

△ site mean, reversed polarity

Site: 78.06 - US 101, Kamilche cutoff.

Demagnetization level: 150 oe.

FISHER ON SAMPLE DIRECTIONS

Site: 7.8.78.1 -- Black Lake Blvd. A Demagnetization level: NRM

NE¼ sec. 29, T. 18 N., R. 2 W.

Sample number	Declination	Inclination
200	5.26	78.12
201	321.82	80.49
202	273.68	67.31
203	359.15	84.43
204	309.61	81.92
205	330.88	82.41
206	290.83	56.42

R= 6.85 Site declination= 306.52 Site inclination= 77.85

Alpha 95= 8.35 Delta= 11.85 Kappa= 40.19

Site latitude= 47.0° Site longitude= 123.0°

Paleolatitude= 56.33°N Paleolongitude= 157.98°W DELP= 14.74

DECLM= 15.68

Black Hills Project

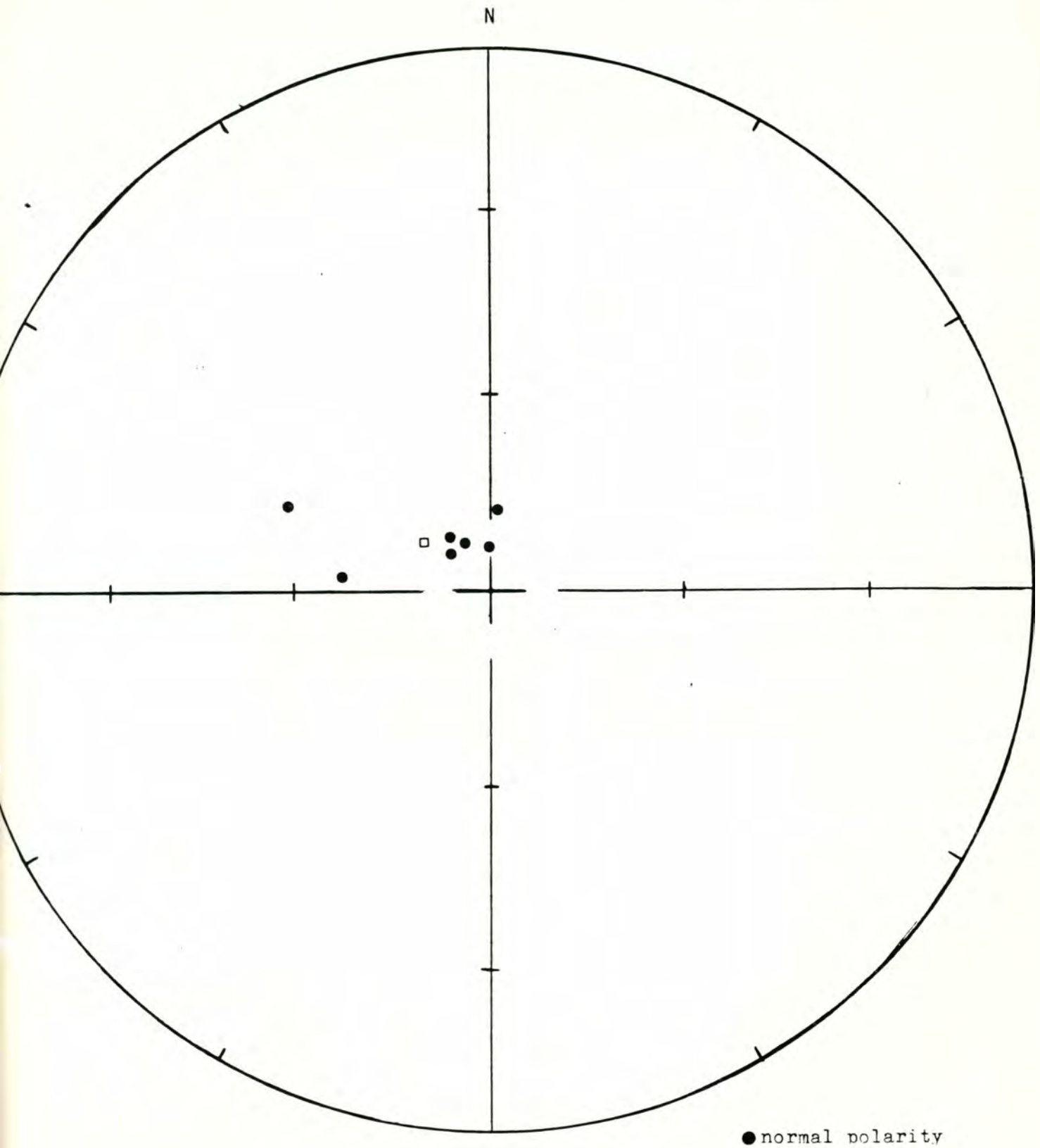

● normal polarity

○ reversed polarity

□ site mean, normal polarit

△ site mean, reversed polarity

Site: 7.8.78.1 - Black Lake Blvd. A

Demagnetization level: NRM

FISHER ON SAMPLE DIRECTIONS

Site: 7.8.78.1 -- Black Lake Blvd. A Demagnetization level: 200 oe.

NE¼ sec. 29, T. 18 N., R. 2 W.

Sample number	Declination	Inclination
200	41.1	81.11
201	43.18	87.75
202	320.50	83.81
203	7.84	85.52
204	45.04	81.52
205	12.12	72.83
206	253.68	74.25

R= 6.91 Site declination= 357.82 Site inclination= 84.83

Alpha 95= 6.36 Delta= 9.02 Kappa= 69.27

Site latitude= 47.0° Site longitude= 123.0°

Paleolatitude= 57.25°N Paleolongitude= 123.72°W DELP= 12.41

DECLM= 12.56

Black Hills Project

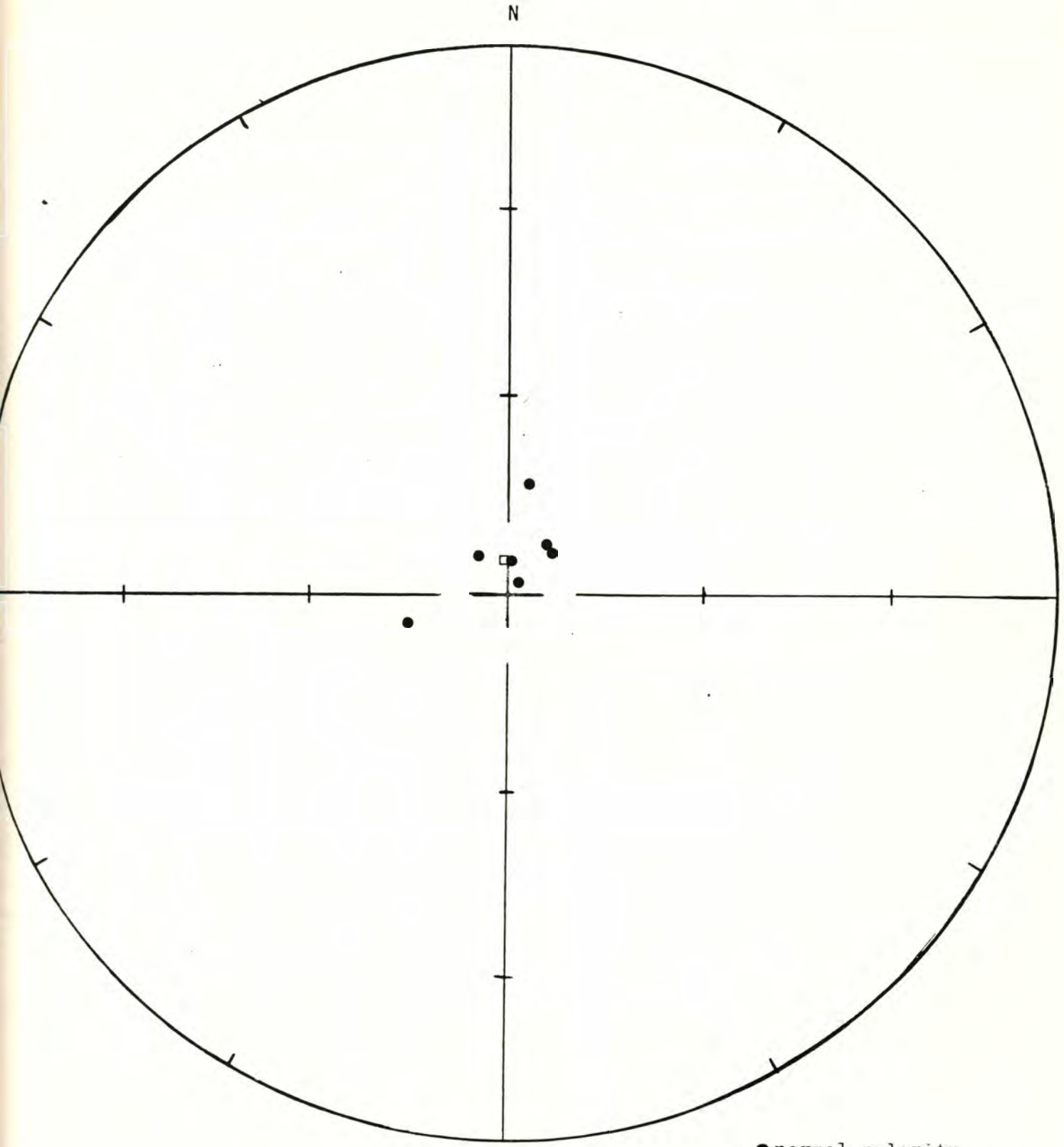

● normal polarity

○ reversed polarity

□ site mean, normal polarit

△ site mean, reversed polarity

Site: 7.8.78.1 - Black Lake Blvd. A

Demagnetization level: 200 oe.

FISHER ON SAMPLE DIRECTIONS

Site: 7.8.78.2 -- Black Lake Blvd. B Demagnetization level: NRM

SW¼ SW¼ sec. 29, T. 18 N., R. 2 W.

Sample number	Declination	Inclination
207	36.30	86.55
208	336.87	73.46
209	236.42	88.09
210	317.79	80.02
211	183.76	28.36
212	278.45	85.91
213	36.89	79.67
214	51.25	78.86

R= 7.38 Site declination= 207.26 Site inclination= 88.43

Alpha 95= 14.72 Delta= 22.68 Kappa= 11.31

Site latitude= 47.0° Site longitude= 123.0°

Paleolatitude= 44.19°N Paleolongitude= 125.0°W DELP= 29.36

DECLM= 29.40

Black Hills Project

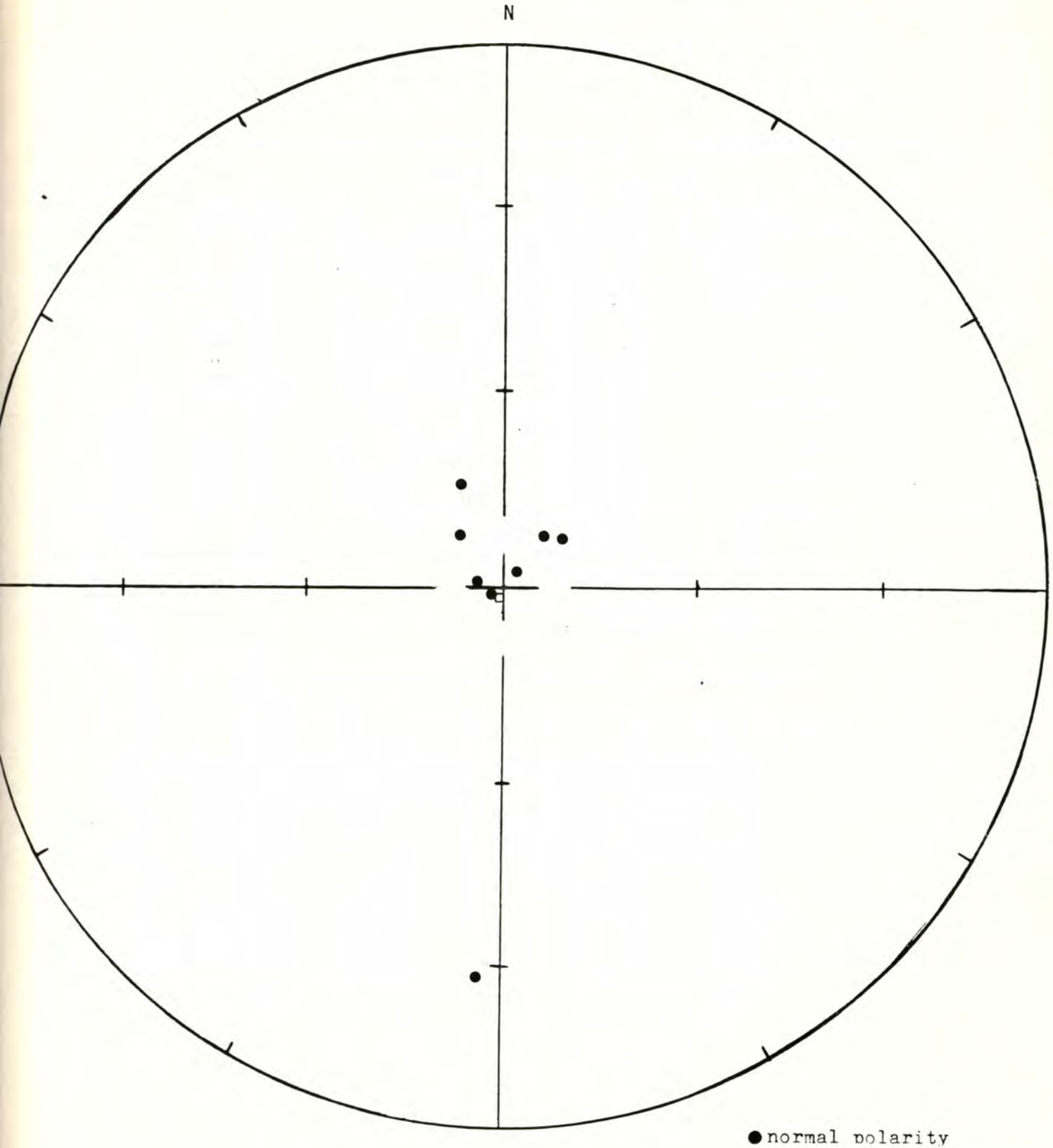

● normal polarity

○ reversed polarity

□ site mean, normal polarit

△ site mean, reversed polarity

Site: 7.8.78.2 - Black Lake Blvd. B

Demagnetization level: NRM

FISHER ON SAMPLE DIRECTIONS

Site: 7.8.78.2 -- Black Lake Blvd. B Demagnetization level: 100 oe.

SW¼ SW¼ sec. 29, T. 18 N., R. 2 W.

Sample number	Declination	Inclination
207	124.93	78.07
208	346.62	79.39
209	46.06	80.31
210	20.52	84.21
211	0	83.50
212	355.38	81.28
213	9.54	86.41
214	50.11	87.33

R= 7.95 Site declination= 26.81 Site inclination= 84.92

Alpha 95= 4.09 Delta= 6.27 Kappa= 146.11

Site latitude= 47.0° Site longitude= 123.0°

Paleolatitude= 55.75°N Paleolongitude= 114.94°W DELP= 8.0

DECLM= 8.10

Black Hills Project

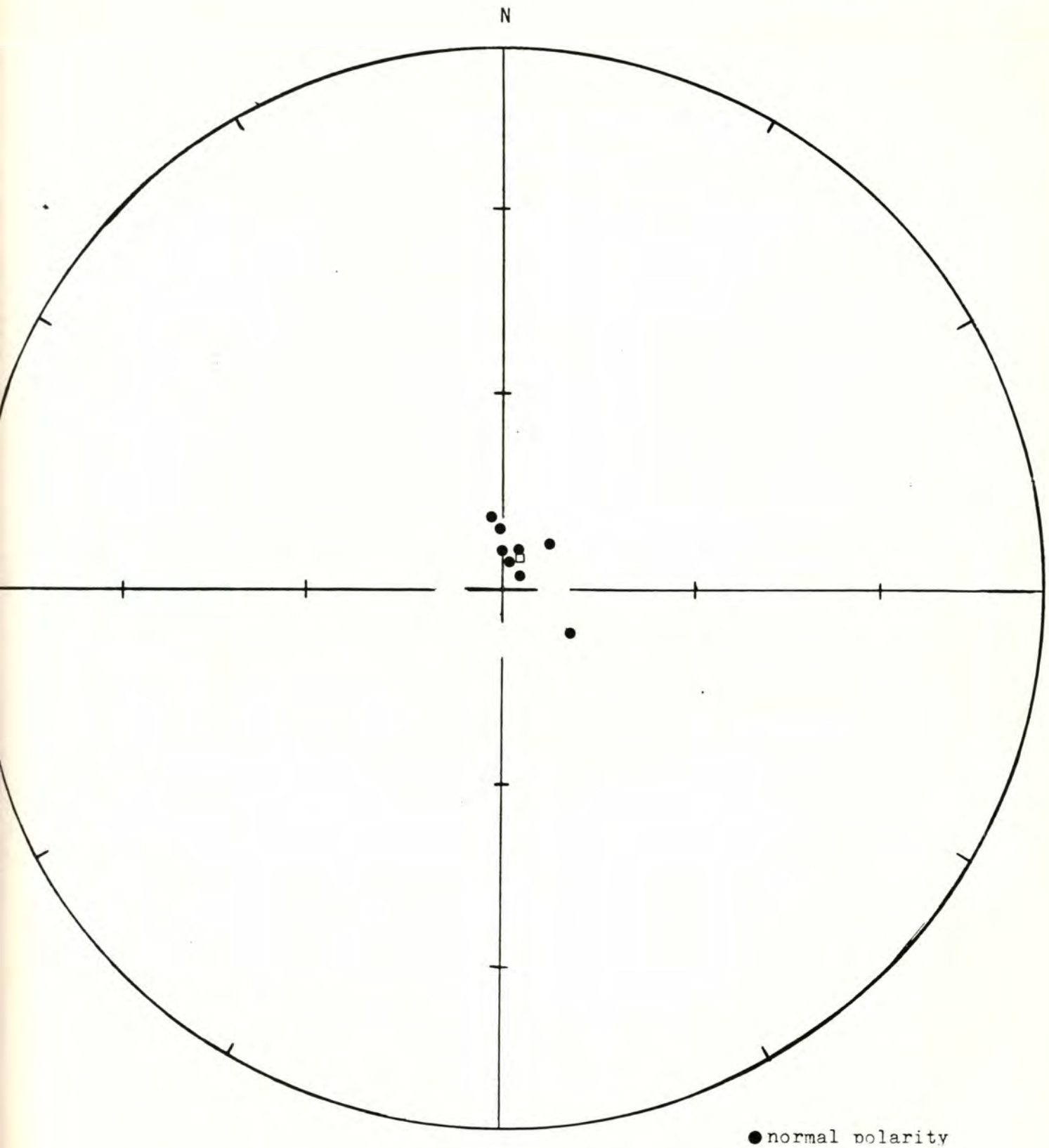

● normal polarity

○ reversed polarity

□ site mean, normal polarit

△ site mean, reversed polarity

Site: 7.8.78.2 - Black Lake Blvd. B

Demagnetization level: 100 oe.

TECTONIC CORRECTION ON SAMPLE DIRECTIONS

Pole on site mean

Site: 7.8.78.2 Demagnetization level: 100 oe.

Dip azimuth: 322 (N52E) Dip angle: 6 (W)

Sample number	Declination	Inclination	Cor. dec.	Cor. inc.
207	124.93	78.07	109.23	83.56
208	346.62	79.39	337.90	73.74
209	46.06	80.31	16.29	78.10
210	20.52	84.21	350.82	79.72
211	0	83.50	341.90	78.18
212	355.38	81.28	342.00	75.88
213	9.54	86.41	339.52	81.17
214	50.11	87.33	345.72	83.35

R= 7.95 Site declination=351.49 Site inclination= 80.64

Alpha 95= 4.10 Delta= 6.28 Kappa= 146.04

Site latitude= 47.0°N Site longitude= 123.0°W

Paleolatitude= 64.93°N Paleolongitude= 129.27°W DELP= 7.59

DECLM= 7.88

WITH TECTONIC CORRECTION

Black Hills Project

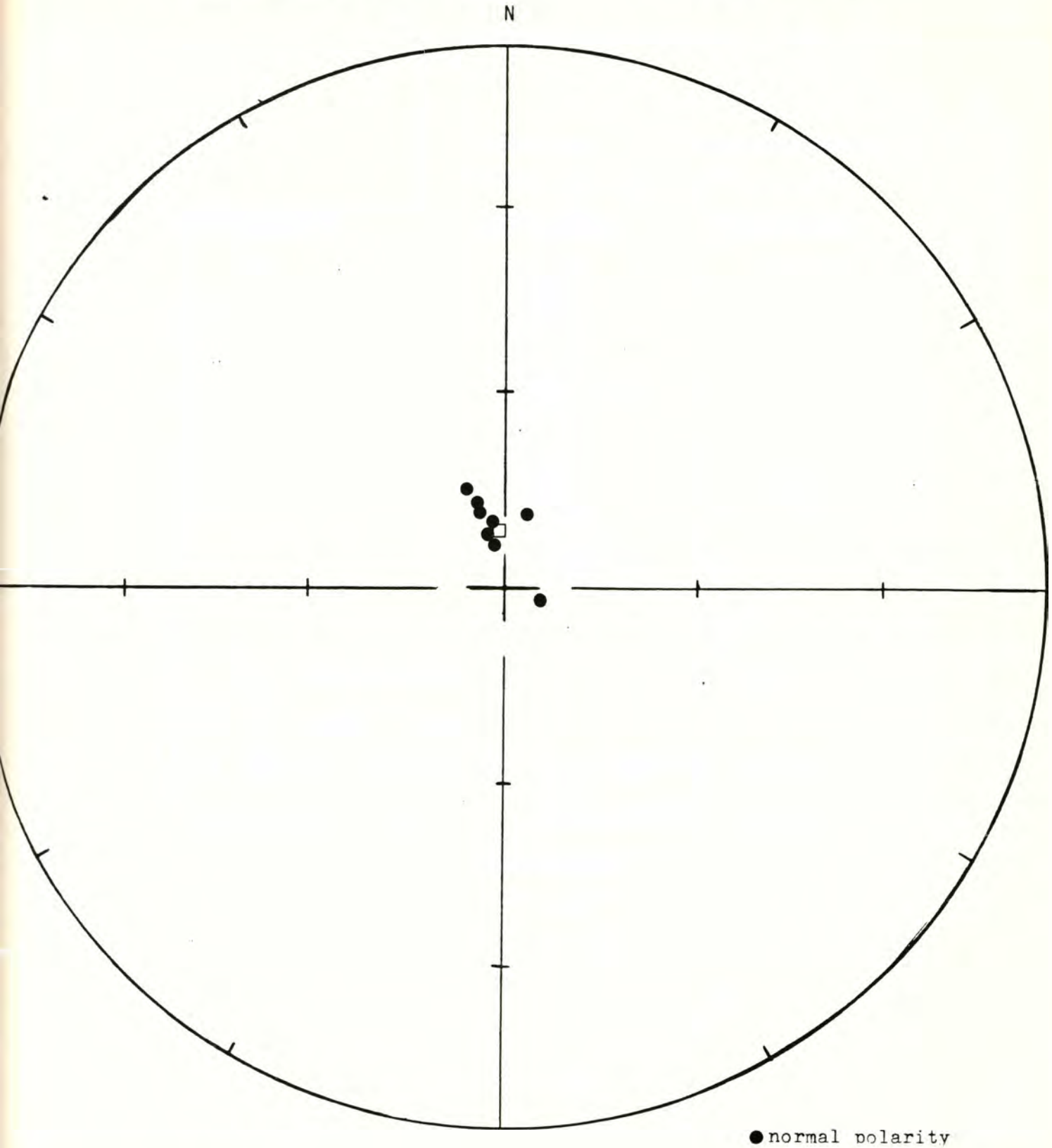

● normal polarity

○ reversed polarity

□ site mean, normal polarit

△ site mean, reversed polarity

Site: 7.8.78.2

Demagnetization level: 100 oe.

FISHER ON SAMPLE DIRECTIONS

Site: 7.9.78.1 -- SR 410, Mud Bay Demagnetization level: NRM

SE¼ SW¼ sec. 12, T. 18 N., R. 3 W.

Sample number	Declination	Inclination
215.21	232.21	76.60
216	342.22	65.85
217	5.83	73.30
218	319.73	70.87
219	355.04	88.77
220	330.18	73.21
221	321.18	67.90
222	170.69	-6.51

R= 7.25 Site declination= 336.09 Site inclination= 69.42

Alpha 95= 16.23 Delta= 25.05 Kappa= 9.30

Site latitude= 47.05° Site longitude= 123.06°

Paleolatitude= 73.60°N Paleolongitude= 182.62°W DELP= 23.68

DECLM= 27.72

Black Hills Project

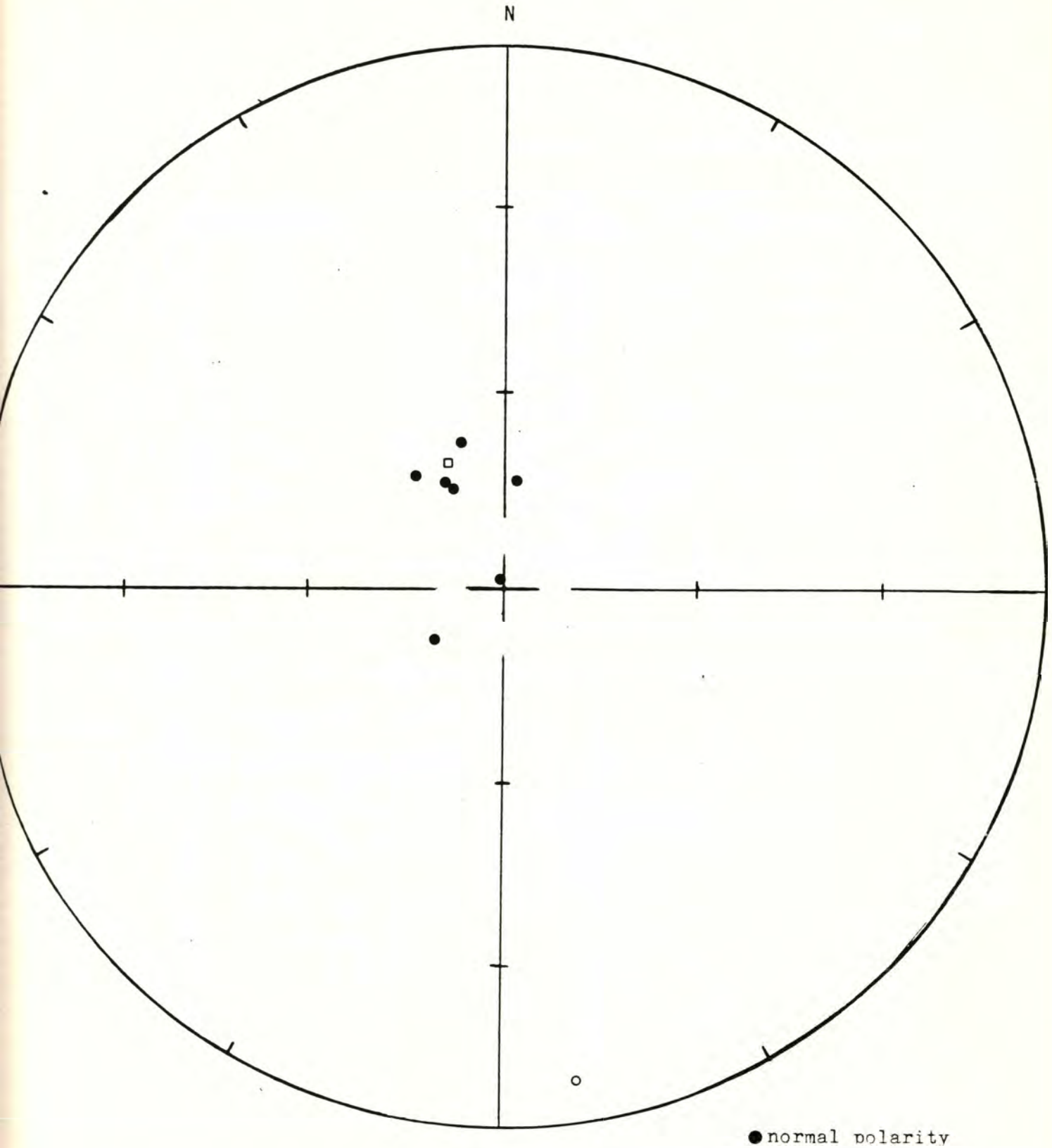

● normal polarity

○ reversed polarity

□ site mean, normal polarit

△ site mean, reversed polarity

Site: 7.9.78.1 - SR 410, Mud Bay.

Demagnetization level: NRM

FISHER ON SAMPLE DIRECTIONS

Site: 7.9.78.1 -- SR 410, Mud Bay Demagnetization level: 300 oe.

SE¼ SW¼ sec. 12, T. 18 N., R. 3 W.

Sample number	Declination	Inclination
215	331.86	76.77
216	315.93	55.76
217	340.35	76.51
218	319.17	74.11
219	354.58	62.98
220	1.52	75.02
221	327.37	70.27
222*	169.87	-7.51

*Sample eliminated from site mean.

R= 6.91 Site declination= 334.33 Site inclination= 70.99

Alpha 95= 6.51 Delta= 9.24 Kappa= 66.04

Site latitude= 47.05° Site longitude= 123.06°

Paleolatitude= 72.02°N Paleolongitude= 175.83°W DELP= 9.88

DECLM=11.34

Black Hills Project

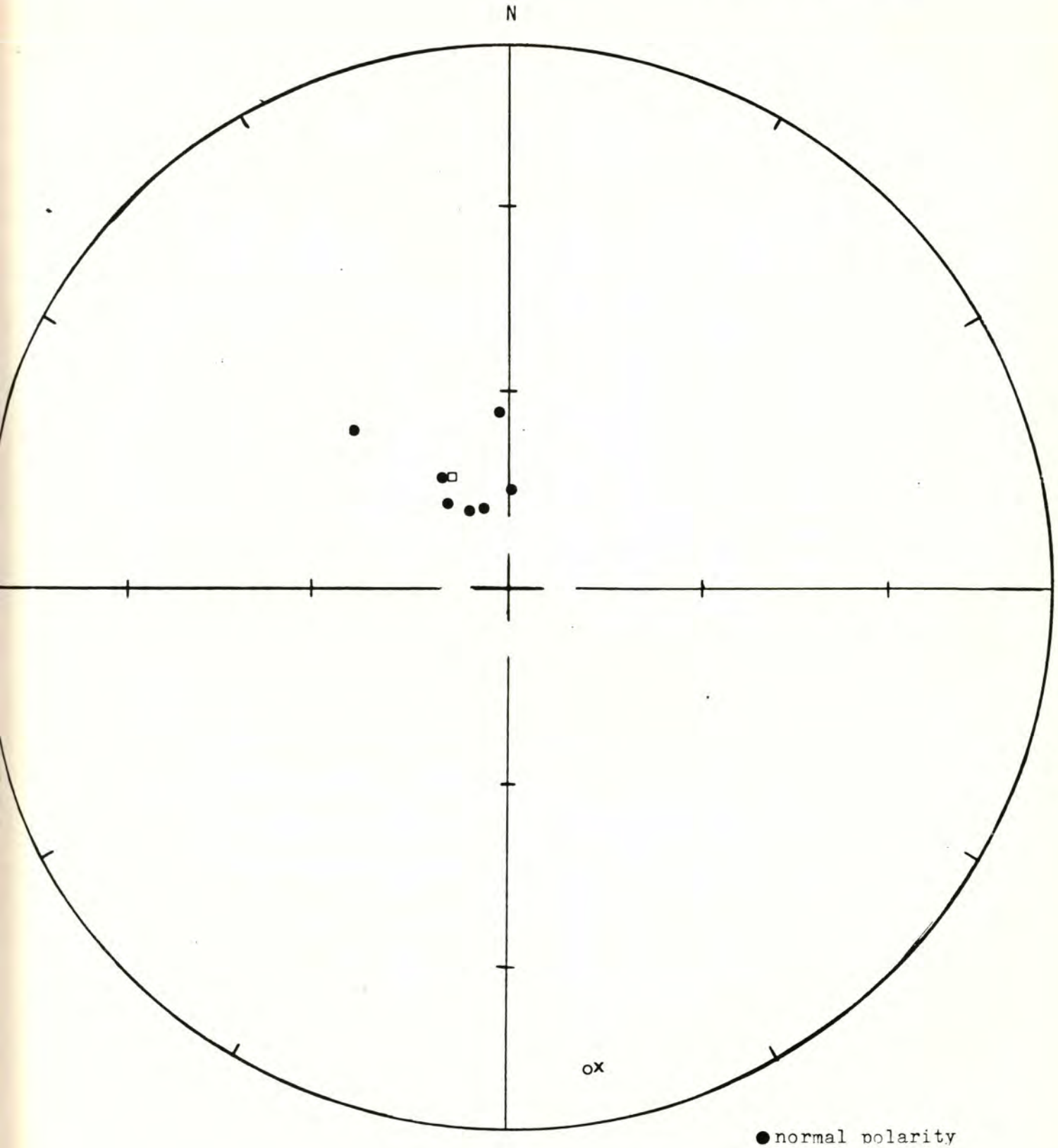

Site: 7.9.78.1 - SR 410, Mud Bay

Demagnetization level: 300 oe.

● normal polarity

○ reversed polarity

□ site mean, normal polarity

△ site mean, reversed polarity

× Sample 222 eliminated from site mean.

TECTONIC CORRECTION ON SAMPLE DIRECTIONS

Pole on site mean

Site: 7.9.78.1 Demagnetization level: 300 oe.

Dip azimuth: 326 (N56E) Dip angle: 9 (E)

Sample number	Declination	Inclination	Cor. dec.	Cor. inc.
215	331.86	76.77	329.55	67.80
216	315.93	55.76	319.20	47.14
217	340.35	76.51	334.76	67.68
218	319.17	74.11	321.56	65.15
219	354.58	62.98	348.17	54.83
220	1.52	75.02	348.71	67.10
221	327.37	70.27	326.96	61.27

R= 6.91 Site declination= 332.06 Site inclination= 62.06

Alpha 95= 6.40 Delta= 9.08 Kappa= 68.42

Site latitude= 47.05^{o}N Site longitude= 123.06^{o}W

Paleolatitude= 69.87^{o}N Paleolongitude= 146.62^{o}E DELP= 7.71

DECLM= 9.93

WITH TECTONIC CORRECTION

Black Hills Project

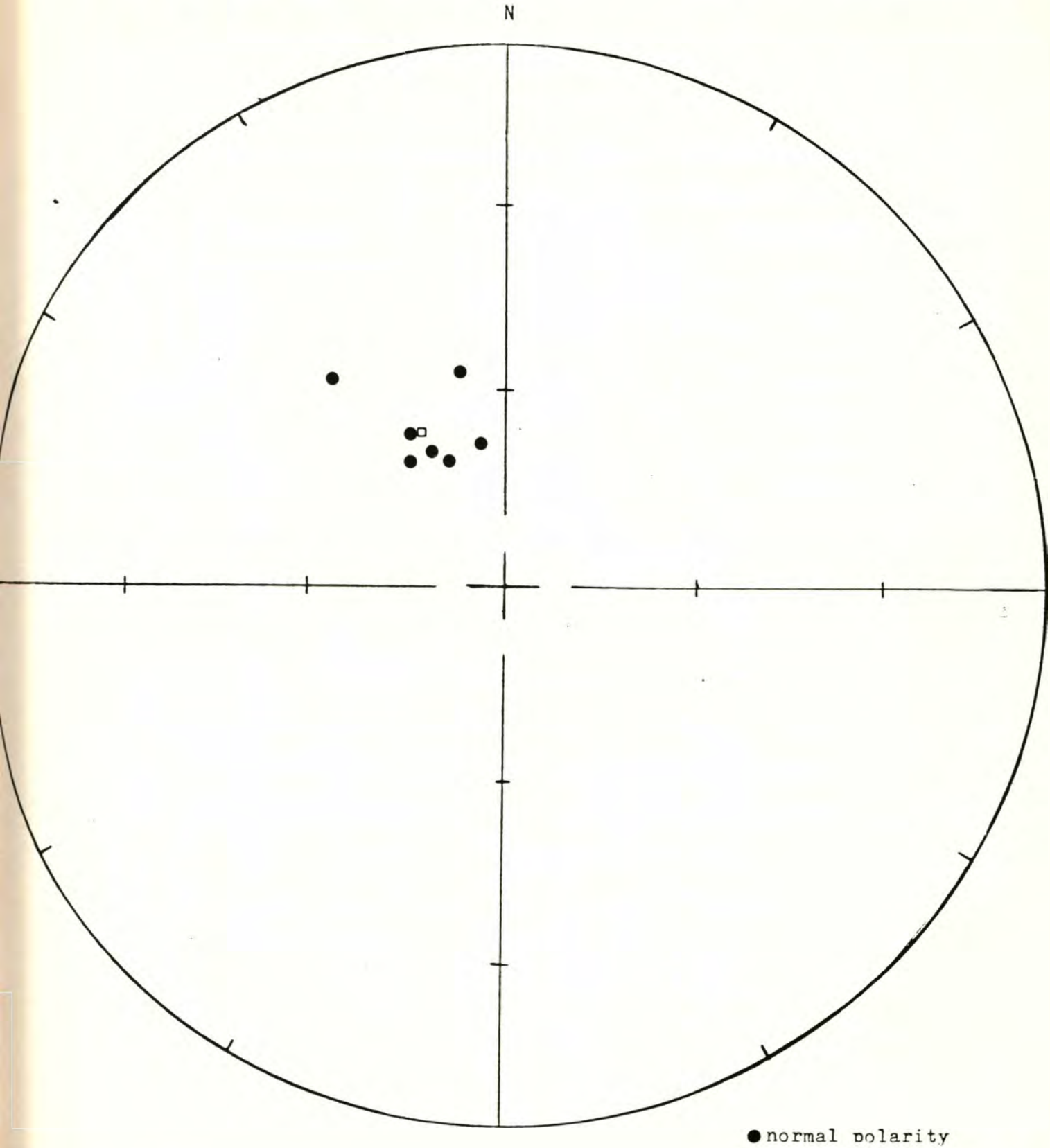

● normal polarity

○ reversed polarity

□ site mean, normal polari

△ site mean, reversed polarity

Site: 7.9.78.1

Demagnetization level: 300 oe.

FISHER ON SAMPLE DIRECTIONS

Site: 7.9.78.2 -- Capitol Peak Road A Demagnetization level: NRM

SW½ sec. 14, T. 17 N., R. 4 W.

Sample number	Declination	Inclination
223	21.58	38.77
224	26.06	44.11
225	27.58	39.11
226	38.69	44.18
227	12.77	46.41
228	40.53	54.41
229	23.71	38.70

R= 6.93 Site declination= 26.88 Site inclination= 43.99

Alpha 95= 5.74 Delta= 8.14 Kappa= 85.12

Site latitude= 46.88° Site longitude= 123.25°

Paleolatitude= 60.04°N Paleolongitude= 2.14°E DELP= 4.49

DECLM= 7.18

Black Hills Project

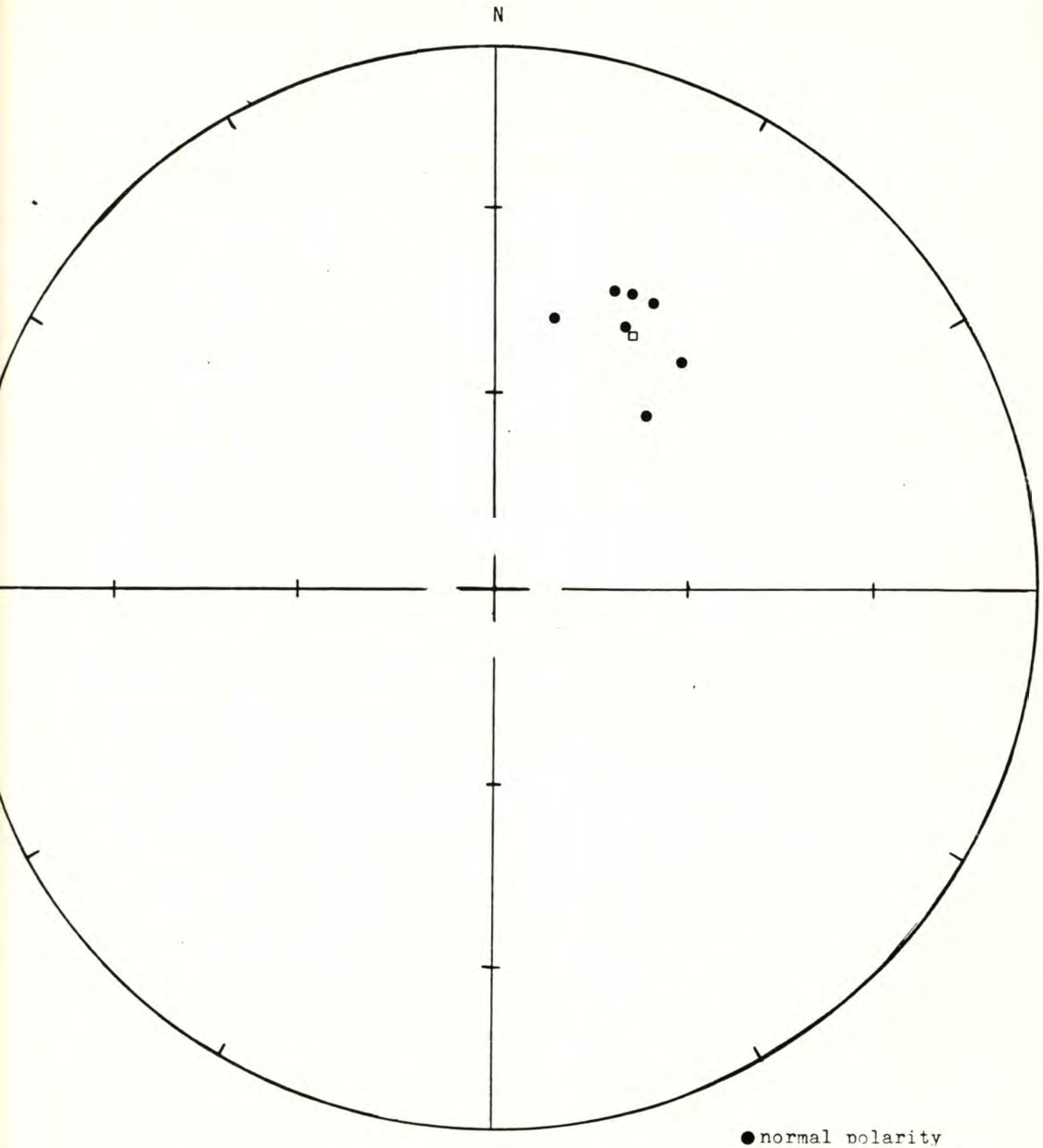

● normal polarity

○ reversed polarity

□ site mean, normal polarit

△ site mean, reversed polarity

Site: 7.9.78.2 - Capitol Peak Road A

Demagnetization level: NRM

FISHER ON SAMPLE DIRECTIONS

Site: 7.9.78.2 -- Captiol Peak Road A Demagnetization level: 100 oe.

SW½ sec. 14, T. 17 N., R. 4 W.

Sample number	Declination	Inclination
223	19.90	40.05
224	24.63	44.18
225	31.88	43.08
226	34.67	33.60
227	16.66	34.29
228	20.71	39.80
229	23.10	37.32

R= 6.96 Site declination= 24.48 Site inclination= 39.07

Alpha 95= 4.29 Delta= 6.08 Kappa= 152.26

Site latitude= 46.88° Site longitude= 123.25°

Paleolatitude= 58.31°N Paleolongitude= 9.78°E DELP= 3.05

DECLM= 5.12

Black Hills Project

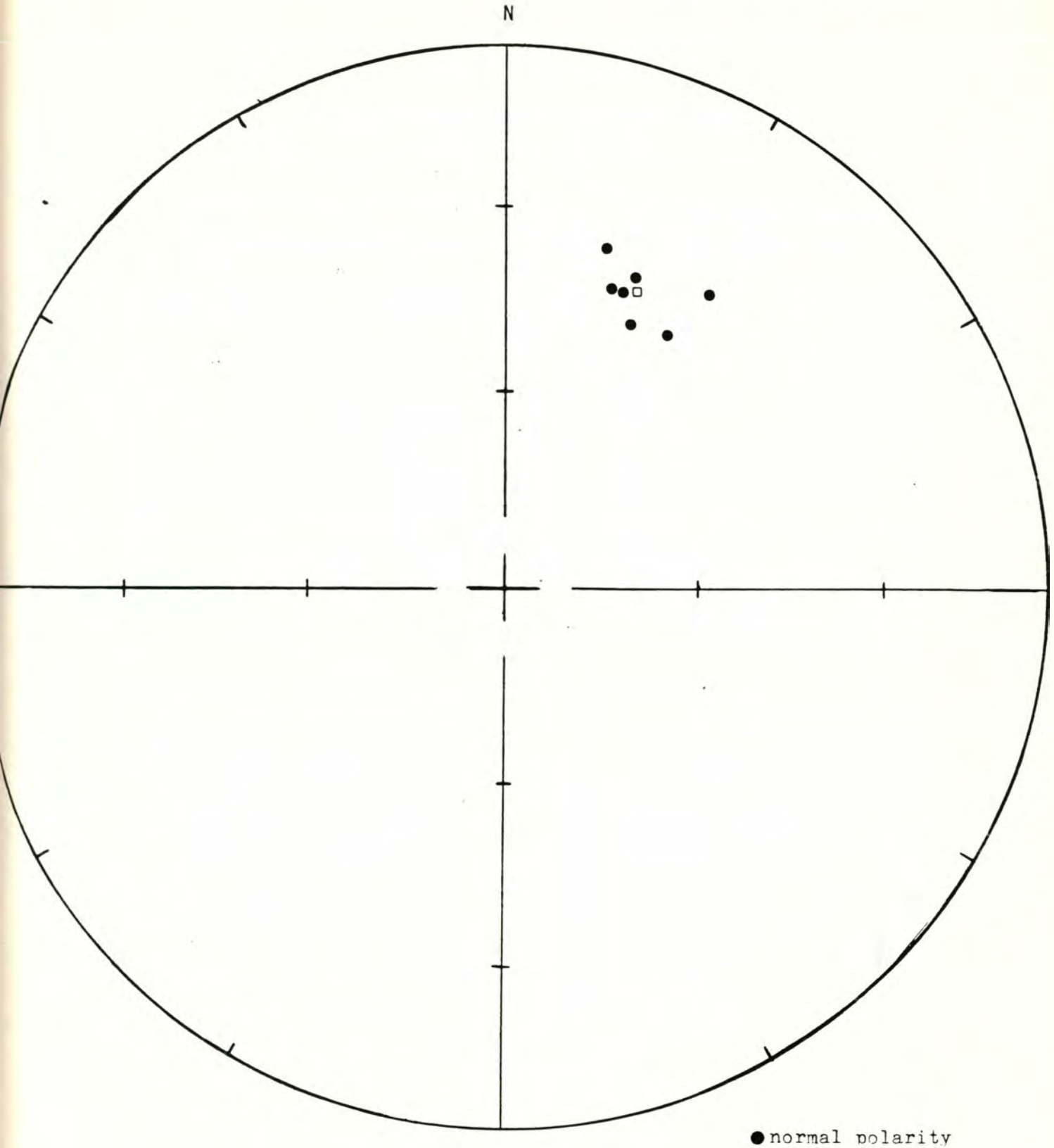

● normal polarity

○ reversed polarity

□ site mean, normal polarit

△ site mean, reversed polarity

Site: 7.9.78.2 - Capitol Peak Road A

Demagnetization level: 100 oe.

TECTONIC CORRECTION ON SAMPLE DIRECTIONS

Pole on site mean

Site: 7.9.78.2 Demagnetization level: 100 oe.

Dip azimuth: 227 (N43W) Dip angle:9 (W)

Sample number	Declination	Inclination	Cor. dec.	Cor. inc.
223	19.9	40.05	15.65	47.91
224	24.63	44.18	20.44	52.38
225	31.88	43.08	29.09	51.71
226	34.67	33.60	33.07	42.37
227	16.66	34.29	12.89	41.91
228	20.71	39.80	16.61	47.73
229	23.10	37.32	19.66	45.44

R= 6.96 Site declination= 21.00 Site inclination= 47.28

Alpha 95= 4.29 Delta= 6.08 Kappa= 152.30

Site latitude= 46.88^{o}N Site longitude= 123.25^{o}W

Paleolatitude= 65.33^{o}N Paleolongitude= 7.73^{o}E DELP= 3.60

DECLM= 5.56

WITH TECTONIC CORRECTION

Black Hills Project

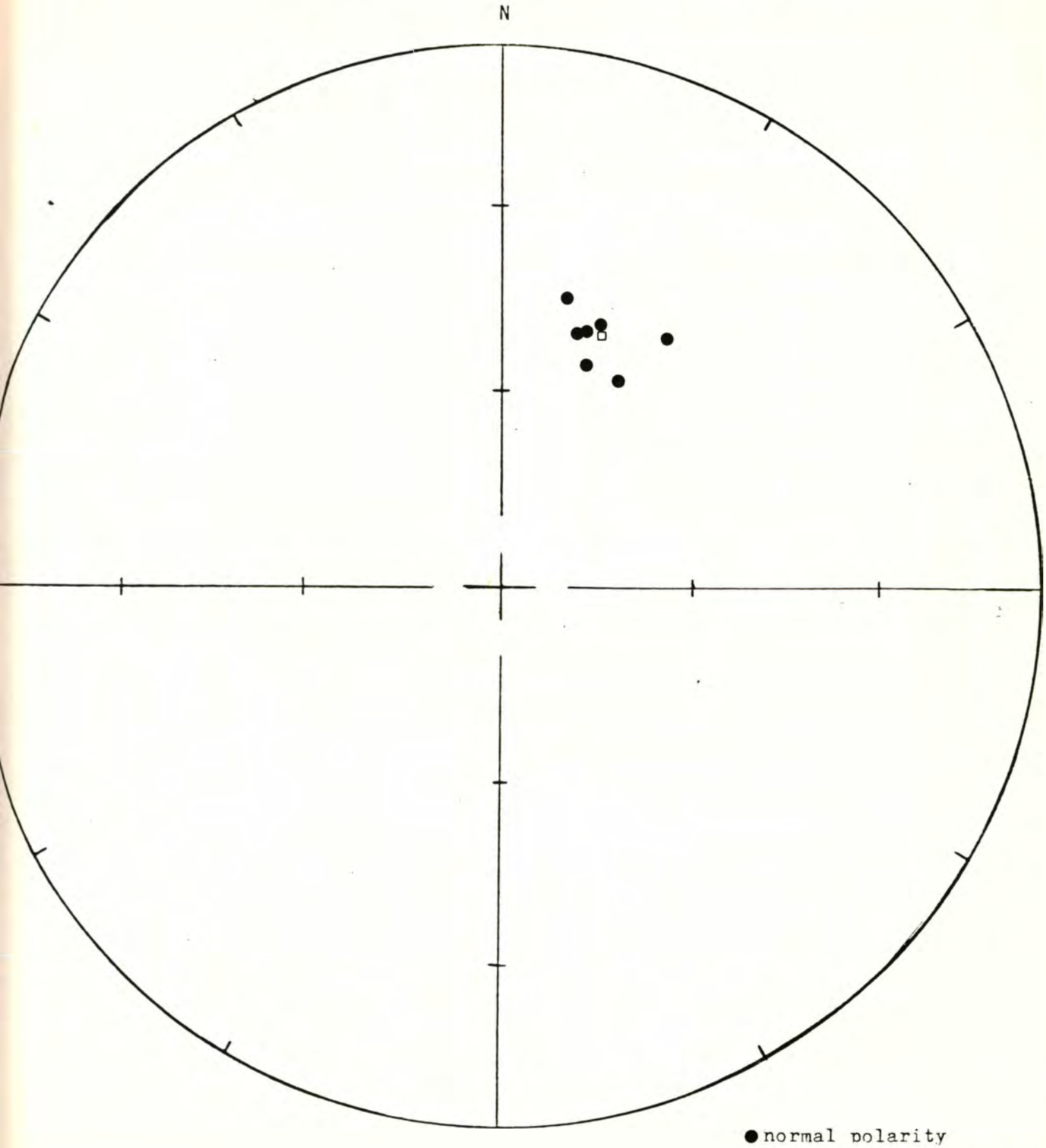

● normal polarity

○ reversed polarity

□ site mean, normal polari

△ site mean, reversed polarity

Site: 7.9.78.2

Demagnetization level: 100 oe.

FISHER ON SAMPLE DIRECTIONS

Site: 7.9.78.3 -- Iron Creek Demagnetization level: NRM

NE¼ sec. 16, T. 17 N., R. 4 W.

Sample number	Declination	Inclination
230	334.76	34.09
231	253.49	31.82
232	249.77	25.44
233	225.78	10.62
234	211.14	25.37
235	193.59	17.84
236	131.76	72.91

R= 5.86 Site declination= 230.08 Site inclination= 35.38

Alpha 95= 23.08 Delta= 33.18 Kappa= 5.26

Site latitude= 46.88° Site longitude= 123.25°

Paleolatitude= 9.74°S Paleolongitude= 170.41°W DELP= 15.42

DECLM= 26.68

Black Hills Project

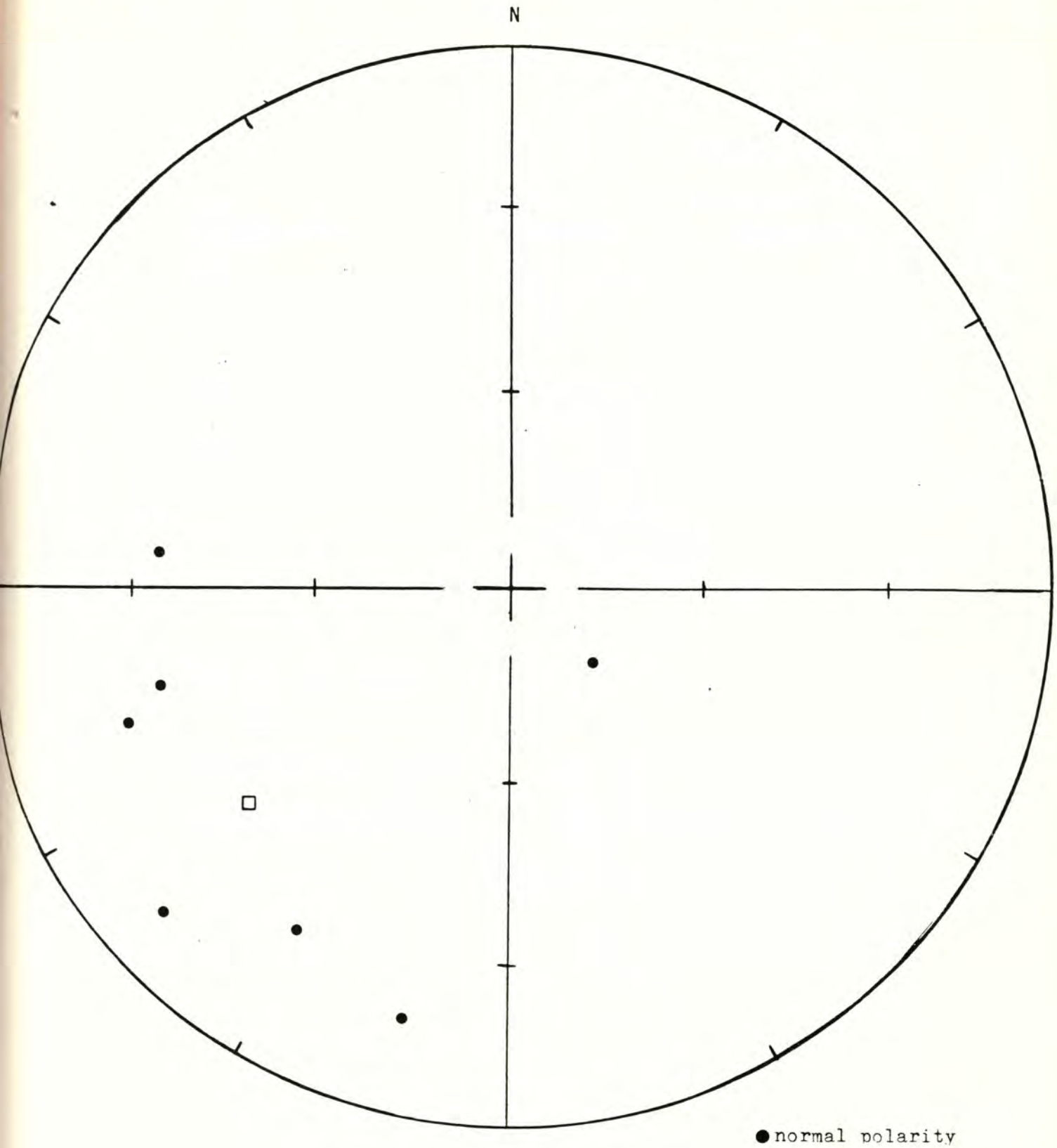

● normal polarity
○ reversed polarity
□ site mean, normal polarit
△ site mean, reversed polarity

Site: 7.9.78.3 - Iron Creek

Demagnetization level: NRM

Black Hills Project

FISHER ON SAMPLE DIRECTIONS

Site: 7.9.78.3 -- Iron Creek Demagnetization level: 100 oe.

NW¼ sec. 16, T. 17 N., R. 4 W.

Sample number	Declination	Inclination
230	35.91	61.89
231	37.96	63.85
232	31.64	67.71
233*	239.57	75.67
234	41.89	70.61
235	30.46	67.48
236	42.68	67.96

*Sample eliminated from site mean.

R= 5.99 Site declination= 36.63 Site inclination= 66.65

Alpha 95= 2.61 Delta= 3.38 Kappa= 477.96

Site latitude= 46.88° Site longitude= 123.25°

Paleolatitude= 65.64°N Paleolongitude= 52.29°W DELP= 3.55

DECLM= 4.31

Black Hills Project

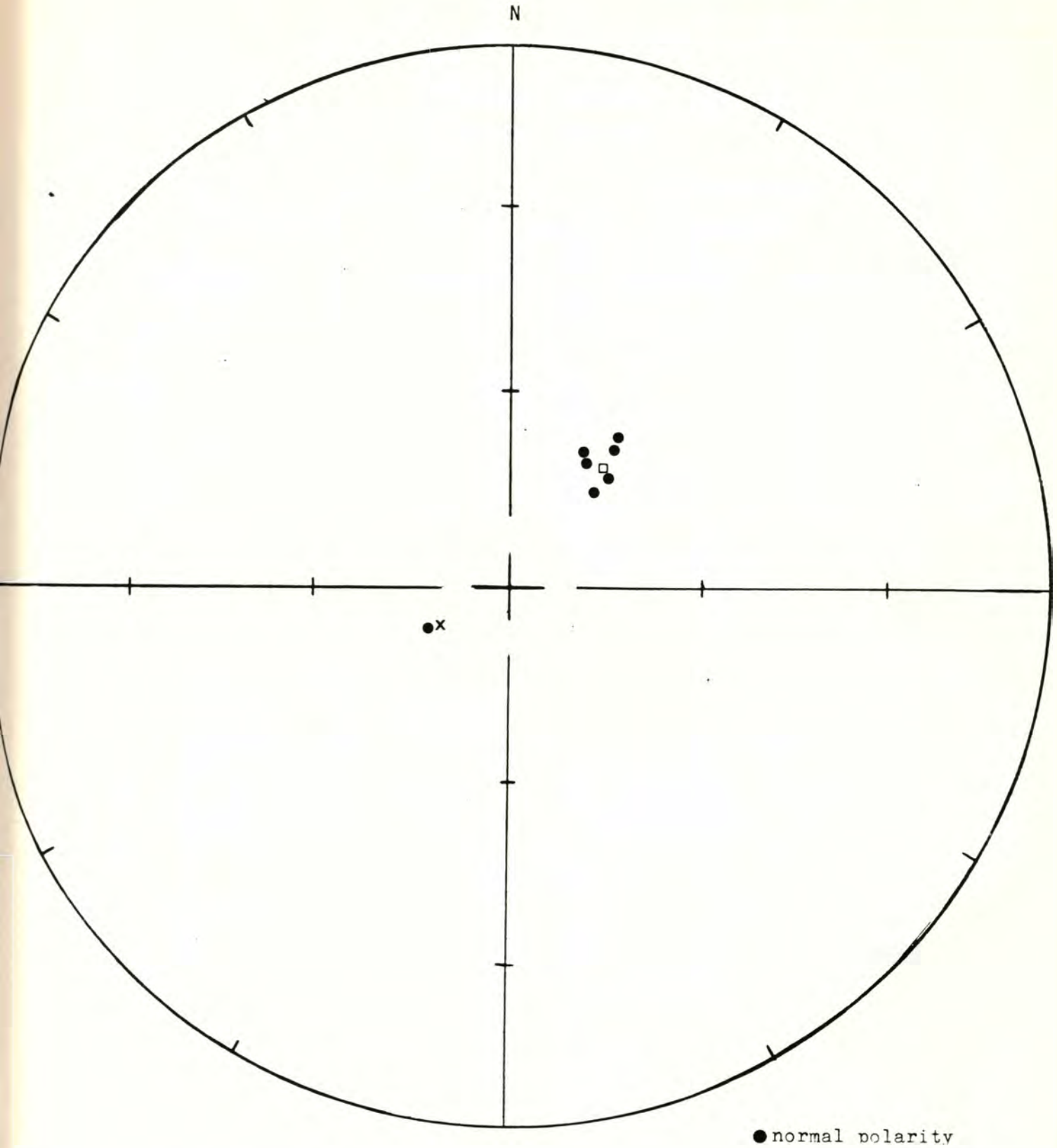

Site: 7.9.78.3 - Iron Creek

Demagnetization level: 100 oe.

● normal polarity

○ reversed polarity

□ site mean, normal polarit

△ site mean, reversed polarity

x Sample 233 eliminated from site mean.

TECTONIC CORRECTION ON SAMPLE DIRECTIONS

Pole on site mean

Site: 7.9.78.3 Demagnetization level: 100 oe.

Dip azimuth: 213 (N57W) Dip angle: 5 (W)

Sample number	Declination	Inclination	Cor. dec.	Cor. inc.
230	35.91	61.89	36.49	66.88
231	37.96	63.85	39.06	68.83
232	31.64	67.71	31.26	72.71
234	41.89	70.61	44.85	75.53
235	30.46	67.48	29.77	72.47
236	42.68	67.96	45.37	72.87

R= 5.99 Site declination= 37.57 Site inclination= 71.64

Alpha 95= 2.61 Delta= 3.38 Kappa= 477.87

Site latitude= 46.88°N Site longitude= 123.25°W

Paleolatitude= 65.20°N Paleolongitude= 69.75°W DELP= 9.25

DECLM= 10.53

WITH TECTONIC CORRECTION

Black Hills Project

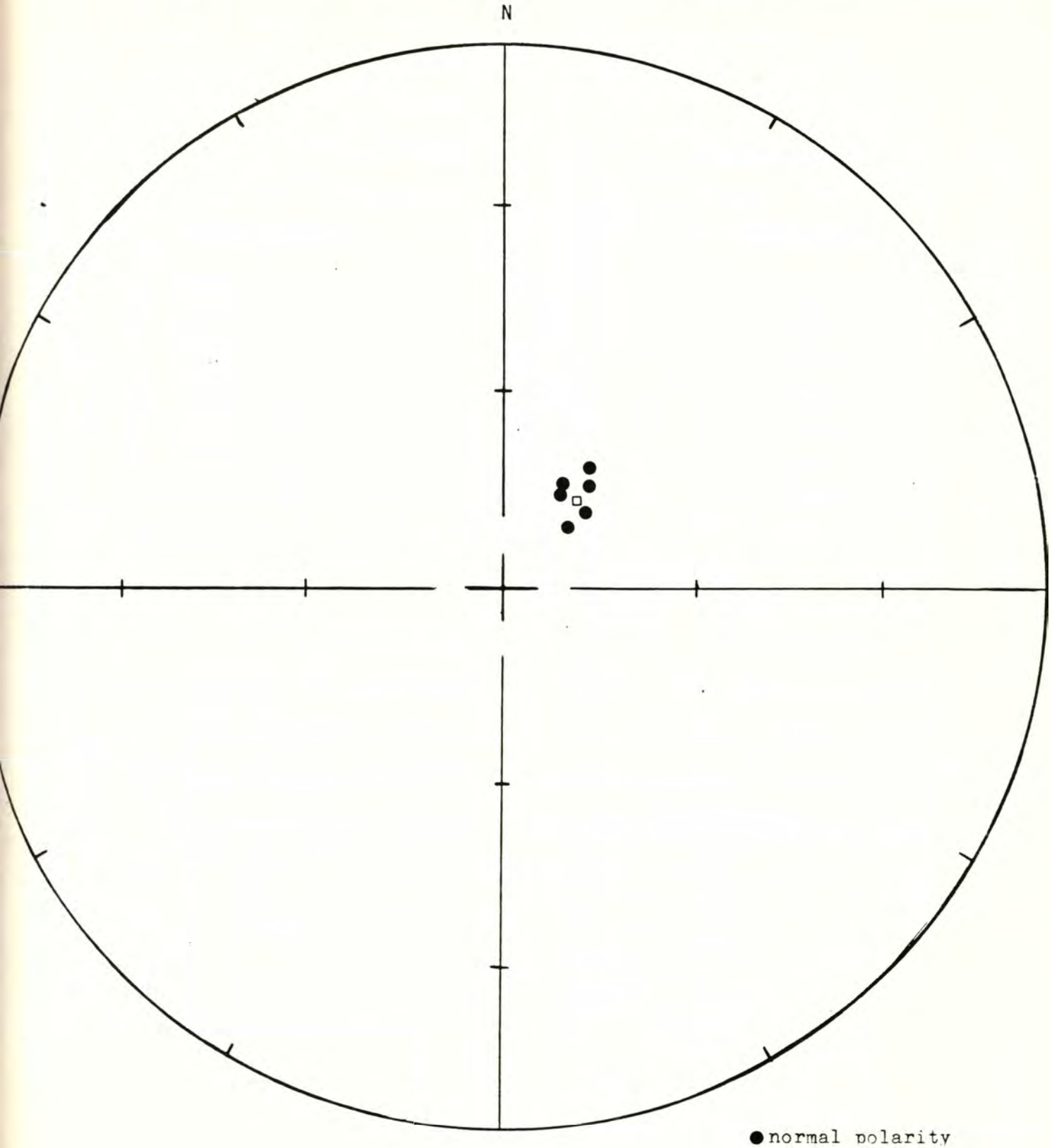

● normal polarity

○ reversed polarity

□ site mean, normal polarit

△ site mean, reversed polarity

Site: 7.9.78.3

Demagnetization level: 100 oe.

Black Hills Project

FISHER ON SAMPLE DIRECTIONS

Site: 7.9.78.4 -- Summit Lake south Demagnetization level: NRM

NW¼ NE¼ sec. 18, T. 18 N., R. 3 W.

Sample number	Declination	Inclination
237	160.37	-81.28
238	122.89	-78.16
239	137.07	-78.64
240	166.58	-79.99
241	148.47	-72.64
242	148.75	-69.35
243	162.20	-75.36

R= 6.97 Site declination= 149.17 Site inclination= -76.83

Alpha 95= 3.52 Delta= 5.00 Kappa= 225.51

Site latitude= 47.0° Site longitude= 123.0°

Paleolatitude= 65.59°N Paleolongitude= 154.72°W DELP= 6.09

DECLM= 6.55

Black Hills Project

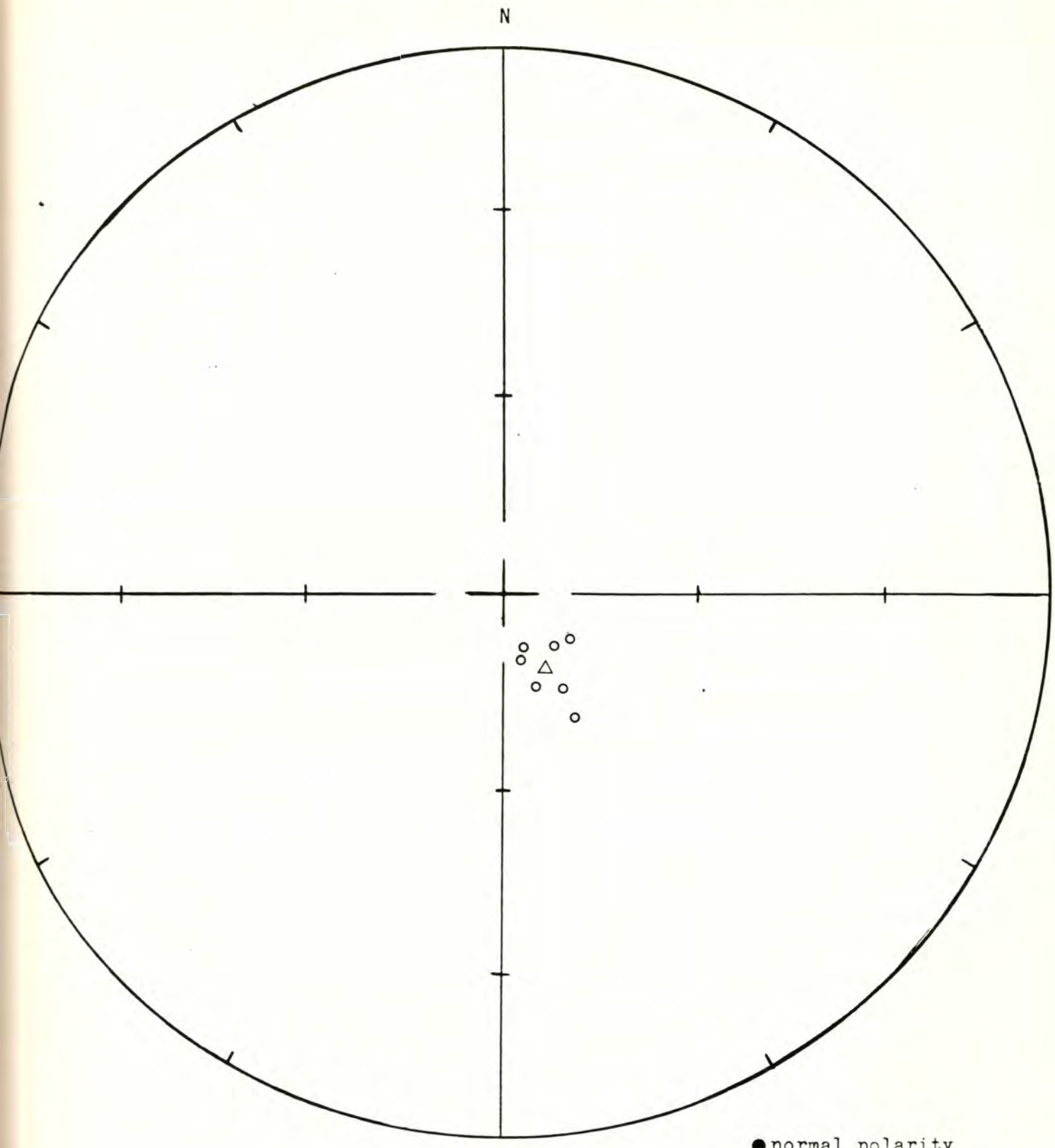

● normal polarity

○ reversed polarity

□ site mean, normal polarit

△ site mean, reversed polarity

Site: 7.9.78.4 - Summit Lake south

Demagnetization level: NRM

FISHER ON SAMPLE DIRECTIONS

Site: 7.9.78.4 -- Summit Lake south Demagnetization level: 800 oe.

NW¼ NE¼ sec. 18, T. 18 N., R. 3 W.

Sample number	Declination	Inclination
237	182.84	-67.26
238	213.83	-86.31
239	166.91	-63.78
240	182.30	-76.53
241	169.04	-67.21
242	210.43	-59.20
243	95.83	-78.25

R= 6.83 Site declination= 178.45 Site inclination= -73.45

Alpha 95= 8.84 Delta= 12.55 Kappa= 35.85

Site latitude= 47.0° Site longitude= 123.0°

Paleolatitude= 77.69°N Paleolongitude= 126.73°W DELP= 14.21

DECLM= 15.85

Black Hills Project

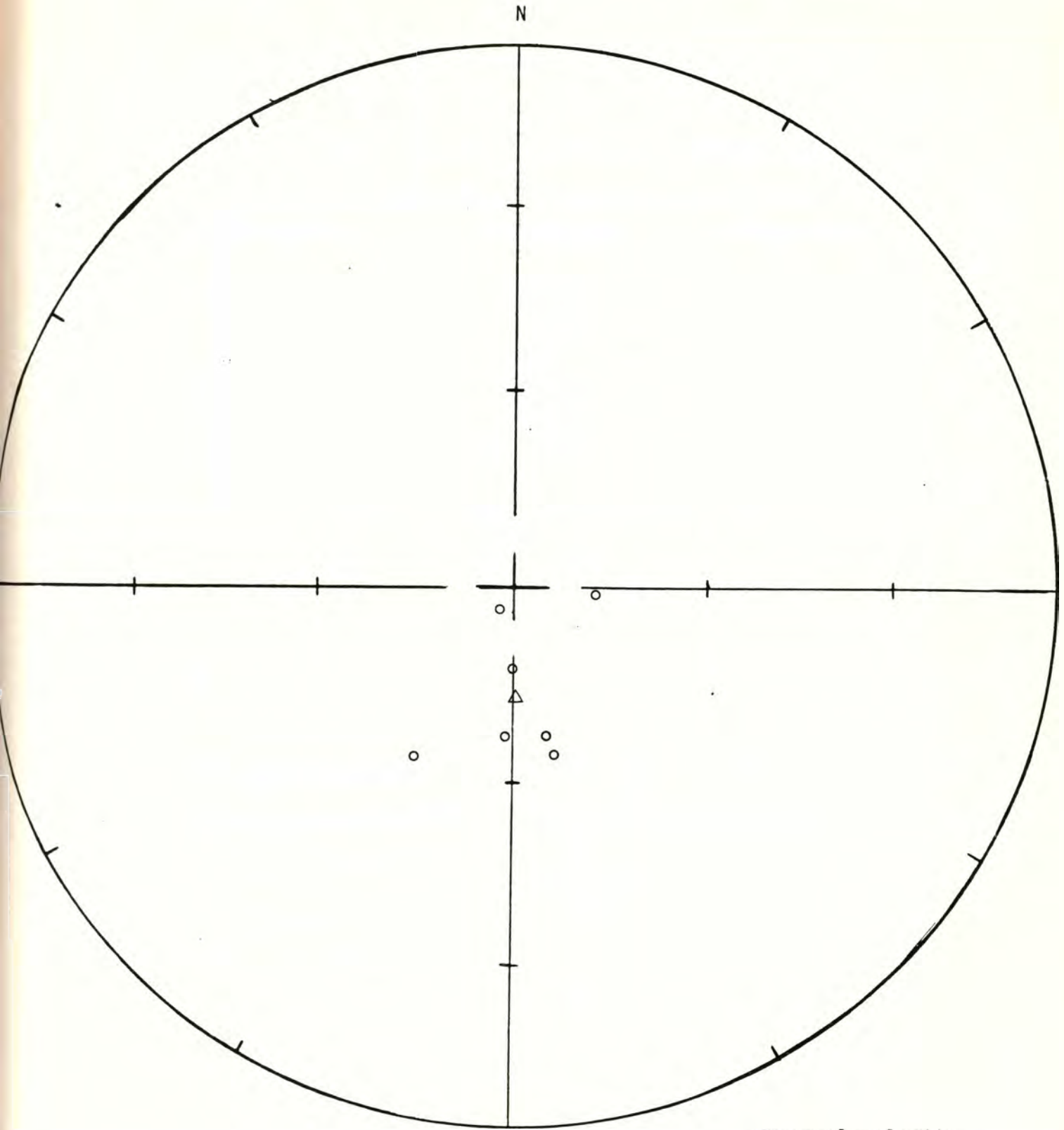

● normal polarity

○ reversed polarity

□ site mean, normal polarit

△ site mean, reversed polarity

Site: 7.9.78.4 - Summit Lake south

Demagnetization level: 800 oe.

FISHER ON SAMPLE DIRECTIONS

Site: 7.10.78.1 -- Shaker Church Road Demagnetization level: NRM

NE¼ NE¼ sec. 11, T. 18 N., R. 3 W.

Sample number	Declination	Inclination
244	171.74	-73.92
245	167.17	-77.44
246	42.54	6.16
248	192.54	-69.57
249	179.81	-81.93
250	51.61	-73.47

R= Site declination= 163.39 Site inclination= -80.29

Alpha 95= 10.25 Delta= 11.88 Kappa= 37.34

Site latitude=47.0° Site longitude= 123.0°

Paleolatitude= 64.63°N Paleolongitude= 135.48°W DELP= 18.89

DECLM= 19.68

Black Hills Project

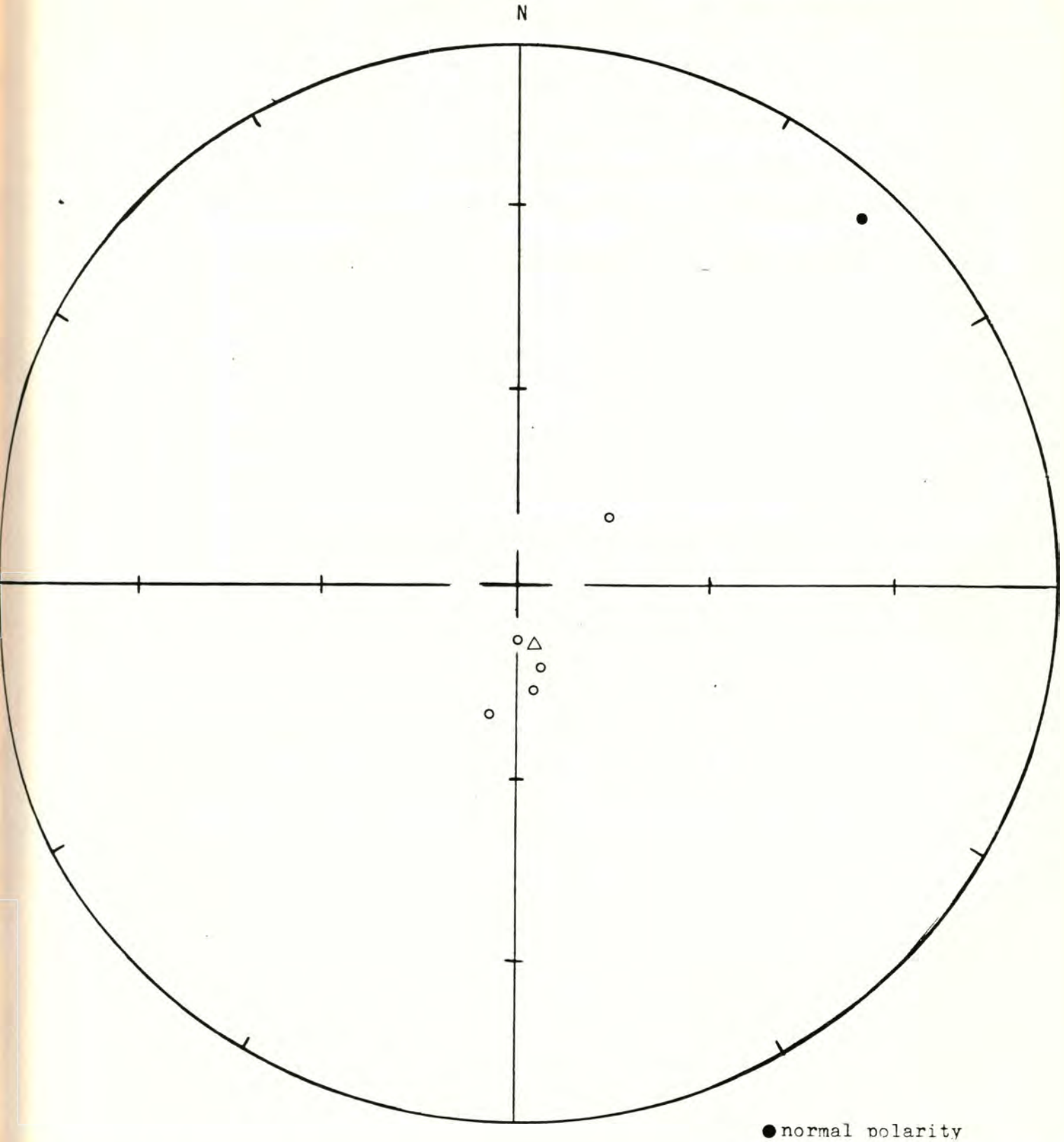

● normal polarity

○ reversed polarity

□ site mean, normal polarit

△ site mean, reversed polarity

Site: 7.10.78.1 - Shaker Church Road

Demagnetization level: NRM

FISHER ON SAMPLE DIRECTIONS

Site: 7.10.78.1 -- Shaker Church Road Demagnetization level: 200 oe.
NE¼ NE¼ sec. 11, T. 18 N., R. 3 W.

Sample number	Declination	Inclination
244	140.28	-74.44
245	177.27	-72.29
248	204.35	-69.27
249	175.62	-79.86
250	282.53	-65.11
246*		

*Sample 246 is eliminated from site mean.

R= 4.84 Site declination= 201.30 Site inclination= -78.28

Alpha 95=12.37 Delta= 14.36 Kappa= 25.60

Site latitude= 47.0° Site longitude= 123.0°

Paleolatitude= 66.78°N Paleolongitude= 102.32°W DELP= 22.01

DECLM= 23.34

Black Hills Project

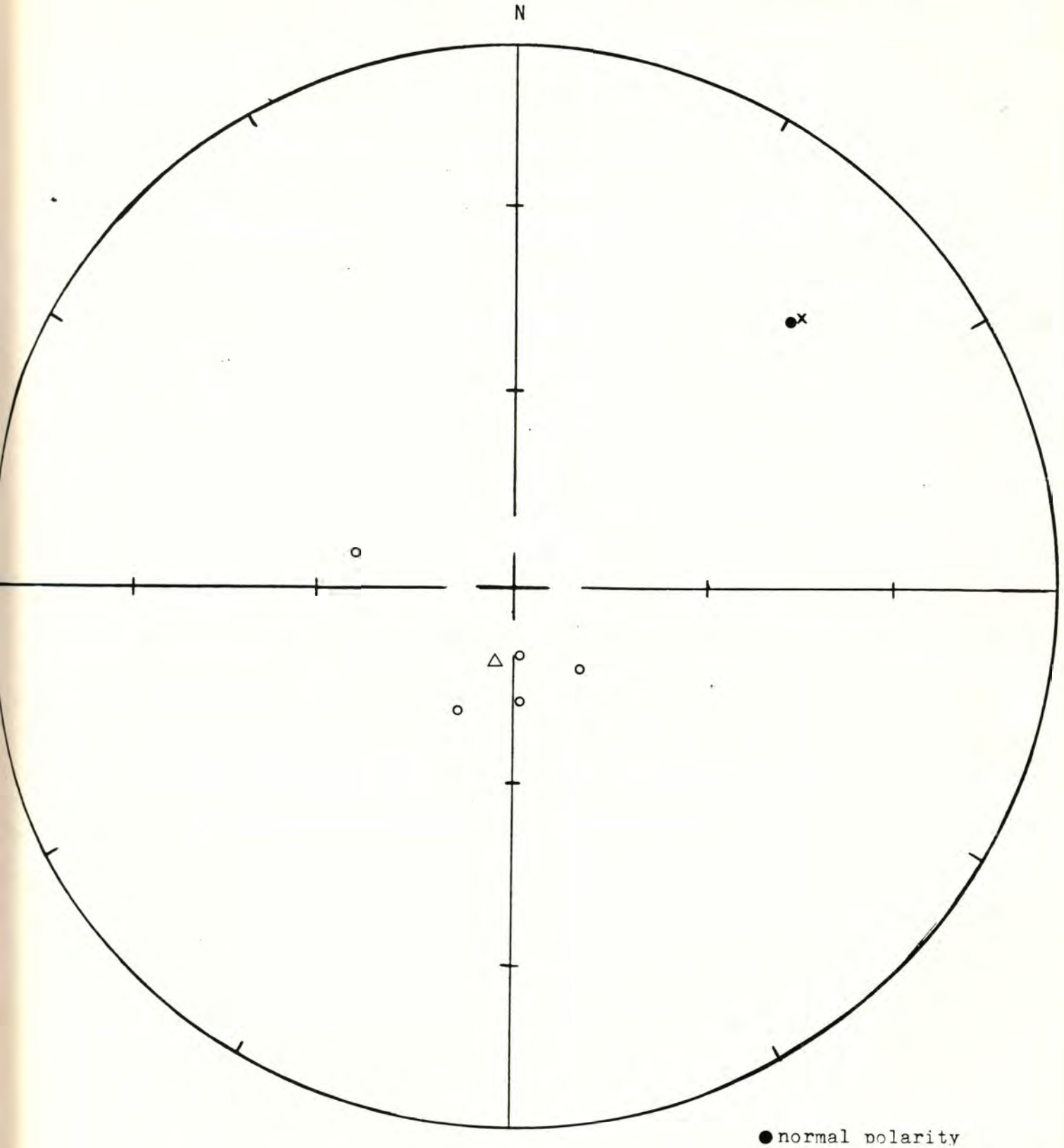

Site: 7.10.78.1 - Shaker Church Road

Demagnetization level: 200 oe.

● normal polarity

○ reversed polarity

□ site mean, normal polarit

△ site mean, reversed polarity

x sample 246 eliminated from site mean.

Black Hills Project

FISHER ON SAMPLE DIRECTIONS

Site: 7.10.78.2 -- Bordeaux Road Demagnetization level: NRM

NW¼ NW¼ sec. 9, T. 16 N., R. 3 W.

Sample number	Declination	Inclination
251	234.62	-75.59
252	225.66	-80.79
254	254.14	-78.31
255	332.34	-75.45
256	212.50	-78.88
257	105.14	27.05
258	56.80	-42.68
259	5.92	-45.81

R= Site declination= 51.38 Site inclination= -79.93

Alpha 95= 27.01 Delta= 42.31 Kappa= 3.36

Site latitude= 46.9° Site longitude= 123.0°

Paleolatitude= 33.05°N Paleolongitude= 141.18°W DELP= 49.48

DECLM= 51.70

Black Hills Project

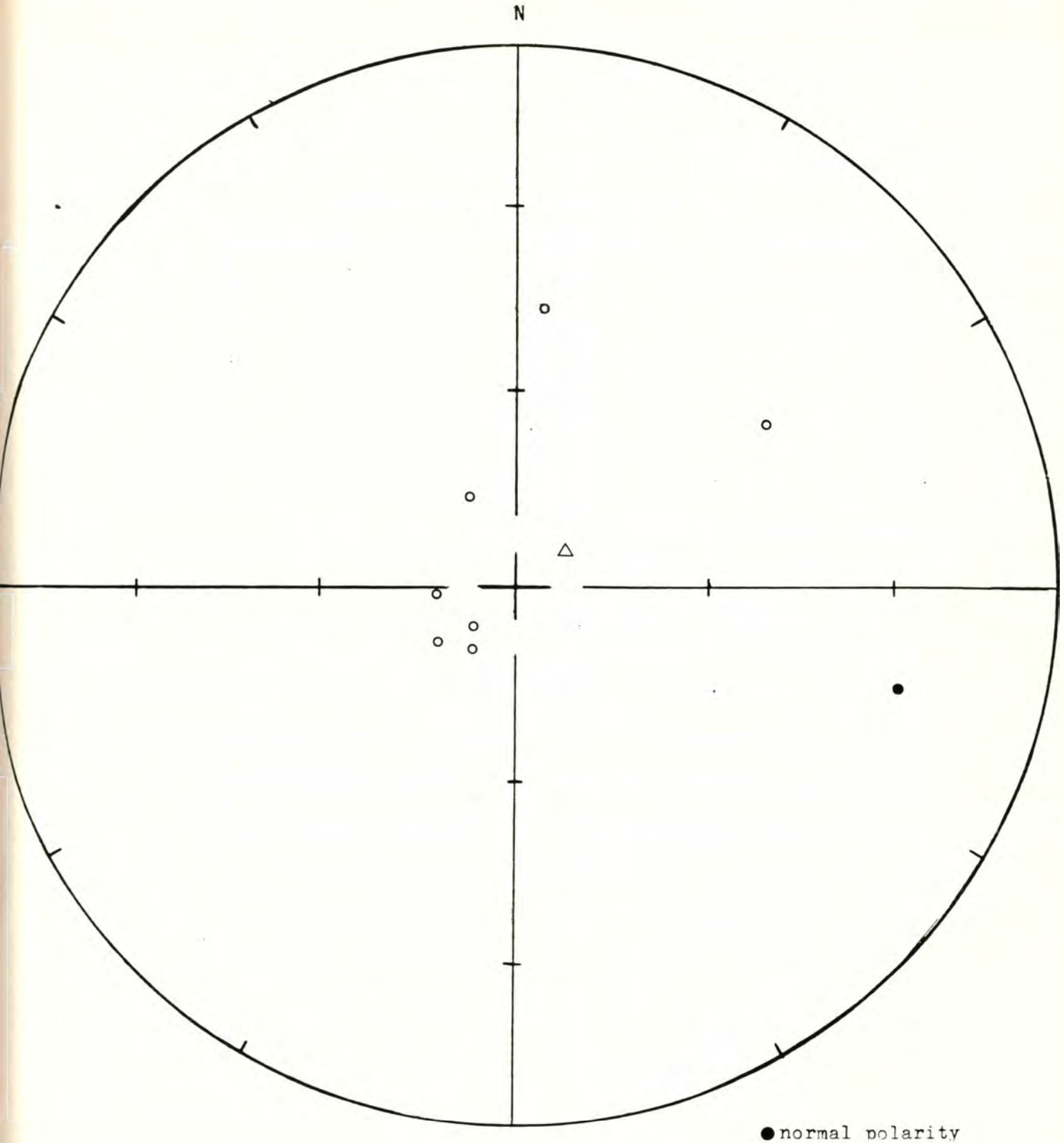

● normal polarity

○ reversed polarity

□ site mean, normal polarit

△ site mean, reversed polarity

Site: 7.10.78.2 - Bordeaux Road

Demagnetization level: NRM

FISHER ON SAMPLE DIRECTIONS

Site: 7.10.78.2 -- Bordeaux Road Demagnetization level: 200 oe.

NW¼ NW¼ sec. 9, T. 16 N., R. 3 W.

Sample number	Declination	Inclination
251	224.9	-77.83
252	235.64	-80.03
254	237.80	-77.08
255	239.76	-77.96
256	213.21	-77.65
258	231.57	-79.60

Samples 257 and 259 cannot be measured after demagnetization.

R= 6.0 Site declination= 230.34 Site inclination= -78.51

Alpha 95= 1.67 Delta= 2.16 Kappa= 1177.70

Site latitude= 46.9° Site longitude= 123.0°

Paleolatitude= 57.21°N Paleolongitude= 90.71°W DELP= 2.98

DECLM= 3.12

Black Hills Project

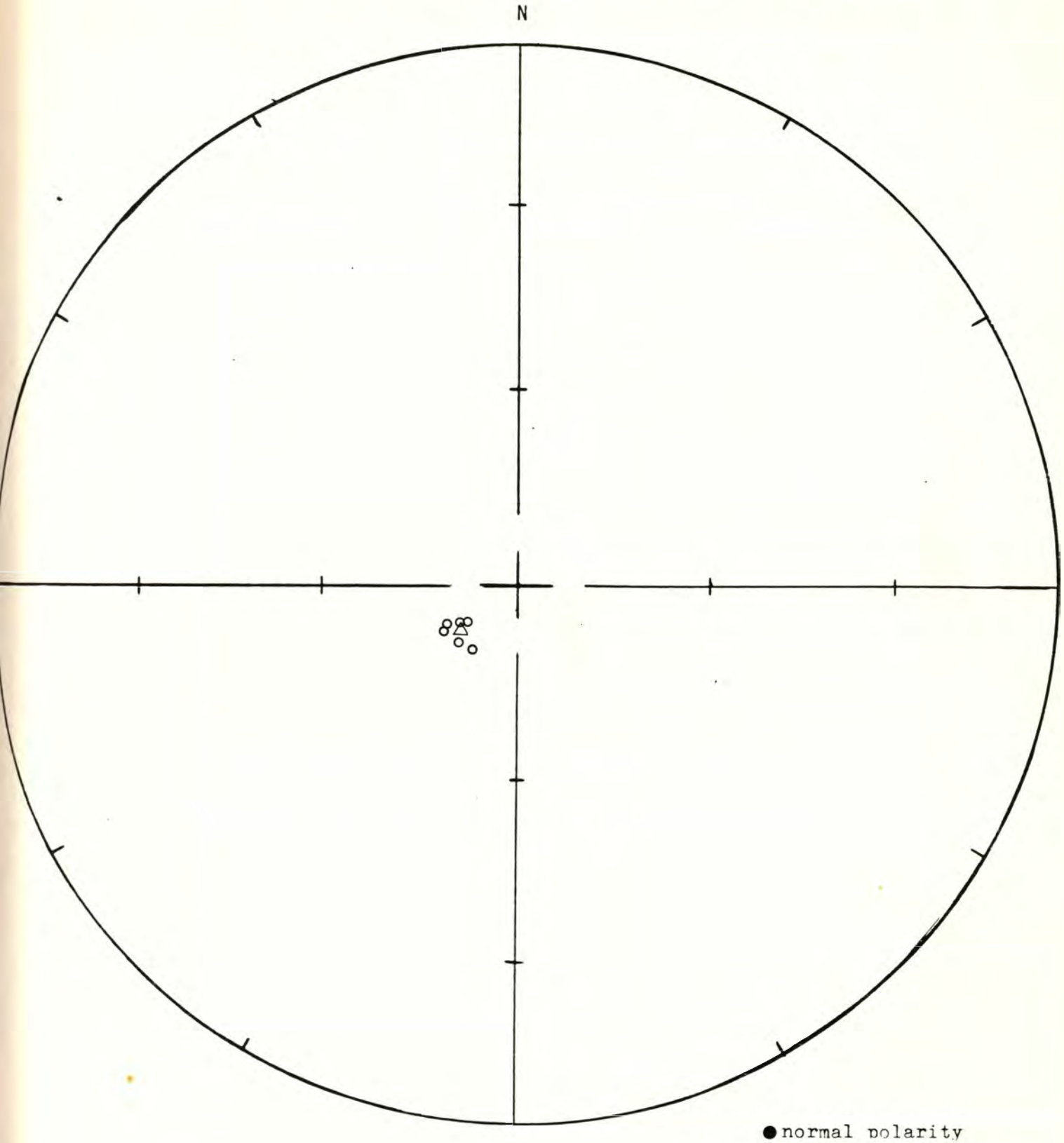

● normal polarity

○ reversed polarity

□ site mean, normal polarit

△ site mean, reversed polarity

Site: 7.10.78.2 - Bordeaux Road

Demagnetization level: 200 oe.

Two samples could not be measured following demagnetization.

FISHER ON SAMPLE DIRECTIONS

Site: 7.10.78.3 -- Sherman Valley Road Demagnetization level: NRM south

SW¼ sec. 35, T. 17 N., R. 4 W.

Sample number	Declination	Inclination
260	40.65	72.47
261	168.12	2.84
262	22.08	64.53
263	339.30	72.25
264	1.33	70.22
265	351.23	74.86
266	81.14	51.76

R= 5.68 Site declination= 58.82 Site inclination= 77.70

Alpha 95=24.82 Delta= 35.76 Kappa= 4.55

Site latitude= 46.9° Site longitude= 123.12°

Paleolatitude= 54.16°N Paleolongitude= 87.38°W DELP= 43.68

DECLM= 46.56

Black Hills Project

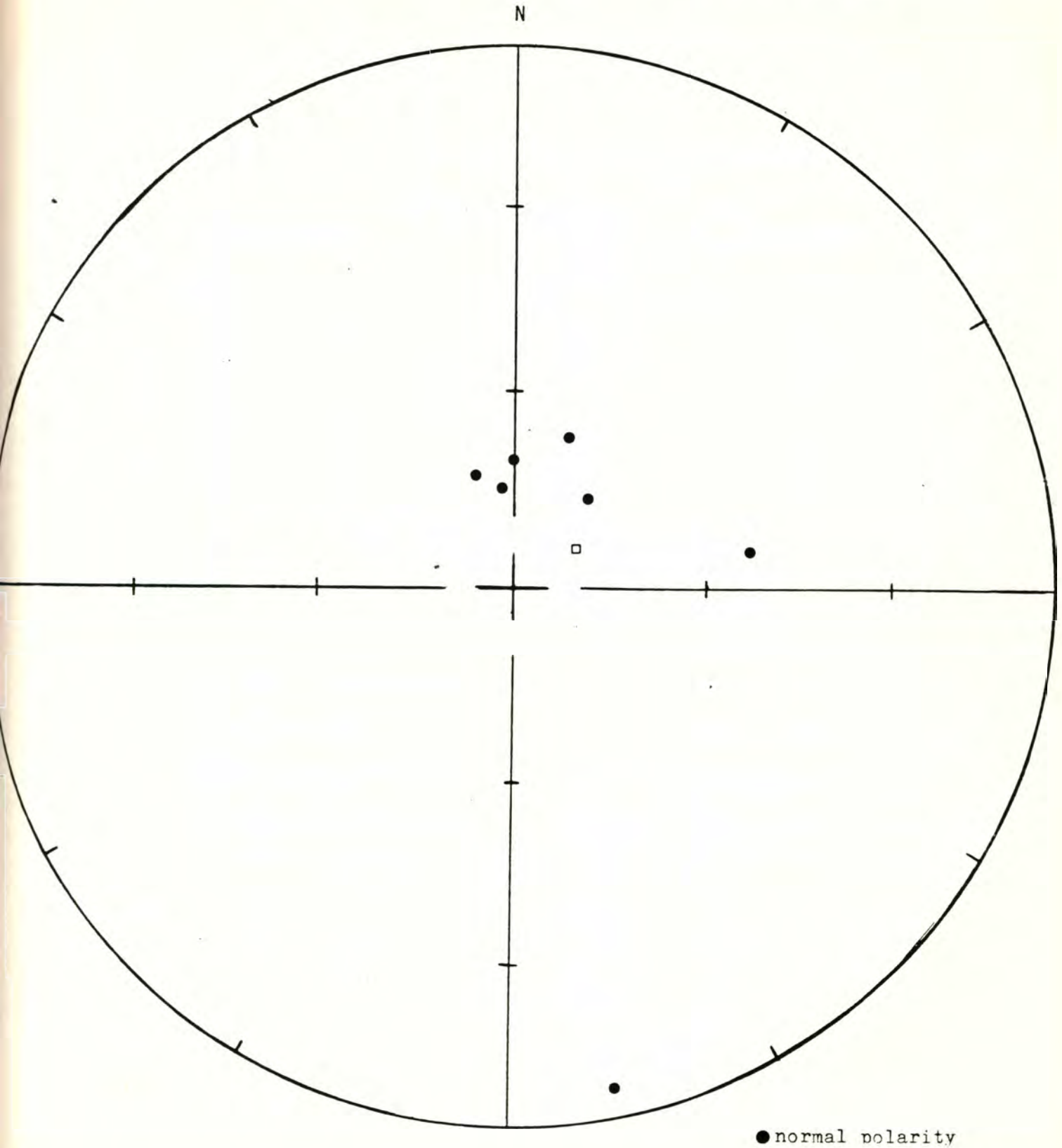

● normal polarity

○ reversed polarity

□ site mean, normal polarit

△ site mean, reversed polarity

Site: 7.10.78.3 - Sherman Valley Road south

Demagnetization level: NRM

FISHER ON SAMPLE DIRECTIONS

Site: 7.10.78.3 -- Sherman Valley Road Demagnetization level: 300 oe.
south

SW¼ sec. 35, T. 17 N., R. 4 W.

Sample number	Declination	Inclination
260	48.32	76.76
261*	168.90	2.42
262	33.46	74.68
263	346.56	67.55
264	14.58	71.42
265	11.57	70.76
266	29.62	72.83

*Sample eliminated from site mean.

R= 5.96 Site declination= 17.68 Site inclination= 73.30

Alpha 95= 5.05 Delta= 6.54 Kappa= 128.05

Site latitude= 46.9° Site longitude= 123.12°

Paleolatitude= 73.96°N Paleolongitude= 88.69°W DELP= 8.10

DECLM= 9.04

Black Hills Project

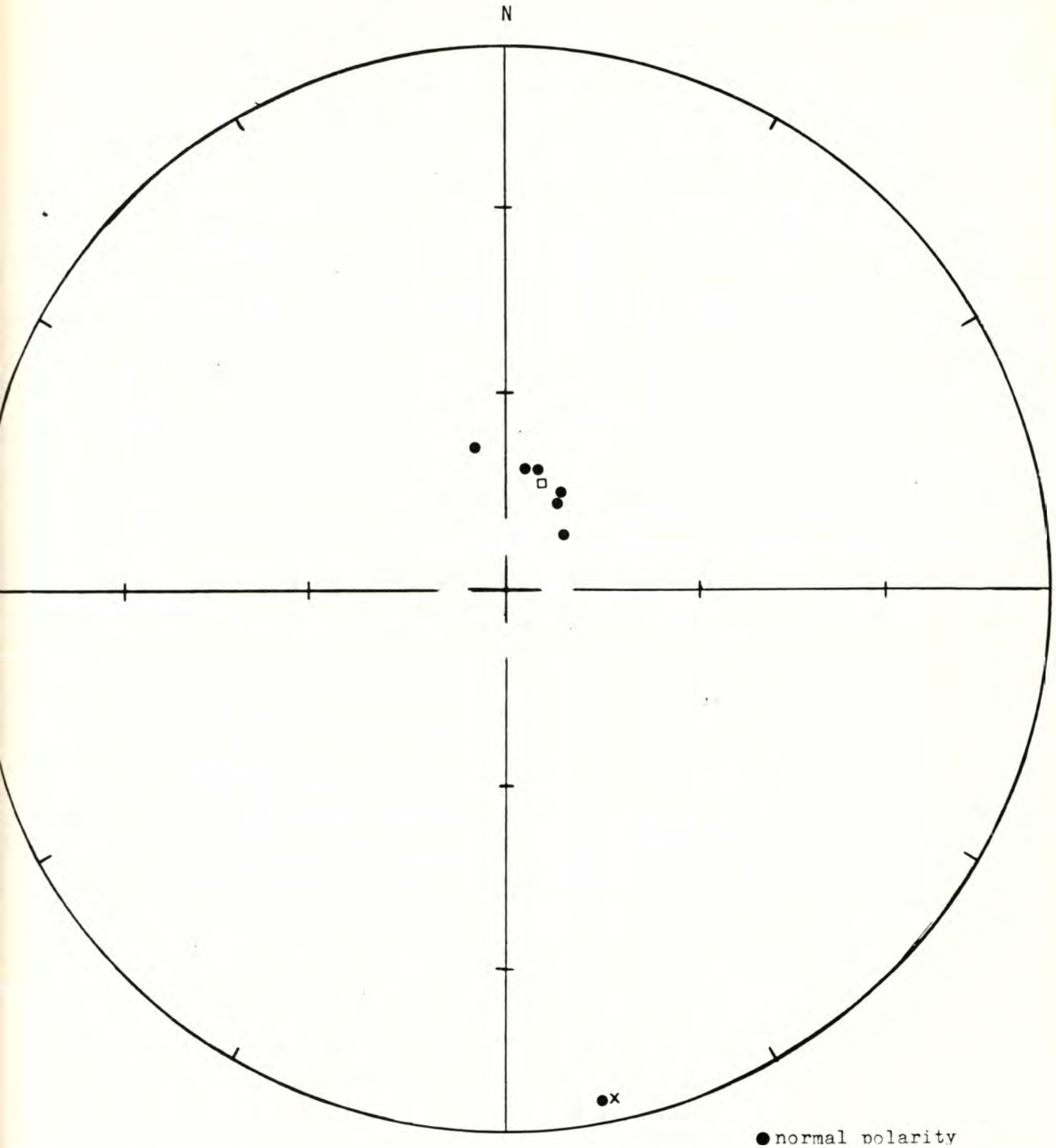

Site: 7.10.78.3 - Sherman Valley Road south

Demagnetization level: 300 oe.

● normal polarity

○ reversed polarity

□ site mean, normal polarity

△ site mean, reversed polarity

× Sample 261 is eliminated from site mean.

TECTONIC CORRECTION ON SAMPLE DIRECTIONS

Pole on site mean

Site: 7.10.78.3 Demagnetization level: 300 oe.

Dip azimuth: 247 (N23W) Dip angle: 7 (W)

Sample number	Declination	Inclination	Cor. dec.	Cor. inc.
260	48.32	76.76	29.82	83.03
262	33.46	74.68	11.69	79.77
263	346.56	67.55	329.48	67.68
264	14.58	71.42	354.03	74.69
265	11.57	70.76	351.57	73.72
266	29.62	72.83	10.00	77.66

R= 5.96 Site declination= 354.61 Site inclination= 76.78

Alpha 95= 5.05 Delta= 6.54 Kappa= 128.09

Site latitude= 46.9°N Site longitude= 123.12°W

Paleolatitude= 71.83°N Paleolongitude= 130.48°W DELP= 8.73

DECLM= 9.39

WITH TECTONIC CORRECTION

Black Hills Project

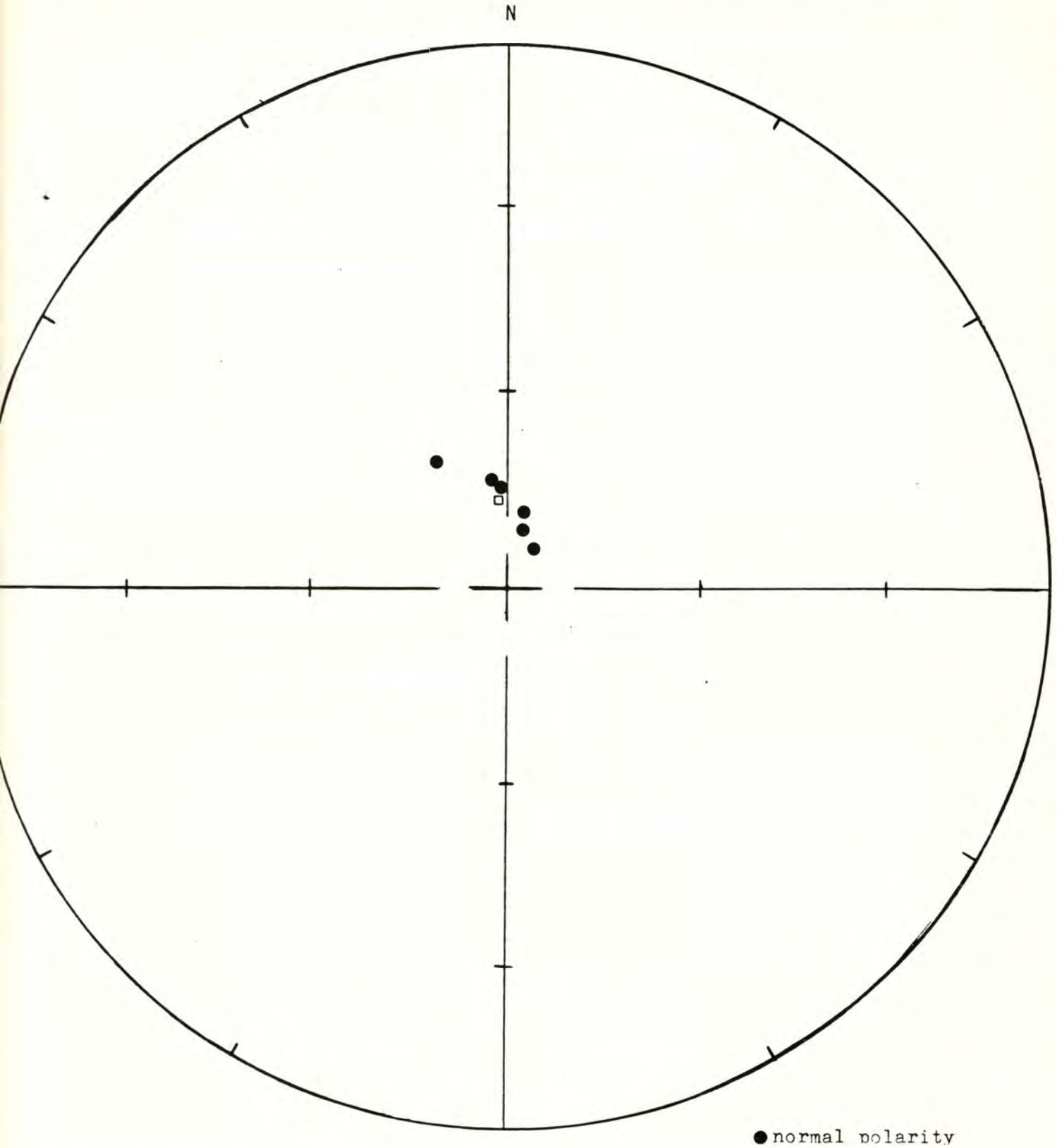

● normal polarity

○ reversed polarity

□ site mean, normal polarit

△ site mean, reversed polarity

Site: 7.10.78.3

Demagnetization level: 300 oe.

FISHER ON SAMPLE DIRECTIONS

Site: 7.10.78.4 -- Sherman Valley Road Demagnetization level: NRM north

NE¼ sec. 13, T. 17 N., R. 4 W.

Sample number	Declination	Inclination
267	194.71	46.50
268	17.55	52.16
269	21.22	48.48
271	8.07	55.36
272	16.72	50.39
273	19.26	46.21

R= 5.21 Site declination= 17.42 Site inclination= 61.58

Alpha 95= 22.78 Delta= 29.81 Kappa= 6.29

Site latitude= 46.9° Site longitude= 123.12°

Paleolatitude=76.99°N Paleolongitude= 20.80°W DELP= 27.12

DECLM= 35.15

Black Hills Project

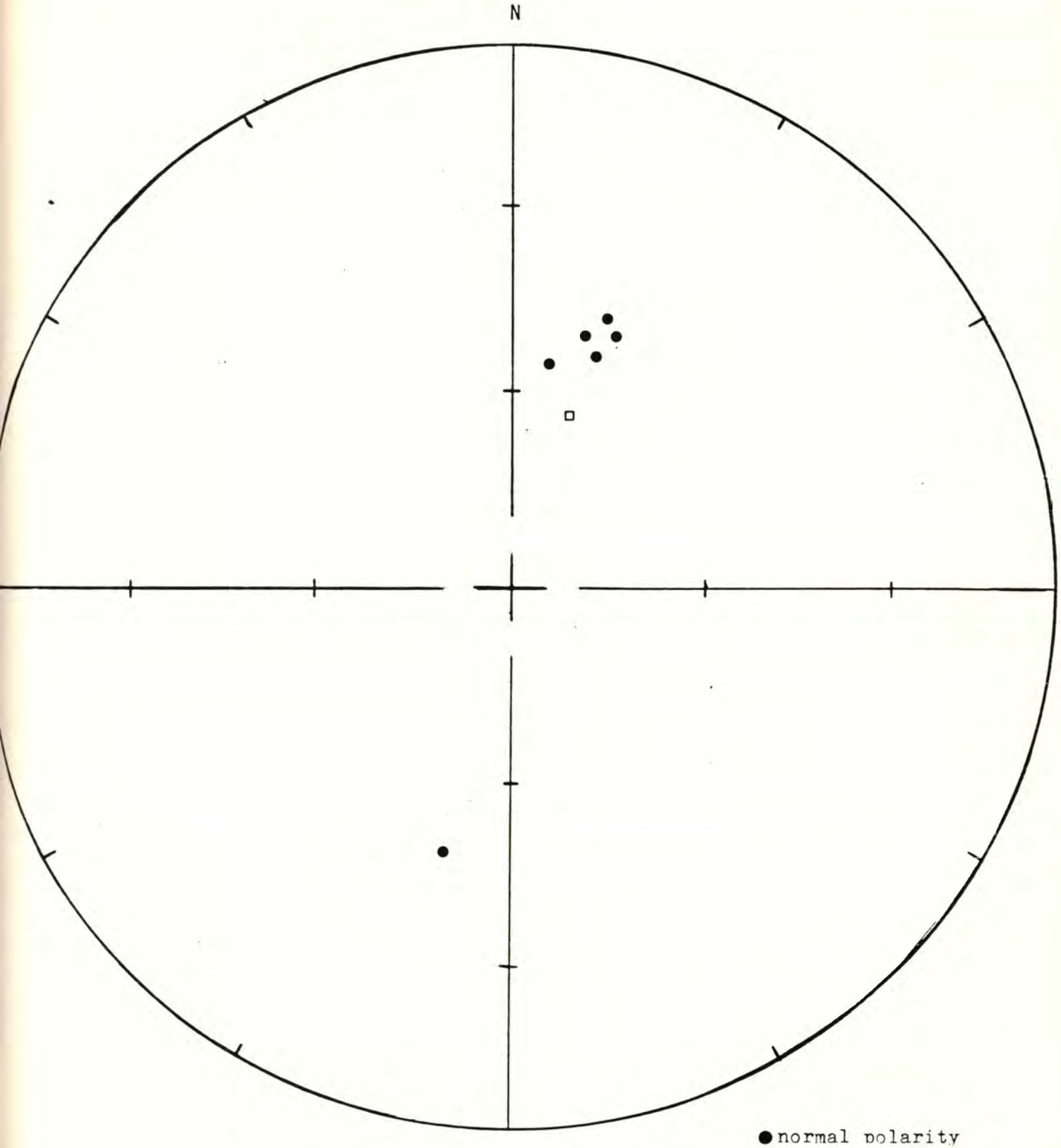

● normal polarity

○ reversed polarity

□ site mean, normal polarit

△ site mean, reversed polarity

Site: 7.10.78.4 - Sherman Valley Road north

Demagnetization level: NRM

FISHER ON SAMPLE DIRECTIONS

Site: 7.10.78.4 -- Sherman Valley Road south Demagnetization level: 300 oe.

NE¼ sec. 13, T. 17 N., R. 4 W.

Sample number	Declination	Inclination
267*	198.81	48.63
268	17.66	54.01
269	11.30	50.66
271	5.90	53.87
272	4.92	51.65
273	16.32	48.31

*Sample eliminated from site mean.

R= 4.99 Site declination= 11.28 Site inclination= 51.82

Alpha 95= 3.32 Delta= 3.85 Kappa= 355.21

Site latitude= 46.9° Site longitude= 123.12°

Paleolatitude= 73.18°N Paleolongitude= 22.10°E DELP= 4.66

DECLM= 6.83

Black Hills Project

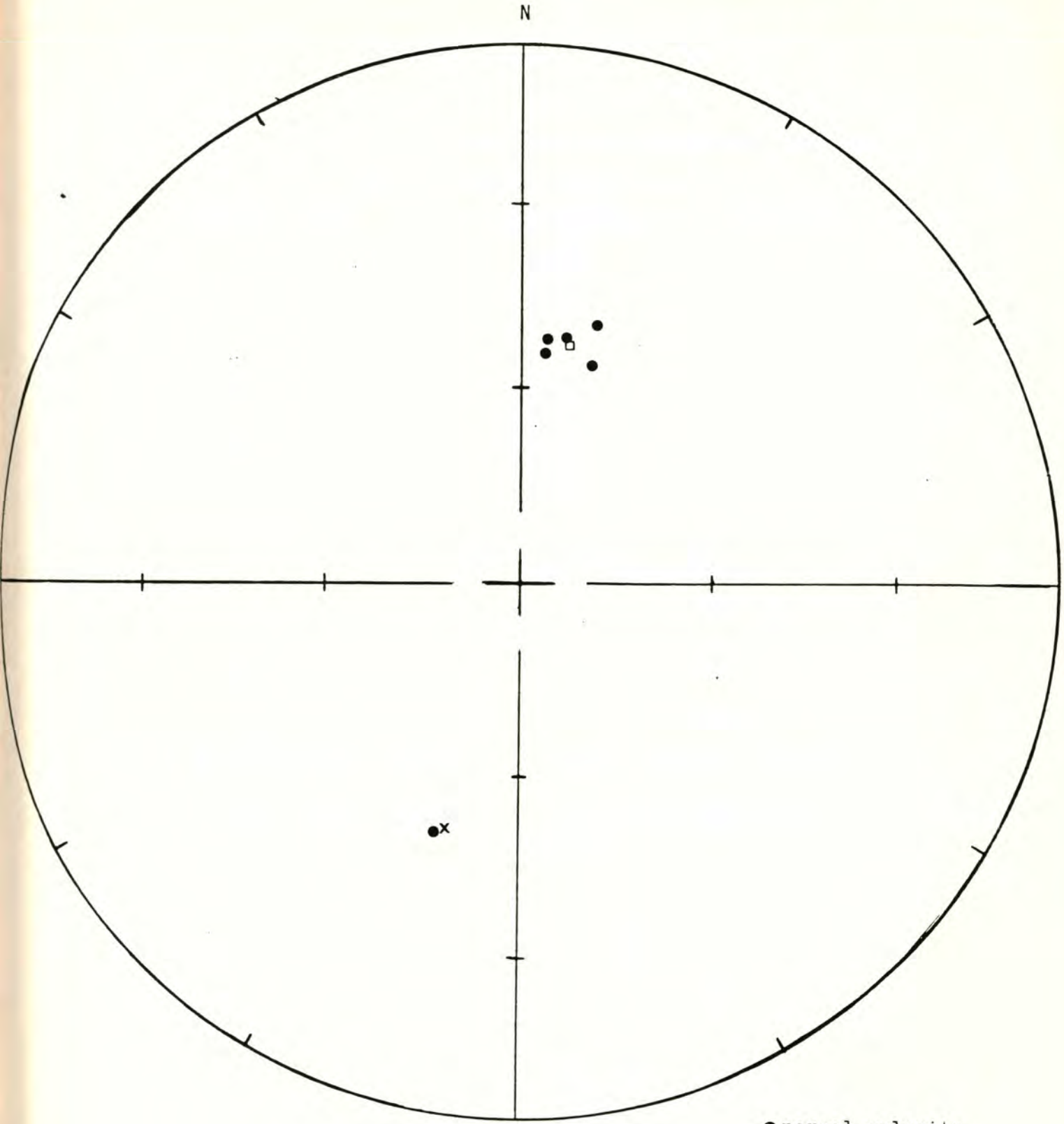

Site: 7.10.78.4 - Sherman Valley Road north

Demagnetization level: 300 oe.

● normal polarity

○ reversed polarity

□ site mean, normal polarit

△ site mean, reversed polarity

×Sample 267 is eliminated from site mean.

FISHER ON SAMPLE DIRECTIONS

Site: 8.6.78.1 -- US 12, Oakville quarry Demagnetization level: NRM

NW¼ NE¼ sec. 25, T. 16 N., R. 4 W.

Sample number	Declination	Inclination
274	250.29	-66.63
275.	245.12	-57.04
276	244.05	-51.17
277	242.36	-53.45
278	197.21	-52.64
279	324.53	9.72
280	238.09	-39.66

R= 6.05 Site declination= 219.39 Site inclination= -54.71

Alpha 95= 21.02 Delta= 30.14 Kappa= 6.34

Site latitude= 46.83° Site longitude= 123.25°

Paleolatitude= 41.93°N Paleolongitude= 33.69°W DELP= 4.86

DECLM= 7.41

Black Hills Project

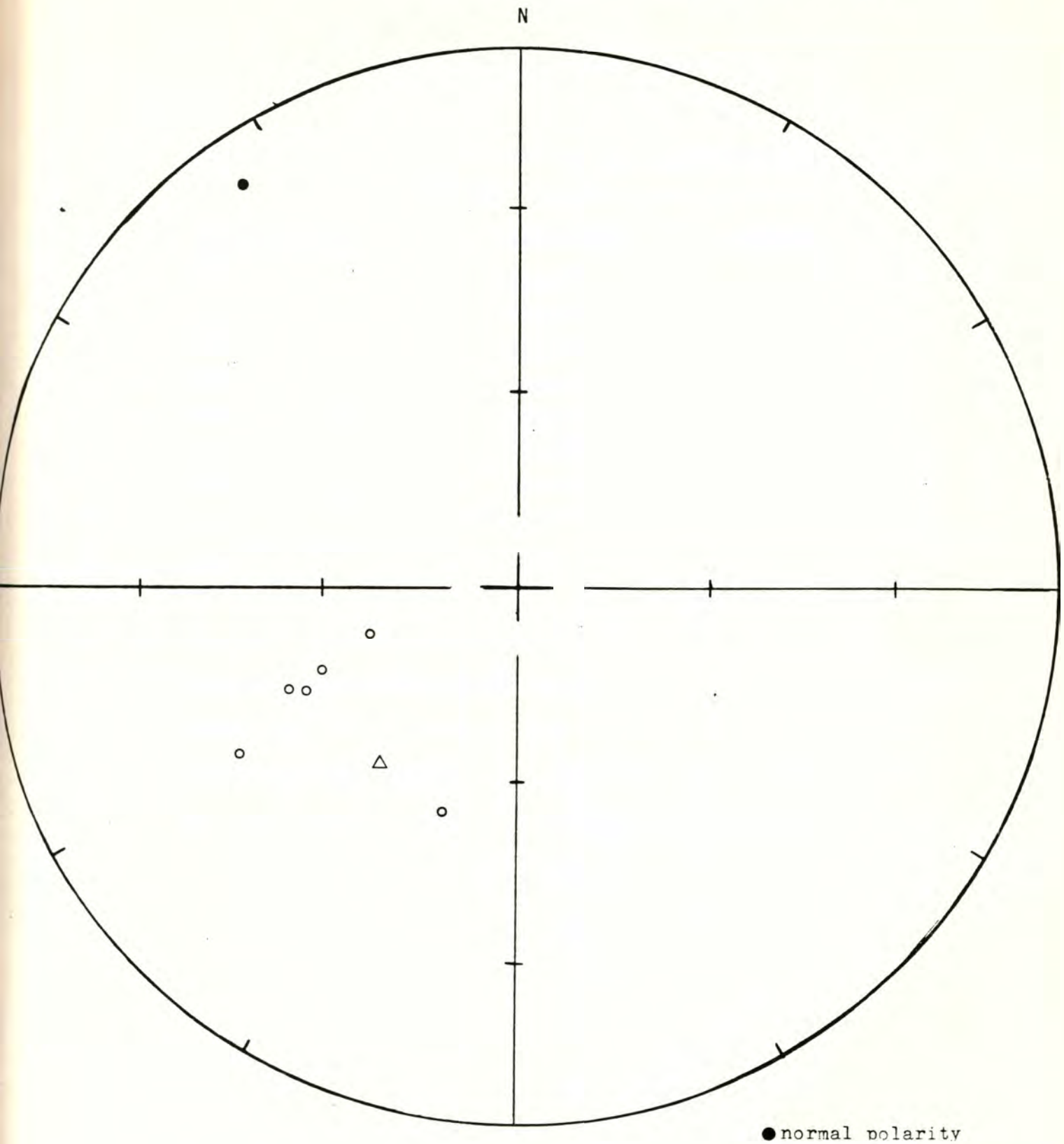

● normal polarity

○ reversed polarity

□ site mean, normal polarity

△ site mean, reversed polarity

Site: 8.6.78.1 - US 12, Oakville quarry.

Demagnetization level: NRM

FISHER ON SAMPLE DIRECTIONS

Site: 8.6.78.1 -- US 12, Oakville quarry Demagnetization level: 300 oe.
NW¼ NE¼ sec. 25, T. 16 N., R. 4 W.

Sample number	Declination	Inclination
274	238.34	-55.02
275	238.59	-55.28
276	241.36	-51.33
277	243.26	-52.59
278	229.94	-47.35
279	242.75	-32.37
280	236.09	-44.36

R= 6.93 Site declination= 238.66 Site inclination= -48.44

Alpha 95= 5.64 Delta= 8.01 Kappa= 87.91

Site latitude= 46.83° Site longitude= 123.25°

Paleolatitude= 41.93°N Paleolongitude= 33.69°W DELP= 4.86

DECLM= 7.41

Black Hills Project

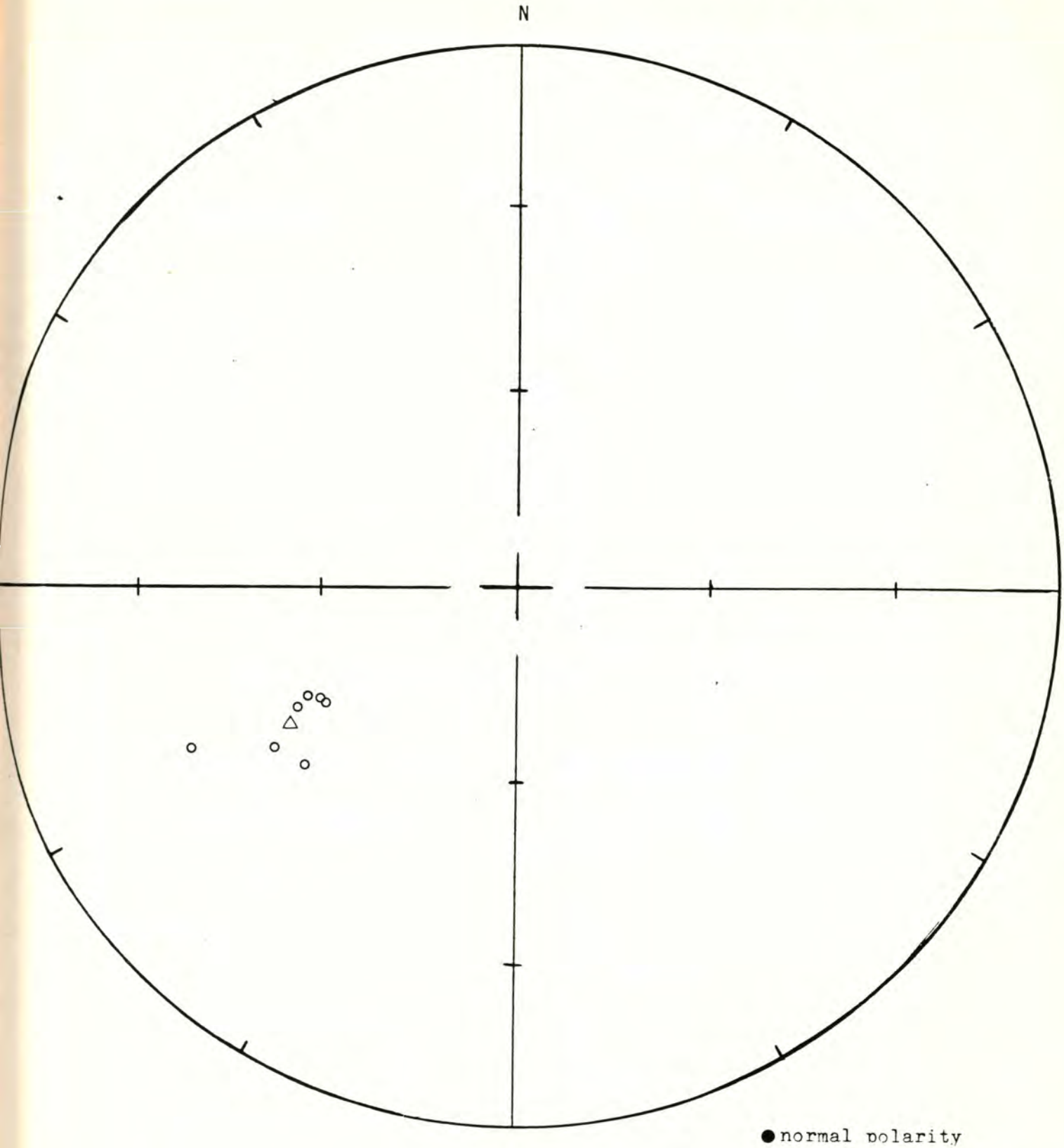

Site: 8.6.78.1 - US 12, Oakville quarry.

Demagnetization level: 300 oe.

● normal polarity

○ reversed polarity

□ site mean, normal polarit

△ site mean, reversed polarity

FISHER ON SAMPLE DIRECTIONS

Site: 8.6.78.2 -- US 12, Gibson Creek Demagnetization level: NRM

NW¼ sec. 34, T. 17 N., R. 5 W.

Sample number	Declination	Inclination
281	47.03	47.42
282	22.84	67.40
283	357.83	30.49
284	34.13	58.98
285	33.05	51.78
286	186.10	-30.50
287	19.99	53.87

R= 6.70 Site declination= 20.79 Site inclination= 49.91

Alpha 95= 11.86 Delta= 16.88 Kappa= 19.90

Site latitude= 46.88° Site longitude= 123.3°

Paleolatitude= 67.25°N Paleolongitude= 4.61°E DELP= 10.57

DECLM= 15.84

Black Hills Project

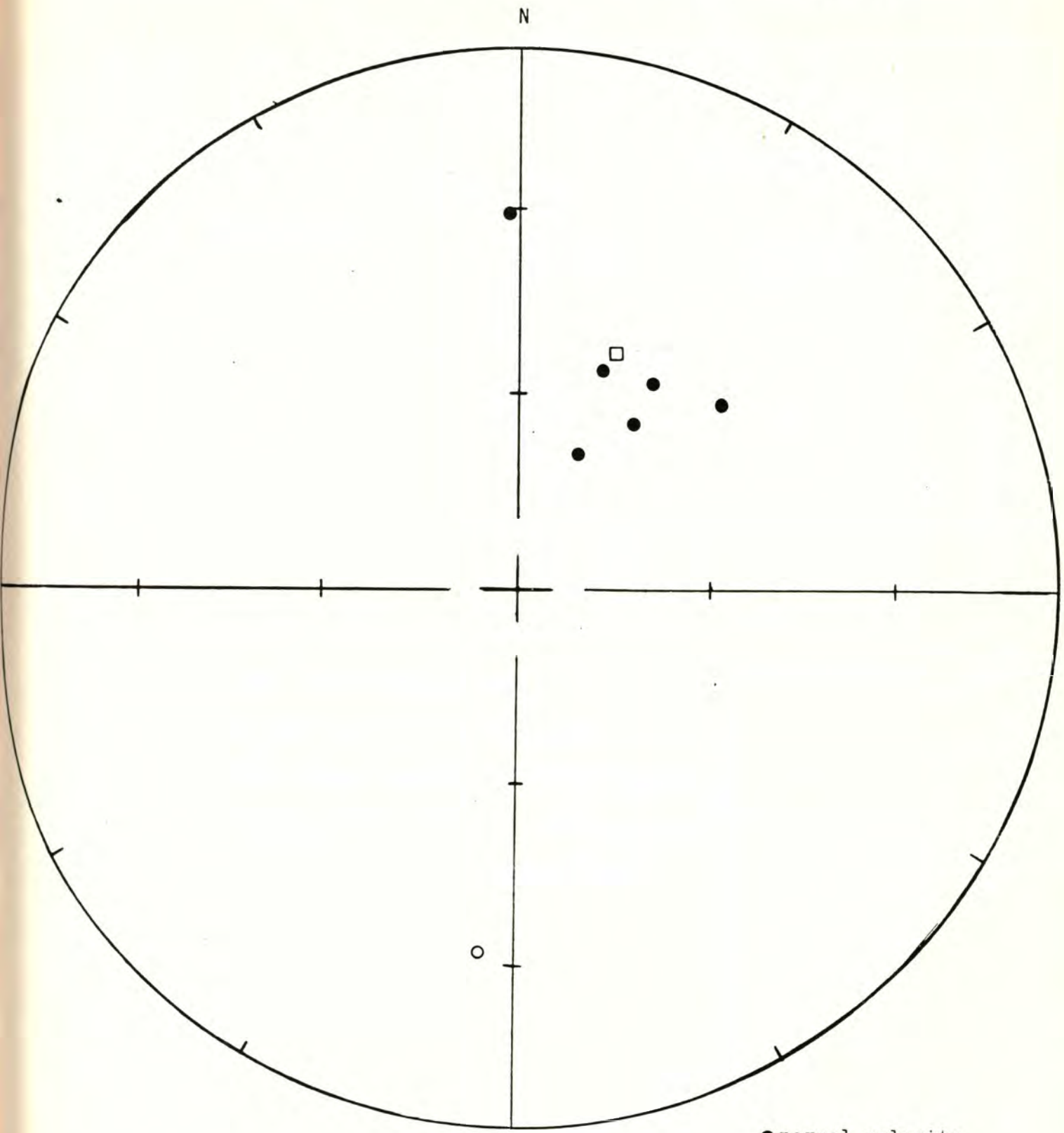

● normal polarity

○ reversed polarity

□ site mean, normal polarit

△ site mean, reversed polarity

Site: 8.6.78.2 - US 12, Gibson Creek

Demagnetization level: NRM

FISHER ON SAMPLE DIRECTIONS

Site: 8.6.78.2 -- US 12, Gibson Creek Demagnetization level: 300 oe.
NW¼ sec. 34, T. 17 N., R. 5 W.

Sample number	Declination	Inclination
281	20.03	49.31
282	34.0	62.60
283	6.46	29.23
284	30.78	48.69
285	28.88	49.84
286	30.95	52.42
287	349.74	62.43

R=6.80 Site declination= 20.18 Site inclination= 51.54

Alpha 95= 9.56 Delta= 13.58 Kappa= 30.65

Site latitude= 46.88° Site longitude= 123.3°

Paleolatitude= 68.72°N Paleolongitude= 3.15°E DELP= 9.04

DECLM= 13.27

Black Hills Project

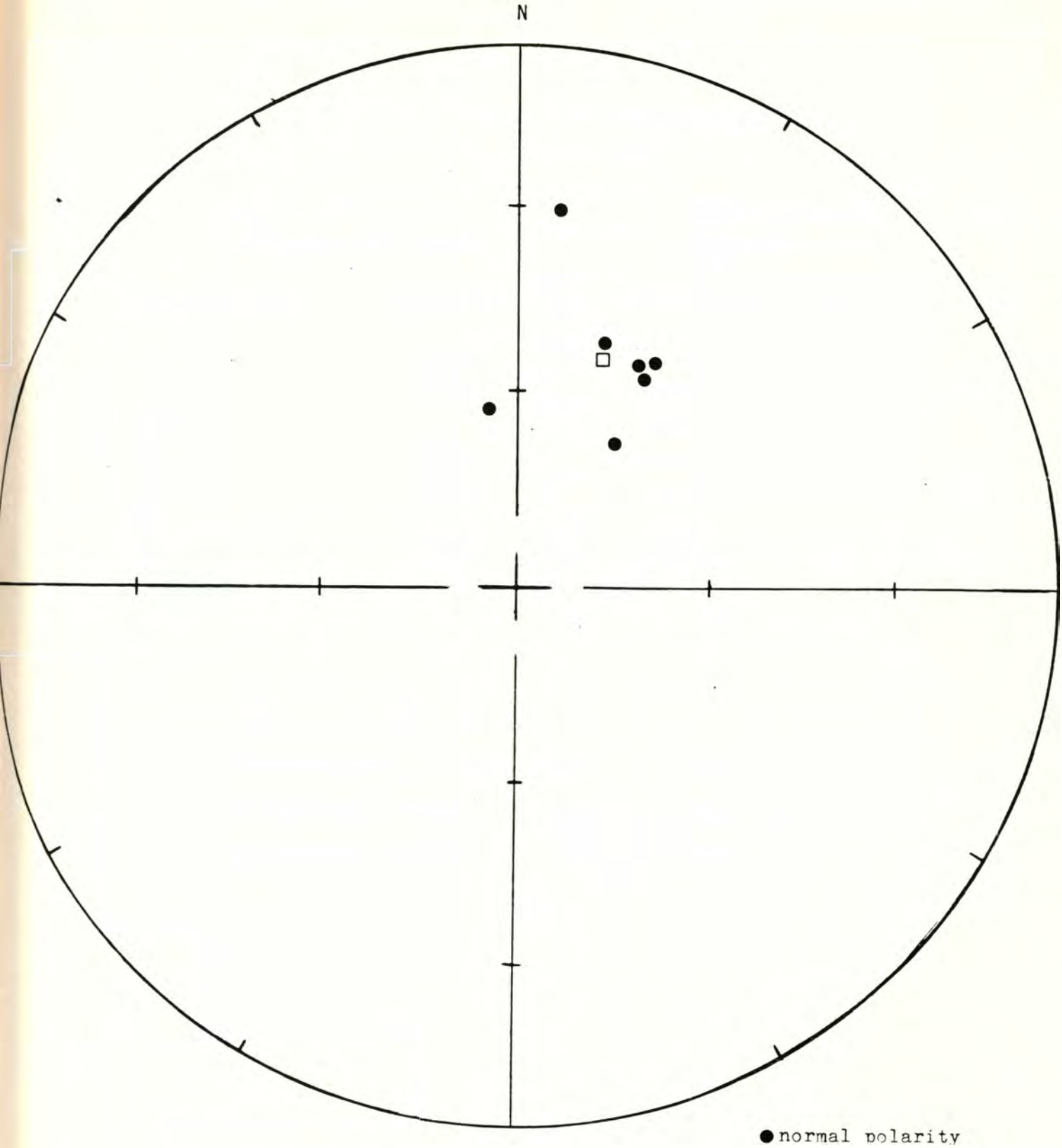

● normal polarity

○ reversed polarity

□ site mean, normal polarit

△ site mean, reversed polarity

Site: 8.6.78.2 - US 12, Gibson Creek

Demagnetization level: 300 oe.

TECTONIC CORRECTION ON SAMPLE DIRECTIONS

Pole on site mean

Site: 8.6.78.2 Demagnetization level: 300 oe.

Dip azimuth: 308 (N38E) Dip angle: 10 (W)

Sample number	Declination	Inclination	Cor. dec.	Cor. inc.
281	20.03	49.31	10.00	45.38
282	34.00	62.60	15.97	60.31
283	6.46	29.23	2.30	23.68
284	30.78	48.69	20.05	46.50
285	28.88	49.84	17.87	47.30
286	30.95	52.42	18.75	50.13
287	349.73	62.43	339.94	54.39

R= 6.80 Site declination= 9.36 Site inclination= 47.57

Alpha 95= 9.56 Delta= 13.58 Kappa= 30.65

Site latitude= 46.88°N Site longitude= 123.30°W

Paleolatitude= 70.39°N Paleolongitude= 31.54°E DELP= 8.08

DECLM= 12.43

WITH TECTONIC CORRECTION

Black Hills Project

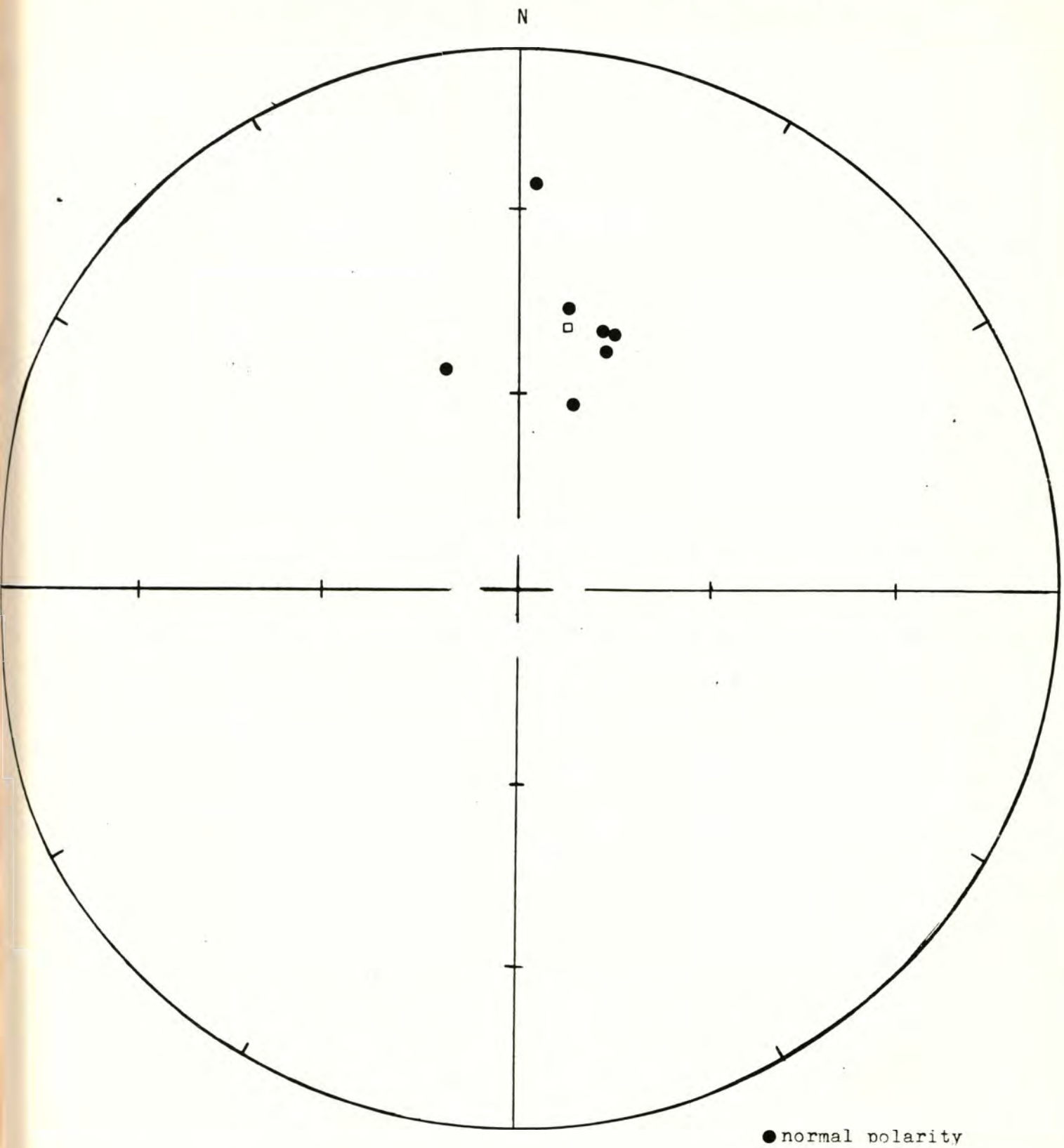

● normal polarity

○ reversed polarity

□ site mean, normal polarit

△ site mean, reversed polarity

Site: 8.6.78.2

Demagnetization level: 300 oe.

FISHER ON SAMPLE DIRECTIONS

Site: 8.7.78.1 -- Cedar Creek Road A Demagnetization level: NRM

SW¼ sec. 8, T. 16 N., R. 4 W.

Sample number	Declination	Inclination
288	8.19	54.12
289	13.88	51.01
290	13.46	53.03
291	6.58	51.30
292	24.14	55.56
293	22.16	53.37
294	25.08	55.89

R= 6.98 Site declination= 16.01 Site inclination= 53.67

Alpha 95= 3.18 Delta= 4.52 Kappa= 276.05

Site latitude= 46.88° Site longitude= 123.25°

Paleolatitude= 72.50°N Paleolongitude= 7.41°E DELP= 3.10

DECLM= 4.45

Black Hills Project

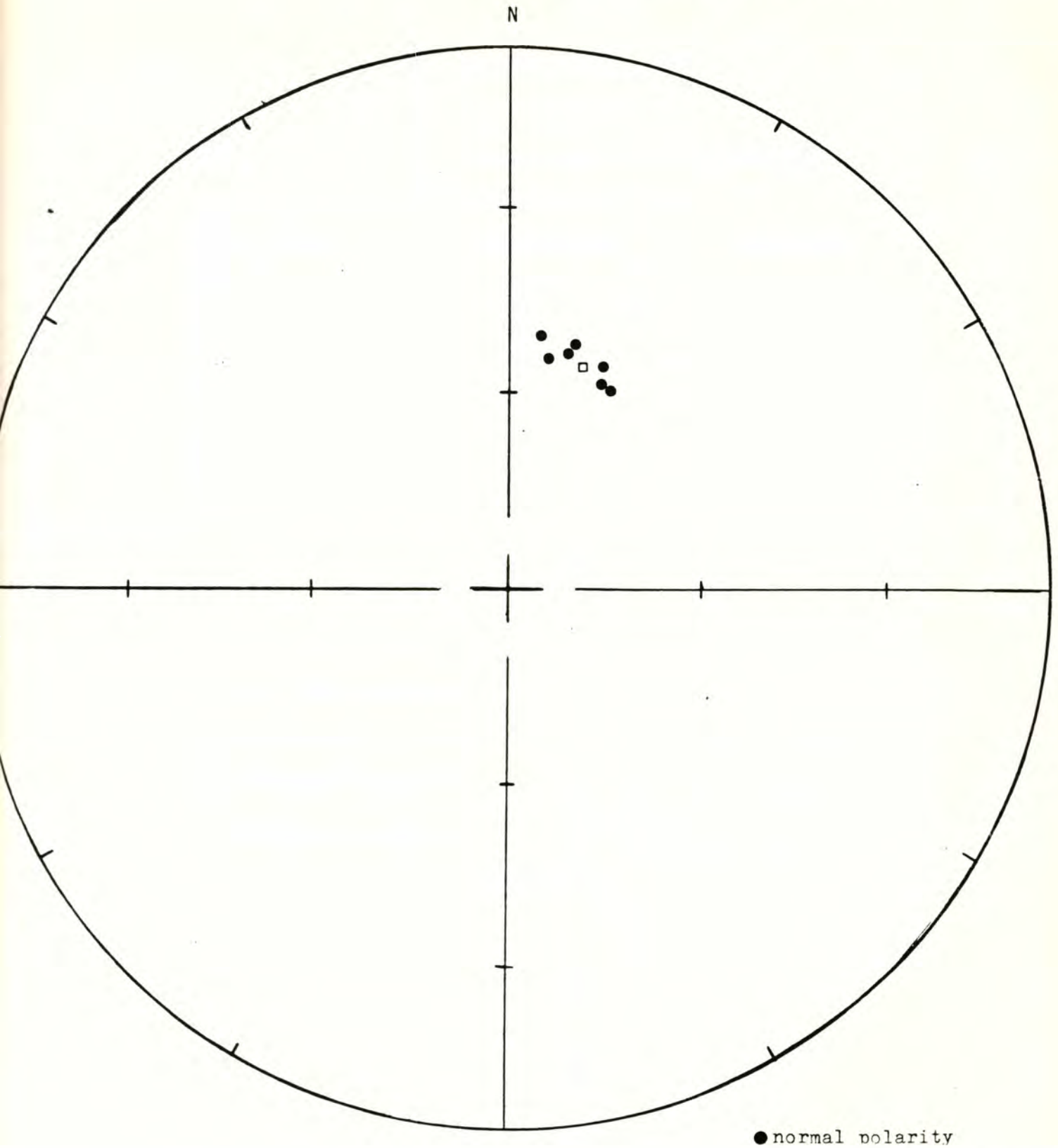

● normal polarity

○ reversed polarity

□ site mean, normal polarity

△ site mean, reversed polarity

Site: 8.7.78.1 - Cedar Creek Road A

Demagnetization level: NRM

FISHER ON SAMPLE DIRECTIONS

Site: 8.7.78.1 -- Cedar Creek Road A Demagnetization level: 600 oe.
SW¼ sec. 8, T. 16 N., R. 4 W.

Sample number	Declination	Inclination
288	12.21	46.96
289	12.55	48.91
290	18.63	51.58
291	15.46	54.20
292	17.54	51.58
293	21.29	55.28
294	30.42	47.09

R= 6.98 Site declination= 18.31 Site inclination= 50.95

Alpha 95= 3.41 Delta= 4.84 Kappa= 240.36

Site latitude= 46.88° Site longitude= 123.25°

Paleolatitude= 69.29°N Paleolongitude= 7.60°E DELP= 3.12

DECLM= 4.61

Black Hills Project

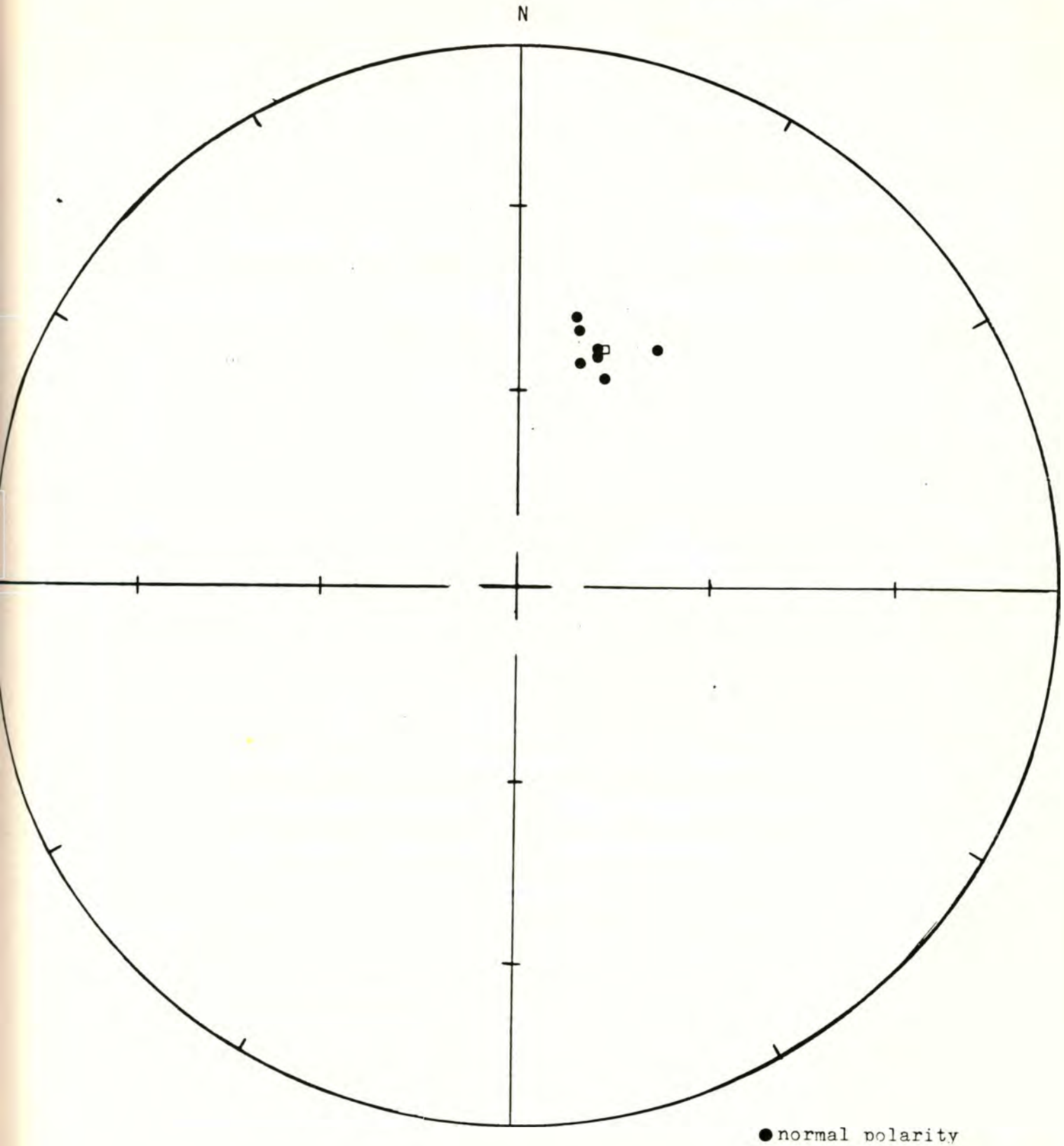

● normal polarity

○ reversed polarity

□ site mean, normal polarit

△ site mean, reversed polarity

Site: 8.7.78.1 - Cedar Creek Road A

Demagnetization level: 600 oe.

TECTONIC CORRECTION ON SAMPLE DIRECTIONS

Pole on site mean

Site: 8.7.78.1 Demagnetization level: 600 oe.

Dip azimuth: 232 (N38W) Dip angle: 15 (W)

Sample number	Declination	Inclination	Cor. dec.	Cor. inc.
288	12.21	46.96	358.00	57.32
289	12.55	48.91	357.25	59.24
290	18.63	51.58	3.13	63.01
291	15.46	54.20	357.02	64.83
292	17.54	51.58	1.72	62.80
293	21.29	55.28	3.82	67.03
294	30.42	47.09	21.31	60.61

R= 6.98 Site declination= 3.14 Site inclination= 62.35

Alpha 95= 3.41 Delta= 4.84 Kappa= 240.25

Site latitude= 46.88°N Site longitude= 123.25°W

Paleolatitude= 86.10°N Paleolongitude= 21.14°E DELP= 4.14

DECLM= 5.32

WITH TECTONIC CORRECTION

Black Hills Project

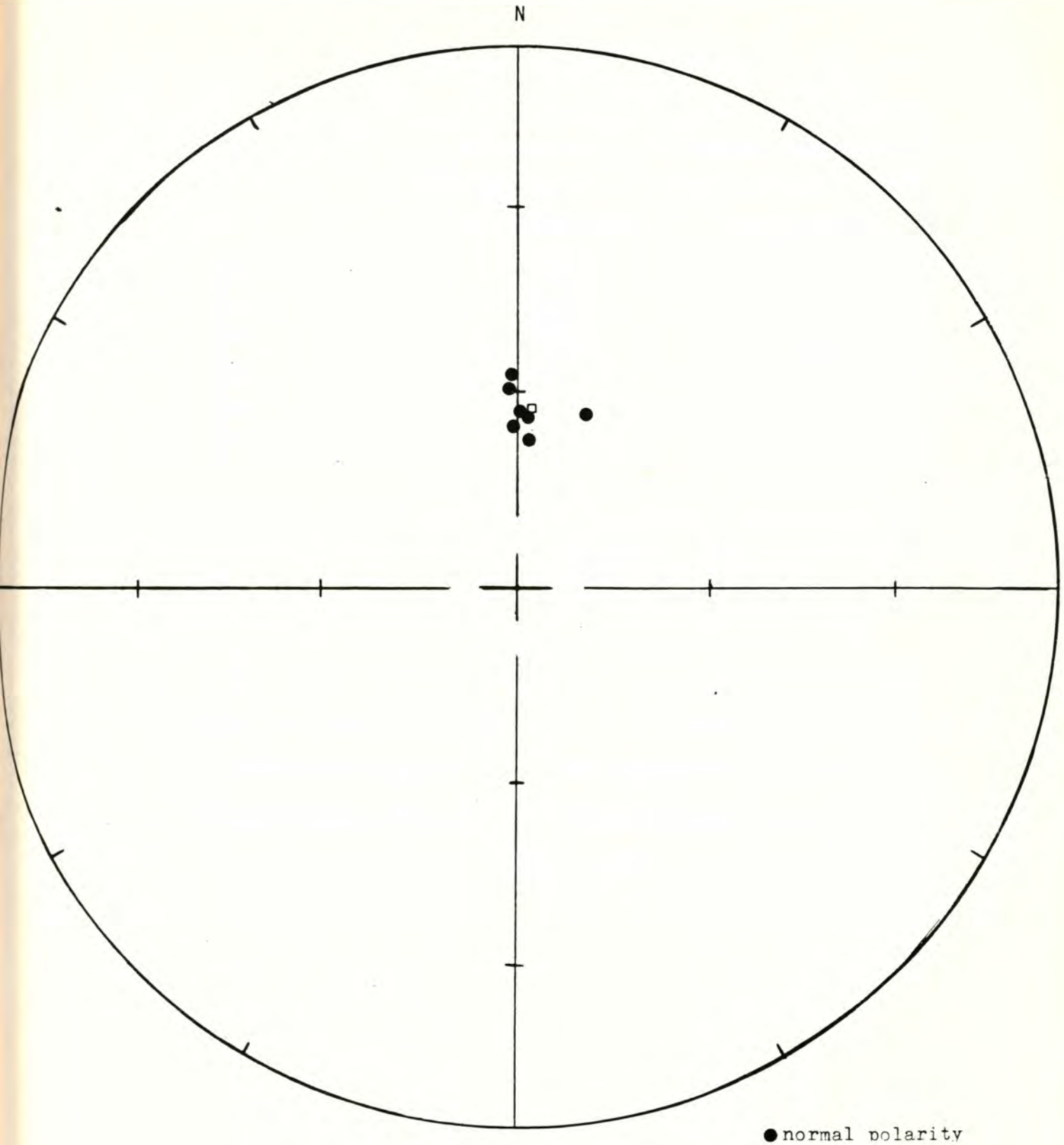

● normal polarity

○ reversed polarity

□ site mean, normal polarit

△ site mean, reversed polarity

Site: 8.7.78.1

Demagnetization level: 600 oe.

FISHER ON SAMPLE DIRECTIONS

Site: 8.7.78.2 -- Cedar Creek B Demagnetization level: NRM

SE¼ SE¼ sec. 7, T. 16 N., R. 4 W.

Sample number	Declination	Inclination
295	330.62	38.66
296	224.19	11.40
297	343.03	54.99
298	3.85	89.70
299	18.07	48.90
300	34.59	18.52

R= 4.33 Site declination= 350.74 Site inclination= 50.78

Alpha 95= 33.07 Delta= 43.87 Kappa= 2.99

Site latitude= 46.88° Site longitude= 123.25°

Paleolatitude= 73.05°N Paleolongitude= 84.83°E DELP= 30.07

DECLM= 44.60

Black Hills Project

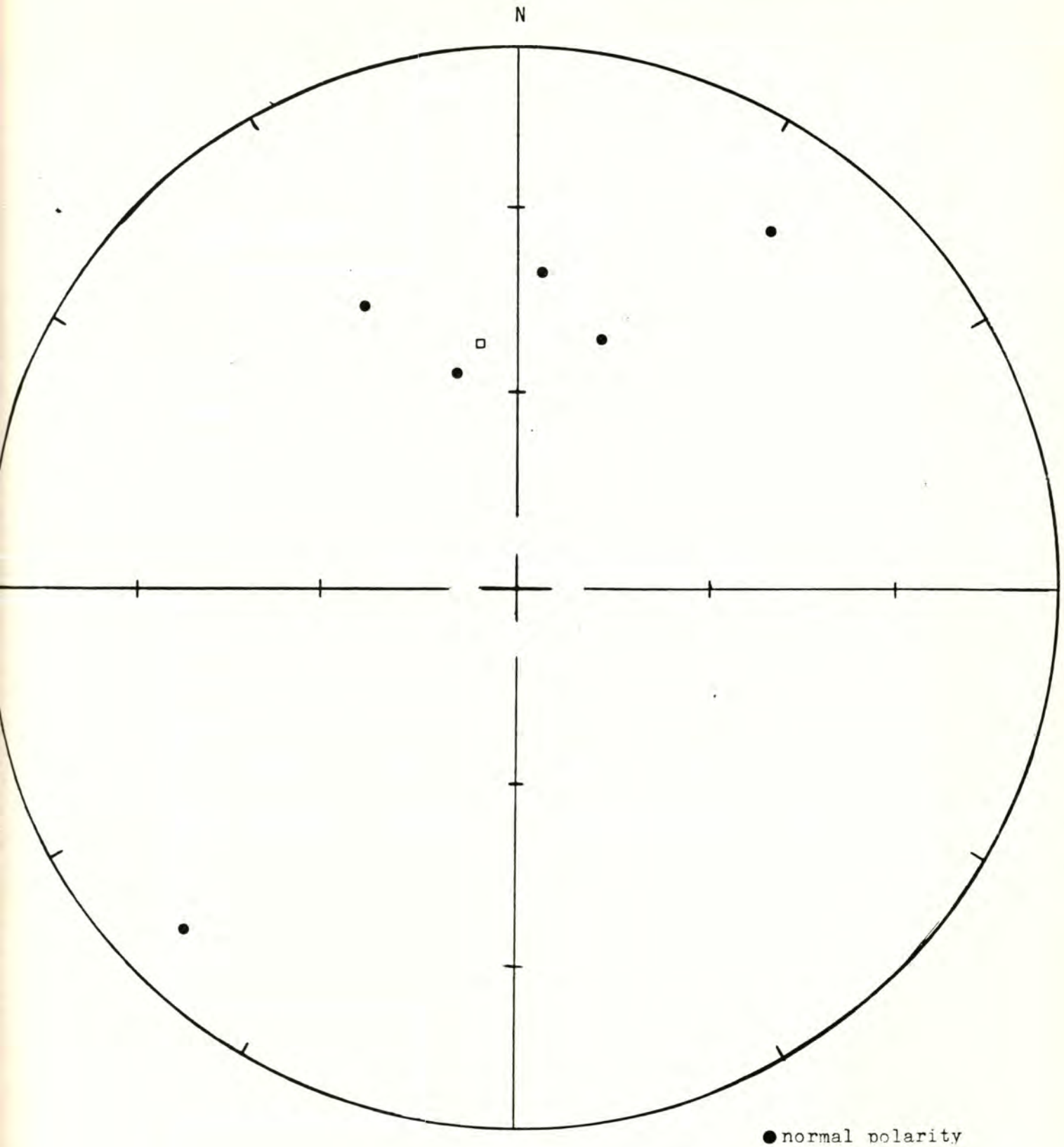

● normal polarity

○ reversed polarity

□ site mean, normal polarit

△ site mean, reversed polarity

Site: 8.7.78.2 - Cedar Creek B

Demagnetization level: NRM

FISHER ON SAMPLE DIRECTIONS

Site: 8.7.78.2 -- Cedar Creek B Demagnetization level: 600 oe.

SE¼ SE¼ sec. 7, T. 16 N., R. 4 W.

Sample number	Declination	Inclination
295	335.82	54.33
296*	288.38	63.10
297	16.21	48.90
298	6.04	41.11
299	13.57	50.11
300	14.06	42.19

*Sample eliminated from site mean.

R= 4.91 Site declination= 6.21 Site inclination= 48.21

Alpha 95= 9.27 Delta= 10.74 Kappa= 45.61

Site latitude=46.88° Site longitude= 123.25°

Paleolatitude= 71.69°N Paleolongitude= 39.26°E DELP= 7.95

DECLM= 12.14

Black Hills Project

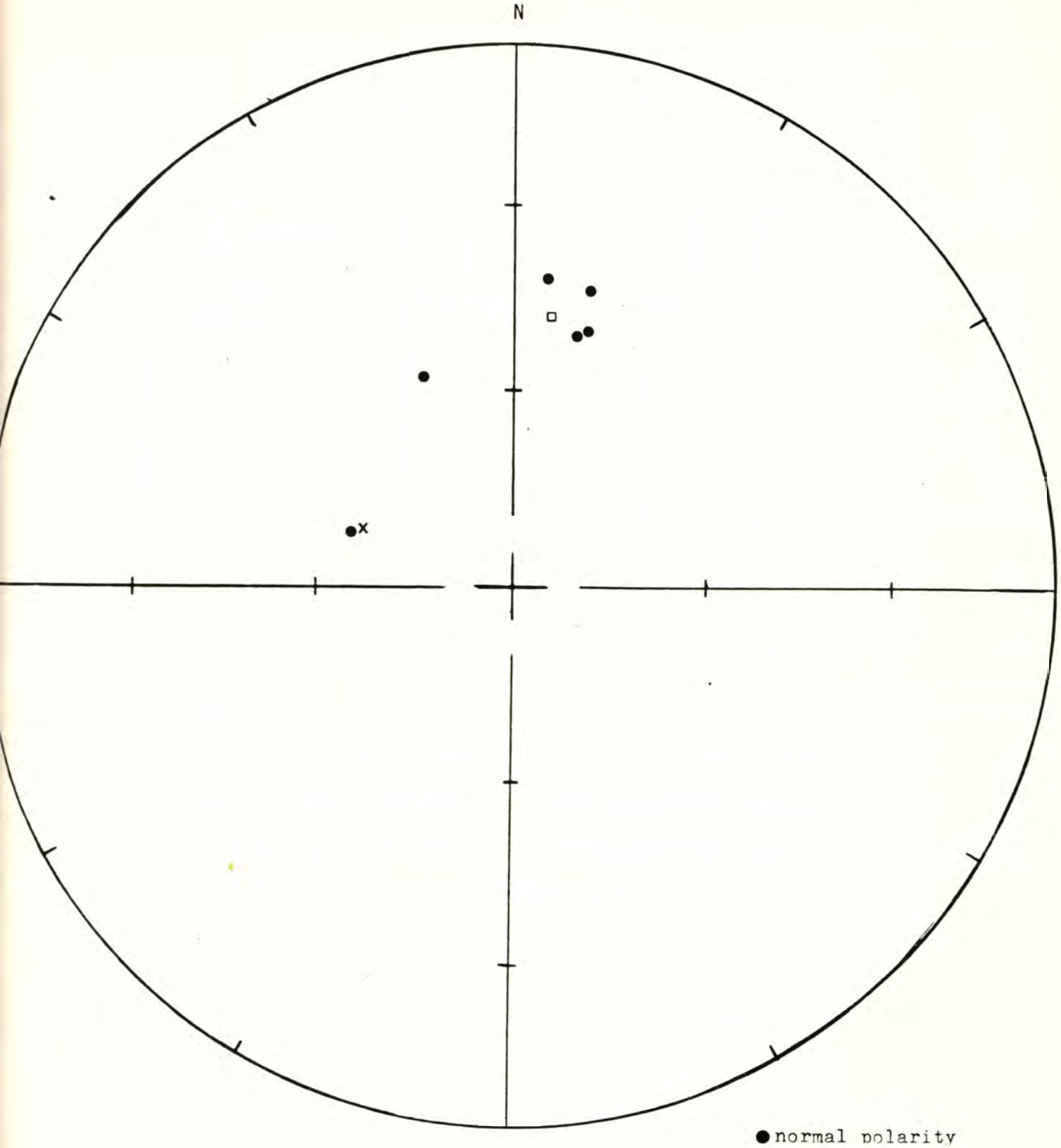

Site: 8.7.78.2 - Cedar Creek B

Demagnetization level: 600 oe.

● normal polarity

○ reversed polarity

□ site mean, normal polarit

△ site mean, reversed polarity

X Sample 296 is eliminated from site mean.

TECTONIC CORRECTION ON SAMPLE DIRECTIONS

Pole on site mean

Site: 8.7.78.2 Demagnetization level: 600 oe.

Dip azimuth: 232 (N38W) Dip angle: 15 (W)

Sample number	Declination	Inclination	Cor. dec.	Cor. inc.
295	335.82	54.33	314.38	55.16
297	16.21	48.90	1.78	59.99
298	6.04	41.11	353.79	50.41
299	13.57	50.11	357.72	60.59
300	14.06	42.19	2.61	53.12

R= 4.91 Site declination= 350.18 Site inclination= 57.19

Alpha 95= 9.27 Delta= 10.75 Kappa= 45.60

Site latitude= 46.88°N Site longitude= 123.25°W

Paleolatitude= 78.39°N Paleolongitude= 98.80°E DELP= 5.32

DECLM= 7.29

WITH TECTONIC CORRECTION

Black Hills Project

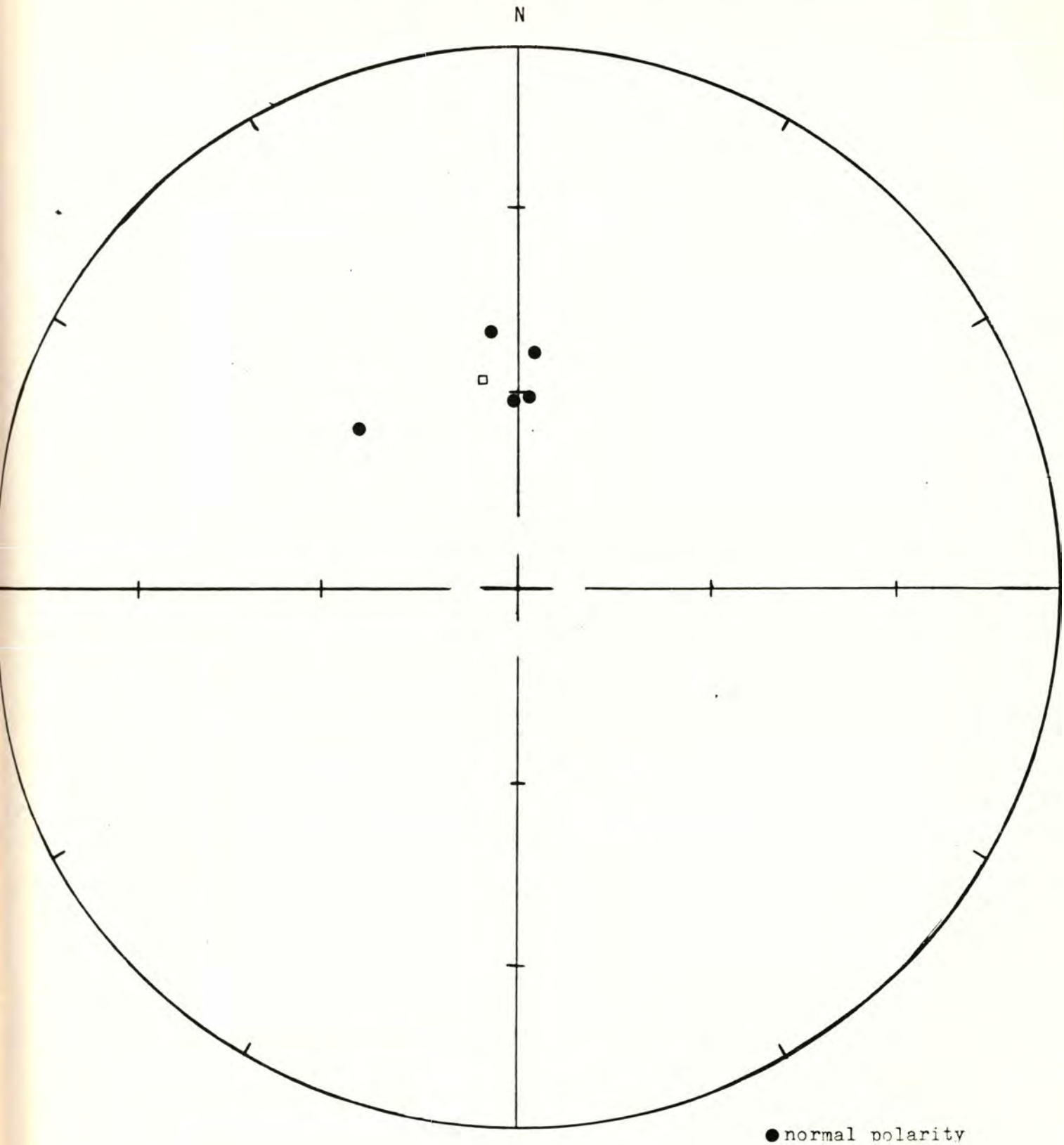

● normal polarity

○ reversed polarity

□ site mean, normal polarit

△ site mean, reversed polarity

Site: 8.7.78.2

Demagnetization level: 600 oe.

FISHER ON SAMPLE DIRECTIONS

Site: 8.7.78.3 -- Cedar Creek Road C Demagnetization level: NRM

NW¼ sec. 9, T. 16 N., R. 4 W.

Sample number	Declination	Inclination
301	4.92	43.09
302	49.99	32.81
303	44.42	46.74
304	23.19	50.73
305	350.64	48.27
306	33.20	51.76

R= 5.77 Site declination= 25.37 Site inclination= 47.60

Alpha 95= 12.33 Delta= 16.0 Kappa= 21.50

Site latitude= 46.9° Site longitude= 123.12°

Paleolatitude= 63.15°N Paleolongitude= 0.57°E DELP= 10.43

DECLM= 16.03

Black Hills Project

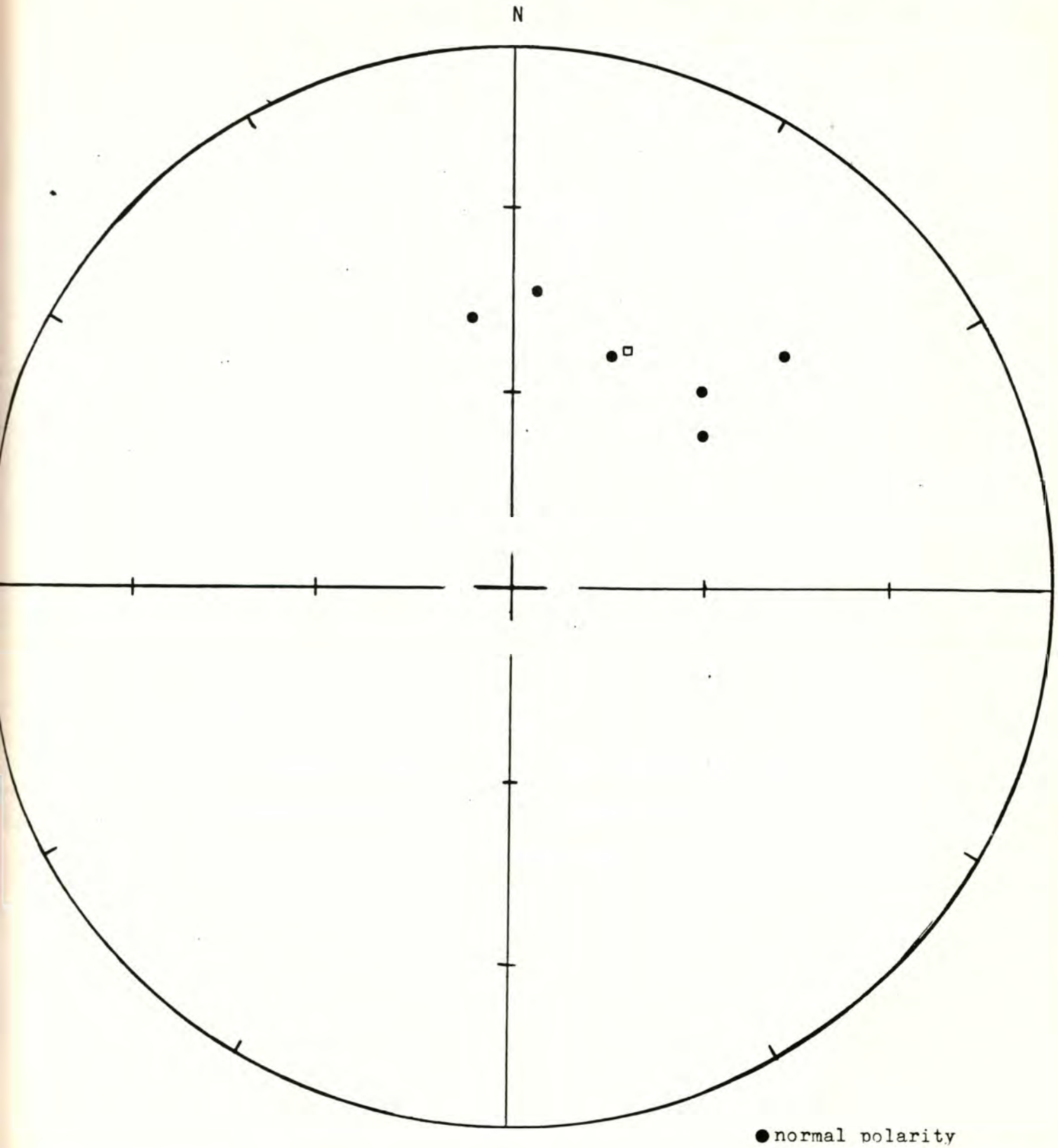

● normal polarity

○ reversed polarity

□ site mean, normal polarit

△ site mean, reversed polarity

Site: 8.7.78.3 - Cedar Creek Road C

Demagnetization level: NRM

FISHER ON SAMPLE DIRECTIONS

Site: 8.7.78.3 -- Cedar Creek Road C Demagnetization level: 400 oe.
NW¼ sec. 9, T. 16 N., R. 4 W.

Sample number	Declination	Inclination
301	32.62	30.36
302	28.16	44.56
303	27.48	46.83
304	30.34	49.36
305	27.02	58.43
306	43.77	51.56

R= 5.92 Site declination= 31.58 Site inclination= 47.01

Alpha 95= 7.21 Delta= 9.34 Kappa= 62.83

Site latitude= 46.9° Site longitude= 123.12°

Paleolatitude= 59.1°N Paleolongitude= 7.11°W DELP= 6.02

DECLM=9.32

Black Hills Project

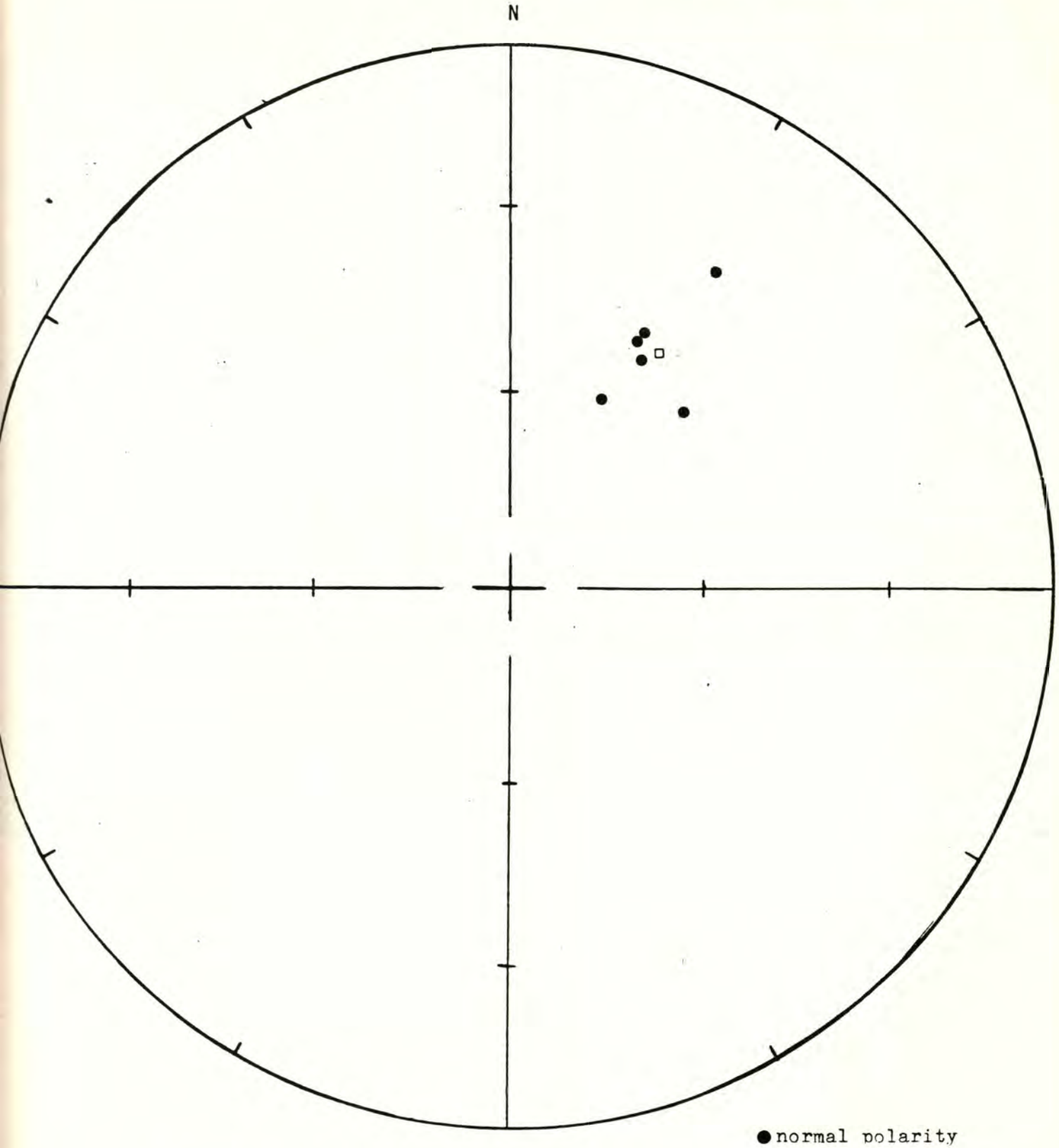

● normal polarity

○ reversed polarity

□ site mean, normal polarit

△ site mean, reversed polarity

Site: 8.7.78.3 - Cedar Creek Road C

Demagnetization level: 400 oe.

FISHER ON SAMPLE DIRECTIONS

Site: 8.23.78.1 -- Monroe Creek Demagnetization level: NRM

SW¼ NE¼ sec. 15, T. 17 N., R. 4 W.

Sample number	Declination	Inclination
307	354.77	38.44
308	6.04	56.28
309	3.96	53.54
310	11.37	58.74
311	21.69	49.96
312	353.13	53.73
313	5.86	51.18

R= 6.93 Site declination= 4.87 Site inclination= 52.07

Alpha 95= 5.85 Delta= 8.30 Kappa= 81.76

Site latitude= 46.9° Site longitude= 123.12°

Paleolatitude= 75.31°N Paleolongitude= 40.51°E DELP= 5.49

DECLM= 8.01

Black Hills Project

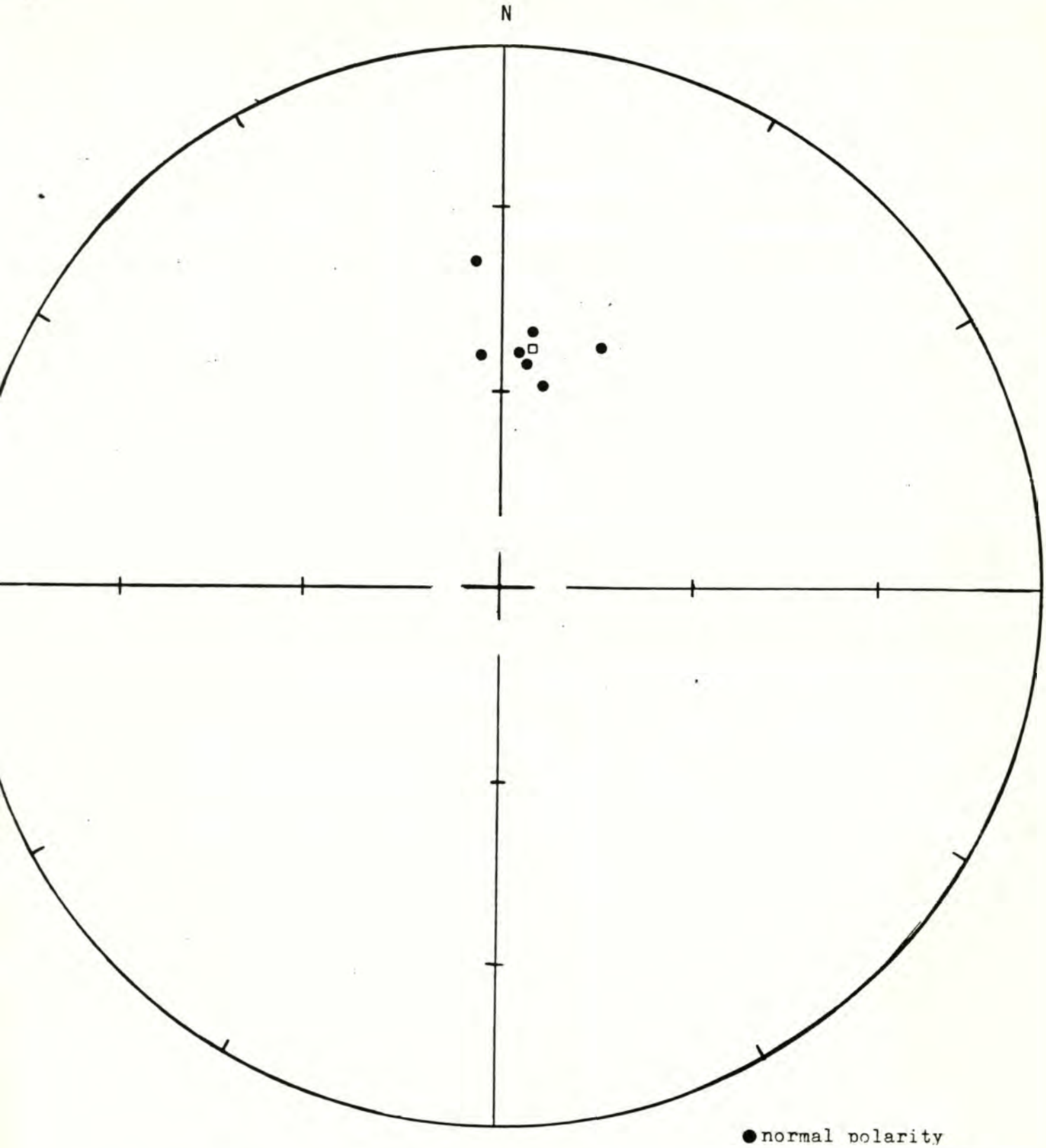

● normal polarity

○ reversed polarity

□ site mean, normal polarit

△ site mean, reversed polarity

Site: 8.23.78.1 - Monroe Creek

Demagnetization level: NRM

FISHER ON SAMPLE DIRECTIONS

Site: 8.23.78.1 -- Monroe Creek Demagnetization level: 300 oe.

SW¼ NE¼ sec. 15, T. 17 N., R. 4 W.

Sample number	Declination	Inclination
307	10.59	54.68
308	5.13	49.24
309	6.73	47.05
310	18.33	58.73
311	11.02	54.55
312	354.99	61.62
313	7.22	57.74

R= 6.96 Site declination= 7.82 Site inclination= 54.96

Alpha 95= 4.20 Delta= 5.96 Kappa= 158.56

Site latitude= 46.9^{o} Site longitude= 123.12^{o}

Paleolatitude= 77.18^{o}N Paleolongitude= 26.92^{o}E DELP= 4.23

DECLM= 5.96

Black Hills Project

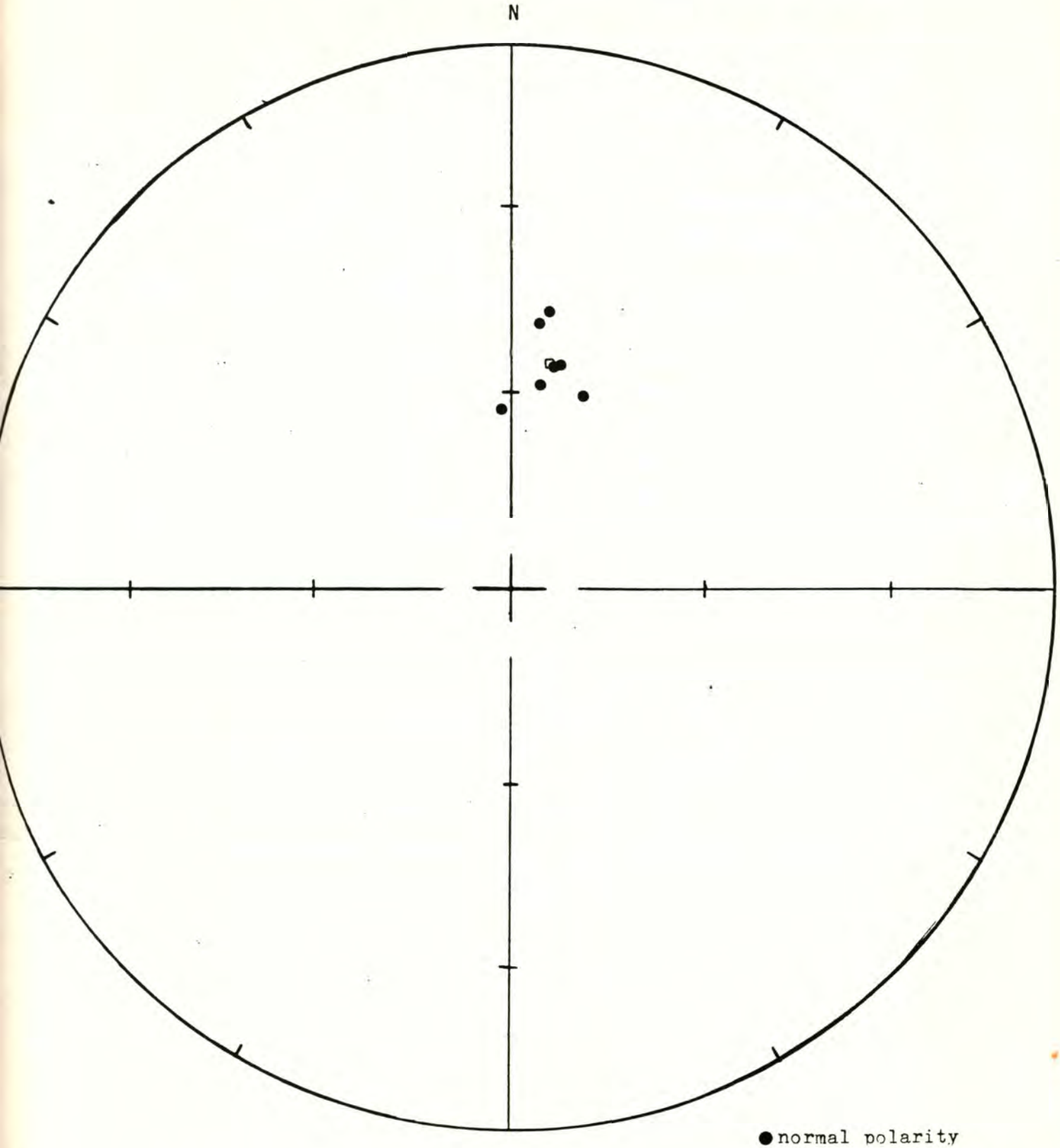

● normal polarity

○ reversed polarity

□ site mean, normal polarit

△ site mean, reversed polarity

Site: 8.23.78.1 - Monroe Creek

Demagnetization level: 300 oe.

TECTONIC CORRECTION ON SAMPLE DIRECTIONS

Pole on site mean

Site: 8.23.78.1 Demagnetization level: 300 oe.

Dip azimuth: 228 (N42W) Dip angle: 13 (W)

Sample number	Declination	Inclination	Cor. dec.	Cor. inc.
307	10.59	54.68	354.92	63.94
308	5.13	49.24	351.67	57.74
309	6.73	47.05	354.65	55.93
310	18.33	58.73	1.89	69.11
311	11.02	54.55	355.55	63.89
312	354.99	61.62	330.01	67.16
313	7.22	57.74	348.28	66.19

R= 6.96 Site declination= 351.29 Site inclination= 63.69

Alpha 95= 4.20 Delta=5.96 Kappa= 158.51

Site latitude= 46.90°N Site longitude= 123.12°W

Paleolatitude= 83.76°N Paleolongitude= 135.39°E DELP= 5.29

DECLM= 6.66

WITH TECTONIC CORRECTION

Black Hills Project

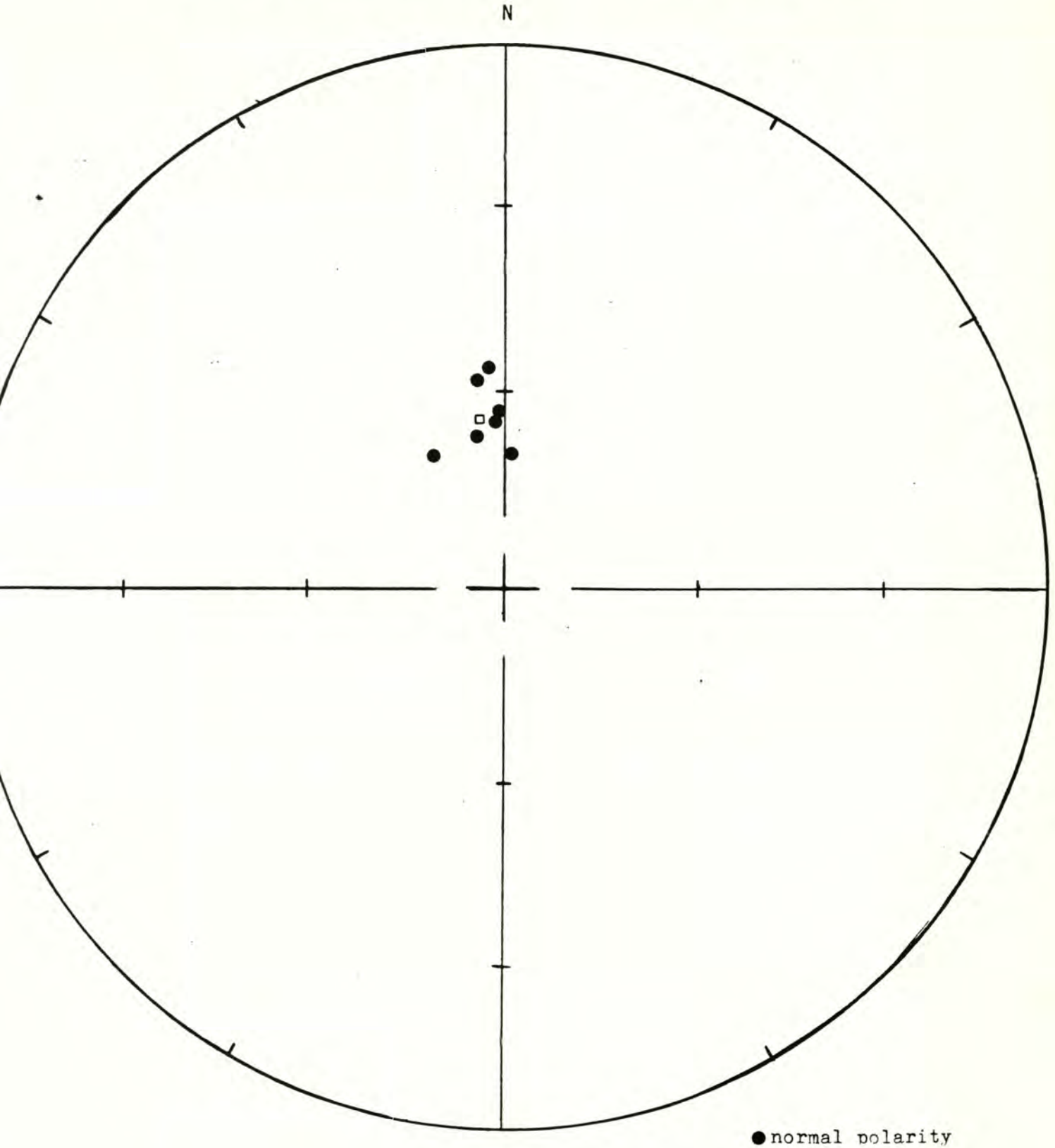

● normal polarity

○ reversed polarity

□ site mean, normal polarit

△ site mean, reversed polarity

Site: 8.23.78.1

Demagnetization level: 300 oe.

FISHER ON SAMPLE DIRECTIONS

Site: 8.23.78.2 -- Countyline Demagnetization level: NRM

secs. 10, 11, T. 17 N., R. 4 W.

Sample number	Declination	Inclination
314	3.0	41.38
315	38.0	54.51
316	41.51	53.85
317	34.12	50.71
318	26.42	54.42
319	28.35	52.51
320	39.46	58.85

R= 6.91 Site declination= 29.10 Site inclination= 53.04

Alpha 95= 6.58 Delta= 9.34 Kappa= 64.65

Site latitude= 46.9° Site longitude= 123.12°

Paleolatitude= 64.34°N Paleolongitude= 12.4°W DELP= 6.31

DECLM= 9.12

Black Hills Project

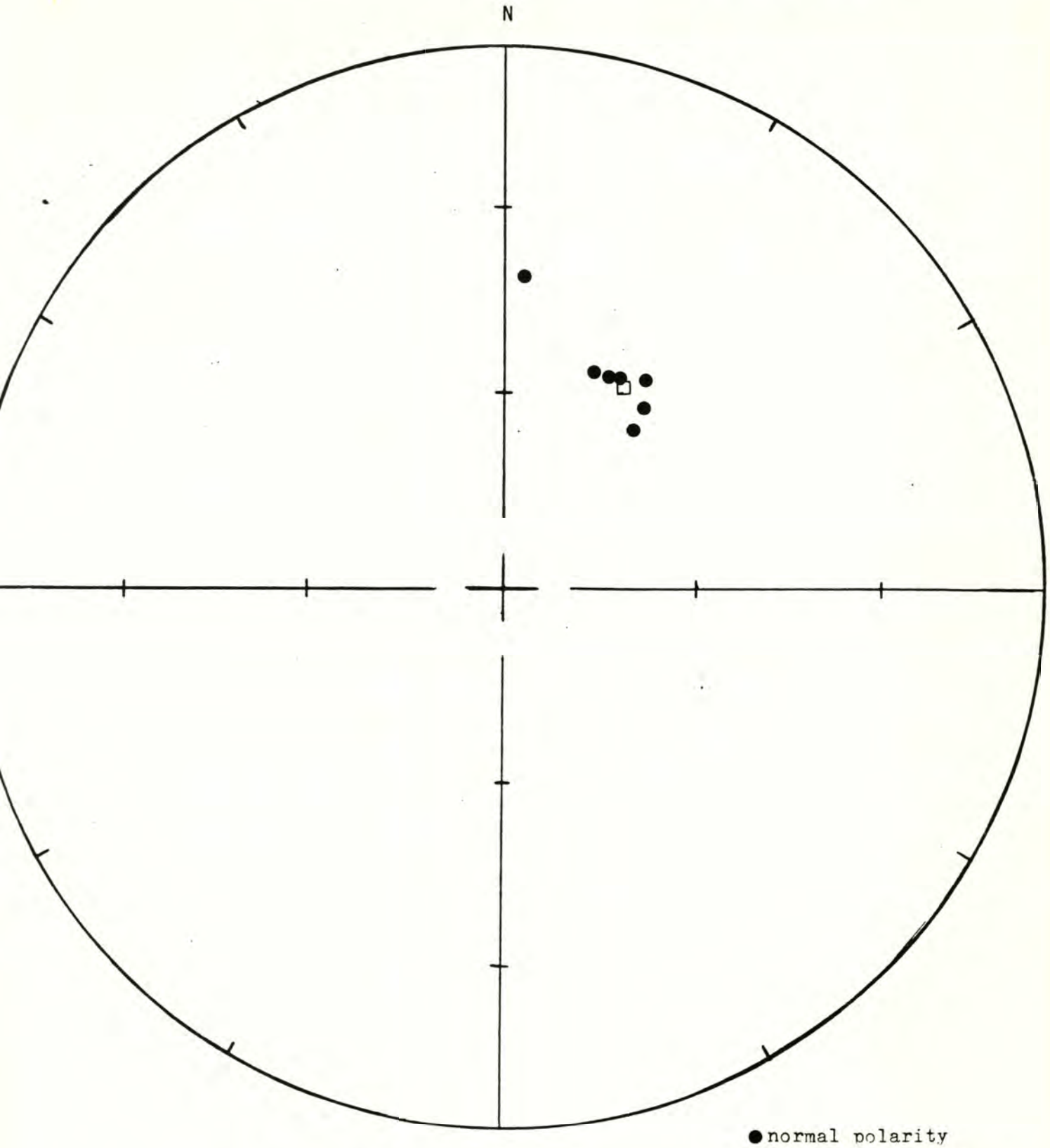

● normal polarity

○ reversed polarity

□ site mean, normal polarit

△ site mean, reversed polarity

Site: 8.23.78.2 - Countyline

Demagnetization level: NRM

FISHER ON SAMPLE DIRECTIONS

Site: 8.23.78.2 -- Countyline Demagnetization level: 400 oe.

secs. 10, 11, T. 17 N., R. 4 W.

Sample number	Declination	Inclination
314	0.51	51.51
315	15.23	47.84
316	29.29	49.70
317	27.46	57.34
318	14.40	51.17
319	29.55	53.77
320	13.70	56.70

R= 6.95 Site declination= 18.46 Site inclination= 52.99

Alpha 95= 4.84 Delta= 6.86 Kappa= 119.68

Site latitude= 46.9° Site longitude= 123.12°

Paleolatitude= 70.68°N Paleolongitude= 3.97°E DELP= 4.64

DECLM= 6.70

Black Hills Project

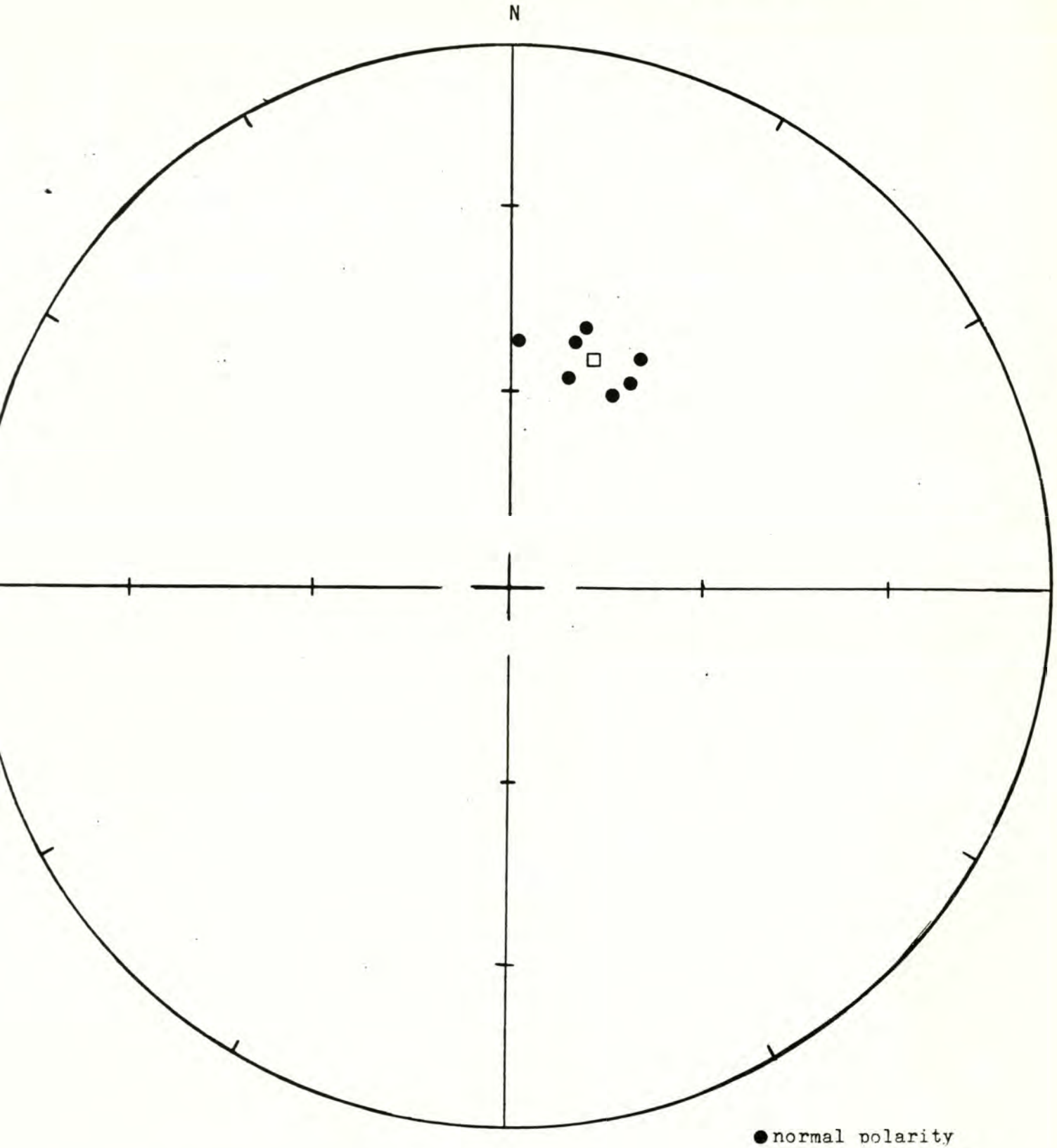

Site: 8.23.78.2 - Countyline

Demagnetization level: 400 oe.

● normal polarity

○ reversed polarity

□ site mean, normal polarit

△ site mean, reversed polarity

TECTONIC CORRECTION ON SAMPLE DIRECTIONS

Pole on site mean

Site: 8.23.78.2 Demagnetization level: 400 oe.

Dip azimuth: 228 (N42W) Dip angle: 13 (W)

Sample number	Declination	Inclination	Cor. dec.	Cor. inc.
314	0.51	51.51	344.99	59.01
315	15.23	47.84	4.52	58.13
316	29.29	49.70	22.00	61.75
317	27.46	57.34	16.00	69.07
318	14.40	51.17	1.88	61.23
319	29.55	53.77	20.86	65.80
320	13.70	56.70	357.37	66.41

R= 6.95 Site declination= 6.09 Site inclination= 63.63

Alpha 95= 4.84 Delta= 6.86 Kappa= 119.63

Site latitude= 46.90°N Site longitude= 123.12°W

Paleolatitude= 85.46°N Paleolongitude= 13.94°W DELP= 6.08

DECLM= 7.67

WITH TECTONIC CORRECTION

Black Hills Project

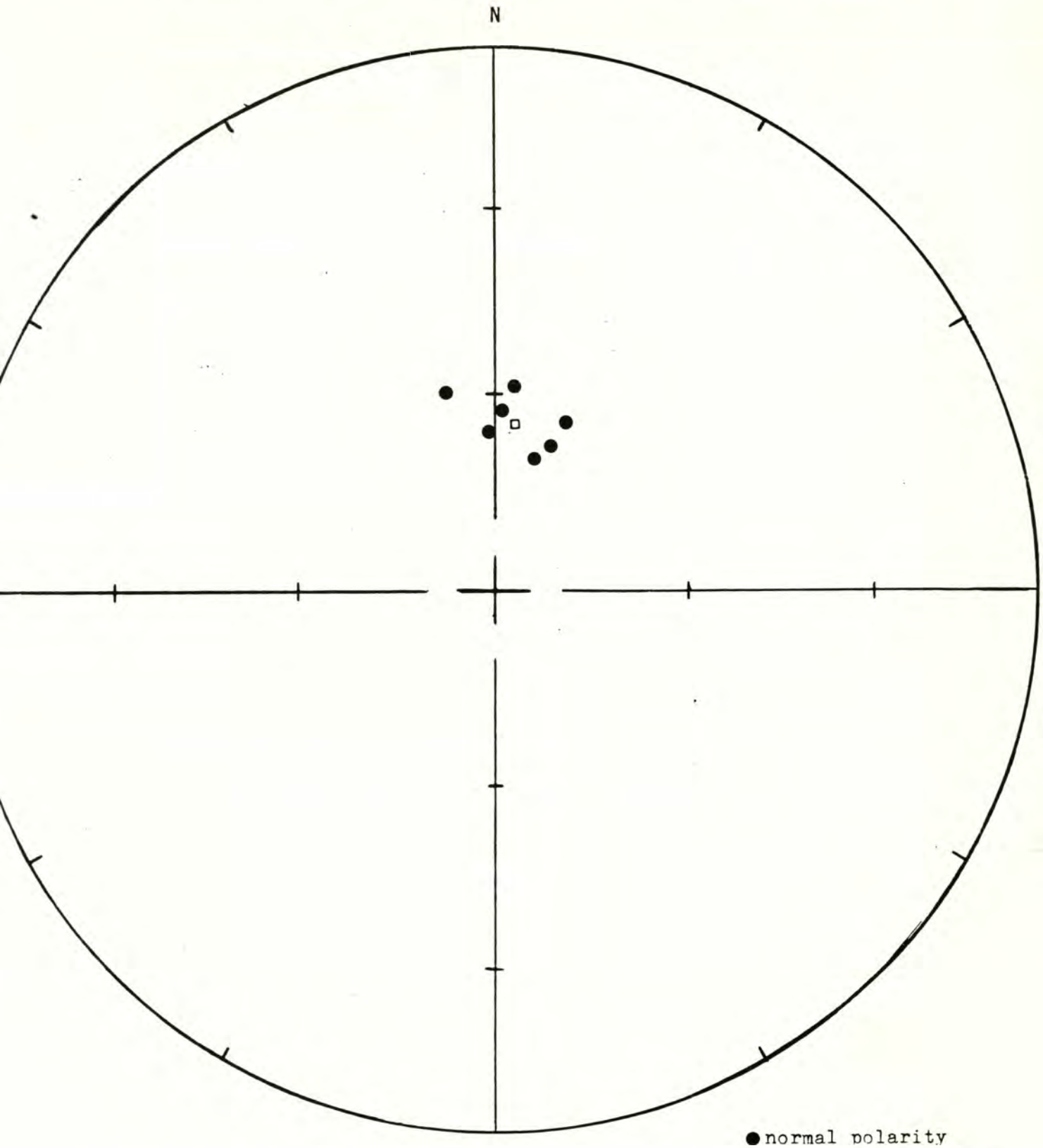

● normal polarity

○ reversed polarity

□ site mean, normal polari

△ site mean, reversed polarity

Site: 8.23.78.2

Demagnetization level: 400 oe.

FISHER ON SAMPLE DIRECTIONS

Site: 9.8.78.1 -- Capitol Peak Demagnetization level: NRM

SW¼ sec. 12, T. 17 N., R. 4 W.

Sample number	Declination	Inclination
321	9.11	61.95
322	60.76	57.86
323	20.71	54.25
324	0.07	73.80
325	39.36	43.99
326	16.28	59.96

R= 5.84 Site declination= 27.43 Site inclination= 60.07

Alpha 95= 10.22 Delta= 13.25 Kappa= 31.30

Site latitude= 46.9° Site longitude= 123.12°

Paleolatitude= 69.50°N Paleolongitude= 26.35°W DELP= 11.70

DECLM= 15.46

Black Hills Project

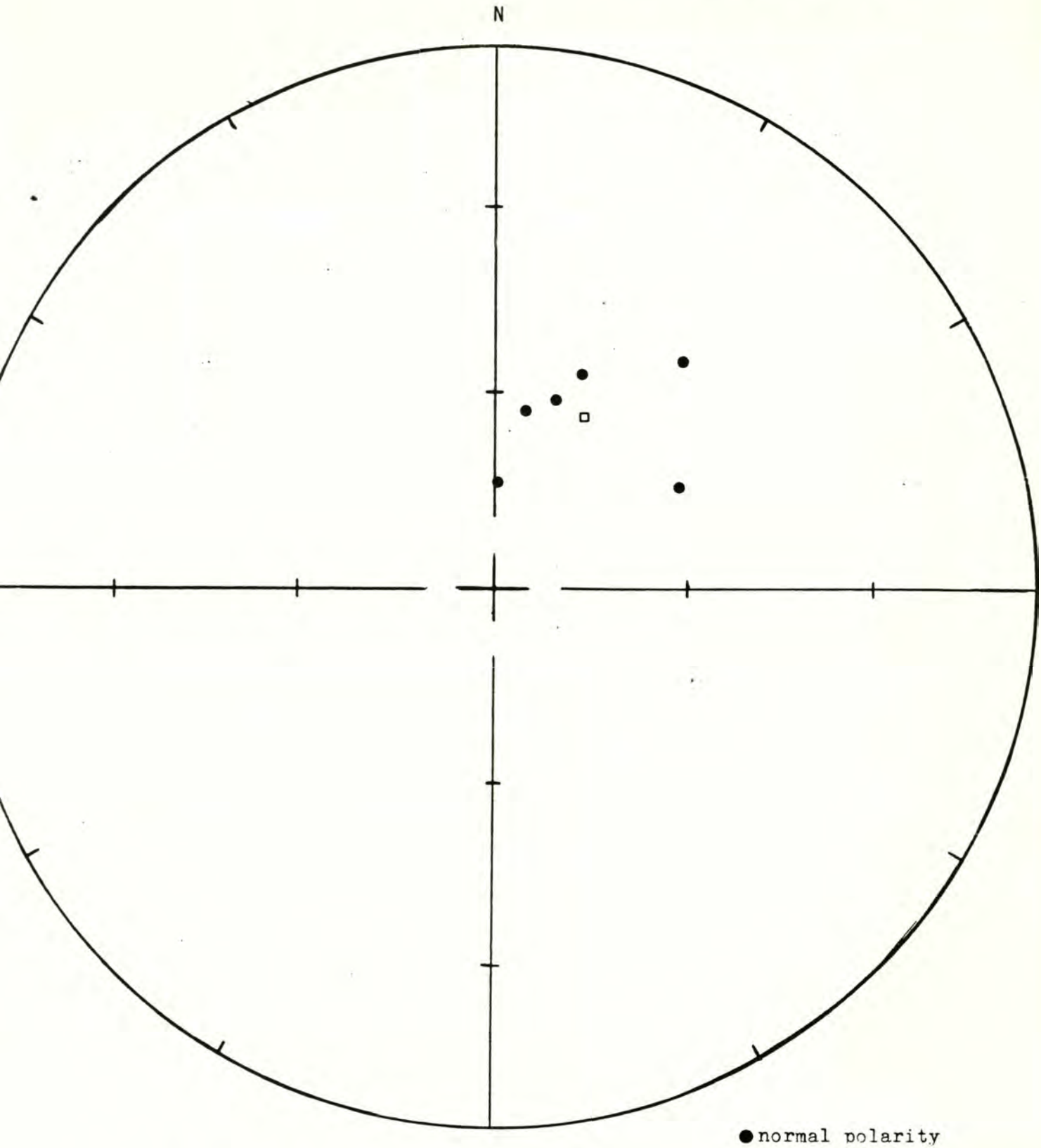

● normal polarity

○ reversed polarity

□ site mean, normal polarit

△ site mean, reversed polarity

Site: 9.8.78.1 - Capitol Peak

Demagnetization level: NRM

FISHER ON SAMPLE DIRECTIONS

Site: 9.8.78.1 -- Capitol Peak Demagnetization level: 200 oe.

SW¼ sec. 12, T. 17 N., R. 4 W

Sample number	Declination	Inclination
321	43.35	61.26
322	32.65	60.17
323	42.79	54.23
324	37.19	57.72
325	45.82q	51.73
326	40.18	56.73

R= 5.99 Site declination= 40.55 Site inclination= 57.05

Alpha 95= 3.11 Delta=4.03 Kappa= 337.03

Site latitude= 46.9° Site longitude= 123.12°

Paleolatitude= 58.99°N Paleolongitude= 30.68°W DELP= 3.30

DECLM=4.53

Black Hills Project

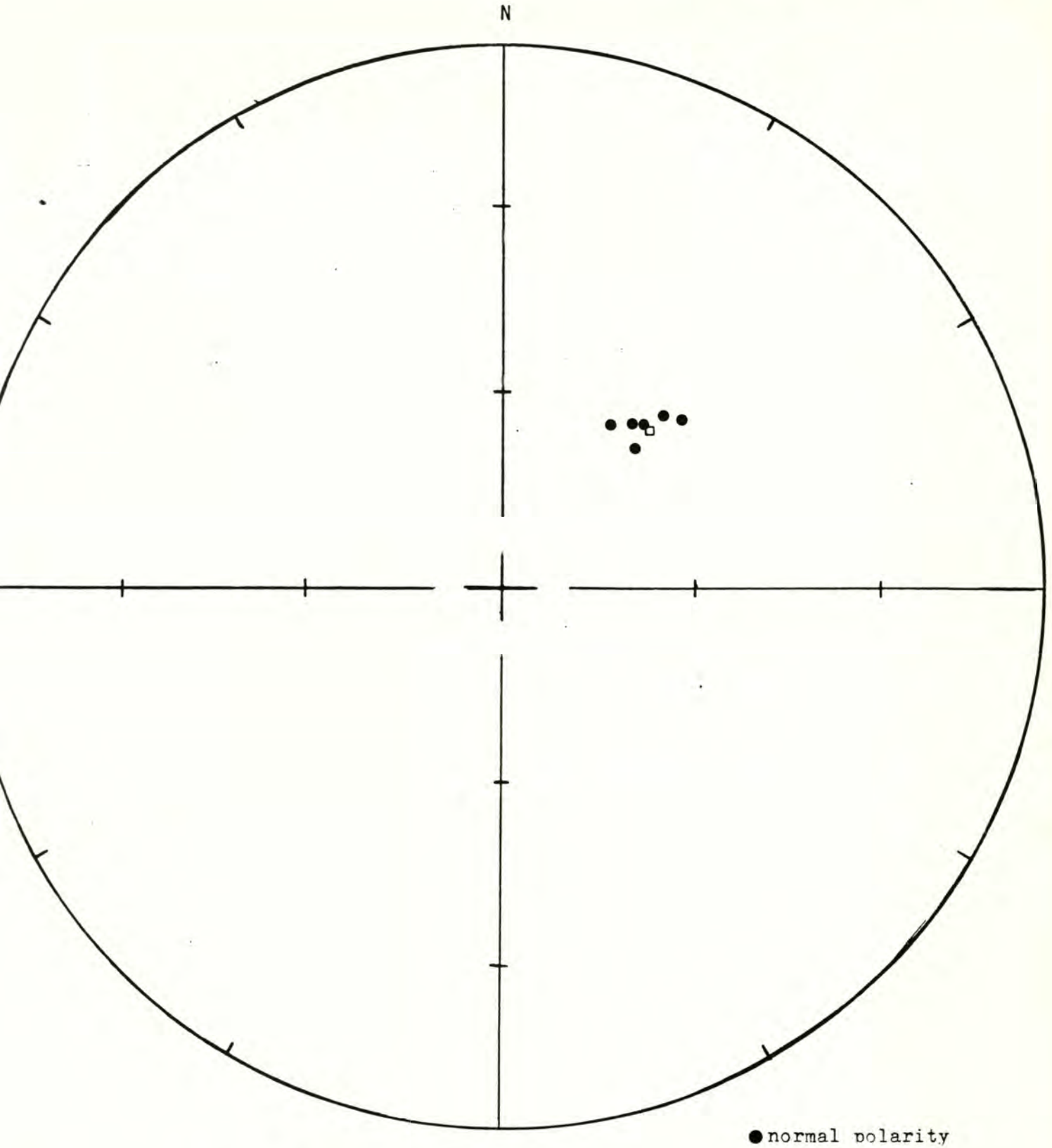

● normal polarity

○ reversed polarity

□ site mean, normal polarit

△ site mean, reversed polarity

Site: 9.8.78.1 - Capitol Peak

Demagnetization level: 200 oe.

FISHER ON SAMPLE DIRECTIONS

Site: 9.8.78.2 -- Hell Creek Demagnetization level: NRM

SW¼ sec. 21, T. 17 N., R. 4 W.

Sample number	Declination	Inclination
328	130.35	13.78
329	116.06	27.46
330	122.19	1.01
331	138.68	28.16
332	110.51	31.29
333	31.26	34.30
334	115.17	72.17

R= 5.84 Site declination= 113.42 Site inclination= 33.48

Alpha 95= 23.24 Delta= 33.42 Kappa= 5.19

Site latitude= 46.9° Site longitude= 123.12°

Paleolatitude= 1.64°S Paleolongitude= 62.48°W DELP= 15.05

DECLM= 26.45

Black Hills Project

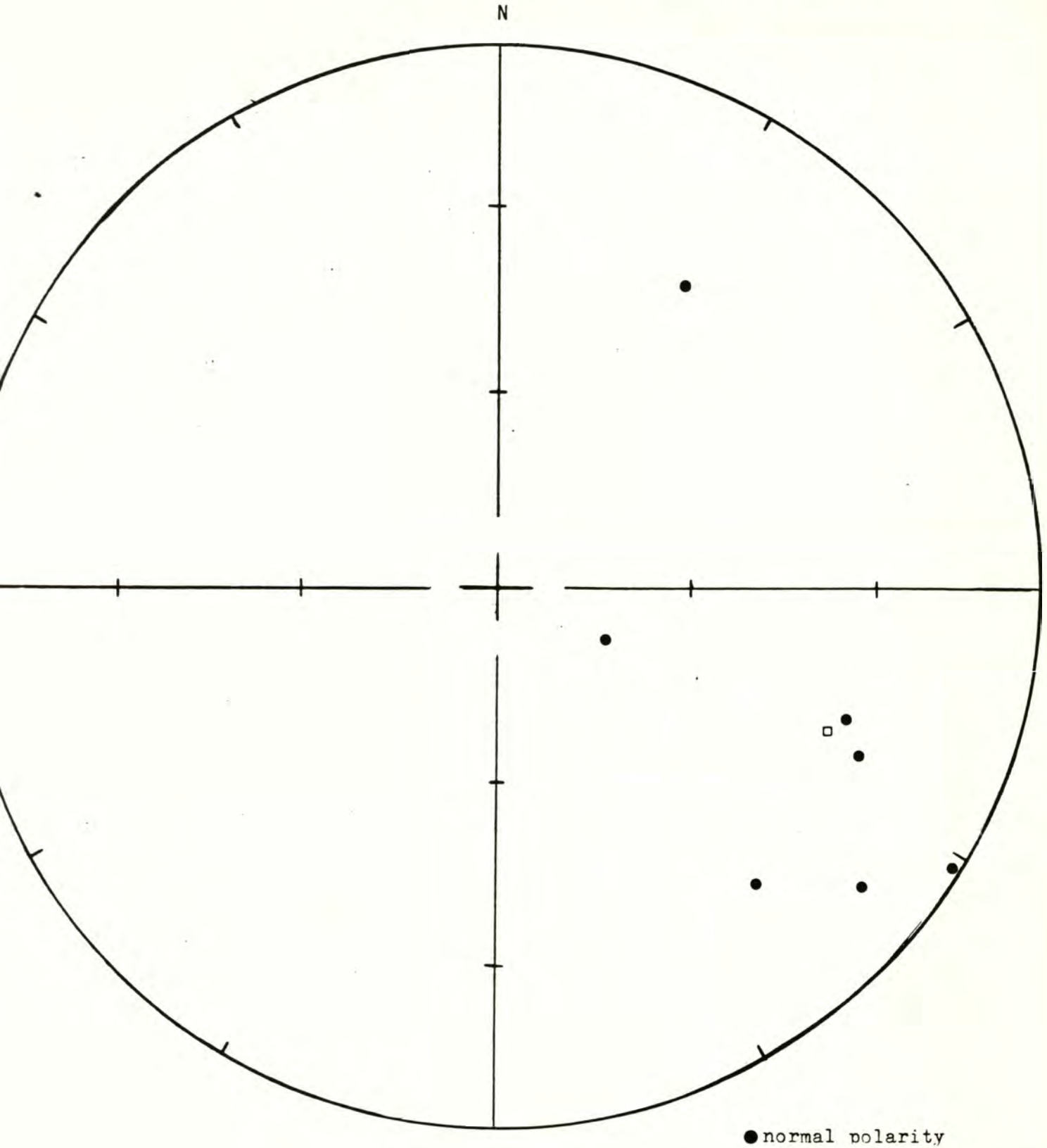

● normal polarity

○ reversed polarity

□ site mean, normal polarit

△ site mean, reversed polarity

Site: 9.8.78.2 - Hell Creek

Demagnetization level: NRM

FISHER ON SAMPLE DIRECTIONS

Site: 9.8.78.2 -- Hell Creek Demagnetization level: 400 oe.

SW¼ sec. 21, T. 17 N., R. 4 W.

Sample number	Declination	Inclination
328	49.50	47.80
329	48.04	43.54
330	61.84	50.27
331	47.22	49.13
332	39.51	52.59
333	47.26	44.35
334	68.50	49.59

R= 6.95 Site declination= 51.62 Site inclination= 48.53

Alpha 95= 4.72 Delta= 6.70 Kappa= 125.57

Site latitude= 46.9° Site longitude= 123.12°

Paleolatitude= 46.78°N Paleolongitude= 28.25°W DELP= 4.08

DECLM= 6.21

Black Hills Project

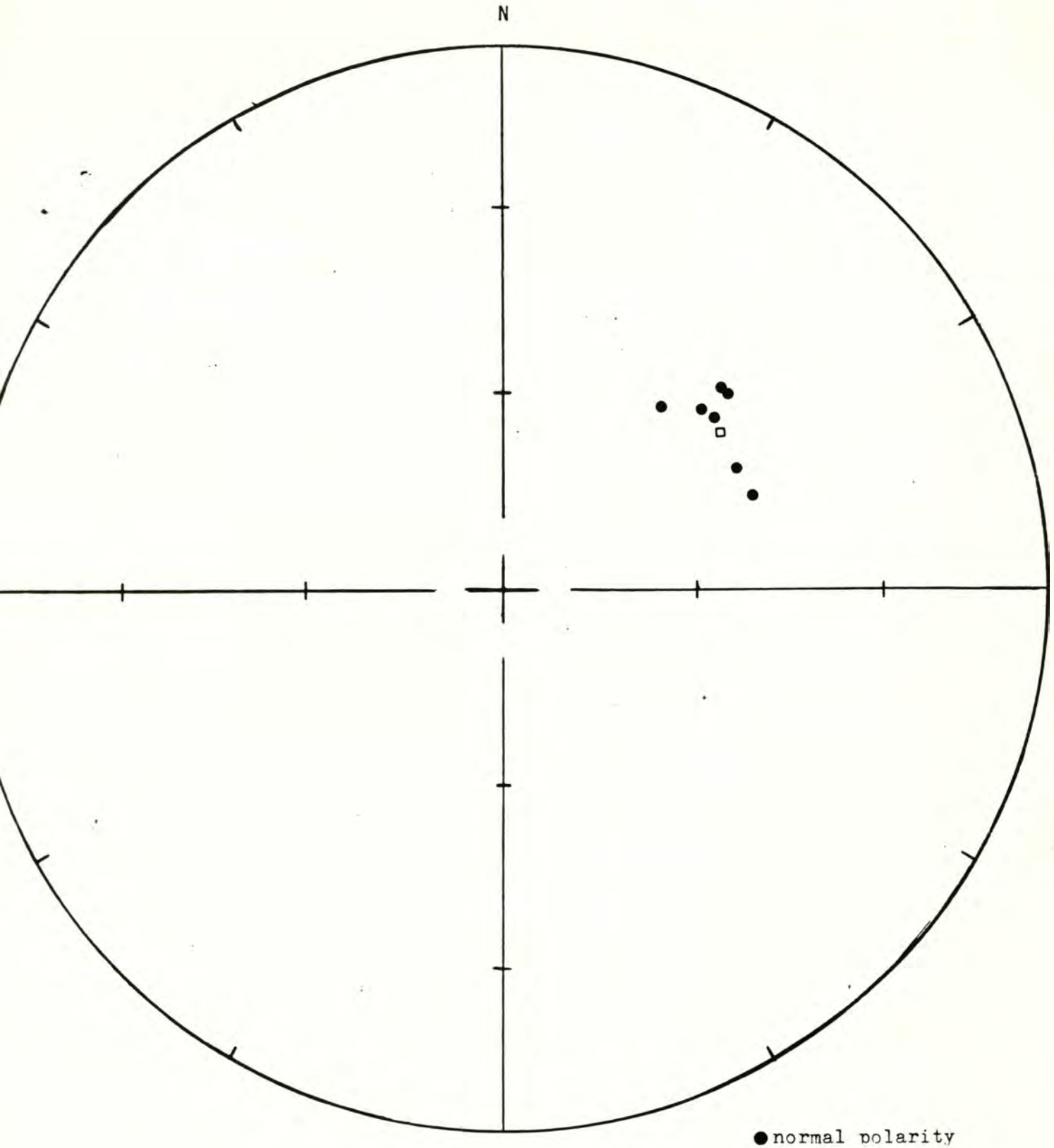

● normal polarity

○ reversed polarity

□ site mean, normal polarit

△ site mean, reversed polarity

Site: 9.8.78.2 - Hell Creek

Demagnetization level: 400 oe.

TECTONIC CORRECTION ON SAMPLE DIRECTIONS

Pole on site mean

Site: 9.8.78.2 Demagnetization level: 400 de.

Dip azimuth: 210 (N60W) Dip angle: 13 (W)

Sample number	Declination	Inclination	Cor. dec.	Cor. inc.
328	49.50	47.80	56.47	59.80
329	48.04	43.54	53.49	55.72
330	61.84	50.27	73.44	60.63
331	47.22	49.13	53.82	61.33
332	39.51	52.59	43.92	65.33
333	47.26	44.35	52.66	56.59
334	68.50	49.59	81.32	58.87

R= 6.95 Site declination= 59.50 Site inclination= 60.29

Alpha 95= 4.72 Delta= 6.70 Kappa= 125.62

Site latitude= 46.90°N Site longitude= 123.12°W

Paleolatitude= 47.90°N Paleolongitude= 47.95°W DELP= 5.44

DECLM= 7.16

WITH TECTONIC CORRECTION

Black Hills Project

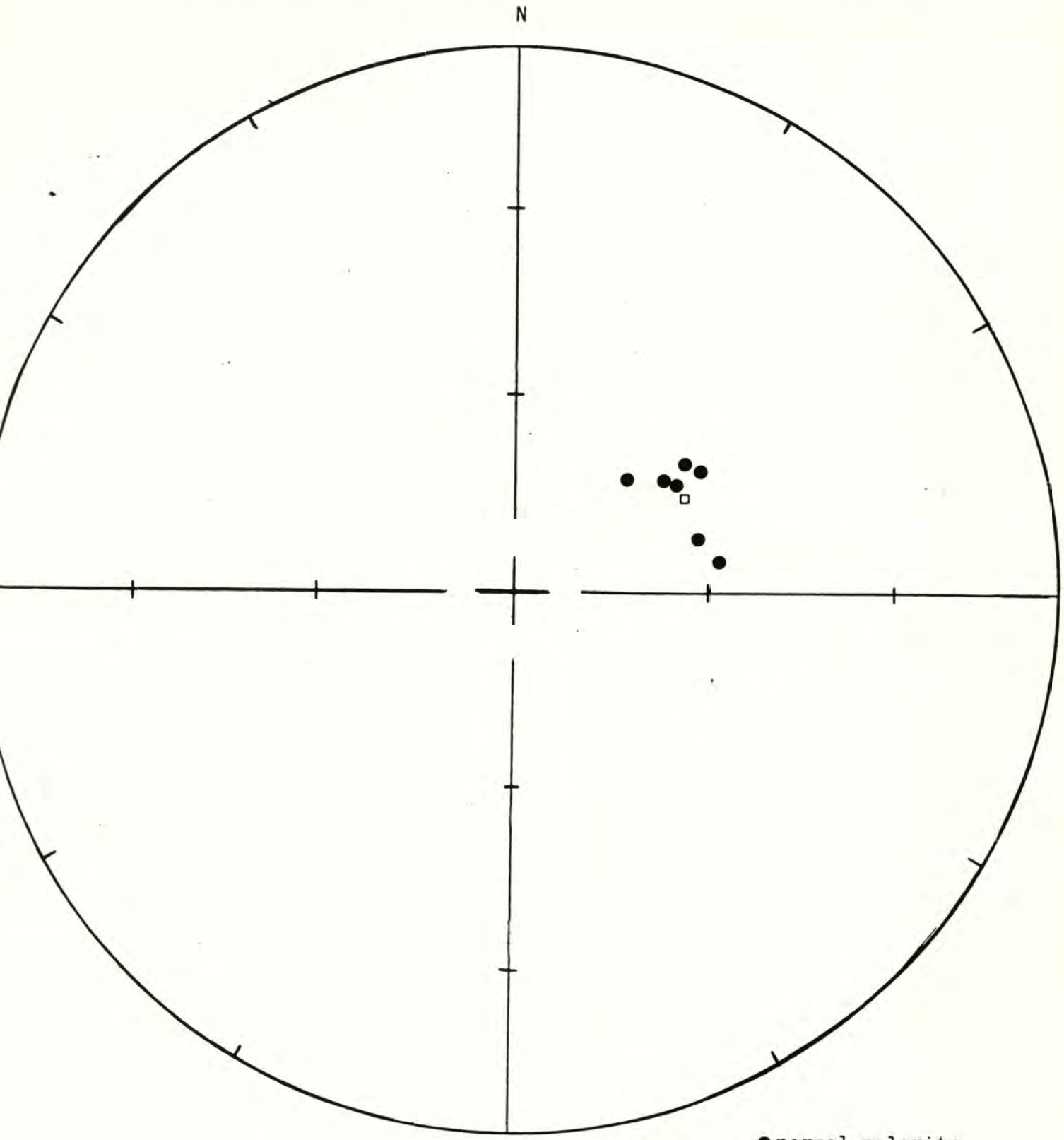

● normal polarity

○ reversed polarity

□ site mean, normal polarit

△ site mean, reversed polarity

Site: 9.8.78.2

Demagnetization level: 400 oe.

FISHER ON SAMPLE DIRECTIONS

Site: 9.11.78.1 -- Porter Creek campground Demagnetization level: NRM

NW¼ NW¼ sec. 12, T. 17 N., R. 5 W.

Sample number	Declination	Inclination
335	71.16	45.27
336	70.12	53.04
337	68.71	47.27
338	89.76	48.06
339	76.93	55.91
340	80.40	52.62
341	76.73	47.45

R= 6.97 Site declination= 76.21 Site inclination= 50.15

Alpha 95= 4.02 Delta= 5.70 Kappa= 173.59

Site latitude= 46.9° Site longitude= 123.25°

Paleolatitude= 30.99°N Paleolongitude= 46.87°W DELP= 3.60

DECLM= 5.38

Black Hills Project

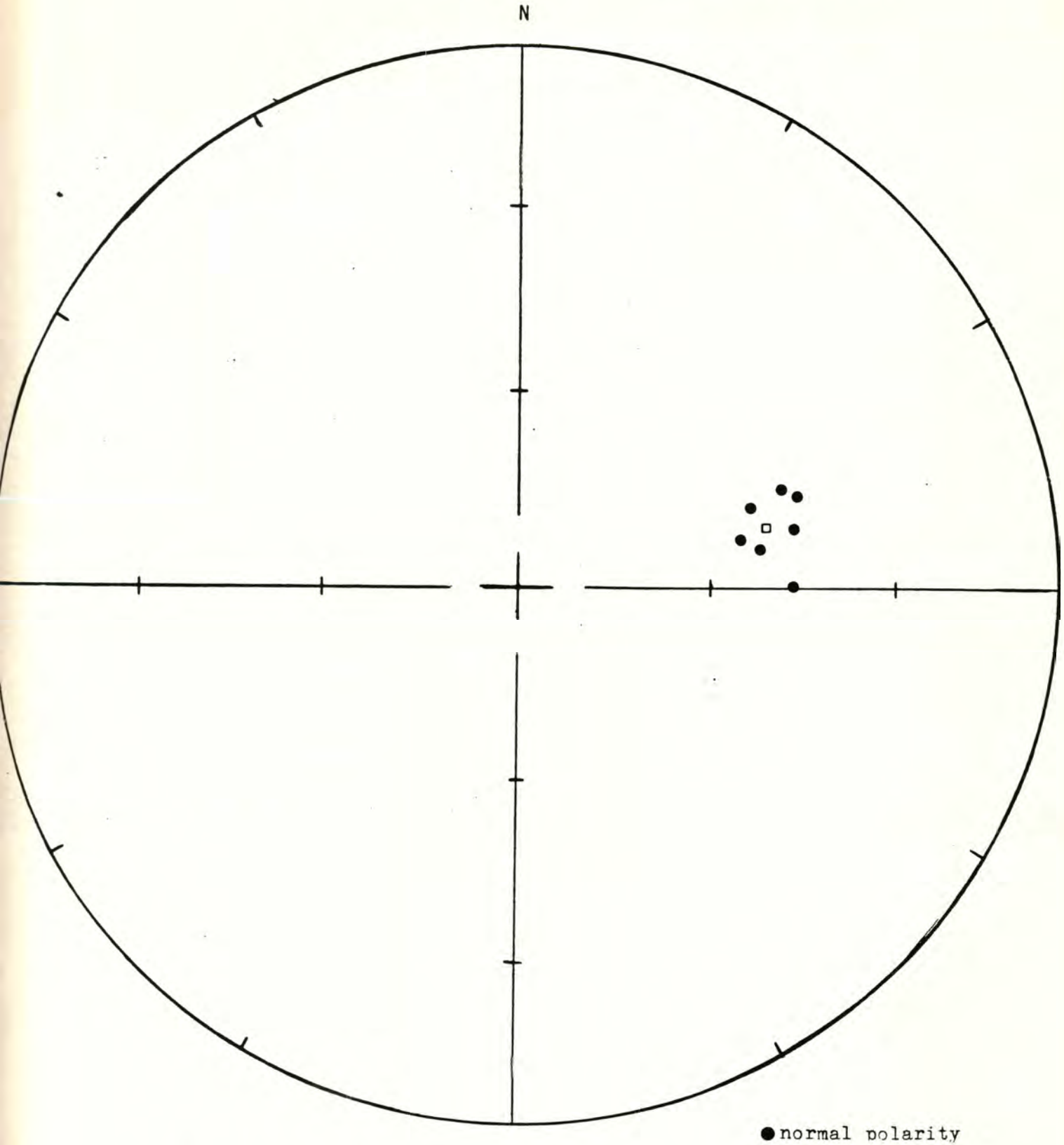

● normal polarity

○ reversed polarity

□ site mean, normal polarit

△ site mean, reversed polarity

Site: 9.11.78.1 - Porter Creek campground

Demagnetization level: NRM

FISHER ON SAMPLE DIRECTIONS

Site: 9.11.78.1 -- Porter Creek campground Demagnetization level: 500 oe.

NW¼ NW¼ sec. 12, T. 17 N., R. 5 W.

Sample number	Declination	Inclination
335	74.82	48.0
336	74.68	48.11
337	69.45	43.15
338	80.22	50.32
339	82.15	59.19
340	87.90	52.81
341	75.68	46.74

R= 6.96 Site declination= 77.41 Site inclination= 49.89

Alpha 95= 4.19 Delta= 5.95 Kappa= 159.11

Site latitude= 46.9° Site longitude= 123.25°

Paleolatitude= 30.05°N Paleolongitude=47.42°W DELP= 3.74

DECLM= 5.60

Black Hills Project

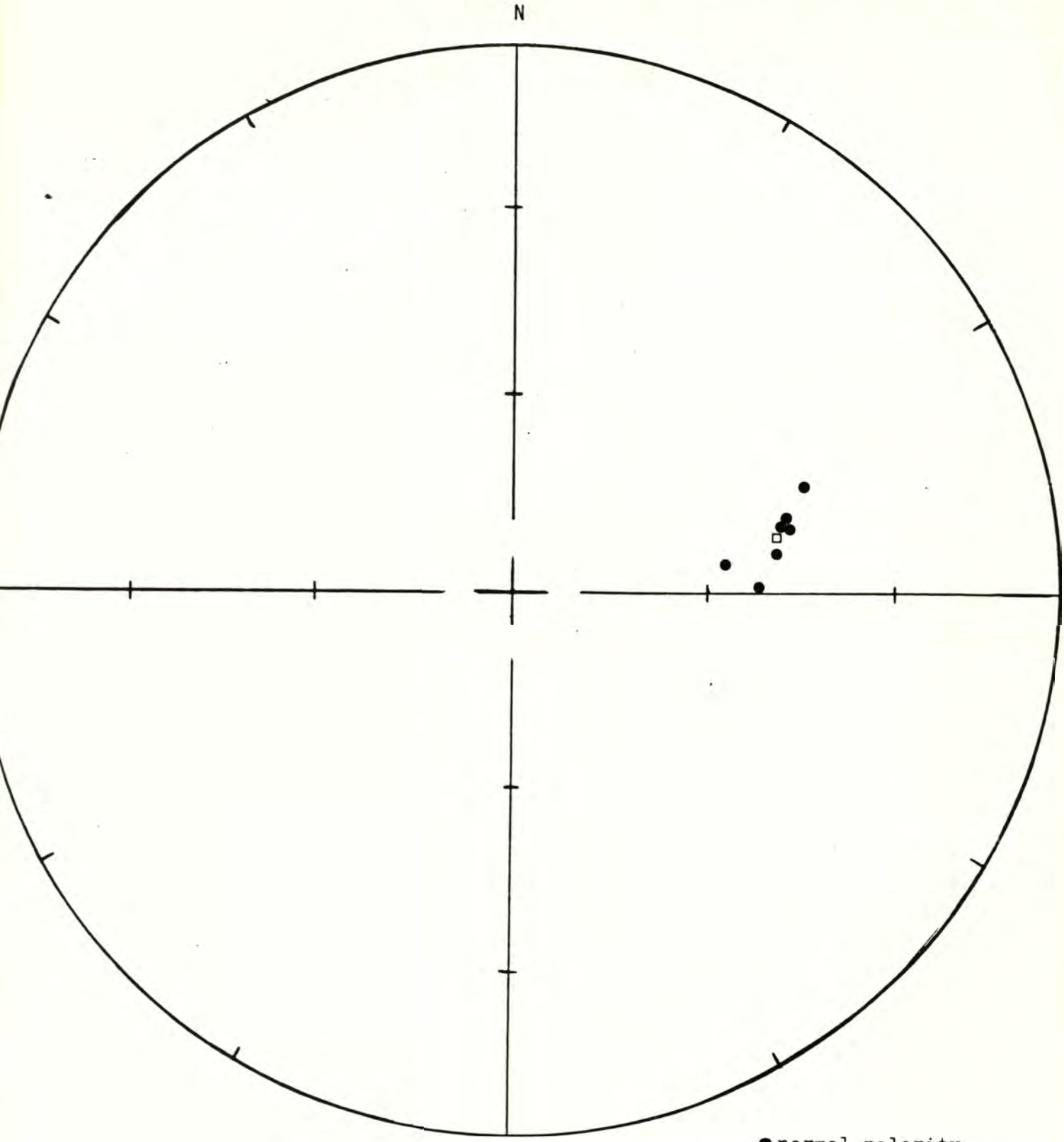

● normal polarity

○ reversed polarity

□ site mean, normal polarit

△ site mean, reversed polarity

Site: 9.11.78.1 - Porter Creek campground

Demagnetization level: 500 oe.

TECTONIC CORRECTION ON SAMPLE DIRECTIONS

Pole on site mean

Site: 9.11.78.1 Demagnetization level: 500 oe.

Dip azimuth: 289 (N19E) Dip angle: 9 (W)

Sample number	Declination	Inclination	Cor. dec.	Cor. inc.
335	74.82	48.00	67.87	55.14
336	74.68	48.11	67.68	55.24
337	69.45	43.15	63.00	49.77
338	80.22	50.32	73.59	57.96
339	82.15	59.19	72.88	66.89
340	87.90	52.81	82.28	61.05
341	75.68	46.74	69.19	53.99

R= 6.96 Site declination= 70.38 Site inclination= 57.27

Alpha 95= 4.19 Delta= 5.95 Kappa= 159.16

Site latitude= 46.9°N Site longitude= 123.25°W

Paleolatitude= 39.01°N Paleolongitude= 50.16°W DELP= 4.46

DECLM= 6.12

WITH TECTONIC CORRECTION.

Black Hills Project

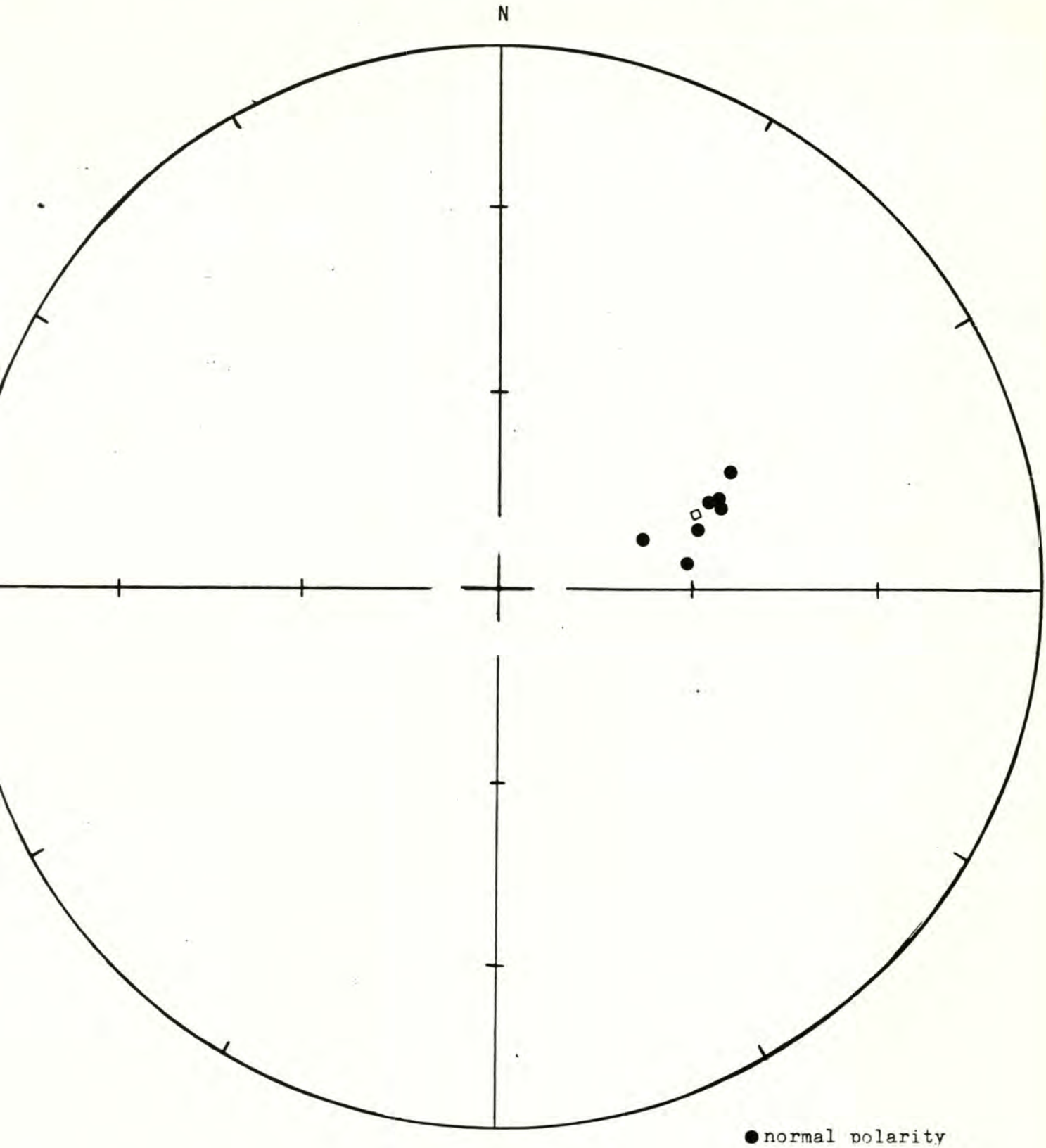

● normal polarity

○ reversed polarity

□ site mean, normal polarit

△ site mean, reversed polarity

Site: 9.11.78.1

Demagnetization level: 500 de.

FISHER ON SAMPLE DIRECTIONS

Site: 9.27.78.1 -- Porter Creek Road B Demagnetization level: NRM

NE¼ SW¼ sec. 18, T. 17 N., R. 4 W.

Sample number	Declination	Inclination
342	198.46	7.56
343	72.31	66.17
344	321.95	-3.88
345	62.54	56.49
346	96.27	36.07
347	67.24	61.37
348	151.81	26.79

R= 5.21 Site declination= 125.64 Site inclination= 47.85

Alpha 95= 28.88 Delta= 41.87 Kappa= 3.36

Site latitude= 46.9° Site longitude= 123.25°

Paleolatitude= 0.26°N Paleolongitude= 77.90°W DELP= 24.57

DECLM= 37.67

Black Hills Project

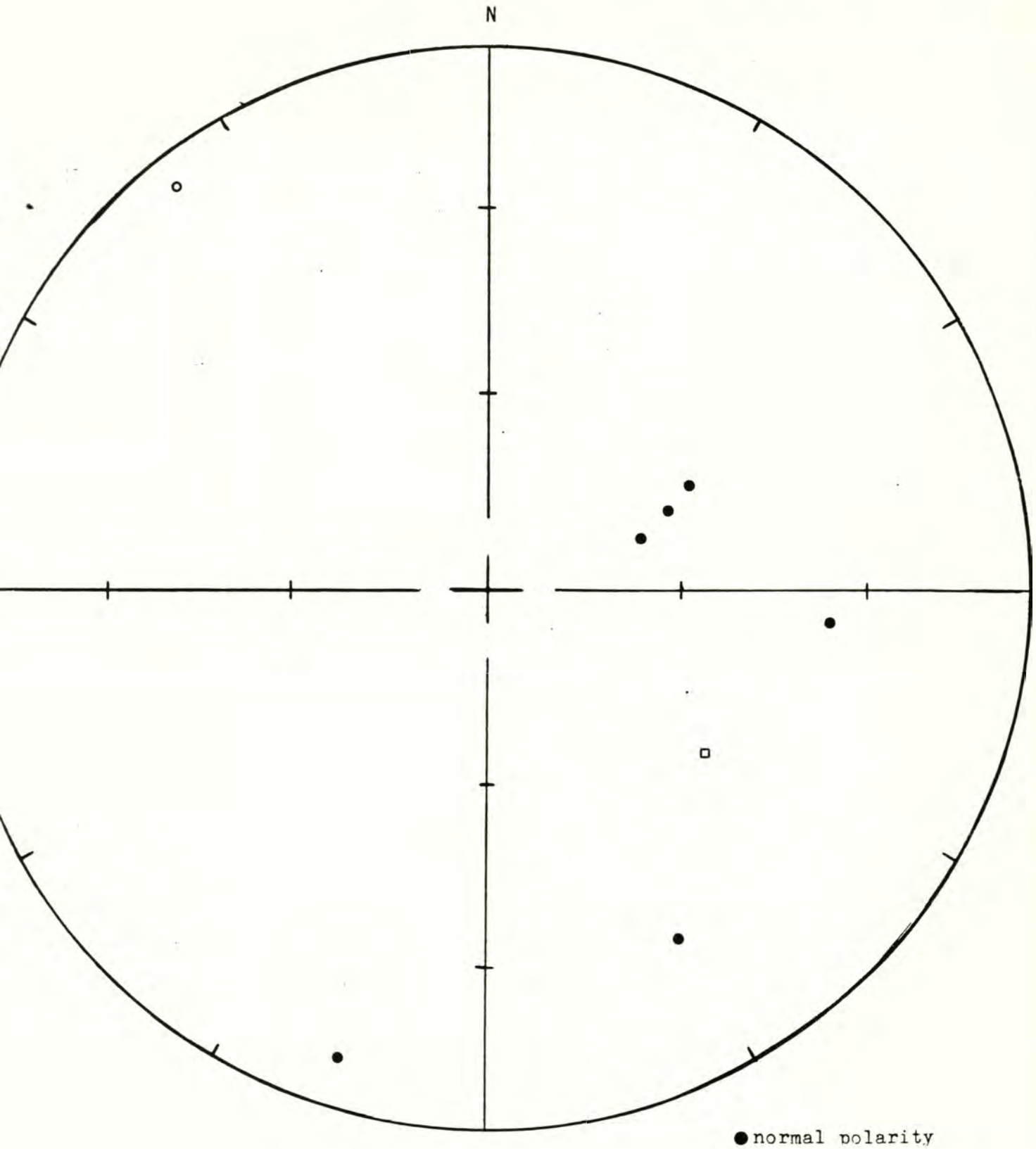

● normal polarity

○ reversed polarity

□ site mean, normal polarit

△ site mean, reversed polarity

Site: 9.27.78.1 - Porter Creek Road B

Demagnetization level: NRM

FISHER ON SAMPLE DIRECTIONS

Site: 9.27.78.1 -- Porter Creek Road B Demagnetization level: 400 oe.
NE¼ SW¼ sec. 18, T. 17 N., R. 4 W.

Sample number	Declination	Inclination
342	67.45	55.96
343	75.25	59.07
344	65.45	62.51
345	65.43	54.45
346	48.28	59.11
347	53.86	61.38
348	65.38	59.68

R= 6.97 Site declination= 63.18 Site inclination= 59.15

Alpha 95= 3.53 Delta= 5.01 Kappa= 224.24

Site latitude= 46.9° Site longitude= 123.25°

Paleolatitude= 44.84°N Paleolongitude= 48.45°W DELP= 3.95

DECLM= 5.28

Black Hills Project

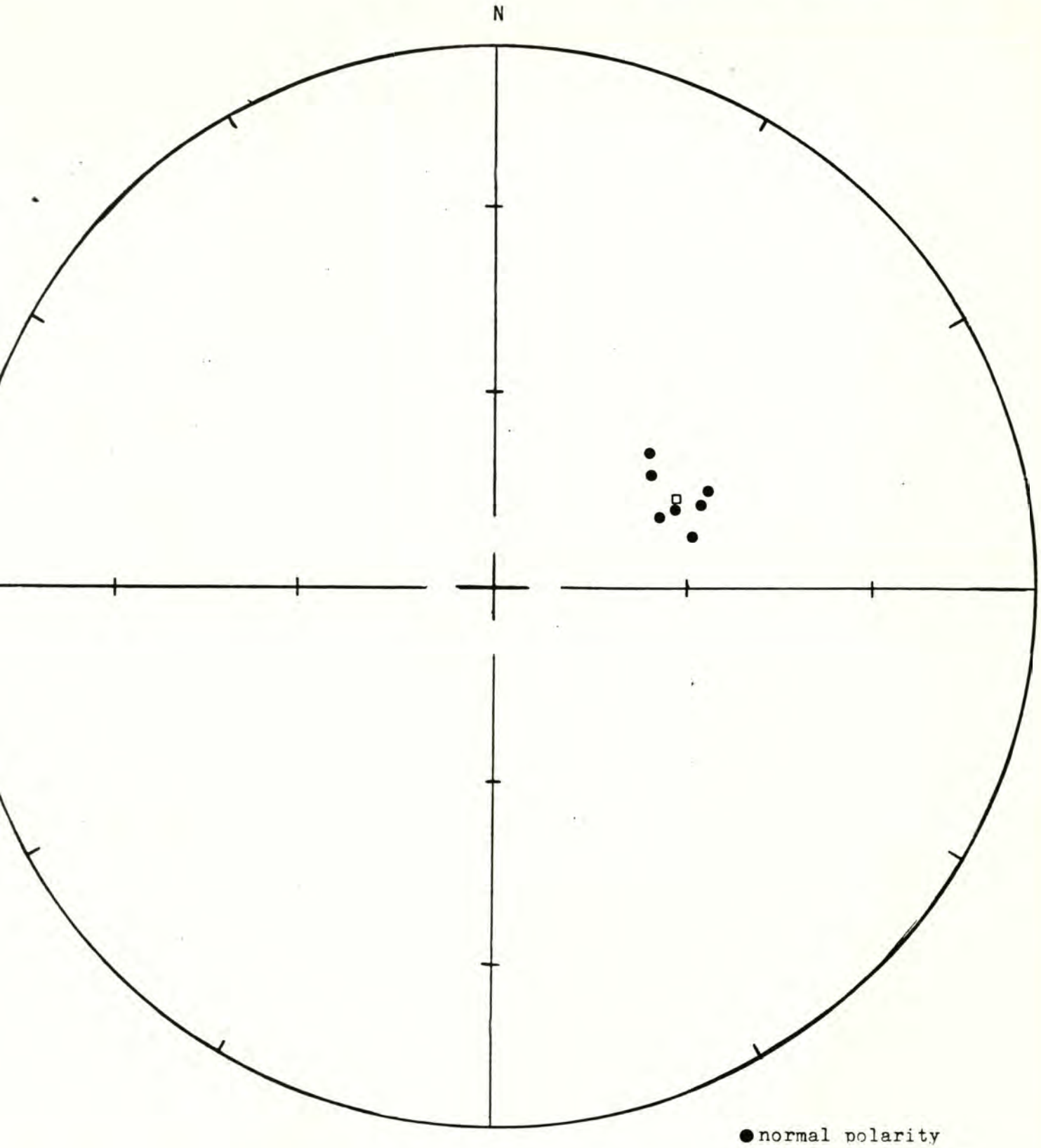

● normal polarity

○ reversed polarity

□ site mean, normal polarit

△ site mean, reversed polarity

Site: 9.27.78.1 - Porter Creek Road B

Demagnetization level: 400 oe.

FISHER ON SAMPLE DIRECTIONS

Site: 10.9.78.1 -- Camp Wedekind Demagnetization level: NRM

SE¼ NW¼ sec. 21, T. 17 N., R. 4 W.

Sample number	Declination	Inclination
349	86.0	60.74
350	203.69	72.61
351	310.95	82.94
352	37.55	65.97
353	47.12	70.68
354	310.39	78.54
355	5.87	52.36

R= 6.58 Site declination= 31.01 Site inclination= 78.49

Alpha 95= 13.99 Delta= 19.94 Kappa= 14.30

Site latitude= 46.83° Site longitude= 123.25°

Paleolatitude= 63.72°N Paleolongitude= 97.22°W DELP= 25.0

DECLM= 26.45

Black Hills Project

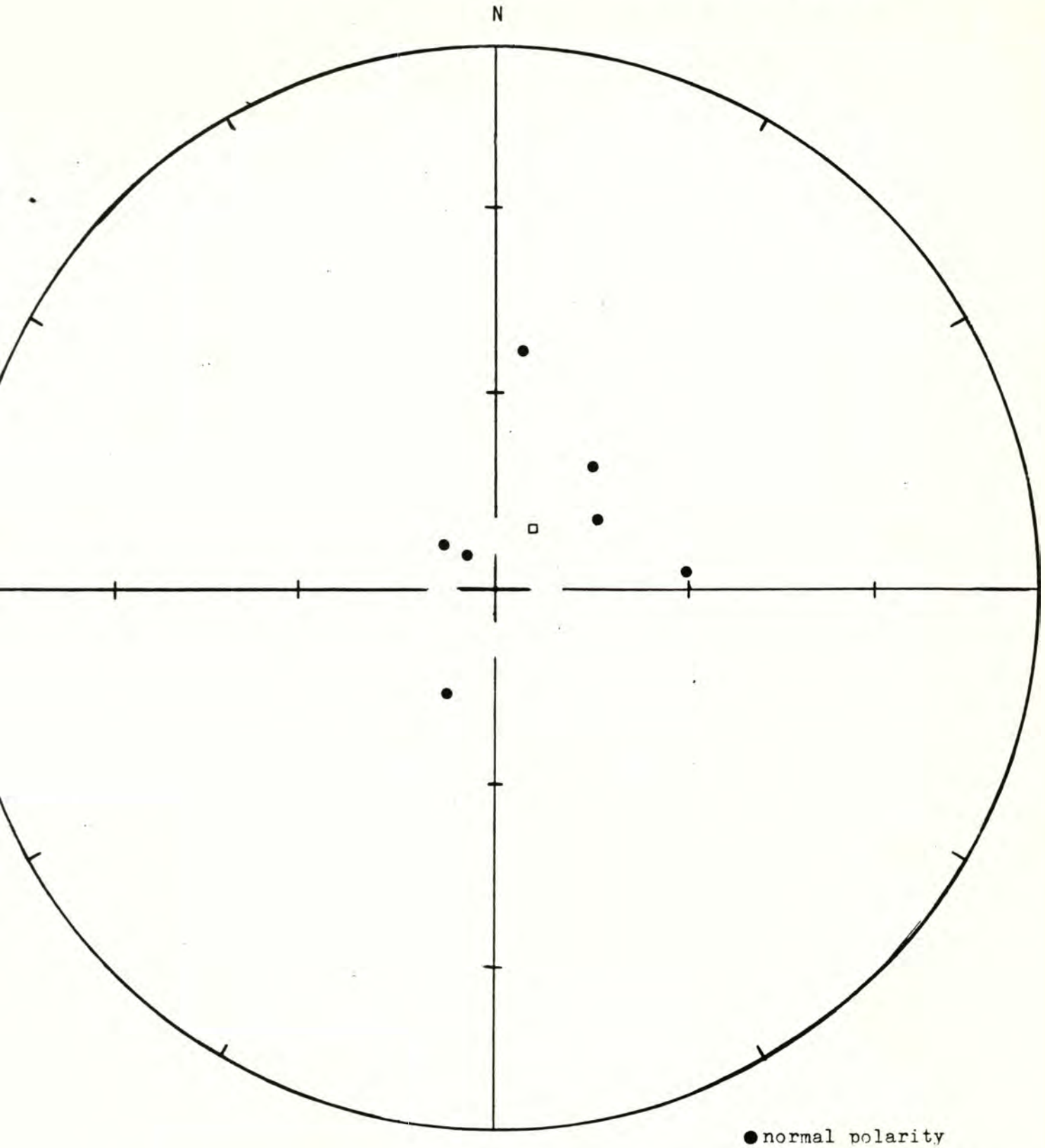

● normal polarity

○ reversed polarity

□ site mean, normal polarit

△ site mean, reversed polarity

Site: 10.9.78.1 - Camp Wedekind

Demagnetization level: NRM

FISHER ON SAMPLE DIRECTIONS

Site: 10.9.78.1 -- Camp Wedekind Demagnetization level: 400 oe.

SE¼ NW¼ sec. 21, T. 17 N., R. 4 W.

Sample number	Declination	Inclination
349	42.18	59.69
350	61.69	66.68
351	38.57	68.32
352	43.43	67.91
353	52.28	61.45
354	58.66	70.50
355	40.12	54.77

R= 6.96 Site declination= 47.43 Site inclination= 64.43

Alpha 95= 4.50 Delta= 6.39 Kappa= 138.04

Site latitude= 46.83° Site longitude= 123.25°

Paleolatitude= 57.88°N Paleolongitude= 49.99°W DELP= 5.78

DECLM=7.21

Black Hills Project

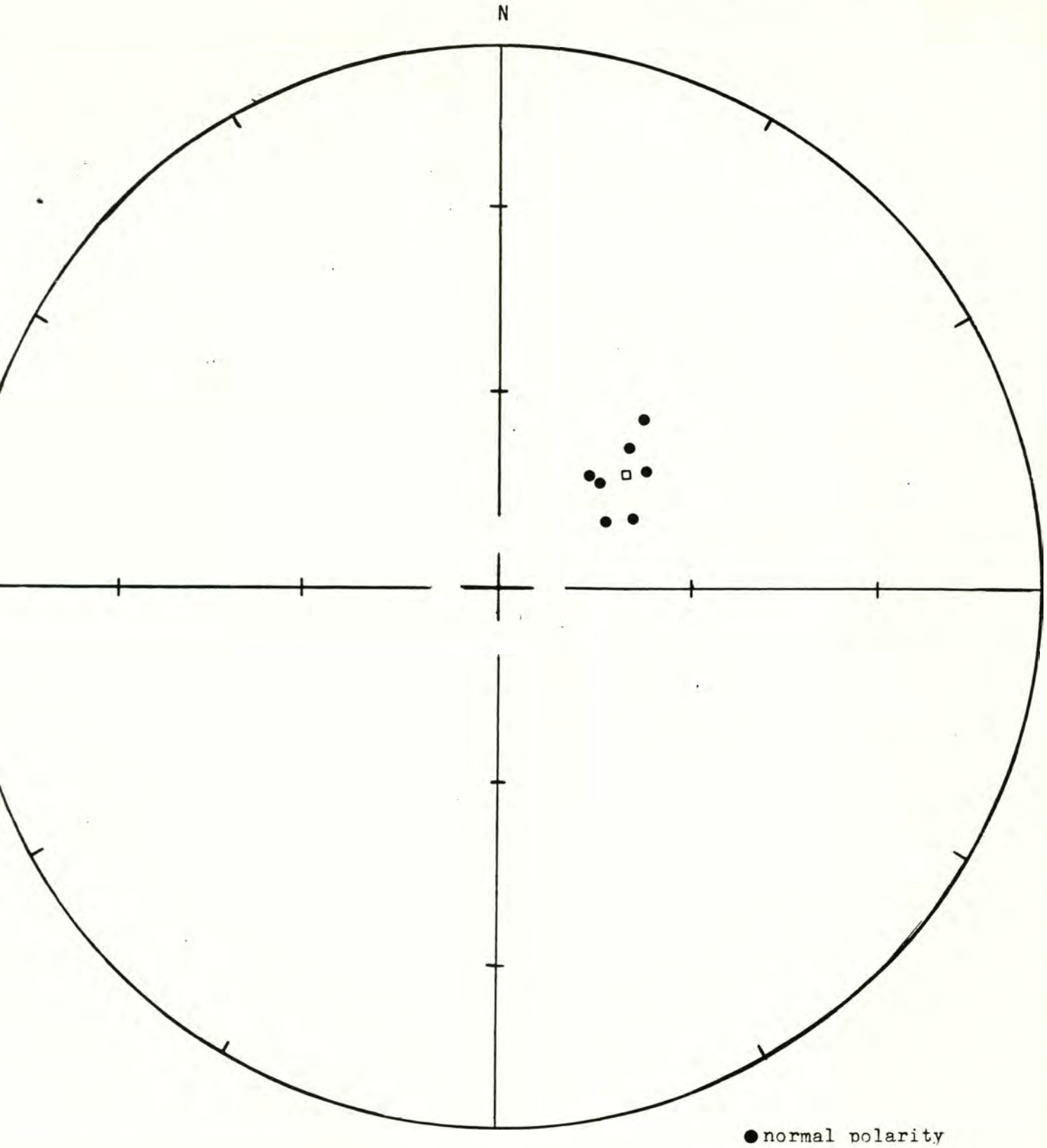

Site: 10.9.78.1 - Camp Wedekind

Demagnetization level: 400 oe.

● normal polarity

○ reversed polarity

□ site mean, normal polarit

△ site mean, reversed polarity

TECTONIC CORRECTION ON SAMPLE DIRECTIONS

Pole on site mean

Site: 10.9.78.1 Demagnetization level: 400 oe.

Dip azimuth: 210 (N60W) Dip angle: 13 (W)

Sample number	Declination	Inclination	Cor. dec.	Cor. inc.
349	42.18	59.69	50.39	72.20
350	61.69	66.68	89.68	76.06
351	38.57	68.32	50.54	80.97
352	43.43	67.91	60.55	80;11
353	52.28	61.45	67.83	72.82
354	58.66	70.50	95.38	79.86
355	40.12	54.77	45.34	67.47

R= 6.96 Site declination= 63.10 Site inclination= 76.31

Alpha 95= 4.50 Delta= 6.39 Kappa= 138.04

Site latitude= 46.83°N Site longitude= 123.25°W

Paleolatitude= 52.30°N Paleolongitude= 83.56°W DELP= 7.71

DECLM= 8.33

WITH TECTONIC CORRECTION

Black Hills Project

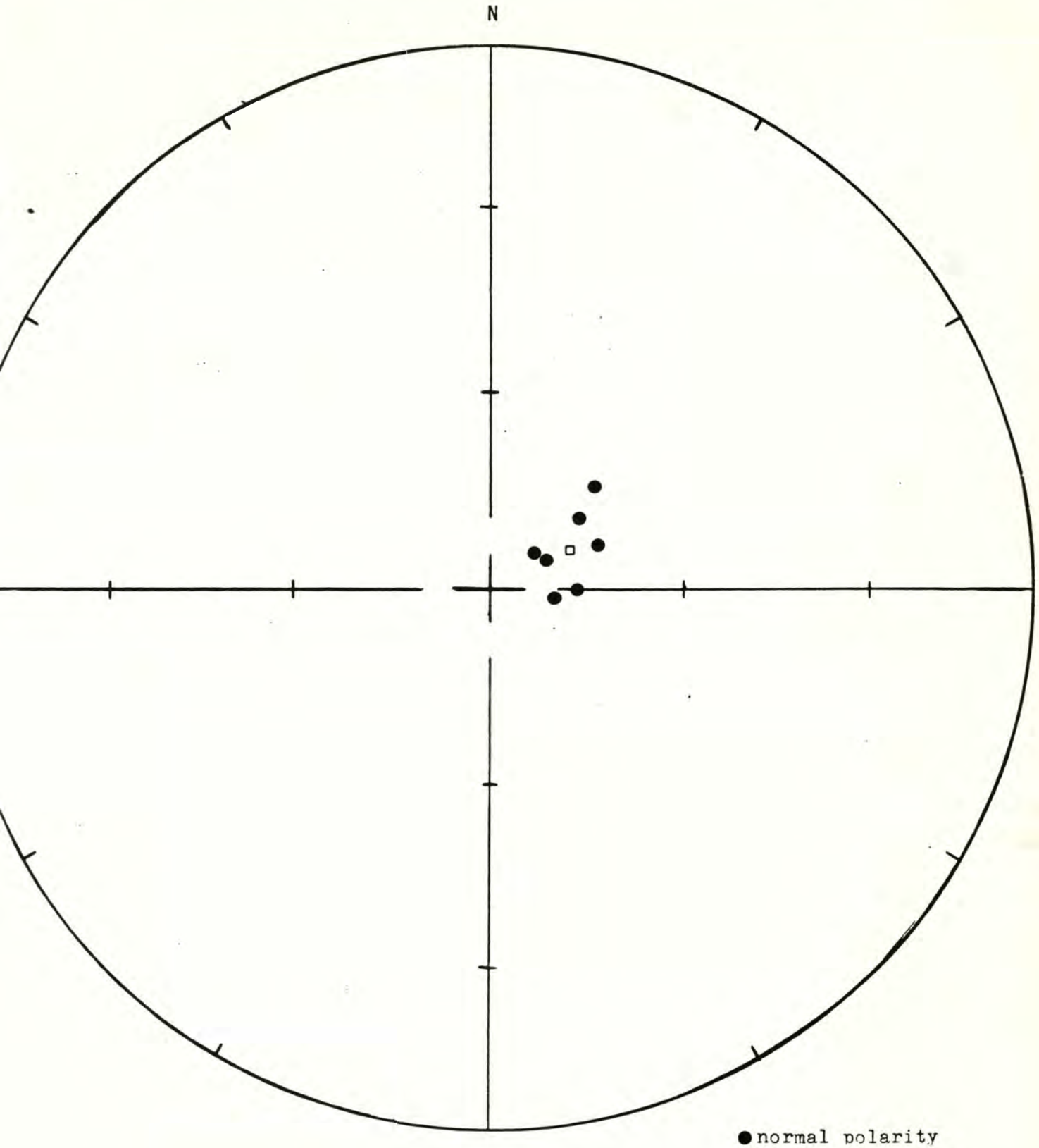

● normal polarity

○ reversed polarity

□ site mean, normal polarit

△ site mean, reversed polarity

Site: 10.9.78.1

Demagnetization level: 400 oe.

FISHER ON SAMPLE DIRECTIONS

Site: 10.9.78.2 --Porter Creek Road A Demagnetization level: NRM

SE¼ sec. 12, T. 17 N., R. 4 W.

Sample number	Declination	Inclination
356	94.54	16.67
357	93.24	9.60
358	85.46	22.21
359	89.86	27.10
360	77.83	28.97
361	80.47	63.77
362	71.53	23.81

R= 6.68 Site declination= 85.25 Site inclination= 27.38

Alpha 95= 12.22 Delta= 17.39 Kappa= 18.76

Site latitude= 46.9° Site longitude= 123.25°

Paleolatitude= 13.76°N Paleolongitude= 39.92°W DELP= 7.26

DECLM= 13.32

Black Hills Project

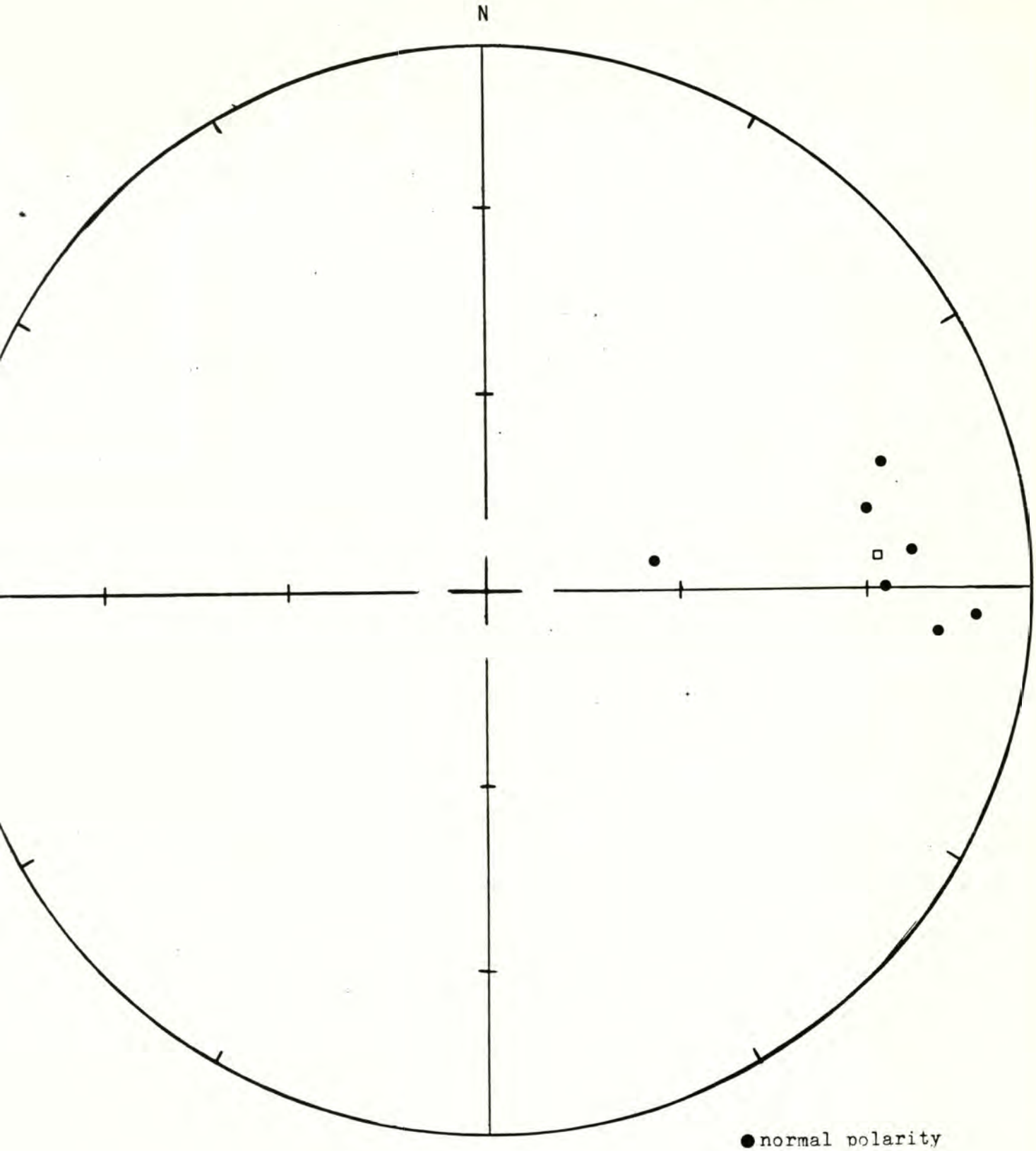

● normal polarity

○ reversed polarity

□ site mean, normal polarit

△ site mean, reversed polarity

Site: 10.9.78.2 - Porter Creek Road A

Demagnetization level: NRM

FISHER ON SAMPLE DIRECTIONS

Site: 10.9.78.2 -- Porter Creek Road A Demagnetization level: 300 oe.
SE¼ sec. 12, T. 17 N., R. 4 W.

Sample number	Declination	Inclination
356	88.45	24.24
357	83.37	18.90
358	86.37	24.54
359	86.09	25.36
360	80.67	21.80
361	85.58	27.27
362	93.41	38.16

R= 6.95 Site declination= 86.11 Site inclination= 25.79

Alpha 95= 4.58 Delta= 6.50 Kappa= 133.24

Site latitude= 46.9° Site longitude= 123.25°

Paleolatitude= 12.51°N Paleolongitude= 39.86°W DELP= 2.67

DECLM=4.95

Black Hills Project

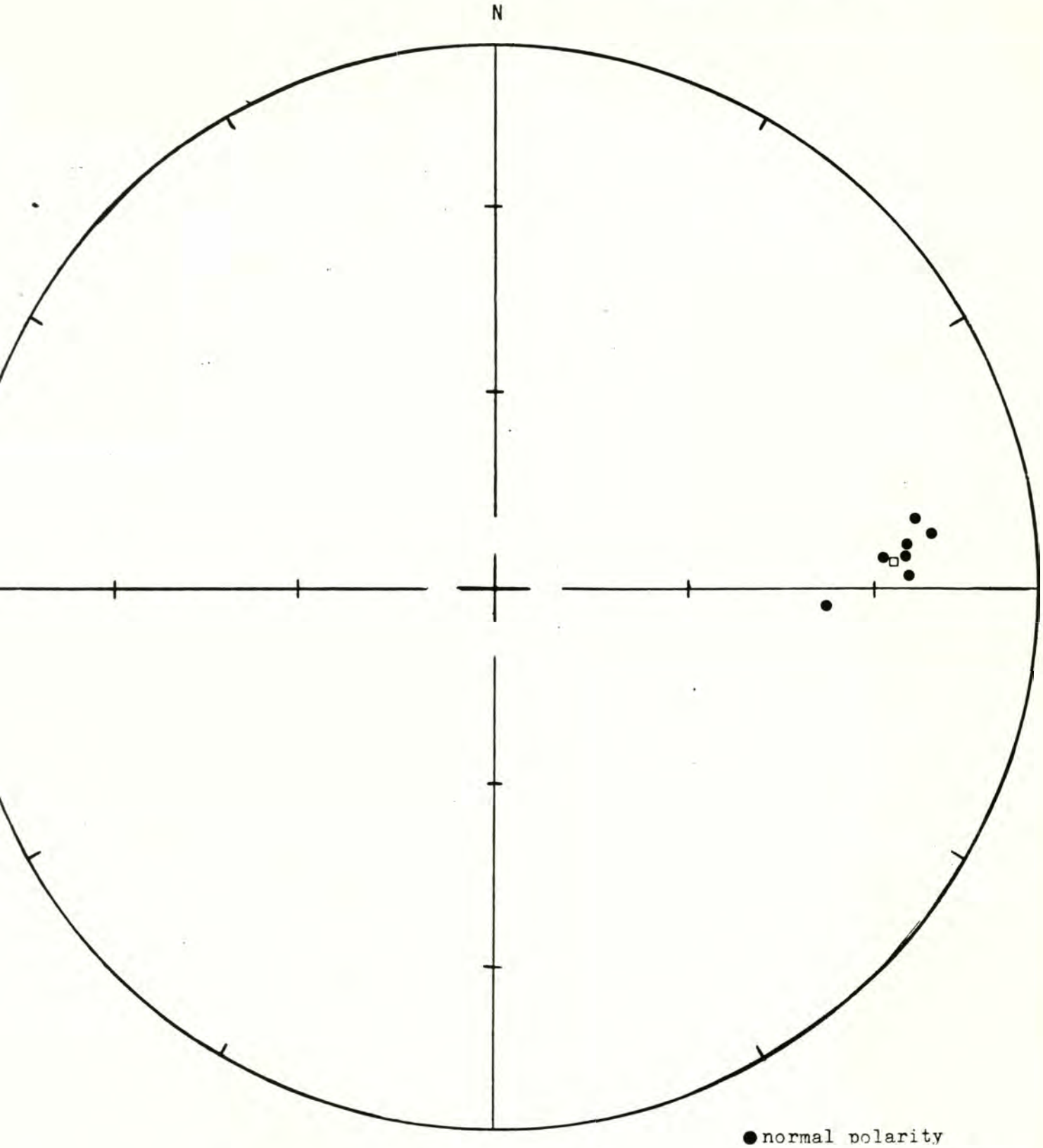

● normal polarity

○ reversed polarity

□ site mean, normal polarit

△ site mean, reversed polarity

Site: 10.9.78.2 - Porter Creek Road A

Demagnetization level: 300 oe.

TECTONIC CORRECTION ON SAMPLE DIRECTIONS

Pole on site mean

Site: 10.9.78.2 Demagnetization level: 300 oe.

Dip azimuth: 300 (N30E) Dip angle: 40 (W)

Sample number	Declination	Inclination	Cor. dec.	Cor. inc.
356	88.45	24.24	64.78	54.49
357	83.37	18.90	64.06	47.67
358	86.37	24.54	61.87	53.61
359	86.09	25.36	60.69	54.11
360	80.67	21.80	57.89	48.26
361	85.58	27.27	58.00	55.32
362	93.41	38.16	51.90	67.71

R= 6.96 Site declination= 60.26 Site inclination= 54.46

Alpha 95= 4.57 Delta= 6.50 Kappa= 134.20

Site latitude= 46.90°N Site longitude= 123.25°W

Paleolatitude= 44.14°N Paleolongitude= 40.86°W DELP= 4.54

DECLM= 6.44

WITH TECTONIC CORRECTIONS

Black Hills Project

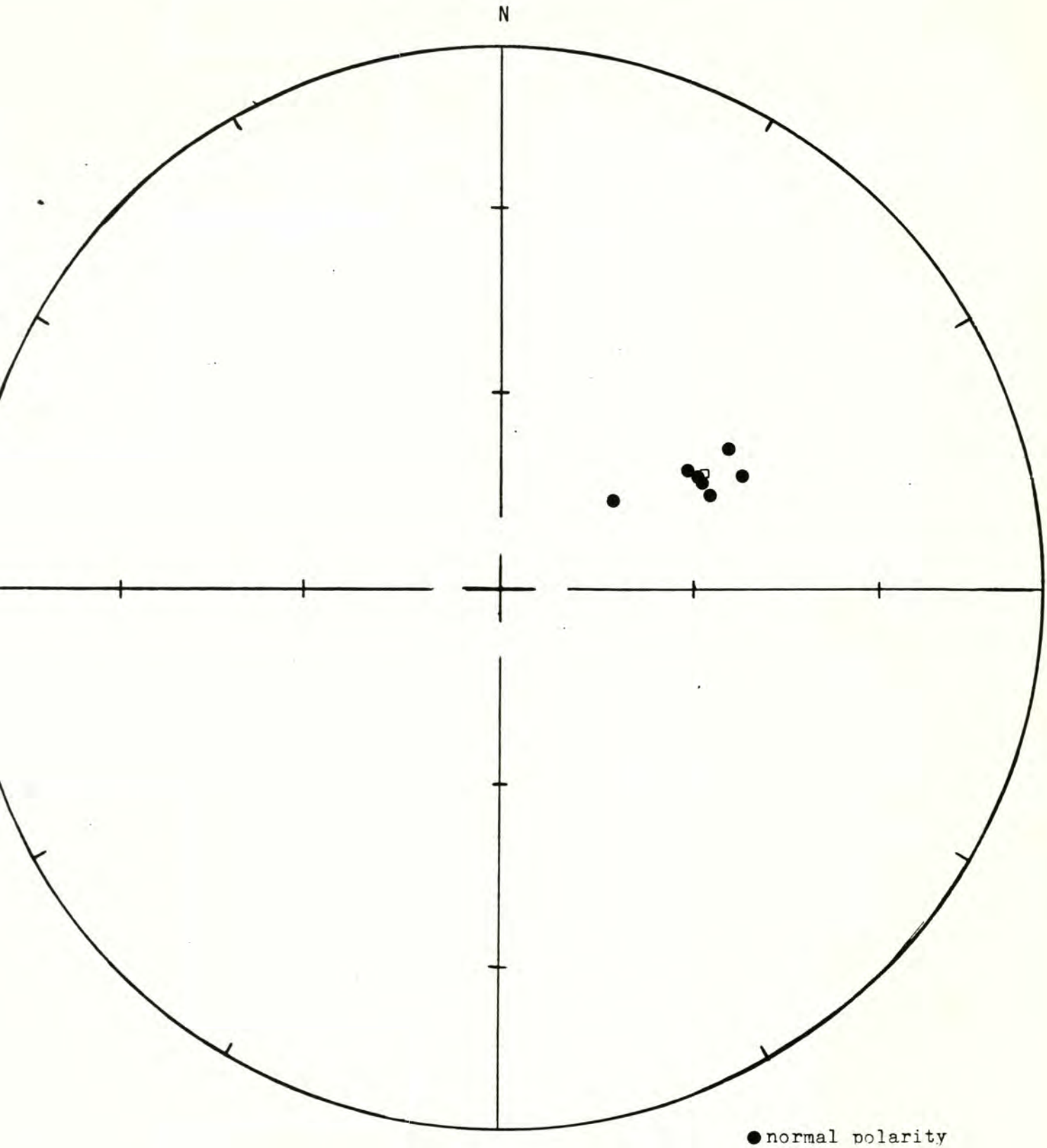

● normal polarity

○ reversed polarity

□ site mean, normal polarit

△ site mean, reversed polarity

Site: 10.9.78.2

Demagnetization level: 300 oe.

FISHER ON SAMPLE DIRECTIONS

Site: 10.15.78.1 -- Cloquallum Road Demagnetization level: NRM

SW¼ sec. 14, T. 19 N., R. 5 W.

Sample number	Declination	Inclination
363	242.55	-46.79
364	243.83	-35.11
365	235.42	-41.87
366	333.92	22.58
367	257.84	-40.89
368	246.84	-45.86

R= 5.3 Site declination= 231.12 Site inclination= -44.74

Alpha 95= 21.45 Delta= 28.04 Kappa= 7.10

Site latitude= 47.12° Site longitude= 123.30°

Paleolatitude= 45.08°N Paleolongitude= 24.34°W DELP= 17.07

DECLM= 27.06

Black Hills Project

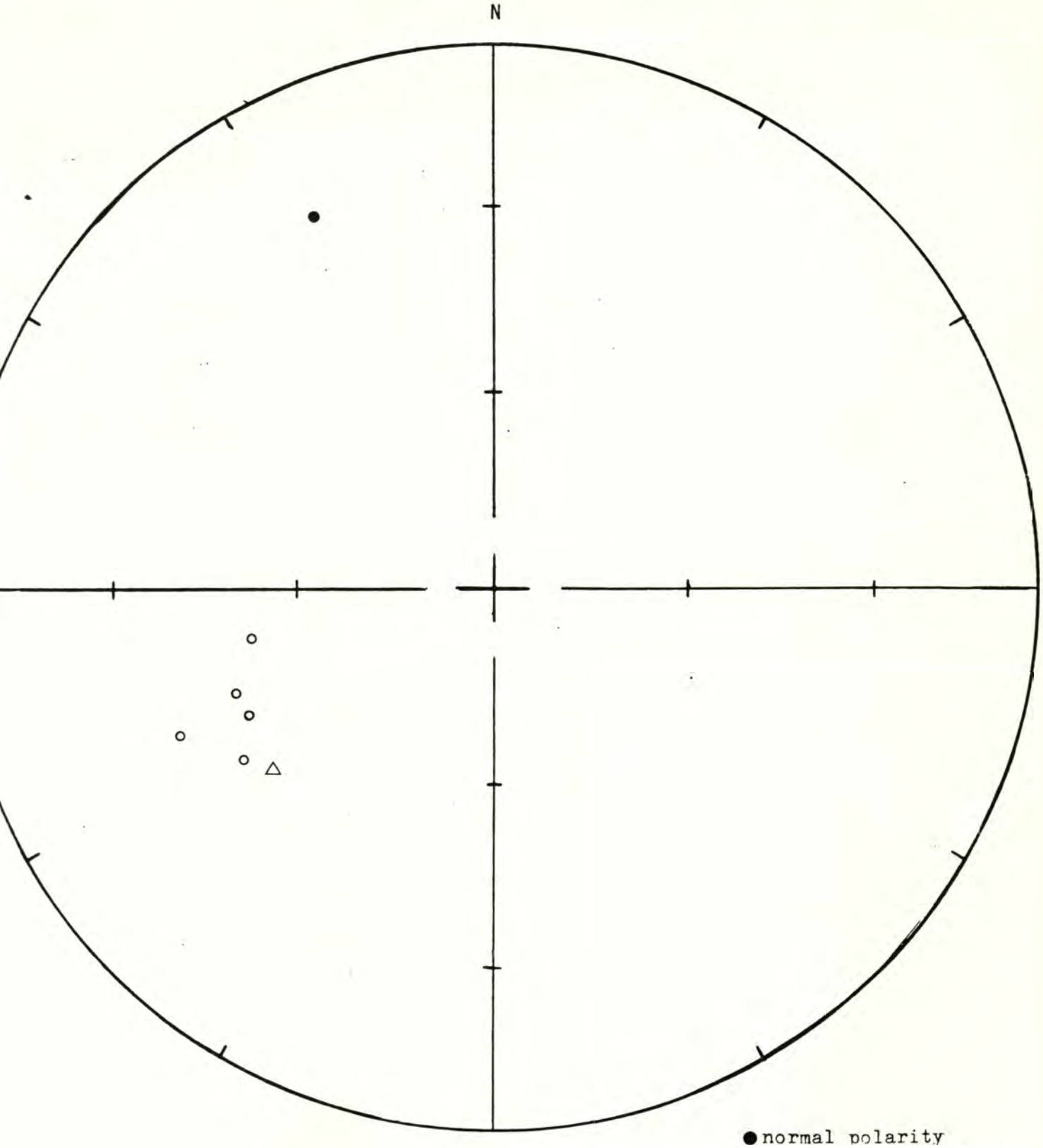

● normal polarity

○ reversed polarity

□ site mean, normal polarit

△ site mean, reversed polarity

Site: 10.15.78.1 - Cloquallum Road

Demagnetization level: NRM

FISHER ON SAMPLE DIRECTIONS

Site: 10.15.78.1 -- Cloquallum Road Demagnetization level: 300 oe.
SW¼ sec. 14, T. 19 N., R. 5 W.

Sample number	Declination	Inclination
363	247.07	-58.22
364	243.41	-52.73
365	243.5	-46.85
366	264.95	-56.5
367	251.31	-46.84
368	246.21	-51.63

R=5.97 Site declination= 249.11 Site inclination= -52.35

Alpha 95=4.77 Delta= 6.18 Kappa= 143.59

Site latitude= 47.12° Site longitude= 123.30°

Paleolatitude= 37.02°N Paleolongitude= 44.19°W DELP= 4.50

DECLM= 6.55

Black Hills Project

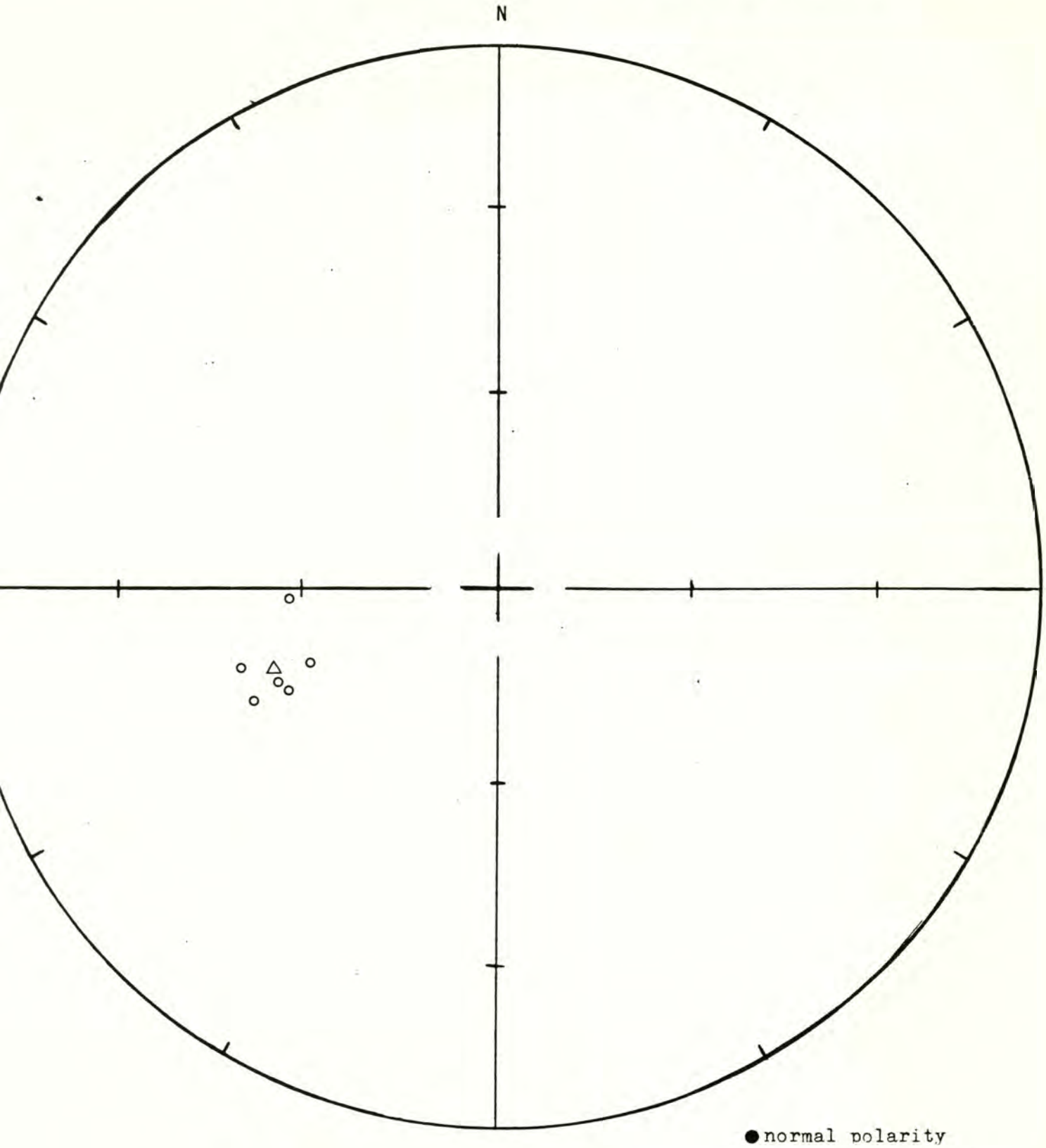

● normal polarity

○ reversed polarity

□ site mean, normal polarit

△ site mean, reversed polarity

Site: 10.15.78.1 - Cloquallum Road

Demagnetization level: 300 oe.

FISHER ON SAMPLE DIRECTIONS

Site: 10.22.78.1 -- SR 108, Kamilche Valley Demagnetization level: NRM

NW¼ NW¼ sec. 19, T. 19 N., R. 3 W.

Sample number	Declination	Inclination
369	14.63	46.96
370	66.32	31.72
371	9.06	57.37
372	357.81	34.92
373	0.58	63.68
374	266.03	73.19
375	111.54	23.02

R= 5.71 Site declination= 32.88 Site inclination=59.42

Alpha 95= 24.54 Delta= 35.34 Kappa= 4.65

Site latitude= 47.12° Site longitude= 123.12°

Paleolatitude= 65.45°N Paleolongitude= 28.94°W DELP= 27.63

DECLM= 36.82

Black Hills Project

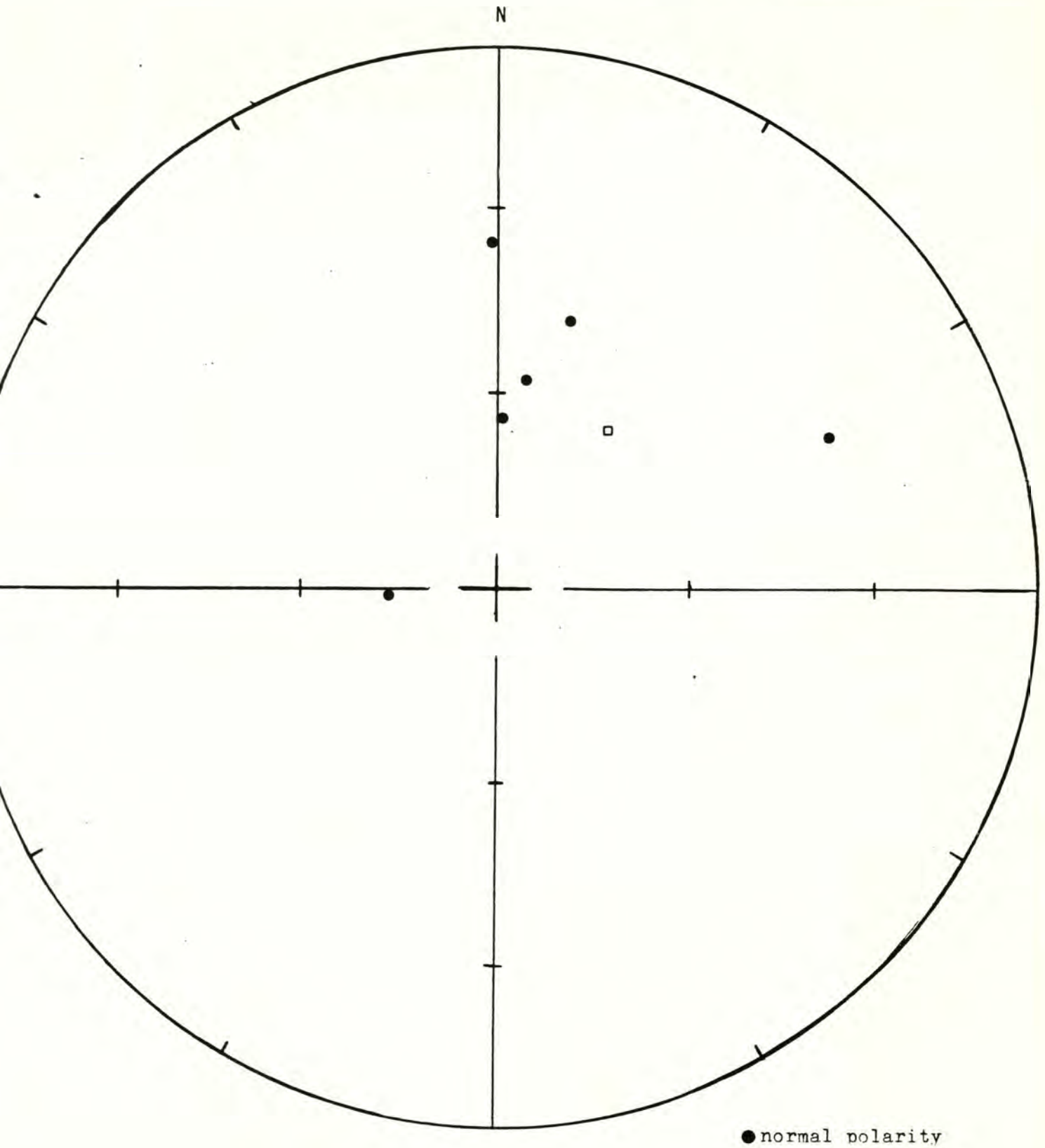

● normal polarity
○ reversed polarity
□ site mean, normal polarit
△ site mean, reversed polarity

Site: 10.22.78.1 - SR 108, Kamilche Valley

Demagnetization level: NRM

FISHER ON SAMPLE DIRECTIONS

Site: 10.22.78.1 -- SR 108, Kamilche Valley Demagnetization level: 200 oe.

NW¼ NW¼ sec. 19, T. 19 N., R. 3 W.

Sample number	Declination	Inclination
369	37.26	49.40
370	30.54	51.72
371	23.65	51.29
372	29.47	39.58
373	32.66	63.23
374	31.86	56.56
375	31.18	36.56

R= 6.92 Site declination= 30.86 Site inclination= 49.83

Alpha 95= 6.25 Delta= 8.88 Kappa= 71.57

Site latitude= 47.12° Site longitude= 123.12°

Paleolatitude= 61.17°N Paleolongitude= 9.34°W DELP= 5.56

DECLM= 8.34

Black Hills Project

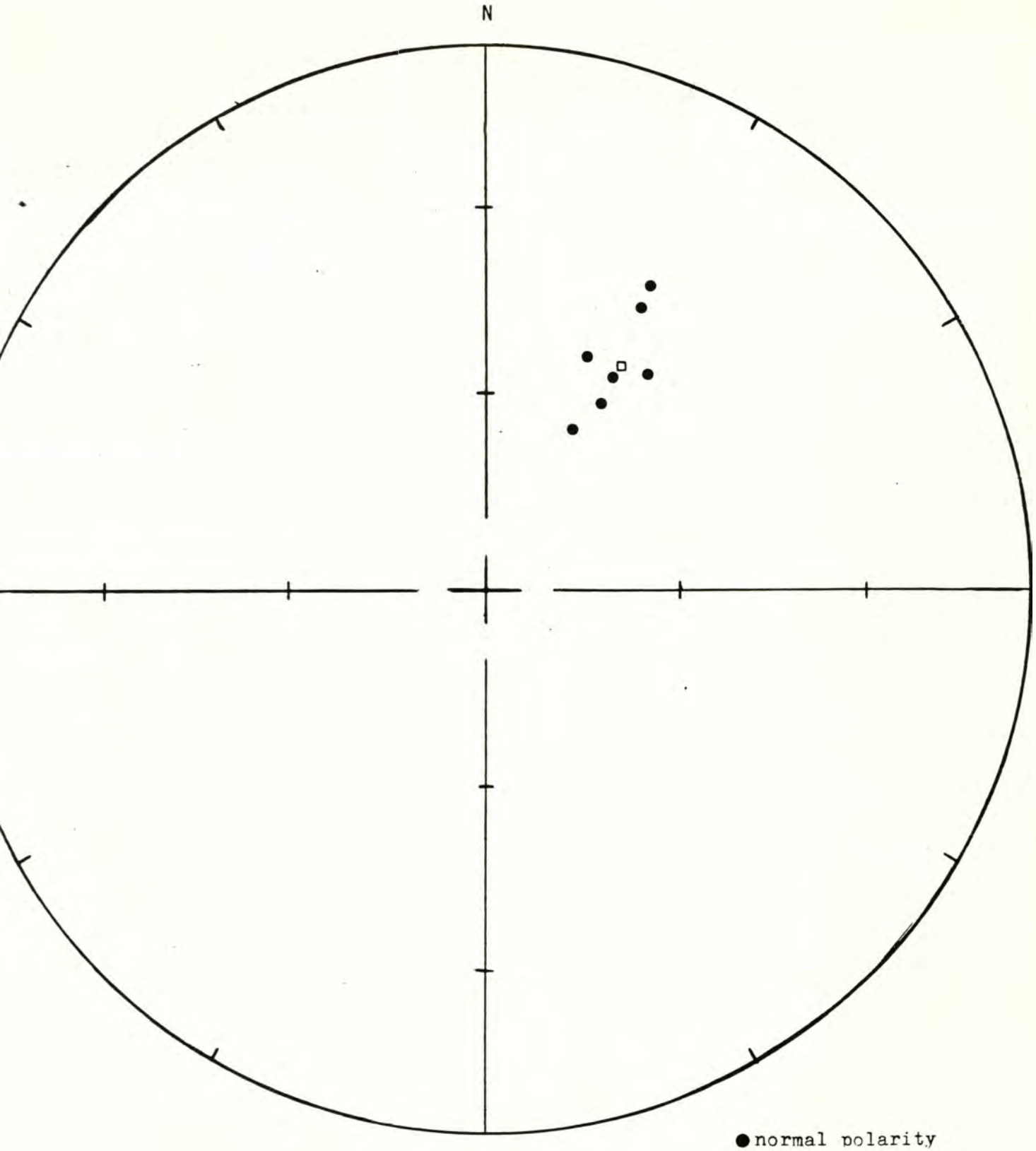

● normal polarity

○ reversed polarity

□ site mean, normal polarit

△ site mean, reversed polarity

Site: 10.22.78.1 - SR 108, Kamilche Valley

Demagnetization level: 200 oe.

TECTONIC CORRECTION ON SAMPLE DIRECTIONS

Pole on site mean

Site: 10.22.78.1 Demagnetization level: 200 oe.

Dip azimuth: 298 (N28E) Dip angle: 17 (W)

Sample number	Declination	Inclination	Cor. dec.	Cor. inc.
369	37.26	49.40	17.26	49.18
370	30.54	51.72	9.82	49.35
371	23.65	51.29	4.32	47.08
372	29.47	39.58	15.74	37.96
373	32.66	63.23	1.27	59.83
374	31.86	56.56	7.23	53.98
375	31.18	36.56	18.69	35.64

R= 6.92 Site declination= 11.35 Site inclination= 47.74

Alpha 95= 6.26 Delta= 8.88 Kappa= 71.57

Site latitude= 47.12°N Site longitude= 123.12°W

Paleolatitude= 69.68°N Paleolongitude= 27.11°E DELP= 5.31

DECLM= 8.16

WITH TECTONIC CORRECTION

Black Hills Project

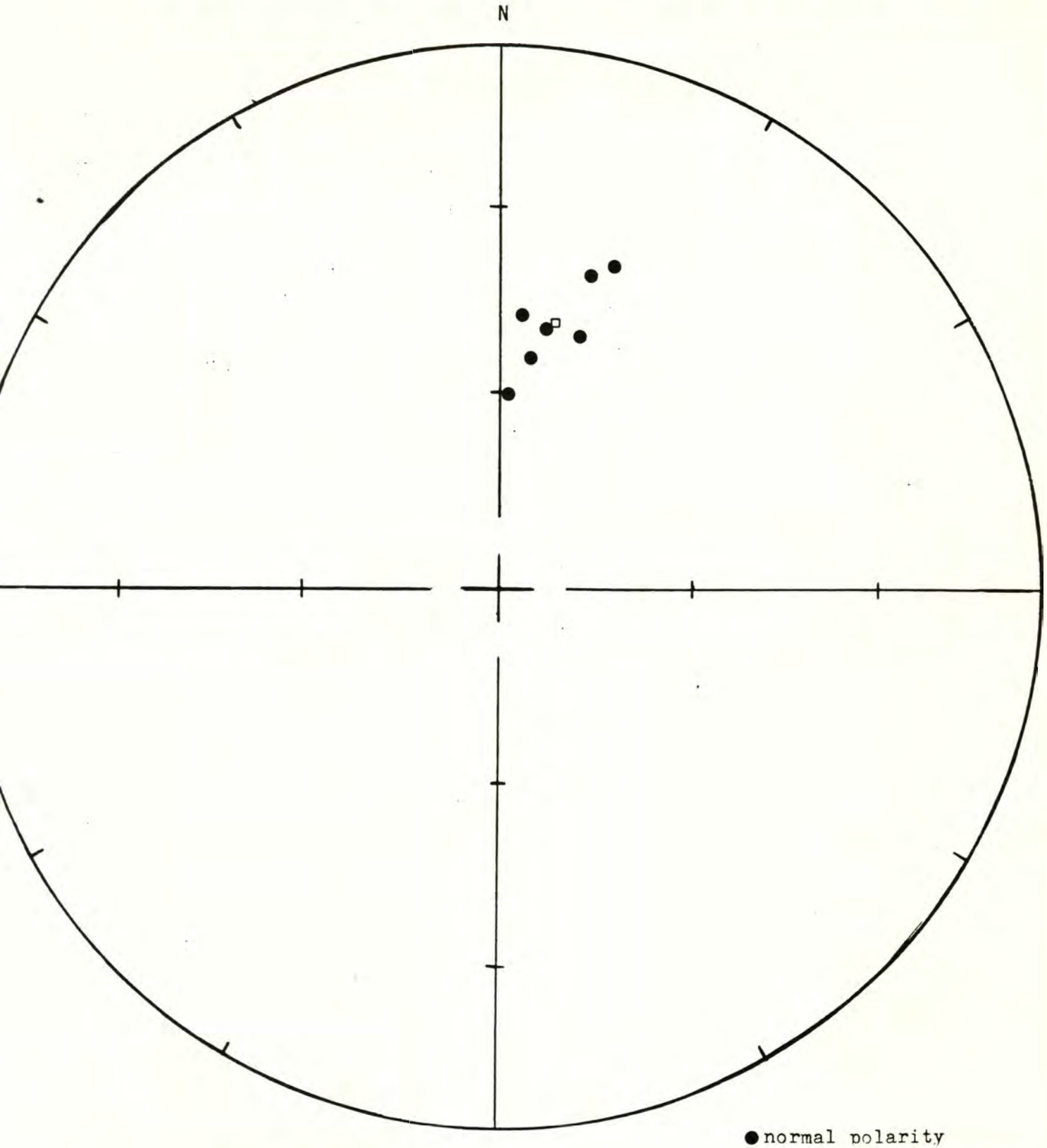

● normal polarity

○ reversed polarity

□ site mean, normal polarit

△ site mean, reversed polarity

Site: 10.22.78.1

Demagnetization level: 200 oe.

FISHER ON SAMPLE DIRECTIONS

Site: 10.23.78.1 -- SR 108, McCleary Demagnetization level: NRM

SW¼ NE¼ sec. 1, T. 18 N., R. 5 W.

Sample number	Declination	Inclination
376	205.41	-16.66
377	263.43	-64.44
378	285.69	-65.52
379	313.22	-39.88
380	270.48	-7.64
381	249.26	-64.26
382	184.29	-37.84

R= 5.59 Site declination= 249.6 Site inclination= -51.64

Alpha 95= 25.61 Delta= 36.94 Kappa= 4.27

Site latitude=47° Site longitude= 123.25°

Paleolatitude= 36.27°N Paleolongitude= 43.88°W DELP= 23.76

DECLM= 34.89

Black Hills Project

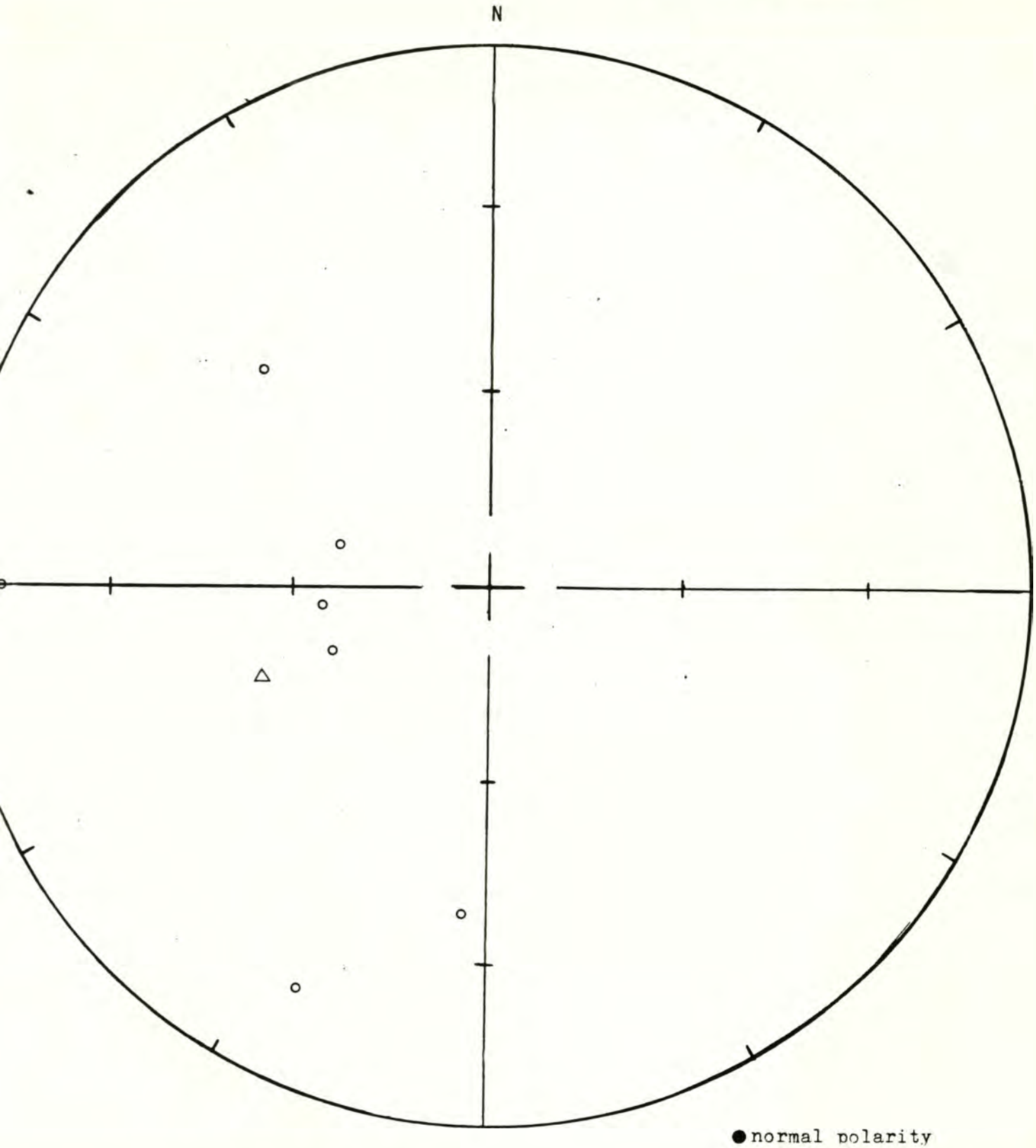

● normal polarity

○ reversed polarity

□ site mean, normal polarit

△ site mean, reversed polarity

Site: 10.23.78.1 - SR 108, McCleary

Demagnetization level: NRM

FISHER ON SAMPLE DIRECTIONS

Site: 10.23.78.1 -- SR 108, McCleary Demagnetization level: 300 oe.
SW¼ NE¼ sec. 1, T. 18 N., R. 5 W.

Sample number	Declination	Inclination
376	234.51	-55.46
377	246.04	-57.5
378	232.02	-59.98
379	262.06	-66.78
380	228.06	-58.11
381	247.38	-64.24
382	247.22	-58.92

R= 649655 Site declination= 241.55 Site inclination= -60.55

Alpha 95= 4.47 Delta= 6.34 Kappa= 140.16

Site latitude= 47° Site longitude= 123.25°

Paleolatitude= 46.73°N Paleolongitude= 49.44°W DELP= 5.18

DECLM= 6.81

Black Hills Project

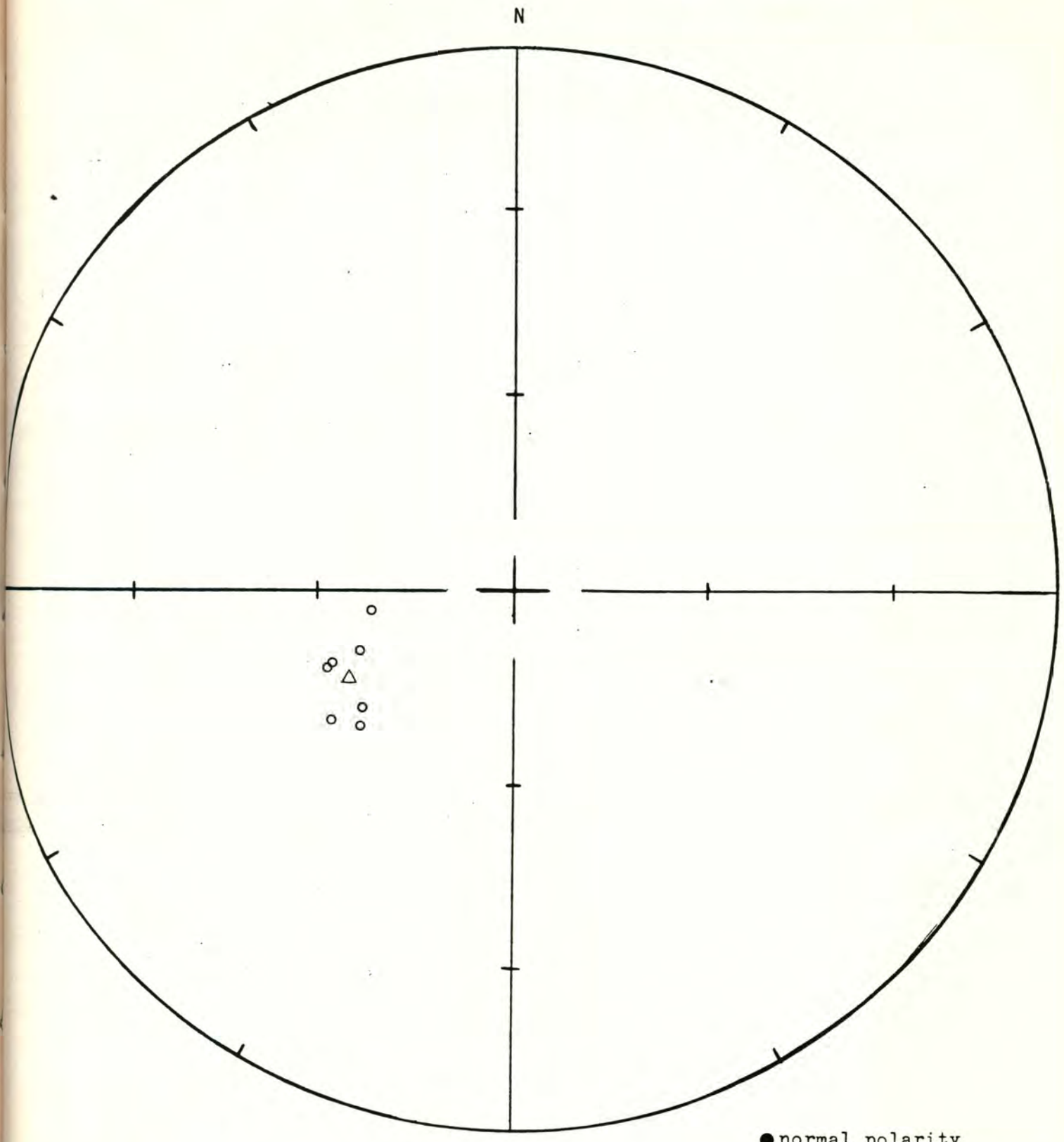

● normal polarity

○ reversed polarity

□ site mean, normal polarit

△ site mean, reversed polarity

Site: 10.23.78.1 - SR 108, McCleary

Demagnetization level: 300 oe.

FISHER ON SAMPLE DIRECTIONS

Site: 10.23.78.2 -- Summit Lake north Demagnetization level: NRM

NW¼ NE¼ sec. 8, T. 18 N., R. 3 W.

Sample number	Declination	Inclination
383	317.56	-24.1
384	256.79	-62.80
385	251.03	-69.06
386	238.34	-61.08
387	229.84	-61.08
388	233.14	-60.24
389	238.98	-66.0

R= 6.49 Site declination= 258.03 Site inclination= -62.58

Alpha 95= 15.37 Delta= 21.93 Kappa= 11.85

Site latitude= 47^{o} Site longitude= 123^{o}

Paleolatitude= 37.54^{o}N Paleolongitude= 60.33^{o}W DELP=18.79

DECLM= 24.03

Black Hills Project

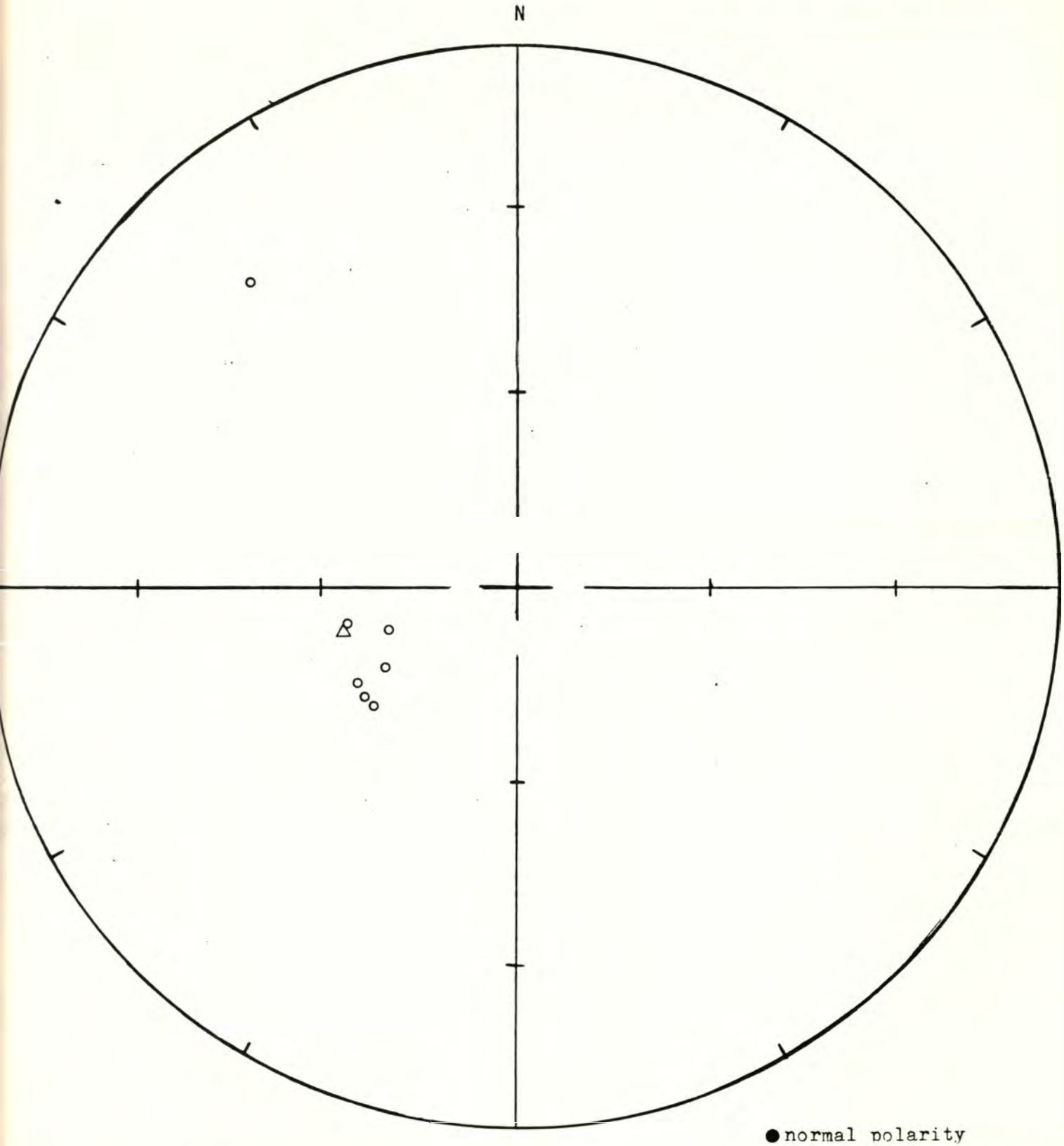

● normal polarity

○ reversed polarity

□ site mean, normal polarit

△ site mean, reversed polarity

Site: 10.23.78.2 - Summit Lake north

Demagnetization level: NRM

FISHER ON SAMPLE DIRECTIONS

Site: 10.23.78.2 -- Summit Lake north Demagnetization level: 500 oe.
NW¼ NE¼ sec. 8, T. 18 N., R. 3 W.

Sample number	Declination	Inclination
383*	299.85	-53.77
384	250.49	-68.36
385	243.06	-62.62
386	231.33	-48.39
387	236.35	-58.45
388	221.48	-61.69
389	238.64	-81.77

*Rejected from site mean.

R= 5.89 Site declination= 235.68 Site inclination= -63.81

Alpha 95= 8.38 Delta= 10.87 Kappa= 46.48

Site latitude= 47.0° Site longitude= 123.0°

Paleolatitude= 52.28°N Paleolongitude= 51.79°W DELP= 10.58

DECLM= 13.32

Black Hills Project

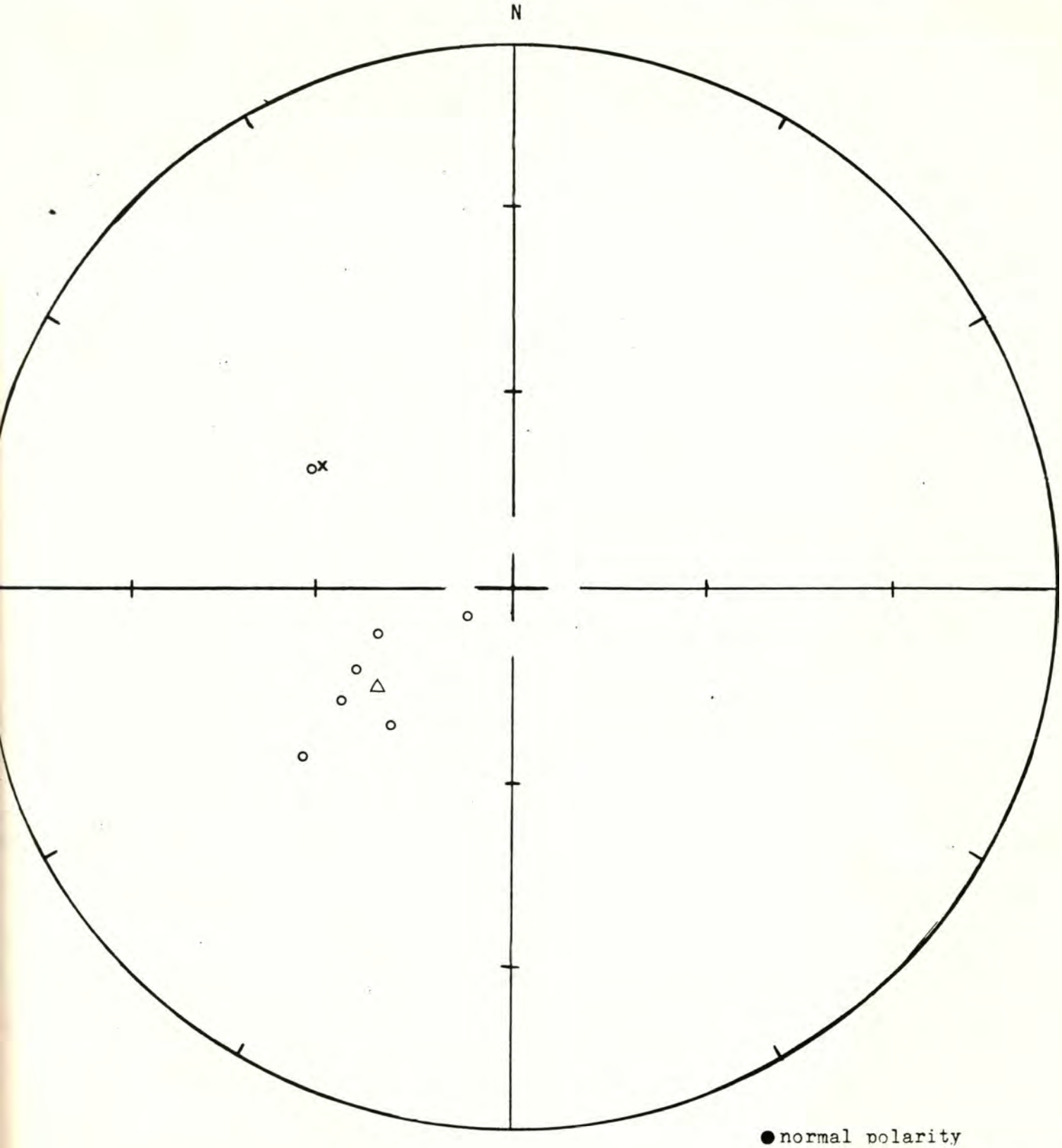

Site: 10.23.78.2 - Summit Lake north

Demagnetization level: 500 oe.

● normal polarity

○ reversed polarity

□ site mean, normal polarit

△ site mean, reversed polarity

× Sample 383 eliminated from site mean.

TECTONIC CORRECTION ON SAMPLE DIRECTIONS

Pole on site mean

Site: 10.23.78.2 Demagnetization level: 500 oe.

Dip azimuth: 216 (N54W) Dip angle: 12 (W)

Sample number	Declination	Inclination	Cor. dec.	Cor. inc.
384	250.49	-68.36	279.51	-76.51
385	243.06	-62.62	260.09	-72.50
386	231.33	-48.39	236.44	-59.83
387	236.35	-58.45	247.01	-69.32
388	221.48	-61.69	225.23	-73.60
389	238.64	-81.77	0.25	-84.59

R= 5.89 Site declination= 250.05 Site inclination= -74.61

Alpha 95= 8.38 Delta= 10.86 Kappa= 46.49

Site latitude= 47.0°N Site longitude= 123.0°W

Paleolatitude= 48,84°N Paleolongitude= 79.46°W DELP= 13.84

DECLM= 15.23

WITH TECTONIC CORRECTION

Black Hills Project

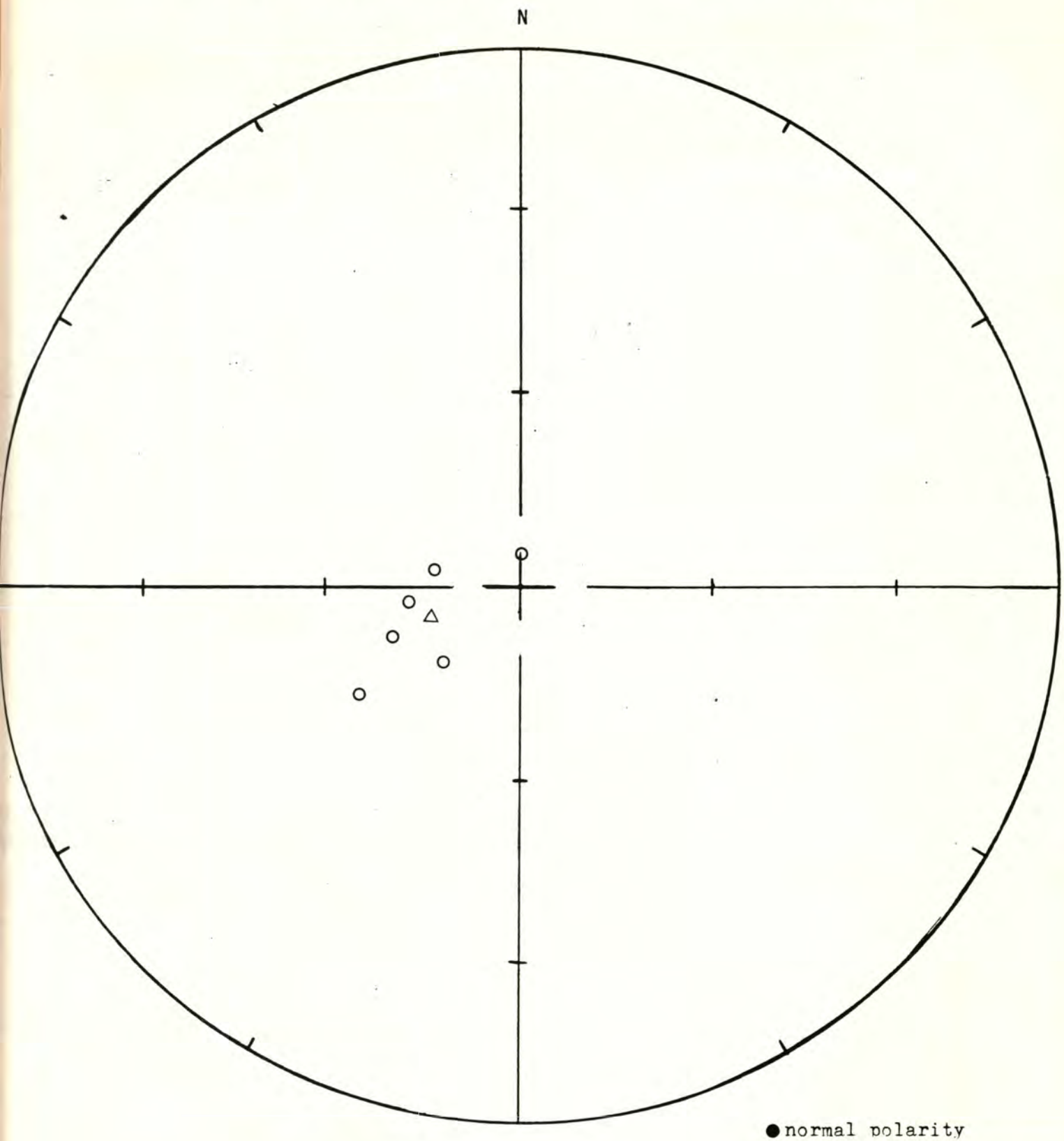

● normal polarity

○ reversed polarity

□ site mean, normal polari

△ site mean, reversed polarity

Site: 10.23.78.2

Demagnetization level: 500 oe.

FISHER ON SAMPLE DIRECTIONS

Site: 10.28.78.1 -- Kennedy Falls Demagnetization level: NRM
SE¼ NE¼ sec. 1, T. 18 N., R. 4 W.

Sample number	Declination	Inclination
390	206.88	-66.34
391	130.35	-81.07
392	174.39	-85.13
393	357.07	80.10
394	35.09	-73.67
395	85.81	-11.81
396	62.95	-39.88

R= 5.96 Site declination= 92.07 Site inclination= -72.66

Alpha 95= 22.01 Delta= 31.61 Kappa= 5.77

Site latitude= 47° Site longitude= 123,12°

Paleolatitude= 39.3°N Paleolongitude= 166.28°W DELP= 34.76

DECLM= 39.12

Black Hills Project

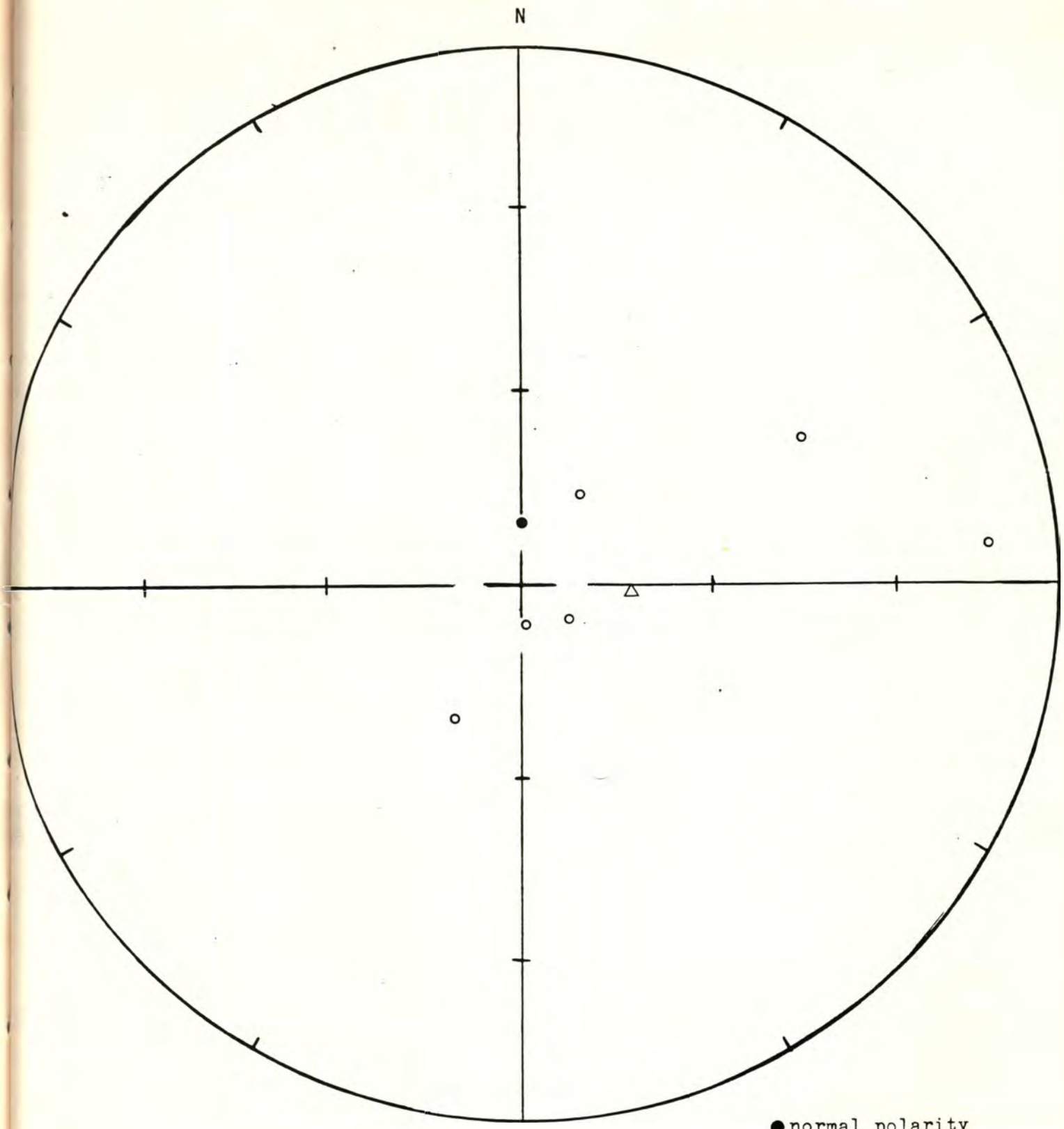

● normal polarity

○ reversed polarity

□ site mean, normal polarit

△ site mean, reversed polarity

Site: 10.28.78.1 - Kennedy Falls

Demagnetization level: NRM

FISHER ON SAMPLE DIRECTIONS

Site: 10.28.78.1 -- Kennedy Falls Demagnetization level: 500 oe.

SE¼ NE¼ sec. 1, T. 18 N., R. 4 W.

Sample number	Declination	Inclination
390	194.53	-69.62
391	0.62	-72.58
392	106.49	-76.22
393*	145.49	-44.64
394	252.29	-79.88
395*	1.40	-14.32
396	35.56	-70.17

R= 4.79 Site declination= 56.07 Site inclination= -87.49

Alpha 95= 14.26 Delta= 16.56 Kappa= 19.28

Site latitude= 47° Site longitude= 123.12°

Paleolatitude= 44.05°N Paleolongitude= 128.9°W DELP= 28.36

DECLM= 28.44

Black Hills Project

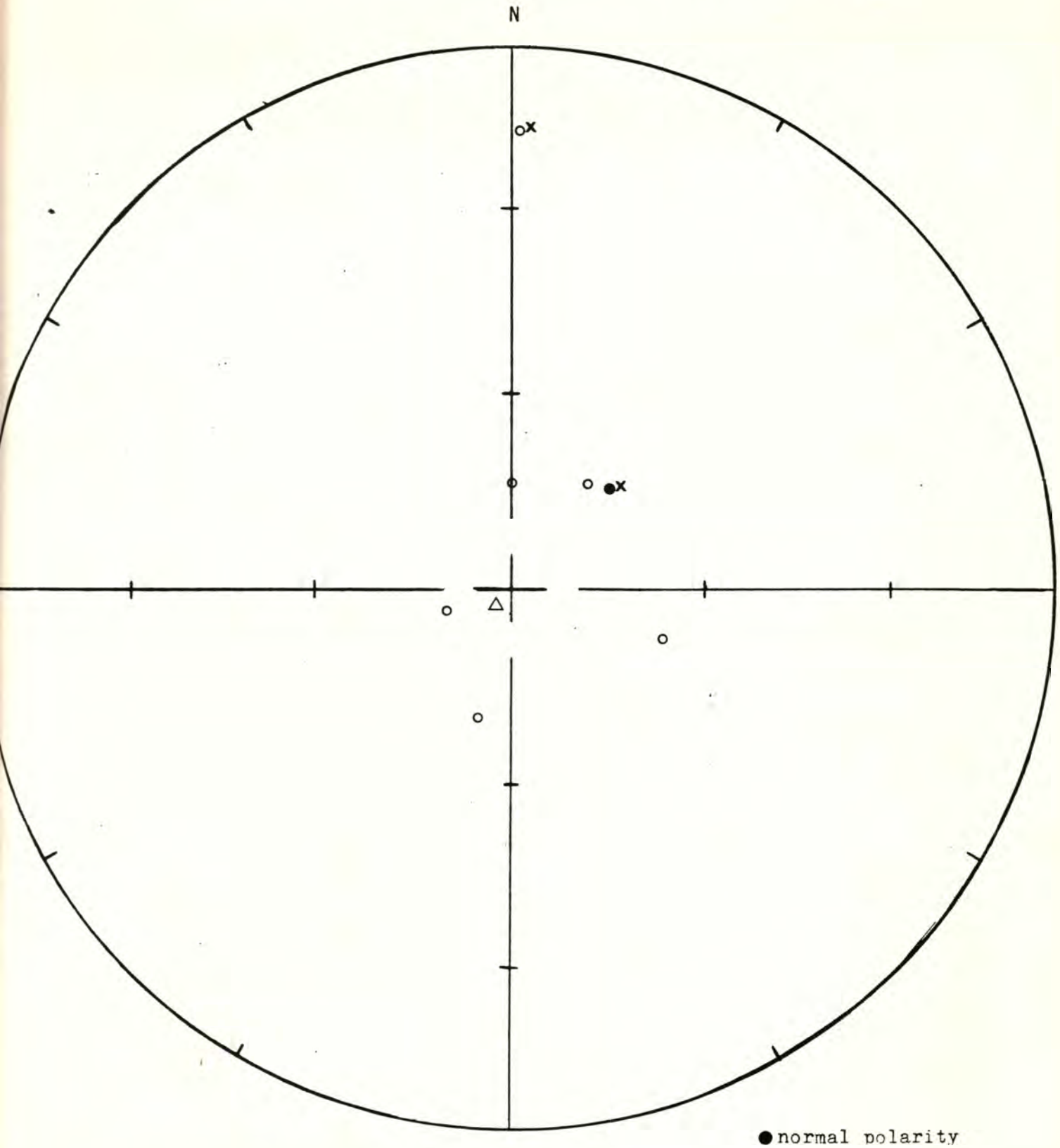

Site: 10.28.78.1 - Kennedy Falls

Demagnetization level: 500 oe.

● normal polarity

○ reversed polarity

□ site mean, normal polarit

△ site mean, reversed polarity

✕ Samples 393, 395 eliminated from site mean.

FISHER ON SAMPLE DIRECTIONS

Site: 7.7.79.1 -- Independence Valley Demagnetization level: NRM
SW¼ NW¼ sec. 15, T. 15 N., R. 4 W.

Sample number	Declination	Inclination
501	79.14	-33.54
502	128.28	-64.64
503	91.41	-36.84
504	96.86	-0.42
505	45.79	11.26
506	100.43	-43.31
507	62.91	-0.53

R= 4.89 Site declination= 98.97 Site inclination= -37.15

Alpha 95= 31.37 Delta= 45.68 Kappa= 2.84

Site latitude= 46.75° Site longitude= 123.25°

Paleolatitude= Paleolongitude= DELP=

DECLM=

Black Hills Project

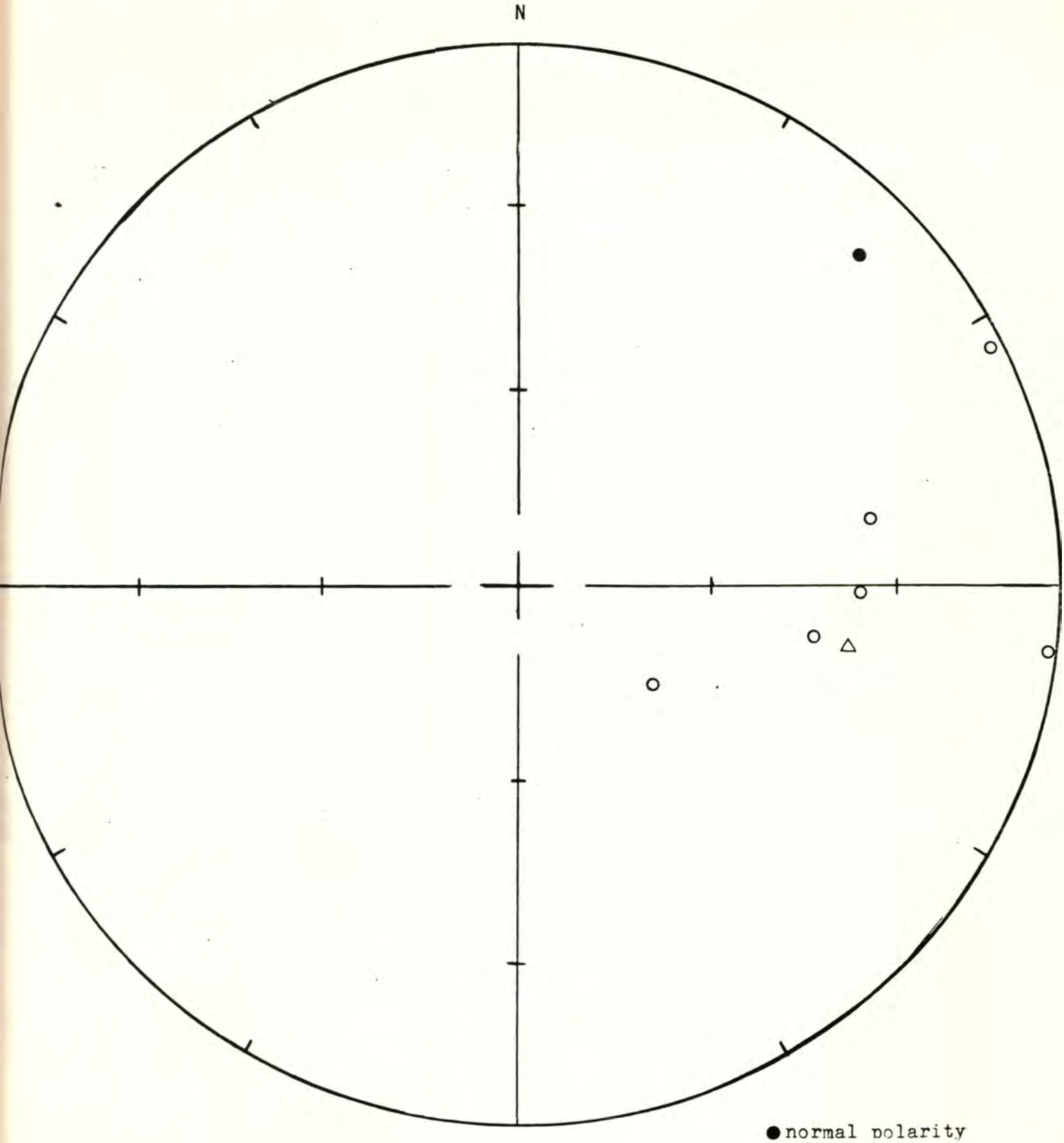

● normal polarity

○ reversed polarity

□ site mean, normal polarit

△ site mean, reversed polarity

Site: 7.7.79.1 - Independence Valley

Demagnetization level: NRM

FISHER ON SAMPLE DIRECTIONS

Site: 7.7.79.1 -- Independence Valley Demagnetization level: 400 oe.
SW¼ NW¼ sec. 15, T. 15 N., R. 4 W.

Sample number	Declination	Inclination
501	143.6	-56.69
502	164.76	-63.15
503	133.11	-52.51
504	129.85	-34.36
505	120.01	-50.29
506*	74.56	-25.23
507*	59.12	-27.34

*Samples rejected from site mean.

R= 4.87 Site declination= 135.9 Site inclination= -52.27

Alpha 95= 11.09 Delta= 12.87 Kappa= 31.86

Site latitude= 46.75° Site longitude= 123.25°

Paleolatitude= 53.96°N Paleolongitude= 140.17°E DELP=10.45

DECLM= 15.23

This site is rejected.

Black Hills Project

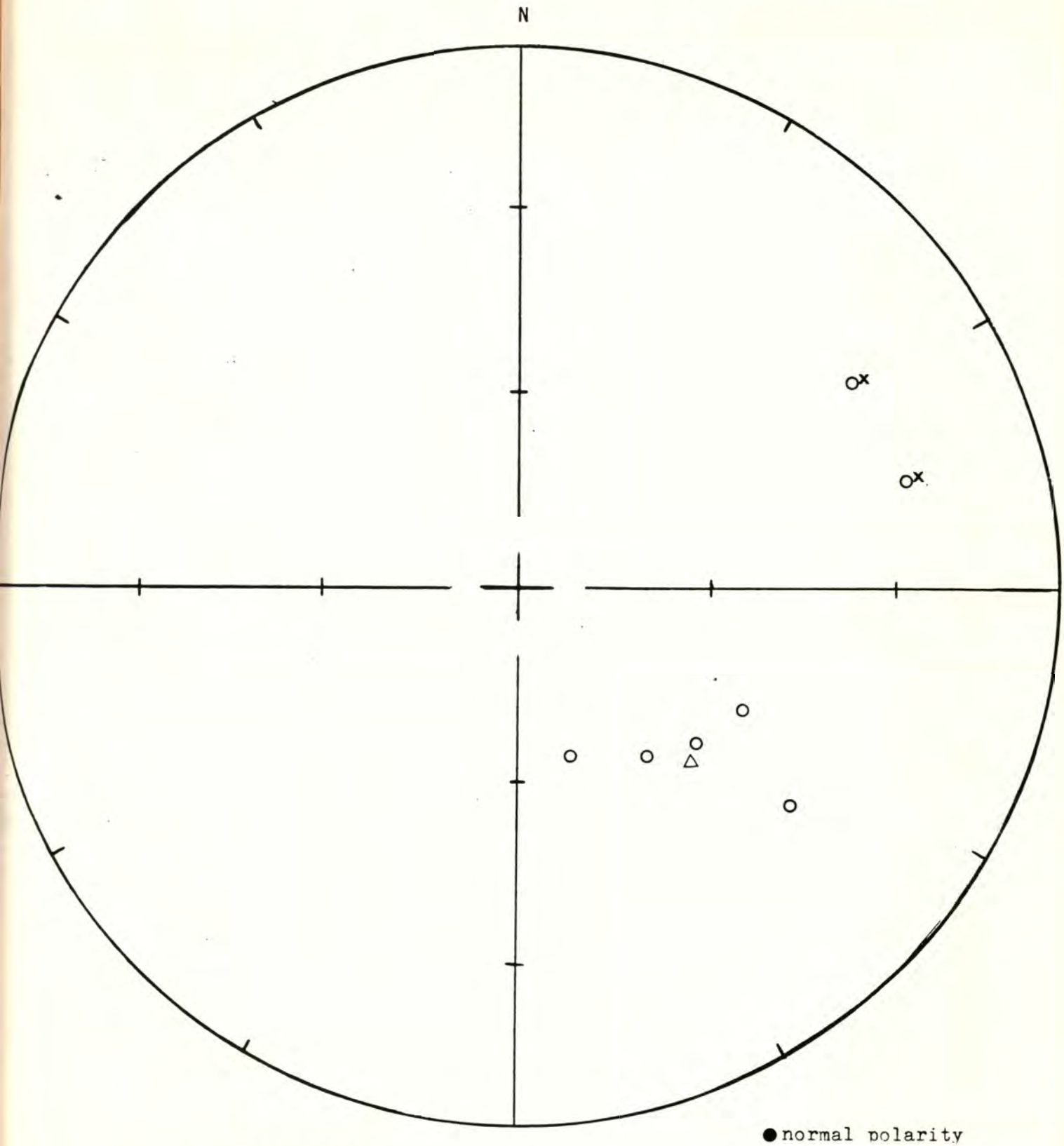

Site is rejected.

Site: 7.7.79.1 - Independence Valley

Demagnetization level: 400 oe.

● normal polarity

○ reversed polarity

□ site mean, normal polarit

△ site mean, reversed polarity

X Samples 506, 507 eliminated from site mean.

FISHER ON SAMPLE DIRECTIONS

Site: 7.8.79.1 -- Gate quarry. Demagnetization level: NRM

SW¼ NW¼ sec. 26, T. 16 N., R. 4 W.

Sample number	Declination	Inclination
508	14.92	49.10
509	3.30	50.12
510	13.16	44.64
511	10.28	54.09
512	23.32	47.46
513	175.17	-14.57

R= 5.80 Site declination= 9.06 Site inclination= 43.91

Alpha 95= 11.36 Delta= 14.74 Kappa= 25.31

Site latitude= 46.85° Site longitude= 123.12°

Paleolatitude= 67.66°N Paleolongitude= 34.96°E DELP= 8.89

DECLM= 14.21

Black Hills Project

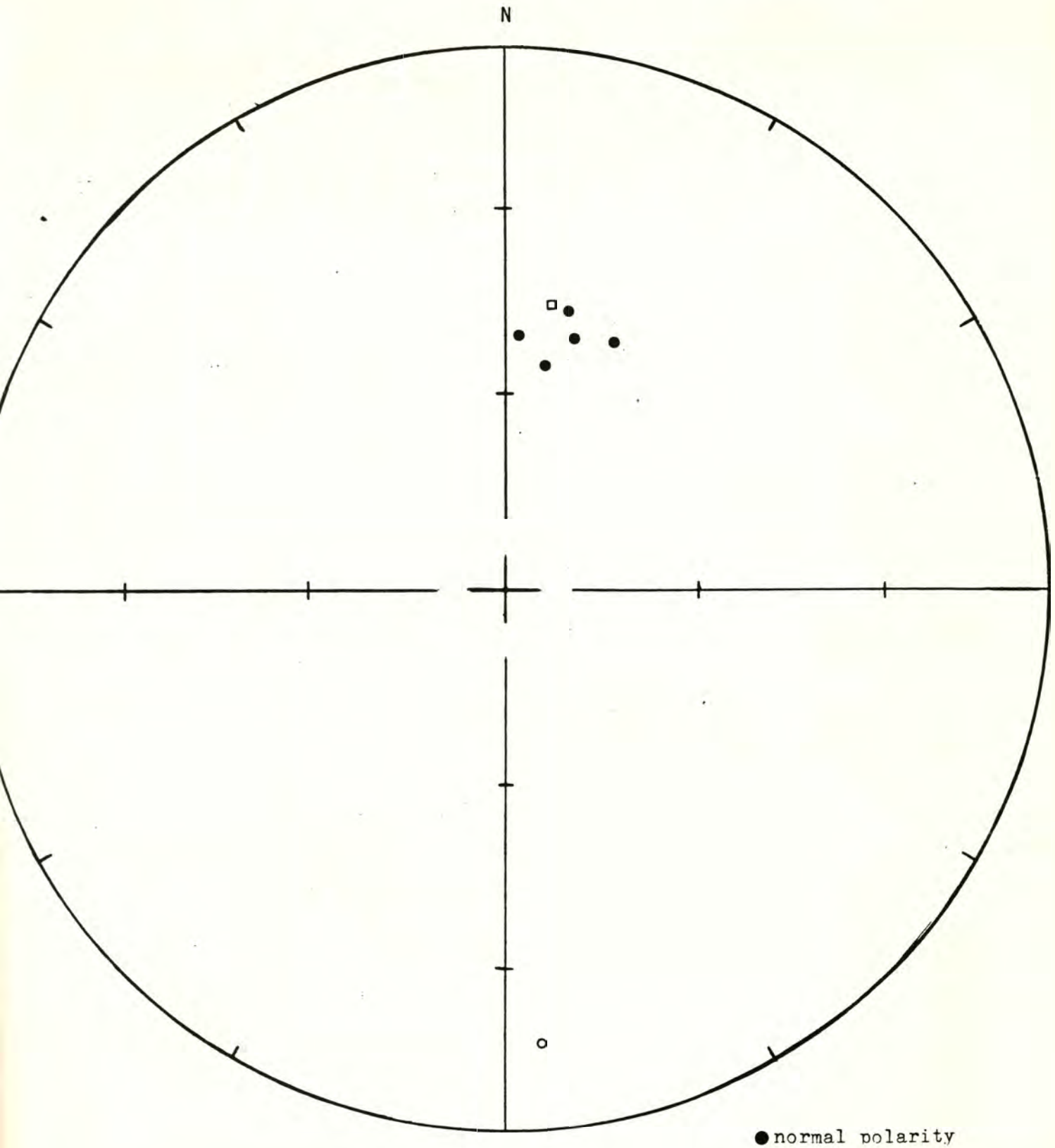

● normal polarity

○ reversed polarity

□ site mean, normal polarit

△ site mean, reversed polarity

Site: 7.8.79.1 - Gate quarry.

Demagnetization level: NRM

FISHER ON SAMPLE DIRECTIONS

Site: 7.8.79.1 -- Gate quarry. Demagnetization level: 400 oe.

SW¼ NW¼ sec. 26, T. 16 N., R. 4 W.

Sample number	Declination	Inclination
508	18.97	45.55
509	9.24	51.12
510	7.18	47.22
511	18.25	50.71
512	5.04	66.91
513*	167.91	-8.42

*Sample eliminated from site mean.

R=4.95 Site declination= 12.36 Site inclination= 52.41

Alpha 95= 7.20 Delta= 8.34 Kappa= 75.62

Site latitude= 46.85° Site longitude= 123.12°

Paleolatitude= 73.27°N Paleolongitude= 18.31°E DELP= 6.80

DECLM= 9.90

Black Hills Project

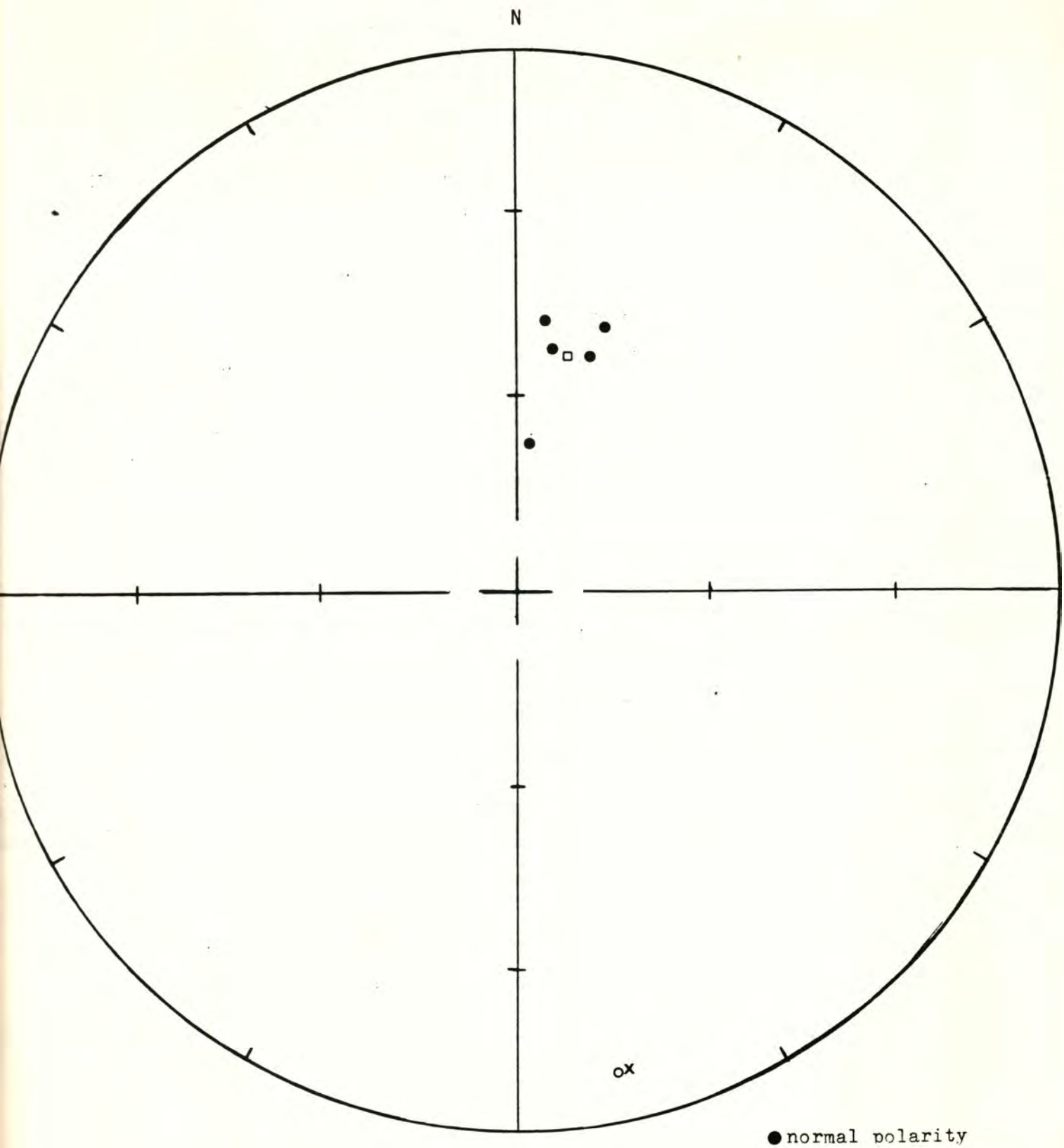

Site: 7.8.79.1 - Gate quarry

Demagnetization level: 400 oe.

● normal polarity

○ reversed polarity

□ site mean, normal polarit

△ site mean, reversed polarity

× Sample 513 is eliminated from site mean.

TECTONIC CORRECTION ON SAMPLE DIRECTIONS

Pole on site mean

Site: 7.8.79.1 Demagnetization level: 400 oe.

Dip azimuth: 222 (N48W) Dip angle: 28 (W)

Sample number	Declination	Inclination	Cor. dec.	Cor. inc.
508	18.97	45.55	352.49	68.89
509	9.24	51.12	328.50	69.25
510	7.18	47.22	332.85	65.48
511	18.25	50.71	342.20	72.84
512	5.04	66.91	278.65	73.60

R= 4.95 Site declination= 329.67 Site inclination= 71.54

Alpha 95= 7.20 Delta= 8.34 Kappa= 75.61

Site latitude= 46.85°N Site longitude= 123.12°W

Paleolatitude= 69.15°N Paleolongitude= 175.11°W DELP= 11.07

DECLM= 12.63

WITH TILT CORRECTION

Black Hills Project

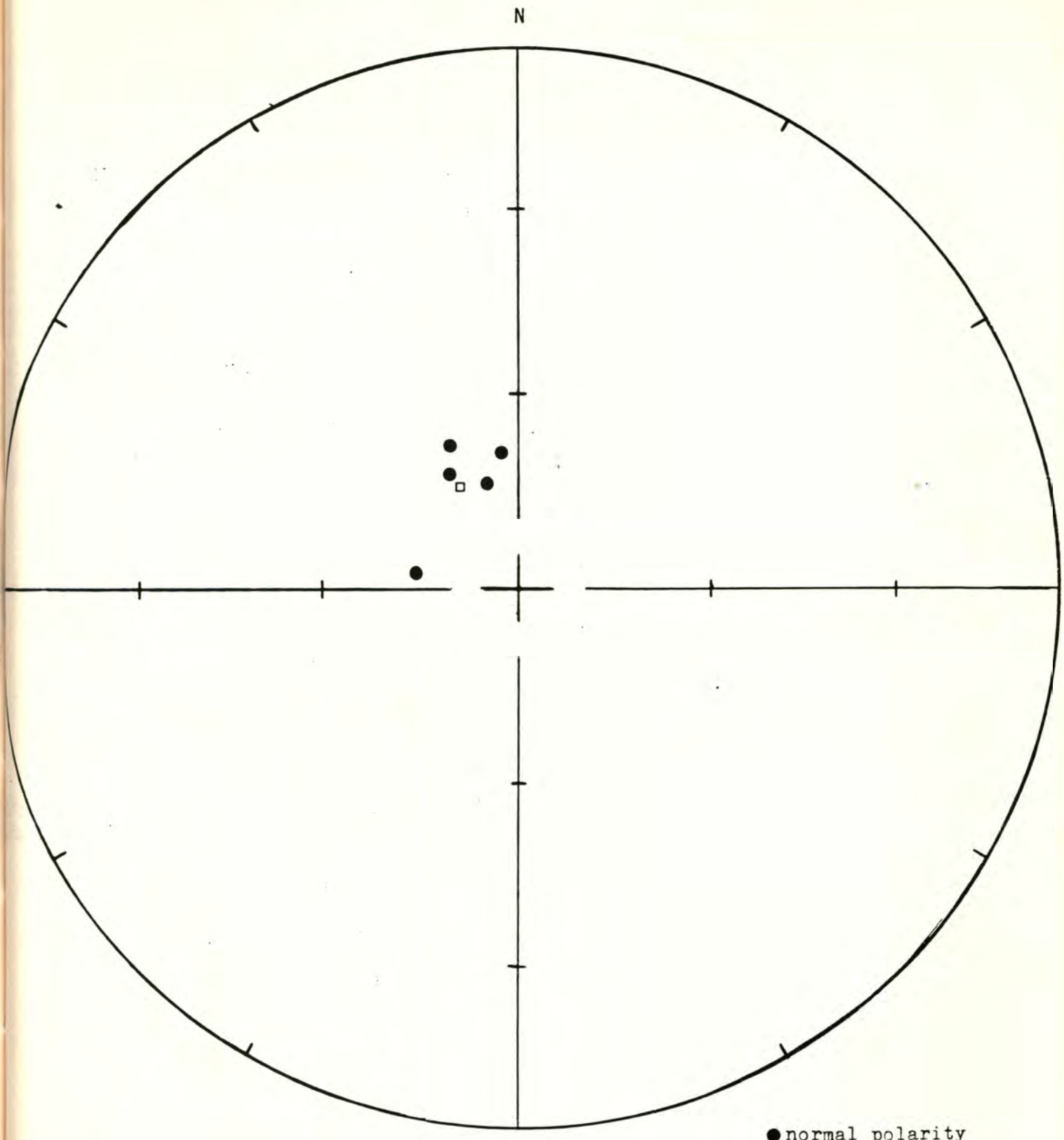

● normal polarity

○ reversed polarity

□ site mean, normal polarit

△ site mean, reversed polarity

Site: 7.8.79.1

Demagnetization level: 400 oe.

FISHER ON SAMPLE DIRECTIONS

Site: 7.8.79.2 -- Black River Demagnetization level: NRM

SW¼ SW½ sec. 20, T. 16 N., R. 3 W.

Sample number	Declination	Inclination
514	185.39	-77.16
515	185.96	-64.96
516	185.06	-41.60
517	201.75	-75.34
518	19.23	60.31
519	302.63	70.13
520	186.79	-72.47

R= 6.78 Site declination= 183.05 Site inclination= -67.68

Alpha 95= 10.06 Delta= 14.30 Kappa= 27.68

Site latitude= 46.83° Site longitude= 123.12°

Paleolatitude= 85.72°N Paleolongitude= 96.24°W DELP= 14.04

DECLM= 16.81

Black Hills Project

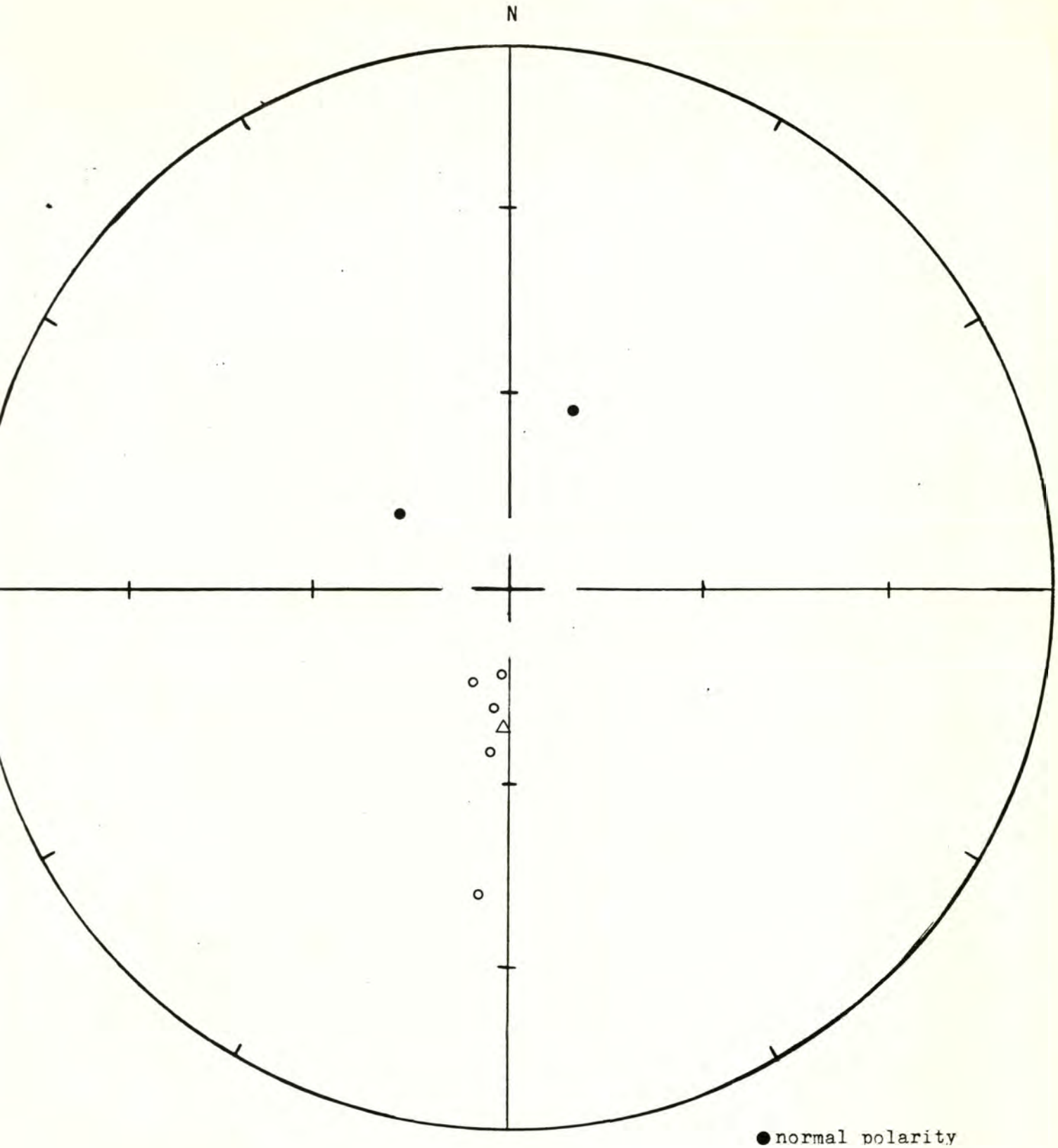

● normal polarity

○ reversed polarity

□ site mean, normal polarit

△ site mean, reversed polarity

Site: 7.8.79.2 - Black River

Demagnetization level: NRM

FISHER ON SAMPLE DIRECTIONS

Site: 7.8.79.2 -- Black River Demagnetization level: 300 oe.

SW¼ SW½ sec. 20, T. 16 N., R. 3 W.

Sample number	Declination	Inclination
514	191.03	-79.42
515	172.06	-75.46
516	220.33	-80.70
517	233.08	-77.07
518	157.27	-69.30
519	160.73	-61.11
520	199.13	-70.63

R= 6.90 Site declination= 183.10 Site inclination= -75.01

Alpha 95= 6.78 Delta= 9.62 Kappa= 60.95

Site latitude= 46.83° Site longitude= 123.12°

Paleolatitude= 74.9°N Paleolongitude= 117.5°W DELP=11.29

DECLM= 12.37

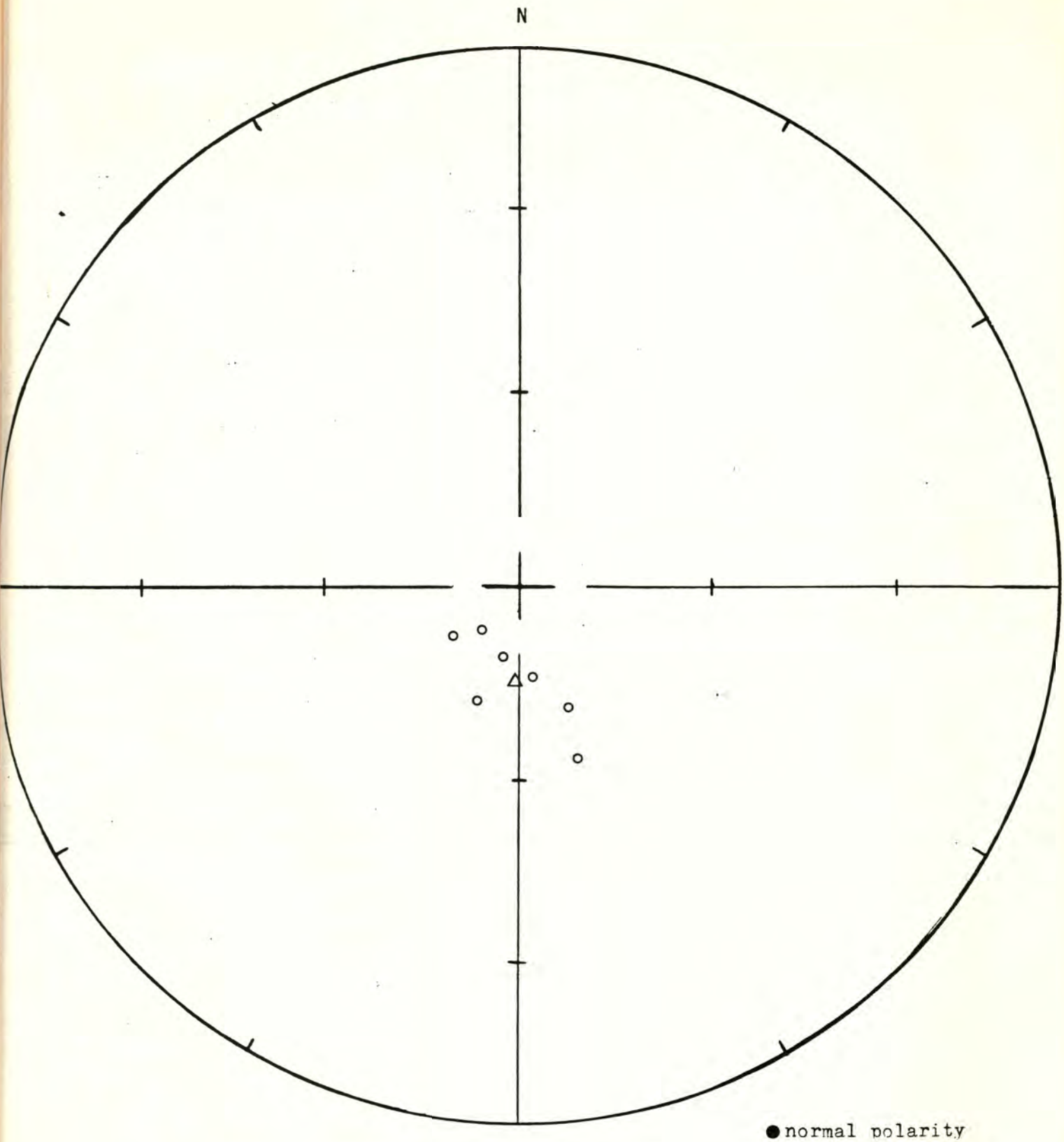

● normal polarity
○ reversed polarity
□ site mean, normal polarit
△ site mean, reversed polarity

Site: 7.8.79.2 - Black River

Demagnetization level: 300 oe.

APPENDIX F:

LIST OF PALEOMAGNETIC POLES REFERENCED IN FIGURE 1

Code	Paleopole	Age	Reference
AD	Andesite dikes, B.C.	K	*EPB- 10-086
AJ	Alaskan Jurassic rocks	J	EPB- 9-156
CM	Copper Mt. intrusion, B.C.	K	EPB- 8-302
CC	Captain Cove pluton, B.C.	K	Symons, 1977
EB1	Ecstall-Butedale pluton, B.C.	K	Symons, 1977
EB2	" - Hawkesbury warp	K	Symons, 1977
FB	Finger Bay lavas, Alaska	Te	EPB- 11-451
FD	Franciscan dunite, Calif.	J	EPB- 10-067
FF	Franciscan Fm., Calif.	J	EPB- 10-067
FM	Fleming Fiord Fm., Greenland	Tru	EPB- 8-241
FP	Franciscan peridotite, Calif.	J	EPB- 10-066
GB	Guichon batholith, B.C.	K	EPB- 8-132
GD	Gil Island complex, B.C.	K	Symons, 1977
HS	Howe Sound plutons, B.C.	K	EPB- 10-183
KB	Karmutsen Fm., B.C.	Tru	EPB- 8-261
KQ	Kasik-Quotton plutons, B.C.	Te	Symons, 1977
MP	Mary's Peak sill, Oregon	29 m.y.	EPB- 11-312
MT	Masset Fm., B.C.	66 m.y.	Hicken and Irving, 1977
NG	Nikolai greenstone, Alaska	Tru	Hillhouse, 1977
PM	Pliocene muds, Baja Calif.	Tp	EPB- 11-374
SC	Batholith, Calif.	121 m.y.	EPB- 10-161
SD	Sappington dike, Mont.	K	EPB- 10-048
SH	Shemya Island lavas, Alaska	Te	EPB- 11-450
SP	Stevens Pass granodiorite, WA.	85 m.y.	EPB- 10-118
SR	Siletz River Series, Oregon	Te	Simpson and Cox, 1977
ST	Stevens Island pluton, B.C.	102 m.y.	Symons, 1977
TF	Tyee-Flournoy Fm., Oregon	Te	Simpson and Cox, 1977
TS	Twin Sisters dunite, Wash.	Te	EPB- 11-657
YB	Yachats Basalt, Oregon	Te	Simpson and Cox, 1977

Ages: K= Cretaceous, J= Jurassic, Te= Eocene, Tp= Paleocene,
Tru= upper Triassic. *Earth Physics Branch catalog number

References for paleopoles in Figure 1:

Earth Physics Branch Catalogs of paleomagnetic directions and poles: All ages, first issue, Hicken, A., Irving, E., Law, L.K., and Hastie, J. (1972) Publications of the Earth Physics Branch, Energy, Mines, and Resources, Ottawa; Mesozoic, fourth issue (1976) Geomagnetic Series No. 6; Cenozoic, fifth issue, (1976) Geomagnetic Series No. 10.

Hicken, A., and Irving, E., 1977, Tectonic rotations in western Canada: Nature, v. 268, p. 219-220.

Hillhouse, J. W., 1977, Paleomagnetism of the Triassic Nikolai Greenstone, McCarthy Quadrangle, Alaska: Can. Jour. Earth Sci., v. 14, p. 2578-2592.

Simpson, R. W., and Cox, A., 1977, Paleomagnetic evidence for the tectonic rotation of the Oregon Coast Range: Geology, v. 5, p. 585-589.

Symons, D. T. A., 1977, Paleomagnetism of Mesozoic plutons in the westernmost complex of British Columbia: Can. Jour. Earth Sci., v. 14, p. 2127-2139.